UNIVERSIDAD AUTÓNOMA DE MADRID

FACULTY OF SCIENCE

Department of Applied Physical Chemistry

DEVELOPMENT OF ADVANCED ANALYTICAL METHODS FOR THE ANALYSIS OF FOOD COMPLEX MATRICES BY COMPREHENSIVE TWO-DIMENSIONAL LIQUID CHROMATOGRAPHY COUPLED TO MASS SPECTROMETRY (LC × LC-MS).

LIDIA MONTERO GARCÍA

PhD Thesis

INSTITUTE OF FOOD SCIENCE RESEARCH

(CIAL, CSIC-UAM)

Madrid, 2017

UNIVERSIDAD AUTÓNOMA DE MADRID

FACULTY OF SCIENCE

Department of Applied Physical Chemistry

DEVELOPMENT OF ADVANCED ANALYTICAL METHODS FOR THE ANALYSIS OF FOOD COMPLEX MATRICES BY COMPREHENSIVE TWO-DIMENSIONAL LIQUID CHROMATOGRAPHY COUPLED TO MASS SPECTROMETRY (LC × LC-MS).

PhD Dissertation presented by:

LIDIA MONTERO GARCÍA

To apply for the degree of:

DOCTOR IN BIOLOGY AND FOOD SCIENCE.

Work performed under the supervision of:

Dra. Elena Ibáñez Ezequiel

Dr. Miguel Herrero Calleja

Institute of Food Science Research

(CIAL-CSIC)

Academic supervisor:

Tiziana Fornari Reale

Universodad Autónoma de Madrid

(UAM)

INSTITUTO DE INVESTIGACIÓN
EN CIENCIAS DE LA ALIMENTACIÓN

CSIC
Consejo Superior de Investigaciones Científicas

UAM
UNIVERSIDAD AUTÓNOMA
DE MADRID

Elena Ibáñez Ezequiel, Research Professor of the Spanish National Research Council (CSIC) at the Institute of Food Science Research (CIAL),

And

Miguel Herrero Calleja, Tenured Scientist of the Spanish National Research Council (CSIC) at the Institute of Food Science Research (CIAL),

CERTIFY:

That the research work entitled: "**Development of advanced analytical methods for the analysis of food complex matrices by comprehensive two-dimensional liquid chromatography coupled to mass spectrometry (LC × LC-MS)**" presented by **Lidia Montero García**, has been performed under their supervision at the Department of Bioactivity and Food Analysis of the Institute of Food Science Research (CIAL). This dissertation is submitted in fulfilment of the requirements for the degree of doctor at Autonomous University of Madrid.

Madrid, 10 May 2017

Elena Ibáñez Ezequiel

Miguel Herrero Calleja

c/ Nicolás Cabrera, 9 • Campus de Cantoblanco • UAM • 28049 • Madrid
Tlf.: 91 001 79 00 • **Fax:** 91 001 79 05 • **www.cial.uam-csic.es**

CONTENTS

Abbreviations I

Summary V

Resumen VII

Structure of the PhD Dissertation IX

CHAPTER 1. INTRODUCTION 1

1.1. Food analytical chemistry. 3

1.1.1. Nutritional value and food composition. 4

1.1.2. Food safety. 6

1.1.3. Food quality and traceability. 7

1.2. Analytical techniques for the characterization of foods and natural products. 8

1.3. Multidimensional liquid chromatography (MDLC). 12

1.3.1. Historical perspective of MDLC. 12

1.3.2. Principles of MDLC. 13

1.3.2.1. Off-line, on-line and stop-flow 2DLC. 14

1.3.2.2. Types of 2DLC. 16

1.3.3. On-line comprehensive two-dimensional liquid chromatography (LC × LC) – theory. 18

1.3.3.1. Concepts of orthogonality in comprehensive two-dimensional liquid chromatography. 19

1.3.4. Peak capacity. 28

1.3.4.1. Effect of ^{1}D undersampling on peak capacity. 31

1.3.4.2. Effect of ^{2}D band broadening on peak capacity. 34

1.3.5. On-line LC × LC instrumentation. 35

1.3.5.1. Types of interfaces. 36

1.3.6. Challenges and requirements of the LC × LC instrumentation. 44

1.3.6.1. First dimension. 45

1.3.6.2. Second dimension 46

1.3.6.3. Interface. 51

1.3.7. Data analysis in on-line LC × LC. 55

1.3.7.1. Detectors. 55

1.3.7.2. Detection issues in on-line LC × LC. 56

1.3.7.3. On-line LC × LC data acquisition and data treatment. 57

1.3.8. On-line LC × LC applications in food analysis. 59

1.3.8.1. LC × LC for the analysis of phospholipids. 60

1.3.8.2. LC × LC for the analysis of triacylglycerols. 60

1.3.8.3. LC × LC for the analysis of phenolic compounds. 61

1.3.8.4. LC × LC for the analysis of carotenoids. 65

CHAPTER 2. AIMS AND WORK PLAN. 67

CHAPTER 3. CHEMICAL CHARACTERIZATION OF PROANTHOCYANIDINS BY HILIC × RP-DAD-MS/MS 73

3.1. Introduction. 75

3.1.1. Chemical structure of proanthocyanidins. 75

3.1.2. Chemical characterization of proanthocyanidins. 76

3.1.3. Detection of proanthocyanidins. 79

3.1.4. MDLC for the chemical characterization of proanthocyanidins. 80

3.2. Characterization of grape seed procyanidins by comprehensive two-dimensional hydrophilic interaction × reversed phase liquid chromatography coupled to diode array detection and tandem mass spectrometry. 81

3.3. Profiling of phenolic compounds from different apple varieties using comprehensive two-dimensional liquid chromatography. 95

3.4. Downstream valorization and comprehensive two-dimensional liquid chromatography-based chemical characterization of bioactives from black chokeberries (*Aronia melanocarpa*) pomace. 107

3.5. Profiling of *Vitis vinifera L.* canes (poly)phenolic compounds using comprehensive two-dimensional liquid chromatography. 119

3.6. General discussion. 155

3.6.1. Influence of method parameters. 155

3.6.2. Chemical characterization of proanthocyanidins-rich food-related samples by HILIC × RP. 164

CHAPTER 4. CHEMICAL CHARACTERIZATION OF PHLOROTANNINS BY HILIC × RP-DAD-MS/MS 173

4.1. Introduction 175

4.1.1. Phlorotannins in brown algae. 175

4.1.2. Chemical structure of phlorotannins. 176

4.1.3. Chemical characterization of phlorotannins. 178

4.1.4. Detection of phlorotannins. 181

4.2. Separation and characterization of phlorotannins from brown algae *Cystoseira abies-marina* by comprehensive two-dimensional liquid chromatography. 183

4.3. Anti-proliferative activity and chemical characterization by comprehensive two-dimensional liquid chromatography coupled to mass spectrometry of phlorotannins from the brown macroalga *Sargassum muticum* collected on North-Atlantic coasts. 193

4.4. General discussion. 207

4.4.1. Influence of method parameters. 207

4.4.2. Chemical characterization of phlorotannins from brown algae by HILIC × RP. 215

CHAPTER 5. CHEMICAL CHARACTERIZATION OF SAPONINS BY HILIC × RP-DAD-MS/MS. 223

5.1. Introduction. 225

5.1.1. Chemical structure of saponins. 226

5.1.2. Chemical characterization of saponins. 227

5.1.3. Licorice as a source of triterpene saponins. 228

5.2. Metabolite profiling of licorice (*Glycyrrhiza glabra*) from different locations using comprehensive two-dimensional liquid chromatography coupled to diode array and tandem mass spectrometry detection. 231

5.3. Focusing and non-focusing modulation strategies for the improvement of on-line two-dimensional hydrophilic interaction chromatography × reversed phase profiling of complex food samples. 249

5.4. General discussion. 291

5.4.1. Chemical characterization of the secondary metabolite profile of licorice samples and geographical origin assessment. 292

5.4.1.1. Influence of method parameters. 293

5.4.1.2. Chemical characterization of secondary metabolites from licorice by HILIC × RP. 296

5.4.2. Improvement of the HILIC × RP profiling of licorice. 302

5.4.2.1. Non-focusing modulation. 303

5.4.2.2. Focusing modulation. 306

CHAPTER 6. General conclusions / Conclusiones generals 311

REFERENCES 323

ANNEXES 357

ABBREVIATIONS

<β>	Peak broadening factor
σ	Standard deviation of the peak width
$^{1}\sigma$	Average standard deviation of the first dimension
$^{2}\sigma$	Average standard deviation of the second dimension
^{1}D	First dimension
^{1}dc	Internal column diameter of the first dimension
1DLC	One-dimensional liquid chromatography
^{1}F	First dimension flow rate
$^{1}n_c$	^{1}D individual peak capacity
$^{1}t_G$	First dimension gradient time
^{2}D	Second dimension
^{2}dc	Internal column diameter of the second dimension
2DLC	Two-dimensional liquid chromatography
$^{2D}n_c$	Theoretical peak capacity of the two-dimensional liquid chromatography system
$^{2D}n_{c,corrected}$	Practical peak capacity corrected by orthogonality
$^{2D}n_{c,\ practical}$	Practical peak capacity of the two-dimensional liquid chromatography system
^{2}F	Second dimension flow rate
$^{2}n_c$	^{2}D individual peak capacity
$^{2}t_c$	Second dimension time
$^{2}t_G$	Second dimension gradient time
$^{2}t_{reeq}$	second dimension equilibration time
ACN	Acetonitrile
Ag^{+}-LC	Silver ion liquid chromatography
A_o	Orthogonality
APCI	Atmospheric pressure chemical ionization

API	Atmospheric pressure ionization interface
CCC	Counter current chromatography
CCS	Collision cross section
CE	Capillary electrophoresis
CS	"Continuous shifting" second dimension gradient
DAD	Diode array detector
DMBA	Dimethoxybenzaldehyde assay
DP	Degree of polymerization
EFSA	European Food Safety Authority
ELSD	Evaporative light scattering detector
ESI	Electrospray ionization
EU	European Union
FD	Fluorescence detector
FIF	"Full in fraction" second dimension gradient
GC	Gas chromatography
GPC	Gel permeation chromatography
GRAM	Generalized rank annihilation method
HILIC	Hydrophilic liquid interaction chromatography
HPLC	High performance liquid chromatography
HRF	Heterocyclic ring fission
HRMS	High resolution mass spectrometry
i.d.	Internal diameter
IEX	Ion exchange chromatography
IM	Ion mobility
LC	Liquid chromatography
LC/a × m/LC	Active modulation
LC × LC	Comprehensive two-dimensional liquid chromatography

LC–LC	Heart-cutting liquid chromatography
LC × LC-MS	Comprehensive two-dimensional liquid chromatography coupled to mass spectrometry
LC-MS	Liquid chromatography coupled to mass spectrometry
LTM	Low thermal mass resistive heating
MALDI	Matrix assisted laser desorption/ionization
MCR-ALS	Multivariate curve resolution-alternating least squares
MDLC	Multidimensional liquid chromatography
MRLs	Maximum residue limits
MS	Mass spectrometry
MS/MS	Tandem mass spectrometry
NARP-LC	Non-aqueous reversed phase liquid chromatography
n_c	Peak capacity
NMR	Nuclear magnetic resonance
NP	Normal phase
PARAFAC	Parallel factor analysis
PCA	Principal component analysis
PEG	Polyethylene glycol
PFP	Pentafluorophenyl
PGUs	Phloroglucinol units
PLE	Pressurized liquid extraction
PUFAs	Polyunsaturated fatty acids
QTOF	Quadrupole Time-of-flight mass analyzer
RDA	Retro-Diels-Alder
RP	Reversed phase
SEC	Size exclusion chromatography
SFC	Supercritical fluid chromatography

SFE	Supercritical fluid extraction
SIF	"Segment in fraction" second dimension gradient
SPE	Solid phase extraction
Sz_x	Distance of each separated peak in the 2D and each asterisk lines of the "*asterisk equations method*"
TAGs	Triacylglycerols
t_G	Gradient time
TOF	Time-of-flight mass analyzer
$t_{Rnorm(i)}$	Normalized first and second dimension retention times
t_s	Sampling time
UHPLC	Ultra-high pressure liquid chromatography
UV-Vis	Ultraviolet–visible spectroscopy
$\overline{w}$	Average peak width

Summary

The importance of the development of novel analytical techniques lies in the growing needs and new applications that are arising in the analytical field, which require high resolving power in order to provide with enough information to characterize complex samples. In Food analysis, samples are commonly heterogeneous and are typically composed of multi-component mixtures of different chemical nature that are present in a wide range of concentrations. Moreover, some food samples contain significant amounts of compounds belonging to similar chemical families, involving very diverse mixtures of closely related compounds that are very difficult to be analyzed. Therefore, analytical techniques that are able to provide the maximum information about those samples are essential to address the new food analysis challenges.

In this regard, multidimensional liquid chromatography groups very powerful separation techniques that provide significantly increased values of peak capacity compared to one-dimensional conventional analytical platforms. The use of multidimensional techniques coupled to mass spectrometry in food applications is gaining importance due to the benefits of the enhanced separation and identification potential that can be achieved for samples that present hundreds, or even thousands, of compounds.

In this Doctoral Dissertation, the impressive analytical power of on-line comprehensive two-dimensional liquid chromatography (LC × LC) for the separation of very complex natural mixtures of compounds from different food sources is demonstrated. In particular, three main groups of secondary metabolites contained in seven different food-related samples deriving from plants and algae are exhaustively studied in this PhD Thesis, namely, proanthocyanidins, phlorotannins and triterpene saponins. These three groups have in common an important structural complexity due to the polymeric nature of proanthocyanidins and phlorotannins as well as to the very high variability of isomers and closely related structures in the case of triterpene saponins. Different on-line LC × LC methods based on the orthogonal coupling HILIC × RP were developed for each sample, and good separations, achieving high peak capacity values and orthogonality degrees were attained. Specifically, the separation of

complex mixtures of proanthocyanidins together with other polyphenolic compounds in grape seeds, apples, chokeberries and grapevine canes is presented in Chapter 3. On the other hand, the separation and characterization of typical polymeric phenolic compounds exclusively found in brown algae, namely phlorotannins, are studied in detail in Chapter 4, and their content on two different algae species (i.e., *Cystoseira abies-marina* and *Sargassum muticum*) is determined. Lastly, a new method is developed for the profiling of the secondary metabolite pattern present in licorice (*Ghlyzyrrhiza glabra*), including the presence of triterpene saponins as well as different polyphenols. Subsequently, different strategies based on the use of focusing and non-focusing modulation procedures are studied with the aim to produce quantitative improvements on resolving power and sensitivity, using licorice as a model complex food sample. These last two studies are contained in Chapter 5.

In addition, the development of LC × LC-based methods for the exhaustive chemical characterization of these interesting compounds helps to determine the native composition of the studied food-related samples, considering that sample preparation steps were reduced for their analysis. Thus, this analytical approach is demonstrated as very useful to correlate chemical composition with the potential biological properties that are attributed to the studied compounds. Moreover, this methodology is also capable to produce typical 2D profiles that could be applied to the determination of metabolic markers for geographical authentication assessment of valuable food products.

In conclusion, the results contained in this PhD Dissertation contribute to increase the knowledge on the composition of the seven analyzed food-related samples for future researches as well as to support with new data and applications the use of LC × LC as a promising analytical technique in the Food analysis field. These contributions have given rise to the publication of 8 original research articles (6 published/accepted and 2 submitted) included in international SCI journals within the Analytical Chemistry and Food Science and Technology categories.

Resumen

La importancia del desarrollo de nuevas técnicas analíticas reside en la aparición de nuevas aplicaciones y crecientes necesidades que están surgiendo en al campo analítico, las cuales requieren un alto poder de resolución que proporcione la información necesaria para caracterizar muestras complejas. En el análisis de alimentos, normalmente las muestras tratadas son heterogéneas y están compuestas por mezclas formadas por gran variedad de componentes de diferente naturaleza química, presentes en la misma en un amplio rango de concentraciones. Además, algunas muestras alimentarias contienen cantidades significativas de compuestos que pertenecen a familias químicas muy similares, dando lugar a diversas mezclas de compuestos estrechamente relacionados que resultan difíciles de analizar. Por lo tanto, para abordar los nuevos retos del análisis de alimentos son esenciales técnicas analíticas capaces de proporcionar la mayor información sobre dichas muestras.

En este sentido, la cromatografía de líquidos multidimensional agrupa técnicas de separación muy poderosas que proporcionan altos valores de capacidad de pico comparado con técnicas analíticas unidimensionales convencionales. El uso de técnicas multidimensionales acopladas a espectrometría de masas para aplicaciones alimentarias está ganando una gran importancia debido al elevado potencial de separación e identificación que son capaces de alcanzar para muestras que presentan cientos, o incluso miles, de compuestos.

En la presente Tesis Doctoral, se demuestra el enorme poder de separación de la cromatografía de líquidos bidimensional completa (LC × LC) para el análisis de mezclas naturales muy complejas procedentes de diferentes fuentes alimentarias. En particular, se presenta el estudio de tres principales grupos de metabolitos secundarios presentes en siete muestras alimentarias derivadas de plantas y algas: proantocianidinas, florotaninos y saponinas triterpénicas. Estos tres grupos tienen en común su gran complejidad estructural debido a la naturaleza polimérica de las proantocianidinas y los florotaninos, así como a la enorme variabilidad de isómeros y estructuras estrechamente relacionas de las saponinas triterpénicas. Para cada una de las muestras se ha desarrollado un método LC × LC diferente basado en el

acoplamiento ortogonal HILIC × RP, obteniéndose buenas separaciones y alcanzando altos valores de capacidad de pico y elevado grado de ortogonalidad.

Concretamente, en el Capítulo 3 se presenta la separación de mezclas complejas de proantocianidinas junto con otros compuestos fenólicos de semillas de uva, manzanas, Aronia negra y sarmientos de vid. Por otro lado, en el Capítulo 4 se detalla la separación y caracterización de compuestos fenólicos poliméricos típicos y exclusivamente presentes en algas marrones; en este capítulo se determina el contenido en florotaninos de dos especies de algas (*Cystoseira abies-marina* and *Sargassum muticum*). Por último, se desarrolla un nuevo método para estudiar el perfil de metabolitos secundarios en regaliz (*Ghlyzyrrhiza glabra*), incluyendo saponinas triterpénicas y diferentes polifenoles. Posteriormente, se estudiaron diferentes estrategias de modulación con y sin efecto de enfoque con el objetivo de generar mejoras cuantitativas en el poder de resolución y sensibilidad, utilizando la muestra de regaliz como modelo de muestra alimentaria compleja. Estos dos últimos estudios están incluidos en el Capítulo 5.

Así mismo, el desarrollo de métodos basados en LC × LC para la caracterización química exhaustiva de estos interesantes compuestos ayudó a determinar la composición nativa de las muestras alimentarias estudiadas, considerando que se redujeron los procesos de preparación de la muestra para su análisis. De esta manera, ha sido posible demostrar la gran utilizad de esta técnica para correlacionar la composición química de la muestra con sus potenciales propiedades biológicas.

En conclusión, los resultados obtenidos en esta Tesis Doctoral contribuyen a incrementar el conocimiento sobre la composición de las siete muestras alimentarias analizadas para futuras investigaciones, así como para apoyar con nuevos datos y aplicaciones el uso de LC × LC como una técnica analítica prometedora en el campo del análisis de alimentos. Estas contribuciones han dado lugar a la publicación de 8 artículos de investigación originales (6 publicados/aceptados y 2 actualmente en proceso de revisión) en revistas incluidas en el SCI (en las categorías de Química Analítica y Ciencia y Tecnología de los Alimentos).

Structure of the PhD Dissertation

This Doctoral Dissertation is structured in four main parts containing six Chapters as explained below:

- **General introduction**, where a broad view of the analytical technique aim of this study, as well as its main theoretical and practical fundamentals, are described (Chapter 1).
- **Aim and work plan**, where the main objective and the related partial objectives developed within the scope of this Dissertation are summarized. Besides, the work plan followed to achieve those objectives is explained (Chapter 2).
- **Results and discussion**. In this part of the Dissertation, the results obtained during the PhD period are presented. Results are divided in three chapters (Chapter 3-5). Each chapter groups the results obtained for the different studied groups of compounds and is divided in several sections:
  i. An introduction to the importance of the studied compounds, their chemical structure, chemical characterization as well as the background and the need of using multidimensional liquid chromatography for their study.
  ii. The publications derived from the studies carried out during this PhD.
  iii. A general discussion, where the main results of the included works in each chapter are discussed and integrated.

- **General conclusions**, where the most relevant findings achieved during this PhD Thesis work are summarized (Chapter 6).

CHAPTER 1.

Introduction

1.1. FOOD ANALYTICAL CHEMISTRY.

Analytical Chemistry is defined as "the science of chemical measurement. Its objective is the generation, treatment and evaluation of signals from which information is obtained on the composition and structure of matter" (Danzer 2007). When this concept is applied to food, the definition refers to the application of chemical measurements to obtain information about properties and characteristics of foods and its components, including for instance, composition and physicochemical characteristics, giving rise to one important branch on analytical chemistry, the food analytical chemistry.

Food analysis involves the interaction between modern food science and nutrition as well as different food-related aspects, such as food nutritional value, food safety, quality control or traceability through the employment of advanced food strategies (Ibáñez and Cifuentes 2014). Figure 1.1 outlines the main areas in which food analysis has an important influence. All these issues are well established under the Foodomics concept, defined as "a discipline that studies the food and nutrition domains through the application and integration of advanced -omics technologies to improve consumer's well-being, health and confidence" (Cifuentes 2009). Although food analytical chemistry also includes very well-known conventional analytical techniques, the use of modern food analysis and Foodomics is closely related to the implementation of advanced strategies and analytical tools. Among these techniques, hyphenated analytical tools based on the coupling of separation techniques and spectroscopic techniques, such as those described in this PhD Dissertation, are pointed out.

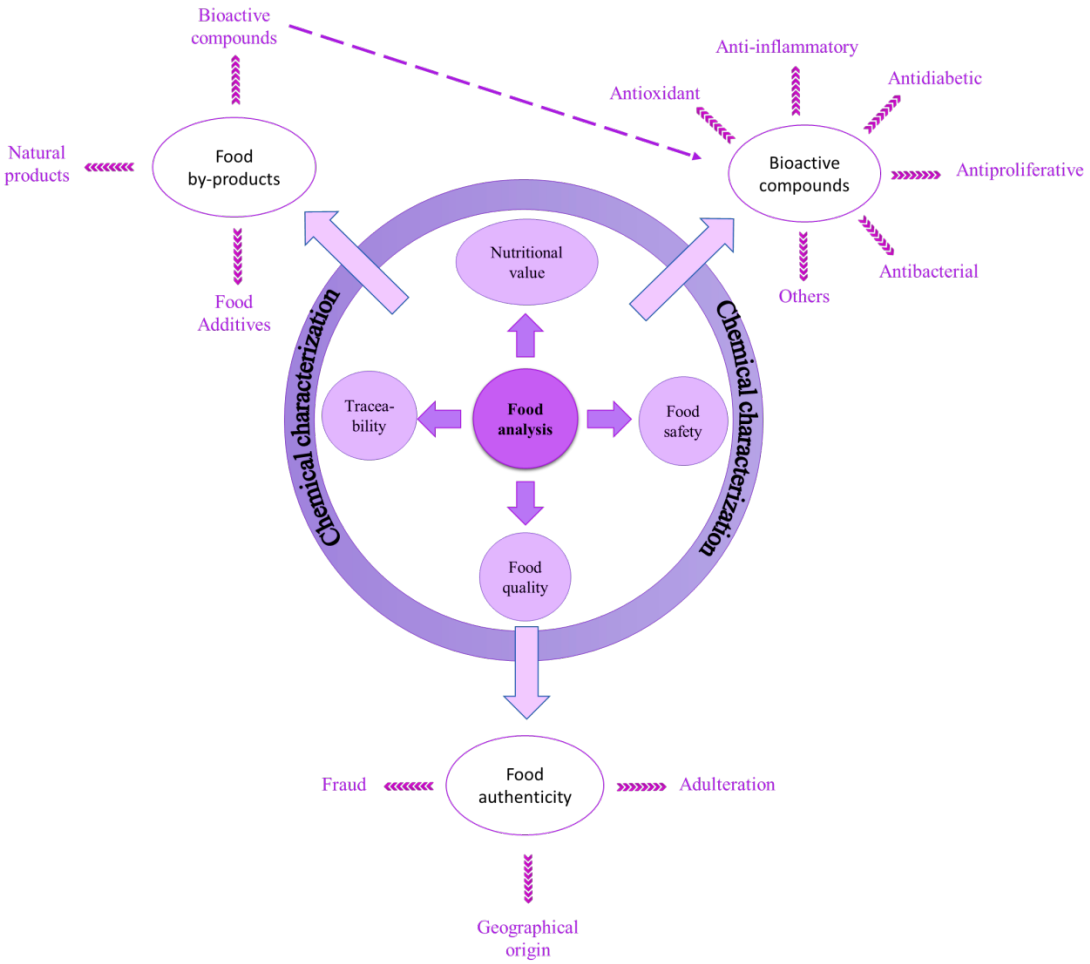

Figure 1.1. Main fields of application of food analysis.

1.1.1. NUTRITIONAL VALUE AND FOOD COMPOSITION.

Due to the fact that new foodstuffs are continuously appearing in the market, the identification and quantification of the food nutrients profile is mandatory. The European Union (EU) is undertaking a big effort to regulate the nutritional information of food, in particular of novel foods and functional foods with health-related claims. To manage the new nutritional information, the EU formed in 2002 the European Food Safety Authority (EFSA), which is the responsible body to propose a regulation for the nutritional and health claims designation in foods (Regulation (EC) No 1924/2006). Thanks to this regulation and to the increase on the available nutritional information, consumers are gradually more interested on knowing the nutritional characteristics of products present in the market (Kaur et al. 2016). Besides, the increment in the prevalence of diet-related diseases in developed countries, such as metabolic

syndrome, type 2 diabetes, cardiovascular, liver and kidney diseases or some types of cancer, has caused the increase on research related to the potentially positive or negative effects of some food components on health, associated with a well-balanced diet (Ard et al. 2016; de la Iglesia et al. 2016).

Therefore, although the determination of the energetic balance and the main macronutrients such as carbohydrates, lipids and proteins is critical, the specification of micronutrients like vitamins and minerals is also considered essential (Visioli et al. 2007). Moreover, nowadays, important attention is paid on some secondary metabolites that are not traditionally considered nutrients, mainly found in plants and algae; due to the potential health-promoting effects that a wealth of scientific reports is attributing to those components, their precise characterization might also be worth. Hence, to satisfy the demand about information of food nutritional value and health-related bioactivity, powerful analytical tools able to provide with high throughput, resolution power and sensitivity, are required to proceed with the chemical characterization of food products.

Secondary metabolites have the primary function of protecting plants and algae against environmental stresses. Some of these components belong to diverse chemical classes, such as phenolic compounds, carotenoids, alkaloids, saponins, glucosinolates, or terpenes, among others. Due to the already mentioned potential positive effects on human health, at present, different natural sources are being proposed for the recovery of bioactive compounds that could be later on introduced into new foods. The compounds that may confer these new properties are usually called functional ingredients, and the new foods in which are contained, functional foods. In this regard, the chemical characterization of natural products and extracts in which those compounds are found has a key role in the elucidation of the effects that these compounds may provide; in fact, a close relationship between phytochemical composition and bioactivity exists. At present, the number of described bioactive metabolites is continuously growing as new natural sources are studied. The extraction from the natural matrix and the development of fast and efficient analytical methods may be the first steps for the determination of its biological function (Kris-Etherton et al. 2004; Brusotti et al. 2014; Cieśla and Moaddel 2016; Sánchez-Camargo et al. 2017).

In addition to the use of natural sources to attain bioactive compounds, the use of agrifood-related wastes and by-products is of high interest nowadays. Food wastes represent a serious problem in the food industry due to the huge quantity of residues generated during processing. For instance, in the fruit-related industry, the amount of generated wastes can reach 20-50%, depending on the kind of fruit. However, many studies have described the still high nutrient value of those residues, considering that there are still important amounts of phytochemicals, such as pectins, fiber, carbohydrates, lipids, vitamins, carotenoids, phenolic compounds or essential oils, among others (Hernández-Santos et al. 2015; Asif et al. 2016; Esparza-Martínez et al. 2016, De Ancos et al. 2015). Thus, the wastes obtained during food processing could be valorized through the generation of high-added value compounds. However, to find an appropriate destination for these valorized by-products is essential to carry out an exhaustive study of their chemical composition in order to obtain the necessary knowledge about their potential. For this reason, the development of advanced analytical methods is also focused on the study of food-related by-products.

1.1.2. FOOD SAFETY.

Food safety refers to the control of the constituents that can be present in food and may pose a risk for human health. The main food hazards are contaminants such as pesticides, fungicides, toxins and environmental pollutants, pathogenic microorganisms or some natural food constituents like allergens or anti-nutritional compounds (Lawal et al. 2016). The absence of a regulation about the control of the presence of these contaminants in food could lead to serious health problems because of the interaction between these risk factors and human diet (Bhat 2008). For this reason, in 2002, the European Commission established, at European level, the analytical methods validation requirements for the detection and quantification of specific contaminants (Regulation (EC) No 178/2002), as well as stringent food safety-related legislation that sets the maximum residue limits (MRLs) for food contaminants, such as pesticides (Regulation (EC) No 396/2005), veterinary drug residues (Regulation (EC) no 37/2010) and other compounds (Regulation (EC) No 1881/2006). The aim of these regulations was to control agricultural, processing and market practices in order to limit the consumer

exposure to these harmful contaminants. Consequently, accurate, sensitive, robust and fast analytical methods able to detect very low concentrations of those contaminants in a variety of very complex samples are a necessity to comply with the regulatory requirements (Castro-Puyana and Herrero 2013). At present, hyphenated techniques coupling separation tools (chromatography) and spectroscopic techniques (mass spectrometry) are the most-widely used analytical approaches to this aim.

1.1.3. FOOD QUALITY AND TRACEABILITY.

Food quality is related to the food attributes responsible for the value of the product and it is one of the most important parameters for food consumers. There are many parameters that can define the food quality: food components, aroma, flavor, taste or color. The main difficulty in the establishment of food quality is that all these parameters depend not only on each specific product and process but also on the particular consumer perception. Consequently, there is a strong subjective influence. Traditionally, this has meant that food quality assessment has mainly been carried out through the application of subjective tools, such as sensory panels. However, at present, new approaches are being developed in order to provide objective measures of food quality. Thus, this field is one of which modern analytical chemistry is needed (Castro-Puyana et al. 2013b; Wang et al. 2013).

Traceability lies in the monitoring of all the steps along the agri-food chain, from the raw material to the consumer; in other words, this process is known as "from farm to fork". The traceability process arises from the food safety and quality concepts, with the main goal of providing all the required information about production, transport and storage to keep safety incidents under control. It is accomplished by registering complete and accurate information of a product and its components at every step of the food processing chain. Chemical characterization plays an essential role across the traceability process as its application is able to provide with the monitoring of the information about food composition data in each processing step, as well as it allows following the history of the product and support food labeling (Kok et al. 2012; Doğu and Şİrelİ 2016).

Advanced analytical tools are also employed nowadays to assess the geographical origin of certified products, which is a characteristic that lies between the fields of food quality and traceability. In this regard, the chemical characterization of the phytochemical composition can also be useful for the determination of geographical origin, as the present phytochemical compounds will vary as the plant adapts itself to the environmental conditions. Therefore, the metabolite profile of the food products might vary according to the climate of the geographical area where they are produced and, in consequence, a classification by zones or an identification of the geographical origin of a product can be done by the study of the whole metabolite content (fingerprinting), the analysis of the profile of a specific phytochemical group (profiling) or by searching specific metabolic markers of a particular region (Cuadros-Rodríguez et al. 2016). To this aim, chemical characterization in combination with chemometric analyses can be a useful tool to ensure food authentication and quality control with the aim of protecting high-value products against frauds (Danezis et al. 2016; Pardo-Mates et al. 2017; Siddiqui et al. 2017).

1.2. ANALYTICAL TECHNIQUES FOR THE CHARACTERIZATION OF FOODS AND NATURAL PRODUCTS.

As it has been pointed out in the previous section, food chemical characterization is essential not only for the evaluation and determination of food characteristics and their composition, but also for the study and assessment of safety, quality and traceability of foods. The measurement of these parameters is usually carried out by the employment of analytical tools that provide qualitative and quantitative information about the compounds of interest (Di Stefano et al. 2012).

From an analytical point of view, foods are complex matrices, since they can be considered as a mixture of a wide variety of compounds of different chemical nature. Therefore, the analytical methods used to characterize and to determine the composition of foods require the use and implementation of advanced analytical techniques able to provide with appropriate robustness, efficiency and sensitivity (Cifuentes 2012).

Nowadays, one of the most growing groups of applications devoted to food chemical characterization involves the separation and characterization of food components from plant origin as well as from algae, due to the increasing interest in natural products (Milledge et al. 2016; Waltenberger et al. 2016; Sánchez-Camargo et al. 2017). This interest is related to the potential health benefits that are ascribed to some micronutrients and secondary metabolites present in those matrices. In this regard, modern analytical tools should be employed to support studies in which the bioactivity of those components is investigated.

The separation and characterization of the metabolite profiles of plants and algae is a significant analytical challenge due to the huge quantity of diverse metabolites present in natural products and extracts and, even more, considering that secondary metabolites are usually present at low concentrations. To facilitate the analysis, proper sample preparation steps should be usually followed, for instance, extraction, clean-up, saponification, hydrolysis or derivatization. However, sometimes, these steps produce a modification of the native composition, due to the strong conditions that are frequently applied. As a result, the chemical pattern later on determined may not completely correspond to the natural composition. For this reason, whenever possible, analytical methods in which there is no sample preparation or pretreatments are preferred.

To reach all these requirements and to provide detailed chemical characterization of such complex samples, very efficient analytical techniques are needed. Capillary electrophoresis (CE), gas chromatography (GC), liquid chromatography (LC) and supercritical fluid chromatography (SFC) are the most used separation techniques for the elucidation of natural extracts and foods composition (Cifuentes 2012; Gallo and Ferranti 2016). These techniques can be coupled to different detectors, which determine the sensitivity and the detection limits of the technique (Locatelli et al. 2012).

However, due to the complexity of food samples, these techniques alone cannot often provide all the required information for the characterization. Thus, the use of these techniques in combination to other techniques such as nuclear magnetic resonance (NMR) and mass spectrometry (MS) is, in practice, indispensable to increase the identification capabilities of

those tools as well as to provide structural information of compounds present in the complex sample (Wishart 2008; Sarker and Nahar 2012; Cai et al. 2016).

Within all the analytical techniques, the hyphenation between LC and MS (LC-MS) is highlighted as one of the most extended tools for the chemical characterization in food and natural products analysis (Wu et al. 2013; Cai et al. 2016). LC offers good reproducibility, selectivity and versatility thanks to the great diversity of available separation mechanisms (normal phase (NP), reversed phase (RP), hydrophilic liquid interaction (HILIC), size exclusion chromatography (SEC) or ion exchange chromatography (IEX)). The capacity of LC to separate analytes of very different physicochemical properties is another reason why LC is widely extended; for example LC allows the separation of compounds from low to high molecular weight, metabolites with a wide range of polarity, as well as with different acid-base properties (Di Stefano et al. 2012; Núñez et al. 2012). The characteristics of versatility and selectivity achievable by LC are essential for the characterization of natural food extracts, because, as complex matrices, they are composed of metabolites with very different chemical nature and diverse dynamic range. For example, these metabolites can present polarities ranging from highly non-polar compounds such as fatty acids, triacylglycerols or carotenoids, to completely polar compounds, as may be the case of phenolic compounds or carbohydrates. On the other hand, when MS is coupled to LC, provides molecular weight information and even structural information if tandem MS (MS/MS) experiments of the previously separated compounds are employed (Cai et al. 2016). With MS, the analysis of compounds with a wide range of polarity is also possible, thanks to the use of atmospheric pressure ionization (API) interfaces (electrospray ionization, ESI, and atmospheric pressure chemical ionization, APCI), that are the most commonly employed ionization sources in food analysis. APCI is more suited for the ionization of low and moderate polarity compounds whereas ESI is used for polar compounds (Wu et al. 2013; Schmitz 2016). For instance LC-MS has been widely employed for the characterization of phenolic compounds from many different natural sources such as cocoa (Ali et al. 2015; Cádiz-Gurrea et al. 2017), apples (Sánchez-Rabaneda et al. 2004; De Paepe et al. 2013; Alarcón-Flores et al. 2014), citrus, berries (Del Bubba et al. 2012; Ancillotti et al. 2016; Tian et al. 2017) grapes (Ribeiro et al. 2015), aromatic plants (Herrero et al. 2010;

Spiridon et al. 2011; Vallverdú-Queralt et al. 2014b), green leafy vegetables (Schmidt et al. 2010; Khanam et al. 2012), and algae (Ferreres et al. 2012; Liu and Gu 2012; Steevensz et al. 2012), among many other natural products (Capriotti et al. 2015; Lucci et al. 2016).

LC-MS has also provided good results in the determination of the carotenoid profile of microalgae (Castro-Puyana et al. 2013a; Crupi et al. 2013; Gilbert-López et al. 2015), tomato and related products (Daood et al. 2014; Vallverdú-Queralt et al. 2014a; Gentili et al. 2015) and carrots (Saha et al. 2015), alkaloids from honey (Betteridge et al. 2005; Bretanha et al. 2014; Kast et al. 2014), cereals (Krska et al. 2008) and tea (Mathon et al. 2014) or saponins from black beans (Guajardo-Flores et al. 2012), tea (Matsui et al. 2009), soy (Gu et al. 2002b; Kamo et al. 2014; Krishnamurthy et al. 2014), ginseng (Stavrianidi et al. 2017) or licorice (Montoro et al. 2011), among other multiple sources.

In many cases, the complexity of food samples and the analytical problems that a high number of different compounds produce are greater than the separation power that conventional LC can provide. Hence, an increase in the efficiency as well as methods that provide higher resolution are required.

In this regard, separation efficiency can be improved by the increment of the column length and by decreasing the size of the stationary phase particles. However, in practice, these efficiency improvements are related to a significant increase of the analysis times and a growing system backpressure that cannot be borne by the conventional high performance liquid chromatography (HPLC) instruments. Several improvements have appeared to partially solve these conflicts, for example, the use of high temperatures to decrease the mobile phase viscosity, the use of monolithic columns that produce lower backpressure because of their lower column resistance factor, or the most important instrumental improvement, the development of ultra-high pressure liquid chromatography (UHPLC) instruments, able to cope with pressures up to 1400 bar. The use of these instruments allows running separations on columns equipped with sub-2 μm particles (Guillarme et al. 2010; Vivó-Truyols et al. 2010; Núñez et al. 2012), that may significantly increase efficiency and performance compared to conventional instruments and columns (Fekete et al. 2014).

In spite of these advancements, there are samples that are simply too complex to be analyzed in a one-dimensional procedure. In those situations, separation techniques that may offer higher resolving power than conventional HPLC, or even UHPLC, systems are required. In this sense, the coupling of two or more chromatographic systems becomes an attractive alternative.

1.3. MULTIDIMENSIONAL LIQUID CHROMATOGRAPHY (MDLC).

1.3.1. HISTORICAL PERSPECTIVE OF MDLC.

Multidimensional liquid chromatography appeared as a response to the necessity of resolving extremely complex samples such as peptides and proteins or polymers. Chromatographic approaches based only on one separation system may offer just part of the information of such complex samples, but important information may remain concealed due to the use of a poor resolving power comparing with the complexity of the sample (Cohen and Schure 2008).

One of the first approaches to MDLC was developed by Consden et al. (1944). This application consisted on a planar two-dimensional paper chromatography for the separation of amino acids. The analysis comprised, firstly, the elution of the sample in one direction of the paper by the use of a particular solvent as mobile phase, arising a partial separation of the amino acids in one dimension. Then, when the cellulose was dried, another different solvent was applied in a direction at right angle to the first to further separate the sample. The main novelty was the increase on the separation space, since compounds could be separated into a separation area instead to one-dimensional space. Short time before, some advances of two-dimensional column chromatography were applied for the purification of chlorophylls (Strain and Manning 1942) and for the separation of amino acids (Wachtel and Cassidy 1943).

After these first approaches, the possibility of gaining separation power through the use of two-dimensional space generated great interest, and therefore, new applications and improvements emerged over the time. The main effort was focused on the employment of chromatographic columns, since column chromatography enables greater control of the separation procedure, providing automation, higher reproducibility, speed and efficiency. Besides, other important advantage of the use of columns is their much easier coupling to

detectors, which is critical to characterize the separated analytes (Cohen and Schure 2008). Therefore, the demand of more sophisticated instruments started to be critical.

These improvements helped to expand the use of two-dimensional techniques to other analytical fields besides proteins and polymers applications; for example, to the pharmaceutical, environmental, food and natural products fields as well as to the analysis of biological samples.

The first real coupling of two columns with the aim of performing a multidimensional separation was implemented by Erni and Frei (1978). They employed a coupling between a gel permeation chromatography (GPC) and a reversed phase separation for the separation of plant extracts. It was the first time that an automatic transfer of fractions from one column to the other was utilized, giving the key for the development of the following MDLC methods until date. Twelve years later, in 1990, Bushey and Jorgenson, developed a MDLC method that may be considered the foundations of the present MDLC (Bushey and Jorgenson 1990).

At the beginning, MDLC analysis implied very long analysis times (from several hours to days), which meant that this technique was not very useful to be routinely applied. However, in recent years, important improvements in the instruments employed for MDLC have greatly decreased the analysis times thanks to the incorporation of high performance and ultra-high pressure liquid chromatographs as well as innovations in columns dimensions and stationary phase particles technology. Furthermore, until recently, the vast majority of the MDLC applications were carried out in instruments assembled by the user, but currently, the growing impact of the increased separation power shown by 2D applications, has led to the emergence of commercial MDLC instruments that offer a great variety of operational modes.

1.3.2. PRINCIPLES OF MDLC.

The higher separation power provided by MDLC is the result of the employment of two or more independent liquid phase separation systems (dimensions) for the separation of a sample. In particular, in two-dimensional liquid chromatography (2DLC), a conventional separation is carried out on the first dimension (^{1}D) and fractions of its eluent are continuously collected

and successively injected and analyzed in the second dimension (^{2}D). Both dimensions should present different and, if possible, even independent retention mechanisms, thus being orthogonal. This way, compounds that coelute and cannot be separated when just one-dimensional system is employed (because of their similar retention behavior and affinity for the stationary phase) can be resolved by the use of a second separation procedure (Dugo et al. 2008a; François et al. 2009; Herrero et al. 2009).

Although the chemistry of the stationary phases selected in each dimension is a relevant condition for obtaining an orthogonal approach, the separation degree also depends on the interaction of the intrinsic properties of the sample analytes and the analytical conditions. Samples that present a mixture of compounds with different chemical behavior are randomly separated into the chromatographic space. Related to this, the number of chemical variables that the compounds of the sample present is referred to as sample dimensionality. That means that if a sample contains compounds with only one chemical variable, a one-dimensional separation would be enough to resolve its components, and a 2D system would not contribute with any additional improvement in the separation. However, when the sample presents different dimensions, additional separation systems are needed and the employment of multidimensional separation is justified. The way to obtain a complete separation of such complex composition is the employment of multidimensional chromatography, and the selection of the adequate separation mechanisms involved in the system as function of the sample dimensionality (Giddings 1995).

1.3.2.1. Off-line, on-line and stop-flow 2DLC.

The transfer of fractions from the ^{1}D to the ^{2}D can be performed off-line, if the effluent of the ^{1}D is collected and reinjected manually in the ^{2}D. Alternatively, the transfer can be performed through an on-line coupling, when the effluent of the ^{1}D is continuously and automatically injected in the ^{2}D.

The off-line mode presents some advantages, for instance, it does not require specific instrumentation, as well as it enables the use and combination of a high variety of separation

mechanisms in both dimensions, avoiding the problem of the solvent incompatibility (that will be detailed below); besides, longer analysis time for the ^{2}D separation can be employed, achieving a higher efficiency and therefore a high peak capacity (Yang et al. 2016). However, the off-line process also presents some disadvantages: it is time-consuming due to the very long analysis times, and there is a chance to introduce errors related to sample manipulation that could lead to low reproducibility (Dugo et al. 2008a; Marchetti et al. 2008). On the other hand, on-line 2DLC has the advantage to provide shorter analysis times and an automated transfer of the ^{1}D fractions into the ^{2}D column by an adequate interface (also called modulator). The challenges of the on-line approaches are the need for dedicated instrumentation and the limitations related to the coupling of two chromatographic systems, such as the incompatibility of the mobile phases employed in each dimension, the necessity of a very fast rate of ^{1}D sampling and consequently, very fast ^{2}D analysis (Malerod et al. 2010).

An intermediate system between on-line and off-line MDLC is the so-called stop-flow or stop-and-go 2DLC. In stop-flow systems, the coupling of the two columns is made on-line, but the analysis of the ^{2}D are carried out more similarly to an off-line system. The system consists on the interruption of the flow rate of the ^{1}D separation every time that a fraction from the ^{1}D is injected in the ^{2}D column; the ^{1}D separation is maintained stopped until the end of the ^{2}D analysis, when the ^{1}D separation will be reactivated until the next fraction of ^{1}D effluent is collected. Compared to the off-line mode, stop-flow mode presents the advantage of the automatic transfer of fractions between dimensions, which improves the robustness and reproducibility of the 2D methods (Guiochon et al. 2008). On the other hand, the advantage of stop-flow mode over on-line mode is the availability of longer analysis times to perform the ^{2}D separations, which can be translated into higher efficiency and separation power. On the opposite side, the main drawback of stop-flow systems is the long analysis time of the overall 2D method as a consequence of the interruption of the ^{1}D separation, and the successive long ^{2}D analyses. Besides, stopping the ^{1}D flow rate during long periods of time leads to ^{1}D band broadening due to diffusion effects, causing a loss in the ^{1}D efficiency.

Although off-line and stop-flow 2DLC are simpler approaches and generate high separation power, the reduction on the total analysis time, the higher reproducibility and the automation

that on-line 2DLC provides makes it a more promising technique for the separation of complex samples.

1.3.2.2. Types of 2DLC.

Depending on the number of fractions from the ^{1}D separation that are transferred to the ^{2}D, 2DLC can be classified in two main groups: heart-cutting liquid chromatography (LC–LC) and comprehensive two-dimensional liquid chromatography (LC × LC).

In heart-cutting mode, only one or a few target ^{1}D peaks are sampled and subsequently injected into the ^{2}D separation. Usually, LC–LC is employed in known samples that present analytes of interest coeluting under a peak. The objective is to collect these unresolved peaks and submit them to a further separation in a ^{2}D, with different column selectivity, to resolve coelutions (Murphy and Schure 2008).

On the other hand, comprehensive mode involves the entire separation of the whole sample through the ^{1}D and ^{2}D. That is, as the ^{1}D separation is taken place, little fractions of its effluent are continuously collected, injected and analyzed in the ^{2}D. This process is usually done at high frequency. Under this mode, ^{2}D separates the unresolved analytes present in each ^{1}D fraction. LC × LC is very useful for the study of very complex samples, allowing to obtain as much information as possible in a single analysis, in order to, for example, carry out profiling or fingerprinting studies (François et al. 2009; Jandera 2012). In Figure 1.2 the fundamentals and comparison of LC–LC and LC × LC modes are represented.

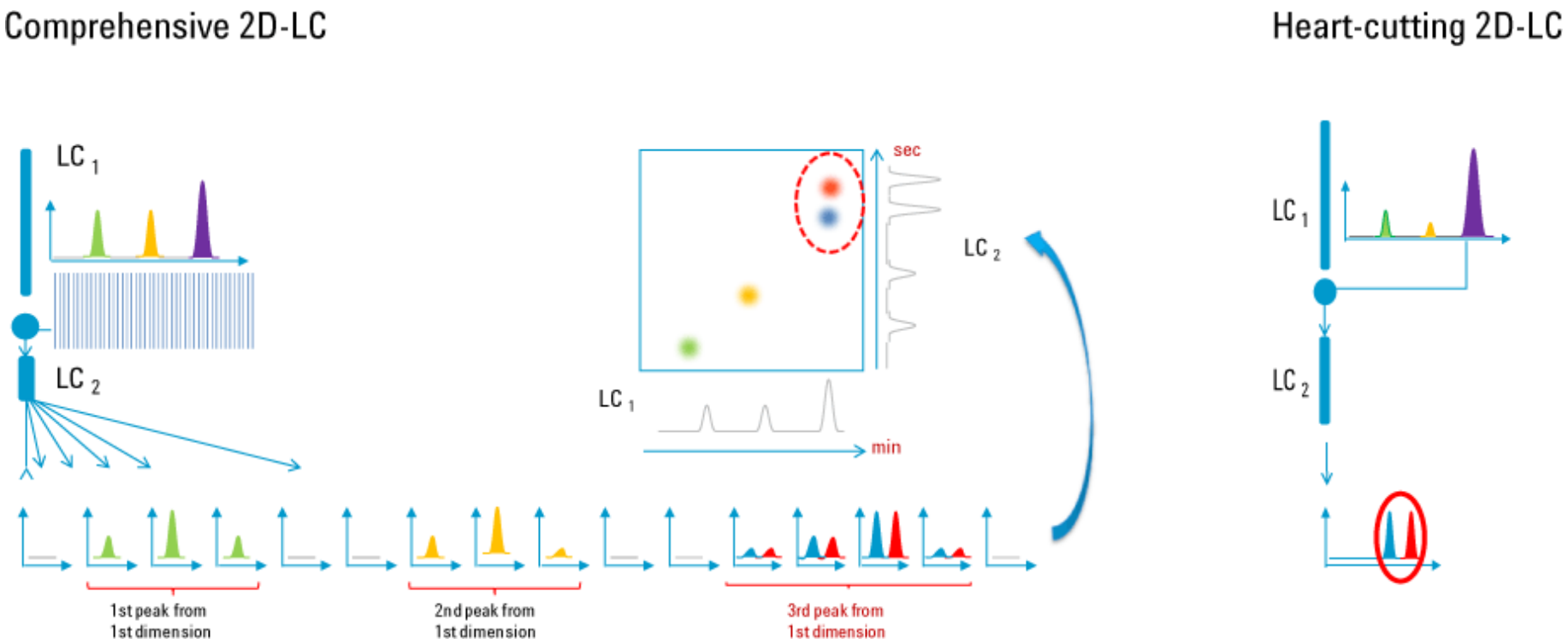

Figure 1.2. Comparison of the two 2DLC modes: comprehensive 2DLC (LC × LC) and heart-cutting 2DLC (LC–LC). Adapted from Carr and Stoll (2015), copyright 2015, Agilent Technologies, Inc.

Therefore, making a direct comparison between both 2DLC modes, LC – LC is simpler and very useful for resolving target compounds present in a complex sample, but it is limited to provide further separation of just target compounds. On the other hand, LC × LC is a very useful analytical technique in order to achieve the maximum information of a sample composition, providing an impressive separation power. Nevertheless, the main shortcomings of LC × LC are that the use of complex instrumentation is needed as well as that requires exhaustive and difficult method optimization (Stoll and Carr 2016).

The present Doctoral Dissertation is focused on the on-line LC × LC mode applied to the chemical characterization of complex natural extracts and food-related products. Therefore, the theoretical and practical fundamentals of the on-line LC × LC mode are described in the following sections.

1.3.3. ON-LINE COMPREHENSIVE TWO-DIMENSIONAL LIQUID CHROMATOGRAPHY (LC × LC) – THEORY.

As mentioned before, on-line LC × LC provides the great advantage of increasing the resolving power, allowing the separation of a large number of compounds in relatively short analysis times. The transfer of the entire ^{1}D effluent and its analysis into the ^{2}D, where a further separation is carried out, is responsible for this higher separation power.

An interface or modulator, usually one or two switching valves, which allows the simultaneous and continuous collection of the ^{1}D effluent and the injection of fractions into the ^{2}D, performs the physical on-line coupling between the two dimensions.

The comprehensiveness of a 2DLC method was stablished by tree main rules that must be met (Schoenmakers et al. 2003):

i. Every part of the sample is subjected to two different separations.
ii. Equal percentages (either 100% or lower) of all sample components pass through both columns and eventually reach the detector.

iii. The separation (resolution) obtained in the first dimension is essentially maintained in the second dimension.

The first condition reflects the difference between LC–LC and LC × LC, while the second condition refers to the fact that in the case that a split is used during the separation process, the split has to affect equally to all components, and the resulting chromatogram has to be a "faithful representation" from what would be attainable with 100% transfer of the sample. Lastly, the third condition refers to one of the most important conditions, essential to obtain a good resolution in LC × LC: the importance of not losing the gained separation on the ^{1}D during the fraction transfer process from the ^{1}D to the ^{2}D. In practice, this third condition is not completely possible due to some instrumental-related limitations. This fact has a critical importance, and consequently, it will be extensively explained and described in Section 1.3.4.1.

Many factors are involved in the LC × LC chromatographic process, and their optimization is essential to attain a successful 2D separation. Some of these factors are efficiency, retention and selectivity. Ultimately, these parameters are covered by two terms: orthogonality and peak capacity. The goal of every LC × LC method is to achieve the highest possible degree of orthogonality in order to obtain the maximum possible peak capacity.

1.3.3.1. Concepts of orthogonality in comprehensive two-dimensional liquid chromatography.

In multidimensional chromatography, orthogonality refers to the combination of retention mechanisms that offer different selectivity for the separation of a sample. In other words, orthogonality measures the different separation properties of the two involved mechanisms. Therefore, the ideal degree of orthogonality is achieved when the involved separation systems provide completely non-correlated retention (Jandera 2012).

The use of different separation mechanisms improves the separation capability allowing the separation of the sample compounds by two independent retention behaviors depending on the properties of the different compounds. At the same time, components that cannot be separated by one of the employed columns (or dimensions), can be well resolved in the other dimension. Therefore, the degree of orthogonality of a multidimensional system will determine the

potential separation that can be attainable. In fact, the degree of orthogonality is closely related to the maximum peak capacity that multidimensional chromatography can provide with, as it will be explained below (Section 1.3.4).

1.3.3.1.1. *Orthogonality calculation.*

A measure of orthogonality is a good parameter to evaluate the quality of a LC × LC separation, and it can be employed for the comparison between analyses when the development and optimization of a new method is being carried out. Moreover, it is also important to calculate the orthogonality of new advanced LC × LC systems in order to quantitatively estimate the correlation between dimensions and the separation space coverage (Schure and Davis 2015).

Numerous studies have proposed different methods for the calculation of orthogonality (Liu et al. 1995; Slonecker et al. 1996; Van Gyseghem et al. 2003; Gilar et al. 2005; Vivó-Truyols and Schoenmakers 2006; Nowik et al. 2013). However, many of them are applied to estimate the orthogonality achieved by a particular LC × LC method after its application, on the obtained 2D chromatogram, due to the lack of predictive models. Hence, the selection of the phase system (stationary and mobile phases) to be employed is mostly based on the analyst experience (Bedani et al. 2012). Some of these mathematical models are commented hereunder.

The degree of similarity of the two chromatographic systems is related to the effective area available for the separation in the 2D chromatogram. This area can be geometrically calculated using the "*retention space angle*" (Figure 1.3). A complete orthogonal coupling would be achieved with a 90º retention space angle; this would mean that the complete 2D space could be available for peak spreading (Pasch 2000).

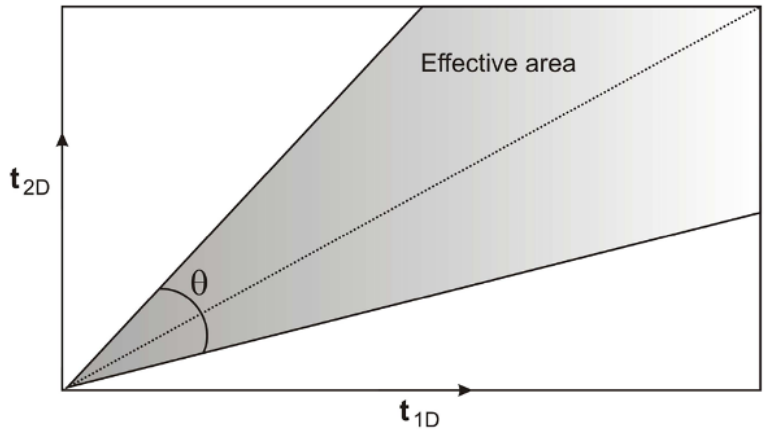

Figure 1.3. Effective area in a comprehensive 2D separation limited by the angle θ, characterizing the orthogonality of 2D systems. Adapted from Jandera (2012a), copyright 2012 Springer.

Other methods for the calculation of orthogonality consist of the division of the 2D separation space in equal rectangular bins with a defined size (Figure 1.4) (Gilar et al., 2005). The area of the bins is established by plotting the normalized retention times of the peaks of a real 2D separation and assigning a normalized area to each data point. Then, an orthogonality value is calculated considering the percentage of bins corresponding to peaks relative to the total number of bins. When two completely correlated separation mechanisms are coupled, the data points are lined up along the diagonal, and the surface coverage is 10% (Figure 1.4A). On the other hand, when an ideal (and hypothetical) separation system is performed with two totally non-correlated dimensions, equal distribution of data points through the separation space would be achieved, covering 100% of the surface (Figure 1.4B). A more realistic situation is represented in Figure 1.4C, where data are randomly distributed, in a way that some bins contain more than one peak and some of the separation space is not used. This method is known as *Bin Counting method* (Gilar et al. 2005). It has been widely employed and it has served as the basis for the development of new methods for the calculation of the orthogonality (Davis et al. 2008; Schure 2011).

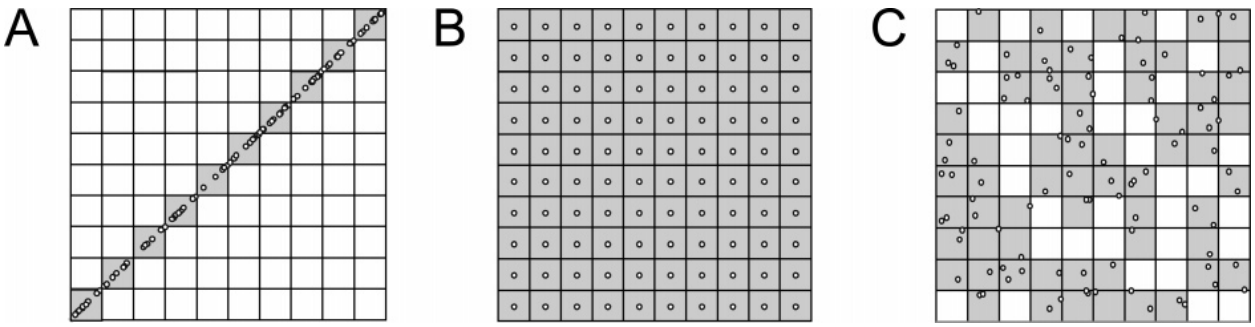

Figure 1.4. Geometric orthogonality concept. Hypothetical separation of 100 analytes in 10 × 10 normalized separation space. (A) Non-orthogonal system, 10% area coverage represents 0% orthogonality. (B) Hypothetical ordered system, full area coverage. (C) Random, ideally orthogonal, system, area coverage is 63% representing the 100% orthogonality. Adapted from Guilar et al. (2005), copyright 2005 American Chemical Society.

Recently, the "*asterisk equations method*", a practical and fast procedure to calculate the orthogonality degree, has been reported by Camenzuli and Schoenmakers (2014). This method has been selected to estimate the orthogonality achieved using the diverse set-ups studied in the different applications described in the present Dissertation. The orthogonality calculation is simply based on the experimental measurement of peak retention times; thus, only the area covered by peaks is considered. It is an objective method since does not require any decision of setting parameter values as it is the case of many of the different models described until date. In practice, the method consists on crossing the 2D space by four lines (Z_-, Z_+, Z_1 and Z_2 lines) forming an asterisk as shown in Figure 1.5. The distance of each separated peak (normalized ^{1}D and ^{2}D times of each peak) to the four Z lines is considered (Sz_x). The spread of components around Z_1 line (Sz_1) is related with the dispersion along the x-axis, that is, in the ^{1}D; the spread of peaks in relation to Z_2 line (Sz_2) measures the ^{2}D separation, while Z_- and Z_+ (Sz_- and Sz_+, respectively) consider the peak dispersion in both dimensions. Consequently, the method describes the use of the separation space, or in other words, estimates how much of the available space is occupied by peaks.

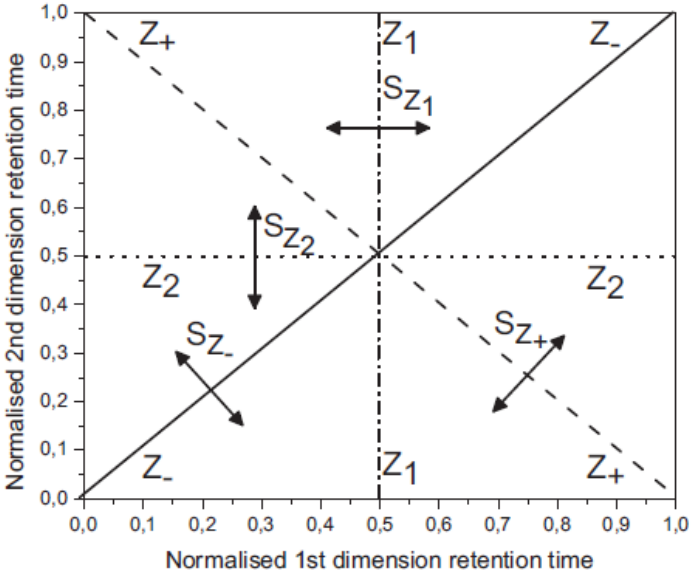

Figure 1.5. Graphical representation of the principles underlying the asterisk equations. S_{Zx} terms refer to the standard deviation of the distances of peaks from the Z_x line. Adapted from Camenzuli and Schoenmakers (2014), copyright 2014 Elsevier.

The distances of each peak regarding to the four lines (Sz_x) are calculated by the following equations:

$$Sz_{-} = \sigma \{ {}^{1}t_{R,norm(i)} - {}^{2}t_{R,norm(i)} \} \quad \text{(Eq. 1)}$$

$$Sz_{+} = \sigma \{ {}^{2}t_{R,norm(i)} - (1 - {}^{1}t_{R,norm}) \} \quad \text{(Eq. 2)}$$

$$Sz_{1} = \sigma \{ {}^{1}t_{R,norm(i)} - 0.5 \} \quad \text{(Eq. 3)}$$

$$Sz_{2} = \sigma \{ {}^{2}t_{R,norm(i)} - 0.5 \} \quad \text{(Eq. 4)}$$

Where σ is the standard deviation of the value between brackets and $t_{Rnorm(i)}$ is the normalized ^{1}D and ^{2}D retention time of each peak, described by:

$$t_{R,norm(i)} = \frac{t_{R(i)} - t_{R,first}}{t_{R,last} - t_{R,first}} \quad \text{(Eq. 5)}$$

To calculate the Z values, the terms Sz_x are then entered in the following equations:

$$Z_{-} = |1 - 2.5|Sz_{-} - 0.4|| \quad \text{(Eq. 6)}$$

$$Z_{+} = |1 - 2.5|Sz_{+} - 0.4|| \quad \text{(Eq. 7)}$$

$$Z_1 = 1 - |2.5 \times Sz_1 \times \sqrt{2} - 1| \qquad \text{(Eq. 8)}$$

$$Z_2 = 1 - |2.5 \times Sz_2 \times \sqrt{2} - 1| \qquad \text{(Eq. 9)}$$

The spread of peaks around each Z line is equally important, so all Z values are included in the main asterisk equation to calculate the overall degree of orthogonality (A_o).

$$A_O = \sqrt{Z_- \times Z_+ \times Z_1 \times Z_2} \qquad \text{(Eq.10)}$$

A_O value is expressed as percentage, in a way that the more the spread of peaks around the four Z lines the higher the A_O value will be obtained, meaning that if A_O = 100% the LC × LC system presents a complete orthogonality degree.

1.3.3.1.2. *Orthogonal couplings in LC × LC.*

Several different couplings of retention mechanisms have shown to produce successful orthogonal two-dimensional separations, such as the coupling between NP mode and RP separations (NP × RP), SEC coupled to RP (SEC × RP), IEX coupled to RP (IEC × RP), HILIC and RP (HILIC × RP), or even the application of two RP separation modes (RP × RP). RP is the most frequently employed separation mode for the ^{2}D as a result of its separation capabilities and selectivity for a wide variety of compounds, as well as its high MS compatibility (Li et al. 2015). In practice, C_{18}-based stationary phases provide with appropriate efficiency and fast re-equilibration after the end of the analysis, which is a highly valued characteristic for fast gradient ^{2}D separations.

Amongst the mentioned couplings, NP × RP, RP × RP and HILIC × RP are those that have more frequently been employed in food analysis.

1.3.3.1.2.1. Normal phase coupled to reversed phase (NP × RP).

The coupling between NP and RP is one of the most orthogonal combinations due to the fact that both separation modes possess completely non-correlated retention characteristics. NP is

characterized for employing polar stationary phases and it is used for the separation of non-polar compounds, while RP-compatible stationary phases are mostly non-polar and are mainly used for the separation of medium and high polarity compounds. Thus, NP × RP involves the use of two completely independent separation mechanisms that are ideal to separate samples containing compounds with hydrophilic-lipophilic properties.

However, the coupling between these two separation modes is not easy to implement mainly due to the incompatibility problems of the mobile phases employed in both dimensions. NP usually employs very non-polar solvents as mobile phases, which can be even immiscible with the highly aqueous initial solvent composition of RP (Herrero et al. 2009). Even when miscible, both solvent compositions will be essentially incompatible as the elution strength in each dimension is the opposite. To partially solve this shortcoming, several strategies have been developed such as the use of evaporative interfaces between both dimensions allowing the evaporation of the solvent of the fraction eluted from the ^{1}D before injection in the ^{2}D (Tian et al. 2008).

The use of long microbore columns in the ^{1}D have also been studied to reduce the volume transferred to the ^{2}D thanks to the possibility of using very low ^{1}D flow rates. That way, the fraction transferred is completely dissolved in the ^{2}D flow rate (Dugo et al. 2004). Another strategy that has been employed to overcome the solvent incompatibility issue was developed by Wei et al. (2009). In this case, partially compatible mobile phases were selected in both dimensions as well as a high temperature in the ^{2}D to decrease the viscosity of the mobile phases, increasing the miscibility between them.

1.3.3.1.2.2. Reversed phase coupled to reversed phase (RP × RP).

In contrast to other couplings, RP × RP employs two related separation mechanisms that, a priori, may not provide enough different retention between the two dimensions to be considered as an orthogonal separation. However, on the contrary, RP × RP is the most extended coupling among the whole LC × LC applications published so far, since a difference in the linked functional groups (C_{18}, phenyl, cyano, amino, among others) in both dimensions

and careful selection of the mobile phases employed in each case, can offer a good degree of orthogonality. The main advantage of the coupling of two similar separation mechanisms is that the mobile phases employed in both dimensions are completely compatible, minimizing one of the most important drawbacks of the coupling of two individual chromatographic systems (Li et al. 2015).

Theoretical models have been applied for selecting the two RP conditions that may provide the best orthogonality, comparing the selectivity of each column. These models are mainly based on the study of the solute-column retentions and interactions, such as hydrophobicity, steric interactions, hydrogen-bond contribution, and ion-exchange activity (Snyder et al. 2004). Other RP × RP applications have also taken into consideration the influence of the mobile phase composition, pH, buffer concentration or temperature on the selectivity. Retention and selectivity on two RP systems can significantly vary with the modification of the mobile phase compositions or pH. For instance, Gilar et al. (2005) reported that the orthogonality achievable by the combination of two RP columns for the separation of peptides is limited by the correlation of the retention mechanism as well as by the scarce difference in selectivity between the tested stationary phases, giving as a result a poor coverage of the 2D separation space. However, a great increase in RP × RP orthogonality was gained by employing mobile phases with different pH in each dimension, showing that for the separation of charged compounds, pH is a leading parameter to generate a good orthogonal separation (Gilar et al. 2005).

1.3.3.1.2.3. Hydrophilic interaction chromatography coupled to reversed phase (HILIC × RP).

Traditionally, HILIC has been employed for the separation of highly polar compounds. It is considered an alternative to NP, since HILIC, as well as NP, employs polar stationary phases, and shows an increased retention for highly polar compounds. The main difference with NP is that, in HILIC, highly organic-aqueous polar solvents are used as mobile phases (usually aqueous mixtures of 97-40% of acetonitrile (ACN)), avoiding the use of typical non-polar toxic solvents employed in NP. Therefore, the solvents employed in HILIC are more similar, and often compatible, to those used in RP modes (Alpert 1990; Dejaegher et al. 2008; Bernal et al. 2011).

Online coupling of HILIC and RP is one of the most orthogonal separation modes combination because it involves the coupling of a polar stationary phase (HILIC) with a non-polar one, as it occurs in the case of NP × RP. However, the important advantage that HILIC × RP provides with respect to NP × RP, is the good miscibility of the mobile phases of each dimension. Therefore, HILIC and RP may offer largely different selectivity and a high orthogonality degree.

Nevertheless, although the solvents employed in both dimensions are miscible, the hyphenation of HILIC and RP in an on-line mode is still complicated, mainly due to the opposite elution strength in each dimension. This means that weaker organic solvents, typically acetonitrile, employed in the ^{1}D (HILIC), are stronger solvents for the ^{2}D (RP). Considering that the solvent composition of the fractions transferred is fixed by the gradient elution of the ^{1}D, problems related to decrease in retention, band broadening and peak distortion may occur during the ^{2}D separations. These deleterious effects are attributed to the injection of a plug of strong solvent in a weaker ^{2}D mobile phase, which produces a loss of the efficiency and separation of the ^{2}D (Jandera et al. 2012).

The most employed strategy to face the solvent incompatibility issue is to carry out the ^{1}D separation at a very low flow rates (10-100 μL min^{-1}) with narrow-bore or microbore columns (~1.0 mm i.d.) in order to collect small volumes of effluent, while very high flow rates (2-5 mL min^{-1}) are employed in the ^{2}D, in a way that injection solvent effect is reduced (Jandera et al. 2012). Apart from this approach, several innovations have been developed to reduce the solvent incompatibility effects, with the aim to remove the ^{1}D solvent before the injection on the ^{2}D columns, or producing the so-called on-column focusing effect on the top of the ^{2}D columns to generate a narrow injection band. To carry out these strategies, several modifications of the instrument have to be performed such as evaporative interfaces or introducing make-up flows of weak solvents after the ^{1}D separation. A more extensive description of these additional instrument solutions and some other innovations are included in Section 1.3.6.

1.3.4. PEAK CAPACITY.

The key demand to chromatography for the separation of samples presenting mixtures of compounds with high complexity is that the system has to be able of produce proper resolution. The more accepted way of measuring the resolving power achieved by a chromatography-based system, is the calculation of the peak capacity.

Peak capacity (n_c) is the main way to measure the separation capability of a chromatographic system, and is defined as the maximum number of peaks with the same width that can be separated with exactly the same required distance to achieve the minimum stated resolution, in a determined chromatographic space (Davis and Giddings 1983).

Peak capacity strongly depends on the elution mode because, under isocratic mode, peaks tend to widen as the retention time increases, whereas in gradient mode the bandwidth of all peaks is essentially maintained throughout the entire chromatogram. Accordingly, as can be deduced from Eq. 11, peak capacity is higher in separations performed under gradient mode because narrower bandwidths are attained, and consequently, more peaks can fit in the same separation space.

$$n_c = 1 + \frac{t_G}{\overline{w}} \qquad \text{(Eq. 11)}$$

Where t_G, is the gradient time and $\overline{w}$ is the average peak width.

This term should be considered as a theoretical measure of the separation capability, that is, as the ideal or the maximum number of resolvable peaks. However, in practice, peaks are not regularly spaced on the chromatogram, but they appear at random retention times, leading to overlapping. Therefore, the number of separated peaks in practice is much lower than the value of theoretical peak capacity calculated (Davis and Giddings 1983). Davis and Giddings (1983), statistically determined that the number of peaks in a chromatographic separation cannot exceed more than 37% of its peak capacity because overlapping. Otherwise, the resolution is compromised.

Taking this theory in consideration, when a multiple-component complex sample has to be analyzed, conventional one-dimensional liquid chromatography (1DLC) techniques are limited by the maximum n_c that can offer. For this reason, for the resolution of a complex sample,

extremely high peak capacities are needed. This theory lays the foundations of the necessity of two-dimensional separations, considering that the separation power can be immensely increased if different chromatographic systems are coupled. This is a direct consequence of the contribution of the peak capacity of each dimension towards the total separation power (Stoll et al. 2007; François et al. 2009).

If ideal 2D separations could be achieved, the peak capacity of a 2DLC system would be calculated by the so-called *product rule*, that consists of the product of the individual peak capacities of each dimension (Eq. 12):

$$^{2D}n_c = {}^{1}n_c \times {}^{2}n_c \qquad \text{(Eq. 12)}$$

Being $^{2D}n_c$ the theoretical peak capacity of the 2DLC system; and $^{1}n_c$ and $^{2}n_c$ the ^{1}D and ^{2}D individual peak capacities, respectively.

The ideal conditions that should be met to reach this peak capacity are, i) the coupling between two completely independent orthogonal separation mechanisms, and, ii) the analysis of a sample with all its compounds separated with the same resolution along the whole chromatographic space without leaving any baseline zone.

Unfortunately, the absolute non-correlation between two separation systems as well as the existence of samples with such a degree of sample dimensionality is difficult, if not impossible, to achieve. Moreover, usually samples of natural origin for which a complete knowledge about their composition is not available are analyzed. In addition, these samples contain compounds with different chemical attributes, and thus, defining the dimensionality may be impossible (Stevenson et al. 2010). Therefore, as can be deduced, the attainment of a good distribution of the peaks throughout the 2D space, and hence a high peak capacity, will depend on both, the orthogonality provided by the two columns, and the composition of the sample.

Even if this estimate to the calculation of peak capacity is not attainable in reality, the *product rule* allows noticing the enormous increment in peak capacity that MDLC is able to produce in comparison with 1DLC (Figure.1.6).

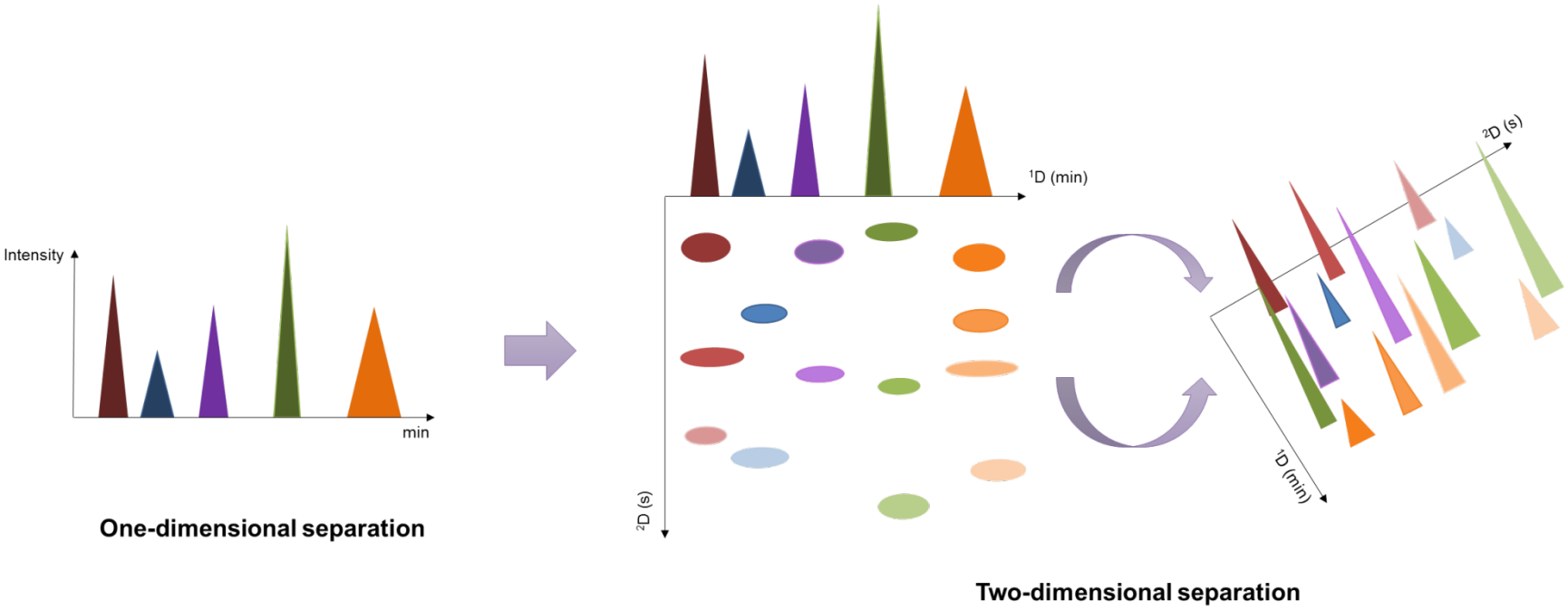

Figure 1.6. Peak capacity gain of MDLC with respect to 1DLC.

During a two-dimensional separation process, some intrinsic separation phenomena have a critical influence on the attainable theoretical peak capacity. These are the effects of ^{1}D undersampling and the ^{2}D band broadening (Bedani et al. 2012).

1.3.4.1. Effect of ^{1}D undersampling on peak capacity.

One of the theoretical foundations in MDLC defines the sampling rate at which the transfer of ^{1}D effluent into the ^{2}D column should be done. That theoretical approach implies that the sampling must be done in a way that during the ^{2}D analysis, the achieved separation during ^{1}D is not lost.

Murphy et al. (1998) studied the effect of the frequency of the sampling rate in relation to the number of cuts along a ^{1}D peak width (considering that the peak width at baseline of a well-defined Gaussian peak is 8σ). Moreover, they considered the relevance of where these cuts start along the ^{1}D, that is, the so-called sampling phase. The relevance of where the sampling phase is done leads to the undersampling problem. When the sampling rate starts at some point at the end of a ^{1}D peak width and it lasts enough time to include the first part of the adjacent ^{1}D peak width, an inevitable remix of these two previously well resolved peaks will occur during the storage of the fraction in the modulator. Hence, part of the resolution gained in the ^{1}D resolution is lost and, as a consequence, a decrease in the peak capacity is observed (Figure 1.7).

This problem could be straightforwardly improved setting shorter sampling times, but, on the contrary, shorter sampling times will imply faster ^{2}D analyses and a general loss of the ^{2}D resolution. Murphy et al. (1998), theoretically and experimentally established that an 8σ peak width should be sampled and injected in the ^{2}D column at least 4 times to minimize the effect of where the sampling phase starts and to solve the remix problem. This is commonly known as Murphy's rule. The aim of the application of this development is to achieve a compromise to obtain the highest resolution at the shortest analysis time.

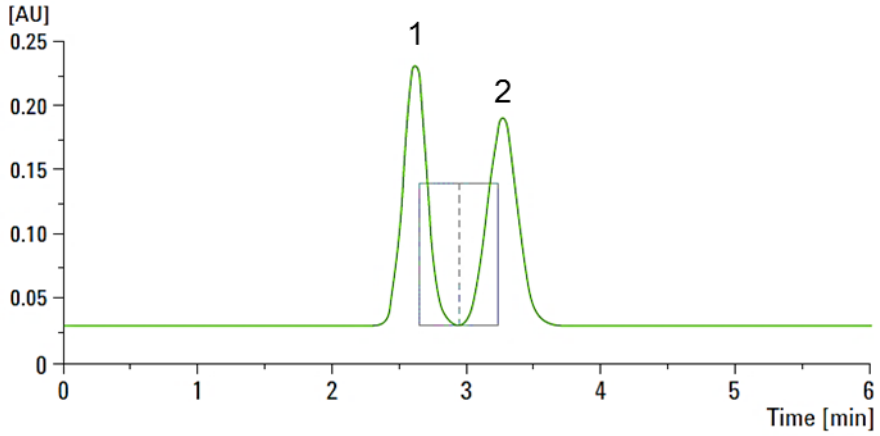

Figure 1.7. Sampling phase in which the end of peak 1 and the beginning of peak 2 are sampled in the same fraction; then, these previously well resolved peaks will be mixed during the transfer process. Adapted from Carr and Stoll (2015), copyright 2015, Agilent Technologies, Inc.

Studies like the work proposed by Murphy are focused on not losing and maintaining as much as possible the ^{1}D peak capacity through short modulation times.

Other authors have paid attention on the modulation period as a parameter to improve the ^{2}D peak capacity and its effect on the ^{1}D separated peaks, and consequently, on the maximization of the whole 2D peak capacity. Horie et al. (2007) reported that the expected 2D peak capacity clearly decreases when modulation periods are stablished at 1.5 times the average standard deviation of the ^{1}D ($^{1}\sigma$) or less, while longer modulation periods produce a progressive reduction on the 2D peak capacity. Besides, they determined the optimum modulation period as a function of the ^{1}D peak width, the ^{2}D column length or the use of packed columns or monolithic columns in the ^{2}D as well as the particle size of the packed columns. They proved that for all ^{1}D peak widths and ^{2}D columns lengths the optimum modulation period was in the range 2.2–4 $^{1}\sigma$.

After the model proposed by Murphy et al. (1998), several authors tried to quantify the undersampling effect in order to consider the decrease that this phenomenon produces over the theoretical peak capacity calculated by the product rule (Eq. 12).

For instance, Davis et al. (2008b) defined the effect of ^{1}D peak band broadening that occurs when using slow sampling frequencies, that is, when undersampling arises. Besides, they

considered the random distribution of the peaks as well as the randomness of the sample phase. All these deliberations where included in the mathematical factor <β>, described as a function of the sampling time (t_s) and $^1\sigma$ before sampling.

$$<\beta>=\sqrt{1+0.21\left(\frac{t_s}{^1\sigma}\right)^2} \qquad \text{(Eq. 13)}$$

Continuing with this theoretical development, Li et al. (2009) proposed to correct the peak capacity, calculated through the product rule, by <β>.

Considering the ^{1}D peak width (w) equal to 4σ, they reorganized the <β> factor as follows:

$$<\beta>=\sqrt{1+3.35\left(\frac{t_s}{w}\right)^2} \qquad \text{(Eq. 14)}$$

According to Eq. 11, and considering that gradient elution is employed in both dimensions, while, ts is equal to the ^{2}D analysis time (^2t_c) that is the sum of the time of the ^{2}D gradient time plus the equilibration time (Eq. 15), <β> can be expressed as Eq. 16.

$$t_s = {}^2t_c = {}^2t_G + {}^2t_{reeq} \qquad \text{(Eq. 15)}$$

$$<\beta>=\sqrt{1+3.35\left(\frac{^2t_c\times\ ^1n_c}{^1t_G}\right)^2} \qquad \text{(Eq. 16)}$$

After that, with the aim to correct the theoretical peak capacity, <β> was included in Eq. 12, hereafter referred as practical peak capacity:

$$^{2D}n_{c,practical}=\frac{^1n_c\times\ ^2n_c}{<\beta>}=\frac{^1n_c\times\ ^2n_c}{\sqrt{1+3.35\times\left(\frac{^2t_c\times\ ^1n_c}{^1t_G}\right)^2}} \qquad \text{(Eq. 17)}$$

With these equations, Li et al. concluded that, in practice, the Murphy's rule of 4 samplings per peak may be sometimes difficult to achieve because short modulation times lead to better maintaining the ^{1}D peak capacity but at the cost of very fast sampling rates and consequently, extremely fast ^{2}D analyses. Thus, it can be concluded that in practice, under LC × LC conditions, a certain degree of ^{1}D undersampling is almost impossible to be avoided.

Although the fact of undersampling is inevitably present in LC × LC, there are some optimizations that can help to reduce its unwanted effects. From Eq. 16 it can be deduced that some parameters can contribute to its improvement, for instance, the use of gradient elution in both dimensions, the increment of the ^{1}D gradient time ($^{1}t_G$) using lower ^{1}D flow rates or, as mentioned before, the fact that shorter $^{2}t_c$ are translated into higher ^{1}D peak capacity. However, it is important to emphasize that the reduction of $^{2}t_c$ leads to loses of $^{2}n_c$ due to the reduction on the available ^{2}D separation time gradient (Seeley 2002; Bedani et al. 2012). Hence, one of the most important optimizations that has to be carefully studied during the development of a LC × LC method is the compromise between undersampling and the optimum ^{2}D analysis time and resolution.

1.3.4.2. Effect of ^{2}D band broadening on peak capacity.

The trade-off between solving undersampling and having appropriate modulation times for a convenient ^{2}D analysis time, sometimes produces large eluted fractions from the ^{1}D, leading to large ^{2}D injection volumes. The effect of injecting large volumes (compared to total column volume) in the ^{2}D is a possible cause of band broadening.

Second dimension band broadening can be even more pronounced when the internal column diameter of the ^{1}D (^{1}dc) is larger than the internal diameter of ^{2}D column (^{2}dc). Thus, maximizing the ratio ^{2}dc/^{1}dc leads to a lower band broadening effect. In addition, the use of ^{2}dc larger than ^{1}dc allows maintaining a higher ^{2}D flow rate than the one used in ^{1}D which contributes to a general improvement of 2D separations thanks to the fact that the ^{2}D flow rate reduces the strength of the ^{1}D solvent, helping to produce a desired focusing effect on the head of the ^{2}D column. The focusing factor is an important parameter that has to be taken into account when the optimization of the LC × LC is being carried out. The injection of the ^{1}D fraction in the ^{2}D column dissolved in the ^{1}D mobile phase can yield to a poor retention of the analytes, because the use of orthogonal columns implies that the weak solvent for the ^{1}D will be the strong solvent for the ^{2}D. Thus, a clear solvent strength mismatch occurs. That way, the injection of analytes in the ^{2}D dissolved in a strong solvent, together with the use of high ^{2}D flow rates can produce a rapid elution of part of the injected volume without any retention

and/or with band broadening, given rise to a loss of efficiency and resolution and, consequently to a loss of ${}^{2}n_c$. For this reason, injection of analytes dissolved in a weak solvent is desired to form a narrow band on the top of the ^{2}D column that allows a good retention and the subsequent elution, i.e., producing on-column focusing. As can be deduced from the information presented in this section, a reduction on ^{2}D band broadening will be translated on higher values of ^{2}D peak capacity, and thus, an improvement on ${}^{2D}n_c$.

Several implementation advances have been developed so far to improve the on-column focusing, and consequently, to reduce the deleterious effect of ^{2}D band broadening. Some of them will be further detailed (Section 1.3.6).

1.3.5. ON-LINE LC × LC INSTRUMENTATION.

The conventional LC × LC instrumentation consists of three sections:

i. First dimension formed by an injector, a LC pump and a chromatographic column, that can be coupled or not to a detector.

ii. Second dimension with another LC pump, a column and a detector.

iii. Interface or modulator that connects both dimensions; usually consists of one or more switching valves.

As already mentioned, until just a few years ago, the vast majority of the LC × LC available equipment were lab-made instruments due to the lack of commercial LC × LC chromatographs. These instruments mainly consisted of two independent HPLC chromatographs coupled through the selected interface. The advantage that these lab-made configurations provide is the versatility to modify each part of the set-up as a function of the desired application; for example, ^{2}D pumps could be substituted, when possible, by UHPLC pumps in order to be able to configure very fast ^{2}D analysis. Nevertheless, they also present drawbacks, such as the complex software compatibility of two LC instruments, the limitation of the maximum pressure that the interfaces support, or the high dwell volume of the instrument

employed in the ^{1}D, that greatly affects to the gradient elution under typical suboptimal ^{1}D flow rates, among others.

Currently, due to the increasing acceptance and knowledge about the benefits of on-line 2DLC, commercial 2DLC instruments have been developed by different brands, with many of the drawbacks of the traditional LC × LC instruments solved.

1.3.5.1. Types of interfaces.

The interface is the critical point to achieve a satisfactory LC × LC analysis. The most difficult task in the development of a LC × LC method is the connection of the two chromatographic systems. It is in the interface where all the interactions between the two dimensions are physically established and, therefore, the interface has to control all the parameters and compromises that must be taken into account to carry out a successful two-dimensional coupling.

In particular, the function of the interface is the continuous collection of ^{1}D effluent and its transfer to the ^{2}D. Some of the most important compromises that the interface has to deal with are: i) the relationship between the ^{1}D flow rate and the ^{2}D injection volume, which is determined by the time elapsed between modulations, and, ii) the possible incompatibility between mobile phases from each dimension.

Depending on the LC × LC application, several interface designs have been employed to solve the challenges that the particular LC × LC method implies.

1.3.5.1.1 *Non-focusing interfaces.*

The vast majority of LC × LC couplings are performed by means of electronically-controlled switching valves. The set-up can be performed by one or multiple valves configuration. Figure 1.8 shows the schemes corresponding to the most-used configurations.

When only one valve is involved in the hardware, 8-, 10- and 12-port 2-position switching valves are the most common traditional options (Figure 1.8A). On the other hand, a multi-valve design with two 6-port 2-position switching valves has also been employed as an alternative

configuration design (Figure 1.8B). From all of them, the 10-port valve is, possibly, the most often valve employed as interface (Figure 1.8A). However, in recent years, a new valve combination is gaining importance, based on a 4-port duo valve (Figure 1.8C). The number of LC × LC applications that employ this new valve has increased as a result of the introduction of commercial LC × LC chromatographs in the market that incorporate this improved design (Cesla and Krenková 2017). The advantages associated to their use are mainly fast operation and to be able to avoid the use of jumpers between connections that slightly increase the transfer volume and flow path length from one position to the other (see comparison between Figure 1.8A and C).

In general, these valves are equipped with two loops with identical internal volume. One loop is connected to the exit of the ^{1}D column and collects its effluent during the time that the valve is maintained in the same position (sampling time or modulation time). The other loop is connected to the ^{2}D pumps and the entrance of the ^{2}D column, in a way that the ^{2}D mobile phase pumped pushes the content of the loop towards the ^{2}D column, where is injected and, subsequently, separated. Therefore, the ^{2}D analysis time (including gradient and re-equilibration) has to be equal to the modulation time. When the valve is operated (modulation), the loops exchange their function.

The time elapsed between modulations together with the ^{1}D flow rate, determines the volume of the stored ^{1}D fraction, and therefore, the injection volume of the ^{2}D. This volume has to be kept as small as possible to avoid possible ^{2}D separation problems (Stoll and Carr 2016). As it has been already mentioned, large volumes can result in band broadening and in a loss of $^{2}n_c$, although injecting too small volumes may result in sensitivity issues (Bedani et al. 2012).

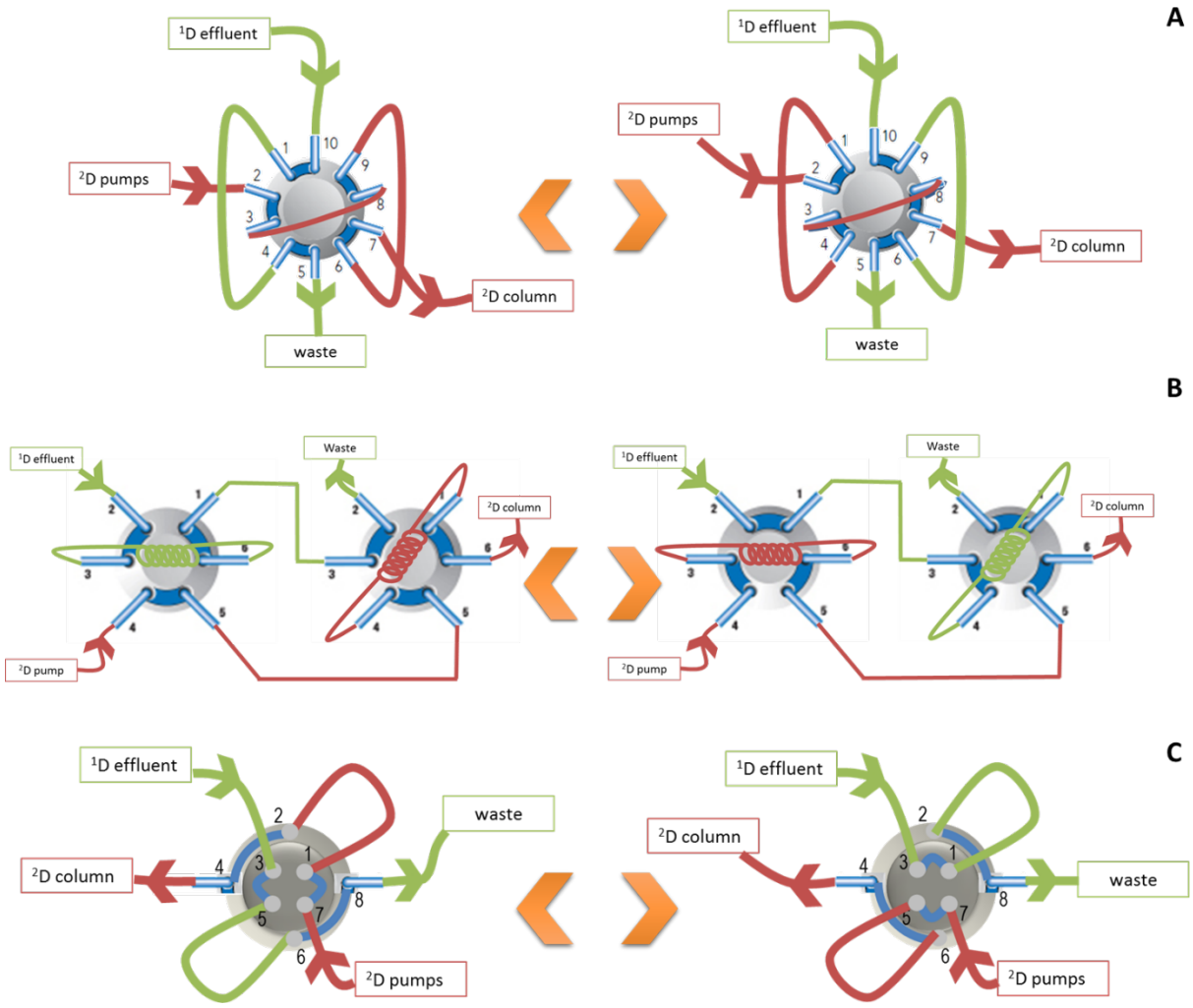

Figure 1.8. Schemes of three of the most-employed valve-based modulators in on-line LC × LC. A) 10-port, 2-position switching valve; B) two 6-port-, 2-position switching valve; C) 4-port duo valve.

Due to their simplicity and reproducibility, valves equipped with injection loops are the most frequently used interfaces. In any case, the use of loops connected to the valve, is linked to the need of short ^{2}D analysis times and very fast ^{2}D separations, resulting in a reduction of ^{2}D peak capacity, as previously explained. With the aim to permit longer ^{2}D analysis times, other valve configurations have been developed. For example, the use of two parallel ^{2}D columns instead of loops was applied by Cacciola et al. (2006) for the separation of phenolic compounds of beer. They employed a 10-port, 2-position switching valve with two identical C_{18} columns as ^{2}D. Each ^{2}D analysis lasted 6 min, which is advantageous to gain ^{2}D peak capacity; however, it implies very long modulation times compared with those of the loop-based interfaces. Therefore, less modulations of the ^{1}D effluent are possible, leading to significant undersampling, and hence, losses of the ^{1}D separation (Cacciola et al. 2006). Moreover, two columns even produced from the same batch are never identical, thus, producing a lack of reproducibility or drifts for successive modulations. Another alternative for reducing the modulation time was developed by François et al. (2008). For this application two 10-port, 2-position switching valves, one equipped with sampling loops and the other with two ^{2}D columns, two detectors and two ^{2}D pumps were needed, besides of two ^{2}D columns. With this approach, the authors were able to use sampling times of 1 min, whereas the ^{2}D analysis time was optimized in 2 min, enabling a higher resolution compared to the same analysis employing regular sampling loops in the interface (François et al. 2008).

Although the strategies involving two parallel ^{2}D columns provide good results in terms of resolution and peak capacity, they present serious drawbacks already mentioned, such as severe ^{1}D undersampling in the first case described (Cacciola et al. 2006) or the need of a very sophisticated instrumentation in the second one (François et al. 2008).

1.3.5.1.2 *Focusing interfaces.*

In some LC × LC applications, very different separation systems are coupled to obtain a good degree of orthogonality like NP × RP or HILIC × RP. However, the coupling of these separation modes leads the use of incompatible mobile phases. Currently, the development of strategies

that partially solve this problem is one of the LC × LC trends that rises most interest. Besides of the use of slow ^{1}D flow rates to transfer as small as possible aliquots of the incompatible solvent into the ^{2}D, several instrumental developments focused in the interface have been studied.

A promising alternative option to the loop configuration is the use of two trapping columns with stationary phase similar to the ^{2}D stationary phase. The selection of the nature of the trapping columns is a very important concept to keep in mind; trapping columns should not offer too strong retention of the analytes, otherwise, they could not be easily desorbed by the ^{2}D mobile phase. However, in the opposite case, some analytes may not be effectively retained in the trapping columns, and therefore they can be lost (Egeness et al. 2016). If the correct trapping columns are used, this approach enables the reduction of the band broadening of peaks in the ^{2}D. This effect is due to the trapping of compounds of the collected fraction in a very short column (trap) with the same selectivity than the ^{2}D column, thus, promoting a concentration effect prior to their injection in the ^{2}D column. Moreover, their elution would be related to a focusing effect and the subsequent injection of narrow bands (Cacciola et al. 2007), further improving ^{2}D performance.

One of the most successful approaches consists in the implementation of the previous design. It is based on the use of two trapping columns in the switching valve together with a make-up flow that dilutes the ^{1}D effluent before its entrance in the interface with a weaker solvent, suitable for the ^{2}D separation (Winther and Reubsaet 2005; Vonk et al. 2015; Gargano et al. 2016). This procedure is an implementation of the use of trapping columns with the only requirement of an additional LC pump easily set to deliver the make-up flow at a fixed rate. The decrease of the mobile phase strength of the ^{1}D fraction with a weaker solvent produces an on-column focusing in the trapping column. That way, analytes are efficiently retained in the trapping column during the loading position of the valve and they will be eluted by the initial ^{2}D mobile phase when the valve changes to the injection position. Therefore, analytes are injected in the ^{2}D dissolved in a mobile phase completely compatible with the stationary phase, which produces narrower peaks and higher efficiency. Moreover, sensitivity can be greatly improved not only because of the pre-concentration of the fraction in the trapping columns, but also because this design allows to use ^{1}D columns with broader internal diameter than

microbore or capillary columns, and therefore, it is possible to load more sample in the ^{1}D column. Another important advantage is that thanks to the decrease of the ^{1}D mobile phase strength, couplings between separation mechanisms that caused severe incompatibility problems until date, could be employed. Gargano et al. (2016) defined this modulation procedure as active modulation (LC/a × m/LC) in contrast with "passive modulation" of the conventional loop interfaces.

An interesting interface design adapted to focusing modulation is the vacuum-assisted evaporation interface. It was employed by Tian et al. (2008) for the coupling of a NP separation in the ^{1}D and a RP in the ^{2}D. The interface consisted on a 10-port 2-position switching valve where vacuum was connected on the waste port. This way, at the same time that the loop was being filled with the ^{1}D effluent, the solvent was evaporated by the application of vacuum at 25°C, leaving the analytes deposited on the internal wall of the loop. Then, when the valve was actuated, the ^{2}D mobile phase desorbed the compounds and were injected in a compatible solvent into the ^{2}D column. By removing the solvent from the ^{1}D, the excessive dilution encountered in LC × LC is circumvented and ^{2}D band broadening can be reduced. Although this application proved to be successful, further development of this type of interface has not been followed, considering that the risk of sample loss is prominent with this type of vacuum evaporative modulators. In fact, Tian et al. (2008) reported a recovery as low as 50% for some analytes.

Thermal modulation is another innovative interface. It involves heat transfers, analyte retentions, and elution velocity controlled by temperature. Up to now, this is the only interface presented not based on a conventional switching valve design. It consists of a modulator formed by three parts: a trapping column with the same stationary phase as the ^{2}D column, a low thermal mass (LTM) resistive heating, similar to the heating modules used in gas chromatography, and a longitudinally modulated cryogenic system adapted to hold the LTM. By applying heating and cooling cycles, analytes were captured in the trap column and eluted to the ^{2}D column. Thermal modulation produced narrower bands in the ^{2}D compared to a conventional switching valve system. Besides, this design reduced the pressure fluctuations produced by switching valves because of the change of the valve position. These fluctuations

cause the brief interruption of the ^{2}D flow rate and therefore a slight pressure drop, which ultimately can reduce column lifetime. The main limitation of the thermal modulation is that the ^{2}D analysis time is restricted by the cycles of the modulator, and analysis shorter than 40 s could not be performed, in addition to its sophisticated design (Creese et al. 2017).

In Table 1.1 the main advantages and disadvantages of all the described interfaces are summarized

Table 1.1. Comparison of the different interfaces employed in on-line LC × LC.

Interface	Description	Pros	Cons
Sampling loops	One 8-, 10-, 12-port 2-position switching valve or 4-port duo valve or two 6-port 2-position switching valves equipped with two sampling loops with identical volume	› Versatility › Simple configuration › High reproducibility	› No focusing effect › Short ^{2}D analysis time required
Two parallel ^{2}D columns	Use of two ^{2}D columns directly connected to the valve	› Longer ^{2}D analysis, higher $^{2}n_c$	› Severe ^{1}D undersampling due to long modulation times › Lack of reproducibility or drift appearance because of non-identical ^{2}D columns
Trapping columns	One of the possible configurations for switching valves using two trapping columns with similar ^{2}D column selectivity.	› Focusing effect › Reduction of ^{2}D band broadening	› Potential loss of some components due to unefficient trapping › Short ^{2}D analysis time required
Active modulation (LC/a × m/LC)	Use of trapping columns with the incorporation of a make-up flow at the exit of the ^{1}D effluent, before entering the trap	› Reduction of the ^{1}D effluent solvent strength › Effective trap retention › Strong focusing effect › Increase on selectivity	› Need of an additional pump › Short ^{2}D analysis time required
Vacuum-assisted evaporation	Conventional loop interface with the incorporation of heat and vacuum connected to the valve.	› Complete removal of ^{1}D solvent, making compatible the coupling of almost all separation modes	› High risk of sampling loss
Thermal modulation	Modulator formed by a trapping column with the same stationary phase than the ^{2}D column, a LTM and a longitudinally modulated cryogenic system.	› Reduction of ^{2}D band broadening	› ^{2}D analysis time limited by the modulator cycles › Very sophisticated instrumentation

1.3.6. CHALLENGES AND REQUIREMENTS OF THE LC × LC INSTRUMENTATION.

The efforts to achieve a satisfactory LC × LC separation are turned towards the gain of higher peak capacity and maximum orthogonality degree as well as to increase sensitivity, considering that current set-ups produce a great dilution of the sample since very high flow rates are typically employed in ^{2}D, which directly affect the limits of detection.

To face these challenges, the operating conditions in the different parts of the LC × LC instruments should be adapted to some requirements and criteria, including stationary phases, mobile phases, column dimensions, flow rates and frequency of the sample transfer fractions, among others (Jandera et al. 2008).

The goal of every LC × LC method development is to maximize the three main parameters, i.e., peak capacity, orthogonality and sensitivity, which imply a multi-objective task. The difficulty to optimize all the involved parameters is that all of them are closely related and somewhat connected, and thus, the modification of one factor affects the others. This implies that each part of the instrument is subjected to important challenges. These are described in the following sections, and summarized in Table 1.2.

Table 1.2. Challenges and solutions of the three main parts of an on-line LC × LC instrument found during method development.

	Challenge		Solution	Advantage	Disadvantage
^{1}D	Undersampling		› Narrow or microbore columns with low flow rates	› Broad separation with wide ^{1}D peaks to allow 3-4 samplings per peak	Sub-optimal ^{1}D flow rates
	^{2}D band broadening	Solvent incompatibility	› Narrow or microbore columns with low flow rates	› Low volume of ^{1}D effluent to modulator	Reduced sensitivity
		^{2}D injection volume	› Narrow or microbore columns with low flow rates › Split the ^{1}D effluent prior modulation	› Collection of small fractions of ^{1}D effluent › Optimal ^{1}D flow rates	
^{2}D	Undersampling	Short ^{2}D analysis time	› Short partially porous or monolithic columns › ^{2}D UHPLC	› Columns that provide high efficiency and produce lower backpressure › Short efficient columns with smaller ^2d_c that allow lower ^{2}D flow rates › Great ^2n_c increase.	Need of very high ^{2}D flow rates Smaller ^2d_c could produce ^{2}D band broadening problems
	2D band broadening	Solvent incompatibility	› ^2d_c larger than ^1d_c with very fast 2D flow rates › SIF and CS system gradients in 2D	› Dilution of the 1D solvent in 2D mobile phase › 2D mobile phase adaptation to 1D mobile phase	Reduced sensitivity SIF requires re-equilibration time. CS could produce band broadening.

Interface	Undersampling		› Short modulation times	› Fast sampling rate of the ^{1}D separation	Short ^{2}D analysis times
	^{2}D band broadening	Focusing effect	› LC/a × m/LC	› Pre-concentration of the analytes. › Increased sensitivity.	Short ^{2}D analysis time.
		Solvent incompatibility	› Vacuum-assisted evaporation	› Elimination of ^{1}D solvent	Risk of sample loss
			› Thermal modulation	› Elimination of ^{1}D solvent	Very sophisticated instrumentation
			› LC/a × m/LC	›Elimination of ^{1}D solvent	Additional LC pump

1.3.6.1. First dimension.

1.3.6.1.1. *First dimension challenges.*

In the ^{1}D, the separation of the compounds present in the sample has to be broadly distributed along the ^{1}D chromatogram to provide wide peaks that can be sampled 3–4 times to meet Murphy's rule (Murphy et al. 1998) in order to reduce the effect of the ^{1}D undersampling and to maintain the separation obtained in the ^{1}D.

The ^{1}D flow rate, together with the modulation time, is one of the parameters that directly determine the fraction volume that will be transferred to the ^{2}D. As explained above, the volume of the fraction injected into the ^{2}D column should be as minimum as possible. Some authors recommend that this volume should not exceeded the 10% of the ^{2}D column void volume (Gargano et al. 2016).

There are several ways to keep small fraction volumes and to provide the needed ^{1}D separation to avoid a loss on ^{1}D resolution during the sampling process. The most common is the implementation of the ^{1}D separation at very low flow rates, often run at suboptimal efficiencies. That way, a good broad ^{1}D separation is achieved and small aliquots of the ^{1}D effluent are collected in the interface. For instance, if the separation in the ^{1}D lasts 120 min, which is rather common in LC × LC, the aim would be to achieve ^{1}D peaks with $^{1}\sigma$ of about 0.5–1 min and modulation times shorter than 2.4 min. These parameters were established by Bedani et al. (2012) and, this way, a compromise to solve the conflict between the length of the sampling time related to the ^{2}D analysis time was found. Bedani et al. (2012) also reported another important contribution: exceeding the $^{1}n_c$ value above 50 is not useful for a fixed total analysis time, because higher values of $^{1}n_c$ would mean narrower ^{1}D peaks, and therefore, faster sampling rates would be needed, implying a reduction of the available ^{2}D analysis time, with the consequent decrease of the $^{2}n_c$ (Bedani et al. 2012).

1.3.6.1.2. *First dimension requirements.*

To carry out successful separations at low flow rate, the use of long ^{1}D columns with narrow internal diameter such as capillary or microbore columns is highly recommended (Dugo et al.

2006c; Cacciola et al. 2011; Jandera et al. 2012). Some LC instruments employed in the ^{1}D are not able to provide reproducible gradients at the low flow rates required for these applications, because of their high total dwell volume. An alternative to solve this problem is the use of a flow-splitter placed between the ^{1}D pump and the injection valve. As a result, adequate flow rates for these LC systems are used in the pump and, thanks to the split, the required low flow rate arrives to the column (Stoll et al. 2007). Unfortunately, this solution means that most of the ^{1}D solvent is wasted. The use of very narrow diameter ^{1}D columns leads to a compromise of the detection sensitivity since the mass of sample that can be injected in these narrow columns is relatively small.

Other works have developed a strategy where ^{1}D separation works at typical HPLC flow rates (0.3-0.5 mL min^{-1}) (Filgueira et al. 2011). The flow rate is then spitted after the ^{1}D column and before the interface. The main advantage of the post-^{1}D flow splitting system is that ^{1}D separation is more robust, reproducible and better efficiencies can be obtained, as well as that it allows essential independence of the modulation time, collected volume and, therefore, of the ^{2}D analysis time. Filgueira el al. (2011) achieved a 4-fold increase in the $^{1}n_c$ in comparison with a splitless system. However, the gain in $^{1}n_c$ can produce a loss of total $^{2D}n_c$, due to the fact that narrow ^{1}D peaks lead to the undesired undersampling of the ^{1}D. In other cases, even low ^{1}D flow rates are splitted after the column, the goal is to collect very small ^{1}D fraction eluents (e.g., 2 µL) in order to reduce as much as possible the ^{2}D injection volume. This split has to be reproducible and robust along the whole 2D analysis in order to affect equally to all components (Beelders et al. 2012). A common disadvantage to both strategies is that part of the sample is discarded during the split, so loss of sample is produced and only a discrete part of the analytes reaches the detector, which significantly affects the sensitivity.

1.3.6.2. Second dimension.

1.3.6.2.1. *Second dimension challenges.*

The $^{2}n_c$ peak capacity and the speed of analysis are two critical parameters since the shorter the ^{2}D analysis, the more the ^{1}D is sampled and thus the better the ^{1}D separation can be

maintained, although, at the same time, the incidence of the available time gradient in the ${}^{2}n_c$ is significant. Thus, shorter analysis times usually mean smaller ${}^{2}n_c$ values. In fact, ^{2}D separation has shown to have more relevance in the total performance of the LC × LC system than the ^{1}D separation (Uliyanchenko et al. 2012).

As above pointed out, the high sampling rate establishes the available ^{2}D analysis time, because the separation of a fraction transferred to the ^{2}D has to be finished before the next fraction is injected. Moreover, when gradient elution mode is selected in the ^{2}D, the ^{2}D analysis time has to include also the re-equilibration of the ^{2}D column, in order to maintain the ^{2}D column under identical initial conditions when the next fraction is injected. Hence, the ^{2}D analysis has to be performed as fast as possible. This implies that the ^{2}D analysis has to be performed at high flow rates, which greatly affects the sensitivity of the system since the analytes are largely diluted in the ^{2}D mobile phase.

Moreover, as already mentioned, other challenge related to ^{2}D is the possible poor compatibility of mobile phases, which affects the separation obtained in the ^{2}D that is susceptible to suffer band broadening. Hence, one of the targets of LC × LC method optimization is to achieve on-column focusing on the top of the ^{2}D.

1.3.6.2.2. *Second dimension requirements.*

Regarding the ^{2}D injection band broadening problem, it is possible to achieve a minimization of the ${}^{2}\sigma$ by maximizing the ratio ${}^{2}d_c/{}^{1}d_c$. When a ^{2}D column with a broad internal diameter is coupled to a ^{1}D narrower internal diameter column, the difference in the flow rates employed in each dimension (lower enough in the ^{1}D) helps to reduce the effect of the ^{1}D mobile phase strength by diluting the sample in the ^{2}D mobile phases. However, larger ${}^{2}d_c$ imply greater dilution of the sample as well as sensitivity losses (Bedani et al. 2012).

Working at high flow rates implies a significant increase of the system backpressure. For this reason, LC instruments that can cope with very high backpressures, as well as columns that generate smaller pressure drops are essential. Hence, to deal with very fast flow rates not only ^{2}D columns with relatively large internal diameters are required, but also short efficient

columns are indispensable. In this regard, monolithic columns can be a very useful alternative, since they generate lower column resistance, and, therefore, lower backpressure (Cacciola et al. 2006; Kivilompolo and Hyötyläinen 2008). In addition, the innovation in column technology has opened an excellent solution to cover the needs of the ^{2}D: the development of partially-porous particles. These new particles consist on a solid core and a superficial porous shell, in which the functional groups of the stationary phase are bound. As a consequence, the diffusion path through the particles is significantly reduced, together with the molecular diffusivity of analytes. These columns show higher efficiency than their conventional counterparts, and facilitate the use of high flow rates since the mass-transfer is faster. Another positive side-effect of using shorter diffusion paths is that smaller pressure drops are generated compared to conventional fully-porous particles (Cavazzini et al. 2007; Cunliffe and Maloney 2007; Marchetti et al. 2007).

Temperature can also help to carry out fast analyses since high temperature reduce the viscosity of the solvents and improve diffusion coefficients, diminishing the operation pressure. Besides, temperature also produces improvements on the LC × LC performance and therefore on the peak capacity (Stoll and Carr 2005).

On the other hand, $^{2}n_c$ can be greatly increased by employing gradient elution programs. Jandera et al. (2008) described that gradient elution could offer a peak capacity four times higher than isocratic elution. The gradient has to cover the whole mobile phase range to elute the most retained compounds in very fast cycles including the re-equilibration time.

Second dimension gradient elution can also influence the orthogonality of the LC × LC separation. ^{1}D column separates the complex mixture of compounds present in the sample as function of its selectivity; however, due to the use of a non-correlated separation mechanisms in ^{2}D, usually, the compounds that are firstly eluted from the ^{1}D are highly retained in the ^{2}D and, *vice versa*, compounds strongly retained in the ^{1}D elute fast in the ^{2}D. Consequently, peaks would not efficiently cover the whole 2D space unless orthogonal mechanisms are coupled. A practical strategy to cover the 2D space is to adapt the ^{2}D gradient to the eluted compounds of the ^{1}D along the whole LC × LC analysis time. In that sense, ^{2}D gradient types can be classified

as "full in fraction" (FIF) (Figure 1.9A), "segment in fraction" (SIF) (Figure 1.9B) and "continuous shifting" (CS) gradients (Figure 1.9C) (Jandera et al. 2010).

FIF gradient comprises the use of the same ^{2}D gradient step along the whole LC × LC analysis (Figure 1.9A). This type of ^{2}D gradient provides narrow peak widths. However, with this gradient the coverage of the 2D space can be scarce because of the different affinities of compounds on the two dimensions. Furthermore, the analysis time available for the separation is less than the modulation time because each ^{2}D analysis has to include a post-gradient re-equilibration time, so as can be deduced of Eq. 15, the time for the separation is described by Eq. 18:

$$^{2}t_{G} = t_{s} - {}^{2}t_{reeq} \qquad \text{(Eq. 18)}$$

Where t_G is the ^{2}D gradient time or the time available for the separation, ts is the sampling time or modulation time, and $^{2}t_{reeq}$ is the time need to re-equilibrate the column to the initial conditions before the next ^{2}D analysis.

In contrast, SIF gradient consists on the application of several segments of ^{2}D gradients along the whole ^{2}D time, in a way that the initial and the end composition of the gradient is modified according to the ^{1}D mobile phase and therefore with the nature of eluted compounds (Figure 1.9B). This modification allows a greater coverage of the 2D space. Moreover, with this method a focusing effect can be obtained thanks to the modification of the ^{2}D mobile phase as function of the ^{1}D mobile phase. The main drawback of this procedure, as in FIF gradient, is the consideration of the re-equilibration time in the ^{2}D analysis time.

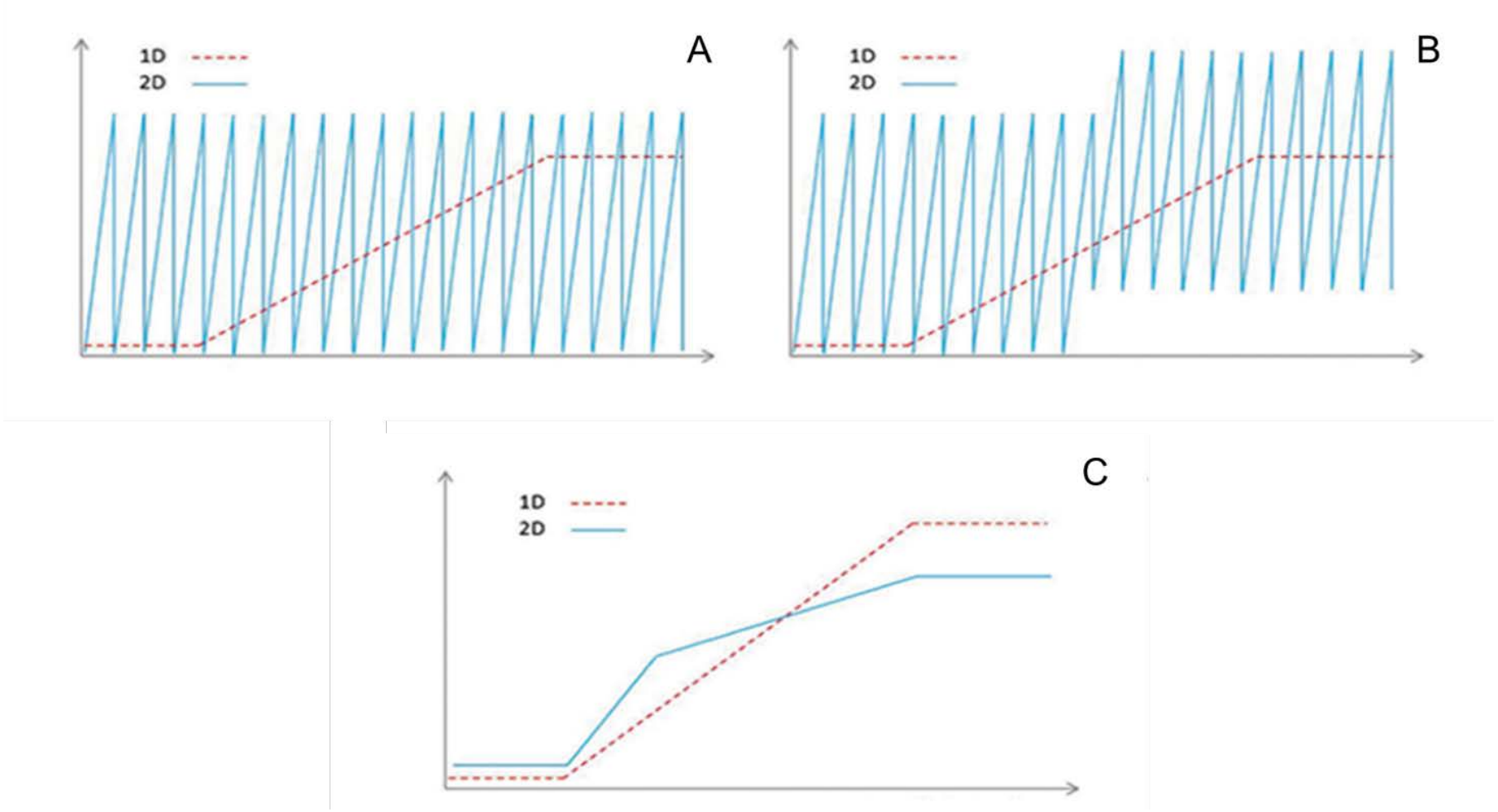

Figure 1.9. The different 2D gradient types that can be used to improve the 2D space coverage, A) FIF, B) SIF and C) CS gradients. Adapted from Li et al. (2013), copyright 2013, Springer.

On the other hand, CS, also called parallel gradient, employs only one ^{2}D gradient during the ^{2}D analysis, unlike FIF and SIF that use repetitive ^{2}D gradients in each modulation (Figure 1.9C). The advantages of this method is that the ^{2}D column does not require a re-equilibration during the analysis because it employs a continuous gradient, so CS offers a more efficient use of the second dimension analysis time since the whole ^{2}D analysis time is accessible for the separation. Besides, the initial ^{2}D mobile phase of each ^{2}D analysis is modified during the whole analysis time. However, it presents the disadvantage of possible band broadening due to quasi-isocratic ^{2}D gradient in each ^{2}D analysis.

Finally, other implementation that can be considered to increase the speed of the ^{2}D analysis is the use of UHPLC instruments in the ^{2}D. The use of UHPLC involves employing columns with sub-2 μm particles, which result in a gain of efficiency and in shorter analysis times, at the cost of higher pressure drops. Thus, the use of UHPLC in the ^{2}D with short columns containing sub-2 μm particles increases the $^{2}n_c$ and allows the use of lower flow rates when columns with smaller internal diameter are employed, enhancing the sensitivity (Huidobro et al. 2008; Kivilompolo and Hyötyläinen 2008; Sarrut et al. 2014). Vivó-Truyols et al. (2010) reported an increase in the peak capacity of 15-20% when UHPLC is used in one of the two dimensions and of 25-30% if UHPLC is used in both dimensions, compared to the use of a conventional HPLC × HPLC system. At the same time, a reduction of 25% and 35 % of total analysis time is achieved when UHPLC is employed in one or in both dimensions, respectively.

1.3.6.3. Interface.

1.3.6.3.1. *Interface challenges.*

As the interface is the responsible for the physical contact between ^{1}D and ^{2}D mobile phases, the interface has to face many challenges. An ideal modulation interface should mix and solve the incompatibility between mobile phases, focus the ^{1}D elution fraction as well as re-inject it in a relatively short time.

Besides, sensitivity could also be improved when a pre-concentration of the analytes and a good focusing of them is carried out in the interface.

1.3.6.3.2. *Interface requirements.*

As explained in Section 1.3.5.1, different interface designs have been developed, generally with different aims: i) to produce short sampling times to achieve the maximum possible number of samplings of the ^{1}D effluent in order to avoid undersampling; ii) to increase the $^{2}n_c$, and/or, iii) to generate a focusing effect (see Table 1.1).

Many efforts have been made to achieve the "ideal modulator"; however, the transfer process of two completely different dimensions, each of them with its particular criteria and requirements is far from straightforward. All the developed interfaces contribute to enhance one of the necessities of the interface performance, but unfortunately, at the cost of some other requirements that are negatively influenced. The most promising approach could arguably be the new LC/a × m/LC procedure, since it meets with all the needs of and ideal modulator with the only drawback of incorporating an easily to be implemented instrumental modification.

1.3.7. DATA ANALYSIS IN ON-LINE LC × LC.

1.3.7.1. Detectors.

Detection in LC × LC is not different from other LC systems. As in conventional HPLC, the kind of detector coupled to the instrument depends on the properties of the analytes to be determined. Some LC × LC applications use two detectors, one at the end of each dimensions (Dugo et al. 2004) although in the vast majority of LC × LC applications, only one detector is used to register the signal after the ^{2}D separation. At this point, it is worth to note that registering the ^{1}D separation is just useful during the LC × LC method development in order to monitor the optimization of the separation. Once optimized and coupled to the ^{2}D, is not necessary to monitor the ^{1}D separation anymore.

A variety of detectors have been coupled to LC × LC: absorbance (UV-Vis) (Filgueira et al. 2011), diode array detector (DAD) (Cacciola et al. 2007; Kivilompolo and Hyötyläinen 2008; Cesla et al. 2009) or evaporative light scattering detector (ELSD) (van der Klift et al. 2008; Mondello et al. 2011). These detectors monitor the separation, and some of them give useful information for sample characterization, for example UV-Vis spectra. However, due to the complexity of the samples analyzed by LC × LC, in many occasions, the information provided by these detectors is not enough to carry out the identification of hundreds or even thousands of peaks. In this regard, the coupling of LC × LC to MS (LC × LC-MS) is completely essential. The hyphenation between LC × LC and MS utilizes the same systems and principles than 1DLC. However, some considerations have to be taken into a count (Dugo et al. 2011):

i. When very high ^{2}D flow rates are employed, the flow rate must be splitted before its entrance into the MS, because the ionization sources employed in LC × LC (ESI and APCI) are not able to cope with such high flow rates.
ii. Acquisition rate fast enough to adapt to the fast ^{2}D separation is recommended. Although mass spectrometers of low resolution (quadrupole, ion trap) are able to provide adequate acquisition speeds, the use of state-of-the-art high resolution mass spectrometry analyzers (time-of-flight (TOF) or hydride analyzers such as QTOF or Orbitrap) is the best choice for LC × LC data acquisition.

In this regard, MS could be considered as an additional dimension. Furthermore, very recently ion mobility (IM) has been employed as a fourth dimension, since its capability to separate compounds according to their shape-to-charge ratio offers a further separation of the compounds after their 2DLC separation and before the MS analysis. Besides, IM, as high resolution mass spectrometry (HRMS) through the exact mass, greatly increase the certain identification of compounds by the characteristic collision cross section (CCS) values, allowing the separation of analytes with the same molecular weight that cannot be differentiated by MS, but are different in size and shape (isobaric compounds) (Stephan et al. 2016a, 2016b).

1.3.7.2. Detection issues in on-line LC × LC.

As it has been previously mentioned, detection sensitivity is one of the most important weaknesses of LC × LC. This issue is worsened when samples containing compounds at low concentrations are analyzed. Low sensitivity of LC × LC is mainly due to the dilution of the sample components during the analysis by two consecutive separation processes; in fact, the dilution in LC × LC is multiplied by two in comparison with 1DLC. This is even more pronounced, considering the typical high ^{2}D flow rates (Horváth et al. 2009).

In 1999, Schure evaluated the dilution effect occurred at the detector in LC × LC focusing on a concrete separation zone and comparing with the same zone analyzed in 1DLC. A 100-fold greater dilution produced in the LC × LC analysis was reported. Currently, several instrumental improvements have been developed with respect to 1999, and therefore, sensitivity has been enhanced, although it remains being a severe limitation for LC × LC. Recently, Stoll et al. (2015) studied the detection sensitivity effect specifically due to all the parameters that influence the transfer process between both dimensions that they called "interface conditions". For this evaluation, authors tested four loop-based set-ups, including one set-up with flow-splitting after ^{1}D column plus make-up flow before the interface with loops of 80 µL volume, whereas the other three set-ups consisted on flow-splitting systems with different loops volumes (40, 20 and 7 µL). It could be concluded that the volume and the solvent composition of the fraction injected in the ^{2}D had a huge impact on the sensitivity. Hence, due to the

amount of sample injected as well as to the focusing effect produced, the use of make-up flows provided better sensitivity.

In summary, a careful selection of the interface parameters and set-ups can lead to the detection of low-concentrated analytes (Stoll et al. 2015).

1.3.7.3. On-line LC × LC data acquisition and data treatment.

Data treatment is one of the most complex aspects of using LC × LC because, although the same detectors as 1DLC are used, working with 2D data is far from being as easy as 1D data.

The way in which the LC × LC separation is performed in practice, together with the large amount of data produced during the analysis requires special data treatment. In principle, the detector coupled to the ^{2}D column, registers and monitors each ^{2}D individual analysis, producing a one dimensional linear chromatogram formed by numerous short ^{2}D analyses. Once the LC × LC analysis is finished, the one-dimensional chromatogram has to be transformed into a two-dimensional image, usually by using dedicated software, that "cuts" each ^{2}D analysis and place them side by side giving rise to a 2D plot where the x-axis represents the ^{1}D separation while the y-axis the ^{2}D. After that, a 3D image can be represented, where the third dimension is based on signal intensity. Figure 1.10 shows a scheme of the LC × LC acquisition data procedure.

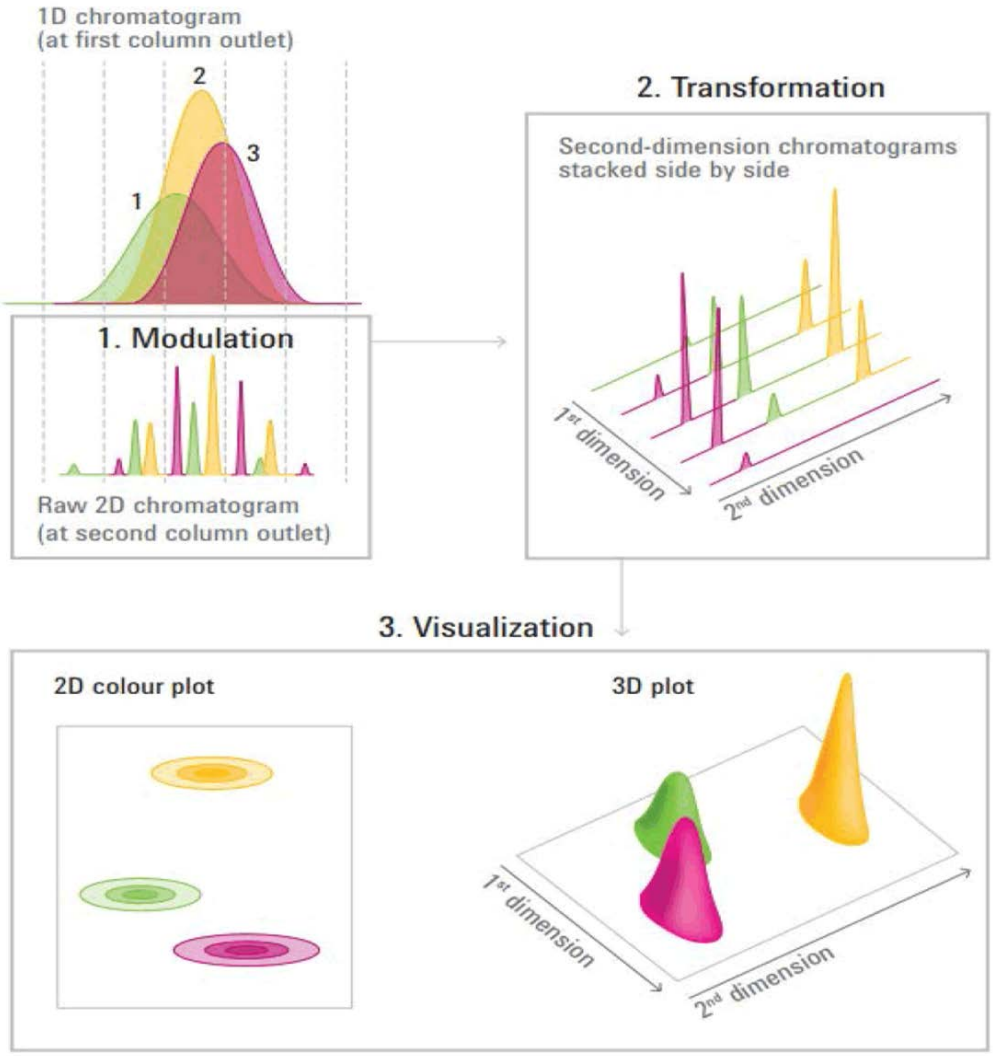

Figure1.10. Data acquisition and elaboration procedure followed in a typical LC × LC analysis. Adapted from Carr and Stoll (2015), copyright 2015, Agilent Technologies, Inc.

Unfortunately, until date, the available software (both home-made and commercial) do not provide with all the tools needed to obtain the whole 2D data information and they still present some limitations and difficulties:

i. When two detectors are coupled in tandem, for instance a DAD coupled to MS, four sets of information are involved: the information provided by both detectors as intensity, as well as the information of the two retention times of each peak (the retention time in the ^{1}D and in the ^{2}D). Moreover, the acquisition of spectra (UV-Vis and/or MS, for instance) may increase even more the complexity of the collected information after just one analysis. The structure of the complex matrix of data can

only be performed by employing complex and sophisticated chemometric tools such as parallel factor analysis (PARAFAC), the generalized rank annihilation method (GRAM), or multivariate curve resolution–alternating least squares (MCR–ALS). Although, these models are powerful tools to analyze and visualize 2D data, there is no commercial software that applies these methods to 2D data. Therefore, usually, the information from each detector must be treated separately.

ii. Moreover, the fact that each ^{1}D peak is sampled 3–4 times means that its area in the linear chromatogram is divided in 3–4 ^{2}D peaks corresponding to the same compound, which hampers the quantification and the data treatment in LC × LC.

iii. Statistical comparison of 2D chromatograms is not possible, since the software is not able to align and normalize the chromatograms, which in the most of the cases is critical because the high probability of slightly different retention times.

Consequently, significant progress in the available 2D data treatment software in order to comply with these requirements is expected in the future.

1.3.8. ON-LINE LC × LC APPLICATIONS IN FOOD ANALYSIS.

The field of food analysis holds the fourth place amongst the LC × LC applications presented so far, behind protein and peptides analysis, pharmaceutical approaches and very close to polymer analysis, whereas environmental analysis stands in fifth place (Carr and Stoll 2015).

The vast majority of the LC × LC food applications developed up to date are directed to the analysis of very complex food matrices. In most of them, sample preparation steps and/or pretreatments are minimized or even avoided, which is considered a great advantage for the chemical characterization of food samples, bearing in mind that the analysis of an intact sample allows to obtain its native chemical composition (Herrero et al. 2009). Numerous LC × LC food applications have been already reported, and can be classified as a function of the analyzed compounds.

1.3.8.1. LC × LC for the analysis of phospholipids.

Phospholipids are amphiphilic molecules, since their chemical structure consists of a glycerol backbone which presents two fatty acids linked in positions sn-1 and sn-2 (non-polar "tails" of the molecule), while in sn-3 position a phosphate group is bound (polar "head" of the molecule). These molecules present a huge chemical variability as a result of the combination of different fatty acids that can present different lengths and degree of unsaturation, and on the other side, because the polar head (phosphate group) can be linked to other molecules. For example, inositol giving phospatidylinositol, serine producing phosphatidylserine or ethanolamine producing phosphatidylethanolamine.

Phospholipids are present in foods like milk or eggs, and have important physiological functions in animals, such as structural and metabolic functions, as well as several functional activities like regulation of the inflammatory reactions, chemopreventive and chemotherapeutic activity on some types of cancer, and inhibition of cholesterol absorption. For these reasons, these components are considered important biomolecules for the health promotion (Contarini and Povolo 2013). As can be deduced of its complexity, the chemical characterization of this group of molecules is compromised by several difficulties.

LC × LC analysis of phospholipids is usually carried out coupling a HILIC separation in the ^{1}D and a RP separation in the ^{2}D through stop-flow and heart-cutting methods (Dugo et al. 2013; Sun et al. 2015). This coupling is able to provide successful separations by phospholipid classes in the ^{1}D-HILIC, whereas each individual species belonging to each phospholipid class are separated as function of their fatty acid chains in the ^{2}D-RP. However, due to the complexity involved in phospholipid analysis, no on-line LC × LC methods have been presented so far.

1.3.8.2. LC × LC for the analysis of triacylglycerols.

Triacylglycerols (TAGs) structurally consist of a glycerol backbone, which is esterified with three medium or long-chain fatty acids. The different TAGs are represented by total carbon number, fatty acids lengths and positions, number of double bonds and the position and configuration related to each fatty acid (Mondello et al. 2011). Hence, the determination of

TAG composition in natural matrices can be challenging and complicated due to the diverse nature of these mixtures derived from the large number of compounds usually observed in the TAGs fraction (Dugo et al. 2006b). In this regard, 2DLC allows the separation of TAGs as a function of their different chemical characteristics and behavior in each dimension.

The main stationary phases employed in 2DLC are non-aqueous reversed phase liquid chromatography (NARP-LC) and silver ion liquid chromatography (Ag^+-LC). In Ag^+-LC, TAGs are separated according to the number and the distribution of the double bonds of the fatty acids present in the TAG molecule. Under NARP-LC, TAGs elute according to their partition number, a parameter that involves the total carbon number of the three fatty acids and the number of double bonds. The complexity of these analytes as well as some mobile phase mismatches and on-column focusing problems make this on-line coupling a big challenge (Dugo et al. 2006a; Mondello et al. 2011). Besides, due to the mentioned difficulties several stop-flow methods have been applied for the chemical characterization of particularly difficult TAG mixtures (HolCapek et al. 2009; Beccaria et al. 2015).

1.3.8.3. LC × LC for the analysis of phenolic compounds.

Phenolic compounds are secondary metabolites widespread in plants. The growing interest in phenolic compounds is due to their potential role in the prevention of several diseases associated to oxidative stress, such as cancer, cardiovascular and neurodegenerative diseases (Tucker and Robards 2008). Within this group, flavonoids and non-flavonoids compounds are included. Among them, flavonoids are further divided in flavonols, flavones, isoflavones, flavanones, anthocyanins, flavanols, whereas non-flavonoids compounds are divided in phenolic acids, stilbenes and lignans. Usually, polyphenols occur in nature in very complex mixtures, composed by a variety of very closely related structures. Therefore, their chemical characterization requires separations with high resolving power.

LC × LC has been widely employed for the analysis of food and beverage samples rich in phenolic compounds, such as vegetable and fruit extracts (Cacciola et al. 2011; Kalili et al. 2013), beers and wines (Cacciola et al. 2007; Hájek et al. 2008; Donato et al. 2016). RP × RP is

the most-frequently used coupling for their separation, although recently, HILIC × RP is gaining interest (Dugo et al. 2008a; Cacciola et al. 2017). In Table 1.3 the main HILIC × RP applications for the characterization of phenolic compounds in foodstuffs are summarized.

Table 1.3. On-line HILIC × RP applications for the analysis phenolic compounds in food-related samples.

Food or beverage	First dimension	Second dimension	Interface	Detection	Reference
Phenolic acids and flavonoids standards	DioEDMA (170 × 0.53 mm, monolithic column). F: adjusted to the ^{2}D analysis time; 40 °C.	C_{18} (50 × 3.0, 2.6 μm) F: 2.5–3 mL/min	› 10-port 2-position switching valve (10 and 20 μL loops). › Modulation time: adjusted to the ^{2}D analysis time.	DAD	Jandera et al. 2012
Wine	Amide (150 × 1 mm, 1.7 μm) F: 1 μL/min	C_{18} (50 × 2.1 mm, 1.3 μm). F: 0.86 mL/min; 60 °C	› 10-port 2-position switching valve (5 μL loops) › Modulation time: 2 min.	ESI-QTOF-MS	Willemse et al. 2015
Phenolic acids and flavonoids standards	BIGMA-MEDSA: 160 × 0.53 mm, monolithic column. F: 3–5 μL/min	C_{18} (50 × 3.0 mm, 2.6 μm) F: 3 mL/min; 50 °C	› 4-port duo valve (10 μL loops). › Modulation time: 1.5 min.	DAD	Hájek et al. 2016
Grape seeds	Diol (250 × 1 mm, 5 μm) F: 25 μL/min	C_{18} (50 × 4.6 mm, 2.6 μm). F: 1.5 mL/min; 50°C	› Post-column flow-split. › 10-port 2-position switching valve (5 μL loops). › Modulation time: 2 min.	FD-ESI-QTOF-MS	Kalili et al. 2013
Phenolic acids and flavonoids standards	BIGMA-MEDSA: 210 × 0.53 mm, monolithic column. F: 2–3 μL/min; 60 °C	C_{18} (30 × 3.0, 2.6 μm). F: 4.5 mL/min; 50 °C	› 10-port 2-position switching valve (10 μL loops). › Modulation time: 1 and 1.5 min.	DAD	Jandera et al. 2013

Cocoa	Diol (250 × 1 mm, 5 µm) F: 25 µL/min	C_{18} (50 × 4.6 mm, 1.8 µm). F: 1.5 mL/min	› Post-column flow-split. › 10-port 2-position switching valve (5 µL loops). › Modulation time: 2–3 min.	DAD	Kalili and De Villiers 2013
Rooibos	Diol (250 × 1 mm, 5 µm). F: 25 µL/min	C_{18} (50 × 4.6 mm, 1.8 µm). F: 1.2 mL/min	› Post-column flow-split. › 10-port 2-position switching valve (5 µL loops). › Modulation time: 2 min.	DAD	Beelders et al. 2012

PEG, polyethylene glycol; F, flow rate; FD, fluorescence detector

1.3.8.4. LC × LC for the analysis of carotenoids.

Carotenoids are natural pigments synthesized by plants, algae and some microorganisms that are responsible for the yellow, orange and red typical colors of many fruits and vegetables. These compounds constitute an important source of natural colorants for the food industry. Moreover, carotenoids have been pointed out to possess several beneficial health effects, including potent antioxidant activity that could protect cells against oxidative damage and therefore, reduce the prevalence of some diseases; furthermore, some of them have provitamin A activity (Shan 2016).

The chemical structure of carotenoids is based on a polyterpenoid skeleton generally formed by the assembling of 8 isoprenoid units, giving rise to a long chain with conjugated double bonds (Rao and Rao 2007). Carotenoids can be classified in two groups: carotenes, consisting of a hydrocarbon chain without any additional functional groups (e.g., β-carotene), and, xanthophylls that present different oxygenated functional groups such as hydroxyl, keto, or epoxy groups (e.g., lutein and zeaxanthin). In addition, cyclations can occur in one or both ends of the molecule. Xanthophylls can be found in their free form or, most-commonly, in a more stable esterified form with one or two fatty acids (Fraser and Bramley 2004; Saini et al. 2015; Petry and Mercadante 2016). As a result, a large number of chemical structures can arise, making LC × LC an analytical solution for carotenoids characterization in complex food samples.

NP × RP is the preferred option for carotenoids analysis; under NP conditions, carotenoids are separated in groups in order of their polarities (from non-polar to polar carotenoids), whereas in RP mode, carotenoids elute according to their increasing hydrophobicity. In the case of carotenoid esters, these are retained according to their fatty acid chain length (Cacciola et al. 2016a). The separation power of NP × RP for the analysis of carotenoids has been shown for several food sources, such as citrus essential oils (Dugo et al. 2006c) and juices (Dugo et al. 2009), peppers (Cacciola et al. 2012), red mamey (Cacciola et al. 2016c), as well as for the characterization and evaluation of stability of carotenoids of overriped fruits such as banana, nectarine and persimmon-apple (Cacciola et al. 2016b).

It is worth to mention that, traditionally, to simplify the analysis of carotenoids in foods and food-related products, a saponification step is carried out. This pretreatment allows releasing all the present carotenoids into their free forms. However, this procedure is well-known for producing some degradations and modifications in the native composition. For this reason, the direct analysis of the original carotenoid mixture is more interesting, in order to have a real picture of the native composition of these components. The impressive separation power provided by LC × LC compared to one-dimensional chromatography has allowed the determination of the native carotenoid composition of different food samples, such as citrus (Dugo et al. 2008b; Dugo et al. 2008c; Dugo et al. 2009). In this regard, interestingly, the typical carotenoid composition acquired by LC × LC could be also related to the freshness degree of orange juices, as native epoxycarotenoid esters suffered rearrangements from 5,6- to 5,8-epoxides with time, partially due to the natural acidity of the juices (Dugo et al. 2009).

CHAPTER 2.

Aims and work plan.

Modern Food Analytical Chemistry was born in the 20th century with the emergence of separation techniques, such as gas chromatography and liquid chromatography, able to individually separate and determine the different food components. After that, the use of spectroscopic techniques hyphenated to those separation systems gained an essential role for the chemical characterization of complex food samples as well as for the identification of minor components contained in food.

Nowadays, food analysis is involved in many researches carried out within the Food Science domain, including important topics such as food and health, food safety, food quality as well as traceability. The development of this field is also pushing to the generation of new advanced analytical tools and methods that are able to cope with the important challenges that Food Science is facing today. Among them, new methods able to provide with appropriate robustness, efficiency and sensitivity are constantly sought.

In this regard, multidimensional techniques, and more specifically, comprehensive two-dimensional liquid chromatography (LC × LC) may play a key role, since this technique is able to provide with impressive resolving power and, in addition, if coupled to MS, this tool is really interesting for the identification of unknown compounds, which may be very useful to meet the current Food Science needs. Although LC × LC is a well-established and mature analytical technique, the use of this technique both in food analysis as well as in other fields is not widespread, partially due to the instrumental requirements and the in-depth knowledge required to properly develop and apply new methods. Consequently, the development of new analytical methods directed towards the analysis of very complex food samples, usually not attainable by conventional one-dimensional LC, as well as the study of new advancements to improve the technical and practical implementation of this technique are of great interest at present.

For this reason, this PhD Thesis is aimed to make a significant contribution to increase the available knowledge and to extend the use of LC × LC to unexplored complex food samples in order to achieve the characterization of potentially bioactive compounds, to obtain complex 2D profiles that could be used for geographical origin authentication of valuable natural

products, as well as to explore new strategies for the practical implementation of LC × LC in order to further increase its analytical performance.

Therefore, the **main objective** of this PhD Thesis is:

To develop novel on-line LC × LC methods for the chemical characterization of secondary metabolite profiles of complex natural food sources, taking advantage of the enhanced resolving power that this technique is able to provide for the identification of potentially bioactive compounds.

In order to achieve this main objective, the following partial objectives have been established:

i. To increase the analytical separation power for the chemical characterization of proanthocyanidins, together with other different polyphenols, from different natural sources, including grape seeds, apples, chokeberries and grapevine canes through the application of HILIC × RP methods.
ii. To develop on-line LC × LC methods to reveal, for the first time, the native phlorotannin composition of the brown algae *Cystoseira abies-marina* and *Sargassum muticum*.
iii. To establish a novel HILIC × RP methodology to characterize the triterpene saponin profile of licorice as well as its complex phenolic composition, in order to obtain typical secondary metabolite profiles that could be related to the geographical origin of different samples.
iv. To improve the coupling between two orthogonal separation modes such as HILIC and RP in on-line LC × LC approaches by applying different focusing and non-focusing modulation strategies in order to increase resolving power, sensitivity as well as overall performance.

To achieve this aims, the work plan followed in this Thesis is schematically represented bellow (Figure 2.1):

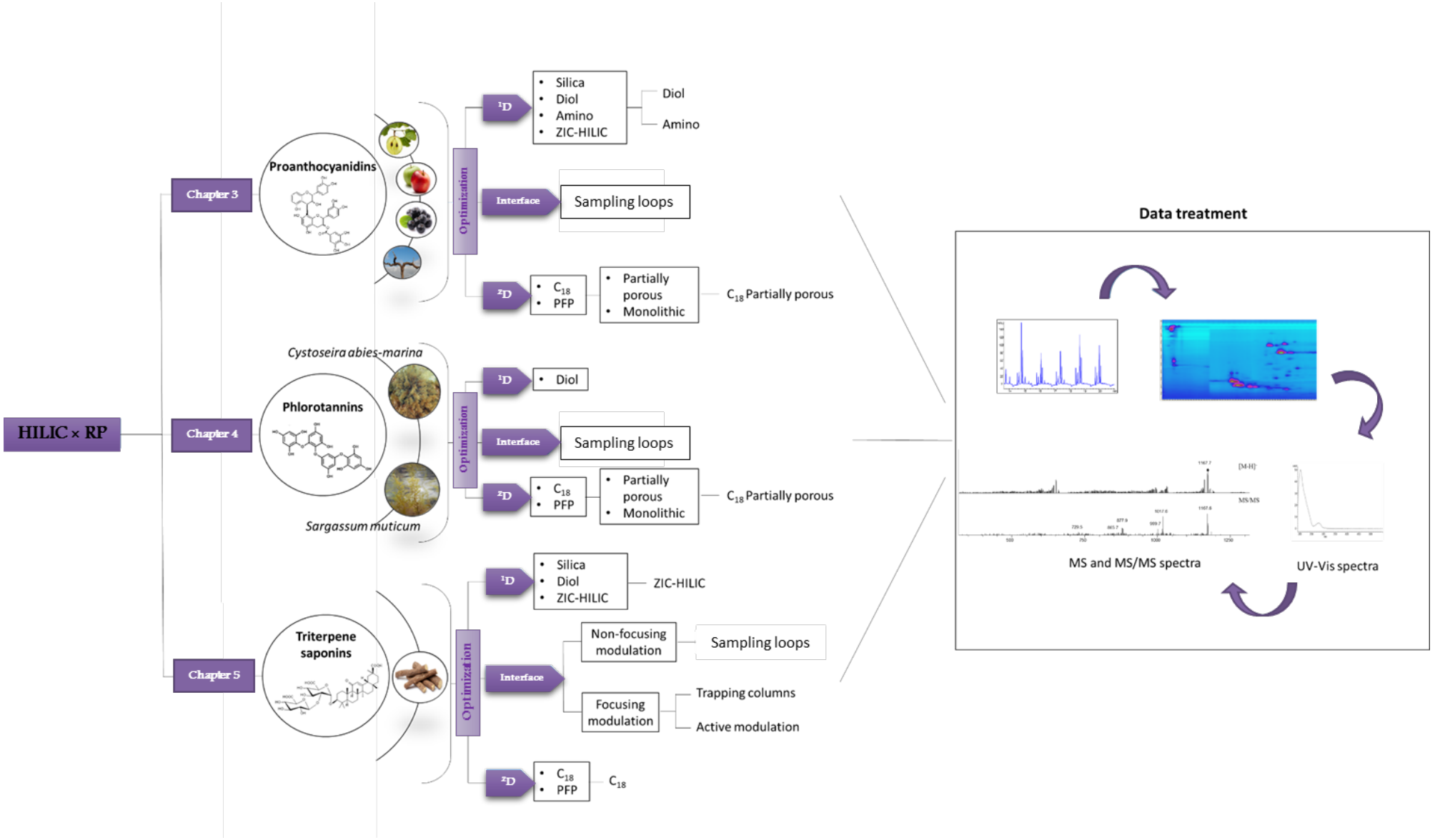

Figure 2.1. Work plan followed in this PhD Thesis.

Firstly, in Chapter 3, the study of the chemical composition of proanthocyanidins in several food-related matrices is reported. To achieve this goal, the separation of proanthocyanidins under HILIC mode, its on-line comprehensive coupling to a RP separation mode, as well as the UV-Vis and MS/MS data obtained from the analyses were studied, in order to get a high separation and identification power. Four proanthocyanidin-rich food samples were studied and their proanthocyanidins composition was determined, together with the presence of other polyphenols, through the careful optimization of the different parameters that affect the LC × LC separation (Chapter 3, Sections 3.2, 3.3, 3.4 and 3.5).

After that, the employment of on-line LC × LC for the separation of phlorotannins from brown algae is presented in Chapter 4. This Chapter describes the separation and identification of those phenolic compounds using LC × LC for the first time. To do that, the chemical structure of these complex molecules and their separation under HILIC × RP coupling were considered. Besides, data treatment of the UV-Vis spectra as well as their particular MS and MS/MS spectra was carried out for the identification of these interesting compounds (Chapter 4, Sections 4.2 and 4.3).

Finally, the optimization of a new HILIC × RP method for the study of the composition of triterpene saponins from licorice is presented in Chapter 5. The optimization of the separation of the triterpene saponins and other phenolic compounds contained in licorice was carried out attaining complex 2D secondary metabolites profiles. The chromatographic behavior of those components present in licorice in different HILIC- and RP-compatible stationary phases was studied, as well as their identification by combining the DAD, MS and MS/MS data acquired (Chapter 5, Section 5.2). These profiles were utilized to establish typical metabolite patterns depending on the geographical origin of 5 different samples. Moreover, this sample was employed as a model food sample to carry out an in-depth study about the influence of different types of modulation including focusing and non-focusing strategies on the overall performance of HILIC × RP methods. After this study, new separation conditions that allowed a significant increase on resolving power and sensitivity were attained (Chapter 5, Section 5.3).

CHAPTER 3.

Chemical characterization of proanthocyanidins by HILIC × RP-DAD-MS/MS

3.1. Characterization of grape seed procyanidins by comprehensive two-dimensional hydrophilic interaction × reversed phase liquid chromatography coupled to diode array detection and tandem mass spectrometry.

3.2. Profiling of phenolic compounds from different apple varieties using comprehensive two-dimensional liquid chromatography.

3.3. Downstream valorization and comprehensive two-dimensional liquid chromatography-based chemical characterization of bioactives from black chokeberries (*Aronia melanocarpa*) pomace.

3.4. Profiling of *Vitis vinifera* L. canes (poly)phenolic compounds using comprehensive two-dimensional liquid chromatography.

3.1. INTRODUCTION – PROANTHOCYANIDINS.

Proanthocyanidins are the second most-abundant group of phenolic compounds after lignans (Gu et al. 2003). The widespread presence of proanthocyanidins in plants makes them an important part of the human diet; particularly, these components are common and abundant in fruits, legume seeds, nuts, cereal grains and in several beverages, such as tea, wine, beer or cider. Their typical astringent character is due to their ability to form complexes with salivary proteins; in fact, this characteristic property helps to easily recognize food sources rich in proanthocyanidins (Santos-Buelga and Scalbert 2000; Gu et al. 2003; Rasmussen et al. 2005). Besides astringency, proanthocyanidins are responsible of other food quality parameters such as bitterness, sourness, sweetness, aroma, and color (Jaganath and Crozier 2009).

Several beneficial health effects have been attributed to proanthocyanidins including antioxidant, anticancer, cardioprotective, antimicrobial, antiviral, neuro-protective and anti-inflammatory activities, among others (Cos et al. 2004; Jeong and Kong 2004; Aron and Kennedy 2008; Singh et al. 2011). These bioactivities are responsible for the interest that these compounds have recently raised as potential source for disease prevention through diet.

3.1.1. CHEMICAL STRUCTURE OF PROANTHOCYANIDINS.

Proanthocyanidins are oligomers and polymers that may reach high molecular weights, composed of flavan-3-ols, that present the typical C6-C3-C6 flavonoind skeleton. These units are mainly linked by C-C bonds (B type proanthocyanidins) or can also be doubly linked by an additional ether C-O-C bond (A type proanthocyanidins). The size of the proanthocyanidins is described by their degree of polymerization (DP). The DP composition naturally found widely varies among sources and even depending on the tissue zone of the plant. Generally, foods present proanthocyanidins with an average degree of polymerization ranging from 1 to 10, or greater than 10 (Aron and Kennedy 2008).

There are three common flavan-3-ol units that can be combined into proanthocyanidin structures: catechin and its isomer epicatechin, gallocatechin and its isomer epigallocatechin, and afzelechin and its isomer epiafzelechin (Figure 3.1A). Besides, these unis can be esterified with gallic acid, giving rise to 3-O-galloylated units. The proanthocyanidins that are uniquely constituted by (epi)catechin are termed procyanidins, and are the most extended proanthocyanidin group in food sources. On the other hand, those conformed by (epi)gallocatechin and (epi)afzelechin are named prodelphinidins and propelargonidins, respectively. These two groups are more heterogeneous and commonly appear in foods coexisting with procyanidins. Figure 3.1 shows the basic chemical structure of the three proanthocyanin types and some polymers examples.

3.1.2. CHEMICAL CHARACTERIZATION OF PROANTHOCYANIDINS.

The characterization of proanthocyanidins is a very challenging task due to the exponential increase of number of different but closely related compounds considering the DP, the specific composition in flavan-3-ols units and their isomeric forms, as well as the different degree of galloylation (Hümmer and Schreier 2008).

Regarding to chromatographic separation, proanthocyanidins from food plants have traditionally been analyzed by different one-dimensional liquid chromatography separation modes, namely RP, counter current chromatography (CCC), SEC or NP.

Under RP mode, the different isomers of dimers and trimers of proanthocyanidins can be separated, but this separation is not carried out in order of increasing DP and it is limited to small oligomers (DP < 4). High DP structures are not separated and commonly elute as a wide unresolved hump (Rzeppa et al. 2011) at the end of the analysis.

Flavan-3-ol	R1	R2	R3	R4	R5
Afzelechin	H	OH	H	H	OH
Epiafzelechin	H	OH	H	OH	H
Catechin	H	OH	OH	H	OH
Epicatechin	H	OH	OH	OH	H
Gallocatechin	OH	OH	OH	H	OH
Epigallocatechin	OH	OH	OH	OH	H

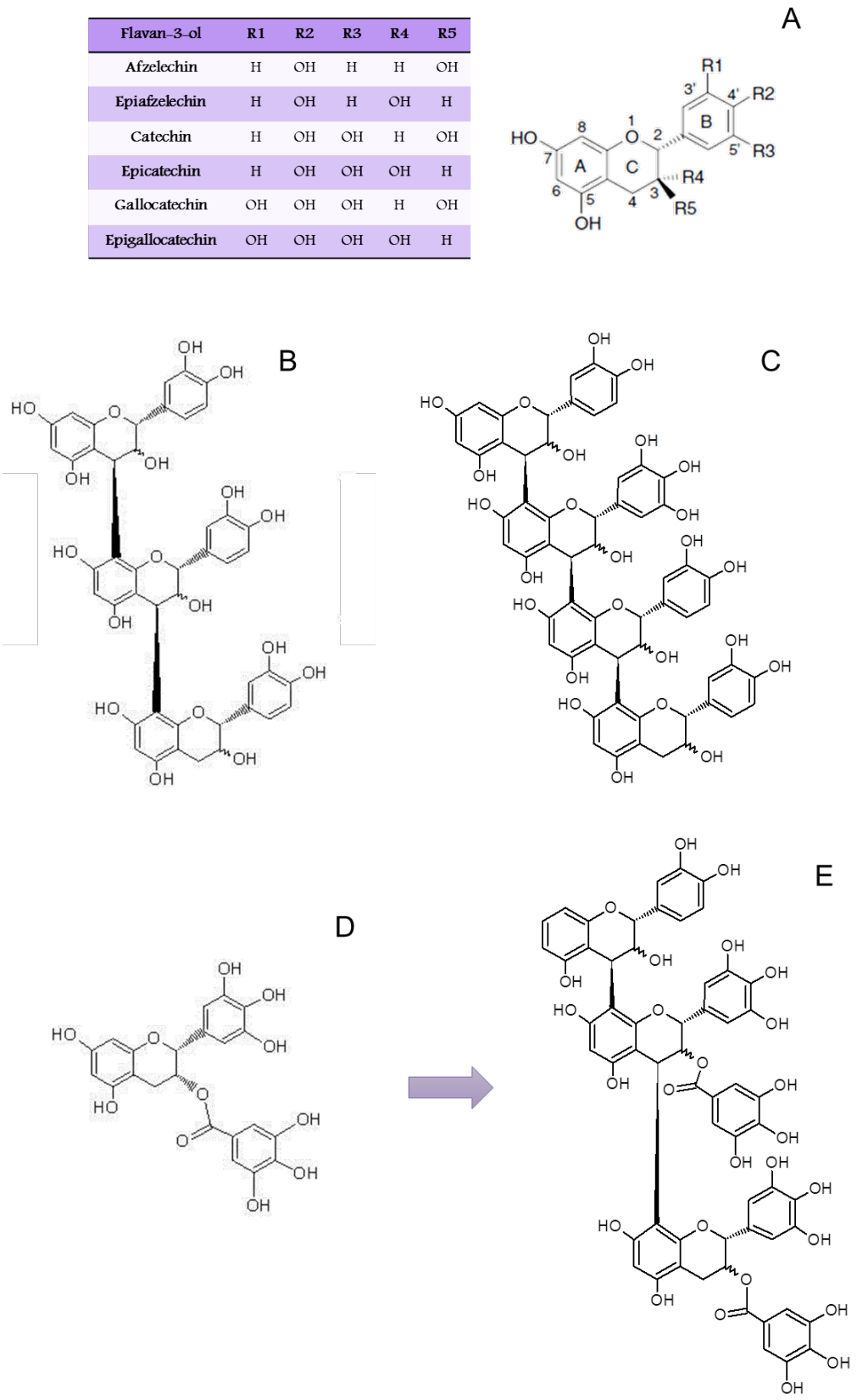

Figure 3.1. A) Chemical structure of the main types of proanthocyanidins found in foods. B) Procyanidin trimer, formed only by (epi)catechin units. C) Prodelphinidin tetramer formed by three (epi)catechin units and one (epi)gallocatechin unit. D) (epi)gallocatechin gallate unit. E) Prodelphinidin trimer digallate formed by one (epi)catechin unit and two (epi)gallocatechin gallate units.

On the other hand, CCC, SEC and NP allow the separation of proanthocyanidins in agreement to their DP (CCC and NP in increasing order of DP, while SEC separates proanthocyanidins in decreasing order of DP). However, the separation efficiency of CCC and SEC is lower than NP (Yanagida et al. 2003). NP provides high efficiencies for the separation of proanthocyanidins from monomers to oligomers and small polymers up to DP = 10. However, under NP mode, the separation of different isomers containing the same DP is not possible. Moreover, when polymers with DP > 10 are present in the sample, the very complex composition makes impossible their separation under NP conditions and, hence, coelute in a large peak at the end of the chromatogram. Usually, silica bonded stationary phases have been employed for the NP separation of proanthocyanidins from apple, grape, berries and cocoa, using dicloromethane–methanol as mobile phase (Gu et al. 2002a; Counet et al. 2004; Hellstro and Mattila 2008). The use of those mobile phases also implies negative connotations, since the use of chloride solvents presents important hazards for the analyst, the environment and increases disposal costs.

In this sense, HILIC entails significant improvements for the analysis of proanthocyanidins as an alternative to NP. Under HILIC mode, proanthocyanidins are basically separated like in NP, that is, in increasing DP order, due to the interactions of the proanthocyanidins with polar stationary phases. However, this mode presents a huge advantage over NP in the replacement of toxic organic solvents by acidified aqueous acetonitrile and methanol mobile phases. In particular diol-bonded particles have shown very good capability in terms of resolution allowing the separation of proanthocyanidins with a DP up to 10 employing more environmentally favorable solvents (Kelm et al. 2006; Robbins et al. 2009).

In any case, as it can be deduced from the above-explained, there is not a universal one-dimensional HPLC method for the appropriate separation of very complex mixtures of proanthocyanidins, as those found in food and food-related matrices. In summary, it can be affirmed that one-dimensional HPLC cannot provide with the enough resolution for the direct analysis and characterization of proanthocyanidins-rich foods.

3.1.3. DETECTION OF PROANTHOCYANIDINS.

Different detection methods can be used during the HPLC analysis of proanthocyanidins. Fluorescence detection has been employed in different applications (Wallace and Giusti 2010; Rodríguez-Mateos et al. 2011; Verardo et al. 2015). This detection provides a very high sensitivity for the determination of proanthocyanidins. However, DAD also offers good sensitivities monitoring the separation at 280 nm; this fact together with the possibility of registering UV-Vis spectra are responsible for the widespread use of DAD for the analysis of these compounds (Guerrero et al. 2009; Liu and White 2012; Zhang et al. 2017). However, none of both types of detection methods are able to provide enough information for the precise identification of oligomers and polymers, considering that these molecules are based on the links of very related monomers with similar UV-Vis spectra (Hümmer and Schreier 2008). Hence, the hyphenation with MS is essential for the characterization of the proanthocyanidin composition of food matrices.

The MS analysis of proanthocyanidins is usually carried out using ESI as ionization technique, working under negative ionization mode. Several MS analyzers have been employed coupled to HPLC for the identification of these complex compounds such as triple quadrupole (Hosseinian et al. 2007; Weber et al. 2007; Ortega et al. 2008), ion trap (Määttä-Riihinen et al. 2005; González-Manzano et al. 2006), TOF (Pongsuwan et al. 2008), or Orbitrap (Piccinelli et al. 2016). Thanks to the use of MS, the information needed for the identification of the type of proanthocyanidin (procyanidin, prodelphinidin or propelargonidin) as well as for the elucidation of the DP and degree of galloylation can be obtained, mostly if tandem MS experiments are carried out. However, the identification by MS also presents difficulties, even when HRMS is employed. This is due to the fact that the proanthocyanidins with the same DP and flavan-3-ol composition have the same molecular weight and the same MS/MS fragmentation patterns, and hence, the identification of the exact isomer composition of the molecule is not possible (Valls et al. 2009). Comparison with retention times of commercial standards, when available, is essential for the unequivocal identification.

MALDI-TOF-MS has been also used for the characterization of proanthocyanidins as a stand-alone technique, without any previous chromatographic separation step (Monagas et al. 2010).

3.1.4. MDLC FOR THE CHEMICAL CHARACTERIZATION OF PROANTHOCYANIDINS.

As a possible solution for the lack of resolving power experienced by one-dimensional HPLC separation methods, the use of different MDLC procedures have been explored in order to produce significant gains in separation power. Proanthocyanidins from different food sources have been analyzed by 2DLC, such as cocoa, apples and red grape seeds (Kalili and de Villiers 2009; Kalili and De Villiers 2013; Kalili et al. 2013). The proanthocyanidins present in these three samples consist of polymers of (epi)catechin units, that is, procyanidin-rich samples, and only grape seeds presented galloylated procyanidins. For the comprehensive two-dimensional LC analysis of procyanidins, the use of HILIC × RP coupling has been proposed under different modes, namely, off-line, stop-flow and on-line. The comparison between the three modes for the separation of cocoa procyanidins (Kalili and De Villiers 2013) showed that off-line and stop-flow modes provided very high peak capacity values (1959 and 1528, respectively), but at the cost of very long and non-practical analysis times (13.3 h). The on-line mode provided a peak capacity value of 591 in 1.7 h, meaning a peak production rate of 4.56 peaks min^{-1}, which is a more appropriate performance. The on-line HILIC × RP method applied for the characterization of grape seed procyanidins allowed the separation of completely resolved peaks of procyanidins up to DP = 7 in 100 min. These works confirmed the utility of LC × LC for the separation of complex polymers such as proanthocyanidins.

Following this idea, the development of different on-line LC × LC methods directed towards the chemical characterization of proanthocyanidins in different complex food samples was carried out during this PhD Thesis. The following sections describe the developed applications for the analysis and characterization of procyanidins in grape seeds (Section 3.2) and apples (Section 3.3). Moreover, samples of increasing complexity were also targeted involving, in addition, the presence of other phenolic compounds. Thus, the development of a new LC × LC method for the secondary metabolite profiling of chokeberry is described in Section 3.4, comprising the simultaneous separation and identification of proanthocyanidins, anthocyanins, flavonoids and phenolic acids, whereas the complete composition on proanthocyanidins and stilbenoids of grapevine canes is presented in Section 3.5.

3.2. Characterization of grape seed procyanidins by comprehensive two-dimensional hydrophilic interaction × reversed phase liquid chromatography coupled to diode array detection and tandem mass spectrometry.

Montero, L., Herrero, M., Prodanov, M., Ibáñez, E., Cifuentes, A.

Analytical and Bioanalytical Chemistry 2013, *405*, 4627–4638.

Anal Bioanal Chem (2013) 405:4627–4638
DOI 10.1007/s00216-012-6567-5

ORIGINAL PAPER

Characterization of grape seed procyanidins by comprehensive two-dimensional hydrophilic interaction × reversed phase liquid chromatography coupled to diode array detection and tandem mass spectrometry

Lidia Montero · Miguel Herrero · Marin Prodanov · Elena Ibáñez · Alejandro Cifuentes

Received: 21 August 2012 / Revised: 15 October 2012 / Accepted: 12 November 2012 / Published online: 8 December 2012

Abstract In this work, the development and optimization of a new methodology to analyze grape seed procyanidins based on the application of two-dimensional comprehensive LC is presented. This two-dimensional method involves the use of a microbore column containing a diol stationary phase in the first dimension coupled to either a C_{18} partially porous short column or a C_{18} monolithic column in the second dimension. The orthogonal hydrophilic interaction × reversed phase liquid chromatography (HILIC×RP-LC) system is interfaced through a ten-port two-position switching valve. The optimized HILIC×RP-LC separation followed by diode array and tandem mass spectrometry detection (HILIC×RP-LC-DAD-MS/MS) made possible the direct analysis of a complex grape seed extract and allowed the tentative identification of 43 flavan-3-ols, including monomers and procyanidin oligomers till a polymerization degree of 7 units with different galloylation degrees. To the best of our knowledge, this is the first time that this powerful analytical technique is employed to characterize complex procyanidin samples. This work successfully demonstrates the great capabilities of the HILIC×RP-LC-DAD-MS/MS coupling for the direct analysis of very complex natural samples like grape seeds.

Keywords Flavan-3-ols · Grape seed procyanidins · HILIC · LC × LC · Mass spectrometry · Procyanidins · Two-dimensional comprehensive LC

Published in the topical collection *Nutraceuticals and Separations* with guest editor Luigi Mondello.

L. Montero · M. Herrero (✉) · E. Ibáñez · A. Cifuentes
Laboratory of Foodomics, Institute of Food Science Research (CIAL, CSIC-UAM), Nicolás Cabrera 9, Campus Cantoblanco, 28049 Madrid, Spain
e-mail: m.herrero@csic.es

M. Prodanov
Department of Production and Characterization of Novel Foods, Institute of Food Science Research (CIAL, CSIC-UAM), Nicolás Cabrera 9, Campus Cantoblanco, 28049 Madrid, Spain

Introduction

Flavan-3-ol polymers, more frequently known as proanthocyanidins or condensed tannins, are a complex group of phenolic compounds widely distributed in the plant kingdom and the second most abundant group of natural plant phenolic compounds after lignin [1]. This wide group of compounds is divided into different smaller categories depending on the monomers included in their composition [2]. The main group belongs to procyanidins, which are basically composed by catechin and epicatechin units, which are the largest class of proanthocyanidins [3]. Besides, monomeric forms esterified with gallic acid are also found in nature, such as catechin, epicatechin, gallocatechin, and epigallocatechin gallates. This fact makes even more complex the number of possible combinations for the different proanthocyanidins forms, increasing considerably the chemical diversity of these components and, therefore, the complexity of their analysis. Procyanidins are among the most common phenolic compounds in grapes, which can be found both in skins and seeds [4]. In fact, grape seeds are an important natural source of these components, although they exist in other important food sources, such as cocoa, apples, peanuts, or berries [5]. *Vitis vinifera* grape seed procyanidins

are particularly interesting because of their unlimited structural diversity based on the combination of only three elemental units, i.e., catechin, epicatechin, and epigallocatechin (Fig 1). This is due to the stereochemistry of the asymmetric carbons C_2 and C_3 of the flavan skeleton, the type of interflavan bond (C_4-C_8 and C_4-C_6, B-type procyanidins), the length of the polymer chain (degree of polymerization), the degree of galloylation, and the position of the gallic acid ester [6].

Grape procyanidins have a critical importance in winemaking as these compounds have been demonstrated to have a great contribution to the astringency of wines as well as to other organoleptic properties, such as improving color stability of red wines [7]. Besides, it has been suggested that the galloylation degree of the contained procyanidins could increase wine coarseness [8]. Nevertheless, the increasing interest on this class of compounds nowadays is mainly due to their important functional and bioactive activities, such as antioxidant, antibacterial [9], anti-inflammatory [10], or anti-cancer [11] effects. These important technological and biological properties have raised interest in developing new methods to analyze these compounds.

However, due to their huge chemical complexity and diversity, the analysis of procyanidins is very difficult and typically requires the use of a purification step before chromatographic separation followed by mass spectrometry (MS) to identify the multiple compounds present. Different strategies have been explored for their separation, being the most commonly applied reversed phase high-performance liquid chromatography (RP-LC). In this case, mainly C_{18} columns are employed, although the complete resolution of all the possible components present on this type of complex profiles is quite difficult to achieve, even using very lengthy gradient elutions (from 60 to 120 min) [12,13]. Besides, the elution order does not correspond to their polymerization degree [5]. Although this RP-LC mode could be well suited for monomers and oligomers, the separation of procyanidins with a degree of polymerization (DP) higher than 4 is usually not possible. In general, polymers with higher DP cannot be separated and coelute in a large unresolved peak. In order to partially solve this problem, other separation modes, such as normal phase LC, have been also employed. In this case, procyanidins can be separated according to their polymerization degree [5]. This approach has been also followed to separate procyanidins from grapes [14], among other food samples [15]. The NP approach has been shown to be useful to separate up to DP 10, for instance, to analyze procyanidins from cocoa and chocolate products [16,17] or different berries [18,19]. However, when the sample is more complex, as grape seeds, it is not possible to have proper resolution between peaks, due to the huge number of isomers and because the degree of galloylation of the polymers varies. Besides, all the compounds which present the same DP coelute. As an evolution of these latter methods, hydrophilic interaction LC (HILIC) has been also employed in order to overcome the problems related to the solvents needed in NP. HILIC acceptance is increasing in the last years because it enables to achieve separation similar to those obtained in NP using solvents compatible with RP [20]. The use of water in the mobile phase allows the formation of a water-enriched layer partially immobilized on the polar stationary phase. Subsequently, the separation is achieved, mainly, by partitioning between the organic-rich mobile phase and the water-enriched layer, although other interactions might also occur [21]. However, despite the development of different methods based on the use of these separation methods, the complete analysis of procyanidins still remains unresolved.

To avoid the lack of resolution provided by the mentioned monodimensional separation strategies, bidimensional approaches might be utilized. Comprehensive two-dimensional LC (LC×LC) is characterized by an enhanced resolving power, which can be very useful for the analysis of complex samples [22]. This technique has been already applied for the separation and characterization of different food-related complex matrices [23,24]. In LC×LC, the sample is subjected to two independent separation processes, so that different fractions from the first dimension are continuously transferred to the second dimension for further separation. This approach is far from being straightforward because multiple parameters have to be optimized [25–27]. For instance, very fast analyses are needed in the second dimension to be able to handle all the fractions coming from the first one, and consequently, very high flow rates should be employed. In order to keep the system backpressure under attainable conditions, two types of columns are typically employed in the second dimension in comprehensive two-dimensional LC systems: monolithic columns and partially porous columns. Monolithic columns are formed by a porous continuous gel with a porosity typically 15 % higher than a conventional packed columns. On the other hand, partially porous columns are packed with particles with 2.7 μm of diameter containing a solid core of 1.7 μm and a superficial porous section of 0.5 μm. These particles provide a decrease on analyte diffusivity into the column compared to conventional fully porous particles, allowing higher mass transfer rates and higher flow rates without compromising the column efficiency and generating significantly less backpressure. Two-dimensional LC in off-line mode has already been applied to the separation of procyanidins from apple and cocoa [28]. In that work, a first dimension HILIC separation was coupled to a RP-based separation in the second dimension. However, in the mentioned work, fractions eluting from the first dimension were collected and, later on, injected in a second dimension making the procedure lengthy and laborious.

The aim of the present work is to develop a new LC×LC method to automatically analyze grape seed procyanidins without any previous pretreatment. To do that, the performance of different HILIC and RP columns is tested and

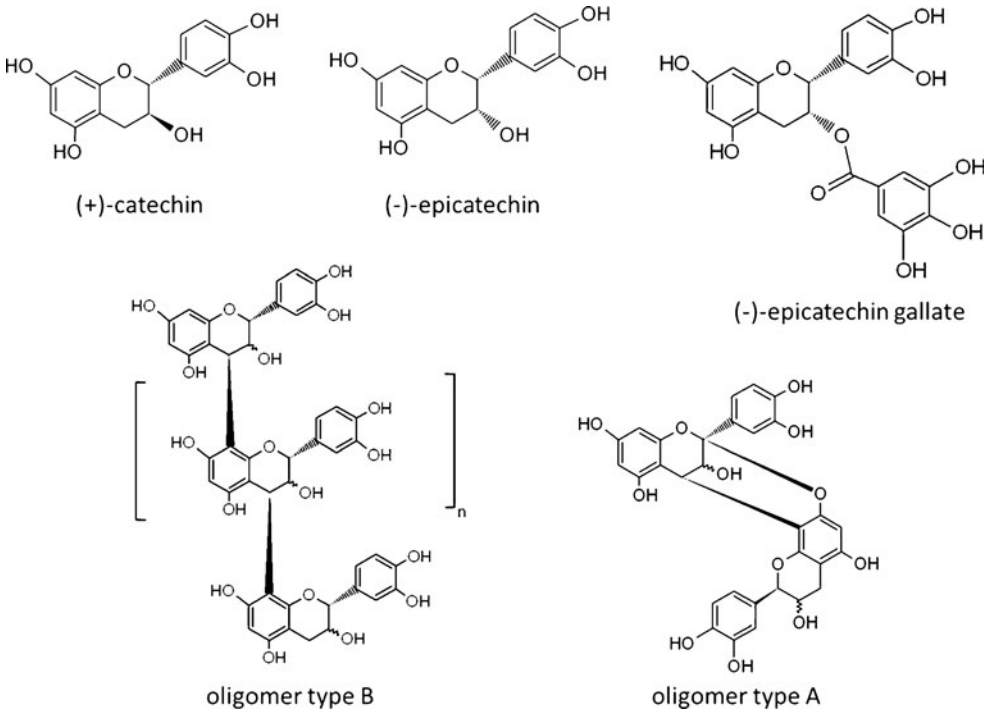

Fig. 1 Chemical structure of the main flavan-3-ols forming part of grape seed procyanidins

compared in both dimensions, and all the parameters involved in this challenging coupling closely studied. By using this novel LC×LC-DAD-MS/MS approach, it is possible to separate and identify 46 different phenolic compounds, mostly, grape seed procyanidins, in a single chromatographic run.

Experimental

Samples and chemicals

Grape seeds (*V. vinifera* L., cv. Malvar) were from the El Encín plantation (IMIDRA, Madrid, Spain). All the solvents employed (acetonitrile, methanol, and 2-propanol) were of HPLC-grade and acquired from Lab-Scan (Dublin, Ireland). Formic acid was supplied by Sigma-Aldrich (Madrid, Spain), whereas acetic acid was purchased from Scharlab (Barcelona, Spain). Water employed was Milli-Q grade obtained from a Millipore system (Billerica, MA). (+)-Catechin, (−)-epicatechin, ethyl gallate, and procyanidin B_1 reference samples were acquired from Extrasynthèse (Genay, France) and gallic acid from Scharlab (Barcelona, Spain).

Sample preparation

A fast and simple extraction protocol was followed for the extraction of proanthocyanidins from grape seeds [29]: briefly, 80 g of finely ground grape seeds was weighted and added to 90 mL of extraction solvent (methanol/water 80:20, *v*/*v*). The solution was sonicated for 15 min. Afterwards, the solution was left to stand protected from light for 2 h, and then, it was again sonicated for 15 min. The extract was centrifuged at 8,000 rpm for 20 min. The supernatant was recovered and filtered through 0.45-μm nylon syringe filters (Symta, Madrid, Spain). Lastly, after evaporation of methanol in a Rotavapor R-210 (Buchi Labortechnik AG, Flawil, Switzerland), the extract was lyophilized using a freeze-dryer (Labconco Corporation, MO). The extraction yield obtained after extraction was 2.75 % (dry weight basis).

For the LC×LC analysis of procyanidins, a 50-mg/mL solution of the dried extract was prepared in methanol and filtered (0.45 μm). Then, 300 μL of this solution was added to 700 μL ACN to obtain a 15-mg/ml solution which was filtered again (0.20 μm, Symta) and finally injected.

LC×LC instrumentation

Comprehensive two-dimensional LC analyses were carried out on an Agilent 1200 series liquid chromatograph (Agilent Technologies, Santa Clara, CA) equipped with a diode array detector and an autosampler. In order to have robust and reproducible low flow rates and gradients in the first dimension, a Protecol flow splitter (SGE Analytical Science, Milton Keynes, UK) was placed between the first dimension pumps and the autosampler. Besides, an additional LC pump (Agilent 1290 Infinity) was coupled to this instrument to perform the second dimension separation through an electronic controlled two-position ten-port switching valve. In addition, an Agilent 6320 Ion Trap mass spectrometer equipped with

an electrospray interface was coupled on-line and operated in negative ionization mode using the following conditions: dry temperature, 350 °C; mass range, *m/z* 90–2,200 Da; dry gas flow rate, 12 L/min; and nebulization pressure, 40 psi. The LC data were elaborated and visualized in two and three dimensions using LC Image software (version 1.0, Zoex Corp., Houston, TX).

LC×LC separation conditions

Different columns and conditions were tested for the optimization of the HILIC×RP separation of grape seed procyanidins. In the first dimension, a Syncronis HILIC column (250×2.1 mm, 5 μm d.p., Thermo Scientific, Waltham, MA) and a Lichrospher diol-5 (150×1.0 mm, 5 μm d.p., HiChrom, Reading, UK) column were tested. Under the optimum conditions, the diol column with a precolumn with the same stationary phase was employed using 15 μl/min as flow rate. The mobile phases employed were (A) acetonitrile/acetic acid (98:2, *v*/*v*) and (B) methanol/water/acetic acid (95:3:2, *v*/*v*/*v*) eluted according to the following gradient: 0 min, 0 % B; 5 min 20 % B; 10 min, 30 % B; 30 min, 50 % B; 40 min, 50 % B; 50 min, 80 % B; 75 min, 100 % B; 85 min, 100 % B. The injection volume was 20 μl.

In the second dimension separation, two different columns were tested. The optimum separation conditions were optimized separately. In first place, a partially porous column Ascentis Express C_{18} (50×4.6 mm, 2.7 μm d.p., Supelco, Bellefonte, CA) was employed. During the whole LC×LC separation, 1.3-min repetitive second dimension gradients were employed, being also 1.3 min the modulation time programmed in the switching valve. Water (0.1 % formic acid, A) and acetonitrile/methanol (50:50, *v*/*v*, B) were the mobile phases, using a repetitive gradient consisting of: 0 min, 0 % B; 0.1 min, 15 % B; 0.3 min, 25 % B; 1 min, 45 % B; 1.01 min, 0 % B. The flow rate was 3 mL/min.

The second column tested in the second dimension was a C_{18} monolithic column (100×4.6 mm, Onyx C_{18}, Phenomenex, Torrance, CA), and it was also eluted using 1.3-min repetitive gradients. Two different gradient profiles were employed throughout the analysis. During the first 52 min, the mobile phase employed consisted of water (0.1 % formic acid, A) and methanol (B) eluted according to the following gradient: 0 min, 0 % B; 0.1 min, 15 % B; 0.3 min, 25 % B; 1.0 min, 45 % B; 1.01 min, 0 % B. From minute 52 till the end of the analysis, the mobile phase composition was changed to water (0.1 % formic acid, A) and acetonitrile/methanol (B) using the following program: 0 min, 0 % B; 0.1 min, 15 % B; 0.3 min, 25 % B; 0.8 min, 45 % B; 0.9 min, 90 % B; 1.0 min, 0 % B. In this case, the flow rate was 4 mL/min.

In all cases, 280 nm was the wavelength used to monitor the separations, although UV–vis spectra were collected from 190–550 nm using a sampling rate of 20 Hz in the diode array detector. The MS was operated under negative ESI mode. The flow eluting from the second dimension column was splitted before the MS instrument, introducing approximately 600 μL/min into the MS detector.

Results and discussion

The coupling of a HILIC column in the first dimension to a RP-LC column in the second dimension to separate grape procyanidins by LC×LC is, theoretically, a promising alternative. However, this coupling is far from being straightforward due to numerous technical difficulties that arise during the method development [30]. For this reason, an initial individual optimization of the two intended dimensions was carried out. Once the preliminary conditions were independently obtained for both columns, their coupling was set up and fine-tuned, as well as the electrospray conditions prior to MS analysis. Data from DAD and MS were combined to chemically characterize the grape seed sample studied.

Optimization of the first dimension separation

To achieve a proper LC×LC separation of procyanidins, it was decided to employ a HILIC column in the first dimension in order to obtain a first distribution of the grape seed components according to their increasing DP. This novel approach would allow the coupling to a RP-based second dimension avoiding problems related to solvent immiscibility. Nevertheless, as in every comprehensive multidimensional system, some requirements should be met in order to have a good coupling depending on the chosen configuration. One of the most successful multidimensional approaches is to use a switching valve as interface between dimensions equipped with two identical sample loops to transfer the fractions collected from the first dimension to the second dimension [24]. This setup was chosen in this work. In this kind of systems, the first dimension separation has to be carried out at very low flow rates so that enough time is allowed to fill one of the loops while the fraction previously collected in the other loop is being analyzed in a fast second dimension. For this reason, the optimization of the first dimension separation implies great difficulties, mainly related to the proper distribution of wide peaks throughout the chromatogram and the effective translation of the gradient program to the column at those very low flow rates. In this sense, obviously, the nature of the column employed is of great importance as it will influence how the components of the sample will interact with the whole chromatography system during the analysis. To achieve the separation of the procyanidins present in the grape seed

sample studied, two different columns were tested from the wide group of stationary phases available to carry out HILIC separations [31], a silica column and a bonded diol column. Different mobile phases and elution gradients were studied, always keeping a small proportion of water during the separation. In any case, the retention obtained in the silica column was stronger making very difficult the correct separation of the procyanidins under the desired conditions. The diol column offered better capabilities in this application, allowing a better separation and distribution of the different procyanidin oligomers during the first dimension analysis. The particular conditions were optimized by changing the mobile phases employed as well as the gradients and flow rates and also studying the influence of the sample solvent. This factor was shown to have a critical importance on the separation. In fact, at the beginning of the optimization, the sample was injected dissolved in methanol, which is a good solvent to dissolve the procyanidins' oligomers and polymers. However, considering the narrow dimensions of the column employed (150×1.0 mm), the introduction of the sample in methanol, with higher eluotropic power than the acetonitrile-rich initial mobile phase (under HILIC conditions), prevented the separation as the components of the sample did not have enough time to interact with the stationary phase and eluted practically unretained. For this reason, the sample was firstly prepared more concentrated in methanol and then diluted in acetonitrile (to maintain the same concentration). This change modified completely the behavior of the chromatographic process allowing the separation of the different components. In Fig 2, a typical first dimension chromatogram obtained under optimum conditions is shown. As it can be observed, flavan-3-ols were grouped and distributed along the analysis according to their different DP, as it was expected. In fact, this behavior has been previously observed in other applications in which this type of stationary phase was used just in one dimension [1,17,19].The flow rate employed was 15 μl/min. This flow rate was selected as it was low enough to permit the transfer of a relatively low volume of the first dimension eluate to the second dimension separation.

Optimization of the second dimension separation

The second dimension separation conditions should allow the fast separation of the components present on each fraction of the first dimension transferred. The length of the second dimension analysis directly influences the volume being transferred in each fraction as each first dimension fraction cannot be transferred until the second dimension analysis is not finished and the second dimension column is prepared. For this reason, 20 μl was the fraction volume targeted from the beginning of the second dimension optimization, to keep a reasonable injection volume in these analyses. This fact is interesting because even if the solvents employed in both dimensions of a HILIC×RP coupling are compatible, the strength of the solvents relative to the two different stationary phases brings about an important problem. Indeed, the stronger solvent in the first dimension will be the weaker one in the second dimension and vice versa. Considering the flow rate employed in the first dimension (15 μl/min), ca. 1.3 min was available for the separation and re-equilibration of the second dimension column after injecting the mentioned 20 μl from the first dimension. Thus, very fast analyses are needed, and consequently, very high flow rates should be employed. In order to keep the system backpressure under attainable conditions, two types of columns have been mainly employed in the second dimension in comprehensive LC systems: monolithic columns and partially porous columns. In this work, both types of columns with C_{18} stationary phases were studied carrying out a preliminary optimization of the separation conditions for each column injecting 20 μl of the whole sample. Different mobile phases (acetonitrile, methanol, acetonitrile/methanol 80:20, *v*/*v*, and acetonitrile/2-propanol 80:20, *v*/*v*), flow rates (2–4 ml/min), gradients, and temperatures (30–55 °C) were tested. According to the obtained results, mobile phases composed by (A) water (0.1 % formic acid) and (B) acetonitrile/methanol eluted at 3 ml/min were selected for the partially porous column, whereas (A) water (0.1 % formic acid) and (B) methanol eluted at 4 ml/min were chosen for the monolithic column. The gradients employed are described in the "Experimental" section. The separation temperature did not influence significantly the separation, and only slight decreases on the system backpressure were observed. For this reason, 30 °C was selected as the separation temperature. At the optimum analysis conditions, the backpressures observed were under the instrument working interval, ranging from 150 to 320 bar for the monolithic and partially porous columns, respectively. Using both sets of conditions, it was possible to accomplish the second dimension separation in 1.3 min, including the time for column reconditioning. Therefore, this time could be selected as modulation time. To this time corresponds the transfer of a volume of 19.5 μl of eluate from the first dimension. In this regard, it is important to note that although the sample solvent has great importance on the analysis obtained in the second dimension, as it can be observed in Fig 3a, in LC×LC the second dimension injection solvent cannot be selected as it is imposed by the fractions eluting from the first dimension. Consequently, in the present HILIC×RP approach, 19.5 μl of a strong solvent is injected in the second dimension, which deteriorates the separation obtained. To partially solve this problem, the use of loops in the switching valve with different internal diameter was studied. The idea was to take advantage of the miscibility of the solvents employed in HILIC and RP modes to dissolve the first dimension fraction in the second dimension mobile phase in order to avoid the problems

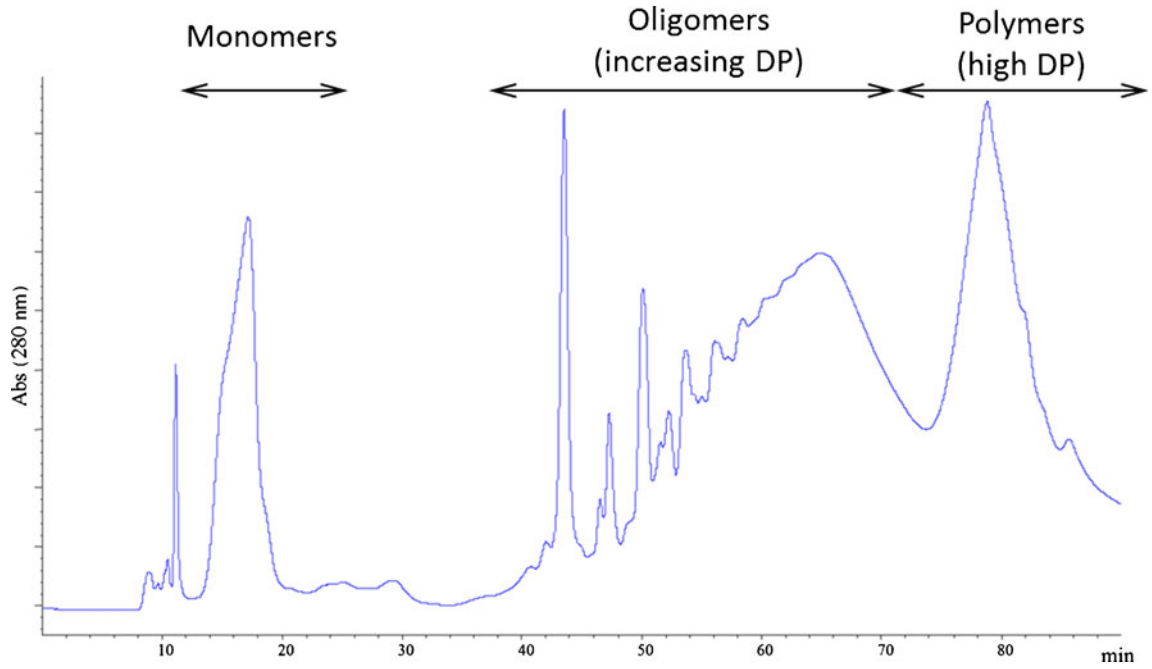

Fig. 2 HILIC chromatogram (280 nm) of a grape seed procyanidins' extract obtained under the optimum first dimension separation conditions using a microbore column (diol stationary phase, 150×1.0 mm, 5 μm). *DP* degree of polymerization

generated by solvent incompatibility. As it is shown in Fig 3b, loops with internal volumes of 20, 30, and 50 μl were tested. It was observed that by using a 30-μl loop, the separation was significantly improved, and at the same time, the volume of injection in the second dimension was kept as low as possible.

Overall HILIC×RPLC-DAD-MS optimization

Under the conditions optimized for each dimension, the negative effect of the differential HILIC and RP solvent strength was successfully solved. Thus, HILIC×RP-LC separations of grape seed procyanidins were carried out using the best conditions for the combinations diol×partially porous columns and diol×monolithic columns. In both cases, the modulation time was 1.3 min corresponding, as mentioned, to 19.5 μl of first dimension eluate being transferred each time and diluted in the second dimension mobile phase up to 30 μl that corresponds to the internal volume of the loop installed on the switching valve. As it can be observed in Figs. 4 and 5, good separations of most of the compounds included in this complex sample were attained. In order to try to improve the separation and ionization yield

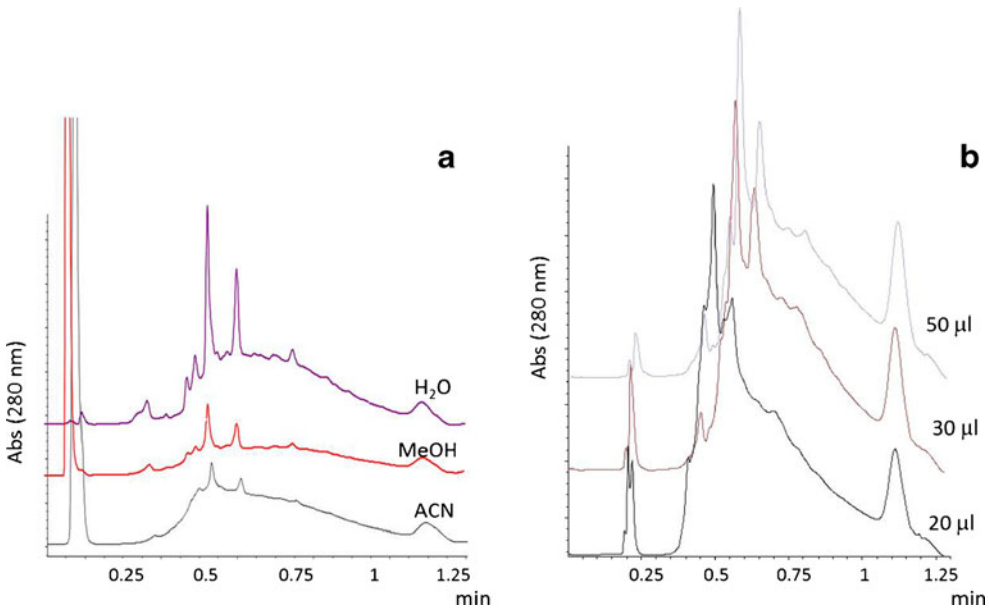

Fig. 3 **a** Effect of the sample solvent on a 2D separation using the partially porous column, and **b** effect of the use of loops with different internal volume installed in the switching valve maintaining 19.5 μl as first dimension transfer volume

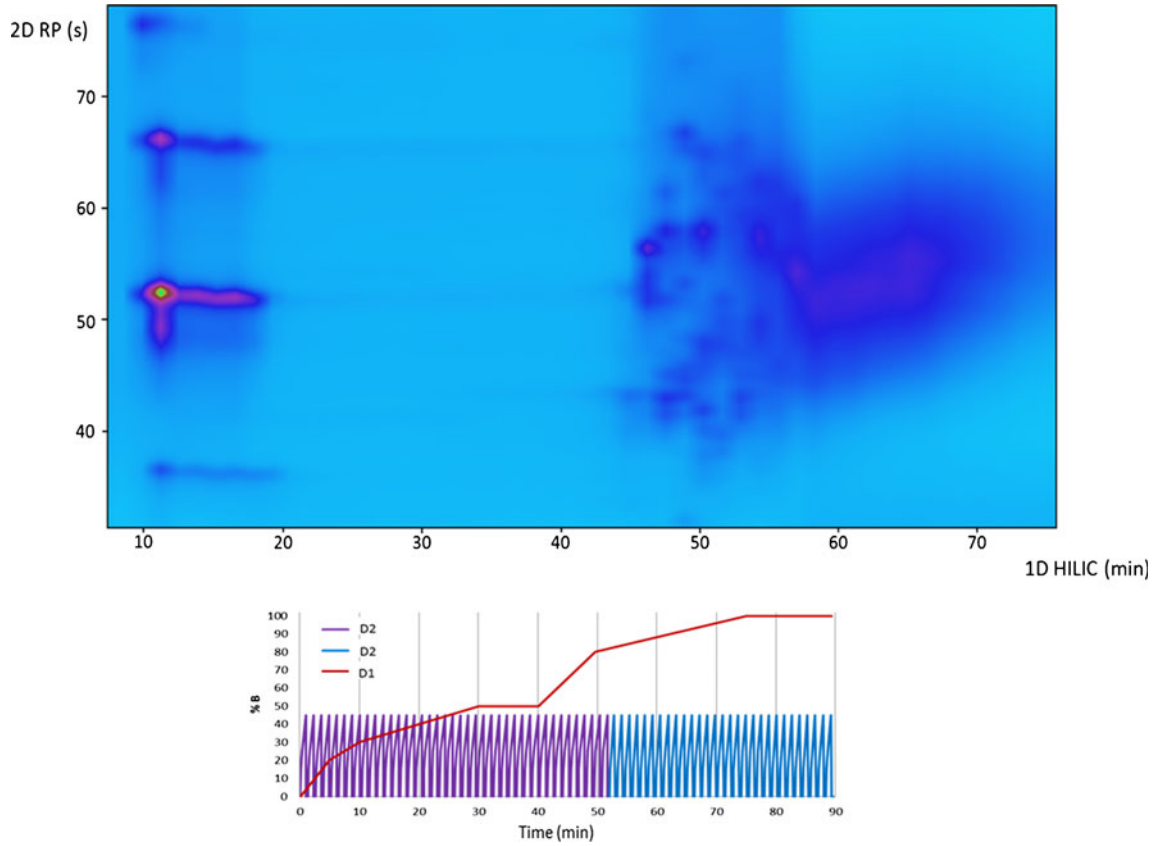

Fig. 4 Two-dimensional HILIC×RP plot (280 nm) of the separation of grape seed procyanidins using a monolithic column in the second dimension. Scheme of the gradients employed during the analysis in both dimensions. *D1*, (A) acetonitrile/acetic acid (98:2, *v*/*v*) and (B) methanol/water/acetic acid (95:3:2, *v*/*v*/*v*); *D2 purple line*, (A) water (0.1 % formic acid) and (B) methanol; *D2 red line*, (A) water (0.1 % formic acid) and (B) acetonitrile/methanol (50:50, *v*/*v*)

in the electrospray of the studied compounds (mainly focusing on those eluting at the end of the first dimension separation, i.e., procyanidins with higher DP), different gradients and mobile phases were tested. In the case of the

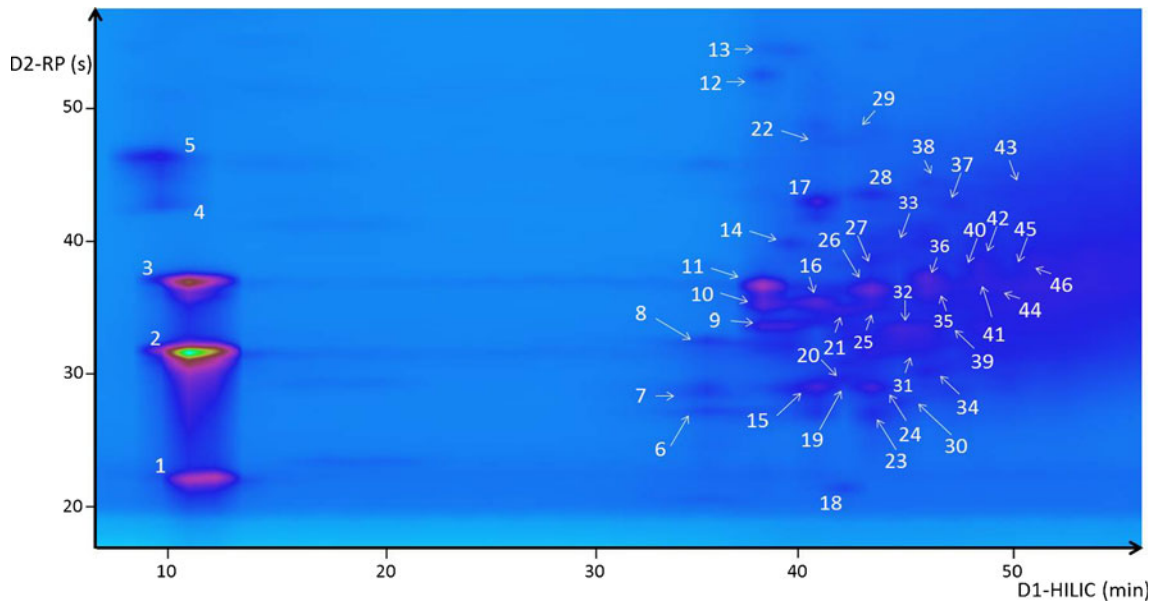

Fig. 5 Two-dimensional HILIC×RP plot (280 nm) of grape seed procyanidins separated using a partially porous column in the second dimension. For peak identification, see Table 1

partially porous column, no significant improvement was observed when the gradient was modified from minute 52. On the other hand, a slight improvement was attained for the monolithic column changing the composition of the mobile phases in this last part of the analysis, above all, regarding the ionization of these components. Thus, after this optimization, when using the monolithic column in the second dimension, water (0.1 % formic acid) and methanol were employed as mobile phases during the first 52 min, while water (0.1 % formic acid) and acetonitrile/methanol were used for the rest of the analysis. Besides, the gradient was also slightly modified, as can be observed in Fig. 4.

Concerning the MS detection of these components, negative ESI ionization was employed as this mode is widely considered as the most suitable to obtain a high response for flavan-3-ols [5]. The particular ionization parameters, namely, dry temperature, dry gas flow rate, and nebulization pressure, were adapted to the second dimension flow rate splitted and introduced into the MS.

It is important to note that the procyanidin polymers with higher DP were not completely resolved. In this sense, although those polymers were eluted at the end of the first dimension analysis, the extremely fast second dimension analyses needed to perform LC×LC did not provide the conditions required to have these compounds properly separated. Nevertheless, it has to be also remarked that procyanidin polymers with DP>4 have not been fully resolved by monodimensional RP [32]. On the other hand, compared to NP procyanidin separations, polymers up to DP 10 could be separated using similar analysis times, although no separation and identification of the compounds possessing the same DP could be obtained using that approach [17]. Instead, compounds are just grouped by DP. Thus, the application of the methodology developed in this work implies a clear and significant improvement over the previously published analytical methods either based on the application of NP or RP.

To proceed with the exhaustive characterization of the natural food sample, the use of the partially porous column in the second dimension was selected as this set of columns allowed using less amount of solvents compared to the set of columns including the monolithic column. Using the optimized method, the peak capacity of the system was studied according to Neue [33]:

$$n_c = 1 + \frac{t_g}{(1/n)\sum_1^n w}$$

where, n is the number of components employed to make the calculations, t_g is the gradient time, and w is the average peak width. Theoretical peak capacity of the separation, assuming that the total peak capacity of the two-dimensional system, n_{c2D}, will be the product of the two independent peak capacities values ($n_{c2D}={}^1n_c \times {}^2n_c$), is 1,435, considering that ${}^1n_c=41$ and ${}^2n_c=35$. As usual, this value assumes that the entire two-dimensional plane might be occupied by peaks, which is not really the case. For this reason, other approaches have been developed to obtain more realistic peak capacity values. Following the equation developed by Li et al. [34], a value of effective peak capacity equal to 875 is obtained:

$$n_{c2D} = \frac{{}^1n_c\,{}^2n_c}{\sqrt{1 + 3.35\left(\frac{{}^2t_c\,{}^1n_c}{{}^1t_g}\right)^2}}$$

This equation takes into account the second dimension time cycle (${}^2t_c$, equal to modulation time in this case, 1.3 min) as well as the influence of undersampling of the first dimension.

In any case, this value clearly shows the extremely high potential and enhanced separation power of the developed method and its application to complex real samples. Besides, it is important to remark the low correlation obtained between the retention mechanisms employed in both dimensions, as it can be clearly appreciated in Figs 4 and 5, thus, assuring high orthogonality.

Characterization of grape seed procyanidins by HILIC×RP-LC-DAD-MS/MS

The development of this HILIC×RP method allowed the comprehensive two-dimensional analysis of procyanidins for the first time. The tentative identification of the separated compounds was carried out combining the information from the two detectors employed, DAD and MS detectors. In Table 1, the data corresponding to the separated compounds as well as their tentative identification are presented. In Fig 5, the two-dimensional chromatogram obtained for the grape seed procyanidins analyzed under optimum conditions is also shown. As it can be observed, the compounds were mainly grouped according to their molecular mass, firstly eluting the monomers and then the different oligomers according to their increasing DP and increasing degree of galoylation (for the same DP) with respect to the first dimension separation.

Although two different detectors were employed, it is important to remark that the UV–vis spectra of the different grape seeds procyanidins were quite similar, thus, not allowing the differentiation among them. Therefore, the information from the MS detector was decisive in order to provide a tentative identification of each separated compound. The first identified compounds were the monomers catechin and epicatechin. Both compounds provided molecular ions with m/z 289 ($[M\text{-}H]^-$). The fragmentation of those ions generated ions at m/z 245 as a result of loss of CO_2. By comparing with commercial standards, peaks 2 and 3 could

Table 1 Main procyanidins tentatively identified on grape seed using the optimized HILIC×RPLC-DAD-MS/MS methodology

Peak	Identification	Total t_R (min)	D2t_R (s)[a]	$[M-H]^-$	$[M-2H]^{2-}$	Main fragments
1	Not identified	10.77	22.2±0.0	418.2		373, 289, 127
2	Catechin	10.92	31.7±0.2	289.7		245
3	Epicatechin	11.02	36.9±0.1	289.3		245
4	Gallic acid ethyl ester	9.81	42.6±0.8	197.0		
5	Not identified	9.87	46.3±0.4	573.3		525, 377, 329, 195
6	Procyanidin dimer	35.55	26.9±0.1	577.3		469, 425
7	Procyanidin dimer	35.58	28.7±0.0	577.8		469, 425
8	Procyanidin dimer	35.65	32.4±0.7	577.3		469, 425
9	Procyanidin trimer	38.26	33.8±0.7	865.3		739, 577
10	Procyanidin dimer monogallate	38.29	35.3±0.3	729.7		577, 559, 407
11	Procyanidin dimer monogallate	38.31	36.7±0.5	729.7		577, 559
12	Procyanidin dimer monogallate	38.58	52.5±1.2	729.2		577, 559, 441
13	Procyanidin dimer monogallate	38.61	54.7±0.8	729.2		577, 559, 441, 407, 289
14	Procyanidin dimer digallate	39.67	39.8±0.4	881.2		729
15	Procyanidin trimer	40.78	28.9±0.3	865.5		739
16	Procyanidin trimer	40.89	35.3±0.5	865.5		739
17	Procyanidin trimer monogallate	41.02	43.0±0.5	1,017.3		891, 847, 729, 577, 441
18	Procyanidin trimer	41.96	21.4±0.0	865.3		739, 695, 577
19	Procyanidin trimer monogallate	42.10	29.9±0.6	1,017.4		729, 865, 999, 577
20	Procyanidin tetramer	42.12	30.9±0.8	1,153		
21	Procyanidin trimer digallate	42.18	35.0±0.5		584.5	999, 880, 1,017, 865, 729
22	Procyanidin trimer monogallate	42.39	47.5±0.2	1,017		
23	Procyanidin tetramer	43.35	26.9±0.5	1,153.5		1,027, 983, 865, 739, 575, 403
24	Procyanidin tetramer	43.38	29.1±0.5		576.7	1,027, 863, 739, 577
25	Procyanidin tetramer	43.48	34.7±0.0	1,153.4		1,027, 983, 865, 739, 575
26	Procyanidin tetramer	43.50	36.2±0.2	1,153.4		1,027, 983, 865, 739, 575
27	Procyanidin tetramer monogallate	43.54	38.5±0.4		652.3	1,179, 1,017, 863, 729, 575
28	Procyanidin tetramer monogallate	43.63	43.7±0.2		652.4	1,179, 1,017, 863, 729, 575
29	Procyanidin tetramer monogallate	43.71	48.4±0.6		652.4	1,179, 1,017, 863, 729, 575
30	Procyanidin tetramer monogallate	44.67	28.0±1.5	1,305.4		
31	Procyanidin tetramer monogallate	44.72	31.4±1.3	1,305.4		
32	Procyanidin pentamer	44.76	33.3±0.2		720.7	1,316, 1,153, 1,027, 863, 729, 577
33	Procyanidin pentamer	44.86	39.4±0.1		720.9	1,316, 1,153, 1,027, 865, 577
34	Procyanidin pentamer	46.01	30.3±1.2		720.8	1,316, 1,153, 1,027, 863, 577
35	Procyanidin pentamer	46.10	35.7±0.7	1,441.5		
36	Procyanidin tetramer digallate	46.13	37.5±0.3		728.5	1,331, 1,169, 1,017, 879, 719, 575
37	Procyanidin pentamer	46.22	43.1±0.1		720.6	1,315, 1,153, 1,027, 863, 577, 441
38	Procyanidin pentamer monogallate	46.24	44.6±0.2		796.4	1,468, 1,304, 1,179, 1,017, 863, 575
39	Procyanidin pentamer	47.31	30.8±1.2	1,141.4		
40	Procyanidin pentamer digallate	47.41	36.6±1.4		872.5	1,575, 1,458, 1,303, 575
41	Procyanidin pentamer digallate	48.65	33.1±2.0		872.6	1,457, 1,327, 1,169, 1,017, 575
42	Procyanidin pentamer digallate	48.72	37.4±1.2		872.7	1,576, 1,457, 1,169, 1,017, 729
43	Procyanidin hexamer monogallate	48.86	45.7±0.6		940.8	
44	Procyanidin hexamer	49.93	31.9±2.8		864.7	1,441, 1,314, 1,151, 575
45	Procyanidin hexamer monogallate	50.01	36.5±2.4		940.8	1,593, 1,441, 1,303, 1,152, 864, 739
46	Procyanidin heptamer	51.32	37.2±2.2		1,008.4	

Peaks as shown in Fig. 5

[a] Mean(s)±SD

be identified as catechin and epicatechin, respectively. Other compounds were detected in the area in which these monomers eluted; peak 1 produced an ion at *m/z* 418.2 ([M-H]$^-$) whose fragmentation generated ions at *m/z* 373, 289, and 127. Peak 4 was tentatively identified as gallic acid ethyl ester, according to its UV–vis spectrum (very similar to that of gallic acid) and the molecular ion detected (*m/z* 197.0, [M-H]$^-$). Different ions at *m/z* 577 ([M-H]$^-$) were detected corresponding to peaks 6, 7, and 8. The fragmentation pattern of these three compounds was the same (see Table 1) giving prominent fragments at *m/z* 469 and 425. These latter fragments would be theoretically formed through a retro-Diels-Alder mechanism ([M-H-152]$^-$) [32] from a procyanidin dimer structure. Thus, according to this information, these peaks were assigned to procyanidin dimers.

Ions with *m/z* of 865 (peaks 9, 15, 16, and 18) were assigned to procyanidins trimers. The fragments derived from these ions consisted on *m/z* 739 and 577, corresponding probably to the loss of a phloroglucinol unit and to the loss of a (epi)catechin molecule, respectively. These fragments have been previously observed in procyanidin trimers [5]. On the other hand, compounds with *m/z* 729 ([M-H]$^-$) generated fragments at *m/z* 577, 559, 441, 407, and 289. The fragments with *m/z* 577 corresponded to the loss of the galloyl group, whereas the fragments at *m/z* 559 would be formed as a result of the subsequent loss of a water molecule. The fragments with *m/z* 441 and 289 were detected as a result of the loss of a (epi)catechin unit and its detection, respectively. The ion at *m/z* 407 would correspond to the loss of water from a fragment formed through a retro-Diels-Alder mechanism from the *m/z* 577 ion. Consequently, these components (peaks 10–13) were tentatively identified as procyanidin dimer monogallates. Besides, a single peak eluting among these components with *m/z* 881.2 ([M-H]$^-$) was detected (peak 14). This compound was assigned to a procyanidin dimer digallate according to the fragment at *m/z* 729 detected after its MS/MS analysis.

Peaks 17, 19, and 22 were tentatively assigned to procyanidin trimer monogallates. The detection of molecular ions ([M-H]$^-$) at *m/z* 1,017 together with the presence of fragments at *m/z* 729 (loss of a (epi)catechin unit), 865 (loss of galloyl group), 577 (loss of a (epi)catechin unit with a galloyl group), and 891 allowed the identification. These fragment ions have been described as common fragments

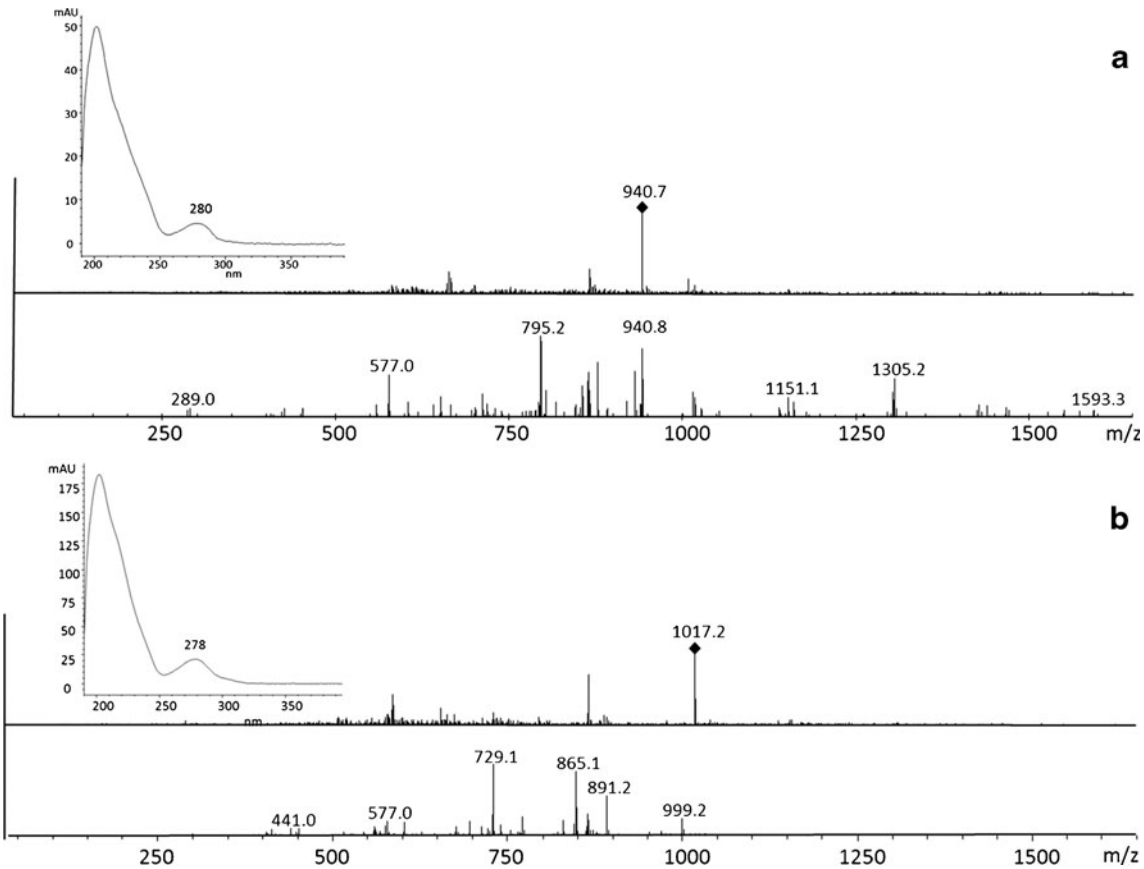

Fig. 6 UV–vis and MS spectra of a procyanidin hexamer monogallate (**a**) and a procyanidin trimer monogallate (**b**). Main detected fragments at *m/z* 940.7 ([M-2H]$^{2-}$): *m/z* 1,593 ([M-H-(epi)catechin]$^-$), *m/z* 1,305 ([M-H-2(epicatechin)]$^-$), *m/z* 1,153 ([M-H-2(epicatechin)-phloroglucinol]$^-$), *m/z* 577 (dimer), *m/z* 289 ((epi)catechin). Main detected fragments of *m/z* 1,017.2 ([M-H]$^-$): *m/z* 865 (([M-H-phloroglucinol]$^-$), *m/z* 729 (([M-H-(epi)catechin]$^-$), *m/z* 577 (dimer)

resulting from these compounds [5]. In Fig. 6b, a typical fragmentation pattern for these compounds is shown. Besides, a doubly-charged ion ($[M\text{-}2H]^{2-}$) with *m/z* 584.5 was also detected. The MS/MS analysis of this compound (peak 21) allowed the detection of fragment ions closely related to loses of galloyl moieties (*m/z* 1,017 and 999), (epi)catechin units (*m/z* 880) and both (*m/z* 729). Consequently, peak 21 was assigned to a procyanidin trimer digallate.

Several procyanidin tetramers and procyanidin tetramer monogallates were found. Procyanidin tetramers were detected either as single-charged ions ($[M\text{-}H]^-$) *m/z* 1,153 (peaks 20, 23, 25, and 26) or doubly-charged ions (*m/z* 576.7, peak 24). In any case, the fragmentation pattern was quite similar producing fragments at *m/z* 1,027 (loss of phloroglucinol unit), 865 (loss of (epi)catechin), 575 (loss of two (epi)catechin units) as well as other typical fragments (*m/z* 739, 403). Likewise, procyanidin tetramer monogallates (peaks 27–31) were mostly detected as doubly-charged ions ($[M\text{-}2H]^{2-}$) at *m/z* 652, although the detection of singly-charged ions was also possible with *m/z* 1,305.4 ($[M\text{-}H]^-$). Moreover, a procyanidin tetramer digallate was also detected as $[M\text{-}2H]^{2-}$ with *m/z* 728.5 (peak 36). The fragments found corresponding to losses similar to those already described confirmed the identification of all these procyanidin tetramers.

The procyanidins with DP 5 detected included pentamers (peaks 32–35, 37, and 39), a procyanidin pentamer monogallate (peak 38) and procyanidin pentamer digallates (peaks 40–42). All these components were detected as doubly-charged ions, with the exception of two procyanidin pentamers that were detected as $[M\text{-}H]^-$ with *m/z* 1,141.5. Concerning the procyanidin pentamers' fragmentation pattern, several fragment ions which confirmed the identification were detected; among them, fragments with *m/z* 1,315 corresponding to a phloroglucinol unit loss, *m/z* 1,153 (matching with a (epi)catechin loss), *m/z* 1,027 (equivalent to a (epi)catechin with a phoroglucinol unit loss), *m/z* 863 (corresponding to the loss of two (epi)catechin units), and *m/z* 577 (matching the loss of three (epi)catechin units). Ions with *m/z* 796.4 and 872.5 were assigned to procyanidin pentamer monogallates and digallates ($[M\text{-}2H]^{2-}$) and presented typical procyanidin oligomer fragments that confirmed the identification.

Lastly, the highest DP compounds identified corresponded to procyanidin hexamer (peak 44, m/z 864.7), procyanidin hexamer monogallates (peaks 43 and 45, m/z 940.8, see Fig 6) and procyanidin heptamer (peak 46, m/z 1008.4) which were detected as doubly-charged ions. Their fragmentation patterns were consistent with those typical of procyanidin oligomers.

Thus, the application of this new two-dimensional comprehensive HILICxRP-LC-DAD-MS method to the analysis of procyanidins from grape seeds allowed the separation and tentative identification of 46 compounds, including gallic acid ethyl ester, catechin, epicatechin and 43 procyanidin oligomers with degree of polymerization of up to 7 and degree of galloylation of up to 2. Although the separation and identification of procyanidin dimers and some trimers is already established in the chromatographic practice, it is not the same with respect to the vast number of galloylated procyanidin oligomers; in fact, one of the most important contributions of the application of the developed two-dimensional method is the separation and tentative identification of 20 non-galloylated procyanidins with DP up to 7, 11 monogalloylated procyanidins with DP from 2 to 6 and 5 digalloylated procyanidins with DP 2 to 5 in a single chromatographic run. According to the best of our knowledge, just as much as 7 monogalloylated and one digalloylated procyanidin dimers and 3 monogalloylated and a digalloylated procyanidin trimers have been previously identified using a single one-dimensional RP-LC method [29,35].

Conclusions

In this work, the development of a new two-dimensional comprehensive HILIC×RP-LC-DAD-MS/MS method to analyze grape seed procyanidins is presented. This application included the use of a microbore column with diol stationary phase for the HILIC separation in the first dimension and either a C_{18} partially porous column or a C_{18} monolithic column to carry out the RP-LC separations in the second dimension. These combinations provided high orthogonality to the multidimensional system. The optimization of this methodology allowed the separation and tentative identification of 46 phenolic compounds including flavan-3-ol monomers (catechin and epicatechin) and procyanidin oligomers up to DP 7. To the best of our knowledge, this is the first time that an on-line two-dimensional comprehensive LC is applied to the separation of procyanidins in such a complex natural sample, like grape seeds. This work also opens new possibilities to the analysis of such complex compounds as proanthocyanidins in other food and natural complex sources.

Acknowledgments M.H. would like to thank MICINN for his "Ramón y Cajal" research contract. The authors want to thank Projects AGL2011-29857-C03-01 and CONSOLIDER INGENIO 2010 CSD2007-00063 FUN-C-FOOD (Ministerio de Educación y Ciencia) for the financial support.

References

1. Kelm MA, Johnson JC, Robbins RJ, Hammerstone JF, Schmitz HH (2006) High performance liquid chromatography separation and purification of cacao (*Theobroma cacao* L.) procyanidins according to degree of polymerization using diol stationary phase. J Agric Food Chem 54:1571–1576

2. Aron PM, Kennedy JA (2008) Flavan-3-ols: nature, occurrence and biological activity. Mol Nutr Food Res 52:79–104
3. Sarnoski PJ, Johnson JV, Reed KA, Tanko JM, O'Keefe SF (2012) Separation and characterization of proanthocyanidins in Virginia type peanut skins by LC-MS^n. Food Chem 131:927–939
4. Hayasaka Y, Waters EJ, Cheynier V, Herderich MJ, Vidal S (2003) Characterization of proanthocyanidins in grape seeds using electrospray mass spectrometry. Rapid Commun Mass Spectrom 17:9–16
5. Valls J, Millan S, Marti MP, Borras E, Arola L (2009) Advanced separation methods of food anthocyanins, isoflavones and flavonols. J Chromatogr A 1216:7143–7172
6. Santos-Buelga C, García-Viguera C, Tomás-Barberán FA (2003) In: Santos-Buelga C, Williamson G (eds) Methods in polyphenol analysis. The Royal Society of Chemistry, Cambridge
7. Monagas M, Gomez-Cordoves C, Bartolome B, Laureano O, Da Silva JMR (2003) Monomeric, oligomeric and polymeric flavan-3-ol composition of wines and grapes from *Vitis vinifera* L. Cv. Graciano, Tempranillo and Cabernet Sauvignon. J Agric Food Chem 51:6475–6481
8. Vidal S, Francis L, Guyot S, Marnet N, Kwiatkowski M, Gawel R, Cheynier V, Waters EJ (2003) The mouth-feel properties of grape and apple proanthocyanidins in a wine-like medium. J Sci Food Agric 83:564–573
9. Yu J, Ahmedna M, Goktepe I (2010) Potential of peanut skin phenolic extract as antioxidative and antibacterial agent in cooked and raw ground beef. Int J Food Sci Technol 45:1337–1344
10. Pallares V, Calay D, Cedo L, Castell-Auvi A, Raes M, Pinent M, Ardevol A, Arola L, Blay M (2012) Additive, antagonistic and synergistic effects of procyanidins and polyunsaturated fatty acids over inflammation in RAW 264.7 macrophages activated by lipopolysaccharide. Nutrition 28:447–457
11. Dinicola S, Cucina A, Pasqualato A, D'Anselmi F, Proietti S, Lisi E, Pasqua G, Antonacci D, Bizzarri M (2012) Antiproliferative and apoptocic effects triggered by grape seed extracts (GSE) versus epigallocatechin and procyanidins on colon cancer cell lines. Int J Mol Sci 13:651–664
12. Bartolomé B, Hernandez T, Bengoechea ML, Quesada C, Gomez-Cordovés C, Estrella I (1996) Determination of some structural features of procyanidins and related compounds by photodiode-array detection. J Chromatogr A 723:19–26
13. Peng Z, Hayasaka Y, Iland PC, Sefton M, Høj P, Waters EJ (2001) Quantitative analysis of polymeric procyanidins (tannins) from grape (*Vitis vinifera*) seeds by reverse phase high-performance liquid chromatography. J Agric Food Chem 49:26–31
14. Hellstrom JK, Mattila PH (2008) HPLC determination of extractable and unextractable proanthocyanidins in plant materials. J Agric Food Chem 56:7617–7624
15. Counet C, Ouwerx C, Rosoux D, Collin S (2004) Relationships between procyanidin and flavor contents of cocoa liquor from different origins. J Agric Food Chem 52:6243–6249
16. Robbins R, Leonczak J, Li J, Johnson JC, Collins T, Kwik-Uribe C, Schmitz HH (2012) Determination of flavanol and procyanidin (by degree of polymerization 1–10) content of chocolate, cocoa liquors, powders and cocoa flavanol extracts by normal phase high-performance liquid chromatography: collaborative study. J AOAC Int 95:1153–1160
17. Robbins R, Leonczak J, Johnson JC, Li J, Kwik-Uribe C, Prior RL, Gu L (2009) Method performance and multi-laboratory assessment of a normal phase high pressure liquid chromatography–fluorescence detection method for the quantitation of flavanols and procyanidins in cocoa and chocolate containing samples. J Chromatogr A 1216:4831–4840
18. Prior RL, Lazarus SA, Gao G, Muccitelli H, Hammerstone JF (2001) Identification of procyanidins and anthocyanins in blueberries and cranberries (*Vaccinium* spp.) using high-performance liquid chromatography/mass spectrometry. J Agric Food Chem 49:1270–1276
19. Khanal RC, Howard LR, Prior RL (2009) Procyanidin composition of selected fruits and fruit by-products affected by extraction method and variety. J Agric Food Chem 57:8839–8843
20. Buszewski B, Noga S (2012) Hydrophilic interaction liquid chromatography (HILIC)—a powerful separation technique. Anal Bioanal Chem 402:231–237
21. Greco G, Crosse S, Letzel T (2011) Study of the retention behavior in zwitterionic hydrophilic interaction chromatography of isomeric hydroxyl- and aminobenzoic acids. J Chromatogr A 1235:60–67
22. Stoll DR (2010) Recent progress in online, comprehensive two-dimensional high-performance liquid chromatography for non-proteomic applications. Anal Bioanal Chem 397:979–986
23. Herrero M, Ibañez E, Cifuentes A, Bernal J (2009) Multidimensional chromatography in food analysis. J Chromatogr A 1216:7110–7129
24. Dugo P, Cacciola F, Kumm T, Dugo G, Mondello L (2008) Comprehensive multidimensional liquid chromatography: theory and applications. J Chromatogr A 1184:353–368
25. Li X, Carr PW (2011) Effects of first dimension eluent composition in two-dimensional liquid chromatography. J Chromatogr A 1218:2214–2221
26. Groskreutz SR, Swenson MM, Secor LB, Stoll DR (2012) Selective comprehensive multi-dimensional separation for resolution enhancement in high performance liquid chromatography. Part I—principles and instrumentation. J Chromatogr A 1228:31–40
27. Donato P, Cacciola F, Tranchida PQ, Dugo P, Mondello L (2012) Mass spectrometry detection in comprehensive liquid chromatography: basic concepts, instrumental aspects, applications and trends. Mass Spectrom Rev 31:523–559
28. Kalili KM, de Villiers A (2009) Off-line comprehensive 2-dimensional hydrophilic interaction × reversed phase liquid chromatography analysis of procyanidins. J Chromatogr A 1216:6274–6284
29. Prodanov M, Vacas V, Hernández T, Estrella I (2010) In Polyphenols communications. A. Ageorges, V. Cheynier, P. Lefer and P. Sarni-Machado (eds.) vol. 2., pp. 592–593.
30. Bedani F, Schoenmakers PJ, Janssen HG (2012) Theories to support method development in comprehensive two-dimensional liquid chromatography—a review. J Sep Sci 35:1697–1711
31. Jandera P (2008) Stationary phases for hydrophilic interaction chromatography, their characterization and implementation into multidimensional chromatography concepts. J Sep Sci 31:1421–1437
32. Rockenbach II, Jungfer E, Ritter C, Santiago-Schübel B, Thiele B, Fett R, Galensa R (2012) Characterization of flavan-3-ols in seeds of grape pomace by CE, HPLC-DAD-MSn and LC-ESI-FTICR-MS. Food Res Int 48:848–855
33. Neue UD (2005) Theory of peak capacity in gradient elution. J Chromatogr A 1079:153–161
34. Li X, Stoll DR, Carr PW (2009) Equation for peak capacity estimation in two-dimensional liquid chromatography. Anal Chem 81:845–850
35. Santos-Buelga C, Francia-Aricha EM, Escribano-Bailón MT (1995) Comparative flavan-3-ol composition of seeds from different grape varieties. Food Chem 53:197–201

3.3. Profiling of phenolic compounds from different apple varieties using comprehensive two-dimensional liquid chromatography.

Montero, L., Herrero, M., E. Ibáñez, E., Cifuentes, A.

Journal of Chromatography A, 2013, *1313*, 275– 283

Journal of Chromatography A, 1313 (2013) 275–283

Contents lists available at ScienceDirect

Journal of Chromatography A

journal homepage: www.elsevier.com/locate/chroma

Profiling of phenolic compounds from different apple varieties using comprehensive two-dimensional liquid chromatography

Lidia Montero, Miguel Herrero*, Elena Ibáñez, Alejandro Cifuentes

Laboratory of Foodomics, Institute of Food Science Research (CIAL, CSIC), Nicolás Cabrera 9, Campus Cantoblanco, 28049 Madrid, Spain

ARTICLE INFO

Article history:
Available online 18 June 2013

Keywords:
Apple
Comprehensive LC
Flavonoids
LC × LC
Phenolic compounds
Procyanidins

ABSTRACT

An innovative analytical approach based on the use of comprehensive two-dimensional liquid chromatography (LC × LC) is applied to obtain the profiling of phenolic compounds in different apple varieties. The method combines the use of hydrophilic interaction liquid chromatography in the first dimension and a reversed phase separation in the second dimension, as well as the use of diode array and mass spectrometry detection. Using this methodology is possible to obtain in less than 50 min the complete profiling of phenolic compounds in a complex food matrix such as apple. In fact, different flavan-3-ols including procyanidin oligomers with degree of polymerization up to 8, as well as several dihydrochalcones, flavonols and a phenolic acid are separated and tentatively identified in these samples in a single run. Besides, the total phenols and total procyanidins amounts were determined using two in vitro assays. Reinette apples presented the highest content on total phenols (6.46 mg galic acid equiv./g dry matter) whereas Granny Smith apples were the richest on total procyanidins (0.73 mg epicatechin equiv./g dry matter). This work shows the great potential of LC × LC for phenolic compounds profiling in complex food samples.

1. Introduction

Natural phenolic compounds are receiving a lot of attention due to their potential beneficial health properties [1]. As a consequence, a great amount of research is being focused on the determination of this kind of compounds [2]. Although, the links between their consumption and the potential influence on health are still not completely understood [3], these effects can be investigated more in depth, i.e., at molecular level, via the recent foodomic approach, which is expected to provide more sounded evidences on the polyphenols bioactivity [4,5].

The profiling of phenolic compounds of a particular sample is usually a tough task, considering the enormous variability of chemical structures included within this wide group of metabolites [2]. Although LC is mainly used for the profiling of phenolic compounds in food-related samples, depending on the relative complexity of the analyzed sample this technique may lack separation power. In this regard, the use of multidimensional techniques significantly improves the separation capabilities compared to their one-dimensional counterparts [6]. Comprehensive two-dimensional liquid chromatography (LC × LC) takes advantage of the combination of two independent separation mechanisms to effectively improve the available resolving power as well as to produce a dramatic increase on peak capacity. To perform this kind of analyses, two different separation processes have to be coupled on-line, so that fractions of the first dimension (D1) eluate are continuously collected and injected into the second dimension (D2). This coupling is not easy, and different strategies have been already developed and applied to improve the hyphenation [7]. Ideally, the most advantageous approaches are composed by two dimensions in which different separation modes are combined, in order to enhance system orthogonality, maximizing the separation power. Due to its characteristics, LC × LC has potential for being a powerful tool for profiling studies, in which the complete composition on a particular class of compounds present on a food sample is studied.

Comprehensive LC has been already employed to analyze a variety of food samples [8,9], including the study of some phenolic compounds from juices [10,11], wines [12,13] and beer [14]. Nevertheless, the complex phenolic compounds pattern of apples has not yet been studied using this technique.

Apples are very rich in phenolic compounds of diverse chemical classes [15] and, up to now, it has not been possible to simultaneously determine the major phenolics present on apple belonging to these different subclasses. In this regard, different methods have been presented focused on the determination of procyanidin oligomers on this sample, using high-speed countercurrent chromatography (HSCCC) [16], size exclusion chromatography (SEC) [17], normal phase LC (NP-LC) [18] or even off-line two-dimensional LC [19]. However, these works were mainly focused on procyanidins, and no other phenolic compounds, also important in

* Corresponding author. Tel.: +34 910 017 946; fax: +34 910 017 905.
E-mail address: m.herrero@csic.es (M. Herrero).

0021-9673/$ – see front matter © 2013 Elsevier B.V. All rights reserved.
http://dx.doi.org/10.1016/j.chroma.2013.06.015

apples, were analyzed in the same run. On the other hand, to analyze other phenolic compounds RP-based approaches have been usually employed [20,21] and, although using these latter methods some procyanidins were also detected, these are just limited to dimers, not being possible the analysis of the whole procyanidin oligomers pattern. Consequently, the complete separation of all compounds of complex food samples like apple, is not attainable using conventional one-dimension LC; for this reason, other multidimensional approaches have been studied, particularly based on the coupling between hydrophilic interaction liquid chromatography (HILIC) and RP separations [22–25].

In this regard, we have recently developed a new HILIC × RP method to characterize grape seed procyanidins [22]; based on that work, in the present manuscript, the method is further optimized and expanded to the detection of several classes of phenolic components, other than procyanidins. The new method was applied to the profiling of phenolic compounds in five different apple varieties. Consequently, the aim of this work was the development of a LC × LC method able to analyze the whole profile of phenolic compounds present in apples, including procyanidin oligomers as well as other flavonoids and phenolic acids, in a single analytical run.

2. Materials and methods

2.1. Samples and chemicals

Five apples (*Malus domestica*) of different varieties (Red Starking, Kanzi, Royal Gala, Reinette and Granny Smith) were purchased in a local supermarket in Madrid, Spain.

Acetonitrile, methanol, and 2-propanol were of HPLC-grade and acquired from Lab-Scan (Dublin, Ireland). Formic acid, sodium carbonate, gallic acid, quercetin, phloridzin dihydrate and 4-dimethylamino cinnamaldehyde (DMAC) were supplied by Sigma–Aldrich (Madrid, Spain), whereas ethanol and acetic acid were purchased from Scharlab (Barcelona, Spain). Folin–Ciocalteu phenol reagent and HCl were acquired from Merck (Darmstadt, Germany). Water employed was Milli-Q grade obtained from a Millipore system (Billerica, MA). (+)-catechin, (−)-epicatechin, procyanidin B1, quercetin-3-O-rutinoside and quercetin-3-O-galactoside reference standards were acquired from Extrasynthèse (Genay, France).

2.2. Sample preparation

Apple phenolic compounds were extracted according to a previously published protocol slightly modified [26]. Briefly, fresh whole apples were cut in small pieces before their lyophilization in a freeze-dryer (Labconco Corporation, MO). 19 g of lyophilized apple powder were extracted with 80 mL of acetone/water (70:30, v/v) during 20 min using magnetic stirring and protected from light. The resulting extract was centrifuged for 20 min at 1900 × *g*, the supernatant was decanted and the precipitate was again extracted following the same procedure. Both supernatants were pooled and 50 mL of water were added before the acetone was removed in a Rotavapor R-210 (Buchi Labortechnik AG, Flawil, Switzerland). Next, phenolic compounds were concentrated using solid phase extraction (SPE). Discovery DSC-18 6 mL SPE cartridges (Supelco, Bellefonte, PA, USA) were conditioned with 3× 5 mL of methanol and with 3× 5 mL of water. Then, 10 mL of sample were loaded in the SPE column, rinsed with 10 mL of water, and the polyphenols were extracted with 2× 5 mL of acetone/water (70:30, v/v). Finally, acetone was evaporated again by rotary evaporation, and the remaining aqueous extract was lyophilized.

2.3. Determination of total phenols content (Folin–Ciocalteu method)

The total phenols content of the different apple samples was measured using the Folin–Ciocalteu assay [27] with some modifications. The total volume of reaction mixture was miniaturized to 1 mL. 600 μL of water and 10 μL of each apple sample (1 mg mL^{-1} of polyphenol extract in methanol) were mixed, to which 50 μL of undiluted Folin–Ciocalteu reagent was subsequently added. After 1 min, 150 μL of 20% (w/v) Na_2CO_3 was added and the volume was made up to 1.0 mL with water. After 2 h of incubation at 25 °C, 300 μL of the mixture was transferred into a well of a 96-well microplate. The absorbance was measured at 760 nm in a microplate spectrophotometer reader Powerwave XS (Bio Tek Instruments, Winooski, VT) and compared to a gallic acid calibration curve (0.032–2 mg mL^{-1}) elaborated in the same manner. Data were presented as the average of triplicate analyses expressed as mg gallic acid equiv. (GAE) g^{-1} dry matter.

2.4. Determination of total procyanidins

To estimate the total procyanidin content in the apple samples, the p-dimethylaminocinnamaldehyde (DMAC) method was employed according to the work by Prior et al. [28] with some modifications. In brief, a DMAC solution (0.1% DMAC reagent (w/v) on a mixture of ethanol/water/HCl 75:12.5:12.5, v/v/v) was prepared immediately before use. 70 μL of each apple sample (0.075 mg mL^{-1} of polyphenol extract in methanol) were mixed with 210 μL of the DMAC solution. The mixture was vortexed, transferred into a well of a 96-well microplate and allowed to react at room temperature for 15 min. After this time, the absorbance was read at 640 nm using a microplate spectrophotometer reader Powerwave XS (Bio Tek). Blanks with 70 μL of methanol instead of sample and a control samples without DMAC solution were also included. Each sample, blank and control was prepared in triplicate. The concentration of total procyanidins was estimated from a calibration curve using epicatechin (0.001–0.02 mg mL^{-1}). Data were presented as the average of duplicate analyses expressed as mg epicatechin equiv. (ECE) g^{-1} dry matter.

2.5. Comprehensive two-dimensional liquid chromatography (LC × LC) analysis of apple phenolic compounds

2.5.1. Instruments

LC × LC analyses were carried out on an Agilent 1200 series liquid chromatograph (Agilent Technologies, Santa Clara, CA) equipped with a diode array detector and an autosampler. In order to have robust and reproducible low flow rates and gradients in the first dimension, a Protecol flow splitter (SGE Analytical Science, Milton Keynes, UK) was placed between the first dimension pumps and the autosampler. Besides, an additional LC pump (Agilent 1290 Infinity) was coupled to this instrument to perform the second dimension separation, hyphenated through an electronic controlled two-position ten-port switching valve. An Agilent 6320 Ion Trap mass spectrometer equipped with an electrospray interface was coupled on-line and operated in negative ionization mode using the following conditions: dry temperature, 350 °C; mass range, *m/z* 90–2200 Da; dry gas flow rate, 12 L min^{-1}; and nebulization pressure, 40 psi. The LC data were elaborated and visualized in two and three dimensions using LC Image software (version 1.0, Zoex Corp., Houston, TX).

2.5.2. LC × LC separation conditions

Samples were prepared by diluting 6 mg of polyphenol extract of each apple variety in 300 μL of methanol and adding 700 μL of acetonitrile to obtain a 6 mg mL^{-1} solution, which was filtered through

0.45-μm nylon syringe filters (Symta, Madrid, Spain) before injection.

In the first dimension, a Lichrospher diol-5 (150 × 1.0 mm, 5 μm d.p., HiChrom, Reading, UK) column was employed with a precolumn with the same stationary phase. The optimized flow rate employed was 21 μL min^{-1}, from minute 0 to 24, and 15 μL min^{-1} from minute 24 to the end of the analysis. The mobile phases employed were (A) acetonitrile/acetic acid (98:2, v/v) and (B) methanol/water/acetic acid (95:3:2, v/v/v) eluted according to the following gradient: 0 min, 0% B; 2 min, 0% B; 5 min, 20% B; 30 min, 20% B; 40 min, 30% B; 50 min, 30% B. The injection volume was 20 μL.

In the second dimension, an Ascentis Express C_{18} (50 × 4.6 mm, 2.7 μm d.p., Supelco, Bellefonte, CA) partially porous column was employed together with a C_{18} precolumn. During the whole LC × LC separation, 78 s-repetitive second dimension gradients were employed, being also 78 s the modulation time programmed in the switching valve. Two different gradient profiles were employed throughout the analysis. During the first 25.4 min of two-dimensional analysis, the mobile phase employed in D2 consisted of water (0.1% formic acid, A) and acetonitrile (B) eluted according to the following gradient: 0 min, 0% B; 0.1 min, 15% B; 0.8 min, 50% B; 1.0 min, 70% B; 1.01 min, 0% B. From minute 25.4 till the end of the analysis, the mobile phase composition was changed to water (0.1% formic acid, A) and acetonitrile/methanol (50:50, v/v) (B) using the following programme: 0 min, 0% B; 0.1 min, 15% B; 0.3 min, 25% B; 1.0 min, 45% B; 1.01 min, 0% B. The flow rate was 3 mL min^{-1}.

The wavelength used to monitor the separations was 280 nm, although UV–vis spectra were collected from 190 to 550 nm during the whole analysis using a sampling rate of 20 Hz in the diode array detector. The MS was operated under negative ESI mode. The flow eluting from the second dimension column was splitted before the MS instrument, so that the flow rate entering the MS detector was approximately 600 μL min^{-1}.

3. Results and discussion

3.1. Optimization of sample preparation for the analysis of phenolic compounds from apple

The first part of this study consisted on the search of optimum extraction conditions to obtain a representative sample of apple phenolic compounds. Apples are very well-known for possessing high amount of procyanidins as well as other phenolic compounds [29]. Although different advanced extraction techniques have been already employed to obtain particular apple polyphenols, such as supercritical fluid extraction [30], microwave-assisted extraction [31] or pressurized liquid extraction [32], for the aim of the present study, a relatively fast and easy extraction method capable of providing with a wide mixture of the entire pattern of phenolic compounds present on these samples was sought. To do this, different extraction methodologies were initially tested, including extraction with ultrasounds as well as magnetic stirring using acetone:water 70:30 (v/v) as extraction solvent. The optimization of the extraction procedure was monitored using a HILIC-based method, which was the basis of the first dimension of a previous LC × LC method involving the separation of procyanidins polymers on grape seeds depending on their degree of polymerization (DP) [22]. The use of magnetic stirring followed by a SPE clean-up and concentration step provided the best results. Once selected the initial methodology for the extraction, the employment of different SPE cartridges with diverse stationary phases was tested in order to find the best conditions to clean-up and increase the recovery of phenolic compounds in the apple extract. Namely, amino, HLB and C_{18} stationary phases were studied. Using the C_{18} cartridges, extracts that produced a better distribution in the HILIC separation as well as higher number of peaks were attained, as it can be observed in Fig. 1A. To have a relatively good separation and wide distribution of the peaks in the first separation is essential to achieve good two-dimensional analyses. Thus, this stationary phase was finally selected to carry out the extraction procedure. Once all the steps of the extraction protocol were optimized, the phenolic compounds-rich extracts from apples were obtained by extracting 19 g of lyophilized apple with 80 mL acetone:water 70:30 (v/v) twice, and the resulting extracts were further concentrated using SPE as detailed above.

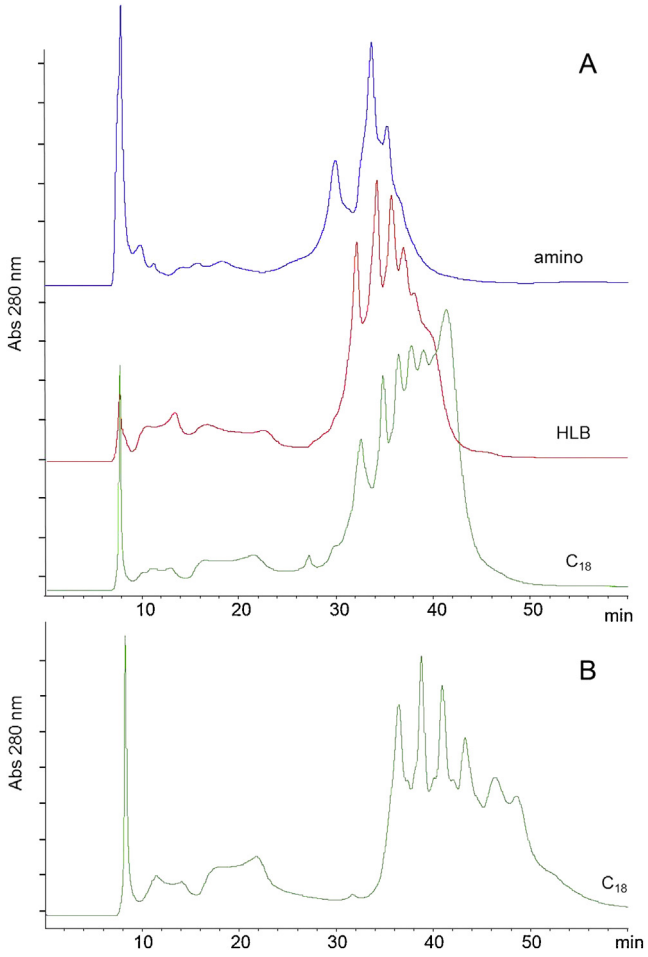

Fig. 1. HILIC chromatograms (280 nm) corresponding to the separation of phenolic compounds from Red Starking apple depending on the nature of the SPE cartridges employed during their extraction (A) and under the optimized conditions used for the comprehensive two-dimensional LC analyses (B).

3.2. HILIC × RP-DAD–ESI-MS analysis of phenolic compounds from apple

The next step consisted on the optimization of the separation method. Although, as it has been already mentioned, apple procyanidins have been previously analyzed using NP-LC [18], SEC [17] and HSCCC [16], all these methods have several drawbacks, mainly involving lengthy analysis times and the impossibility to separate the different procyanidins having the same DP. Since our goal was to separate apple procyanidins together with other phenolic compounds by using an LC × LC approach, a set-up comprising a HILIC separation in the first dimension (D1) coupled to a fast RP-LC separation in the second dimension (D2), previously developed for the separation of grape seeds proanthocyanidins,

was initially tested [22]. However, since evident differences were expected between the compositions of these samples, mainly considering that procyanidins pattern in apples is simpler than in grape seeds whereas apples contain greater amounts of other flavonoids and phenolic acids than grape seeds, no complete separations could be achieved with the original method and further re-optimization of the HILIC × RP method was necessary to obtain a clear profile of the entire phenolic compounds composition from apples. As the optimization of a two-dimensional separation is not an easy task, each dimension was studied separately, although LC × LC analyses during optimization were also necessary, not only to confirm the efficacy of the changes performed but also to suggest further modifications for the fine tuning of the employed conditions.

Firstly, the HILIC separation was optimized modifying the gradient employed in order to get a better distribution of the sample through the available separation space. In this regard, it is important to keep in mind that the chromatographic conditions employed in the D1 will significantly influence the D2. Besides, even if the solvents employed in the two dimensions are miscible or even the same, the use of different separation mechanisms in the two dimensions implies that the weaker solvent in the D1 is the stronger solvent in the D2 and vice versa, which may significantly interfere in the attainment of a successful coupling. For this reason, a maximum injection volume in the D2 of 30 μL was considered, limited by the maximum capacity of the injection loops. Nevertheless, as we formerly showed, the transfer of smaller volumes to the injection loops installed in the switching valve used as interface between injections (<20 μL), allowed the dilution of the D1 eluate with D2 initial mobile phase, producing better peak shapes and significantly less peak distortion in this latter separation [22]. Consequently, 15 μL min^{-1} was selected as flow rate, meaning that the transfer of 19.5 μL into the injection loop would last 78 s, which would be the modulation time as well as the time available to carry out each single D2 separation. Such slow flow rates imply the use of microbore columns so that the needed analytical performance can be attained. After several modifications in the composition and characteristics of the mobile phases and gradients employed, it was decided to maintain the same initial mobile phases using a less steep gradient. Fig. 1B shows the chromatogram obtained under the optimum D1 separation conditions. Final gradient conditions are detailed in Section 2.5.2. As it can be observed comparing with Fig. 1A, the peaks were more evenly distributed during the analysis.

For the D2 conditions optimization, 78 s was fixed as target analysis time. Preliminary LC × LC analyses using the gradients from the original method clearly showed that in the last part (*x* axis) of the 2D plot peaks were clearly and sufficiently separated. However, some peaks were not completely resolved in the initial part of the 2D analysis. To solve this problem, dynamic gradients were employed in the D2 analyses maintaining a flow rate of 3 mL min^{-1}. The LC × LC analysis was divided into two well differentiated zones: from 0 to 25.4 min and from 25.4 to the end of the analysis. The original conditions involving the use of water plus 0.1% formic acid (A) and acetonitrile/methanol 50:50 (v/v) (B) as mobile phases were maintained in the second half of the 2D analysis, while the separation conditions of the initial part (until 25.4 min) were completely re-optimized. Different mobile phases and gradients were employed, finally achieving as optimum conditions the use of water plus 0.1% formic acid (A) and acetonitrile (B) reaching higher proportions of the organic modifier during the separation. The final separation conditions involved in the D2 are specified in Section 2.5.2. In Fig. 2A and B, a comparison between the separations obtained in the first 26 min of the two-dimensional analysis before and after optimization, respectively, is shown. As it can be appreciated, the peaks coeluting around 60–65 s (Fig. 2A) were more clearly resolved (34–43 s) after optimization (Fig. 2B). It is also possible to observe the separation obtained in the last part (25.4 min – end of analysis) of the analysis under the optimum conditions. Moreover, as the relative complexity in these first 26 min in terms of number of different compounds was lower, it was decided to increase the D1 flow rate in order to speed-up the analysis in a certain extent, taking advantage of the volume of the injection loops installed in the switching valve. Thus, the D1 flow rate for the first part of the analysis (Fig. 2B) was established at 21 μL min^{-1}, whereas in the second part (Fig. 2C), D1 flow rate was maintained at 15 μL min^{-1} to take advantage of the dilution effect produced by the partial use of the injection loop volume available, as previously mentioned.

3.3. Profiling of phenolic compounds in different apple varieties

Once the analytical method was optimized, the two-dimensional LC procedure was coupled to MS, including the use of an ESI negative ionization mode in order to assist in the characterization of the apple samples. Five apple varieties, namely Red Starking, Kanzi, Royal Gala, Reinette and Granny Smith, were studied to further demonstrate the applicability of the developed procedure. Table 1 summarizes the main phenolic compounds detected and identified in the five apple varieties studied using the optimized HILIC × RP-DAD–MS/MS methodology. Besides, in Fig. 3 a comparison among the typical profiles obtained for all the samples is shown. As can be observed, the phenolic composition of all samples was dominated by the presence of a high number of different flavan-3-ols, mainly catechin and epicatechin (peaks 1 and 2, respectively) as well as procyanidin oligomers up to a DP = 8. Besides, it was also possible to find several dihydrochalcones (phloretin-glucoside, phloretin-xilosyl-glucoside and hydroxyphloretin-diglycoside, peaks 4, 6, 7, 11, 16, 18, 32), flavonols (quercetin-related compounds, peaks 3, 15, 17, 22–24) and a hydroxycinnamic acid (dicaffeoylquinic acid, peak 5). The identification of the compounds present on the samples was performed thanks to the information provided by the two detectors coupled in series, DAD and MS, as well as the information collected from MS/MS experiments and the use of commercial standards when available. Fig. 4 shows some examples of how the identification was carried out. Among the flavan-3-ols, catechin and epicatechin were correctly identified due to the detection of characteristic ions at *m*/*z* 289.7 and 289.5 ($[M-H]^-$), respectively. These compounds were differentiated by comparing their corresponding retention times with those of their available commercial standards. In the case of procyanidin dimers, trimers and tetramers, their typical molecular ions were detected as $[M-H]^-$ at *m*/*z* 577, 865 and 1153, respectively. In each case, different fragment ions were produced in the MS/MS experiments, which confirmed the assignments; for example, procyanidin dimers presented fragments at *m*/*z* 425, corresponding to a retro-Diels–Alder mechanism ($[M-H-152]^-$) [33], as well as ions of the monomer (*m*/*z* 289). Procyanidin trimers presented fragment ions corresponding to the loss of a phloroglucinol unit (*m*/*z* 739) as well as to the loss of one or two (epi)catechin molecules, *m*/*z* 577 and 289, respectively. On the other hand, procyanidin tetramers were mainly characterized by the presence of ions related to shorter oligomers that would be formed after collision induced dissociation, such as *m*/*z* 865 and 577. Longer procyanidin oligomers could not be detected as monocharged ions. Indeed, procyanidin pentamers, hexamers and heptamers were detected as doubly-charged ions, as can be observed in Table 1. Procyanidin pentamers were detected as *m*/*z* 720 ($[M-2H]^{2-}$) which fragmentations gave rise to ions related to the losses of a phloroglucinol unit, and one, two or three (epi)catechin moieties (*m*/*z* 1315, 1151, 863, 577, respectively), as can be observed in Fig. 4A. Similar fragmentation patterns allowed the identification of ions at *m*/*z* 864 and 1008 ($[M-2H]^{2-}$) as procyanidin hexamers and heptamers, respectively. Lastly in this

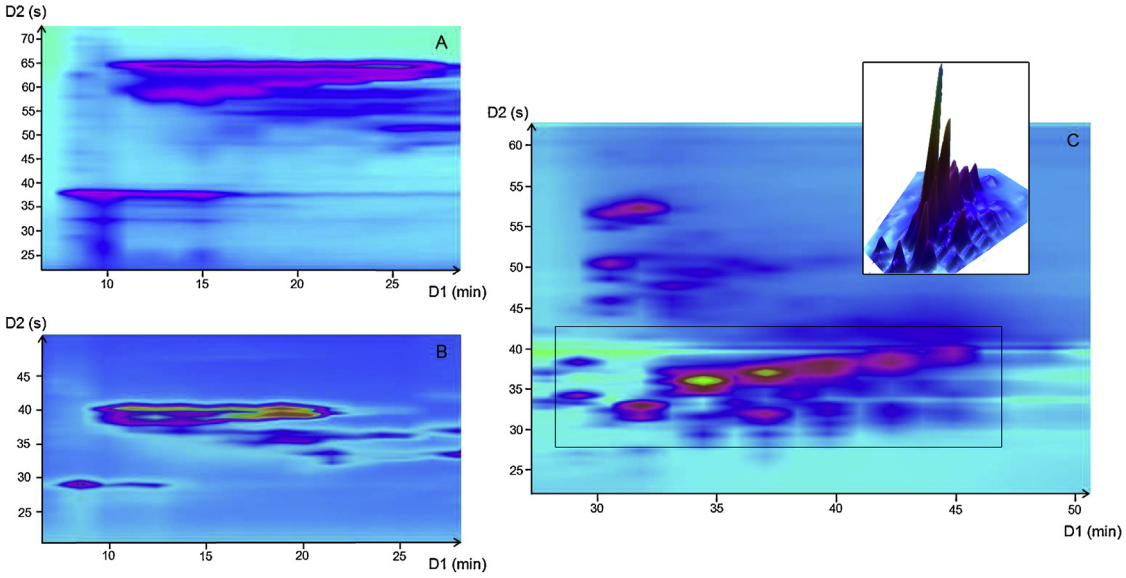

Fig. 2. Two-dimensional plots (280 nm) corresponding to the separation of the first eluting apple phenolic compounds before (A) and after (B) optimization, as well as to the second part of the separation in which a different gradient programme is employed in the optimized HILIC × RP method (C).

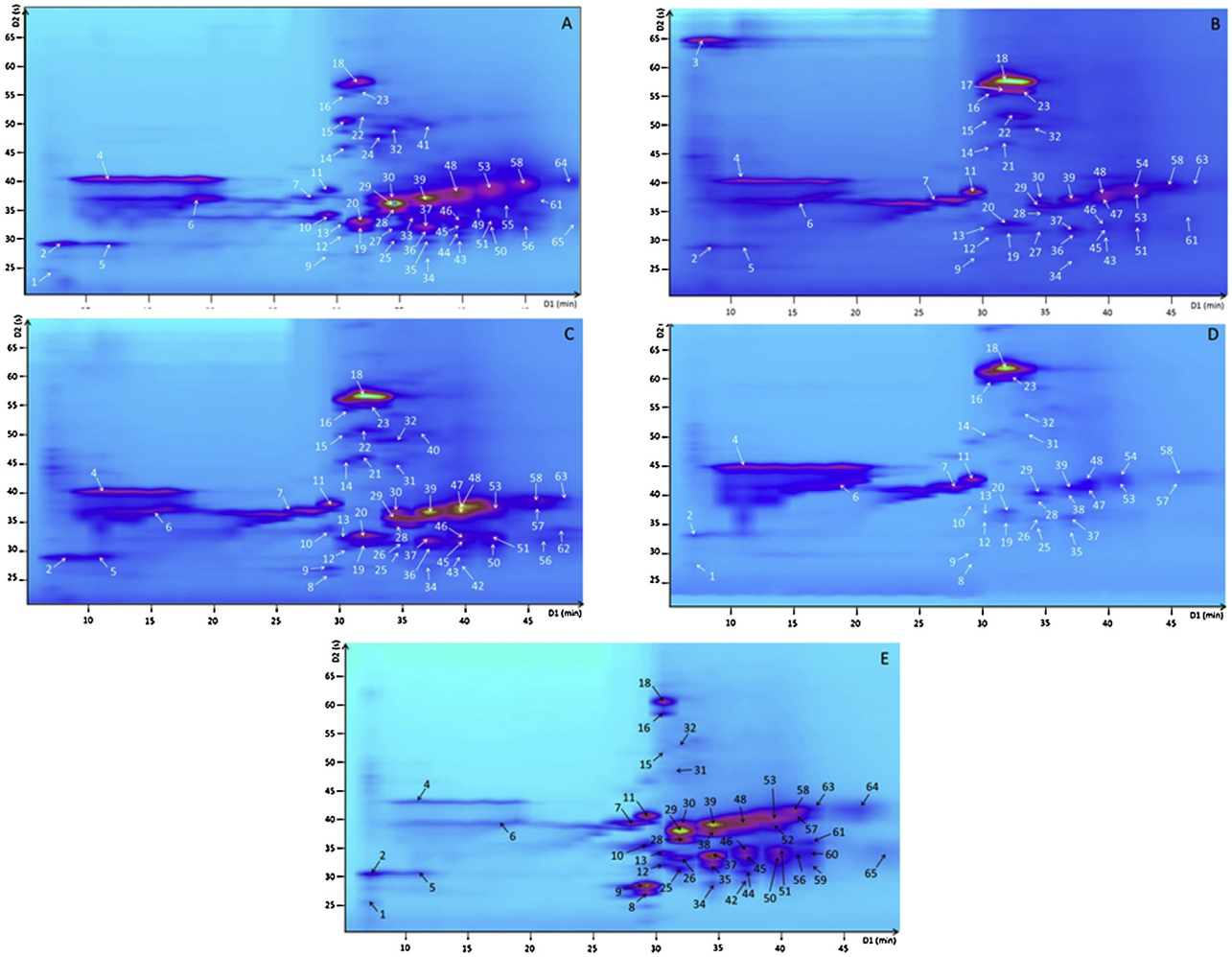

Fig. 3. Comparison of the 2D profiles (280 nm) obtained for the five apple varieties studied using the optimized HILIC × RP-DAD–MS/MS methodology. A, Red Starking; B, Kanzi; C, Royal Gala; D, Reinette; E, Granny Smith. For peak identification see Table 1.

Table 1
Main phenolic compounds tentatively identified in the five different apple varieties studied using the optimized HILIC × RPLC–DAD–MS/MS profiling methodology.

ID	Identification	Total t_R (min)	D2 t_R (s) ± sd	$[M-H]^-$	Main MS/MS fragments	UV–vis maxima (nm)
1	Catechin[c]	6.90	24.17 ± 0.09	289.7	245	280
2	Epicatechin[c]	6.98	28.83 ± 0.16	289.5	245	280
3	Dihydroquercetin rhamnoside	7.57	64.22 ± 0.12	549.3	303	340
4	Phloretin-glucoside[c]	11.07	40.23 ± 0.12	435.6	273, 167	285
5	Dicaffeoylquinic acid	12.18	28.94 ± 0.11	515.4	353, 191	278
6	Phloretin-glycoside	18.82	37.12 ± 0.27	435.8	273	285
7	Phloretin-xylosyl-glucoside	27.91	36.80 ± 0.11	567.4	273	285
8	Procyanidin dimer	29.03	25.79 ± 0.08	577.5	425, 289, 559	280
9	Procyanidin dimer	29.05	27.03 ± 0.15	577.2	425, 289, 559	280
10	Procyanidin dimer	29.16	33.40 ± 0.16	577.2	425, 289, 559	280
11	Phloretin-xylosyl-glucoside	29.23	38.01 ± 0.17	567.3	273, 167	285
12	Procyanidin dimer	30.41	30.40 ± 0.17	577.8	425, 289, 559	280
13	Procyanidin dimer	30.44	32.21 ± 0.20	577.5	425, 289, 559	280
14	Procyanidin dimer	30.66	45.49 ± 0.21	577.5	425, 289, 559	280
15	Quercetin-galactoside[c]	30.73	49.86 ± 0.22	463.3	301	354
16	Phloretin-xylosyl-glucoside	30.80	54.33 ± 0.29	567.4	273	285
17	Quercetin rhamnoside	30.81	54.68 ± 0.04	447.3	301	350
18	Phloretin-xylosyl-glucoside	30.84	56.32 ± 0.33	567.4	273	285
19	Procyanidin dimer	31.72	31.12 ± 0.05	577.3	425, 289, 559	280
20	Procyanidin dimer	31.75	32.75 ± 0.07	577.2	425, 289, 559	280
21	Not identified	31.97	46.02 ± 0.19	599.1	447, 295	280
22	Quercetin-glucoside	32.05	50.84 ± 0.28	463.5	301	356
23	Quercetin glucoside	31.12	55.01 ± 0.09	463.8	301	350
24	Quercetin-rutinoside[c]	33.29	47.58 ± 0.58	609.7	301	350
25	Procyanidin trimer	34.30	29.70 ± 0.23	865.5	739, 577, 289	280
26	Procyanidin trimer	34.32	31.28 ± 0.22	865.6	739, 577	280
27	Procyanidin trimer	34.33	31.47 ± 0.19	865.3	739, 577, 425, 289	280
28	Procyanidin trimer	34.37	34.39 ± 0.23	865.4	739, 577	280
29	Procyanidin trimer	34.40	35.71 ± 0.21	865.3	739, 577, 289	280
30	Procyanidin trimer	34.42	36.96 ± 0.22	865.3	739, 577	280
31	Procyanidin trimer	34.55	44.81 ± 0.18	865.2	739, 577, 289, 245	280
32	Hydroxyphloretin-xylosyl-glucoside	34.62	49.08 ± 0.30	583.2	289, 167	285
33	Procyanidin tetramer	35.66	33.50 ± 0.40	1153.5	1027, 983, 865, 739	280
34	Procyanidin tetramer	36.85	27.29 ± 0.45	1153.3	1027, 983, 865, 739, 575	280
35	Procyanidin tetramer	36.89	29.68 ± 0.37	1153.6	1135, 983, 865, 739, 575	280
36	Procyanidin tetramer	36.91	30.66 ± 0.05	1153.5	1135, 983, 865, 739, 577	280
37	Procyanidin tetramer	36.93	31.79 ± 0.23	1153.5	1135, 983, 865, 739, 575	280
38	Procyanidin tetramer	36.99	35.26 ± 0.08	1153.6	1135, 983, 865, 739, 575	280
39	Procyanidin tetramer	37.01	36.71 ± 0.22	1153.3	1135, 1027, 983, 865, 739, 575	280
40	Procyanidin tetramer	37.23	49.77 ± 0.84	1153.3	1135, 1027, 983, 865, 739, 575	280
41	Procyanidin pentamer	37.28	49.52 ± 0.63	719.8[a]	1315, 1151, 1025, 863, 575, 287	280
42	Procyanidin pentamer	39.46	27.52 ± 0.33	720.4[a]	1315, 1151, 1027, 863, 577, 287, 245	280
43	Procyanidin pentamer	39.49	29.42 ± 0.19	720.6[a]	1315, 1151, 1027, 863, 739, 577, 289, 245	280
44	Procyanidin pentamer	39.50	29.83 ± 1.16	720.5[a]	1315, 1151, 1027, 863, 577, 289	280
45	Procyanidin pentamer	39.53	31.57 ± 0.42	720.6[a]	1315, 1151, 1027, 863, 577, 289	280
46	Procyanidin pentamer	39.54	32.64 ± 0.31	720.4[a]	1315, 1151, 1027, 863, 577, 289	280
47	Procyanidin pentamer	39.61	36.72 ± 0.13	720.5[a]	1315, 1151, 863, 577, 289	280
48	Procyanidin pentamer	39.62	37.49 ± 0.57	720.4[a]	1315, 1151, 1027, 863, 577	280
49	Procyanidin hexamer	40.89	35.15 ± 0.46	864.1[a]	1603, 1315, 1153, 719, 575, 287	280
50	Procyanidin hexamer	42.12	30.94 ± 0.42	864.6[a]	1603, 1441, 1151, 1027, 719, 577, 287	280
51	Procyanidin hexamer	42.14	32.48 ± 0.16	864.5[a]	1603, 1441, 1315, 1153, 719, 575, 289	280
52	Procyanidin hexamer	42.20	36.12 ± 0.08	864.6[a]	1605, 1441, 1315, 1151, 719, 575, 287	280
53	Procyanidin hexamer	42.23	37.73 ± 0.43	864.5[a]	1604, 1441, 1315, 1151, 719, 577, 289	280
54	Procyanidin hexamer	42.25	38.73 ± 0.24	864.6[a]	1603, 1151, 719, 577, 289	280
55	Procyanidin hexamer	43.51	36.62 ± 0.39	864.4[a]	1603, 1441, 1153, 719, 577, 287	280
56	Procyanidin heptamer	44.73	31.98 ± 0.25	1008.5[a]	1729, 1603, 1441, 1316, 1151, 863, 577	280
57	Procyanidin heptamer	44.83	37.56 ± 0.05	1008.7[a]	1727, 1605, 1153, 1027, 865, 739, 577, 287	280
58	Procyanidin heptamer	44.85	39.04 ± 0.28	1008.5[a]	1605, 1439, 1314, 1151, 865, 577, 287	280
59	Procyanidin heptamer	44.70	29.88 ± 0.13	1008.6[a]	1605, 1441, 1153, 863, 575	280
60	Procyanidin heptamer	44.73	31.80 ± 0.17	1008.5[a]	1441, 1153, 863, 575, 287	280
61	Procyanidin heptamer	46.06	33.80 ± 0.36	1008.6[a]	1605, 1441, 1153, 863, 575	280
62	Procyanidin heptamer	46.10	33.77 ± 0.12	1008.6[a]	1605, 1441, 1153, 863, 739, 577	280
63	Procyanidin heptamer	46.15	38.89 ± 0.20	1008.7[a]	1605, 1441, 1315, 1151, 863, 577	280
64	Procyanidin octamer	48.75	39.21 ± 0.62	768.1[b]	1727, 1153, 865, 739, 577, 289	280
65	Procyanidin octamer	49.94	32.69 ± 0.58	768.0[b]	1316, 1153, 863, 575, 287	280

[a] Ions detected as $[M-2H]^{2-}$.
[b] Ions detected as $[M-3H]^{3-}$.
[c] Indicates identification confirmed using commercial standards.

group, two procyanidin octamers were detected in several samples as ($[M-3H]^{3-}$) with m/z 768.

Regarding the rest of identified compounds, two phloretin-glycosides were tentatively identified (peaks 4 and 6) in agreement with the main molecular ion detected at m/z 435.6 ($[M-H]^-$) together with the presence of a fragment corresponding to the loss of an hexoside ($[M-H-162]^-$) matching with phloretin aglycone (m/z 273). Another fragment at m/z 167 derived from phloretin has

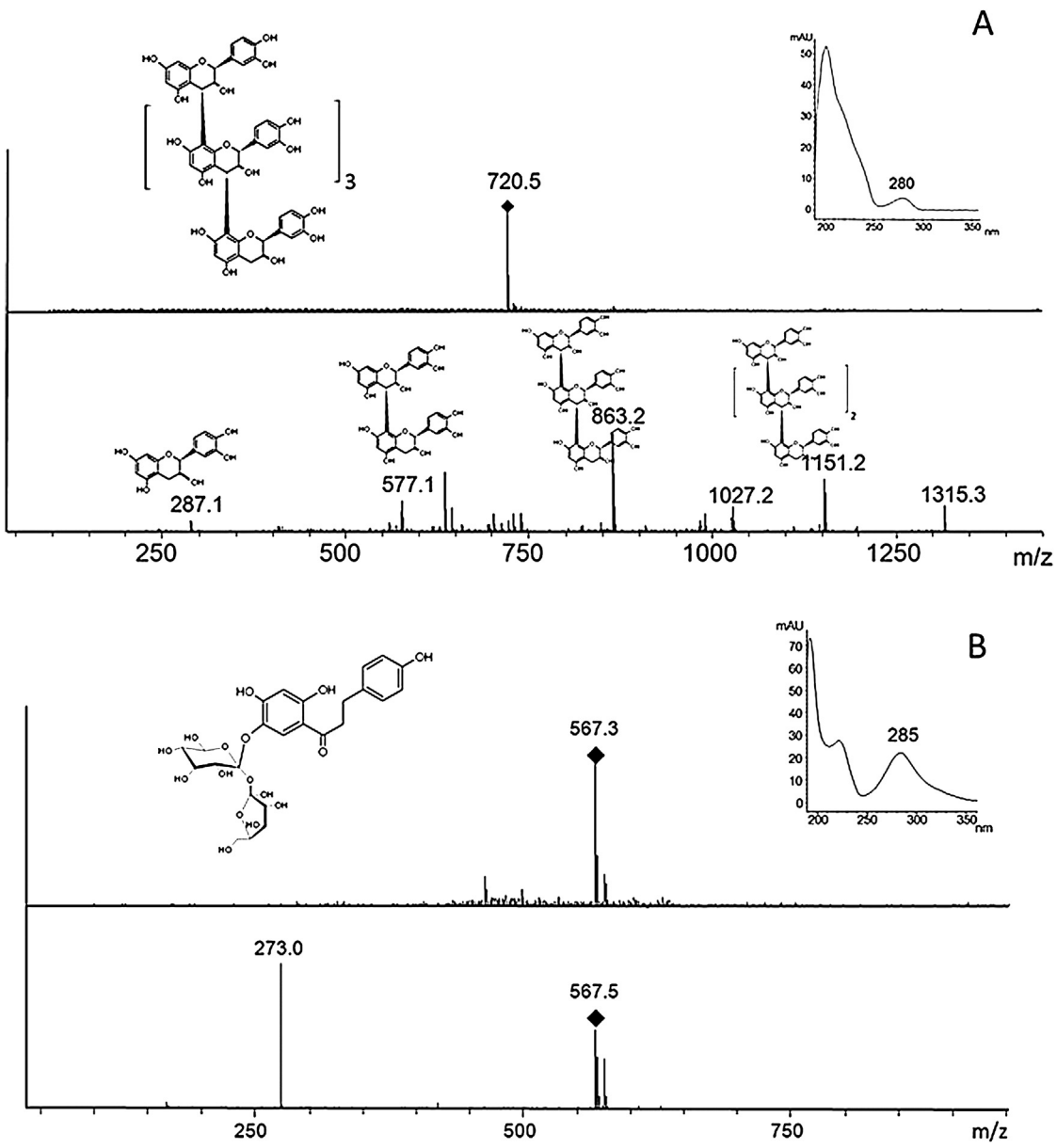

Fig. 4. UV–vis and MS/MS spectra of a procyanidin pentamer (A) and phloretin-xylosyl-glucoside (B).

been also previously detected [34]. Moreover, the UV–vis spectra of these peaks confirmed the identification showing the maximum of absorbance of phloretin (285 nm) as well as the comparison with its corresponding commercial standard. Other dihydrochalcones identified on the samples were phloretin-xylosyl-glucoside (peaks 7, 11, 16 and 18) and hydroxyphloretin-xylosyl-glucoside (peak 32). The identification of these compounds was performed similarly as for phloretin-glucoside, thanks to the detection of their corresponding molecular ions and fragments as well as from the UV–vis spectra obtained (see Fig. 4B). On the other hand, six different quercetin-related flavonols were also tentatively identified. Three of them corresponded to quercetin-glycosides, namely peaks 15, 22 and 23, although peak 15 was tentatively assigned to quercetin-galactoside, according to their elution order [35]. These three compounds presented similar molecular ion at m/z 463 ($[M-H]^-$) and produced a fragment after MS/MS corresponding to quercetin (m/z 301) as well as similar UV–vis absorption maximum at 354 nm. Besides, it was also possible to tentatively assign peak 3 to dihydroquercetin-rhamnoside thanks to the detection of an ion at m/z 549 which produced a fragment at m/z 303. Likewise, quercetin-rhamnoside (peak 17) and quercertin-rutinoside (peak 24) were also identified. All these compounds have been already found in several apple-derived materials [35,36]. Examples of these fragmentation patterns are illustrated in the supporting information (Figure S1).

Supplementary material related to this article found, in the online version, at http://dx.doi.org/10.1016/j.chroma.2013.06.015.

The basic phenolic profiles of the five apple varieties were quite similar (see Fig. 3), formed by groups of peaks belonging to the above-mentioned chemical classes. Nevertheless, the relationships among them were not the same; interestingly, Reinette apples contained higher relative abundance of dihydrochalcones (peaks 4, 6, 7, 11, 16, 18 and 32) than procyanidins. On the other side, Granny Smith apples presented a high number of different procyanidin peaks with significantly higher intensity than other flavonoids. Besides, some characteristic peaks of just one variety could also be detected. In Fig. 5, a reconstructed 2D plot is presented in which it is possible to observe the compounds that were present in all

Table 2
Total phenols amount (given as mg GAE (galic acid equiv.)/g dry matter) and total procyanidins amount (given as mg ECE (epicatechin equiv.)/g dry matter) present in the five studied apple varieties calculated according to the Folin–Ciocalteu and DMAC methods, respectively. Values provided as mean ± sd of three independent assays.

Apple variety	Total phenols (mg GAE/g dry matter)	Total procyanidins (mg ECE/g dry matter)	% Procyanidins
Red Starking	3.57 ± 0.07	0.38 ± 0.00	10.62
Kanzi	1.21 ± 0.13	0.14 ± 0.01	11.19
Royal Gala	1.77 ± 0.07	0.34 ± 0.00	19.41
Reinette	6.46 ± 0.22	0.56 ± 0.01	8.71
Granny Smith	5.45 ± 0.23	0.73 ± 0.00	13.37

the studied samples, as well as those that were markers for only one sample. For instance, dihydroquercitin-rhamnoside (peak 3) and quercetin-rhamnoside (peak 17) were only present in Kanzi apples. Royal Gala apples possessed two differential procyanidin peaks, a tetramer (peak 40) and a heptamer (peak 62), while Red Starking presented a procyanidin tetramer (peak 33), a pentamer (peak 41), two hexamers (peaks 49 and 55) as well as quercetin-rutinoside (peak 24). Granny Smith, possessed three procyanidin oligomers (peaks 52, 59 and 60) that were not present in any other sample. Thus, the only apple variety which did not present at least a differential phenolic compound was Reinette.

In order to quantitatively assess these differences on the phenolic profiles, two in vitro assays were carried out. Firstly, the total phenols amount present on the different samples was determined following the Folin–Ciocalteu method. The obtained results are summarized in Table 2. As it can be observed, the apple variety with the higher phenols content was Reinette (6.46 mg GAE g^{-1} d.m.) followed by Granny Smith and Red Starking, whereas Kanzi presented by far the lowest amount of total phenols (1.21 mg GAE g^{-1} d.m.). A second in vitro assay, based on the reaction with p-dimethylaminocinnamaldehyde (DMAC), was employed to determine the total procyanidin content of the studied samples. DMAC has been shown to specifically react with flavanols, enhancing the sensitivity and accuracy for the determination of procyanidins compared to other procedures [37]. As it can be appreciated in Table 2, Granny Smith was the richest apple variety on this class of compounds, reaching 0.73 mg ECE g^{-1} d.m., followed by Reinette (0.56 mg ECE g^{-1} d.m.). Again, Kanzi was the sample with the lowest amounts of flavan-3-ols. Interestingly, as it was previously pointed out from the analysis shown in Fig. 3, the relationships between procyanidins and other phenolic compounds were not the same among samples. In fact, the apple variety

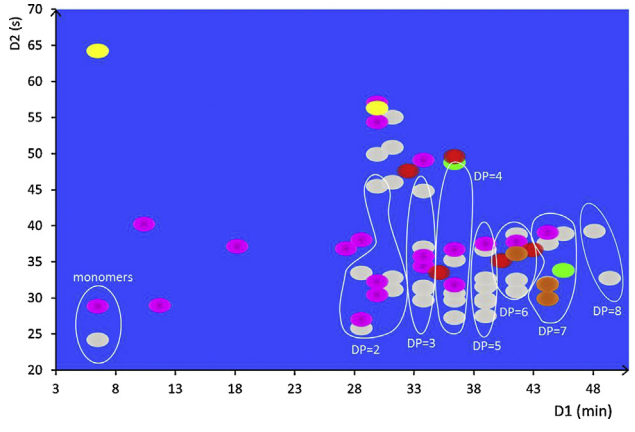

Fig. 5. Reconstructed 2D plot of the phenolic compounds identified in the different apple varieties studied showing the compounds present in all the samples (pink spots), in several apples (grey spots) and those differentially found in just one sample. Kanzi, yellow spots; Royal Gala, green spots; Red Starking, red spots; Granny Smith, orange spots. Circles represent the separation of procyanidins according to their degree of polymerization (DP) in the first dimension. (For interpretation of the references to color in this figure legend, the reader is referred to the web version of the article.)

with the richest content on procyanidins was Royal Gala, with more than 19% of total phenols corresponding to procyanidins; Granny Smith also contained high amounts of procyanidins (13%) whereas Reinette was the sample with the lowest relative abundance of procyanidins (8.7%), in agreement with its corresponding LC × LC analysis. These results corroborate the applicability of the developed methodology based on HILIC × RP-DAD–MS/MS, to characterize complex samples involving a great number of compounds belonging to different chemical classes. It is also worth to mention that the total analysis time needed to obtain the complete phenolic compounds' profile of each sample was less than 50 min, which is a rather fast analysis for a comprehensive two-dimensional method. In fact, these analysis times are directly comparable to other one-dimensional methods aimed to the separation of different phenolic compounds in apples which provided significantly less separation power and information [21,36,38–40]. Besides, the optimized HILIC × RP methodology allowed the separation of procyanidin oligomers in the first dimension according to their DP, and their subsequent differentiation using the second dimension, as can be clearly seen in Fig. 5.

4. Conclusions

In this work, the phenolics profiling of different apple varieties using comprehensive two-dimensional LC is shown for the first time. The developed method, based on a HILIC × RP-DAD–MS/MS coupling was capable to provide the 2D plot of each sample in less than 50 min, allowing the tentative identification of ca. 65 compounds on each studied sample, including flavan-3-ol oligomers up to a DP = 8, dihydrochalcones, flavonols and phenolic acids. By attaining these 2D profiles, a fast visual comparison was possible enabling to distinguish among different phenolic compound classes in a single run, depending on the elution zone of the 2D plane in which they appear. Among the studied samples, Reinette and Granny Smith were the richest cultivars in terms of total phenolic compounds and procyanidins, respectively. Thus, the applicability of 2D LC for the profiling of complex food samples has been demonstrated, opening new possibilities for the application of procedures based on this technique for other target and non-target metabolomics-related studies.

Acknowledgements

M.H. would like to thank MICINN for his "Ramón y Cajal" research contract. The authors want to thank Projects AGL2011-29857-C03-01 and CONSOLIDER INGENIO 2010 CSD2007-00063 FUN-C-FOOD (Ministerio de Educación y Ciencia) for the financial support.

References

[1] J.M. Bueno, F. Ramos-Escudero, P. Saez-Plaza, A.M. Munoz, M.J. Navas, A.G. Asuero, Crit. Rev. Anal. Chem. 42 (2012) 102.
[2] M.J. Montilva, A. Serra, A. Macià, J. Chromatogr. A 1292 (2013) 66.
[3] C. Manach, J. Hubert, R. Llorach, A. Scalbert, Mol. Nutr. Food Res. 53 (2009) 1030.

[4] C. Ibáñez, A. Valdés, V. García-Cañas, C. Simó, M. Celebier, L. Rocamora, A. Gómez, M. Herrero, M. Castro, A. Segura-Carretero, E. Ibáñez, J.A. Ferragut, A. Cifuentes, J. Chromatogr. A 1248 (2012) 139.
[5] V. García-Cañas, C. Simó, M. Herrero, E. Ibáñez, A. Cifuentes, Anal. Chem. 84 (2012) 10150.
[6] P. Dugo, F. Cacciola, T. Kumm, G. Dugo, L. Mondello, J. Chromatogr. A 1184 (2008) 353.
[7] P. Donato, F. Cacciola, P.Q. Tranchida, P. Dugo, L. Mondello, Mass Spectrom. Rev. 31 (2012) 523.
[8] P. Dugo, T. Kumm, F. Cacciola, G. Dugo, L. Mondello, J. Liq. Chromatogr. Rel. Technol. 31 (2008) 1758.
[9] M. Herrero, E. Ibañez, A. Cifuentes, J. Bernal, J. Chromatogr. A 1216 (2009) 7110.
[10] M. Russo, F. Cacciola, I. Bonaccorsi, P. Dugo, L. Mondello, J. Sep. Sci. 34 (2011) 681.
[11] M. Kivilompolo, V. Oburka, T. Hyotylainen, Anal. Bioanal. Chem. 391 (2008) 373–380.
[12] P. Dugo, F. Cacciola, M. Herrero, P. Donato, L. Mondello, J. Sep. Sci. 31 (2008) 3297.
[13] P. Dugo, F. Cacciola, P. Donato, D. Airado-Rodriguez, M. Herrero, L. Mondello, J. Chromatogr. A 1216 (2009) 7483.
[14] T. Hajek, V. Skerikova, P. Cesla, K. Vynuchalova, P. Jandera, J. Sep. Sci. 31 (2008) 3309.
[15] M. Ceymann, E. Arrigoni, H. Scharer, A. Bozzi Nising, R.F. Hurrell, J. Food Compos. Anal. 26 (2012) 128.
[16] X. Cao, C. Wang, H. Rei, B. Sun, J. Chromatogr. A 1216 (2009) 4268.
[17] C. Le Bourvellec, M. Picot, C.M.G.C. Renard, Anal. Chim. Acta 563 (2006) 33.
[18] T. Shoji, S. Masumoto, N. Moriichi, T. Kanda, Y. Ohtake, J. Chromatogr. A 1102 (2006) 203.
[19] K.M. Kalili, A. de Villiers, J. Chromatogr. A 1216 (2009) 6274.
[20] S. Khanizadeh, R. Tsao, D. Rekika, R. Yang, M.T. Charles, H.P.V. Rupasinghe, J. Food Compos. Anal. 21 (2008) 396.
[21] A. Mari, I. Tedesco, A. Nappo, G.L. Russo, A. Molorni, V. Carbone, Food Chem. 123 (2010) 157.
[22] L. Montero, M. Herrero, M. Prodanov, E. Ibañez, A. Cifuentes, Anal. Bioanal. Chem. 405 (2013) 4627.
[23] P. Jandera, T. Hajek, M. Stankova, K. Vynuchalova, P. Cesla, J. Chromatogr. A 1268 (2012) 91.
[24] K.M. Kalili, A. de Villiers, J. Chromatogr. A 1289 (2013) 58.
[25] K.M. Kalili, A. de Villiers, J. Chromatogr. A 1289 (2013) 69.
[26] S.A. Lazarus, G.E. Adamson, J.F. Hammerstone, H.H. Schmitz, J. Agric. Food Chem. 47 (1999) 3693.
[27] M. Kosar, H.J.D. Dorman, R. Hiltunen, Food Chem. 91 (2005) 525.
[28] R.L. Prior, E. Fan, H. Ji, A. Howell, C. Nio, M.J. Payne, J. Reed, J. Sci. Food Agric. 90 (2010) 1473.
[29] W. Huemmer, H. Dietrich, F. Will, P. Schreier, E. Richling, Biotechnol. J. 3 (2008) 234.
[30] I. Hasbay Adil, H.I. Cetin, M.E. Yener, A. Bayindirli, J. Supercrit. Fluids 43 (2007) 55.
[31] X.L. Bai, T.L. Yue, Y.H. Yuan, H.W. Zhang, J. Sep. Sci. 33 (2010) 3751.
[32] H. Wijngaard, N. Brunton, J. Agric. Food Chem. 57 (2009) 10625.
[33] I.I. Rockenbach, E. Jungfer, C. Ritter, B. Santiago-Schübel, B. Thiele, R. Fett, R. Galensa, Food Res. Int. 48 (2012) 848.
[34] S.C. Marks, W. Mullen, G. Borges, A. Crozier, J. Agric. Food Chem. 57 (2009) 2009.
[35] F. Sanchez-Rabaneda, O. Jauregui, R.M. Lamuela-Raventos, F. Viladomat, J. Bastida, C. Codina, Rapid Commun. Mass Spectrom. 18 (2004) 553.
[36] R. Tsao, R. Yang, J.C. Young, H. Zhu, J. Agric. Food Chem. 51 (2003) 6347.
[37] M.J. Payne, W.J. Hurst, D.A. Stuart, B. Ou, E. Fan, H. Ji, Y. Kou, J. AOAC Int. 93 (2010) 89.
[38] D. Pingret, A.S. Fabiano-Tixier, C. Le Bourvellec, C.M.G.C. Renard, F. Chemat, J. Food Eng. 111 (2012) 73.
[39] M. Cam, K. Aaby, J. Agric. Food Chem. 58 (2010) 9103.
[40] Y. Diñeiro Garcia, B. Suarez Valles, A. Picinelli Lobo, Food Chem. 117 (2009) 731.

3.4. Downstream valorization and comprehensive two-dimensional liquid chromatography-based chemical characterization of bioactives from black chokeberries (*Aronia melanocarpa*) pomace.

Brazdauskas, T., Montero, L., Venskutonis, P.R., Ibáñez, E., Herrero, M.

Journal of Chromatography A, 1468 (2016) 126–135

Journal of Chromatography A, 1468 (2016) 126–135

Contents lists available at ScienceDirect

Journal of Chromatography A

journal homepage: www.elsevier.com/locate/chroma

Downstream valorization and comprehensive two-dimensional liquid chromatography-based chemical characterization of bioactives from black chokeberries (*Aronia melanocarpa*) pomace☆

T. Brazdauskas[a], L. Montero[b], P.R. Venskutonis[a], E. Ibañez[b], M. Herrero[b,*]

[a] Kaunas University of Technology, Department of Food Science and Technology, Radvilenu pl. 19, LT-50254 Kaunas, Lithuania
[b] Foodomics Laboratory, Institute of Food Science Research (CIAL, CSIC), Nicolás Cabrera 9, 28049 Madrid, Spain

ARTICLE INFO

Article history:
Received 20 June 2016
Received in revised form
13 September 2016
Accepted 14 September 2016
Available online 15 September 2016

Keywords:
Aronia melanocarpa
Black chokeberry
Biorefinery
LC × LC
Pressurized liquid extraction
Valorization

ABSTRACT

In this work, a new alternative for the downstream processing and valorization of black chokeberry pomace (*Aronia melanocarpa*) which could be potentially coupled to a biorefinery process is proposed. This alternative is based on the application of pressurized liquid extraction (PLE) to the residue obtained after the supercritical fluid extraction of the berry pomace. An experimental design is employed to study and optimize the most relevant extraction conditions in order to attain extracts with high extraction yields, total phenols content and antioxidant activity. Moreover, the PLE extracts were characterized by using a new method based on the application of comprehensive two-dimensional liquid chromatography in order to correlate their activity with their chemical composition. Thanks to the use of this powerful analytical tool, 61 compounds could be separated being possible the tentative identification of different anthocyanins, proanthocyanidins, flavonoids and phenolic acids. By using the optimized PLE approach (using pressurized 46% ethanol in water at 165 °C containing 1.8% formic acid), extracts with high total phenols content (236.6 mg GAE g^{-1} extract) and high antioxidant activities (4.35 mmol TE g^{-1} extract and EC_{50} 5.92 μg mL^{-1}) could be obtained with high yields (72.5%).

1. Introduction

Food-related production represents an important industry worldwide, involving the production of food commodities as well as agricultural-related practices. These foodstuffs production generates a huge amount of wastes and by-products. As in any other industrial activity, wastes in the food industry have been managed looking for alternative uses, being traditionally energy generation or feed production [1]. However, in the last years, different studies have appeared proposing new ways for the valorization of food by-products mainly through the recovery and application of interesting bioactive compounds from them. With these aims in mind, new biorefinery concepts are appearing related to food industry. Biorefinery relies on the development of integrated production processes in which all kinds of materials and by-products are converted in valuable end-products, including energy, biofuels and chemicals [2]. A typical example of food-related biorefinery concept is that applied to algae, in particular microalgae [3], although this concept is nowadays being transferred to other fields involving food production.

Aronia melanocarpa, commonly called black chokeberry, is a plant belonging to Rosaceae family widely distributed around Europe [4]. Berry fruits from this plant are considered as one of the richest natural sources of anthocyanins and proanthocyanidins [5]. A common industrial use of black chokeberries is for juice production. The juice of these berries is highly-valued as it is considered as very rich on polyphenols [6] and it has been even pointed out as being the most antioxidant juice among the polyphenol-rich beverages [7]. Consequently, different studies have dealt with the study of the possible bioactivities associated to these berries' components, including antioxidant activity [8], as well as anti-inflammatory, anticancer, antibacterial or hepatoprotective activities, among others [9,10]. For this reason, different extraction techniques and approaches have been investigated to recover bioactives directly from chokeberries. For instance, maceration [11], ultrasound-assisted extraction [12] or microwave-assisted extraction [13] have been employed in combination with chemometric approaches. However, these approaches may not be directly transferred to waste extraction as technological processes have been demonstrated to have an influence on the final composition

☆ Selected paper from the 40th International Symposium on Capillary Chromatography and 13th GC × GC Symposium (RIVA 2016), 29 May–3 June 2016, Riva del Garda, Italy.

* Corresponding author.
E-mail address: m.herrero@csic.es (M. Herrero).

http://dx.doi.org/10.1016/j.chroma.2016.09.033
0021-9673/

on bioactives in black chokeberry [14]. This is why specific studies have been published using advanced extraction techniques to recover bioactives from black chokeberries by-products, such as juice wastes [15] or tea-related by-products [16].

Up to now, the possibility of using other pressurized approaches has not been comprehensively explored. Among these techniques, supercritical fluid extraction (SFE) and pressurized liquid extraction (PLE) are included. These processes have been recently screened to confirm the potential of black chokeberry products [17]. Whereas SFE, commonly operated with supercritical CO_2, is focused to non-polar components, PLE may be directed to the extraction of high and medium polarity compounds depending on the extraction solvent employed [18]. Thus, the combined use of these techniques may be interesting for the sequential valorization of food-related wastes, such as black chokeberries pomace. For this reason, following some promising initial results [17], the possibility of using PLE to further recover bioactives from the residue after the SFE of black chokeberries pomace is explored in this work. PLE is based on the use of pressurized solvents at high temperatures, maintaining their liquid state. Under those conditions, important gains in terms of mass transfer rates and process time are attained [19]. The generated PLE extracts using environmentally green solvents have been characterized in terms of total phenols content and antioxidant activity and an experimental design has been employed to study the influence of the main parameters involved in the extraction. Moreover, in an effort to correlate the bioactivities observed to the chemical composition of the generated extracts, a new comprehensive two-dimensional liquid chromatography method coupled to diode array and tandem mass spectrometry detection (LC × LC-DAD-MS/MS) has been developed for the chemical characterization of such complex extracts. To the best of our knowledge, this is the first report in which this analytical tool is applied to black chokeberry.

2. Materials and methods

2.1. Samples and chemicals

The dried pomace of black chokeberries was taken from the juice production line of Obuolių namai, (Joint Stock Company, Kaunas Dist, Lithuania). Black chokeberries (*Aronia melanocarpa* [Michx.] Elliott) were collected in the middle of August 2015 in a plantation near the production site. Dried pomace was ground in an ultracentrifugal rotor mill Retsch ZM200 (Retsch, Haan, Germany) to obtain the fraction of ≤0.5 mm particle size. The temperature did not exceed 30 °C during milling. The ground pomace was stored at a temperature of −20 °C until use. Supercritical fluid extraction was performed in a first step using CO_2 at 40 MPa and 40 °C for 150 min, according to Grunovaitė et al. [25]. The obtained raffinate after SFE was dried and stored at −20 °C.

Ultrapure water obtained from a Millipore purification system (Billerica, MA, USA), ethanol (99.5%) provided by VWR Chemicals (Fontenay-sous-Bois, France) and formic acid (98%) purchased from Sigma-Aldrich were used for PLE. 2,2-Diphenyl-1-picrylhydrazyl hydrate (DPPH, free radical, 99%), gallic acid, 6-hydroxy-2,5,7,8-tetramethylchroman-2-carboxylic acid (Trolox, ≥97%), 2,2′-azinobis(3-ethylbenzothiazoline-6-sulfonic acid (ABTS, ≥99%) and dimethyl sulfoxide (DMSO) were purchased from Sigma-Aldrich and acetonitrile from VWR chemicals. The Folin-Ciocalteu phenol reagent was provided by Merck (Darmstadt, Germany).

2.2. Pressurized liquid extraction (PLE)

Extractions were performed using a pressurized liquid extractor (ASE 200, Dionex, Sunnyvale, CA, USA), equipped with a solvent controller unit. Ultrapure water, ethanol and formic acid were used as solvents, as described below. At the beginning of the day, the solvents were sonicated for 10 min to avoid any possible dissolved air. For each extraction, 1 g of dried residue of black chokeberries pomace remaining after SFE were loaded into 11 mL stainless steel extraction cell after being mixed with 4 g of sea sand, employed as dispersive agent. Extraction cells were then filled with 1 g of sea sand and cellulose filters were placed at both ends. The extraction procedure briefly consisted of the following steps: the extraction cell was filled with the selected solvent and the pressure was increased to the desired level; initial instrumentally fixed heat-up time was then applied depending on the extraction temperature (i.e., 5 min when the extraction temperature was 50 °C, 6 min if the extraction temperature was 110 °C, and 8 min when the extraction temperature was 170 °C); static extraction takes place during 20 min, in which all valves remain closed to maintain a constant pressure (10.3 MPa); the extract is collected in a vial and the extraction cell rinsed with 60% of cell volume with the same extracting solvent; finally, extraction cell and lines are purged with pure nitrogen during 60 s. A thorough rinse of the system was applied between the successive extractions to avoid any carry-over from one experimental run into the next. After extraction, solvents were eliminated using a rotary evaporator (Büchi *R*-3000, Flawil, Switzerland) and a freeze-dryer (Labconco Corporation, Missouri, USA), depending on the solvents used. The dried extracts were stored at −20 °C protected from light until analysis.

2.3. Experimental design

PLE from black chokeberry pomace was optimized using a 3-level factorial design 3^3 studying the effects of temperature (50–170 °C), percentage of ethanol in the mixture solvent (0–100%) (*v*/*v*) and percentage of formic acid in the solvent (0–2%) on extraction yield (X_0%), total phenols content (mg GAE/g extract), antioxidant capacity (mM TE/g extract) and DPPH radical scavenging activity (EC_{50}, μg/ml). A total of 29 experiments were conducted in a randomized order, including two center points. The experimental design and data analysis were carried out using response surface methodology with the software Statgraphics Centurion XVI (StatPoint Technologies, Inc., Warrenton, VA, USA). The effects of the independent variables on the response variables in the extraction process were assessed using the pure error, considering a level of confidence of 95% for all the variables. The quadratic model proposed for each response variable (Y_i) was:

$$Y_i = \beta_0 + \beta_1 T + \beta_2 E + \beta_3 F + \beta_{1,1} T^2 + \beta_{2,2} E^2 + \beta_{3,3} F^2 + \beta_{1,2} T \times E + \beta_{1,3} T \times F + \beta_{2,3} E \times F + \text{error} \quad (1)$$

where T is the temperature, E is the solvent composition (percentage of ethanol in the mixture), F is the percentage of acid in the mixture, β0 is the intercept, β_1, β_2 and β_3 are the linear coefficients, $\beta_{1,1}$, $\beta_{2,2}$ and $\beta_{3,3}$ are quadratic coefficients, $\beta_{1,2}$, $\beta_{1,3}$ and $\beta_{2,3}$ are the two factor interaction coefficients, and error is the error variable. Linear models (Eq. (1)) were evaluated considering the percent variation explained by the determination coefficient (R^2), the residual standard deviation (RSD), and the lack-of-fit test for the model from the analysis of variance table, as the significance criteria. The effect of each factor and its statistical significance, for each of the response variables, was analyzed from the standardized Pareto chart. The response surfaces of the respective mathematical models were also obtained, and the significances were accepted at $p \leq 0.05$. A multiple response optimization was carried out by the combination of experimental factors, looking for maximizing the desirability function for the responses.

2.4. In vitro determinations

2.4.1. Total phenols content (Folin-Ciocalteu method)

Total phenols contents (TPC) of the PLE extracts were determined spectrophotometrically by using the Folin–Ciocalteu assay with some modifications, as previously described Montero et al. [20]. The total volume of reaction mixture was miniaturized to 1 mL and methanol was replaced by DMSO due to the low solubility of the extracts in the other solvents. Briefly, 10 μL aliquot of fresh extract solution (5 mg mL^{-1}) and 600 μL ultrapure water were mixed, and 50 μL undiluted Folin–Ciocalteu reagent was subsequently added. After 1 min, 150 μL of 20% (w/v) Na_2CO_3 were added and the volume was brought to 1.0 mL with ultrapure water. The samples were incubated for 2 h at 25 °C in the darkness. Later on, 300 μL of each reaction mixture were transferred to 96–well microplate. The absorbance was measured at 760 nm in a microplate spectrophotometer reader (Synergy HT, BioTek Instruments, Winooski, VT). Standard curves with serial gallic acid solutions (0.031–2 mg mL^{-1}) were used for calibration. The TPC was expressed as mg of gallic acid equivalents (GAE) per g of extract. All analyses were done in triplicate.

2.4.2. Trolox equivalents antioxidant capacity assay (TEAC)

The TEAC was determined using the method described by Re et al. [21] with some modifications. The $ABTS^{\bullet+}$ radical was produced by reacting 7 mM ABTS and 2.45 mM potasium persulfate in the dark at room temperature during 16 h before use. The aqueous $ABTS^{\bullet+}$ solution was diluted with 5 mM phosphate buffer (pH 7.4) to an absorbance of 0.7 (±0.02) at 734 nm. The samples (10 μL, 5 different concentrations from 0.0438 to 1.5 mg mL^{-1}) and 1 mL of $ABTS^{\bullet+}$ solution were mixed in an Eppendorf vial. After incubation for 45 min, 300 μL of the mixture were transferred into a 96-well microplate. The absorbance of end point was measured at 734 nm in a microplate spectrophotometer reader (Synergy HT, BioTek Instruments, Winooski, VT, USA). Trolox was used as reference standard and the results were expressed as TEAC values (mmol of trolox/g extract). These values were obtained from five different concentrations of each extract that were tested in the assay giving a linear response between 20% and 80% of the blank absorbance. All analyses were done in triplicate.

2.4.3. DPPH radical scavenging assay

The DPPH radical scavenging method was carried out adapting the procedure described by Brand-Williams et al. [22], as follows: a stock solution was prepared dissolving 23.5 mg of DPPH in 100 mL of methanol which was further diluted 1:10 with methanol to give the working solution. Both stock and working solutions were stored at 4 °C until use. Five different concentrations of extracts were tested (from 0.0469 to 0.75 mg mL^{-1}). Ten μL of each extract concentration solution were mixed in the 96-well microplate with 290 μL of DPPH diluted solution to complete the final reaction medium (300 μL). The reaction was kept in darkness for 4 h at room temperature. Once the reaction was finished, the absorbance was measured at 516 nm in a microplate spectrophotometer reader (Synergy HT, BioTek Instruments, Winooski, VT, USA). DPPH-methanol solution was used as a control sample. The DPPH concentration remaining in the reaction medium was calculated from a calibration curve. The percentage of remaining DPPH against the extract concentration was then plotted to obtain the amount of antioxidant necessary (expressed in μg mL^{-1}) to decrease the initial DPPH concentration by 50%, that is, the EC_{50} value. Measurements were done by triplicate.

2.5. Comprehensive two-dimensional liquid chromatography (LC × LC) analysis of black chokeberry extracts

2.5.1. Instrumentation

The LC × LC-DAD-MS instrumentation consisted on a first dimension (^{1}D) composed by an Agilent 1200 series liquid chromatograph (Agilent Technologies, Santa Clara, CA) equipped with an autosampler. In order to obtain more reproducible low flow rates and gradients, a Protecol flow-splitter (SGE Analytical Science, Milton Keynes, UK) was placed between the ^{1}D pump and the autosampler. Additionally, a LC pump (Agilent 1290 Infinity) performed the second dimension (^{2}D). Both dimensions were connected by an electronically-controlled two-position ten-port switching valve acting as modulator equipped with two identical 30 μL injection loops. Modulation time of the switching valve was 1.3 min. A diode array detector was coupled after the second dimension in order to register every ^{2}D analysis. Besides, an Agilent 6320 Ion Trap mass spectrometer equipped with an electrospray interface working in positive and negative ionization mode was coupled in series using the following conditions: dry temperature, 350 °C; dry gas flow rate, 12 L min^{-1}; nebulization pressure, 35 psi; mass range, m/z 90–2200 Da. The LC data were elaborated and visualized using LC Image software (version 1.0, Zoex Corp., Houston, TX).

2.5.2. LC × LC separation conditions

The separation on the ^{1}D was carried out on a Hypersil GOLD amino column (150 × 1 mm, 3 μm, Thermo Scientific, Waltham, MA). The mobile phases were (A) ACN/formic acid, 99:1 (*v/v*) and (B) H_2O/formic acid, 95:5 (*v/v*) eluted according to the following gradient: 0 min, 1% B; 60 min, 30% B; 65 min, 40% B; 75 min, 90% B. The flow rate was established at 18 μL min^{-1} and the injection volume was 7 μL, maintaining a column temperature of 25 °C. The modulation time was 1.3 min, the same time as a single ^{2}D analysis. In the ^{2}D separation repetitive 1.3 min analyses were carried out during the whole LC × LC analysis employing an Ascentis Express C_{18} partially porous column (50 × 4.6 mm, 2.7 μm, Supelco, Bellefonte, CA) and using (A) H_2O + 0.1% formic acid and (B) ACN as mobile phases at a flow rate of 3 mL min^{-1}. The repetitive gradients were programmed as follows: 0 min, 0% B; 0.1 min, 5% B, 0.3 min, 15% B; 0.7 min, 40% B; 0.9 min, 50% B, 1 min, 90% B. The separation was carried out at 25 °C and monitored at 280 and 254 nm in the DAD, whereas UV–vis spectra were collected from 190 to 550 nm during the whole analysis using a sampling rate of 20 Hz. The flow eluting from the ^{2}D column was splitted before its entrance on the MS detector, being ca. 0.4 mL min^{-1} the flow rate introduced on the ESI source. The MS detection was carried out in a negative and positive ionization mode using the conditions stated above.

3. Results and discussion

3.1. PLE of black chokeberry pomace

Valorization of food industry-related residues for the production of bioactive compounds reusable in other applications is a hot research topic today. From a biorefinery point of view, it is interesting to develop integrated or coupled processes that can make possible the subsequent reutilization of each residue. In this regard, this work assesses the possibility of using PLE as a downstream extraction technique for the recovery of bioactive compounds from black chokeberry pomace generated as a by-product from juice production that has been already submitted to supercritical fluid extraction using neat CO_2 to recover tocopherols. Thus, PLE is employed as a second step in the valorization chain of black chokeberry pomace.

Table 1
Experimental matrix design conditions (factor levels between parentheses) and results for each response variable studied for the optimization of the PLE of black chokeberry pomace. Values presented are mean ± sd.

Exp. Run	PLE extraction conditions			Response Variables			
	Temp. (°C)	Ethanol (%)	Formic acid (%)	Yield (%)	TPC (mg GAE g^{-1})[a]	TEAC (mmol TE g^{-1})[b]	EC_{50} (μg/ml)[c]
1	50 (−1)	0 (−1)	0 (−1)	24.48	86.69 ± 3.34	1.684 ± 0.067	17.36 ± 0.62
2	50 (−1)	50 (0)	0 (−1)	33.24	200.30 ± 2.85	3.627 ± 0.039	7.16 ± 0.12
3	50 (−1)	100 (+1)	0 (−1)	20.82	181.96 ± 4.03	3.396 ± 0.214	6.33 ± 0.27
4	50 (−1)	0 (−1)	1 (0)	27.63	95.54 ± 0.75	1.860 ± 0.052	17.85 ± 0.35
5	50 (−1)	50 (0)	1 (0)	35.06	201.53 ± 5.40	4.032 ± 0.077	6.39 ± 0.16
6	50 (−1)	100 (+1)	1 (0)	26.35	167.84 ± 4.20	2.878 ± 0.080	6.72 ± 0.22
7	50 (−1)	0 (−1)	2 (+1)	28.40	97.18 ± 1.27	2.752 ± 0.013	11.66 ± 0.57
8	50 (−1)	50 (0)	2 (+1)	36.05	205.53 ± 6.10	4.188 ± 0.152	7.48 ± 0.24
9	50 (−1)	100 (+1)	2 (+1)	26.73	143.40 ± 2.55	2.743 ± 0.076	9.22 ± 0.21
10	110 (0)	0 (−1)	0 (−1)	36.09	183.02 ± 2.75	3.505 ± 0.069	6.95 ± 0.15
11	110 (0)	50 (0)	0 (−1)	42.00	219.19 ± 2.95	4.584 ± 0.018	5.47 ± 0.15
12	110 (0)	100 (+1)	0 (−1)	32.18	198.51 ± 3.09	3.453 ± 0.024	8.04 ± 0.49
13	110 (0)	0 (−1)	1 (0)	39.27	172.68 ± 0.46	3.753 ± 0.022	5.91 ± 0.12
14[d]	110 (0)	50 (0)	1 (0)	49.56	254.89 ± 13.17	4.764 ± 0.142	5.50 ± 0.21
15[d]	110 (0)	50 (0)	1 (0)	49.57	253.28 ± 19.00	4.762 ± 0.285	5.06 ± 0.15
16[d]	110 (0)	50 (0)	1 (0)	50.59	239.98 ± 11.07	4.997 ± 0.174	5.67 ± 0.20
17	110 (0)	100 (+1)	1 (0)	31.79	198.15 ± 12.92	3.931 ± 0.066	7.43 ± 0.34
18	110 (0)	0 (−1)	2 (+1)	44.27	181.43 ± 1.04	3.443 ± 0.069	8.19 ± 0.37
19	110 (0)	50 (0)	2 (+1)	55.21	230.04 ± 4.84	4.650 ± 0.105	5.73 ± 0.22
20	110 (0)	100 (+1)	2 (+1)	35.03	193.56 ± 5.59	3.894 ± 0.014	7.03 ± 0.16
21	170 (+1)	0 (−1)	0 (−1)	48.94	152.14 ± 6.84	3.275 ± 0.141	8.10 ± 0.36
22	170 (+1)	50 (0)	0 (−1)	59.81	258.31 ± 13.34	4.521 ± 0.278	5.61 ± 0.13
23	170 (+1)	100 (+1)	0 (−1)	36.84	204.75 ± 3.53	3.951 ± 0.281	7.39 ± 0.31
24	170 (+1)	0 (−1)	1 (0)	62.67	199.38 ± 11.75	3.320 ± 0.212	7.48 ± 0.37
25	170 (+1)	50 (0)	1 (0)	73.49	221.99 ±1.92	4.404 ± 0.341	5.93 ± 0.24
26	170 (+1)	100 (+1)	1 (0)	39.24	226.67 ± 3.06	4.353 ± 0.223	8.45 ± 0.44
27	170 (+1)	0 (−1)	2 (+1)	64.77	194.75 ± 4.92	3.288 ± 0.216	7.34 ± 0.08
28	170 (+1)	50 (0)	2 (+1)	75.66	227.24 ± 4.73	4.312 ± 0.245	6.62 ± 0.34
29	170 (+1)	100 (+1)	2 (+1)	40.75	227.90 ± 6.01	4.053 ± 0.203	7.65 ± 0.17

[a] mg gallic acid equivalents g^{-1} extract.
[b] mmol trolox equivalents g^{-1} extract.
[c] DPPH assay efficient concentration (μg ml^{-1}).
[d] Experimental design center points.

In this regard, an experimental design is proposed in order to study the significance of the main parameters involved in the extraction, i.e., extraction temperature (50–170 °C), extraction solvent composition (water/ethanol mixtures), acid composition (formic acid, from 0 to 2%). The rest of extraction conditions were kept constant based on our previous experience, as follows: static extraction time, 20 min; extraction pressure, 10.3 MPa. By using a three-level factorial experimental design considering these three factors, the influence of extraction conditions on four different response variables, namely extraction yield, total phenols amount, TEAC value and EC_{50} was studied. Experimental matrix as well as the results obtained at each extraction condition for the four response variables are summarized in Table 1. Results corresponding to the ANOVA for the different responses are included as Supplementary data (Table S1). As it can be observed, the different response variables had diverse behaviors as a consequence of the modification of the extraction factors considered. Extraction yield increased with temperature for all the solvent mixtures considered, reaching a maximum when 50% ethanol containing 2% formic acid was used as solvent at 170 °C. In general, it is possible to observe that 50% ethanol was the solvent mixture that produced higher yields compared to the use of either pure ethanol or pure water. Considering the presence of acid in the solvent, the addition of formic acid significantly increased the attainable yields compared to the extractions in which it was not used. A further increase from 1% to 2% formic acid produced slight increases in extraction yield. TPC of the extracts was also raised at high temperatures, although the effect from 110 to 170 °C was less marked. The richest extract on phenols recovered was produced with 50% ethanol at 170 °C without the addition of acid (258.31 mg GAE g^{-1}). In general, 50% ethanol was clearly the most suitable solvent for the extraction of total phenols. The addition of acid to the solvent was favorable for the extraction of phenols when pure water was employed. In the other cases, no clear effect was observed. Lastly, regarding the antioxidant capacity of the extracts, the most active were found at 110 °C using 50% ethanol containing 1% formic acid (4.997 mmol TE g^{-1} and 5.06 μg mL^{-1} for TEAC and DPPH assays, respectively). For these response variables, temperature was the most influencing factor, observing a significant increase from 50 to 110 °C for the same solvent mixture and then a slight decrease at higher temperatures.

Fig. 1 illustrates the corresponding standardized Pareto charts for the four response variables studied as well as their corresponding response surfaces maintaining constant the formic acid proportion to 1%. Different bar color shadings indicate positive and negative effects whereas the vertical line tests the significance of the effects at the 95% confidence level. As it can be seen, temperature, ethanol proportion in the solvent mixture as well as its quadratic effect are among the most important significant factors for the four response variables. As expected, temperature is the most influencing factor for extraction yield. Moreover, from the response surfaces it is also possible to observe great similarities for the total phenols content and the two antioxidant activity responses. In those variables, an increase on temperature has a positive effect in the low ranges but a negative effect at very high values. In any case, in the four response surfaces is possible to observe a positive effect of the addition of ethanol to the solvent mixture up to a certain point. Looking at the different behaviors and in an effort to determine the most suitable extraction conditions in order to have the best possible values (highest possible extraction yield, TPC, TEAC and lowest possible EC_{50}) a multiple response optimization was carried out considering similar statistical weight

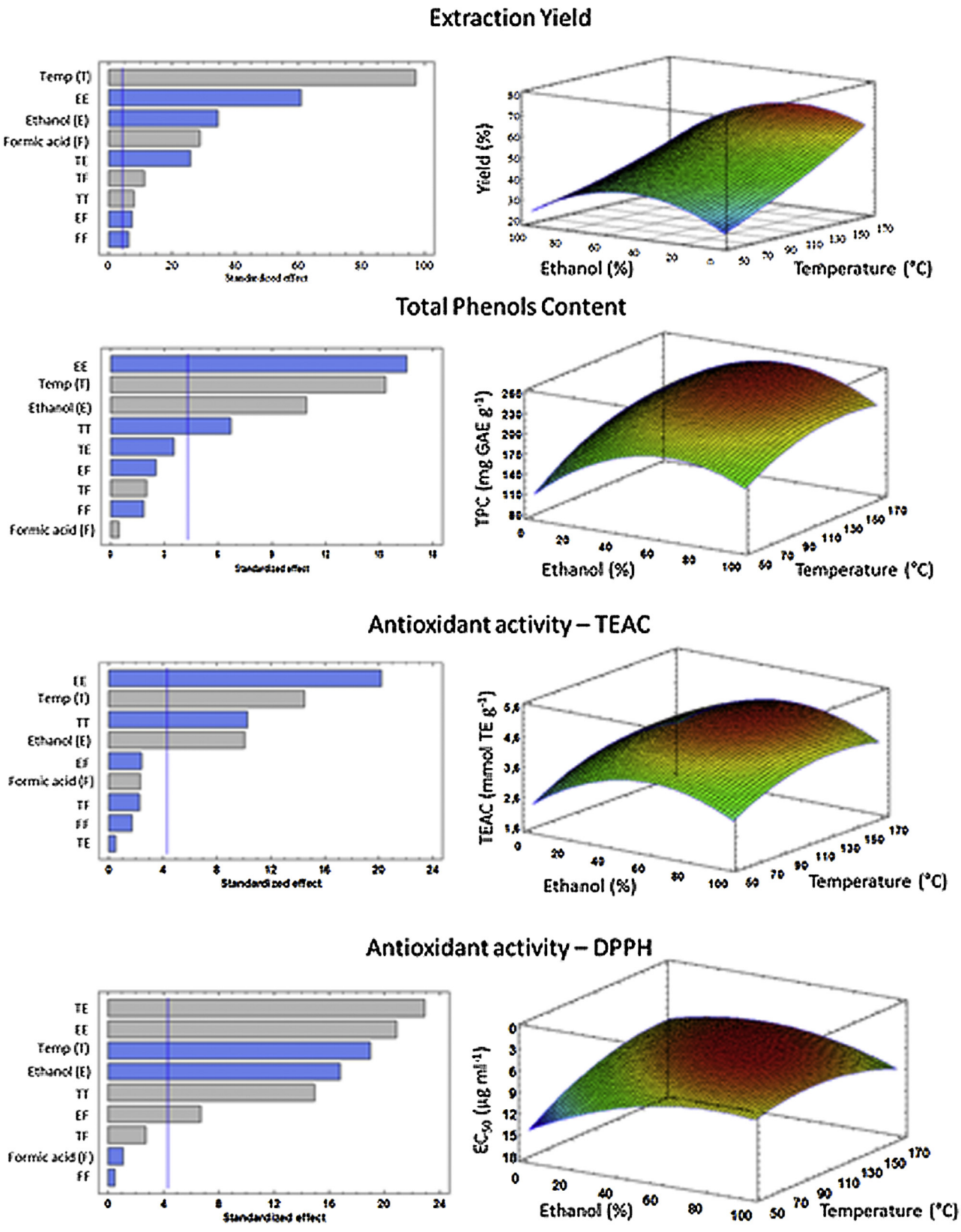

Fig. 1. Standardized Pareto charts for the four response variables studied in the experimental design (grey and blue-shaded bars show positive negative effects, respectively) and their corresponding response surfaces with 1% formic acid.

to the four response variables. Using this approach, the optimum extraction conditions provided by the statistical model involved the extraction with 46% ethanol containing 1.8% formic acid at 165 °C. Using this extraction conditions, the statistical model predicted the values for the four response variables as shown in Table 2. To check the validity of the approach, three independent PLE extractions

Table 2
Optimum PLE conditions provided by the statistical model for the black chokeberry pomace. Values of the response variables predicted and experimentally obtained. Results expressed as mean ± sd of three independent replicates.

	PLE extraction conditions			Response variables			
	Temp. (°C)	Ethanol (%)	Formic acid (%)	Extraction yield (%)	TPC (mg GAE/g extract)	TEAC (mmol Trolox/g extract)	DPPH (EC_{50}, μg/ml)
Predicted	164.9	46.3	1.81	69.00	252.00	4.667	5.33
Experimental	165	46	1.8	72.53 ± 0.02	236.64 ± 3.72	4.346 ± 0.241	5.92 ± 0.23
			Difference (%)	+5.11	−6.10	−6.89	+11.11

were carried out at optimized conditions, and the four response variables determined. The obtained experimental results in the optimum were in good agreement with those predicted, as can be observed in Table 2, thus, confirming the validity of our approach. Based on these results, it can be thus affirmed that PLE in combination with SFE can be a valuable, scalable and environmentally green tool to produce the downstream valorization of a common food by-product such as black chokeberry pomace. The extracts generated possessed very high antioxidant activity and were produced with high extraction yields, which even increases the feasibility of this approach. In any case, to gain more insight on the composition of the attained extracts in order to know which particular compounds could be responsible for such bioactivities, their chemical characterization was studied by using advanced multidimensional analytical techniques.

3.2. Chemical characterization of black chokeberry pomace PLE extracts

Once the usefulness of PLE to obtain bioactive compounds from black chokeberry pomace, and thus, to produce the downstream valorization of this by-product was demonstrated, a new comprehensive two-dimensional liquid chromatography tandem diode array and mass spectrometry detection (LC × LC-DAD-MS) method was set up to separate and identify the compounds contained in the extracts that could be effectively responsible for such bioactivities. The use of this approach is greatly interesting considering the complexity of the bioactive components present in black chokeberry, mainly based on polymeric proanthocyanidins. In fact, up to now, one-dimensional approaches have not been demonstrated to be able to provide a separation power enough to characterize this kind of samples. For this reason, isolation of individual components and subsequent analysis of isolated fractions has been used [5,23,24]. However, the use of LC × LC allows significantly increasing the separation power being possible to resolve very complex samples with multiple closely related components that may coelute using just one separation mechanism. In this regard, although the coupling of two separations based on the same principles (e.g., RP × RP) is feasible, the use of non-correlated separation mechanism in the two dimensions is highly desirable. The combination between HILIC in the ^{1}D and RP in the ^{2}D has already shown a high degree of orthogonality and different methods based on this approach have been developed for the separation of very complex samples [25,26].

Since this is the first time that LC × LC is applied to this kind of sample, an exhaustive optimization of the separation conditions in each dimension was required, testing different stationary and mobile phases. In particular, three different HILIC-compatible stationary phases were tested in ^{1}D, namely silica, diol and amino columns. Fig. 2 shows the separation of the black chokeberry PLE extract obtained after the individual optimization of separation conditions for each column. As can be observed, the amino stationary phase (Fig. 2C) provided the best separation and distribution of the sample along the chromatogram. A wide peak distribution in ^{1}D is preferred in order to allow a good sampling into the ^{2}D. Thus, this column was chosen for the LC × LC set-up. Regarding to the ^{2}D, the availability of different columns for extremely fast separations at high flow rates is more limited. Although a number of stationary phases are available, C_{18} columns are repeatedly selected in different applications because their superior resolving power at those conditions [25]. Besides, this separation mode and stationary phase allow for a very fast column re-equilibration, one of the conditions needed in this kind of two-dimensional set-up. Among C_{18} columns, partially porous stationary phases are well suited for very high flow rates providing high efficiency values at notably lower backpressures compared to fully-porous materials or sub 2 μm particles. Consequently, in the preset work a 5 cm short partially-porous C_{18} column was selected. Different mobile phases (comprising water, ACN, methanol and their mixtures) with or without acid as additive (formic and acetic acids) and different gradients were tested. After optimization, mobile phases composed by (A) H_2O + 2.5% formic acid and (B) ACN were selected. Finally, once the optimum conditions for both dimensions were established, the fine-tuning of the overall LC × LC coupling was carried out employing the selected conditions for each dimension. This optimization consisted of an adjustment of the ^{2}D mobile phase composition as the high percentage of formic acid employed (2.5%) provided a high background MS signal. Consequently, the percentage of acid in the mobile phase was reduced to 0.1%.

The transfer of fractions from the first to the second dimension was performed using identical 30 μL injection loops installed in the switching valve acting as modulator. The use of loops with slightly higher volume than theoretically necessary (23.4 μL in this case) considering modulation time and ^{1}D flow rate has been already demonstrated to be useful to reduce ^{2}D peak distortion related to solvent incompatibility between dimensions [27].

Using those analytical conditions in combination with DAD and MS detectors, a good separation of the complex PLE extracts could be obtained, as it can be appreciated in Fig. 3. A high theoretical peak capacity, calculated according to Li et al. [28], equal to 1693 was obtained. Furthermore, the orthogonality of the optimized method was assessed according to [29]. By using this approach considering the separated and identified compounds (see Fig. 3), an orthogonality value (A_0) of 76% was obtained, thus, confirming the good resolution capabilities obtained. In fact, as it can be inferred from the peak positions in the 2D plane, very low correlation between the separation mechanisms in the two dimensions were achieved. Moreover, it can be deduced that the obtained A_0 value was not even higher due to the relatively low spreading of most peaks from the Z_+ axis [29]. Considering both values, and thus, both undersampling and orthogonality effects on the 2D separation, the "practical" peak capacity obtained was 1287. In any case, like in any other peak capacity calculations, this value should be considered just as a measure of the coupling potential and not a real figure of the peaks that could be separated in practice, as a sample with a chemical pattern so precise to fill all available 2D plane will not exist.

Table 3 summarizes the proposed identification of the 61 peaks separated after the LC × LC analysis of black chokeberry pomace PLE extracts. As it can be observed, in the complex pattern obtained, anthocyanins, proanthocyanidins, flavonoids and phenolic acids could be identified.

Table 3
Tentative identification of the metabolites present in the *Aronia melanocarpa* pomace PLE extract obtained at the optimum extraction conditions (46% ethanol containing 1.8% formic acid at 165 °C).

Peak	Total t_r (min)	t_r ^{2}D (s)	λ max (nm)	Positive ionization		Negative ionization		Identification proposed	Phenolic class
				$[M]^+/[M+H]^+$	Main MS/MS fragments	$[M-H]^-$	Main MS/MS fragments		
1	15.36	63.65	254, 370	349.6	209, 131			NI	
2	17.79	53.05	280	499.8	481, 442, 347, 271			NI	
3	18.86	39.70	258, 294, 510	421.1	375, 288			NI (Cyanidin derivative)	Anthocyanin
4	20.19	41.05	278, 515	419.4	287			Cyanidin arabinoside, cyanidin xyloside	Anthocyanin
5	20.22	43.50		419.2	287, 259			Cyanidin arabinoside, cyanidin xyloside	Anthocyanin
6	21.80	59.90	270	453.5	301, 139			NI	
7	24.08	41.00	515	419.3	287			Cyanidin arabinoside, cyanidin xyloside	Anthocyanin
8	24.10	41.95		419.3	287			Cyanidin arabinoside, cyanidin xyloside	Anthocyanin
9	24.17	46.40	280	291.3	273, 165, 151, 139, 123	289.8	246, 206, 126	(Epi)catechin	Flavanol
10	27.99	41.05	280, 515	419.2	287			Cyanidin arabinoside, cyanidin xyloside	Anthocyanin
11	30.73	50.25	290, 320			305.1	286, 259, 193, 167	(Epi)gallocatechin	Flavanol
12	33.25	44.65	290	439.5	393, 247, 203, 191, 135			NI	
13	37.10	42.05	280, 514	419.2	287			Cyanidin arabinoside, cyanidin xyloside	Anthocyanin
14	38.36	39.35	280, 515	449.3	287			Cyanidin glucoside, cyanidin galactoside	Anthocyanin
15	38.43	44.25		449.2	287			Cyanidin glucoside, cyanidin galactoside	Anthocyanin
16	39.85	51.15	285			550.3	503, 443, 383, 333, 259	NI	
17	39.98	58.45	290	577.3	559, 449, 425, 287			Procyanidin dimer	Proanthocyanidin
18	42.13	49.60	268, 298	479.4	419, 331, 299, 193			NI	
19	43.56	39.50	282, 515	449.3	287			Cyanidin glucoside, cyanidin galactoside	Anthocyanin
20	43.58	40.85	280, 515	449.3	287			Cyanidin glucoside, cyanidin galactoside	Anthocyanin
21	43.78	52.65		435.2	415, 367, 303, 285			Delphinidin arabinoside	Anthocyanin
22	43.82	55.05	275, 380			591.5	531, 465, 439, 303, 215	Prodelphinidin dimer	Proanthocyanidin
23	44.98	46.80	246, 295			433.2	411, 385, 311, 301, 271	Quercetin pentoside	Flavonol
24	45.17	58.30		591.5	573, 465, 477, 438, 419, 287			NI (proanthocyanidin derivative)	Proanthocyanidin
25	46.23	43.50		421.2	401, 383, 287			NI (cyanidin derivative)	Anthocyanin
26	46.24	44.50		450.4	287			Cyanidin glucoside, cyanidin galactoside	Anthocyanin
27	47.59	47.15	280	577.4	409, 289	575.6	467, 449, 424, 330, 288	Procyanindin dimer	Proanthocyanidin
28	47.65	50.65	254, 355	465.2	303	463.8	301	Quercetin glucoside or galactoside	Flavonol
29	47.73	55.70	260, 298	465.0	303	463.7	301	Quercetin glucoside or galactoside	Flavonol
30	48.75	39.20	280, 515	451.7	287			NI (cyanidin derivative)	Anthocyanin
31	48.85	44.65	274	577.9	428	575.4	449, 423, 405, 287, 243	Procyanidin dimer	Proanthocyanidin
32	49.00	54.10	320			593.5	523, 466, 423, 305, 245	Prodelphinidin dimer	Proanthocyanidin
33	50.08	40.50	285			835.5	773, 703, 581, 417, 284	NI	
34	50.16	45.50	274			593.7	575, 449, 421, 289, 247	Prodelphinidin dimer	Proanthocyanidin
35	50.22	49.35	268	735.4	573			NI	
36	51.43	43.45	350			476.4	431, 315, 271	NI	
37	51.56	51.50		625.5	479, 463, 317			Petunidin-*p*-coumaroyl glucoside	Anthocyanin
38	51.65	56.75		404.8	209, 120			NI	
39	52.62	37.70	288			865.7	733, 447, 417, 285	Procyanidin trimer	Proanthocyanidin
40	52.67	39.90	280			865.3	703, 573, 447, 417, 285	Procyanidin trimer	Proanthocyanidin
41	52.72	43.00	300, 325	355.7	163	708.5	353	Chlorogenic acid	Phenolic acid
42	54.02	43.00	296, 324			865.8	733, 703, 576, 447, 417, 285	Procyanidin trimer	Proanthocyanidin
43	55.22	36.85	285			515.6	498, 425, 353	Dicaffeoylquinic acid	Phenolic acid
44	55.41	48.90	256, 355	611.4	479, 465, 449, 317, 303	609.4	533, 464, 362, 346, 302	Quercetin rutinoside, quercetin rhamnosylgalactoside	Flavonol
45	56.63	43.75	267, 300	751.4	589, 453			(Epi)catechin-peonidin-3-*O*-glucoside	Anthocyanin derivative
46	56.68	46.70	280	611.8	465, 449, 303	609.8		Quercetin rutinoside, quercetin rhamnosylgalactoside	Flavonol
47	56.80	54.20	280	611.2	465, 449, 303			Quercetin rutinoside, quercetin rhamnosylgalactoside	Flavonol
48	59.16	39.40	294, 324			356.8	193, 181, 137	NI	
49	59.27	46.35	256, 352	619.5	487, 317			NI	
50	59.30	47.80	255, 352	597.1	465, 435, 303			Quercetin vicianoside	Flavonol
51	60.43	37.55	286, 515	897.4	735	895.8	733, 447, 284	NI (cyanidin hexoside derivative)	Anthocyanin
52	63.14	44.15	270, 338			595.4	577, 505, 475, 385, 355, 301	NI (proanthocyanidin derivative)	Proanthocyanidin
53	63.27	52.35	284, 334	465.3	289			Eriodictyol glucuronide	Flavanone
54	65.62	37.10	280	452.1	365, 288			Eriodictyol hexoside	Flavanone
55	65.80	47.90	280	579.9[a]	848, 803, 735, 451, 427, 289, 247, 179			**Procyanidin tetramer**	**Proanthocyanidin**
56	68.23	37.80	280	482.8	463, 397, 305, 287, 153			NI	
57	68.30	42.00		452.0	288			NI (cyanidin derivative)	Anthocyanin
58	68.41	48.35	280	406.5	389, 319, 183, 139			NI	
59	69.62	43.30	280			1053.8	975, 957, 903, 861, 843, 801, 783, 687, 423	NI	
60	69.71	48.30	280			1035.6	975, 903, 861, 843, 729, 687	NI	
61	72.21	42.70				862.9[b]	1438, 1287, 1103, 801, 730, 669, 575	Procyanidin hexamer	Proanthocyanidin

NI, not identified.

[a] $[M+2H]^{2+}$.

[b] $[M-2H]^{2-}$.

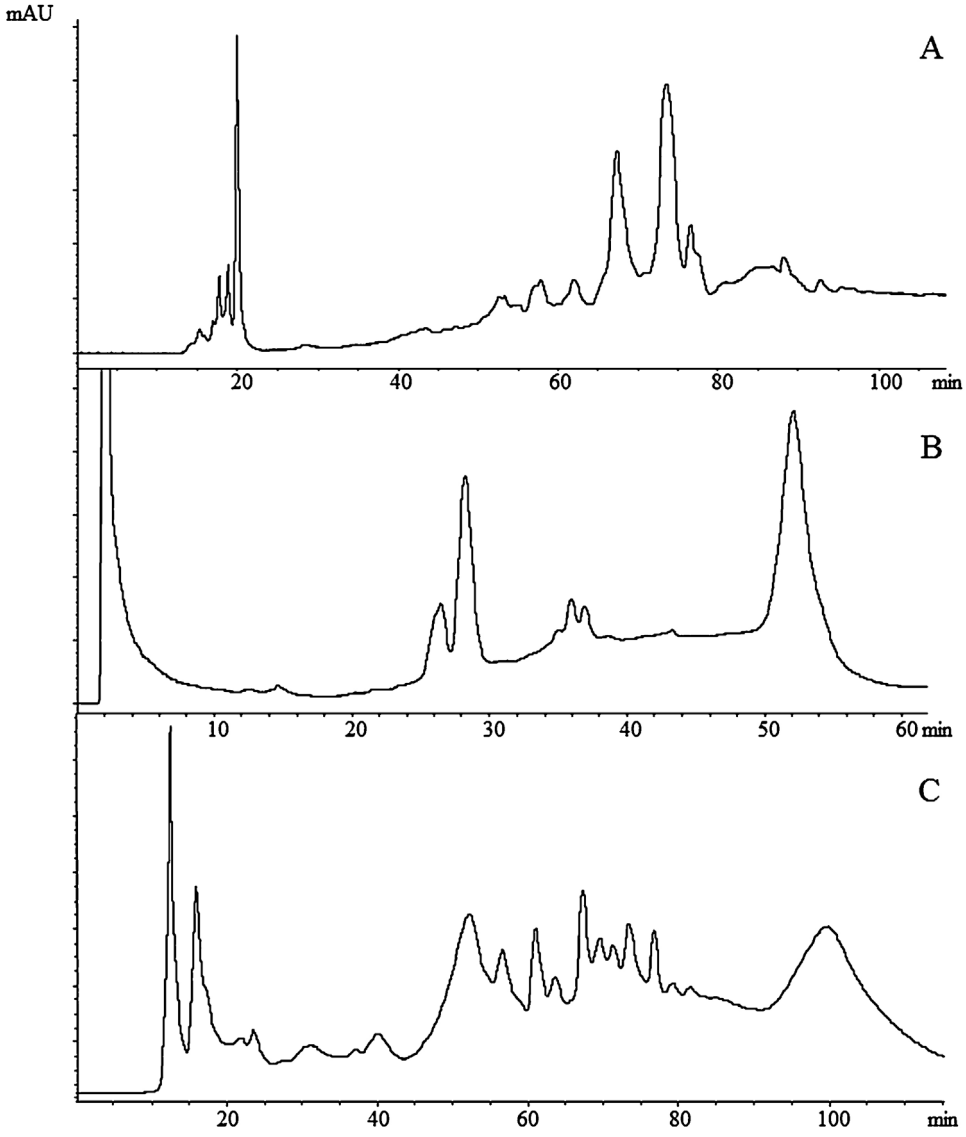

Fig. 2. Chromatograms (280 nm) corresponding to the optimized separations of the black chokeberry PLE extracts under first dimension conditions using different stationary phases: A, silica column (250 × 2.1 mm, 5 μm, Syncronis HILIC, Thermo Scientific) eluted using ACN and H_2O/HCOOH, 97.5:2.5 (*v*/*v*) as mobile phases; B, diol column (150 × 1.0 mm, 5 μm, Lichrospher diol-5, HiChrom) using ACN/HCOOH, 95:5 (v/v) and H_2O/HCOOH, 95:5 (v/v) as mobile phases; C, amino column (150 × 1 mm, 3 μm,, Hypersil GOLD Thermo Scientific) eluted using ACN/HCOOH, 99:1 (*v*/*v*) and H_2O/HCOOH as mobile phases.

3.2.1. Anthocyanins

This group of compounds was the most numerous in the black chokeberry PLE extracts and involved some of the main components separated. Among them, different cyanidin glycosides were tentatively identified. The identification of these peaks was based on characteristics *m*/*z* detected under positive ionization conditions that upon MS/MS fragmentation yielded losses of 162 or 132 Da and fragment ions at *m*/*z* 287, typical from cyanidin aglycone. This was the case for peaks 14, 19 and 20 which were amongst the most intense peaks detected. In this case, *m*/*z* detected at 449.3, with losses of 162 Da clearly indicated the presence of cyanidin glucosides or galactosides. Other separated peaks presented the same fragmentation pattern, and thus, were assigned to different cyanidin glucoside isomers (peaks 15 and 26). Another group of anthocyanins was composed by several cyanidin arabinosides and cyanidin xylosides. In this case, *m*/*z* ions at 419.5 were found, presenting fragment ions of cyanidin aglycone (*m*/*z* 287) (peaks 4, 5, 7, 8, 10 and 13). Unfortunately, under the analytical conditions employed, no conclusive identification of the involved isomers could be concluded. Other cyanidin derivatives could be detected (peaks 3, 25, 30, 57) due to the presence of the fragment at *m*/*z* 287, although no identification could be reached. In any case, cyanidin glycosides have been extensively described in black chokeberry and are regarded as one of the main bioactive compounds present on the chemical composition of these berries [5,8].

Besides, cyanidin-related components, other minor anthocyanins not previously identified in *Aronia melanocarpa* were detected: peak 21 was described as delphinidin arabinoside thanks to the molecular ion detected at *m*/*z* 435.2 and its fragment ions produced, including a delphinidin aglycone ion (*m*/*z* 285); peak 37 was assigned to petunidin *p*-coumaroyl-glucoside, in agreement with its ion at *m*/*z* 625.5 and characteristic fragments at *m*/*z* 479, 463 and 317; and, peak 45 was proposed as a peonidin-related glucoside ((epi)catechin-peonidin glucoside), presenting a molecular ion at *m*/*z* 751.4.

3.2.2. Proanthocyanidins

Proanthocyanidins are another abundant phenolic group present on chokeberry, and in particular, the procyanidin content on chokeberry is widely known [5,8,24]. Procyanidins consist

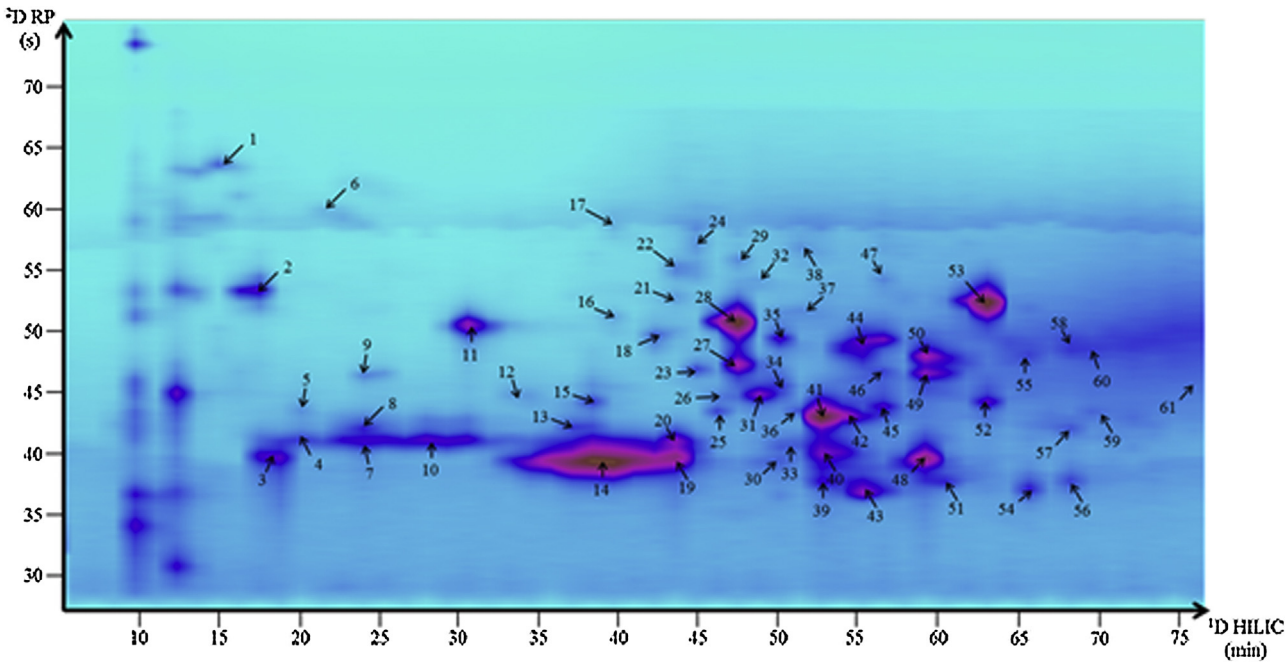

Fig. 3. 2D plot (280 nm) corresponding to the LC × LC separation of the black chokeberry pomace PLE extract obtained at 165 °C using 46% ethanol with 1.8% formic acid. For peak identification, see Table 3. For detailed separation conditions, see Section 2.5.2.

on polymers of different degree of polymerization formed by the monomers catechin, epicathechin and their corresponding galloylated forms.

Among the Proanthocyanidins present on the PLE extracts, several procyanidins with different degree of polymerization were detected under negative and positive ESI mode. In particular, procyanidin dimer (peaks 27 and 31, *m*/*z* 575.4 and 577.3 in negative and positive ionization mode, respectively), trimer (peaks 39, 40 and 42, presenting *m*/*z* at 865), tetramer (peak 55, with a doubly charged ion at *m*/*z* 579.9) and hexamer (peak 61, with $[M-2H]^{2-}$ at *m*/*z* 862.9) forms were tentatively assigned.

Moreover, in this work, other proanthocyanidins have been detected, namely prodelphinidins, which differ from procyanidins because of the presence of (epi)gallocatechins and their galloylated forms on their structure. Different prodelphinidin dimers were tentatively identified due to the detection of molecular ions at *m*/*z* 593.5 (peaks 22, 32 and 34) whereas their fragmentation pattern showed ions at *m*/*z* 575 (loss of 18 Da), 303 (loss of catechin moiety) and 289 (loss of gallocatechin unit). Although this kind of compounds has not been previously described in this sample, the high degree of separation obtained using comprehensive LC allowed their tentative assignment. Moreover, their presence is consistent with the determination of delphinidin glucoside in the extract.

Besides these peaks, others could be assigned to the group of proanthocyanidins thanks to their characteristic fragmentation patterns, although no conclusive identification could be achieved.

3.2.3. *Flavonoids and phenolic acids*

Lastly, several flavonoids were detected in the black chokeberry extract. (Epi)gallocatechin (peak 11) was one of the most intense peaks. This compound was assigned as a result of the detection of an ion at *m*/*z* 305.1 under negative ionization mode, with characteristic fragment ions (see Table 3). Related to this peak, another flavan-3-ol, (epi)catechin (peak 9) was also found. However, the most abundant flavonoid group in the studied sample belongs to flavonols. Different quercetin derivatives (peaks 23, 28, 29, 44, 46, 47 and 50) were detected. Among them, a quercetin glucoside (peak 28) presenting $[M-H]^-$ at *m*/*z* 463.8, quercetin rutinoside (peak 44) with $[M-H]^-$ at *m*/*z* 609.4, and quercetin vicianoside (peak 50, $[M+H]^+$ *m*/*z* 597.1) were the most intense. Other flavonoids present were identified as flavanones, more specifically, eriodictyol glucuronide and eriodictyol glucoside (peaks 53 and 54, respectively) thanks to the detection of characteristic molecular ions under positive ionization as well as fragment ions corresponding to eriodictyol.

Besides flavonoids, the complex chemical pattern of black chokeberry pomace extract included the presence of phenolic acids, which were detected under negative ionization mode. Peak 43 could be identified as dicaffeoylquinic acid in agreement with the molecular ion detected ($[M-H]^-$) at *m*/*z* 515.6 and the MS/MS fragmentation pattern observed (yielding ions at *m*/*z* 498, 425 and 353) whereas peak 41 was tentatively assigned to chlorogenic acid due to the detection of an ion at *m*/*z* 708.5 which could correspond to a $[2M-H]^-$ ion with characteristic fragment at *m*/*z* 353. Ions detected under positive ionization mode (see Table 3) helped to confirm this identification.

Thus, the use of this novel analytical approach has not only permitted the identification of a great variety of compounds in black choberry pomace extracts but also the tentative assignment of some prodelphinidins and anthocyanins not previously described in *Aronia melanocarpa*.

4. Conclusions

PLE has been demonstrated as a useful downstream green process for the valorization of black chokeberry (*Aronia melanocarpa*) pomace after SFE. Optimized conditions involved the use of pressurized 46% ethanol in water as solvent mixture at 165 °C with 1.8% formic acid. High total phenols content (236.6 mg GAE g^{-1} extract) and good antioxidant activities (4.35 mmol TE g^{-1} extract and EC_{50} 5.92 μg mL^{-1}) were obtained with extremely high extraction yields (72.5%). Moreover, the attained extracts were chemically characterized for the first time using a new LC × LC method; 61 different components could be separated, being possible the tentative identification of different anthocyanins, proanthocyanidins, flavonoids and phenolic acids.

Acknowledgements

This work was supported by MINECO, Spain (Project AGL2014-53609-P) and COST action TD1203 'Food Waste Valorisation for Sustainable Chemicals, Materials and Fuels (EUBIS)'.

Appendix A. Supplementary data

Supplementary data associated with this article can be found, in the online version, at http://dx.doi.org/10.1016/j.chroma.2016.09.033.

References

[1] D.S. Martin, S. Ramos, J. Zufía, Valorisation of food waste to produce new raw materials for animal feed, Food Chem. 198 (2016) 68–74.
[2] F. Cherubini, The biorefinery concept: using biomass instead of oil for producing energy and chemicals, Energy Convers. Manage. 51 (2010) 1412–1421.
[3] B. Gilbert-López, J.A. Mendiola, J. Fontecha, L.A.M. van den Broek, L. Sijtsma, A. Cifuentes, M. Herrero, E. Ibáñez, Downstream processing of *Isochrysis galbana*: a step towards microalgal biorefinery, Green Chem. 17 (2015) 4599–6609.
[4] S. Benvenuti, F. Pellati, M. Melegari, D. Bertelli, Polyphenols, anthocyanins, ascorbic acid, and radical scavenging activity of Rubus, Ribes, and Aronia, J. Food Sci. 69 (2004) 164–169.
[5] X. Wu, L. Gu, R.L. Prior, S. McKay, Characterization of anthocyanins and proanthocyanidins in some cultivars of *Ribes Aronia*, and *Sambucus* and their antioxidant capacity, J. Agric. Food Chem. 52 (2004) 7846–7856.
[6] D. Nowak, M. Gośliński, E. Wojtowicz, Comparative analysis of the antioxidant capacity of selected fruit juices and nectars: chokeberry juice as a rich source of polyphenols, Int. J. Food Prop. 19 (2016) 1317–1324.
[7] S.E. Kulling, H.M. Rawel, Chokeberry (*Aronia melanocarpa*)—a review on the characteristic components and potential health effects, Planta Med. 74 (2008) 1625–1634.
[8] P.N. Denev, C.G. Kratchanov, M. Ciz, A. Lojek, M.G. Kratchanova, Bioavailability and antioxidant activity of black chokeberry (Aronia melanocarpa) polyphenols: in vitro and in vivo evidences and possible mechanisms of action: a review, Compr. Rev. Food Sci. Food Saf. 11 (2012) 471–489.
[9] A. Kokotkiewicz, Z. Jaremicz, M. Luczkiewicz, *Aronia* plants: a review of traditional use, biological activities, and perspectives for modern medicine, J. Med. Food. 13 (2010) 255–269.
[10] I. Sainova, V. Pavlova, B. Alexieva, I. Vavrek, E. Nikolova, S. Valcheva-Kuzmanova, T. Markova, M. Krachanova, P. Denev, Chemoprotective, antioxidant and immunomodulatory *in vitro* effects of *Aronia melanocarpa* total extract on laboratory-cultivated normal and malignant cells, J. BioSci. Biotechnol. (2012) 35–43, SE/ONLINE.
[11] N. Čujić, K. Šavikin, T. Janković, D. Pljevljakušić, G. Zdunić, S. Ibrić, Optimization of polyphenols extraction from dried chokeberry using maceration as traditional technique, Food Chem. 194 (2016) 135–142.
[12] L.G. d'Alessandro, K. Kriaa, I. Nikov, K. Dimitrov, Ultrasound assisted extraction of polyphenols from black chokeberry, Sep. Purif. Technol. 93 (2012) 42–47.
[13] V.M. Simić, K.M. Rajković, S.S. Stojičević, D.T. Veličković, N.Č. Nikolić, M.L. Lazić, I.T. Karabegović, Optimization of microwave-assisted extraction of total polyphenolic compounds from chokeberries by response surface methodology and artificial neural network, Sep. Purif. Technol. 160 (2016) 89–97.
[14] N.D. Thi, E.S. Hwang, Effects of drying methods on contents of bioactive compounds and antioxidant activities of black chokeberries (*Aronia melanocarpa*), Food Sci. Biotechnol. 25 (2016) 55–61.
[15] L.G. D'Alessandro, K. Dimitrov, P. Vauchel, I. Nikov, Kinetics of ultrasound assisted extraction of anthocyanins from *Aronia melanocarpa* (black chokeberry) wastes, Chem. Eng. Res. Des. 92 (2014) 1818–1826.
[16] M. Ramić, S. Vidović, Z. Zeković, J. Vladić, A. Cvejin, B. Pavlić, Modeling and optimization of ultrasound-assisted extraction of polyphenolic compounds from *Aronia melanocarpa* by-products from filter-tea factory, Ultrason. Sonochem. 23 (2015) 360–368.
[17] L. Grunovaitė, M. Pukalskienė, A. Pukalskas, P.R. Venskutonis, Fractionation of black chokeberry pomace into functional ingredients using high pressure extraction methods and evaluation of their antioxidant capacity and chemical composition, J. Funct. Foods 24 (2016) 85–96.
[18] M. Herrero, A.P. Sánchez-Camargo, A. Cifuentes, E. Ibáñez, Plants seaweeds, microalgae and food by-products as natural sources of functional ingredients obtained using pressurized liquid extraction and supercritical fluid extraction, Trends Anal. Chem. 71 (2015) 26–38.
[19] M. Herrero, M. Castro-Puyana, J.A. Mendiola, E. Ibáñez, Compressed fluids for the extraction of bioactive compounds, Trends Anal. Chem. 43 (2013) 67–83.
[20] L. Montero, M. Herrero, E. Ibáñez, A. Cifuentes, Profiling of phenolic compounds from different apple varieties using comprehensive two-dimensional liquid chromatography, J. Chromatogr. A 1313 (2013) 275–283.
[21] R. Re, N. Pellegrini, A. Proteggente, A. Pannala, M. Yanga, C. Rice-Evans, Antioxidant activity applying an improved ABTS radical cation decolorization assay, Free Rad. Biol. Med. 26 (1999) 1231–1237.
[22] W. Brand-Williams, M.E. Cuvelier, C. Berset, Use of a free radical method to evaluate antioxidant activity, LWT Food Sci. Technol. 28 (1995) 25–30.
[23] J. Oszmianski, A. Wojdylo, Aronia melanocarpa phenolics and their antioxidant activity, Eur. Food Res. Technol. 221 (2005) 809–813.
[24] R. Taheri, A. Conolly, M.H. Brand, B.W. Bolling, Underutilized chokeberry (*Aronia melanocarpa Aronia arbutifolia*, *Aronia prunifolia*) accessions are rich sources of anthocyanins, flavonoids, hydroxycinnamic acids, and proanthocyanidins, J. Agric. Food Chem. 61 (2013) 8581–8588.
[25] F. Cacciola, S. Farnetti, P. Dugo, P.J. Marriott, L. Mondello, Comprehensive two-dimensional liquid chromatography for polyphenol analysis in foodstuffs, J. Sep. Sci. (2016), http://dx.doi.org/10.1002/jssc.201600704, in press.
[26] T. Hájek, P. Jandera, M. Staňková, P. Cesla, Automated dual two-dimensional liquid chromatography approach for fast acquisition of three-dimensional data using combinations of zwitterionic polymethacrylate and silica-based monolithic columns, J. Chromatogr. A 1446 (2016) 91–102.
[27] L. Montero, M. Herrero, M. Prodanov, E. Ibáñez, A. Cifuentes, Characterization of grape seed procyanidins by comprehensive two-dimensional hydrophilic interaction × reversed phase liquid chromatography coupled to diode array detection and tandem mass spectrometry, Anal. Bioanal. Chem. 405 (2013) 4627–4638.
[28] X. Li, D.R. Stoll, P.W. Carr, Equation for peak capacity estimation in two-dimensional liquid chromatography, Anal. Chem. 81 (2009) 845–850.
[29] M. Camenzuli, P.J. Schoenmakers, A new measure of orthogonality for multi-dimensional chromatography, Anal. Chim. Acta 838 (2014) 93–101.

3.5. Profiling of *Vitis vinifera* L. canes (poly)phenolic compounds using comprehensive two-dimensional liquid chromatography.

Montero, L., Sáez, V., von Baer, D., Cifuentes, A., Herrero, M.

Submitted to Journal of Chromatography A, 2017

Profiling of *Vitis vinifera* L. canes (poly)phenolic compounds using comprehensive two-dimensional liquid chromatography.

Lidia Montero[1], *Vania Sáez*[2], *Dietrich von Baer*[2], *Alejandro Cifuentes*[1], *Miguel Herrero*[1*]

[1]Laboratory of Foodomics, Institute of Food Science Research (CIAL-CSIC), Nicolás Cabrera 9, 28049 - Madrid, Spain.

[2]Dpto. Análisis Instrumental, Facultad de Farmacia, Universidad de Concepción, Chile

Corresponding author: m.herrero@csic.es (M. Herrero)

TEL: +34 910 017 946

FAX: +34 910 017 905

ABSTRACT.

Grapevine canes, a pruning-derived by-product, possess a great amount of bioactive (poly)phenolic compounds belonging to different chemical classes, thus, having a good potential for further valorization. However, in order to properly design valorization strategies, the precise chemical composition of this material has to be known. Up to now, this chemical characterization has been based on analysis of different groups of components individually, due to difficulties related to their huge chemical variability. In this work, a comprehensive two-dimensional liquid chromatography-based method (LC × LC) is developed to obtain the profiles of (poly)phenolic compounds present in grapevine canes from several varieties. Three different set-ups have been tested and compared; the combination of diol and C_{18} columns produced the best results, allowing the characterization of the (poly)phenolic profile in around 80 min. This way, 81 different components were detected in the samples; most of them could be tentatively assigned using the information provided by the DAD and MS detectors employed. Indeed, it has been possible to detect in a single run components belonging to stilbenoids, procyanidins and prodelphinidins of varying degrees of polymerization, some of them not formerly described in this natural source. The method has shown extremely good separation capabilities, and is characterized by high effective peak capacity (842) and orthogonality (A_0 = 78%). The obtained results demonstrate that *Vitis vinifera* L. canes may retain a great potential to be used as an underexploited natural source of bioactive compounds, with potential applications in different fields.

Keywords: Grapevine canes; LC × LC; Phenolic compounds; Proanthocyanidins; Stilbenoids

1. INTRODUCTION.

Management of agricultural and food-related by-products and wastes is an important issue nowadays worldwide. Industrial practices related to food production are responsible for the generation of a huge amount of unwanted materials at different levels. Traditionally, these wastes have been reused for energy generation and/or feed production [1]. Nevertheless, this approach is clearly not efficient enough to deal with such a high amount of by-products. For this reason, different alternatives have appeared in the last years proposing new ways for the valorization of agricultural and food industry by-products [2], considering that a significant part of those wastes are still rich on interesting components, such as bioactives. Indeed, at present, the complete valorization of all the residues and by-products generated in a particular production chain is ideally sought through the application of the modern concept of biorefinery [3].

Among the different agrofood-related by-products, grapevine (*Vitis vinifera* L.) canes are a promising source of different bioactive components, basically, phenolic compounds. Canes are a pruning residue which is not processed for extensive valorization as they are normally burnt or composted [4]. Among the bioactives present in this material, stilbenoids are commonly pointed out [5], although others such as proanthocyanidins are also present. Stilbenoids are non-flavonoid phenolic compounds which are related to defense mechanisms in plants as a response to different stresses. The basic structure of those found in grapevines are based on (*E*)-resveratrol (3,5,4 trihydroxystilbene) chemical structure, which is also the most abundant compound in grapevine canes after post-pruning storage. However, reactions such as photoisomerization, glycosylation and oligomerization are responsible for the complex chemical pattern that can be natively found in the plant [6], including monomers ((*E*)-piceatannol, (*E*)-piceid), dimers ((*E*)-ε-viniferin, (*E*)-ω-viniferin, ampelopsin A, vitisinol C), trimers ((*E*)-miyabenol C), and tetramers ((*E*)-vitisin B, (*Z*)-vitisin B, hopeaphenol, isohopeaphenol), among others. Moreover, the levels of (*E*)-resveratrol and some other related minor stilbenoids are strongly dependent on storage conditions of canes (time, temperature) after pruning. It has been observed that pruning triggers a

very significant increase in stilbenoid levels, mainly (*E*)-resveratrol, in grapevine canes [6,7], which is induced by the stress affecting the vegetal material during post-pruning storage. The increase of the activity of the stilbenoid synthesizing enzyme during this period has been already reported [7], indicating that the biosynthesis is activated. Interestingly, this increase is not observed if the vegetal material is not cut or if it is kept frozen or ground soon after collection [5,6]. Different beneficial health effects and bioactive activities have been ascribed to *(E)*-resveratrol as well as to other stilbenoids [8], thus, highlighting the interest on these natural components.

On the other hand, proanthocyanidins are flavan-3-ol polymers which can be linked through multiple ways and degrees of polymerization, giving rise to extremely complex patterns [9]. As for stilbenoids, proanthocyanidins are regarded as responsible for a number of bioactivities, including antioxidant, hepatoprotective, anti-inflammatory, antibacterial or anticancer effects, among others [10]. Different proanthocyanidins, mainly procyanidins, have been already described in grapevine [11], although the natural chemical variability may still be concealed due to difficulties in their analysis. Consequently, the presence of this complex array of (poly)phenolic compounds makes grapevine canes a potentially interesting material for the development of valorization processes.

However, to produce an efficient valorization of wastes, not only environmentally friendly extraction and processing techniques are needed to obtain the compounds of interest, but also an exhaustive chemical characterization of those materials is required. In fact, it is of utmost importance to precisely know the chemical composition of a particular by-product in order to devise strategies for its valorization. In this regard, the already mentioned extremely complex pattern on bioactives present on grapevine canes implies that the typically used one-dimensional separation approaches may not provide the separation and identification power enough to reveal more in detail the chemical composition of these wastes. It is precisely on this kind of complex natural samples where comprehensive two-dimensional liquid chromatography (LC × LC) may

provide with the required additional separation capabilities. LC × LC is based on the coupling of two independent separation mechanisms that allow significant improvements on resolving power and peak capacity [12]. By using this on-line approach, the entire sample is subjected to two independent separation mechanisms continuously; although different combinations between separation mechanisms may be applied, the one involving hydrophilic interaction chromatography (HILIC) coupled to reversed phase (RP) separations has shown a very good potential for polyphenols analysis [13]. In any case, the application of this coupling is not straightforward due to multiple factors that should be optimized [14-16], being one of the most important the transfer from the first dimension (^{1}D) eluent to the second dimension (^{2}D) continuously, due to solvent incompatibility. Although, this technique has been already employed for the analysis of different types of polyphenols and matrices [17], up to now, it has not been used for the profiling of grapevine canes. Thus, the aim of this work is to profile and characterize the complex mixture of (poly)phenolic compounds contained in grapevine canes, mainly stilbenoids and proanthocyanidins, in a single run through the use of a HILIC × RP method coupled to tandem mass spectrometry. The developed method is then applied to reveal differences on the chemical composition between two red grapevine varieties stored for 3 months after pruning to foster an accumulation of stilbenoids.

2. MATERIALS AND METHODS.

2.1. Samples and chemicals.

Grapevine (*Vitis vinifera L.*) canes from the variety *Pinot Noir* were collected from Itata Valley (Concepción, Chile) and canes from the variety *Cabernet Sauvignon* were from Maipo Valley (Santiago, Chile) in the winter of 2013. After pruning, both samples were stored at room temperature during three months. Then, the grapevine canes were ground and frozen at -20°C. Extraction of (poly)phenolic compounds from dried canes was carried out by solid/liquid extraction. Briefly, 50 mL of acetone/water (80:20, *v/v*) were added to 5 g of ground grapevine

canes. The solution was sonicated (Elma, Singen, Germany) for 15 min. After that, the mixture was kept in the darkness during 2 h and then it was again sonicated for 15 min. Finally, the solution was centrifuged for 20 min at 8000 rpm, the acetone was evaporated under vacuum (Rotavapor R-210, Büchi Labortechnik AG, Flawil, Switzerland) and lastly, the aqueous extract was freeze-dried (Labconco Corporation, MO).

HPLC grade methanol, acetonitrile and acetone were purchased from VWR Chemicals (Barcelona, Spain), whereas acetic and formic acids were acquired from Sigma-Aldrich (Madrid, Spain) and ammonium acetate was from Panreac (Barcelona, Spain). Water employed was Milli-Q grade obtained from a Millipore system (Billerica, MA).

2.2. Instrumentation.

The LC × LC-DAD instrumentation consisted on a first dimension (^{1}D) composed by an Agilent 1200 series liquid chromatograph (Agilent Technologies, Santa Clara, CA) equipped with an autosampler. In order to obtain more reproducible low flow rates and to minimize the gradient delay volume of the pump, a Protecol flow-splitter (SGE Analytical Science, Milton Keynes, UK) was placed between the ^{1}D pump and the autosampler. Additionally, a LC pump (Agilent 1290 Infinity) performed the second dimension (^{2}D) separation. Both dimensions were connected by an electronically-controlled two-position ten-port switching valve (Rheodyne, Rohnert Park, CA, USA) acting as modulator equipped with two identical 30 µL injection loops. Modulation time of the switching valve was 1.3 min. A diode array detector was coupled after the second dimension in order to register every ^{2}D analysis. Besides, an Agilent 6320 Ion Trap mass spectrometer equipped with an electrospray interface working under negative ionization mode was coupled in series using the following conditions: dry temperature, 350 ºC; dry gas flow rate, 12 L min^{-1}; nebulization pressure, 40 psi; mass range, *m/z* 90-2200 Da; ultra scan mode (26000 *m/z* /s). The LC data were elaborated and visualized using LC Image software (version 1.0, Zoex Corp., Houston, TX).

2.3. LC × LC separation conditions.

The ^{1}D separation was optimized using three sets of columns. The best conditions for each column after optimization were:

i) ZIC-HILIC column (150 × 1 mm, 3.5 µm, Merck, Darmstadt, Germany) eluted using acetonitrile (A) and 10 mM ammonium acetate pH 5 (B) as mobile phases, using the following gradient at 15 µL min^{-1}: 0 min, 3% B; 5 min, 3% B; 10 min, 5% B; 15 min, 10% B; 30 min, 20% B; 45 min, 20% B; 50 min, 30% B; 60 min, 30% B; 70 min, 40% B; 80 min, 40% B.

ii) PEG column (150 × 2.1 mm, 5 µm, Supelco, Bellefonte, CA) eluted using methanol (0.1 % formic acid, A) and water (0.1 % formic acid, B) at 20 µL min^{-1} according to the following gradient: 0 min, 40% B; 50 min, 10% B; 70 min, 2% B.

iii) Lichrospher diol-5 (150 × 1.0 mm, 5 µm, HiChrom, Reading, UK) column eluted using acetonitrile (1% formic acid, A) and methanol/10 mM ammonium acetate/acetic acid (95:4:1, B) at 18 µL min^{-1} using the following gradient: 0 min, 2% B; 10 min, 2% B; 15 min, 5% B; 30 min, 20% B; 45 min, 20% B; 50 min, 30% B; 60 min, 30% B; 70 min, 40% B; 80 min, 40% B.

On the ^{2}D, a pentafluorophenyl column (Kinetex PFP column, 50 × 4.6 mm, 2.7 µm, Phenomenex, Torrance, CA, USA) and a C_{18} column (Ascentis Express C_{18} column, 50 × 4.6 mm, 2.7 µm, Supelco, Bellefonte, CA) were used. For LC × LC analysis, the C_{18} column was employed under optimized conditions depending on the stationary phase used in ^{1}D, as follows:

i) diol×C_{18} and PEG×C_{18} set-ups: water (0.1% formic acid, A) and acetonitrile (0.5% formic acid, B) were selected as mobile phases, eluted at 3 mL min^{-1} using the following gradient: 0 min, 2% B; 0.1 min, 2% B; 0.3 min, 10% B; 0.5 min, 25% B; 0.7 min, 40% B; 1 min, 60% B, 1.01 min, 2% B.

ii) ZIC-HILIC×C_{18} set-up: mobile phases employed were composed by water (0.1% formic acid, A) and acetonitrile (0.5% formic acid, B) and were eluted at 3 mL min^{-1} using the following

gradient: 0 min, 0% B; 0.1 min, 2% B; 0.3 min, 5% B; 0.5 min, 15% B; 0.7 min, 25% B; 1 min, 50% B; 1.01, 0% B.

Independently of the column combinations, 2D analyses were performed maintaining a column temperature of 25 ºC. UV-Vis spectra were collected in the range of 190-550 nm using a sampling rate of 20 Hz, while 254, 280 and 330 nm signals were also independently recorded. The effluent from the ^{2}D column was splitted before entering the MS instrument, so that the flow rate introduced in the MS detector was *ca.* 0.6 mL min^{-1}. MS detection was performed as above indicated (section 2.2).

2.4. Calculations.

2.4.1 Peak capacity.

Individual peak capacity for each dimension was calculated according to eq. 1:

$$n_c = 1 + \frac{t_G}{\overline{w}} \qquad (1)$$

where t_G is the gradient time and $\overline{w}$ is the average peak width, equivalent to 4σ. For ^{1}D peak capacity calculations, the average peak width was obtained from 10-15 representative peaks selected along the analysis. Likewise, for ^{2}D peak capacity, as much as possible peaks were considered (14-22 peaks, depending on the analysis). Additionally, $^{1}n_c$ was also calculated considering the broadening factor <β>, giving rise to a corrected ^{1}D peak capacity (eq. 2), considering the influence of the deleterious effect of undersampling. To estimate <β>, the sampling time (t_s) as well as the average width of ^{1}D peaks before modulation were considered:

$$^{1}n_{c,corrected} = \frac{n_c}{\sqrt{1+0.21\left(\frac{t_S}{^{1}\sigma}\right)^{2}}} \qquad (2)$$

For each two-dimensional set-up, different peak capacity values were estimated. First of all, theoretical peak capacity was obtained following the so-called product rule, using eq. 3, considering the individual peak capacities obtained in each dimension:

$$^{2D}n_{c,theoretical} = {}^{1}n_c \times {}^{2}n_c \qquad (3)$$

As eq. 3 does not take into consideration the deleterious effects due to the modulation process as well as possible undersampling, a more realistic peak capacity value was obtained from the equation proposed by Li et al. [18], denominated here as practical peak capacity (eq. 4):

$$^{2D}n_{c,practical} = \frac{^{1}n_c \times {}^{2}n_c}{\sqrt{1+3.35\times\left(\frac{^{2}t_c \, {}^{1}n_c}{^{1}t_G}\right)^2}} \qquad (4)$$

being $^{2}t_c$, the ^{2}D separation cycle time, which is equal to the modulation time. This latter equation also includes the <β> parameter accounting for undersampling. Moreover, to more precisely compare among set-ups and in order to evaluate possible peak clusters along the 2D analysis and, thus, to estimate 2D space coverage, the orthogonality degree (A_0) was considered to offer the denominated 2D corrected (also known as effective) peak capacity, as follows:

$$^{2D}n_{c,corrected} = {}^{2D}n_{c,practical} \times A_0 \qquad (5)$$

2.4.2 Orthogonality.

Different approaches have been developed and published to quantify the orthogonality degree of a two-dimensional set-up [19]. In the present work, system orthogonality (A_0) was calculated according to the method proposed by Camenzuli and Schoenmakers [20], taking into account the spread of each peak along the four imaginary lines that cross the 2D space forming an asterisk, that is Z_1, Z_2 (vertical and horizontal lines) and Z_{-}, Z_{+} (diagonal lines of the asterisk). Z parameters describe the use of the separation space with respect to the corresponding Z line, allowing to semi-quantitatively diagnose areas of the separation space where sample components are clustered, thus, reducing in practice orthogonality. For the determination of each Z parameter, the S_{Zx} value was calculated, as the measure of spreading around the Z_x line, using the retention times of all the separated peaks in each 2D analysis.

3. RESULTS AND DISCUSSION.

Although some previous works dealt with the identification of some stilbenoids [5,21] and proanthocyanidins [22] by one-dimensional reversed phase HPLC in grapevine canes, no comprehensive method has been developed up to now to obtain the (poly)phenolic profile of this material. Consequently, a LC × LC method has been developed to this aim. Based on the literature and our own experience, as well as considering the nature of the compounds expected to be part of that profile (see Figure 1 for examples), the combination between HILIC × RP could be a promising alternative [17,23-25], although the application of RP × RP has also been explored [17]. To perform a proper method optimization, different conditions have been tested independently, firstly looking at the performance achievable by three different stationary phases in the ^{1}D and then, studying their potential when combined with a C_{18} column in the ^{2}D. This method optimization has been performed considering the available materials and instruments, which impose some important constraints, mainly related to the maximum pressure borne by the equipment (400 bar) as well as to the scanning speed of the available detectors (DAD and MS). Thus, method development has been guided taking some compromises, as described below, not only in terms of theory but also in terms of practice (instrumental limitations). Finally, in order to select the most appropriate set-up for the separation of the grapevine cane samples, the obtained results were critically compared in terms of separation capabilities (overall resolution, peak capacity and orthogonality).

3.1 Separation method optimization.

Unlike other previously investigated samples where a phenolic group of compounds was clearly predominant [23-25], the studied samples in the present work are composed of complex mixtures of varying degrees of polymerization of two different groups of polyphenols, i.e., stilbenoids and proanthocyanidins. Due to this different pattern, several stationary phases compatible with HILIC separations were evaluated for their use in ^{1}D separation, namely, diol, ZIC-HILIC and PEG (polyethylene glycol) columns. Diol stationary phases have repeatedly shown to provide

good retention under HILIC mode [17], whereas ZIC-HILIC particles carry zwitterionic functional groups (sulfobetaine) with a charge balance 1:1, also suitable for that separation mode. On the other hand, PEG columns were initially developed for RP, although it has been demonstrated that they can also be run under HILIC conditions with satisfactory results [26]. For this reason, in this work, the performance of the PEG column was studied under both separation modes, as RP × RP has also previously shown relatively good performance in phenolic compounds analysis [13,17]. An independent optimization of the separation conditions was performed for each column, keeping in mind the basic requirements imposed by the 2D set-up used. This LC × LC set-up is based on the use two identical volume sampling loops installed in the switching valve in order to allow the continuous collection and injection of ^{1}D effluent on the ^{2}D. Hence, separations as slow as possible in the ^{1}D are preferred (from 10 to 100 µL min^{-1}, typically) while very fast separations are needed to perform quick ^{2}D separations (3-4 mL min^{-1}) and to maintain the modulation time (and transfer volume) as short as possible. The use of such low flow rates in the ^{1}D limits, in turn, the morphology of the column. It has been repeatedly reported that microbore and narrow columns can provide with the needed efficiency at low flow rates. The characteristics of the columns tested are shown in Table 1. One of the studied grapevine samples was used as a model, and different mobile phases, gradients and flow rates (from 15 to 25 µL min^{-1}) were tested for each column, including acetonitrile/formic acid, acetonitrile/acetic acid, methanol/water/acid or methanol/ammonium acetate buffer mixtures in different proportions. After careful study of the obtained results, the optimum separation conditions for each studied column are reported in Section 2.3. The best conditions involving the use of the PEG column were found under RP conditions. When operated under HILIC-compatible conditions, the PEG column did not produce satisfactory retention of the studied compounds. In any case, it is worth noting that the internal diameter of the available PEG column (2.1 mm) was wider than those from the other tested columns. This fact implies that the used linear velocity is far from optimal values, which means that the obtained separation could

be theoretically further improved, although higher flow rates, which are not practical in this application, would be required. Figure 2 shows typical ^{1}D chromatograms obtained under optimum separation conditions for each column. As can be observed, good peak distributions were obtained with the three tested columns, although the diol column was the only one allowing a separation between stilbenoids and proanthocyanidins. Peak capacity values were calculated for the three optimized separations. Results are given in Table 1. The undersampling correction factor <β> was also considered to reduce the theoretical $^{1}n_c$ as a result of undersampling (Eq. 2), including the sampling time (t_s) later on applied in LC × LC experiments (see below). As can be observed, the diol column produced higher peak capacity values, followed by the PEG and ZIC-HILIC columns (25, 23 and 19, respectively). However, this value should not be the only one taken into consideration to select the best ^{1}D separation method, as increments in ^{1}D peak capacity do not produce enhancements in the two-dimensional peak capacity beyond a certain point because undersampling get worse as a result of narrower ^{1}D peaks (unless $^{1}t_G$ is significantly increased) [27].

The three columns studied in ^{1}D were then tested in a LC × LC set-up in combination with a short partially porous C_{18} column (50 × 4.6 mm, 2.7 µm). The use of relatively short columns with partially porous materials allows obtaining high efficiency values and fast separations, significantly reducing backpressure compared to sub-2 µm columns. In our application, control of pressure as a result of the ^{2}D separations is of utmost importance, as the available switching valve and DAD are not designed to operate at pressures above 400 bar. As can be deduced from the literature [17], C_{18} columns offer unparalleled retention for most of published applications involving a RP separation in ^{2}D. In spite of this, we also studied the possibility of using a PFP (pentafluorophenyl) stationary phase in ^{2}D, maintaining column morphology, although that column did not provide comparable results (data not shown). For each of the studied set-ups, the ^{2}D separation conditions were independently determined; optimum separation conditions are

shown in Section 2.3. Flow rate was always maintained as fast as possible in order to reduce ^{2}D analysis time, although gradients shorter than 1 min did not produced successful separations. On the other hand, higher ^{2}D flow rates were avoided due to increased pressure drop and lack of enough sampling rate in the DAD. For these reason, total ^{2}D analysis times were kept at 1.3 min, in order to allow column re-equilibration for 18 s. Moreover, the transfer volume, determined by the available sampling loop volume was also considered. For the three couplings, two 30 μL loops were employed, which provided higher volume than strictly required according to the ^{1}D flow rate and modulation time employed (Table 1). However, we previously demonstrated that by using this additional space, each fraction being transferred was in practice diluted at the head of the ^{2}D column with ^{2}D initial mobile phase. This dilution effect has been demonstrated to be effective to reduce ^{2}D peak distortion related to solvent incompatibility between dimensions [23], considering that there was a solvent strength mismatch in every LC × LC coupling studied here.

The results obtained after the application of each optimized LC × LC set-up are illustrated in Figure 3. To make a quantitative comparison of the separation capabilities of each combination, the number of separated peaks and overall resolution, peak capacity values, as well as orthogonality were considered. Firstly, it is important to note, that although 1.3 min cycles may seem too long, the conditions applied in both dimensions allowed to minimize possible negative effects due to undersampling. Considering ^{1}D peak widths before modulation, sampling times from ^{1}D to ^{2}D were estimated; obtained values in the three studied set-ups were always faster than the recommended rate by Murphy, Schure and Foley [28] (i.e., 4 cuts per peak, thus, 2σ), as it can be observed in Table 1. Theoretical peak capacity values derived from the application of eq. 3 are shown in Table 1. As it can be noted, the set-up involving the use of the diol column provided the highest values ($^{2D}n_c$ = 1408). Moreover, in order to give more realistic values, the practical peak capacity (according to eq. 4) was also calculated. This way, the effects of undersampling are also considered; these deleterious effects are related to the re-mix of already

separated compounds in the ^{1}D during the collection of the ^{1}D effluent in the modulator. Although one of the premises of LC × LC is that none of the resolution obtained in the ^{1}D is lost in the ^{2}D, in practice this can never be completely achieved [27]; for this reason, the estimation of peak capacity should include the possible losses of ^{1}D peak capacity related to undersampling. Using this approach, practical peak capacity values of the diol × C_{18}, PEG × C_{18} and ZIC-HILIC × C_{18} set-ups were 1080, 961 and 768, respectively. Still, it is important to keep in mind that these peak capacity values are not the real number of peaks that could be separated along the 2D space because there are areas on the 2D chromatogram where peaks do not appear. To evaluate the 2D separation space coverage, orthogonality degree in each set-up was calculated. This parameter gives a measure of the separation quality and allows the comparison between different 2D approaches. System orthogonality (A_0) was calculated taking into account the spread of each peak along the four imaginary lines that cross the 2D space forming an asterisk, that is Z_1, Z_2 (vertical and horizontal lines) and Z_{-}, Z_{+} (diagonal lines of the asterisk) [20]. The ZIC-HILIC × C_{18} coupling provided an A_0 of 70%, due to a good spread of the peaks around Z_1 and Z_2 lines (97 and 91%, respectively). The PEG × C_{18} set-up possessed an A_0 = 45%. This moderated value is related to the poor spread of peaks around the Z_{-} and Z_{+} lines (42 and 60%, respectively) as can be observed in Figure 3B, where a peak clustering occurs on the Z_{-} axis with a low spread. The best orthogonality degree was achieved with the diol × C_{18} coupling obtaining an A_0 of 78% (Figure 3A) corresponding to a high peak spreading around the four axis (93% Z_1, 95% Z_2, 91% Z_{-} and 75% Z_{+}). Interestingly, as expected from theory, those set-ups involving a HILIC × RP coupling (Figures 3A and C) provided with higher orthogonality values than the RP × RP set-up involving the use of the PEG column (Figure 3B), for this application. Considering orthogonality values, corrected peak capacities (eq. 5, $^{2D}n_{c,\,corr}$) attained in the diol × C_{18}, PEG × C_{18} and ZIC-HILIC × C_{18} set-ups were 842, 432 and 538, respectively. The application of this correction factor allows a fairer comparison among set-ups, as the whole coupling is evaluated, not only in terms of each dimension separately but also looking at the 2D separation obtainable

once coupled. Consequently, as can be deduced from Figure 3, the best conditions were produced using HILIC × RP using a diol column in the ^{1}D coupled to a C_{18} column in the ^{2}D. Moreover, as it can also be inferred from Figure 3, the best ^{1}D peak distribution along the available analysis time was obtained using the diol column, thus, further justifying the use of the mentioned set-up in the present application.

3.4. Characterization of the (poly)phenolic profile of grapevine canes by HILIC×RP.

The optimized method was then applied for the characterization of the (poly)phenolic profile of canes of two different grapevine varieties, specifically, *Pinot Noir* and *Cabernet Sauvignon*. The analyzed canes were derived from the pruning of different vineyards. After pruning, the canes were stored at ambient temperature for three months. This period was demonstrated to be useful to promote the synthesis of the bioactives present [6]. The 2D plots of the studied samples under the optimum conditions are shown in Figure 4. In order to characterize the separated components, a MS detector was also hyphenated to the LC × LC instrument. The MS used consisted of an ion trap equipped with an electrospray (ESI) interface working on the negative ionization mode. Although this analyzer provided with useful MS data, this instrument does not provide with high scanning speeds, which are very desirable in LC × LC, considering the fast separations (^{2}D) that are carried out just before detection. Table 2 summarizes the tentatively identified compounds in both grapevine cane extracts as well as the corresponding data related to their UV-Vis and MS spectra. As can be observed from this Table and Figure 4, most peaks were detected in both varieties, although some others were uniquely found in just one of them. Among the assigned compounds, two families were mainly present, namely proanthocyanidins and stilbenoids. In general, compounds eluted from the ^{1}D according to increasing degree of polymerization (DP); monomers and smaller oligomers were predominantly found in the first section of the 2D plot (first 23 min). These compounds were the most abundant in both samples with higher intensities.

Catechin and epicatechin (peaks 5 and 6, respectively) were the only flavan-3-ol monomers detected in the studied samples. These two compounds are the basic components of procyanidins; as can be observed in Table 2, the chemical pattern of procyanidin oligomers in grapevine canes was very complex. Moreover, catechin and epicatechin, together with (epi)gallocatechin, are part of prodelphinidins, the other group of proanthocyanidins found in the studied samples. Several procyanidins with DP 2 and DP 3 could be tentatively assigned thanks to their typical molecular ions at *m/z* 577, 579 and 865, depending on the type of linkage. These compounds also presented characteristic fragment ions corresponding to retro-Diels−Alder (RDA) fission (-152 Da), heterocyclic ring fission (HRF, -126 Da), and quinone methide (QM) fission (-289 Da) [29]. Moreover, other mono- and digalloylated dimers and trimers were also found (peaks 42, 62, 66 and 67). An example of the MS and MS/MS spectra of a procyanidin trimer digallate as well as its proposed fragmentation pattern can be observed in Figure S1. The typical fragmentation pattern of these components which was already described for other samples [23] was the key for their identification, including the presence of fragments derived from different fission pathways [29]. It has to be pointed out that procyanidins are extensively present in different grape-related components, such as skins, seeds and even wine [30]. The other type of proanthocyanidins identified in these samples was prodelphinidins. In this case, different compounds containing a DP from 2 to 5 could be assigned, having also different degree of galloylation. In Table 2, the tentative monomer composition of each prodelphinidin is included in agreement with the molecular ion and main MS/MS fragments detected. For instance, both prodelphinidin dimers detected (peaks 39 and 41) possessed identical molecular ion at *m/z* 593 ($[M-H]^-$), producing MS/MS fragments revealing the presence of (epi)catechin (*m/z* 289) and (epi)gallocatechin (*m/z* 305) (through QM fission). However, in the case of higher molecular weight components, the chemical variability was more complex. For prodelphinidin trimers, three different structures appeared, formed by: two (epi)catechin moieties and one (epi)gallocatechin (peaks 52, 53, 56 and 58) with *m/z* at 881 ($[M-H]^-$); a (epi)catechin unit with

two (epi)gallocatechin moieties (peak 61) with *m/z* at 897 ($[M-H]^-$), and; a galloylated trimer (peak 65). Likewise, different tetramers could be described in the samples with different basic structure and degree of galloylation (peaks 68, 70, 71 and 72). Interestingly, some of these components were detected as doubly-charged ions. It is important to remark that this is the first work in which prodelphinidins are described in grapevine canes. In any case, the clarification of prodelphinidin oligomers is sometimes not possible only with the information provided by the MS and MS/MS spectra due to the fact that these complex molecules may present different degrees of galloylation as well as different number of (epi)gallocatechin molecules. This implies that some different oligomers may have the same *m/z* and main MS/MS fragments, making the unequivocal assignment very difficult. This is the case of peak 72 that presents a $[M-2H]^{2-}$ at *m/z* 828.6 and could correspond to a prodelphinidin tetramer trigallate or to a prodelphidin pentamer monogallate. The MS and MS/MS spectra of this peak are shown in FigS1C and D, as well as the tentatively proposed fragmentation pattern of both identification options. The use of a high resolution MS analyzer would potentially improve the attainable results as well as the identification certainty through the acquisition of accurate mass values.

The other main group of phenolic compounds in grapevine canes are stilbenoids. As can be observed from Table 2, the chemical composition on these compounds was also very complex, involving a great number of different but closely related chemical structures. These components eluted from the ^{1}D according to their increasing size. The most abundant among them was (*E*)-resveratrol (3,5,4'-trihydroxystilbene, peak 1), which was also the most intense peak in general in both samples. Piceatannol (peak 3) was also present in high amounts. Stilbenes monomers, such as resveratrol and piceatannol, present the same MS/MS fragmentation behavior. The fragmentation occurs in the resorcinol ring, which loses two consecutive C_2H_2O, corresponding to one and two neutral losses of 42 Da, respectively [31]. This way, the fragmentation of resveratrol (peak 1, *m/z* 227) is characterized by the production of fragments at *m/z* 187 and 143. Likewise, the fragmentation of piceatannol (peak 3, *m/z* 243) produced fragments at *m/z* 201 and

159. The rest of stilbenoids detected in the grapevine canes samples were formed by more complex structures, with varying degree of polymerization. UV-Vis maxima were also useful to assign the separated components as resveratrol presents a UV absorption maximum at 310 nm, whereas, as the size of stilbenoid oligomers increases, the UV maximum shifts to *ca.* 280-290 nm [32]. The above-commented loss of C_2H_2O under MS/MS fragmentation is also characteristic of stilbenoid oligomers; besides the neutral loss of 42 Da, oligomers may also present typical loses corresponding to 94 Da (C_6H_6O), 106 Da (C_7H_6O) and 110 Da ($C_6H_6O_2$) [31]. For instance, peak 4 (*m/z* 453.7, $[M-H]^-$) was tentatively identified as a resveratrol dimer, being the most important fragments derived from this ion those with *m/z* 411 (loss of 42 Da), 359 (loss of 94 Da) and 347 (loss of 106 Da). In the same way, peak 2 was also assigned as a resveratrol dimer. These two compounds were related to viniferin, although an unequivocal identification could not be reached with the available tools.

Interestingly, a di-glycosylated derivative of this compound was also found in *Pinot Noir* canes (peak 48). This compound, not reported previously in grapevine canes, has been detected in Riesling wine [33]. Viniferin diglycoside was characterized by a molecular ion at *m/z* 777, showing MS/MS fragments corresponding to the loss of one or both glycosidic residues (*m/z* 615 and 454). Moreover, three other dimeric stilbenoid derivatives were also detected (peaks 15, 17 and 18). These possessed an ion at *m/z* 469, which was in agreement of a structure based on the combination of (*E*)-resveratrol and piceatannol. Only one resveratrol trimer was detected (peak 19) in the *Pinot Noir* sample (*m/z* 679, Figure 4A) which contrasts with the detection of 6 different resveratrol tetramers (peaks 22, 23, 26, 27, 29 and 30). All these possessed molecular ions at *m/z* 905 and their structure would be related to hopeaphenol and vitisin [34]. Additionally, two other stilbenoid tetramers were detected at *m/z* 923 (peaks 36 and 37); their fragmentation pattern indicated that were related to viniferol E, including an additional hydroxyl group in their structure compared to the other tetramers. Moreover, two bigger oligomers, i.e., a resveratrol hexamer (peak 55) and a resveratrol heptamer (peak 47, Figure S1A), were detected

in these samples. The generated fragments corresponding to less polymerized resveratrol derivatives helped to assign these components. This is the first report of the presence of these big oligomers in grapevine canes.

Besides these components, other compounds were separated and their MS and MS/MS information collected, although no specific assignment could be obtained (see Table 2). Comparing both samples, quite similar profiles were achieved (Figure 4), being (*E*)-resveratrol, piceatannol and resveratrol dimers the most abundant compounds. Although the precise composition changed between *Pinot Noir* and *Cabernet Sauvignon* canes, from a qualitative point of view all the groups of compounds were similarly represented on both samples. In any case, the variability on the (poly)phenolic composition and content in grapevine canes from different varieties has been already reported [5,34]. However, this method allows to obtain the (poly)phenolic profile of these complex materials involving different group of polyphenol oligomers, which gives a clear idea of the satisfactory separation power of the developed HILIC × RP method. Furthermore, this application confirms the good possibilities that grapevine canes may have for valorization and attainment of valuable natural components with potential applications in the food, nutraceutical and cosmetic industries.

4. CONCLUSIONS.

In this work, a new HILIC × RP-DAD-MS/MS method is developed for the profiling of (poly)phenolic compounds present in grapevine canes from several varieties. By combining a diol column in the ^{1}D with a C_{18} column in the ^{2}D, it is possible to obtain their (poly)phenolic profile in around 80 min. The method has shown extremely good separation capabilities, and is characterized by high effective peak capacity (842) and orthogonality (A_0 = 78%). 81 different components were detected in the samples; most of them could be tentatively assigned using the information provided by the MS and DAD detectors employed. Two main (poly)phenolic groups

are represented, proanthocyanidins and stilbenoids. Thanks to this development, some components, such as prodelphinidins as well as some highly polymerized stilbenoids have been described for the first time in grapevine canes. Consequently, the interest of the application of LC × LC-based approaches to study complex natural mixtures has been once more confirmed. From the obtained results, it can be deduced that *Vitis vinifera* L. canes have a great potential to be used as an underexploited natural source of bioactive compounds, with potential applications in different fields. The developed methodology might also be a very effective tool to better understand the ongoing mechanisms in grapevine canes triggering the significant increase of the concentrations of some stilbenoids after pruning and during cane storage, thanks to its improved separation capabilities.

ACKNOWLEDGEMENTS.

The authors would like to thank Projects AGL2014-53609-P (MINECO, Spain), Grant 1150721 (FONDECYT, Chile) and Project Basal PFB-27 (CONICYT, Chile) for financial support. V.S. thanks CONICYT (Chile) for a Doctoral Fellowship.

REFERENCES.

[1] D.S. Martin, S. Ramos, J. Zufía, Valorisation of food waste to produce new raw materials for animal feed, Food Chem. 198 (2016) 68–74.

[2] R. Ravindran, A.K. Jaiswal, Exploitation of food industry waste for high-value products, Trends Biotechnol. 34 (2016) 58–69.

[3] F. Cherubini, The biorefinery concept: using biomass instead of oil for producing energy and chemicals, Energy Convers. Manag. 51 (2010) 1412–1421.

[4] R. Devesa-Rey, X. Vecino, J.L. Varela-Alende, M.T. Barral, J.M. Cruz, A.B. Moldes, Valorization of winery waste vs. the costs of not recycling. Waste Manage. 31 (2011) 2327−2335.

[5] C. Vergara, D. von Baer, C. Mardones, A. Wilkens, K. Wernekinck, A. Damm, S. Macke, T. Gorena, P. Winterhalter, Stilbene levels in grape cane of different cultivars in Southern Chile: determination by HPLC-DAD-MS/MS Method. J. Agric. Food Chem. 60 (2012) 929−933.

[6] T. Gorena, V. Sáez, C. Mardones, C. Vergara, P. Winterhalter, D. von Baer, Influence of post-pruning storage on stilbenoid levels in *Vitis vinifera* L. canes, Food Chem. 155 (2014) 256–263.

[7] B. Houillé, S. Besseau, V. Courdavault, A. Oudin, G. Glévarec, G. Delanoue, L. Guérin, A.J. Simkin, N. Papon, M. Clastre, N. Giglioli-Guivarc'h, A. Lanoue, Biosynthetic origin of E-resveratrol accumulation in grape canes during postharvest storage, J. Agric. Food Chem. 63 (2015) 1631−1638.

[8] R. Flamini, F. Mattivi, M. De Rosso, P. Arapitsas, L. Bavaresco, Advanced knowledge of three important classes of grape phenolics: Anthocyanins, stilbenes and flavonols. Int. J. Mol. Sci. 14 (2013) 19651-19669.

[9] C. Santos-Buelga, C. García-Viguera, F.A. Tomás-Barberán, On-line identification of flavonoids by HPLC coupled to diode array detector, in: C. Santos-Buelga, G. Williamson (Eds.), Methods in polyphenol analysis. The Royal Society of Chemistry, Cambridge, UK, 2003.

[10] D. Bagchi, A. Swaroop, H.G. Preuss, M. Bagchi, Free radical scavenging, antioxidant and cancer chemoprevention by grape seed proanthocyanidin: an overview. Mutat. Res. 768 (2014) 69-73.

[11] T. Püssa, J. Floren, P. Kuldkepp, A. Raal, Survey of grapevine *Vitis vinifera* stem polyphenols by liquid chromatography-diode array detection-tandem mass spectrometry, J. Agric. Food Chem. 54 (2006) 7488-7494.

[12] D.R. Stoll, Recent progress in online, comprehensive two-dimensional high-performance liquid chromatography for nonproteomic applications. Anal. Bioanal. Chem. 397 (2010) 979–986.

[13] F. Cacciola, P. Donato, D. Sciarrone, P. Dugo, L. Mondello, Comprehensive liquid chromatography and other liquid-based comprehensive techniques coupled to mass spectrometry in food analysis. Anal. Chem. 89 (2017) 414–429

[14] X. Li, P.W. Carr, Effects of first dimension eluent composition in two-dimensional liquid chromatography. J Chromatogr A 1218 (2011) 2214–2221.

[15] S.R. Groskreutz, M.M. Swenson, L.B. Secor, D.R. Stoll, Selective comprehensive multi-dimensional separation for resolution enhancement in high performance liquid chromatography. Part I—principles and instrumentation. J Chromatogr A 1228 (2012) 31–40.

[16] P. Donato, F. Cacciola, P.Q. Tranchida, P. Dugo, L. Mondello, Mass spectrometry detection in comprehensive liquid chromatography: basic concepts, instrumental aspects, applications and trends. Mass Spectrom. Rev. 31 (2012) 523–559.

[17] F. Cacciola, S. Farnetti, P. Dugo, P.J. Marriott, L. Mondello, Comprehensive two-dimensional liquid chromatography for polyphenol analysis in foodstuffs, J. Sep. Sci. 40 (2017) 7-24.

[18] X. Li, D.R. Stoll, P.W. Carr, Equation for peak capacity estimation in two-dimensional liquid chromatography, Anal. Chem. 81 (2009) 845–850.

[19] M.R. Schure, J.M. Davis, Orthogonal separations: Comparison of orthogonality metrics by statistical analysis, J. Chromatogr. A 1414 (2015) 60-76.

[20] M. Camenzuli, P.J. Schoenmakers, A new measure of orthogonality for multi-dimensional chromatography. Anal. Chim. Acta 838 (2014) 93–101.

[21] A. Zhang, L. Wan, C. Wu, Y. Fang, G. Han, H. Li, Z. Zhang, H. Wang. Simultaneous determination of 14 phenolic compounds in grape canes by HPLC-DAD-UV using wavelength switching detection. Molecules 18 (2013) 14241-14257.

[22] N. Vivas, M.F. Nonier, N. Vivas de Gaulejac, C. Absalon, A. Bertrand, M. Mirabel. Differentiation of proanthocyanidin tannins from seeds, skins and stems of grapes (*Vitis vinifera*) and heartwood of Quebracho (*Schinopsis balansae*) by matrix-assisted laser desorption/ionization time-of-flight mass spectrometry and thioacidolysis/liquid chromatography/electrospray ionization mass spectrometry. Anal. Chim. Acta 513 (2004) 247-256.

[23] L. Montero, M. Herrero, M. Prodanov, E. Ibáñez, A. Cifuentes, Characterization of grape seed procyanidins by comprehensive two-dimensional hydrophilic interaction × reversed phase liquid chromatography coupled to diode array detection and tandem mass spectrometry, Anal. Bioanal. Chem. 405 (2013) 4627–4638.

[24] L. Montero, M. Herrero, E. Ibáñez, A. Cifuentes, Profiling of phenolic compounds from different apple varieties using comprehensive two-dimensional liquid chromatography, J. Chromatogr. A 1313 (2013) 275–283.

[25] L. Montero, M. Herrero, E. Ibáñez, A. Cifuentes, Separation and characterization of phlorotannins from brown algae *Cystoseira abies-marina* by comprehensive two-dimensional liquid chromatography, Electrophoresis 35 (2014) 1644–1651.

[26] B. Buszewski, S. Noga, Hydrophilic interaction liquid chromatography (HILIC) – a powerful separation technique, Anal. Bioanal. Chem. 402 (2012) 231-247.

[27] D.R. Stoll, P.W. Carr, Two-dimensional liquid chromatography: a state of the art tutorial, Anal. Chem. 89 (2017) 519–531.

[28] R.E. Murphy, M.R. Schure, J.P. Foley, Effect of Sampling Rate on Resolution in Comprehensive Two-Dimensional Liquid Chromatography. Anal. Chem. 70 (1998) 1585–1594.

[29] H.J. Li, M.L. Deinzer. Tandem mass spectrometry for sequencing proanthocyanidins. Anal Chem 79 (2007) 1739-1748.

[30] Y. Hayasaka, E.J. Waters, V. Cheynier, M.J. Herderich, S. Vidal, Characterization of proanthocyanidins in grape seeds using electrospray mass spectrometry. Rapid Commun. Mass Spectrom. 17 (2003) 9–16.

[31] R. Moss, Q. Mao, D. Taylor, C. Saucier. Investigation of monomeric and oligomeric wine stilbenoids in red wines by ultra-high-performance liquid chromatography/electrospray ionization quadrupole time-of-flight mass spectrometry. Rapid Commun. Mass Spectrom. 27 (2013) 1815-1827.

[32] R.H. Cichewicz, S.A. Kouzi. Resveratrol oligomers: Structure, chemistry, and biological activity, in: Atta-ur-Rahman (Ed.), Studies in natural products chemistry Vol. 26, Bioavtive Natural Productos (Part G) Elsevier Science B.V., Amsterdam, The Netherlands, 2002.

[33] B. Baderschneider, P. Winterhalter, Isolation and characterization of novel stilbene derivatives from Riesling wine, J. Agric. Food Chem. 48 (2000) 2681-2686.

[34] C. Lambert, T. Richard, E. Renouf, J. Bisson, P. Waffo-Teguo, L. Bordenave, N. Ollat, J.M. Merillon, S. Cluzet. Comparative analses of stilbenoids in canes of major *Vitis vinifera* L. cultivars, J. Agric. Food Chem. 61 (2013) 11392-11399.

FIGURE LEGENDS.

Figure 1. Chemical structure of some representative polyphenols present in grapevine (*Vitis vinifera* L.) canes. A) Resveratrol tetramer (Vitisin A); B) Procyanidin trimer digallate; C) Prodelphinidin tetramer (3(E)C-(E)GC).

Figure 2. First dimension chromatograms (280 nm) corresponding to the separation of the polyphenols found in a grapevine cane extract under optimum conditions for each column. For separation conditions, see section 2.3.

Figure 3. Two-dimensional plots and orthogonality values (A_0) obtained using each first dimension column studied (A, diol; B, PEG; C, ZIC-HILIC) coupled to the partially porous C_{18} column in the second dimension under optimized conditions. Dotted lines define area occupied by peaks. For detailed separation conditions, see section 2.3.

Figure 4. Two-dimensional HILIC × RP plots (280 nm) corresponding to the (poly)phenolic profile of Pinot Noir (A) and Cabernet Sauvignon (B) grapevine canes under optimum separation conditions. For peak identification, see Table 2. For detailed separation conditions, see section 2.3.

Table 1. Comprehensive two-dimensional method parameters applied to the profiling of (poly)phenolic compounds from grapevine canes.

		Diol × C_{18}	PEG × C_{18}	ZIC-HILIC × C_{18}
^{1}D	L (mm)	150	150	150
	I.D. (mm)	1.0	2.1	1.0
	Particle size (µm)	5	5	3.5
	Flow rate (µLmin^{-1})	18	20	15
	$\overline{w}$ (min)	3.01	3.60	3.40
	$^{1}n_c$	32	27	23
	<β>	1.28	1.20	1.22
	$^{1}n_c$ corr.	25	23	19
^{2}D	$\overline{w}$ (s)	1.40	1.40	1.49
	$^{2}n_c$	44	44	41
LC × LC	Analysis time (min)	92	92	75
	t_s	1.73σ	1.44σ	1.52σ
	Modulation time (min)	1.3	1.3	1.3
	$^{2}V_{inj}$ (V ^{1}D effluent)	30 µL (23.4 µL)	30 µL (26 µL)	30 µL (19.5 µL)
	Z_1	0.93	0.85	0.97
	Z_2	0.95	0.91	0.91
	Z_-	0.91	0.42	0.72
	Z_+	0.75	0.60	0.77
	A_0	78%	45%	70%
	$^{2D}n_c$ theoretical	1408	1188	943
	$^{2D}n_c$ practical	1080	961	768
	$^{2D}n_c$ corr.	842	432	538

<β>, average ^{1}D broadening factor; $^{1}n_c$ corr.: calculated according to eq. 2; t_s, sampling time; A_0, orthogonality; $^{2D}n_{c,\ theoretical}$: $^{1}n_c \times {}^{2}n_c$; $^{2D}n_{c,\ practical}$: calculated according to eq. 4; $^{2D}n_c$ corr.: $^{2D}n_{c,\ practical} \times A_0$

Table 2. Main polyphenols detected in the grapevine canes samples using the optimized HILIC × RP-DAD-MS/MS method. (E)C, (epi)catechin; (E)gC, (epi)gallocatechin; (E)gCG, (epi)gallocatechin gallate.

Peak	Total t_R (min)	t_R ^{2}D (s)	$[M-H]^-$	λ max (nm)	Main MS/MS fragments	Identification proposed
1	10.03	55.80	227.2	310	210, 186, 159, 143	(*E*)-Resveratrol
2	10.11	60.60	453.0	326	435, 361, 349, 239, 228	Resveratrol dimer
3	11.26	51.50	243.4	324	225, 201, 175, 159	(*E*)-Piceatannol
4	12.70	60.05	453.7	324	435, 411, 359, 347, 339, 253	Resveratrol dimer
5	13.70	41.70	289.7	280	245, 205, 165, 125	Catechin
6	13.73	43.90	289.2	279	245, 205, 125	Epicatechin
7	15.19	53.20	523.3		503, 485, 475, 358, 243	n.i.
8	15.31	60.40	523.2	324	521, 503, 485, 475, 243	n.i.
9	16.27	40.05	433.7	265	385, 223, 205, 179, 153	n.i.
10	16.40	47.75	533.5	310		n.i.
11	16.42	48.85	475.0	268	441, 429, 379, 351, 257	n.i.
12	16.43	49.95	508.4	268	463, 441, 349, 193	n.i.
13	16.51	54.80	521.1	281	485, 475, 387, 357	n.i.
14	16.54	56.35	559.6	310	516, 485, 470, 441, 289	n.i.
15	16.54	56.55	469.3	301	455, 433, 377, 365	Stilbenoid dimer
16	18.99	47.50	475.1	284	454, 377, 349, 255	n.i.
17	19.03	49.65	469.4	301	452, 376, 364, 349, 255	Stilbenoid dimer
18	19.05	50.70	469.4	303	453, 432, 418, 255	Stilbenoid dimer
19	19.23	61.65	679.4	292, 320	661, 586, 452, 345, 257	Resveratrol trimer
20	21.62	48.85	444.6	273	402, 301, 291, 285	n.i.
21	21.81	60.70	695.2	296, 325	601, 575, 467, 453, 241	n.i.
22	29.57	58.10	906.5	284		Resveratrol tetramer
23	29.67	64.30	906.0	284, 325		Resveratrol tetramer
24	33.25	45.00	579.9	280	561, 531, 453, 289, 246	Procyanidin dimer
25	33.30	48.15	549.4		531, 505, 463, 375	n.i.
26	34.66	57.75	906.3	285		Resveratrol tetramer
27	40.02	61.35	905.9	283		Resveratrol tetramer
28	41.05	45.05	577.6	280	559, 451, 425, 407, 289	Procyanidin dimer
29	42.57	58.00	905.8	285		Resveratrol tetramer
30	42.63	61.45	905.8	284, 326		Resveratrol tetramer
31	46.16	39.30	577.7	279	559, 469, 451, 425, 290	Procyanidin dimer
32	46.18	40.80	577.7	280	559, 469, 451, 425, 408, 289	Procyanidin dimer
33	46.21	42.45	577.6	278	559, 469, 452, 426, 333	Procyanidin dimer
34	46.24	44.15	577.7	281	559, 469, 452, 426, 332, 290	Procyanidin dimer
35	46.46	57.25	579.7	282	559, 469, 452, 425, 289	Procyanidin dimer
36	46.47	57.95	923.4	282	903, 827, 693, 479, 469	Stilbenoid tetramer
37	49.04	56.55	923.8	283	903, 829, 693, 469	Stilbenoid tetramer
38	51.48	46.85	757.1	281	605, 405, 230	n.i.
39	53.96	39.50	593.6		575, 465, 453, 439, 407, 305, 289	Prodelphinidin dimer

40	54.20	53.90	939.8		906, 840, 746, 645	n.i.
41	55.28	40.75	593.4		575, 465, 407,305, 289	Prodelphinidin dimer
42	55.36	45.25	729.3	278	665, 603, 577, 559, 441, 407, 289	Procyanidin dimer monogallate
43	55.52	55.05	839.0	285	821, 679, 532	n.i.
44	55.67	64.25	1045.1	286, 325	1027, 988, 758, 602	n.i.
45	56.63	43.65	745.3	278	645, 592, 453, 341	Procyanidin dimer
46	56.79	53.55	839.8	285	820, 679, 593, 532	n.i.
47	58.22	61.40	790.9*	286	1355, 1131, 906, 792, 679, 451	Resveratrol heptamer
48	59.44	56.25	777.6	288	615, 454	Viniferin diglycoside
49	59.52	61.20	781.8*	288	1439, 1351, 1040, 949, 887, 688	n.i.
50	60.49	41.35	865.6	279	847, 739, 713, 695, 577	Procyanidin trimer
51	60.52	43.35	865.8	278	848, 821, 801, 663, 591, 518, 475	Procyanidin trimer
52	60.54	44.30	881.3	278	729, 711, 591, 577, 559, 439	Prodelphinidin trimer (2(E)C--(E)gC) // Procyanidin dimer digallate
53	60.58	47.15	881.5	280	729, 711, 591, 577, 559, 439	Prodelphinidin trimer (2(E)C--(E)gC) // Procyanidin dimer digallate
54	60.63	49.95	897.7	325	877, 801, 725, 605, 589, 578	Dp-3-p-coumaroilglucoside-(epi)catechin
55	60.74	56.25	1359.7	285	1265, 1253, 1131, 906, 813	Resveratrol hexamer
56	61.87	46.00	881.5	281	861, 753, 727, 709, 791, 547	Prodelphinidin trimer (2(E)C--(E)gC) // Procyanidin dimer digallate
57	61.97	52.00	1195.7	282	1043, 905, 707	Resveratrol tetramer + Catechin
58	64.26	33.75	881.3	278	863, 755, 729, 711, 593, 575, 287	Prodelphinidin trimer (2(E)C--(E)gC) // Procyanidin dimer digallate
59	64.50	47.80	1027.6	279	905, 782, 724, 659, 575, 313	
60	64.70	59.90	1175.1		1137, 1027, 944, 843, 729, 592, 493, 381	n.i.
61	65.71	42.60	897.9	280	838, 769, 743, 727, 607, 591, 467, 303	Prodelphinidin trimer ((E)C+ 2(E)gC)
62	65.74	44.25	1017.0	280	999, 955, 891, 866, 847, 740, 729, 696, 678, 602, 559, 451, 407, 289	Procyanidin trimer monogallate
63	65.76	45.35	1015.2	280	997, 967, 851, 789, 713, 610, 427	n.i.
64	66.01	60.60	922.7*	286	1811, 1555, 905, 875 827, 799	n.i.
65	69.53	37.95	1035.2		1015, 907, 881, 863, 847, 755, 745, 729	Prodelphinidin trimer monogallate ((E)C--(E)gCG or (E)CG--(E)C--(E)gC)
66	69.65	44.65	1169.6	280	1151, 1043, 1017, 999, 881, 865, 847, 729, 577	Procyanidin trimer digallate
67	70.90	42.05	1167.7	279	1152, 1017, 999, 877, 865, 742, 729, 591	Procyanidin trimer digallate
68	76.06	39.70	1171.8			Prodelphinidin tetramer (3 (E)C--(E)gC)
69	76.14	44.10	751.9*	278	1377, 1103, 989, 664, 487	n.i.
70	77.30	36.15	1186.5	290		Prodelphinidin tetramer (2 (E)C--2(E)gC)
71	78.71	42.80	735.0*	279	1443, 1339, 1154, 1017, 865, 578, 289	Prodelphinidin tetreamer digallate

72	78.75	45.20	828.6*	282	1492, 1370, 1016, 865, 745, 571	(2(E)CG--(E)C--(E)gC or (E)CG--2(E)C--(E)gCG) Prodelphinidin tetramer trigallate ((E)CG--2(E)gCG--(E)gC or (E)C--3(E)gCG // Prodelphidin pentamer monogallate ((E)CG--4(E)gC or (E)C--(E)gCG--3(E)gC)
73	81.34	44.45	917.9*	282	1541, 1487, 1087, 1029, 841, 576	n.i.
74	82.66	45.55	884.3*	280	1568, 1483, 1316, 1192, 1065, 739, 591	n.i.
75	82.67	46.05	894.9*	281	1618, 1375, 1316, 1179, 816, 603	n.i.
76	83.92	43.30	881.4*	281	1469, 1183, 806, 795, 728, 590, 577, 289	Procyanidin-related
77	83.96	45.60	886.0*	280	1579, 1483, 1354, 1179, 995, 865, 808, 741, 577	Procyanidin-related
78	86.54	44.25	1163.7	280		n.i.
79	86.57	46.30	1171.7	279		n.i.
80	89.16	45.35	1163.5	278		n.i.
81	94.24	38.10	1028.9	278		n.i.

n.i., Not identified; *ions detected as $[M-2H]^{2-}$

Figure 1
Click here to download high resolution image

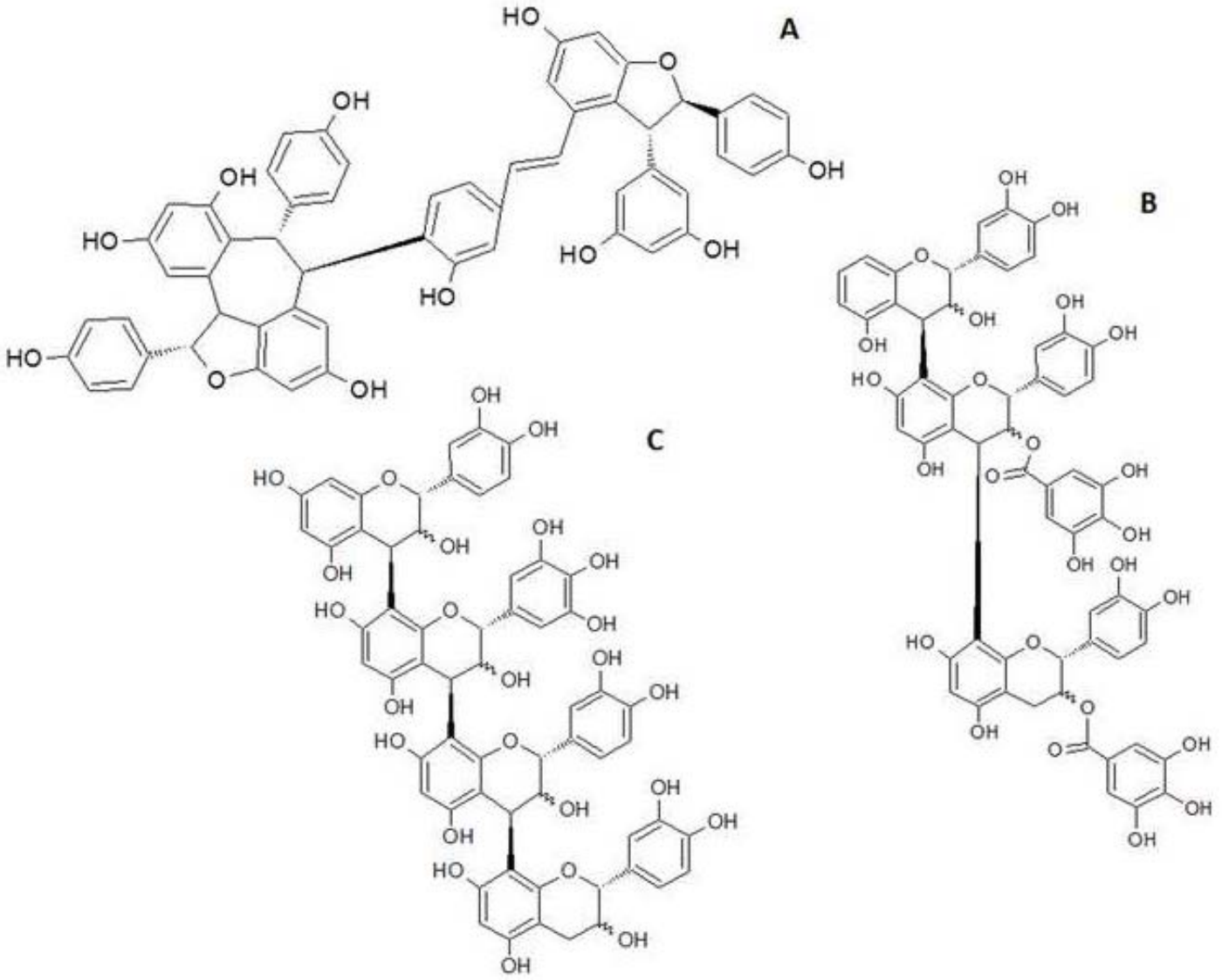

Figure 2
Click here to download high resolution image

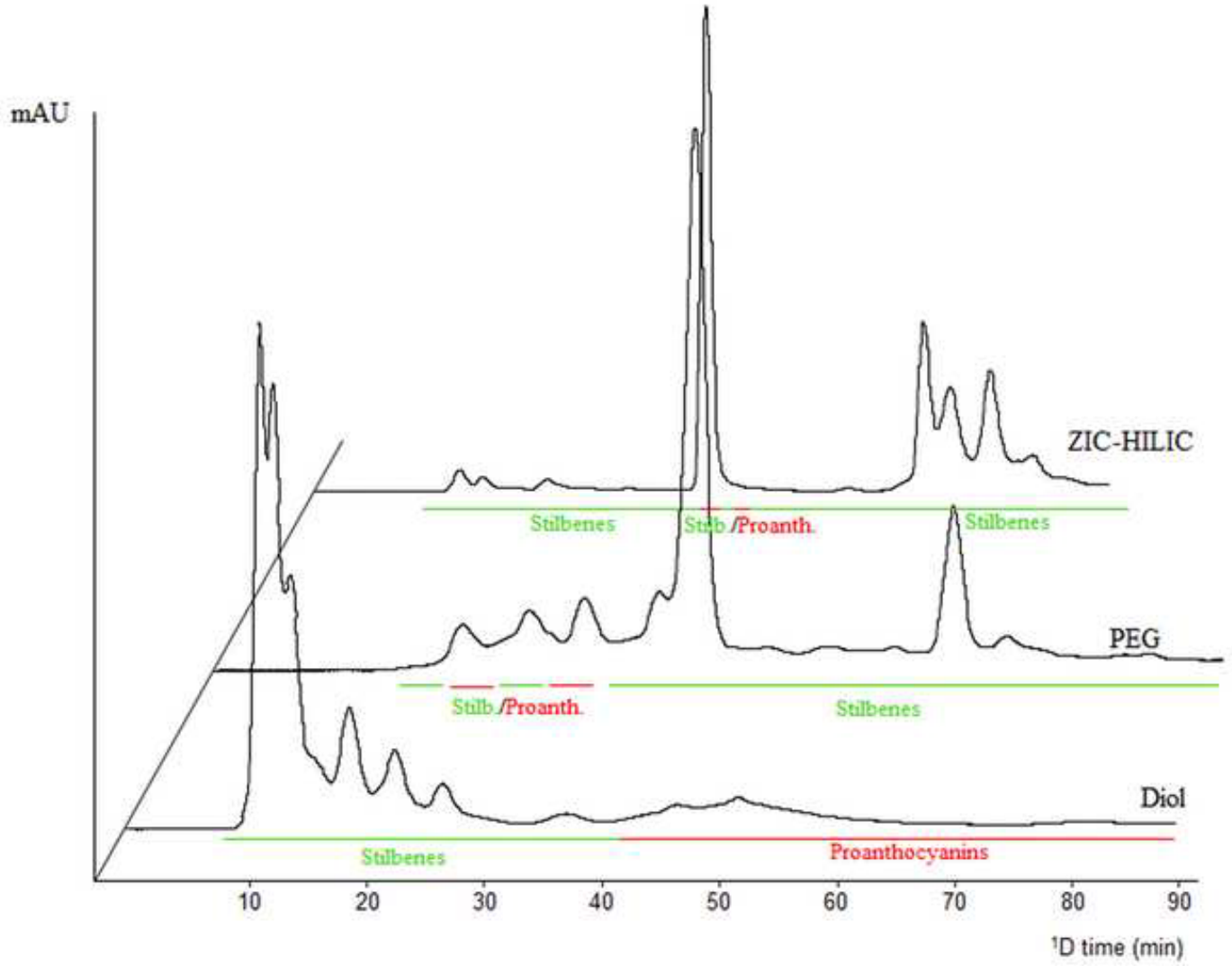

Figure 3
Click here to download high resolution image

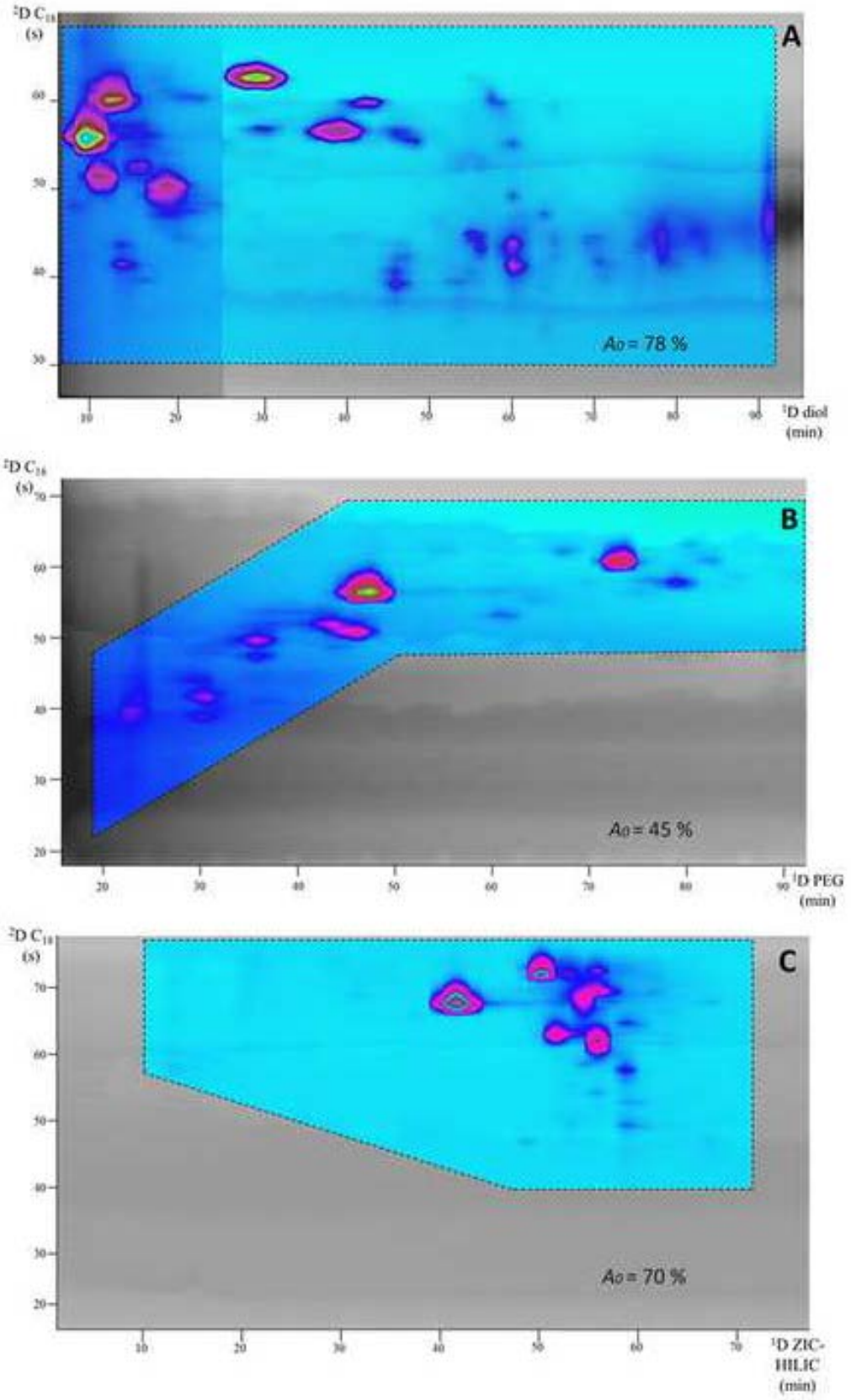

Figure 4
Click here to download high resolution image

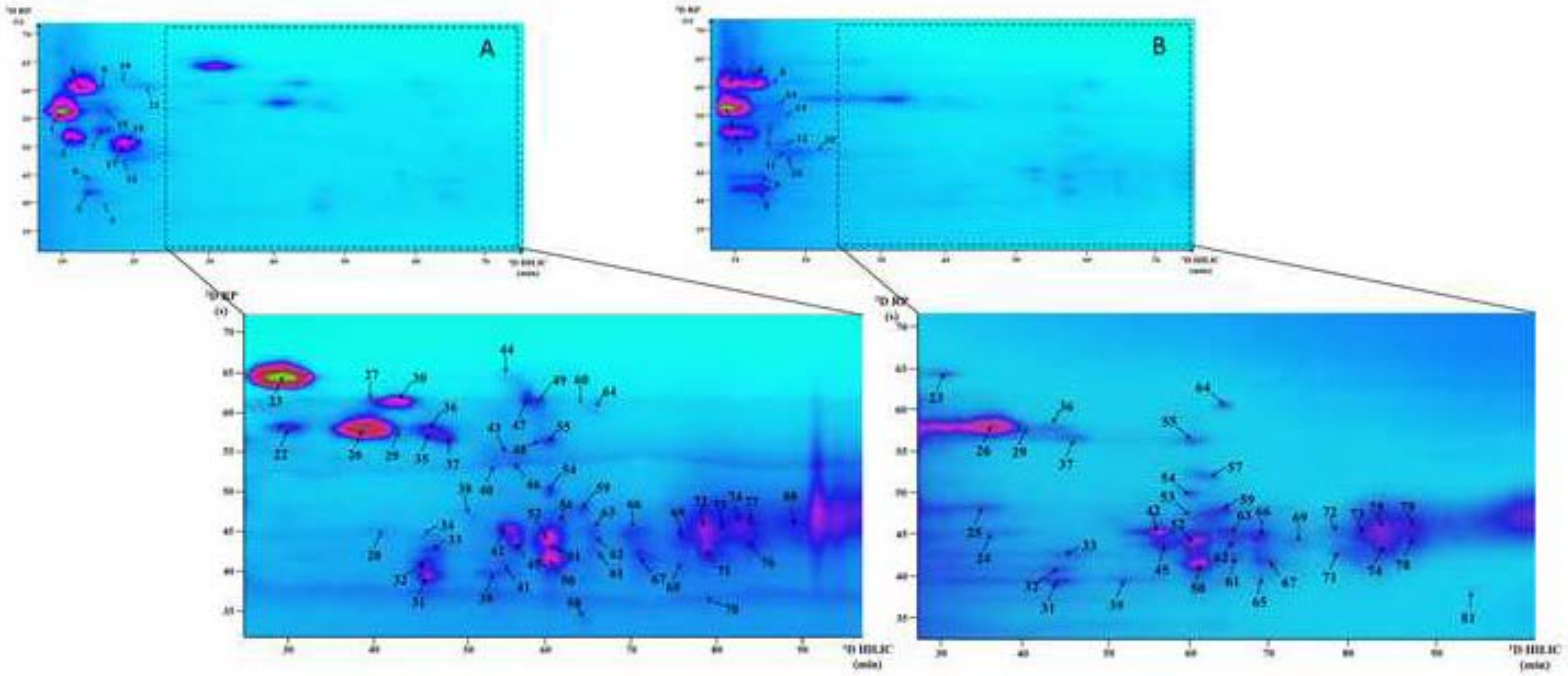

3.6. GENERAL DISCUSSION.

As mentioned, proanthocyanidins are polymeric phenolic compounds that present a complex chemical composition. It is not possible to achieve their complete separation and chemical characterization through only one separation mechanism, since the native proanthocyanidin composition in foods implies a great variability and presents multidimensionality. For this reason, the application of LC × LC for the characterization of these compounds is a good solution to obtain a more comprehensive knowledge on the composition of proanthocyanidins-rich food samples.

In this chapter, an in-depth study of the chemical composition of proanthocyanidins from different agri-food sources, namely grape seeds, apples, chokeberry and grapevine canes, through the application of on-line LC × LC has been carried out. In particular, the separation of these compounds was performed employing HILIC separation mode in the ^{1}D and RP in the ^{2}D. Although this coupling is theoretically able to provide with a high degree of orthogonality, and thus, non-correlated separation mechanisms in both dimensions, its use is far from straightforward. The main difficulty related to this approach, as already described in Chapter 1, relies on the important solvent strength mismatch that takes place during the transfer of ^{1}D effluent to the ^{2}D. This mismatch may produce important peak broadening and/or peak distortion in the ^{2}D separations, thus, generating an important loss on efficiency and separation capabilities. To successfully cope with this problem, exhaustive method optimization is required, which is directly linked to the nature and specific characteristics of each analyzed sample. Consequently, in the following sections, the most-notable aspects related to these optimized methods as well as the main results are described and commented.

3.6.1. INFLUENCE OF METHOD PARAMETERS.

3.6.1.1. Sample preparation.

As in any other analytical procedures, sample preparation is the first step to be considered. Although the use of LC × LC may help to avoid labor-intensive and complicated sample preparation procedures in some applications, depending on the concentration of the targeted

compounds in the real samples, a proper extraction step could be needed. In the case of the samples analyzed within this Chapter, an extraction protocol was employed prior analysis. Conventional solid/liquid extraction methods such as magnetic stirring or ultrasound assisted extraction were employed for the extraction of proanthocyanidin excepting for the extraction of the phenolic content of chokeberry. In that case, environmentally green advanced extraction techniques based on the use of compressed fluids (supercritical fluid extraction, SFE, and pressurized liquid extraction, PLE) were applied, as a part of a biorefinery process proposed to recover valuable ingredients from the residue of the fruit juices industry.

Regarding other sample treatments after extraction, only apple samples required a pre-concentration step consisting on a solid phase extraction (SPE) procedure. This was due to the fact that apples are very complex matrices where numerous macronutrients coexist, including proteins, sugars, lipids as well as secondary metabolites. For the development of that application (Section 3.3), the whole fruits were considered, including pomace and skin, and thus, several macronutrients were co-extracted together with phenolic compounds. The relative amounts of macronutrients compared to polyphenols produced severe interferences in the chromatographic separation. For this reason, the use of liquid/liquid fractionation (Sánchez-Rabaneda et al. 2004) or pre-concentration of the polyphenols has been proposed before their analysis (Shoji et al. 2003; Reis et al. 2012). The rest of the studied samples were directly analyzed before the extraction of the target compounds, without any intermediate additional sample preparation step.

It is worth to mention that the developed applications were directed to the analysis of the entire native proanthocyanidins fraction of each sample, together with other possibly present polyphenols. Due to their great natural complexity, some protocols have been previously developed in which proanthocyanidins are firstly separated from the rest of polyphenols using tedious processes, such as preparative HPLC, and then thiolysis and/or hydrolysis procedures to reduced their diversity (Lazarus et al. 1999). These sample preparation steps are well known for producing substantial modifications in the analyzed components, thus, concealing the actual native composition. By using the LC × LC methods proposed in this Chapter, this kind of

sample pretreatments are avoided, and thus, the native chemical composition may be characterized.

3.6.1.2. ^{1}D separation.

Several stationary phases were tested for the HILIC-based ^{1}D separation of proanthocyanidins in the different samples. For instance, silica and diol stationary phases were tested for the optimization of the separation of grape seed procyanidins; besides these two, an amino HILIC-compatible stationary phase was studied for the chokeberry application, whereas diol, ZIC-HILIC and polyethylene glycol (PEG) stationary phases were tested for the separation of grapevine canes proanthocyanidins. Considering the particular nature of PEG particles, this column was run using both HILIC and RP separation modes. In the case of apple procyanidins, the previously developed method for grape seed procyanidins was re-optimized and adapted for this new sample, due to the satisfactory results obtained.

In general, diol particles have been demonstrated to be very selective for the separation of proanthocyanidins, allowing an elution in increasing order of DP. Diol-bonded stationary phases usually contain neutral hydrophilic 2,3-dihydroxypropyl ligands and show high polarity and hydrogen bonding properties (Jandera 2011). The retention of proanthocyanidins in diol columns was achieved through very slow increments of the proportion of water in the mobile phase during the gradient to elute the larger molecules at the end of the analysis. In agreement with Kelm et al. (2006), diol particles showed stronger retention characteristics and an increase in speciation of the different proanthocyanidins than silica, ZIC-HILIC, PEG and amino stationary phases. Consequently, diol stationary phase was finally selected as ^{1}D column for three out of the four developed applications. In the case of chokeberry, the phenolic profile of this sample contained a large number of different compounds, among them, a high concentration on anthocyanins; in this regard, amino stationary phase provided the maximum separation among the entire pattern of phenolic compounds present in that sample.

As a common aspect to the four studied samples, the same strategy was followed in order to minimize the ^{1}D undersampling effect at the same time that reducing the volume fraction stored in the valve, thus, minimizing the solvent strength mismatch. The mentioned approach was based on the use of micro-bore columns (1 mm i.d.) in the ^{1}D working at very low flow

rates (15–21 μL min^{-1}, depending on the application). These conditions allowed obtaining broad separations along the ^{1}D chromatogram achieving peaks wide enough to be able to comply with Murphy's rule of 3–4 samplings per ^{1}D peak (Murphy et al. 1998). In Table 3.1, the data related to the separation conditions are summarized.

Table 3.1. Comparison of 2D separation data of the four proanthocyanidins-rich samples.

Sample	$^{1}\overline{w}$ (min)	$^{1}n_c$	Optimal sampling rate (min)	$^{2}\overline{w}$ (s)	$^{2}n_c$	$^{2D}n_{c,practical}$	A_O (%)	$^{2D}n_{c,corrected}$
Grape seeds	3.31	19	1.7	1.4	57	875	76	666
Apples	2.86	19	1.4	0.8	95	1334	68	907
Chokeberry	2.77	28	1.4	1.0	82	1693	76	1287
Grapevine canes	3.01	32	1.5	1.4	57	1397	78	1083

$^{1}\overline{w}$ and $^{2}\overline{w}$: average peak width in ^{1}D and ^{2}D, respectively; $^{1}n_c$ and $^{2}n_c$ individual peak capacity of the ^{1}D and ^{2}D calculated according to Eq. 11; Optimal sampling rate corresponding to $2^{1}\sigma$; $^{2D}n_{c,practical}$: calculated according to Eq. 16; A_O, orthogonality; $^{2D}n_{c,corrected}$: practical peak capacity corrected by orthogonality ($^{2D}n_{c,practical} \times A_O$).

3.6.1.3. Interface.

For all the applications a 10-port, 2-position switching valve equipped with two sampling loops of identical internal volume was employed. The minimum required volume of the sampling loops directly depends on the ^{1}D flow rate as well as the modulation time, considering that the volume of ^{1}D effluent to be transferred will be calculated from the product of the ^{1}D flow rate and the total ^{2}D analysis time, which is equal to the modulation time. In turn, the modulation time has to be established considering the already mentioned Murphy's rule. This widely-accepted theory establishes that each ^{1}D peak has to be sampled at least 4 times. Considering that the full width at baseline of a perfectly Gaussian peak is 8σ (being σ its standard deviation), a sampling rate of 2σ would be enough to meet with this requirement (see Figure 3.2). The applied sampling rates in each application considering the modulation time (1.3 min) as well as the average ^{1}D peak width ($\overline{w}$) obtained were 1.7σ, 1.4σ, 1.4σ, and 1.5σ min for the separation of grape seeds, apple, chokeberry and grapevine canes, respectively (Table 3.1). Thus, although 1.3 min may seem a long modulation time, being a possible cause for

severe undersampling with loss of gained ^{1}D resolution, in truth, in every application the system was operated well behind the recommended sampling rate by Murphy's rule. This implies an advantage to maintain the resolution of the ^{1}D separation during the transfer process, allowing using long enough ^{2}D analysis times to obtain the maximum possible ^{2}D separation and resolution (Bedani et al. 2012).

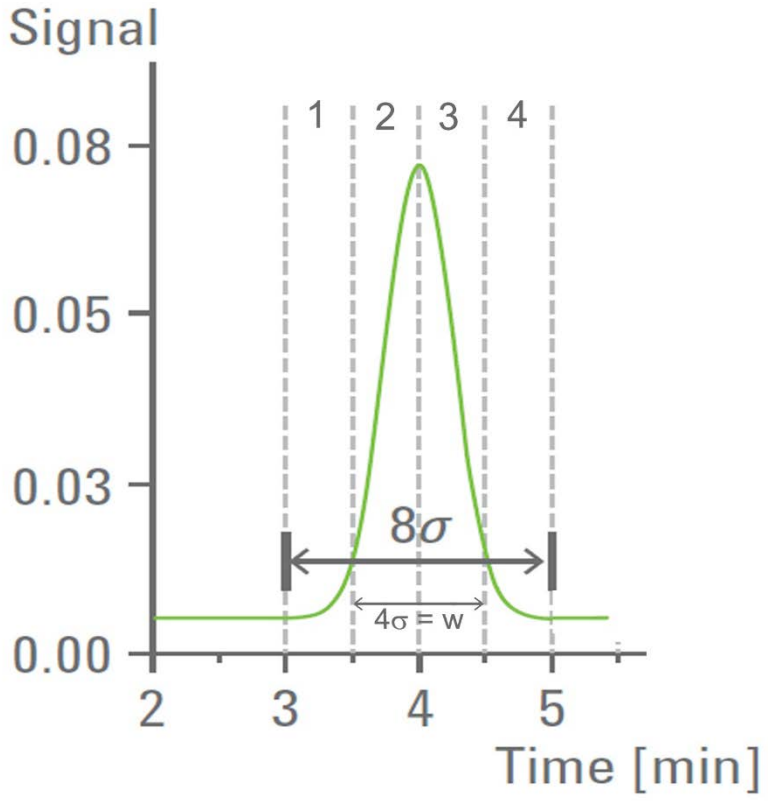

Figure 3.2. Schematic representation of the 8σ peak width of a Gaussian chromatographic peak. Dashed lines indicate a sampling rate of 2σ corresponding to four cuts per peak.

The influence of the volume of the sampling loops installed in the switching valve, and thus, the influence of the fraction solvent transferred onto the ^{2}D separation was studied in the first developed application (Section 3.2), in order to reach an appropriate balance between the solvent in which the collected fraction was transferred to the ^{2}D (to minimize the solvent strength mismatch) and the injection volume in the ^{2}D (to reduce the ^{2}D band broadening). This aspect has a huge relevance in the ^{2}D separation since important deleterious band broadening effects may be produced in the ^{2}D separations as a result of either the transfer of

fractions involving stronger solvents and the injection of large volumes. Consequently, the aim of these experiments was to find a compromise between the injection of a fraction diluted as much as possible and the injection of a volume as reduced as possible.

Considering the ^{1}D flow rate and the sampling time, the ^{1}D effluent to be stored in the sampling loop was 19.5 μL. Thus, the use of 20 μL-loops would be enough to collect the whole fraction; however, in this study, loops with three different volumes (20, 30, 50 μL) were tested. The use of loops with larger internal volume than strictly necessary (19.5 μL) allowed filling the rest of the available volume with the initial ^{2}D gradient mobile phase achieving a partial dilution of the ^{1}D solvent in a completely compatible ^{2}D solvent. This dilution effect allows decreasing the overall fraction solvent strength. Loops with an internal volume of 30 μL were selected; this volume allowed a significant reduction in the fraction solvent strength, not producing any visible peak distortion in the ^{2}D, at the same time that the injection volume (6% of total ^{2}D column void volume) was kept to a minimum to avoid band broadening. Based on the observed results, this dilution strategy was extended to the rest of applications included in the present PhD Dissertation.

3.6.1.4. ^{2}D separation.

Following the set-up selected for proanthocyanidins separation by LC × LC, short RP columns with a broad internal dimeter were selected in the ^{2}D, with the aim to maintain the ratio between the internal diameters of ^{2}D and ^{1}D columns ($^{2}d_c/^{1}d_c$) as high as possible. It has been repeatedly reported that increasing the $^{2}d_c/^{1}d_c$ ratio, significantly reduce the problems associated to solvent incompatibility (Carr and Stoll 2015; Bedani et al. 2012).

The use of partially porous columns as well as monolithic columns in the ^{2}D has been pointed out as very interesting to carry out fast ^{2}D separations with the higher possible efficiency/backpressure relationship. The comparison of the use of these two types of columns was carried out for the separation of procyanidins from grape seeds. The tested partially porous column showed better efficiency and resolution than the monolithic column, both containing C_{18} functional groups. Although the monolithic column provided with good results allowing

smaller pressure drops, the partially-porous materials improved the resolution of some of the separated compounds (Figure 3.3). Consequently, that column (50 × 4.6 mm, 2.7 μm) was selected for further analyses of complex phenolic polymers.

However, recent developments on column technology provide different stationary phases available with diverse selectivity. For this reason, the study of different stationary phases compatible with RP mode that may confer differential selectivity in the ^{2}D were studied for the separation of procyanidins and stilbenoids present in grapevine canes. Namely, C_{18} and pentafluorophenyl (PFP) partially porous columns were tested. Although PFP particles produced the same elution order than C_{18}, this column presented unparalleled better retention and resolution.

In spite of using basically the same column in the ^{2}D for the four food-related matrices studied, the gradient profiles throughout the 2D analysis were optimized for the different applications. In some of them, such as the separation of phenolic compounds in apples, the use of SIF ^{2}D gradient was very useful to carry out good 2D separations, giving rise to a better coverage of the 2D space, and therefore, giving a higher orthogonality. The use of SIF gradient profiles allows a better optimization of the available separation space, since the gradient is modified at different parts of the 2D analysis to adapt to the eluting compounds. Besides, the use of SIF gradients was also considered during the optimization of the different couplings tested for the separation of the grapevine canes. In Figure 3.4, the comparison of using FIF ^{2}D gradient (Figure 3.4A) and SIF ^{2}D gradient (Figure 3.4B) in the analysis of grapevine canes using a PEG column in the ^{1}D and a C_{18} column in the ^{2}D is shown.

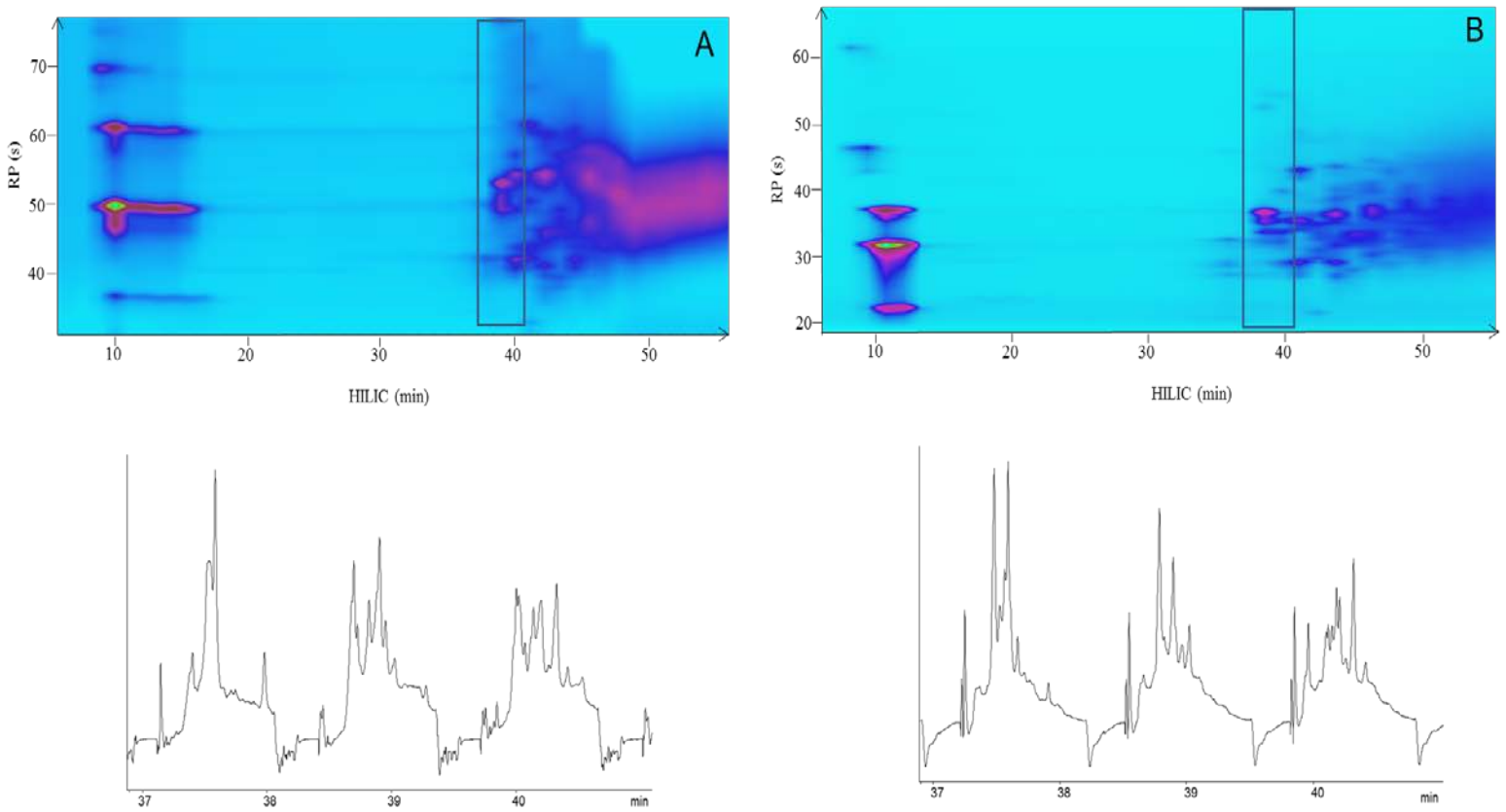

Figure 3.3. Comparison of the HILIC × RP analysis of grape seed procyanidins using a C_{18} monolithic column in the ^{2}D (A) and a C_{18} partially porous column in the ^{2}D (B)

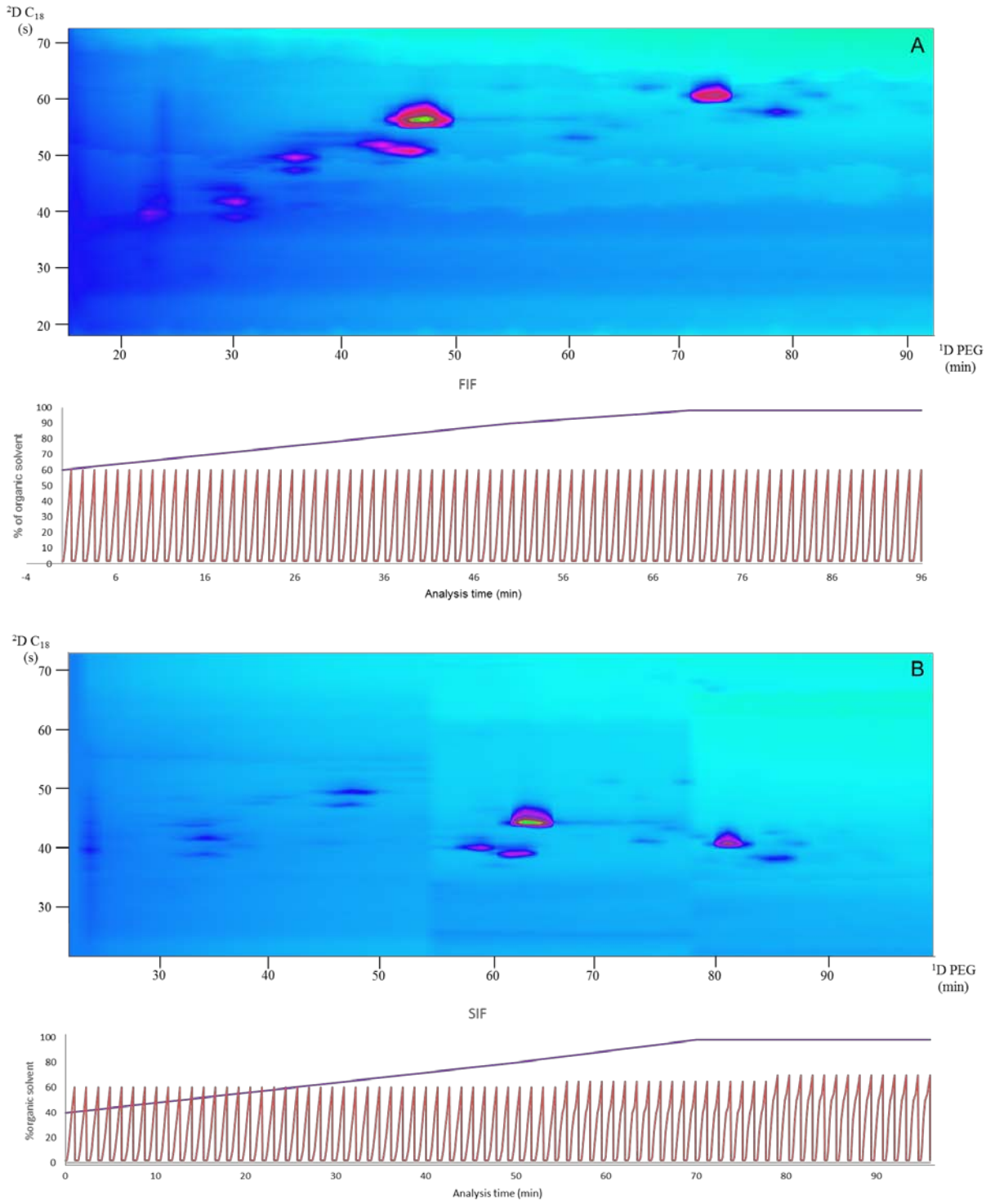

Figure 3.4. 2D plots of the separation of grapevine canes using FIF gradients (A) and SIF (B) gradients in the ^{2}D.

3.6.2. CHEMICAL CHARACTERIZATION OF PROANTHOCYANIDINS-RICH FOOD-RELATED SAMPLES BY HILIC × RP.

The analysis of grape seed procyanidins by the developed diol × C_{18} method enabled the separation of 46 compounds. Among them, procyanidins up to DP = 7 were separated thanks to the use of a diol column in the ^{1}D, as well as different isomers of procyanidins (up to 5 isomers of pentamer monogallate), some of them mono and digalloylated. Some of the tentatively identified compounds in grape seeds, such as several mono and digalloylated procyanidins with high DP were described for the first time.

The MS analysis of proanthocyanidins was carried out under negative ionization mode. Under this ionization mode was possible to identify the catechin and epicatechin monomers at the beginning of the analysis showing an ion at *m/z* 289 ($[M-H]^-$). After the monomer units, the detection of oligomers of procyanidins with increasing DP and galloylation degree was possible thanks to their representative $[M-H]^-$ as well as their fragmentation pathway. Proanthocyanidins can suffer several fragmentation pathways, some of the most common are the characteristic retro-Diels-Alder (RDA) reaction, which produces a loss of 152 Da of the (epi)catechin units and the heterocyclic ring fission (HRF) that produces a loss of 126 Da. Besides, for the identification of the different oligomers, losses of (epi)catechin units and gallic acid molecules (-289 and -152 Da, respectively) were observed.

In the case of apple samples, the diol × C_{18} analysis revealed the complex apple phenolic profile, formed by procyanidins with a DP up to 8, dihydrochalcones, flavonols and hydroxycinnamic acids; one of the main novelties provided by the developed methodology was the separation and identification of the mentioned compounds, belonging to very different phenolic groups, in the same run. All these compounds were identified by their typical UV-Vis and their MS and MS/MS spectra. An example of the MS/MS fragmentation of the different groups detected in the apple profile is shown in Figure 3.5. As can be observed, procyanidins usually show RDA (-152 Da) and HRF (-126 Da) fissions as well as losses of (epi)catechin units (Figure 3.5A). In the case of flavonols, they are present as glycosylated compounds, so their main fragment corresponds to the aglycone, quercetin at *m/z* 301 due to the loss of the

glycosidic units (Figure 3.5B). The same fragmentation pathway was observed in the case of the dihydrochalcones, were the aglycone ion corresponded to phloretin at *m/z* 273 (Figure 3.5C).

Moreover, the developed procedure was applied to the comparison of five apple varieties, looking for differences on the obtained profiles. This way, characteristic 2D plots were obtained for each variety, revealing significant quali- and quantitative differences. These visual differences observed in the 2D plots were further confirmed using quantitative colorimetric assays.

Grapevine (*Vitis vinifera*) canes are a waste of the agrifood industry, which valorization may be of interest, considering that these by-products are still rich in bioactive interesting compounds. In order to fully understand the potential of this matrix, a HILIC × RP method, based on the combination of a diol and C_{18} columns, was applied to gain deeper knowledge on its composition on bioactive compounds. The method developed allowed the separation and identification of mono and digalloylated procyanidins with DP up to 3. For example, peak 67 was tentatively identify as procyanidin trimer digallate presenting a *m/z* 1167.7 ($[M-H]^-$), and fragment ions at *m/z* 1017, 877, 865 and 725 corresponding with the loss of a gallic acid molecule, a (epi)catechin unit, two gallic acid molecules and a (epi)catechin gallate unit, respectively, as can be observed in Figure 3.6.

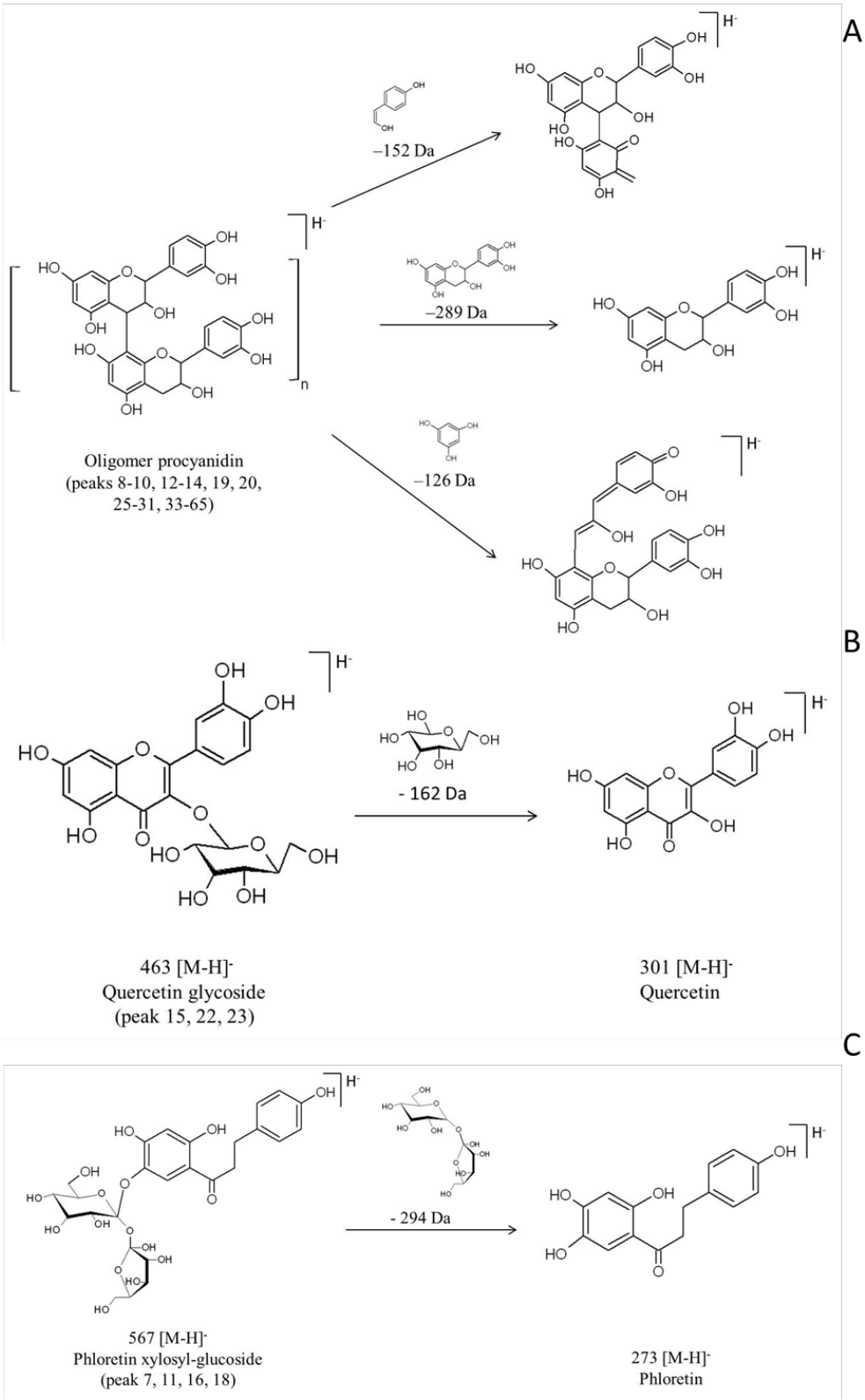

Figure 3.5. Schematic MS/MS fragmentation pathway of three different phenolic compounds found in apple: procyanidins (A), flavonols (B) and dihydrochalcones (C).

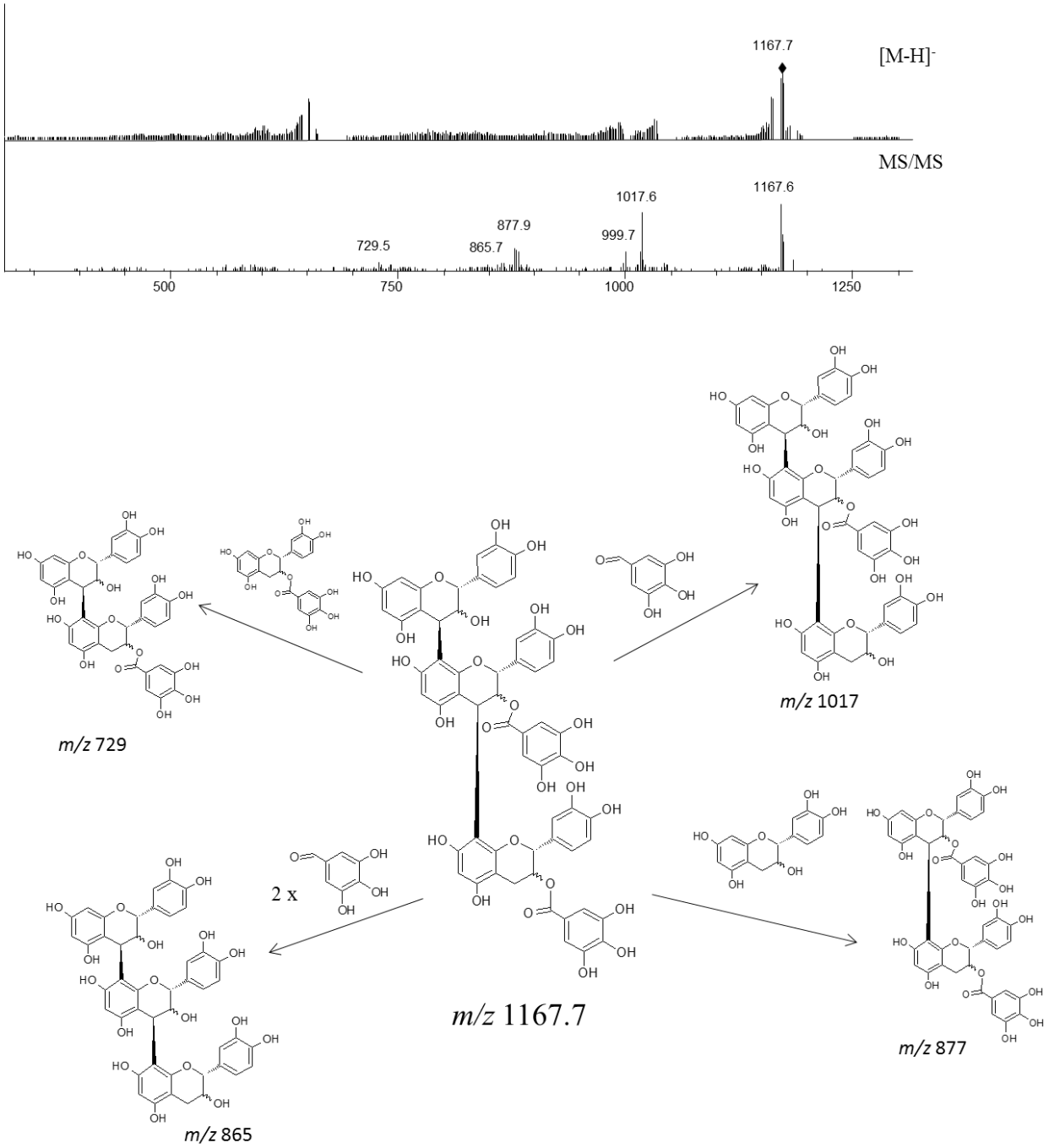

Figure 3.6. MS and MS/MS spectra of a procyanidin trimer digallate as well as its proposed fragmentation pathway.

The very high resolving power that this method provided, also allowed the separation and tentative identification of galloylated prodelphinidins for the first time in this sample. An example of the identification of these new compounds found in grapevine canes is shown in Figure 3.7.

As can be observed in Figure 3.7, this compound presented a $[M-2H]^{2-}$ ion at 828.6 and it was tentatively identified as prodelphinidin tetramer trigallate thanks to the MS/MS observed fragments.

Besides, by using this method, the separation of another kind of complex polymeric phenolic compounds, stilbenes, was also possible. In this regard, the identification of large stilbene polymers that had not been previously described in grapevine canes (stilbene hexamers and heptamers) was attained. For instance, the presence of a $[M-2H]^{2-}$ at *m/z* 790.9 was tentatively assigned to a resveratrol heptamer. The fragmentation pathway of this compound reveal the successive losses of resveratrol units showing losses from 1 to 5 resveratrol units corresponding with the *m/z* ions at 1355 (loss of one resveratrol unit), 1131 (loss of two resveratrol unit), 906 (loss of three resveratrol unit), 679 (loss of four resveratrol unit) and 451 (loss of five resveratrol unit), as schematically represented in Figure 3.8.

In summary, the relevance of the obtained results lies in the high separation power that LC × LC provides, allowing, in a single run, the identification of bioactive compounds in the studied by-products.

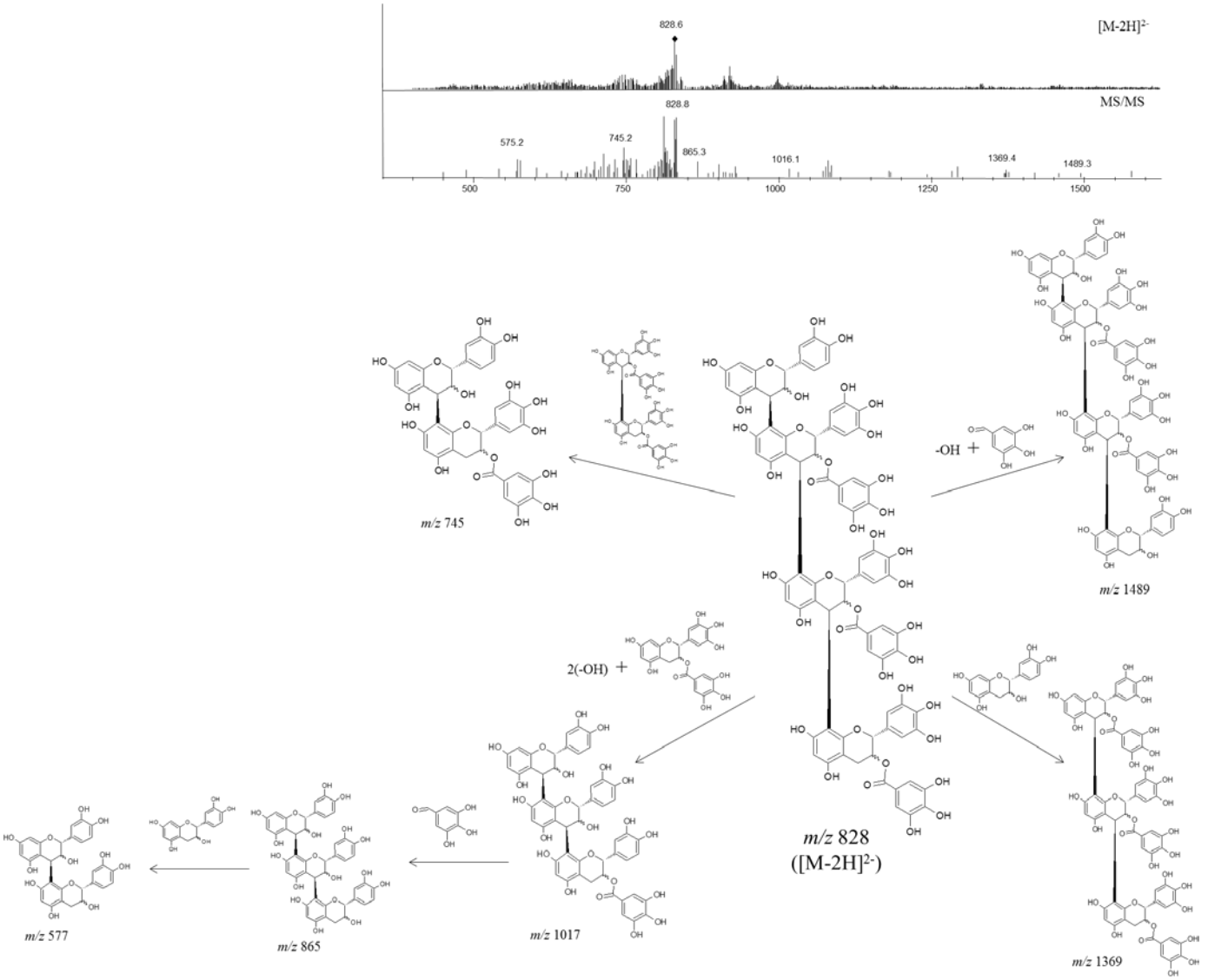

Figure 3.7. MS and MS/MS spectra of a prodelphinidin tetramer trigallate as well as its proposed fragmentation pathway.

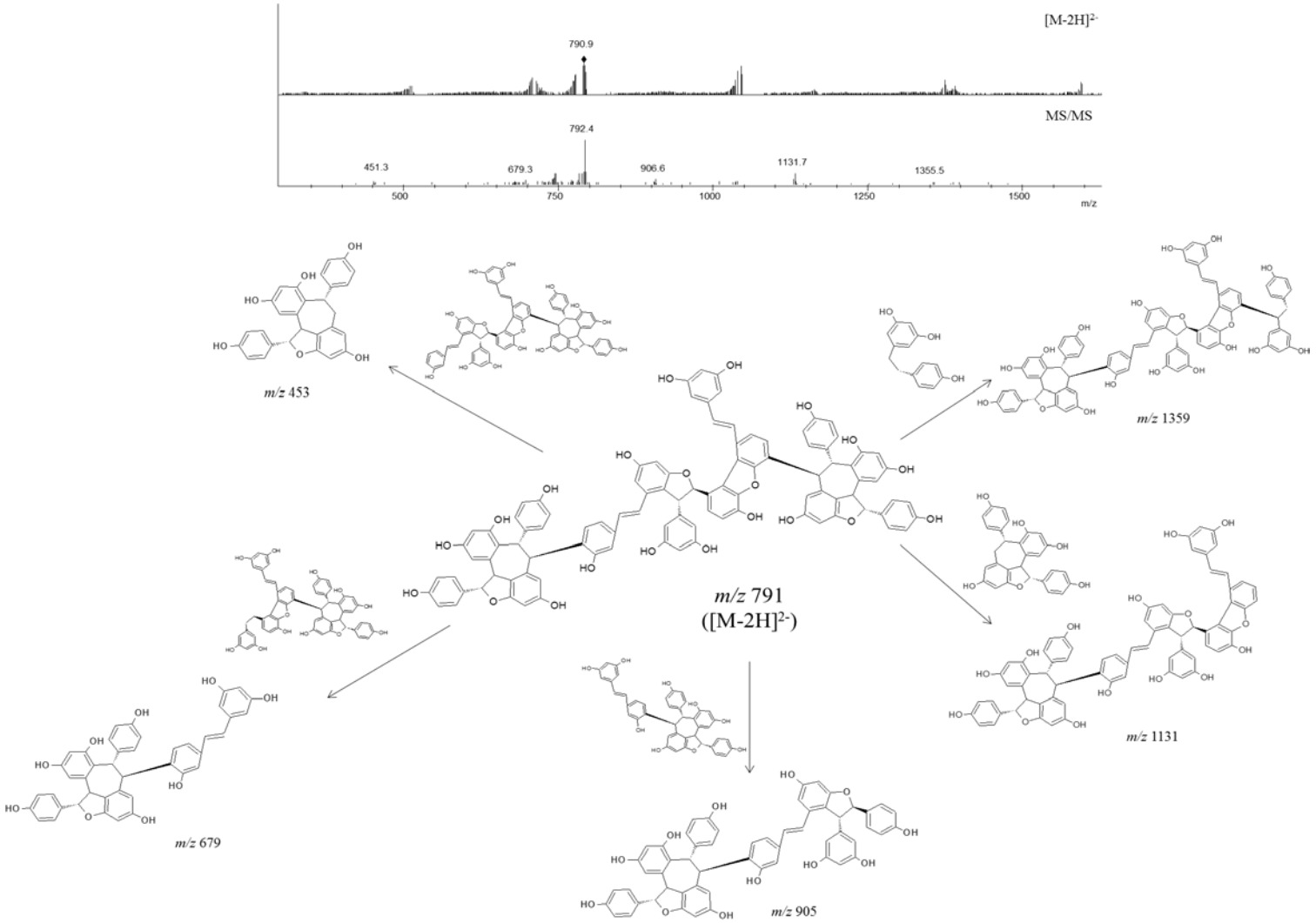

Figure 3.8. MS and MS/MS spectra of a resveratro heptamer as well as its proposed fragmentation pathway.

Lastly, an amino × C_{18} method was developed for the chemical characterization of another agrifood by-product, the residue obtained from the chokeberry (*Aronia melanocarpa*) juice industry. In this work, the chemical characterization of procyanidins up to DP = 6, as well as some prodelphinidin monomers and dimers with different degree of galloylation was achieved. The tentative identification of prodelphinidins in chokeberry was also described for the first time in this work. Besides proanthocyanidins, this method was able to separate in the same analytical run a wide range of phenolic compounds such as a complex mixture of anthocyanins as well as flavonoids and phenolic acids.

In summary, the use of diol × C_{18} combination has been demonstrated to be a very efficient approach for the separation of complex mixtures of proanthocyanidins. These polymeric molecules were separated in increasing order of DP in the ^{1}D HILIC-based separation, while in the ^{2}D RP-based separation, a distribution as a function of their hydrophobicity was obtained. These two separation mechanisms showed very low correlated separation selectivity, allowing a good peak coverage of the 2D space. In table 3.1 the orthogonality values as well as the practical and corrected peak capacity values of the three diol × C_{18} methods are presented. On the other hand, the amino × C_{18} coupling also showed a very good orthogonality degree (A_O = 76%). Moreover, although the developed methods were primarily focused on the separation of proanthocyanidins, by carefully optimizing each procedure, the complete polyphenolic profile was obtained for the different studied samples. In this regard, a further advantage of the used two-dimensional methodology was to obtain the phenolic compounds profile of very complex samples in just one run.

The results obtained in this Chapter open up the possibility for the elucidation and chemical characterization of complex mixtures of proanthocyanidins, considering that these phenolic compounds are widely distributed in nature, enhancing the current one-dimensional methods for the separation of proanthocyanidins through the application of HILIC × RP methods. Further development towards quantification would be of very high interest.

CHAPTER 4.

Chemical characterization of phlorotannins by HILIC × RP-DAD-MS/MS

4.2. Separation and characterization of phlorotannins from brown algae *Cystoseira abies-marina* by comprehensive two-dimensional liquid chromatography.

4.3. Anti-proliferative activity and chemical characterization by comprehensive two-dimensional liquid chromatography coupled to mass spectrometry of phlorotannins from the brown macroalga *Sargassum muticum* collected on North-Atlantic coasts.

4.1. INTRODUCTION.

Algae have been considered as the "plant-based food of the future" (Cardoso et al. 2015) because their composition comprises a wide range of interesting nutrients and secondary metabolites, mainly lipids and polyunsaturated fatty acids (PUFAs), pigments such as carotenoids and chlorophylls, proteins, polysaccharides and phenolic compounds (Stengel et al. 2011; Herrero et al. 2015). For this reason, algae are nowadays considered as a promising source for health promoting compounds.

From a biological point of view, however, algae are far from being just aquatic plants. There are numerous definitions for the organisms commonly considered algae, although some common points are that algae are autotrophic photosynthetic organisms. Their classification is quite complex, and in fact, the organisms traditionally considered algae may belong to three out of the six taxonomic realms for living organisms, *Bacteria, Protista and Plantae*. As a result of the great variability that can be found within algae, these organisms may present dramatic morphological differences, involving unicellular microscopic organisms to huge pluricellular forms that may be tens of meters long. For this reason, a common way to classify algae according to their size implies a division into microalgae (unicellular) and macroalgae, also commonly called seaweeds. Among seaweeds, there is also a huge diversity of species that are usually classified in three categories according to their composition of pigments: green algae (*Chlorophyceae*), red algae (*Rhodophyceae*), and brown algae (*Phaeophyceae*).

4.1.1. PHLOROTANNINS IN BROWN ALGAE.

Macroalgae are well-known as a rich source of some polyphenols. Among the different algae classes, brown algae are considered those with higher amount of these interesting compounds (Heffernan et al. 2015). In fact, brown algae present a variety of phenolic compounds, called phlorotannins, that has only been described in this type of seaweeds (Li et al. 2011; Steevensz et al. 2012; Isaza Martínez and Torres Castañeda 2013; Stiger-Pouvreau et al. 2014).

Phlorotannins present a structural function in algae due to their contribution to the formation and fortification of the cell wall. Their content on brown algae can reach concentrations

ranging 20 to 250 mg g^{-1} of the algae dry weight (Shibata et al. 2004). Besides, as secondary metabolites of algae, other functions have been attributed to these compounds, for instance, a protection function against UV radiation, heavy metal chelation activity or antibacterial, antifouling and anti-herbivory activity (Amsler and Fairhead 2006). As a consequence of theses protective functions, phlorotannins have been studied as potential bioactive compounds to produce positive health effects, such as antioxidant, antiproliferative, anti-HIV, anti-Alzheimer, anti-obesity, antidiabetic or antiallergic effects, among others (Li et al. 2011; Montero et al. 2017). In order to determine relationships between the bioactivity observed and the compound (or compounds) responsible for that bioactivity, and thus, to study the interesting health effects that phlorotannins may confer, an exhaustive chemical characterization of these compounds in the original samples is required. This is an essential requirement to understand which compounds exert the attributed physiological biological action.

4.1.2. CHEMICAL STRUCTURE OF PHLOROTANNINS.

From a chemical and structural point of view, phlorotannins are complex polymeric phenolic compounds composed of phloroglucinol units (PGUs) (1,3,5-trihydroxybenzene), linked to each other by different bonds. The molecular size of phlorotannins is in the range of 126 Da (for phloroglucinol unit) to 650 KDa (for highly polymerized phlorotannins). Depending on the linkages found in their structure, phlorotannins can be classified into: fucols (phenyl linkages), phlorethols (ether bonds), fuhalols (ether bonds and additional hydroxyl groups), fucophlorethols (with ether and phenyl linkages) and eckols and carmalols (dibenzodioxin linkage) (Figure 4.1) (Isaza Martínez and Torres Castañeda 2013). Moreover, the complexity of these polymers increases since some brown algae present halogenated phlorotannins (bromo-, chloro- and iodo- phlorotannins) (La Barre et al. 2010).

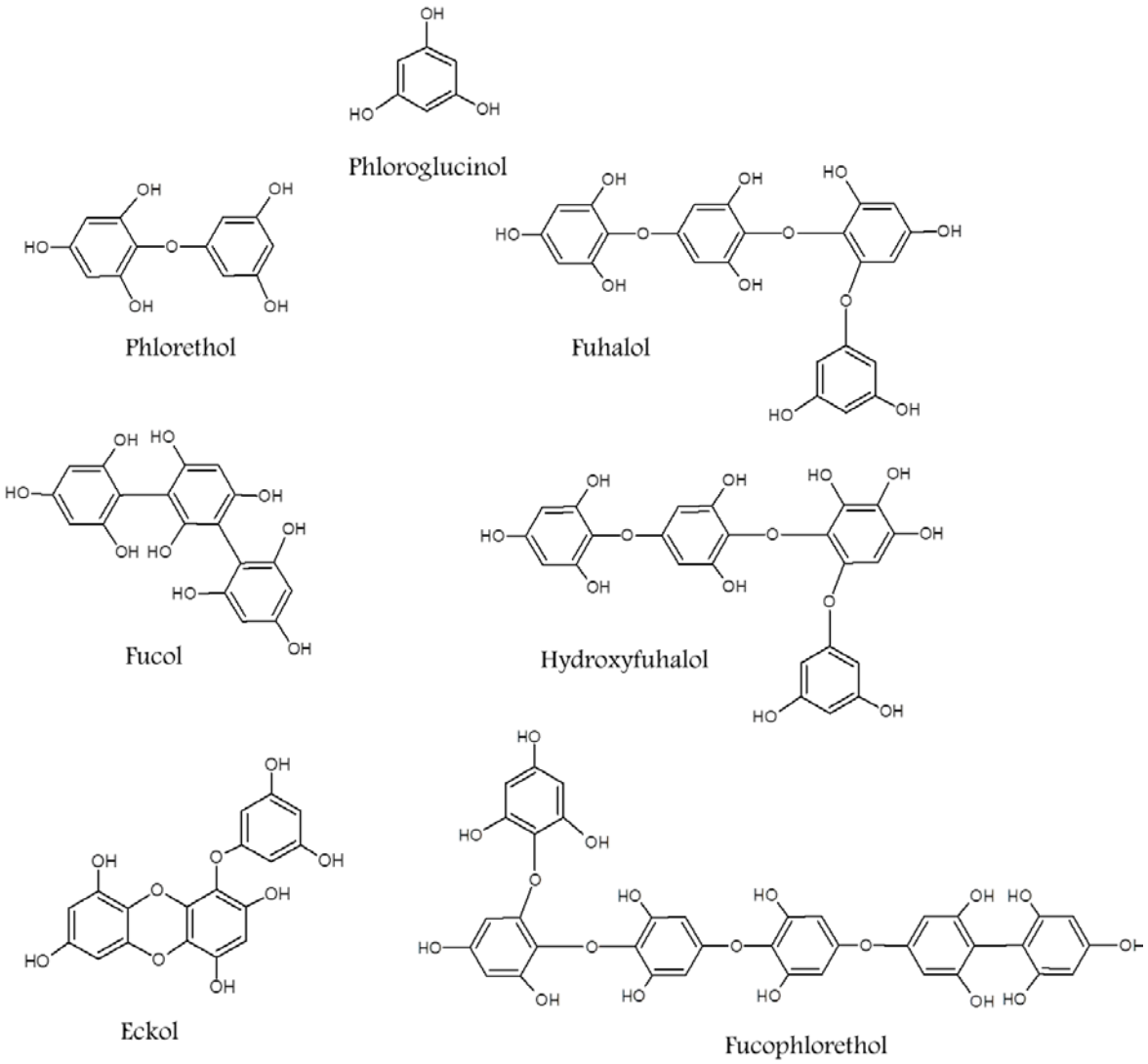

Figure 4.1. Chemical structure of phloroglucinol and structural classes of phlorotannins according to the linkage between phloroglucinol units.

For this reason, the chemical content on phlorotannins in a particular species may reach a very high degree of complexity, as a very diverse chemical variety may be found. These technical difficulties together with the fact that algae are largely unexplored sources, imply that the composition of phlorotannins in brown seaweeds is, to date, essentially unknown. Thus, further efforts in the characterization of these compounds are needed; in this sense, advanced analytical techniques are required for the study of the complex chemical structure and the composition of phlorotannins in individual brown algae species (Heffernan et al. 2015).

4.1.3. CHEMICAL CHARACTERIZATION OF PHLOROTANNINS.

The structural complexity and diversity of phlorotannin fraction greatly increases as the number of PGUs growths as well as with the variety of bond types between units and the positions at which they are linked as can be observed in Figure 4.2 (Kim et al. 2013). This level of complexity extremely hampers the individual identification and chemical characterization of phlorotannins.

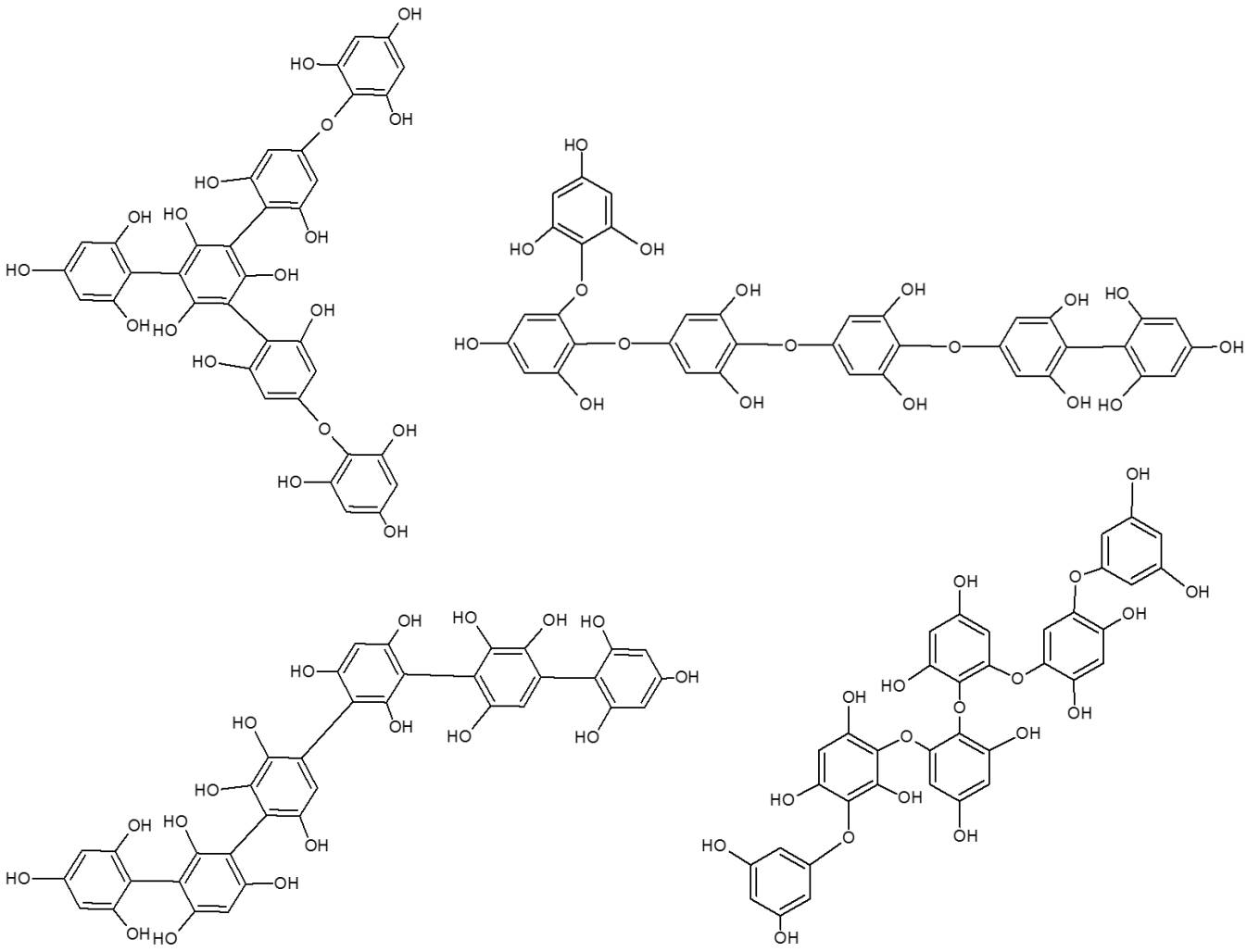

Figure 4.2. Different phlorotannin molecules with the same PGU presenting different types and positions of linkages.

Different analytical techniques have been employed to separate and identify phlorotannins from different brown algae, such as HPLC-DAD-MS (Ferreres et al. 2012; Steevensz et al. 2012; Wang et al. 2012) or UHPLC-DAD-MS (Tierney et al. 2014; Heffernan et al. 2015). Usually, liquid chromatographic separations of phlorotannins are carried out under NP or RP modes. However, similar to proanthocyanidins, the polymeric nature of phlorotannins implies some limitations on their chromatographic separation. RP separation mode allows the separation of relatively short-chain phlorotannins, but presents limited separation power for phlorotannins with higher DP and with an increased number of isomers, that usually coelute in a big and wide peak at the end of the analysis. On the other hand, the NP polar stationary phases produce a more efficient retention of phlorotannins enabling the separation of higher polymerized phlorotannins in increasing DP order. However, NP does not provide good resolution for the separation of different phlorotannins isomers with the same DP. Likewise, very highly polymerized compounds are not separated either, appearing a hump at the end of the analysis containing the larger phlorotannin polymers, as can be observed in Figure 4.3 (Koivikko et al. 2007).

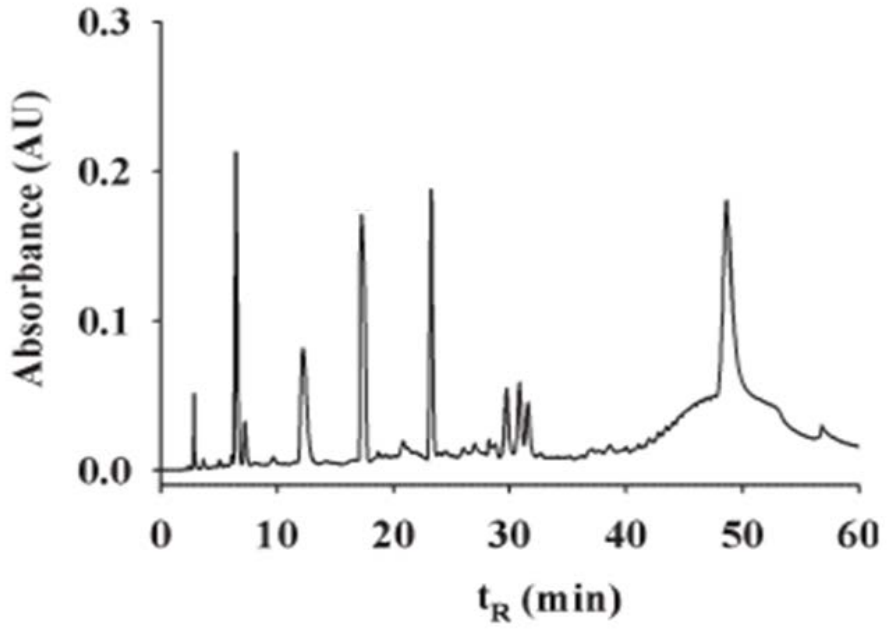

Figure 4.3. Example of a NP-HPLC analysis of phlorotannins from the brown alga *Fucus vesiculosus*. Adapted from Koivikko et al. (2007), Copyright 2007 John Wiley & Sons, Ltd.

Providing a similar elution pattern than NP, HILIC has also been applied for the separation of phlorotannins, achieving a separation in agreement with their DP, up to a limited number of PGUs. However, in contrast to NP, HILIC offers "mixed-mode" retention mechanisms (involving liquid-liquid partition, hydrogen bonds, cation exchanges and electrostatic interactions) that can provide an efficient selectivity of such highly polar compounds (Steevensz et al. 2012).

Hence, in spite of the efforts made to increase the separation of phlorotannins from brown algae, relatively limited characterization of these polymers has been obtained by using one-dimensional liquid chromatography. To date, only the characterization of phlorotannins with a DP up to 16 PGUs with limited capability to separate phlorotannin isomers has been achieved (Steevensz et al. 2012; Heffernan et al. 2015). Therefore, only a small proportion of the phlorotannin composition of brown algae is being analyzed. This fact demonstrates that MDLC might be a potentially useful tool to obtain a better knowledge of the greatly complex chemical structure of phlorotannins as well as on their native composition within individual macroalgae species.

4.1.4. DETECTION OF PHLOROTANNINS.

The most employed detectors coupled to LC for the characterization of phlorotannins are DAD and MS. When DAD is employed, usually the detection of phlorotannins is recorded at 280 nm (Koivikko et al. 2007; Ferreres et al. 2012). Considering that UV spectra of phlorotannins slightly varies as the DP increases, as well as the polymeric nature of these compounds and their huge variety of isomers together with the lack of available commercial standards, make the identification and quantification of the individual compounds an unattainable task.

The use of MS and MS/MS in the analysis of phlorotannins provides information about the DP of the molecules thanks to the determination of the molecular weight. Moreover, in some cases, such as for eckols, fuhalols, hydroxyfuhalols or halogenated phlorotannins, is also possible to obtain some compositional information by closely studying their fragmentation pathways. Hence, in practice, the use of MS becomes essential for the elucidation of the number of PGUs of each separated compound and for the determination of some phlorotannin types (Koivikko

et al. 2007; Steevensz et al. 2012; Heffernan et al. 2015). Nevertheless, the specific structure of each phlorotannin as well as the linkages between the different PGUs within the molecule is not achievable from the MS spectra because, commonly, every phlorotannin with the same DP presents the same molecular weight, independently of the linkage type(s) present in the molecule. Besides, to obtain a good ionization of the different phlorotannins, a good separation prior MS analysis is required, due to fact that very complex mixtures like those of highly polymerized phlorotannins could lead to ionization suppression.

In summary, from the information described in this Section 4.1, MDLC methods coupled to MS may alleviate some of the important issues related to phlorotannin analysis found at present. This way, new methods providing increased separation power as well as enhanced detection/identification capability could be developed and applied to increase the available knowledge on the presence of these complex compounds in brown algae. In this Chapter 4, the optimization and application of on-line LC × LC methods to chemically characterize the complex phlorotannin composition from two brown algae, *Cystoseira abies-marina* (Section 4.2) and *Sargassum muticum* (Section 4.3), are presented. To our knowledge, these Sections show the first applications of on-line LC × LC for the analysis of phlorotannins. Thanks to the use of this technique, phlorotannins belonging to different types (namely, fuhalols, hydroxyfuhalols and phlorethols) with DP up to 17 PGUs could be separated and identified in the studied brown algae.

4.2. Separation and characterization of phlorotannins from brown algae *Cystoseira abies-marina* by comprehensive two-dimensional liquid chromatography.

Montero, L., Herrero, M., Ibáñez. E., Cifuentes, A.

Electrophoresis 2014, *35*, 1644–1651

Lidia Montero
Miguel Herrero
Elena Ibáñez
Alejandro Cifuentes

Laboratory of Foodomics, Institute of Food Science Research (CIAL, CSIC), Campus de Cantoblanco, Madrid, Spain

Received March 14, 2014
Revised March 27, 2014
Accepted March 27, 2014

Research Article

Separation and characterization of phlorotannins from brown algae *Cystoseira abies-marina* by comprehensive two-dimensional liquid chromatography

Phlorotannins are an important class of polyphenolic compounds only found in brown algae. The chemical analysis of these bioactive polyphenols is rather difficult due to the great chemical variability and complexity of the natural composition of these components in algae, forming large phloroglucinol polymers. In the present work, a new approach based on the use of comprehensive 2D LC (LC × LC) is shown to analyze this complex family of compounds. The developed LC × LC methodology is based on the coupling of a hydrophilic-interaction LC (HILIC)-based separation in the first dimension and an RP-based separation in the second dimension. The employment of this online coupling together with DAD and MS/MS allowed the separation and identification of more than 50 compounds in a *Cystoseira abies-marina* brown alga extract. Phlorotannins containing from 5 to 17 phloroglucinol units were identified in this sample by HILIC × RP-DAD-MS/MS. Besides, using the 2,4-dimethoxybenzaldehyde assay, it was possible to determine that the total amount of phlorotannins present in the extract was 40.2 mg phloroglucinol equivalents per gram of extract. To our knowledge, this work is the first demonstration of the usefulness of HILIC × RP-DAD-MS/MS for the determination of phlorotannins.

Keywords:
Brown algae / *Cystoseira abies-marina* / LC × LC / Phlorotannins / Polymeric polyphenols
DOI 10.1002/elps.201400133

Additional supporting information may be found in the online version of this article at the publisher's web-site

1 Introduction

Brown algae (Phaeophyceae) contain a typical kind of secondary metabolites that are classified within the phenolic compounds family, called phlorotannins. These compounds, which may reach a high percentage of the algae dry mass (up to 15%) [1], are formed as polymers of phloroglucinol (1,3,5-trihydroxybenzene) of different size and composition. There exist four main classes of phlorotannins: fuhalols and phlorethols, containing an ether linkage; fucols, containing a phenyl linkage; fucophlorethols, with an ether and a phenyl linkage; and eckols, which possess a benzodioxin linkage [2]. Besides, it is also possible to find quite complex chemical variability with compounds containing different degree of polymerization as well as structure (linearly linked or branched). It is widely accepted that phlorotannins are components of the algal cell walls that may be forming complexes with alginic acid, although it is not completely clear if they exert a chemical defense function or just an influence on cell wall construction [2]. The genus *Cystoseira* comprises more than 30 species and it is one of the most important brown algae genera found in the Mediterranean Sea and Atlantic Ocean ecosystems. *Cystoseira abies-marina* is one of the species already identified as possessing some interesting compounds, such as meroterpenoids [3] and fucoxanthin [4], although it is also a good potential source of phenolic compounds, including phlorotannins.

These latter compounds have recently raised attention as algae have been pointed out as a potential source of bioactive compounds potentially useful for the food and pharmaceutical industries [5]. In this regard, some research has already

Correspondence: Dr. Miguel Herrero, Laboratory of Foodomics, Institute of Food Science Research (CIAL, CSIC), Nicolas Cabrera 9, Campus de Cantoblanco, 28049 Madrid, Spain
E-mail: m.herrero@csic.es
Fax: +34-910-017-905

Abbreviations: D1, first dimension; **D2**, second dimension; **DMBA**, 2,4-dimethoxybenzaldehyde; **HILIC**, hydrophilic-interaction LC; **LC × LC**, comprehensive 2D LC; **PFP**, pentafluorophenyl; **PGU**, phloroglucinol units

Colour Online: See the article online to view Fig. 1 in colour.

hinted that phlorotannins may confer with different bioactivities, including antibacterial [6, 7], antidiabetic [8], antiproliferative [9], anti-inflammatory [10], antioxidant [11–13], as well as chemopreventive activity [14]. Consequently, there is a great interest in determining these compounds in the different species of brown algae that may contain them. Due to the huge chemical variability already mentioned, the analysis of these components is quite complex, and it is rather common to roughly estimate the phlorotannins content in algae by using colorimetric methods [10, 15–17]. To partially solve the problems associated to those methods, mainly, the little information on chemical composition that they provide as well as the relatively low accuracy associated to most colorimetric methods, some approaches involving the use of LC-based methods have been developed [17–20], frequently using MS-based detection. Considering the high degree of hydrophilicity of these polymeric compounds, hydrophilic-interaction LC (HILIC) methods have also been recently applied [2, 21] with the aim to increase the resolution among the different phlorotannins contained in complex algal samples. Despite these efforts, the chemical characterization of brown algae in terms of phlorotannins composition is not well known yet [22].

The use of multidimensional techniques, such as comprehensive 2D LC (LC × LC), may be an effective alternative to carry out this kind of characterization of very complex samples. In fact, this technique has already been shown to possess a great potential to analyze complex food and natural samples [23, 24]. LC × LC is based on the online coupling of two independent separation mechanisms through which the whole sample is analyzed. In this sense, different couplings may be employed in the two dimensions, including, for example, RP, normal phase, or HILIC-based separations [25]. Our group has previously presented two novel LC × LC approaches to separate and identify procyanidins, which are also polymeric phenolic compounds, from complex food matrices such as grape seeds [26] and apples [27], combining the use of a HILIC separation in the first dimension (D1) and an RP approach in the second dimension (D2) together with the employment of MS/MS detection. This type of approach allowed the separation in terms of degree of polymerization in the D1 and according to differential hydrophobicity in the D2. Following this idea, the aim of the present work is to develop a new method based on a HILIC × RP-DAD-MS/MS coupling to separate and identify the phlorotannins present in *C. abies-marina* brown algae. To the best of our knowledge, this is the first time that an LC × LC method is developed and used to analyze phlorotannins.

2 Materials and methods

2.1 Samples and chemicals

Cystoseira abies-marina brown algae were obtained from the Spanish Bank of Algae (Marine Biotechnology Center, University of Las Palmas de Gran Canaria, Gran Canaria, Spain). Algae were sun-dried and stored protected from oxygen, light, and moisture until use.

ACN, methanol, dichloromethane, and 2-propanol were of HPLC-grade and acquired from VWR Prolabo (Barcelona, Spain), whereas acetone was from Lab-Scan (Dublin, Ireland). Acetic acid, formic acid, and 2,4-dimethoxybenzaldehyde (DMBA) were obtained from Sigma Aldrich (Madrid, Spain). Hydrochloric acid was acquired from Probus (Barcelona, Spain), whereas ammonium acetate was supplied from Panreac (Barcelona, Spain). Ultrapure water quality (resistivity of 18.2 MΩcm at 25°C) with 1–5 ppb total organic carbon was produced in-house using a laboratory water purification Milli-Q Synthesis A10 system from Millipore (Billerica, MA, USA). Phloroglucinol and quercetin rutinoside reference standards were purchased from Extrasynthèse (Genay, France).

2.2 Sample preparation

The extraction of the phenolic compounds from *C. abies-marina* was carried out employing a previously described protocol slightly modified [21]. Briefly, the alga was freeze-dried (LyoBeta 15, Telstar, Terrassa, Spain) and ground. A total of 30 g of the dried powder was extracted with 300 mL of acetone/water (70:30, v/v) by magnetic stirring during 45 min in darkness. Afterwards, the supernatant was decanted and the remaining residue was extracted three times more with 100 mL of solvent. The supernatants were pooled and the acetone was removed by rotary evaporation (Rotavapor R-210, Buchi Labortechnik, Flawil, Switzerland). Next, the aqueous extract was defatted three times with dichloromethane (1:1, v/v), collecting the aqueous phases. The phenolic fraction of the aqueous extract was concentrated using Discovery DSC-18 6 mL SPE cartridges (Supelco, Bellefonte, PA, USA). SPE cartridges were conditioned with 12 mL of methanol and 18 mL of water. Then, 12.5 mL of sample was loaded in the SPE cartridge, rinsed with 20 mL of water, and finally, the polyphenols were eluted with 30 mL of acetone/water (70:30, v/v). Lastly, acetone was evaporated again by rotary evaporation, and the remaining aqueous extract was lyophilized.

2.3 Determination of total phlorotannins

To estimate the amount of total phlorotannins content in the brown alga, the DMBA colorimetric assay was employed [10]. Briefly, a DMBA solution was prepared just prior use by mixing equal volumes of 2% DMBA reagent in acetic acid m/v and 6% hydrochloric acid in acetic acid v/v. A total of 50 μL of sample (0.075 mg/mL) was mixed with 250 μL of DMBA solution in a 96-well microplate. The reaction was conducted at room temperature in the dark for 60 min. After this time, the absorbance was read at 515 nm using a microplate spectrophotometer reader Powerwave XS (Bio Tek, Winooski, VT, USA). Blanks with 50 μL of water instead of sample and control samples without DMBA solution were also included. All samples, blanks, and controls were prepared in triplicate. The

concentration of total phlorotannins was estimated from a calibration curve using phloroglucinol (0.98–62.5 μg/mL). Data were presented as the average of triplicate analyses expressed as milligram phloroglucinol equivalents per gram dry matter.

2.4 LC × LC analysis of phlorotannins

2.4.1 Instruments

LC × LC analyses were carried out on an Agilent 1200 series liquid chromatograph (Agilent Technologies, Santa Clara, CA, USA) equipped with a DAD and an autosampler. A Protecol flow splitter (SGE Analytical Science, Milton Keynes, UK) was placed between the D1 pumps and the autosampler in order to have robust and reproducible low flow rates and gradients in the D1. Besides, an additional LC pump (Agilent 1290 Infinity) was coupled to this instrument to perform the D2 separations, hyphenated through an electronically controlled two-position ten-port switching valve. An Agilent 6320 Ion Trap mass spectrometer equipped with an electrospray interface was coupled online and operated in negative ionization mode using the following conditions: dry temperature, 350°C; mass range, *m/z* 90–2200 Da; dry gas flow rate, 12 L/min; nebulization pressure, 40 psi. The LC data were elaborated and visualized in two and three dimensions using LC Image software (version 1.0, Zoex, Houston, TX, USA).

2.4.2 LC × LC separation conditions

Samples were prepared at 12 mg/mL of the extract obtained as described in Section 2.2 in MeOH/ACN (3:7, v/v) and filtered through 0.45 μm nylon syringe filters (Análisis vínicos, Tomelloso, Spain) before injection.

In the D1, a Lichrospher diol-5 (150 × 1.0 mm, 5 μm particle diameter, HiChrom, Reading, UK) column was employed with a precolumn with the same stationary phase. The flow rate employed was 15 μL/min. The mobile phases were (A) ACN/acetic acid (98:2, v/v) and (B) methanol/water/acetic acid (95:3:2, v/v/v) used according to the following gradient: 0 min, 0% B; 3 min, 0% B; 5 min, 7% B; 30 min, 15% B; 70 min, 15% B; 75 min, 25% B; 85 min, 25% B. The injection volume was 20 μL.

In the D2, two different columns were tested, namely an Ascentis Express C_{18} partially porous column (50 × 4.6 mm, 2.7 μm particle diameter, Supelco) with a C_{18} precolumn, and a Kinetex pentafluorophenyl (PFP) partially porous particles column (50 × 4.6 mm, 2.6 μm particle diameter, Phenomenex, Torrance, CA, USA). During the whole LC × LC separation, 78 s repetitive D2 gradients were employed, being also 78 s the modulation time programed in the switching valve. The wavelength used to monitor the separations was 280 nm, although UV–Vis spectra were collected from 190 to 550 nm during the whole analysis using a sampling rate of 20 Hz in the DAD. The MS was operated under negative ESI mode. The mobile phases employed in the D2 analysis of both columns consisted of water (0.1% formic acid, A) and ACN (B) eluted according to the following gradients: 0 min, 0% B; 0.1 min, 10% B; 0.6 min, 30% B; 0.8 min, 50% B; 0.9 min, 70% B; 1 min, 90%; 1.01 min, 0% B; 1.3 min, 0% B for the C_{18} column, and 0 min, 0% B; 0.1 min, 5% B; 0.3 min, 20% B; 0.8 min, 40% B; 0.9 min, 70% B; 1 min, 90%; 1.01 min, 0% B; 1.3 min, 0% B for the PFP column. The flow rate employed was always 3 mL/min. The flow eluting from the D2 column was splitted before entering the MS instrument, so that the flow rate introduced in the MS detector was 600 μL/min.

3 Results and discussion

Phorotannins estimation is commonly carried out by using colorimetric methods [10, 15, 16]. In this work, the DMBA assay was used as a starting point to determine the phlorotannins content in the *C. abies-marina* extract (see Section 2.3). Using this approach, the amount of phlorotannins determined was 40.2 mg phloroglucinol equivalents per gram extract. As mentioned above, comprehensive 2D coupling using a HILIC-based separation in the D1 and an RP-based separation in the D2 could potentially solve many of the problems commonly encountered when analyzing phlorotannins. This combination is characterized by providing a high degree of orthogonality [26] at the same time that completely miscible mobile phases are employed in the two dimensions. Besides, the capabilities of HILIC followed by RP-LC to separate complex mixtures of polymeric phenolic compounds have been already shown, both using online [26, 27] and off-line couplings [28, 29]. Moreover, the online approach followed by the direct hyphenation to several detectors, such as DAD and MS detectors, gives rise to a powerful analytical system whose use is mandatory if complex samples have to be analyzed. In this work, a HILIC × RP-DAD-MS/MS approach is proposed to characterize the phlorotannins composition from brown algae. Since the sample as well as the target compounds have not been previously studied using this approach, a complete optimization of the separation and coupling conditions was first needed.

3.1 HILIC-based D1 separation optimization

The LC × LC instrument setup employed in this work is based on the use of two identical injection loops installed in a ten-port two-position switching valve that is used as modulator. This device makes possible the physical coupling between both dimensions. Under this configuration, one of the injection loops injects the eluate collected from the D1 to the D2 whereas the other loop is collecting new eluate, so that the complete collection and transfer of the whole effluent from the D1 to the D2 is performed. This implies that each D2 separation should be completely finished before the collecting injection loop is filled with the D1 eluate. For this reason, in this kind of couplings, the use of microbore columns in the D1 is highly recommended. By using this kind of columns, a very low D1 flow rate can be employed, in order to give

enough time for the D2 separation to be completed while the transfer volume is maintained as small as possible. To perform the HILIC separation in the D1, a microbore column with diol particles was selected.

To carry out the optimization of the separation, the whole phlorotannins purified extract from *C. abies-marina* was injected and the conditions previously employed to separate the complete profile of apple polyphenols were used [27]. As expected, under these conditions, using a flow rate of 15 μL/min, the separation obtained was not satisfactory. Next, different new gradients using the same mobile phases (A, ACN/acetic acid 98:2, v/v; B, methanol/water/acetic acid 95:3:2, v/v/v) as well as other different mobile phases were tested. Namely, 10 mM ammonium acetate (pH 9) was also tested as mobile phase B as well as other different proportions of methanol and water in that mobile phase. After a close study of the obtained profiles, the mobile phases (A) ACN/acetic acid (98:2, v/v) and (B) methanol/water/acetic acid (95:3:2, v/v/v) were selected optimizing next the gradient in order to obtain a better separation of this complex sample (see Section 2.4.2.). In Supporting Information Fig. 1, a comparison is shown between the initial (Supporting Information Fig. 1A) and the final selected conditions for the D1 analysis (Supporting Information Fig. 1B). As can be observed, the separation of the complex profile obtained is not completely resolved. It is interesting to mention that, at this stage of the LC × LC optimization, a complete baseline separation of all the components in the D1 is not aimed, but only to obtain a good distribution of all of them in the time, to be able to collect those peaks and inject them, and separate their components in the D2.

3.2 RP-based D2 separation optimization

For the D2, two different types of stationary phases and columns were studied with the aim to compare their performances under LC × LC conditions. Namely, a partially porous C_{18} short column that had already shown its potential in LC × LC [26,27,30,31] and a partially porous PFP short column that has been pointed out as a possible new alternative for the efficient separation of phenolic compounds [32, 33]. In this regard, the optimization of the final analytical conditions in each case was carried out separately. To do that, the whole sample was directly injected in the D2 column. Although these analytical conditions are not exactly equal to those taking place during the LC × LC analysis, in which only fractions of the sample will be separated in each D2 analysis, this step injecting the whole sample will provide important information on the D2 conditions that produce a better separation of the sample components. Once these conditions are selected, further confirmation or fine tuning of the separation conditions is needed for directly performing 2D analyses.

The mobile phases selected were water (0.1% formic acid, A) and ACN (B) for both C_{18} and PFP columns, although different gradients were chosen. The use of other solvents in the mobile phase B, such as 2-propanol in different proportions or mixtures between ACN and methanol, did not improve the separations obtained and significantly increased the backpressure obtained (mainly when 2-propanol was used).

3.3 Overall HILIC × RP optimization and method performance

Once the two dimensions were optimized separately, the fine tuning of the coupling conditions was performed. To do that, two identical 30 μL internal volume injection loops were installed in the ten-port two-position switching valve acting as modulator. This internal volume allowed the complete transfer of eluate from the D1 to the D2 in each modulation period (1.3 min, 19.5 μL). In this regard, it is worth to mention that although 20 μL loops would have been enough to collect all the effluent in the modulation time, we have previously observed a beneficial influence when the injection volume in the D2 of HILIC × RP methods was slightly increased [26]. These observations were also confirmed in the present approach. In fact, the dilution of the eluent from the D1 with D2 mobile phase (up to 30 μL) just before the injection permitted to minimize the negative effects on band broadening and retention derived by using as injection solvent a stronger solvent than the initial mobile phase. It is necessary to remark that under LC × LC conditions, being an online system, the injection solvent in the D2 is fixed by the D1 and cannot be modified. Moreover, the setup was completed by coupling an MS detector at the exit of the DAD after the D2 separation. Considering the high flow rates used in the D2, the inclusion of a flow splitter was necessary in order to reduce the flow rate entering the ESI interface to 600 μL/min, which is more suitable for a proper ionization of the target compounds.

Subsequently, the *C. abies-marina* phlorotannins extract was injected and analyzed using the two different optimized setups, namely diol × C_{18} and diol × PFP configurations. Figure 1 shows the obtained 2D-plots corresponding to both configurations. As it can be observed in this figure, both setups were able to provide adequate separations of such a complex mixture. The separation in the D1 (same conditions for both configurations) was produced according to the degree of polymerization of phlorotannins, whereas in the D2, the separation was obtained in terms of relative hydrophobicity. It is possible to observe in the figures how the use of LC × LC permits the resolution of coelutions in both dimensions, such as the coelution of peaks 12, 13, 14, and 17 in the D1, or the coelution of peaks 21, 30, 33, and 44 in the D2 (see Fig. 1A), making possible the separation of components that, otherwise, would not be separated using monodimensional separations.

Although the separation mode and mobile phases were the same, it can be clearly observed how the two tested columns produced different profiles under the selected conditions, showing differential retention. This is mainly due to the use in the PFP short column of fluorine atoms in the

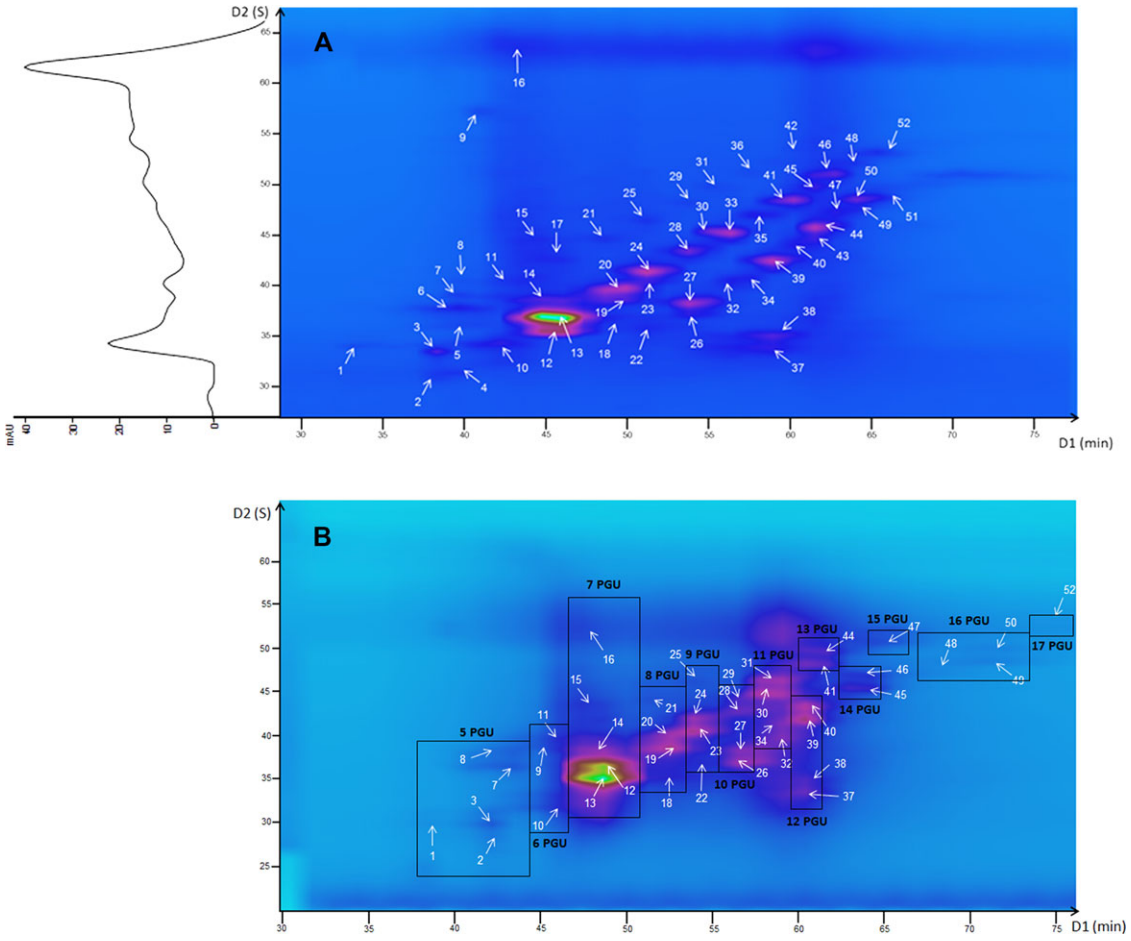

Figure 1. Two-dimensional plot (280 nm) of the *Cystoseira abies-marina* phlorotannins extract obtained using the optimized diol × C_{18} setup (A) and the diol × PFP setup (B). Areas marked correspond to phlorotannins containing the same number of phloroglucinol units (PGU). For peak identification, see Table 1.

periphery of a phenyl ring, which are highly electronegative, in contrast to the long C_{18} alkyl chain. As it can be appreciated in the figure, using the C_{18} column, a better separation among the different peaks could be obtained in the D2 (Fig. 1A), compared to the PFP column (Fig. 1B). To the best of our knowledge, this is the first application of a PFP column in LC × LC, showing acceptable capabilities for its coupling to HILIC separations. Comparing the two separations, different peak capacities values can be obtained. It is important to remark that this value is just a theoretical measure of the performance of the system that does not necessarily describe what actually happens in practice. In fact, although there are several methods for measuring peak capacity in an LC × LC system, normally, it is assumed that the peaks are homogeneously distributed across the 2D plane, which is obviously a great source of error. Anyhow, this value helps to compare different LC × LC setups or methods. In this regard, the two-dimensional peak capacity (n_{c2D}) was measured for the two instrumental setups under the optimized conditions, obtaining values of theoretical peak capacity [34] of 1248 and 902 for the diol × C_{18} and diol × PFP configurations, respectively. Following the approach developed by Li et al. [35], which considers the D2 time cycle as well as the influence of undersampling of the D1 eluate, the values obtained for the diol × C_{18} and diol × PFP were 992 and 739, respectively, showing the great potential capabilities of both developments. Peak capacity values also show the better performance of the C_{18} column in the D2 compared to the PFP column under the selected conditions.

3.4 *Cystoseira abies-marina* phlorotannins characterization

As already mentioned, the main difficulty to analyze phlorotannins is the great heterogeneity and chemical variability within this family of compounds due to the differential degree of polymerization as well as the diverse bonds between monomers. In this regard, the use of LC × LC allows the attainment of a distribution along the D1 in order to separate smaller groups of components into the D2. Table 1 summarizes the information corresponding to the assigned compounds. As it can be observed in Table 1, phlorotannins from a degree of polymerization of 5 phloroglucinol units

Table 1. Peak assignments of the purified *Cystoseira abies-marina* phlorotannins extract analyzed using the diol × C_{18} setup under optimized conditions

Peak	Identification	Total t_R (min)	D2 t_R(s) ± SD	$[M-H]^-$	$[M-2H]^{2-}$	Main MS/MS fragments
1	Phlorotannin–5 PGU	33.07	34.10 ± 0.22	621.6		603, 495, 373, 229
2	Phlorotannin–5 PGU	38.22	31.08 ± 0.14	621.4		603, 479, 353, 247, 229
3	Phlorotannin–5 PGU	38.26	33.33 ± 0.13	621.0		603, 495, 373, 247, 229
4	Phlorotannin–5 PGU	39.52	31.17 ± 0.15	621.7		603, 246, 229
5	Phlorotannin–5 PGU	39.60	35.83 ± 0.16	621.8		603, 495, 230
6	Phlorotannin–5 PGU	39.63	37.60 ± 0.15	621.3		601, 495, 371, 229
7	Phlorotannin–5 PGU	39.65	38.90 ± 0.10	621.3		601, 495, 371, 229
8	Phlorotannin–5 PGU	39.67	40.30 ± 0.10	621.5		601, 495, 229
9	Not identified	41.25	56.98 ± 0.32	941.3		897, 855, 693, 400, 319
10	Phlorotannin–6 PGU	42.17	34.02 ± 0.26	745.4		728, 229
11	Phlorotannin–6 PGU	43.57	40.13 ± 0.15	745.2		727, 601, 479, 353, 229
12	Phlorotannin–7 PGU	44.79	34.88 ± 0.64	869.4		853
13	Phlorotannin–7 PGU	44.81	36.63 ± 0.10	869.4		852
14	Phlorotannin–7 PGU	44.84	38.45 ± 0.10	869.2		851
15	Quercetin rutinoside	44.94	44.23 ± 0.14	609.2		301, 270, 178
16	Not identified	45.26	63.50 ± 0.18	955.9		937, 849, 794
17	Phlorotannin–7 PGU	46.21	42.30 ± 0.10	869.2		852
18	Phlorotannin–8 PGU	48.71	36.70 ± 0.13	993.5		975, 849, 743
19	Phlorotannin–8 PGU	48.74	38.33 ± 0.13	993.9		975, 849
20	Phlorotannin–8 PGU	48.76	39.48 ± 0.13	993.5		975, 849, 743, 621
21	Phlorotannin–8 PGU	48.84	44.38 ± 0.08	993.3		975, 849, 743, 621
22	Phlorotannin–9 PGU	51.29	35.58 ± 0.08	1117.5		1099, 1081, 869, 851, 727, 603
23	Phlorotannin–9 PGU	51.37	40.20 ± 0.10	1117.9		1099, 869, 727
24	Phlorotannin–9 PGU	51.39	41.25 ± 0.00	1117.5		1099, 869, 727, 619
25	Phlorotannin–9 PGU	51.47	46.33 ± 0.03	1117.4		1099, 869, 727, 619
26	Phlorotannin–10 PGU	53.92	36.88 ± 0.23	1241.6		1223, 1205, 993, 975, 603
27	Phlorotannin–10 PGU	53.93	38.15 ± 0.09	1241.8		1223, 1205, 975, 833
28	Phlorotannin–10 PGU	54.02	43.32 ± 0.03	1241.9		1223, 993, 975, 869, 744
29	Phlorotannin–10 PGU	54.10	48.05 ± 0.00	1241.5		1223, 1099, 975, 849, 726, 601
30	Phlorotannin–11 PGU	55.36	45.15 ± 0.17	1365.8		1347, 1117, 991, 868, 727, 618
31	Phlorotannin–11 PGU	55.43	49.52 ± 0.19	1365.5		1347, 1117, 991, 867, 723
32	Phlorotannin–11 PGU	56.58	40.53 ± 0.13	1365.4		1329, 1099, 975, 849
33	Phlorotannin–11 PGU	56.65	45.15 ± 0.05	1365.7		1347, 1117, 973, 867, 727
34	Not identified	57.89	40.55 ± 0.10	1043.8		1025, 925, 907
35	Phlorotannin–12 PGU	57.98	46.88 ± 0.08	1489.6		1453, 1223, 1100
36	Phlorotannin–12 PGU	58.05	50.92 ± 0.24	1490.2		1471, 1453, 1241, 1223, 1115, 867
37	Not identified	59.06	33.65 ± 0.13	1017.3		999, 909, 869, 851
38	Not identified	59.08	34.93 ± 0.08	1018.0		999, 909, 869, 851
39	Phlorotannin–12 PGU	59.21	42.35 ± 0.00		744.3	1241, 1223, 1117, 993, 867, 726, 619, 229
40	Not identified	60.53	43.85 ± 0.17	1017.4		999, 981, 927, 909, 869, 851, 621, 305
41	Phlorotannin–13 PGU	60.61	48.25 ± 0.05		808.4	1453, 1365, 1242, 1116, 1099, 993, 975, 867, 745, 619
42	Phlorotannin–13 PGU	60.69	52.80 ± 1.39		807.6	1365, 1223, 1115, 993, 975, 867, 745, 619, 350, 229
43	Not identified	61.84	44.52 ± 0.14	1142.6		1123, 1051, 1033, 975, 891, 755, 495
44	Not identified	61.86	45.67 ± 0.15	1141.6		1123, 1106, 1051, 1033, 975, 849, 769, 745, 648, 478
45	Phlorotannin–14 PGU	61.93	49.63 ± 0.16	1737.0		1493, 1243, 975, 852
46	Phlorotannin–14 PGU	62.01	53.62 ± 0.73		869.4	1489, 1471, 1241, 991, 850
47	Phlorotannin–15 PGU	63.19	46.65 ± 0.82		930.8	1613, 1594, 1366, 975, 921, 795, 744
48	Phlorotannin–16 PGU	64.49	47.35 ± 0.10		992.6	1737, 1594, 1239, 974, 477
49	Phlorotannin–16 PGU	64.51	48.42 ± 0.08		992.6	1738, 1719, 1598, 1469, 1239, 1095, 975, 354
50	Phlorotannin–16 PGU	64.57	51.85 ± 0.15		992.6	1737, 1720, 1594, 1239, 974, 477
51	Phlorotannin–16 PGU	65.81	48.52 ± 0.15		992.6	1737, 1720, 1490, 974, 931, 622, 494
52	Phlorotannin–17 PGU	65.89	52.95 ± 0.15		1054.0	

For peak numbers, see Fig. 1.
PGU: phloroglucinol units.

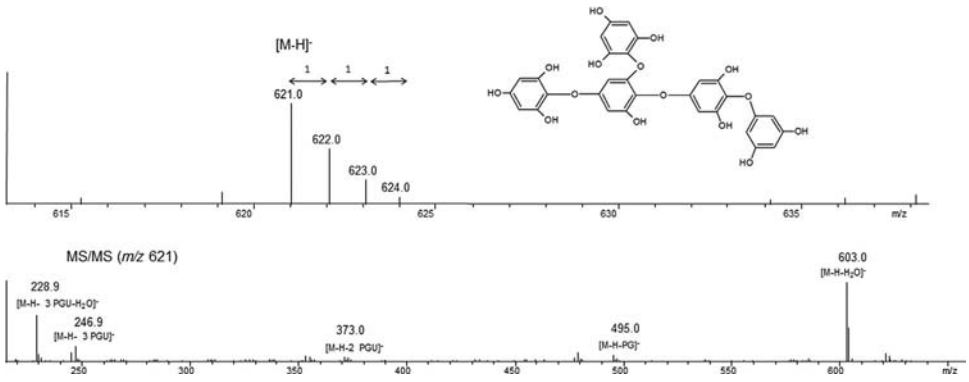

Figure 2. MS spectrum and MS/MS fragmentation pattern of peak 3 (phlorotannin with five PGU) as well as the tentatively proposed chemical structure.

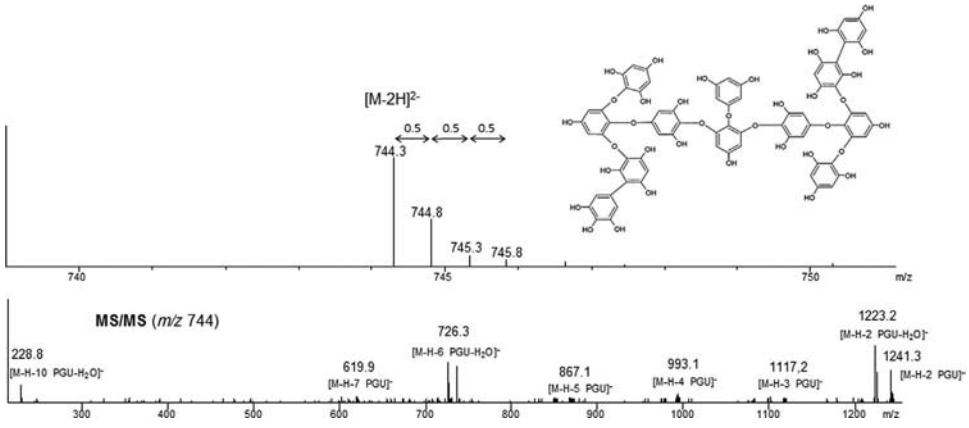

Figure 3. MS spectrum and MS/MS fragmentation pattern of peak 39 (phlorotannin with 12 PGU) as well as the tentatively proposed chemical structure.

(PGU) up to 17 PGU were separated and assigned. In total, 43 different phlorotannins were tentatively identified according to their MS and MS/MS spectra as well as their position in the 2D plane. Besides, a flavonoid, quercetin rutinoside, was also found in the extract. Additionally, eight other compounds were detected in the sample, although no proper identification of these compounds was possible. The highest number of compounds of a same degree of polymerization corresponded to five PGU (peaks 1–8), whereas the most intense compound was a phlorotannin containing seven PGU (peak 13). Phorotannins of less than five PGU were not detected, in line with the phlorotannins composition in other brown algae, where just high degree of polymerization phlorotannins were found [21].

Phlorotannins assignment was performed thanks to the detection of typical $[M–H]^-$ ions together with MS/MS fragments corresponding to phlorotannin structures. Phlorotannins containing five PGU were detected as $[M–H]^-$ at m/z 621, with typical fragments of m/z 603 corresponding to the loss of water, m/z 495 in agreement with the loss of a phloroglucinol, m/z 373 assigned to the loss of two PGU, and m/z 228 that corresponded to a dehydrated fragment containing two PGU. Figure 2 shows the MS spectra as well as the MS/MS fragmentation pattern of peak 3 as well as its tentative chemical structure (branching not unequivocally confirmed). Similar losses and fragments were detected for phlorotannins with 6–11 PGU, except in the compounds containing 7 PGU from which no fragments were clearly produced beyond the loss of a water molecule.

On the other hand, phlorotannins having 13–17 PGU were detected as doubly charged ions, as can be observed in Table 1. The different ion charge states were detected thanks to the presence of specific ions in the MS spectra, as it is highlighted in Figs. 2 and 3 (see in the MS spectra, the isotopes of the molecular ion separated by a difference of 1 or 0.5 for the singly charged or doubly charged, respectively). These latter multicharged compounds were also identified according to the detection of different fragments corresponding to phlorotannin fragments of smaller PGU, which allow confirming the identifications. For example, in the case of phlorotannins of 13 PGU, a doubly charged ion was detected at m/z 807 indicating the possible presence of this type of polymer. The fragmentation pattern of that ion produced ions at m/z 1365 (11 PGU), 1115 (9 PGU), 993 (8 PGU), 975 (8 PGU dehydrated), 867 (7 PGU), 745 (6 PGU), 619 (5 PGU), and 228 (2 PGU dehydrated) that completed the identification. The same behavior was observed for one of the phlorotannins containing 12 PGU (peak 39), as shown in Fig. 3. Moreover, as previously indicated, the relative position of each peak in the 2D plane helped to conclude the identification; as can be observed in Fig. 1B, the different polymers were clearly separated according to their degree of polymerization along the D1 analysis time, the compounds of a similar size being grouped together.

4 Concluding remarks

This contribution shows the first application of LC × LC to analyze phlorotannins, a family of complex algal polyphenolic compounds. The coupling between a HILIC-based separation in the D1 and an RP-based separation in the D2 provides a high degree of orthogonality at the same time that produces a distribution according the degree of polymerization of phlorotannins in the D1 that facilitates their separation in the D2. The optimized HILIC × RP-DAD-MS/MS approach has been demonstrated to be useful for the separation and identification of more than 50 compounds in a *C. abies-marina* brown alga extract. Besides, two different setups involving different D2 columns were tested. Although partially porous C_{18} column produced the best results in terms of separation capabilities, a partially porous PFP column was also applied for the first time in an LC × LC development, with acceptable results. Once this method has been developed and its applicability demonstrated, its future use can be expected for the determination of phlorotannins in different brown algae as well as for determination of the influence of the algal growing conditions on the composition of these bioactive compounds, which currently is an important analytical challenge.

M. H. would like to thank MICINN for his "Ramón y Cajal" research contract. Authors thank the BEA (Banco Español de Algas, Las Palmas de Gran Canaria, Spain) for providing the Cystoseira samples. The authors want to thank Projects AGL2011-29857-C03-01 (MINECO, Spain) and ALIBIRD, S2009/AGR-1469 (Comunidad de Madrid) for the financial support.

The authors have declared no conflict of interest.

5 References

[1] Koivikko, R., Loponen, J., Pihlaja, K., Jormalainen, V., *Phytochem. Anal.* 2007, *18*, 326–332.

[2] Kim, S. M., Kang, S. W., Jeon, J. S., Jung, Y. J., Kim, W. R., Kim, C. Y., Um, B. H., *Food Chem.* 2013, *138*, 2399–2406.

[3] Gouveia, V. L. M., Seca, A. M. L., Barreto, M. C., Neto, A. I., Kijjoa, A., Silva, A. M. S., *Phytochem. Lett.* 2013, *6*, 593–597.

[4] Moraes, E. P., Ruperez, F. J., Plaza, M., Herrero, M., Barbas, C., *Electrophoresis* 2011, *32*, 2055–2062.

[5] Ibañez, E., Cifuentes, A., *J. Sci. Food Agric.* 2013, *93*, 703–709.

[6] Sandsdales, E., Haug, T., Stensvag, K., Styrvold, O. B., *World J. Microbiol. Biotechnol.* 2003, *19*, 777–782.

[7] Lopes, G., Pinto, E., Andrade, P. B., Valentao, P., *PLOS One* 2013, *8*, e72203.

[8] Lee, S. H., Jeon, Y. J., *Fitoterapia* 2013, *86*, 129–136.

[9] Nwosu, F., Morris, J., Lund, V. A., Stewart, D., Ross, H. A., McDougall, G. J., *Food Chem.* 2011, *126*, 1006–1012.

[10] Lopes, G., Sousa, C., Silva, L. R., Pinto, E., Andrade, P. B., Bernardo, J., Mouga, T., Valentao, P., *PLOS One* 2012, *7*, e31145.

[11] Wang, T., Jonsdottir, R., Liu, H., Gu, L., Kristinsson, H. G., Raghavan, S., Olafsdottir, G., *J. Agric. Food Chem.* 2012, *60*, 5874–5883.

[12] Tierney, M. S., Smyth, T. J., Hayes, M., Soler-Vila, A., Croft, A. K., Brunton, N., *Int. J. Food Sci. Technol.* 2013, *48*, 860–869.

[13] Kang, S. M., Lee, S. H., Heo, S. J., Kim, K. N., Jeon, Y. J., *Nutr. Res. Pract.* 2011, *5*, 495–502.

[14] Parys, S., Kehraus, S., Krick, A., Glombitza, K. W., Carmeli, S., Klimo, K., Gerhauser, C., Konig, G. M., *Phytochemistry* 2010, *71*, 221–229.

[15] Stern, J. L., Hagerman, A. E., Steinberg, P. D., Winter, F. C., Estes, J. A., *J. Chem. Ecol.* 1996, *22*, 1273–1293.

[16] Parys, S., Rosenbaum, A., Kehraus, S., Reher, G., Glombitza, K., König, G. M., *J. Nat. Prod.* 2007, *70*, 1865–1870.

[17] Koivikko, R., Eränen, J. K., Loponen, J., Jormalainen, V., *J. Chem. Ecol.* 2008, *34*, 54–64.

[18] Ferreres, F., Lopes, G., Gil-Izquierdo, A., Andrade, P. B., Sousa, C., Mouga, T., Valentao, P., *Mar. Drugs* 2012, *10*, 2766–2781.

[19] Liu, H., Gu, L., *J. Agric. Food Chem.* 2012, *60*, 1326–1334.

[20] Tierney, M. S., Soler-Vila, A., Rai, D. K., Croft, A. K., Brunton, N. P., Smyth, T. J., *Metabolomics*, 2014, *10*, 524–535.

[21] Steevenz, A. J., Mackinnon, S. L., Hankinson, R., Craft, C., Connan, S., Stengel, D. B., Melanson, J. E., *Phytochem. Anal.* 2012, *23*, 547–553.

[22] Isaza Martinez, J. H., Torres Castañeda, H. G., *J. Chromatogr. Sci.* 2013, *51*, 825–838.

[23] Dugo, P., Kumm, T., Cacciola, F., Dugo, G., Mondello, L., *J. Liq. Chromatogr. Rel. Technol.* 2008, *31*, 1758–1807.

[24] Herrero, M., Ibañez, E., Cifuentes, A., Bernal, J., *J. Chromatogr. A* 2009, *1216*, 7110–7129.

[25] Donato, P., Cacciola, F., Tranchida, P. Q., Dugo, P., Mondello, L., *Mass Spectrom. Rev.* 2012, *31*, 523–559.

[26] Montero, L., Herrero, M., Prodanov, M., Ibáñez, E., Cifuentes, A., *Anal. Bioanal. Chem.* 2013, *405*, 4627–4638.

[27] Montero, L., Herrero, M., Ibáñez, E., Cifuentes, A., *J. Chromatogr. A* 2013, *1313*, 275–283.

[28] Kalili, K. M., de Villiers, A., *J. Chromatogr. A* 2009, *1216*, 6274–6284.

[29] Kalili, K. M., de Villiers, A., *J. Chromatogr. A* 2013, *1289*, 58–68.

[30] Dugo, P., Cacciola, F., Herrero, M., Donato, P., Mondello, L., *J. Sep. Sci.* 2008, *31*, 3297–3308.

[31] Dugo, P., Cacciola, F., Donato, P., Airado-Rodriguez, D., Herrero, M., Mondello, L., *J. Chromatogr. A* 2009, *1216*, 7483–7487.

[32] Regos, I., Treutter, D., *J. Chromatogr. A* 2010, *1217*, 6169–6177.

[33] Manns, D. C., Mansfield, A. K., *J. Chromatogr. A* 2012, *1251*, 111–121.

[34] Neue, U. D., *J. Chromatogr. A* 2005, *1079*, 153–161.

[35] Li, X., Stoll, D. R., Carr, P. W., *Anal. Chem.* 2009, *81*, 845–850.

4.3. Anti-proliferative activity and chemical characterization by comprehensive two-dimensional liquid chromatography coupled to mass spectrometry of phlorotannins from the brown macroalga *Sargassum muticum* collected on North-Atlantic coasts.

Montero, L., Sánchez-Camargo, A. P., García-Cañas, V., Tanniou, A., Stiger-Pouvreau, V., Russo, M, Rastrelli, L., Cifuentes, A., Herrero, M., Ibáñez, E.

Journal of Chromatography A 2016, *1428*, 115–125.

Journal of Chromatography A, 1428 (2016) 115–125

Contents lists available at ScienceDirect

Journal of Chromatography A

journal homepage: www.elsevier.com/locate/chroma

Anti-proliferative activity and chemical characterization by comprehensive two-dimensional liquid chromatography coupled to mass spectrometry of phlorotannins from the brown macroalga *Sargassum muticum* collected on North-Atlantic coasts

Lidia Montero[a], Andrea P. Sánchez-Camargo[a], Virginia García-Cañas[a], Anaëlle Tanniou[b], Valérie Stiger-Pouvreau[b], Mariateresa Russo[c], Luca Rastrelli[d], Alejandro Cifuentes[a], Miguel Herrero[a,*], Elena Ibáñez[a]

[a] *Laboratory of Foodomics, Institute of Food Science Research (CIAL-CSIC), Nicolás Cabrera 9, 28049 Madrid, Spain*
[b] *LEMAR UMR 6539 CNRS UBO IRD IFREMER, Université de Bretagne Occidentale (UBO), Institut Universitaire Européen de la Mer (IUEM), Technopôle Brest-Iroise, Rue Dumont d'Urville, Plouzané 29280, France*
[c] *Dipartimento di Agraria, Università Mediterranea di Reggio Calabria, loc. Feo di Vito, 89122 Reggio Calabria, Italy*
[d] *Dipartimento di Farmacia, Università di Salerno, Via Giovanni Paolo II 132, 84084 Fisciano, Italy*

ARTICLE INFO

Article history:
Received 6 May 2015
Received in revised form 23 June 2015
Accepted 12 July 2015
Available online 15 July 2015

Keywords:
Anti-proliferative activity
Brown algae
Comprehensive LC
Phenolic compounds
Phlorotannins
Sargassum muticum

ABSTRACT

In the present work, the phlorotannin composition of different *Sargassum muticum* samples collected at different locations along the North Atlantic coasts as well as the bioactivities related to these components were investigated. After pressurized liquid extraction, the samples collected at the extreme locations of a latitudinal gradient from Portugal and Norway, were found to be the richest on total phenols and, particularly, on phlorotannins, containing up to 148.97 and 5.12 mg phloroglucinol equivalents g^{-1}, respectively. The extracts obtained from these locations were further purified and chemically characterized using a modified HILIC × RP-DAD-MS/MS method. The application of this methodology allowed the tentative identification of a great variability of phlorotannins with different degrees of polymerization (from 3 to 11) and structures, determined for the first time in *S. muticum*. The most-abundant phlorotannins on these samples were fuhalols, hydroxyfuhalols and phlorethols, showing also particularities and important differences depending on the geographical location. Afterwards, the antiproliferative activity of these extracts against HT-29 adenocarcinoma colon cancer cells was studied. Results revealed that the richest *S. muticum* samples in terms of total phlorotannins, i.e., those from Norway, presented the highest activity, showing a good cytotoxic potential at concentrations in the medium micromolar range.

1. Introduction

Phlorotannins are polyphenolic compounds widely recognized to be exclusive from brown seaweeds (Phaeophyceae) [1]. This particular type of polyphenols comprises a very heterogeneous group of polymeric compounds with a great chemical variability [2]. The interest of these compounds is related to their associated bioactivities, such as antioxidant [3–5], anti-inflammatory [6], anti-bacterial [7,8], antidiabetic [9] or anti-adipogenic [10], among others. Moreover, their potential anti-proliferative activity has been pointed out by several researches [11–13]. Phlorotannin content in brown algae can reach up to 15% of dry weight, depending on species, and they may be found in free form or forming complexes with different components of the cell walls, such as alginic acid [14]. From a purely chemical point of view, phlorotannins are made up of phloroglucinol (1,3,5-trihydroxybenzene) units with varying degrees of polymerization that may be linked through different bonds forming several structures and types, namely: fuhalols and phlorethols, which contain ether linkages; fucols, with phenyl linkages; fucophlorethols in which both ether and phenyl linkages are present; and eckols, that possess a benzodioxin linkage. Although their presence in brown algae is widely accepted, it is rather difficult to find studies in which the complete characterization of such complex polymeric structures is carried out. In fact, several

* Corresponding author. Tel.: +34 910 017 946; fax: +34 910 017 905.
E-mail address: m.herrero@csic.es (M. Herrero).

http://dx.doi.org/10.1016/j.chroma.2015.07.053
0021-9673/

approaches have been attempted for the structural elucidation of phlorotannins in their native form; for instance, Stiger-Pouvreau et al. [15] employed one- and two-dimensional nuclear magnetic resonance (NMR) (1H, heteronuclear multiple bond correlation) together with *in vivo* NMR (high-resolution magic-angle spinning, HR-MAS NMR) analyses, to structurally elucidate and fingerprint phlorotannin signals in different Sargassaceae species. Results revealed that these techniques were useful for discriminating among species, giving a differentiated profile but only determining the class of phlorotannins in the sample, without elucidating the entire structure of any compound. In a recent work carried out in our laboratory [16], a new comprehensive two-dimensional liquid chromatography coupled to DAD and tandem mass spectrometry (LC × LC-DAD-MS/MS) methodology was developed based on the coupling of a hydrophilic-interaction chromatography (HILIC)-based separation in the first dimension and an RP-based separation in the second dimension that allowed the separation and identification of more than 50 compounds in a *Cystoseira abies-marina* brown algal extract. By using this approach, phlorotannins containing from 5 to 17 phloroglucinol units were identified in this sample [16]. The application of this methodology to *S. muticum* could therefore imply a definitive step forward for the characterization of its phlorotannin composition.

S. muticum is an invasive brown macroalga widely spread along the European Atlantic coasts [17] Although native from Japan, this macroalga grows well in a variety of different environments, being in fact, one of the most readily available Sargassaceae species in Europe. Considering its availability and the fact that the presence of phlorotannins in *S. muticum* composition has been already confirmed [5,8], this seaweed has been pointed out as a potential sustainable source of bioactive compounds.

Different methods have been tested to extract phlorotannins from brown algae; the classical procedure [1] involves a solid–liquid extraction with large volumes of aqueous mixtures of ethanol or methanol for a long time. New green processes have been previously shown to be suitable for the extraction of bioactive compounds from a variety of different natural sources [18]; among them, centrifugal partition extraction (CPE), supercritical fluid extraction (SFE) and pressurized liquid extraction (PLE) have been employed, and compared to classical solid-liquid extraction, to obtain bioactive phenolic compounds from *S. muticum* [5]. Results demonstrated that PLE can be employed with advantages for obtaining extracts rich in phenolic compounds from brown algae, with high efficiency and complying with the rules of green chemistry. On the other hand, in a recent work carried out in our laboratory, enzyme-assisted extraction (EAE) was studied and compared to an optimized PLE process to try to increase the recovery of phenolic compounds from *S. muticum* [19]. This study showed that EAE did not significantly improve the results directly attainable through the use of PLE.

Thus, in the present work, the previously optimized PLE process [19] was applied to the extraction of phlorotannins from *S. muticum* samples collected at 13 different locations along the North-Atlantic coasts (Portugal, Spain, France, Ireland and Norway) with the aim to study the influence of the growing conditions on the chemical composition of the extracts. The extracts were characterized in terms of total phenol content, total phlorotannin content and antioxidant activity. Besides, a comprehensive two-dimensional liquid chromatography (LC × LC) method was optimized and applied to the richest samples to chemically characterize for the first time the native complex phlorotannin composition of *S. muticum*. Moreover, these extracts were also assayed to test their potential anti-proliferative activity against human colon cancer cells.

2. Materials and methods

2.1. Samples and chemicals

Samples of the brown alga *S. muticum* were collected from April to May 2011 in 13 different sites of five European Atlantic coast countries (Portugal, Spain, France, Ireland and Norway) as already described in Tanniou et al. [8]. The algae were rinsed firstly with filtered seawater and then with distilled water to remove the residual sediments and salts. After that, the samples were dried with absorbent paper and cut into fragments before their freeze-drying. Finally the dry material was powdered and sieved at 250 μm.

The solvents employed were HPLC-grade. Acetonitrile, ethanol, methanol and acetone were acquired from VWR Chemicals (Barcelona, Spain), whereas dichloromethane was acquired from Fluka AG (Buchs, Switzerland) and ethyl acetate from Scharlau (Barcelona, Spain). Ultrapure water was obtained from a Millipore system (Billerica, MA, USA).

Gallic acid, phloroglucinol, acetic acid, formic acid, 2,4-dimethoxybenzaldehyde (DMBA), 6-hydroxy-2,5,7,8-tetramethylchroman-2-carboxylic acid (Trolox) and 2,2′-azino-bis(3-ethylbenzothiazoline-6-sulfonic acid (ABTS) were purchased from Sigma–Aldrich (Madrid, Spain). The Folin–Ciocalteu phenol reagent was provided by Merck (Darmstadt, Germany). Hydrochloric acid was obtained from Probus (Barcelona, Spain). For inhibition of cell proliferation assays, dry purified extracts were dissolved in dimethyl sulfoxide (DMSO) (Sigma–Aldrich) at the appropriate concentrations and stored as aliquots at −80 °C until use.

2.2. Pressurized liquid extraction (PLE)

Firstly, extractions of freeze-dried and ground *S. muticum* samples from 13 different localizations along the North-Atlantic coasts were performed using an accelerated solvent extractor (ASE 200, Dionex, Sunnyvale, CA, USA), equipped with a solvent controller unit. For each extraction, an 11 mL stainless steel extraction cell was employed to load the sample. The extraction cell bottom was loaded with 1 g of sea sand, followed by 1 g of dried brown alga being mixed with the same quantity of sea sand. Subsequently, 1 g of sea sand was added on top as dispersive agent. Before the static extraction period, an instrumentally preset warming-up time of 6 min was used. The extraction conditions applied were based on a previous optimization [19], including the use of ethanol:water (95:5) as extraction solvent at 160 °C and 10.3 MPa for 20 min. Each extraction was carried out by duplicate. After the extraction process, the ethanol was removed by evaporation (Rotavapor R-210, Buchi Labortechnik AG, Flawil, Switzerland) and finally, the extracts were freeze-dried (Labconco Corporation, MO) and kept in the darkness at −20 °C until analysis.

2.3. Phlorotannins purification procedure

In order to obtain concentrated phlorotannin extracts, a purification protocol previously reported by Stiger-Pouvreau et al. [15] was applied to the *S. muticum* samples from Norway and Portugal. The dried extracts were re-dissolved in water and submitted to a liquid-liquid extraction with dichloromethane (1:1, *v/v*) in order to eliminate the lipidic compounds and chlorophylls present in the extract, repeating this step several times until a colorless non-polar fraction was obtained. After that, successive precipitations of proteins and carbohydrates were carried out with acetone and ethanol, respectively, ending with the elimination of the organic solvent using a gentle stream of nitrogen. Finally, phlorotannins were extracted from the water fraction with three rinses with equivalent volumes of ethyl acetate. The ethyl acetate fractions

were pooled and the solvent was evaporated under a stream of nitrogen.

2.4. In-vitro determinations

2.4.1. Total phenol content (Folin–Ciocalteu method)

Total phenol content of the PLE extracts and the purified extracts were measured by the Folin–Ciocalteu method developed by Kosar et al. [20] with some modifications. Briefly, 10 μL of sample (10 mg mL^{-1} in methanol) were transferred to 600 μL of water, and then 50 μL of undiluted Folin–Ciocalteu reagent were added. After 1 min, 150 μL of 20% (*w/v*) Na_2CO_3 were added and the volume was made up to 1 mL with water. The reaction was incubated at 25 °C for 2 h and then 300 μL of the mixture were transferred to a 96-well microplate. The absorbance was measured at 760 nm in a microplate spectrophotometer reader Powerwave XS (Bio Tek Instruments, Winooski, VT) and compared to a phloroglucinol calibration curve (62.5–2000 μg mL^{-1}). The phenolic content was expressed as mg of Phloroglucinol Equivalents (PGE) per g extract. Moreover, total phenol content was also expressed as % dry weight of algae. All analyses were done by triplicate.

2.4.2. Total phlorotannin content (DMBA assay)

To estimate the total phlorotannin content of the algal PLE and purified extracts, the DMBA colorimetric assay was employed [6]. DMBA solution was prepared just prior to use by mixing equal volumes of 2% DMBA reagent in acetic acid (*w/v*) and 6% hydrochloric acid in acetic acid (*v/v*). A total of 50 μL of sample (5 mg mL^{-1}) was mixed with 250 μL of DMBA solution in a 96-well microplate and the reaction was conducted at room temperature for 60 min in the dark. Then, the absorbance was read at 515 nm using a microplate spectrophotometer reader Powerwave XS (Bio Tek, Winooski, VT, USA). Water was used as blank and control samples without DMBA solution were also included. A calibration curve using phloroglucinol (PG) (0.1–46.0 μg mL^{-1}) was employed to estimate the total phlorotannin content. All samples, blanks, and controls were prepared in triplicate. Data are presented as the average of triplicate analyses expressed as milligram phloroglucinol equivalents (PGE) per gram of dry extract.

2.4.3. Trolox equivalents antioxidant capacity assay (TEAC)

The antioxidant capacity of the algal extracts was estimated with the TEAC assay following the ABTS method based on the procedure described by Re et al. [21]. $ABTS^{\bullet+}$ radical was produced by mixing 7 mM ABTS and 2.45 mM potassium persulfate allowing their reaction during 16 h in the dark at room temperature. The aqueous $ABTS^{\bullet+}$ solution was diluted with 5 mM phosphate buffer (pH 7.4) until an absorbance of 0.7 (±0.02) at 734 nm was achieved. 10 μL of sample (5 different concentrations ranging from 0.25 to 2 mg mL^{-1}) and 1 mL of $ABTS^{\bullet+}$ solution were mixed in an eppendorf vial and 300 μL of the mixture were transferred into a 96-well microplate. The absorbance was measured at 734 nm every 5 min during 45 min in a Powerwave XS microplate spectrophotometer reader (BioTek). Trolox was used as reference standard and results were expressed as TEAC values (mM Trolox g^{-1} extract). These values were obtained from five different concentrations of each extract tested in the assay giving a linear response between 20 and 80% of the blank absorbance. All analyses were done in triplicate.

2.5. Anti-proliferative activity against human colon cancer cells

Human colon cancer cell line HT-29 was used in order to measure the anti-proliferative activity of Norway and Portugal purified extracts. HT-29 cells obtained from the ATCC (American Type Culture Collection, LGC Promochem, UK) were grown in McCoy's 5A medium supplemented with 10% heat-inactivated fetal calf serum, 50 U mL^{-1} penicillin G, and 50 U mL^{-1} streptomycin, at 37 °C in humidified atmosphere and 5% CO_2. Cell viability was determined using MTT (3-(4,5-dimethylthiazol-2-yl)-2,5-diphenyltetrazolium bromide) assay. Briefly, HT-29 cells were seeded onto 96-well culture plates at 10,000 cells cm^{-2}, and permitted to adhere overnight at 37 °C. Cells were treated with the vehicle (medium with 0.2% DMSO) or different concentrations of *Sargasssum muticum* purified extracts (from 12.5 to 100 μg mL^{-1}) for 24, 48 and 72 h. After incubation with the extracts, the medium was aspirated and 0.5 mg mL^{-1} of MTT reagent (Sigma–Aldrich) was added to the cells and incubated for 3 h at 37 °C in humidified 5% CO_2/air atmosphere. The medium was then removed, and the purple formazan crystals were dissolved in 100 μL of DMSO. The absorbance at 570 nm was measured in a microplate reader (Multiskan™ FC Microplate Photometer, Thermo Fisher Scientific, Vantaa, Finland). Results are shown as the mean ± 95% confidence interval of at least three independent experiments, each performed in triplicate. Cell viability at the beginning of the treatment (time zero) was used to calculate the following parameters related to cell proliferation: GI50 (50% growth inhibition), TGI (total growth inhibition), and LC50 (50% cell death). These parameters were calculated according to the NIH definitions [22].

2.6. Comprehensive two-dimensional liquid chromatography (LC × LC) analysis of phlorotannins

2.6.1. Instrumentation

An Agilent 1200 series liquid chromatograph (Agilent Technologies, Santa Clara, CA) equipped with an autosampler and a diode array detector was used in the first dimension (D1) of the LC × LC setup. In order to obtain more reproducible low flow rates and gradients, a Protecol flow-splitter (SGE Analytical Science, Milton Keynes, UK) was placed between the first dimension pump and the autosampler. An additional LC pump (Agilent 1290 Infinity) was coupled to perform the second dimension (D2) separations. Both instruments were hyphenated through an electronically controlled two-position ten-port switching valve equipped with two 30 μL injection loops. An Agilent 6320 Ion Trap mass spectrometer equipped with an electrospray interface was online coupled and operated in negative ionization mode using the following conditions: dry temperature, 350 °C; mass range, *m/z* 90–2200 Da; dry gas flow rate, 12 L min^{-1}; nebulization pressure, 40 psi. The LC data were elaborated and visualized in two and three dimensions using LC Image software (version 1.0, Zoex, Houston, TX, USA).

2.6.2. LC × LC separation conditions

Samples of purified extracts of *S. muticum* from Portugal and Norway were prepared at 50 mg mL^{-1} in methanol/acetonitrile (3:7, *v/v*) from the dry extract obtained as described in Section 2.3.

D1 separation was run on a Lichrospher diol-5 (150 × 1.0 mm, 5 μm d.p., HiChrom, Reading, UK) column, following the separation conditions developed in our previous work [16]. Briefly, the mobile phases were (A) acetonitrile/acetic acid (98:2, *v/v*) and (B) methanol/water/acetic acid (95:3:2, *v/v/v*) eluted at 15 μL min^{-1} according to the following gradient: 0 min, 0% B; 3 min, 0% B; 5 min, 7% B; 30 min, 15% B; 70 min, 15% B; 75 min, 25% B; 85 min, 25% B. The injection volume was 5 μL.

D2 consisted on 78 s-repetitive gradients during the whole LC × LC separation, being modulation time of the switching valve also 78 s. In the D2 separation an Ascentis Express C_{18} (50 × 4.6 mm, 2.7 μm, d.p., Supelco, Bellefonte, CA) partially porous column with a C_{18} precolumn was employed, using as mobile phases water (0.1% formic acid, A) and acetonitrile (B) eluted according to the following repetitive gradients: 0 min, 0% B; 0.1 min, 0% B; 0.3 min, 5% B; 0.8 min, 70% B; 0.9 min, 90% B; 1.0 min, 0% B. The flow rate was

Table 1
Extraction yield (%), total phenol content (mg PGE g^{-1} extract), total phlorotannin content (mg PGE g^{-1} extract) and antioxidant activity (mmol TE g^{-1} extract, TEAC assay) of the brown macroalga *Sargassum muticum* PLE extracts according to their collection location. Values presented are mean ± sd. Superscripts mean groups not statistically different ($p > 0.05$) for each response.

Location		Extraction yield (%)	Total phenol content (mg PGE g^{-1})[A]	Total phenol content (% DWalgae)[B]	Total phlorotannins (mg PGE g^{-1})[C]	TEAC value (mmol TE g^{-1})[D]
France	F1	23.7 ± 0.3	75.43 ± 1.56^{a}	1.783 ± 0.029^{d}	3.297 ± 0.337^{c}	0.983 ± 0.018^{c,d}
	F2	17.5 ± 0.4	58.19 ± 3.31^{b}	1.016 ± 0.070^{a}	2.606 ± 0.036^{a}	0.652 ± 0.013^{a}
	F3	27.4 ± 2.5	78.55 ± 0.51^{a}	2.150 ± 0.157^{f}	3.380 ± 0.163^{c}	1.091 ± 0.017^{e}
Portugal	P1	24.9 ± 0.1	145.02 ± 3.05^{e}	3.604 ± 0.060^{h}	4.088 ± 0.239^{d}	2.101 ± 0.047^{g}
	P2	23.2 ± 0.5	119.27 ± 1.39^{f}	2.768 ± 0.068^{g}	4.127 ± 0.129^{d}	1.828 ± 0.025^{f}
Spain	S1	18.7 ± 0.1	79.29 ± 134^{a}	1.481 ± 0.030^{b,c}	2.629 ± 0.091^{a}	0.919 ± 0.023^{b}
	S2	16.2 ± 0.2	77.19 ± 1.64^{a}	1.248 ± 0.022^{a,b}	2.477 ± 0.139^{a}	0.943 ± 0.033^{b,c}
	S3	15.5 ± 0.1	80.46 ± 1.38^{a,c}	1.245 ± 0.026^{a,b}	2.567 ± 0.075^{a}	0.923 ± 0.016^{b}
Ireland	I1	21.3 ± 0.7	86.60 ± 2.44^{c}	1.844 ± 0.064^{d,e}	2.933 ± 0.090^{b}	1.106 ± 0.020^{d}
	I2	21.8 ± 0.6	78.39 ± 5.57^{a}	1.710 ± 0.156^{c,d}	2.670 ± 0.335^{a}	0.889 ± 0.011^{b}
	I3	22.3 ± 1.0	94.08 ± 0.96^{d}	2.098 ± 0.077^{e,f}	3.462 ± 0.095^{c}	1.068 ± 0.007^{e}
Norway	N1	31.5 ± 0.3	148.97 ± 0.85^{e}	4.696 ± 0.034^{i}	5.115 ± 0.145^{e}	2.297 ± 0.050^{h}
	N2	31.6 ± 1.4	146.44 ± 4.54^{e}	4.639 ± 0.274^{i}	4.839 ± 0.134^{f}	2.090 ± 0.032^{g}

[A] mg phloroglucinol equivalents g^{-1} extract.
[B] % dry weight algae.
[C] mg phloroglucinol equivalents g^{-1} extract.
[D] mmol Trolox equivalents g^{-1} extract.

3 mL min^{-1}. UV–vis spectra of the second dimension eluent were registered in the range of 190–550 nm using a sampling rate of 20 Hz, while 280 nm was the wavelength used to monitor the separations. The MS was operated under negative ESI mode. The flow eluting from the second dimension column was split before the MS instrument, so that the flow rate entering the MS detector was 500 μL min^{-1}.

2.7. Statistical analysis

IBM SPSS Statistics software v.19 was employed for data elaboration and statistical analysis using a level of significance set at 95%. One-way analysis of variance (ANOVA), together with Student–Newman–Keuls test, was employed to group samples, based on statistically significant differences. Mean values were compared using the Tukey's test and differences were considered statistically significant if $p < 0.05$.

3. Results and discussion

3.1. Influence of growing conditions on phlorotannin content

In order to study the influence of the particular growing conditions on the chemical composition of the *S. muticum* extracts, an optimized PLE procedure was applied to 13 different algal samples collected along the North-Atlantic coasts, including Portugal, Spain, France, Ireland and Norway locations. The extraction procedure applied included the use of ethanol:water (95:5, *v/v*) as extraction solvent at 160 °C and 10.3 MPa for 20 min. The extracts obtained were firstly characterized in terms of total phenol content, total phlorotannin content and antioxidant activity. Table 1 summarizes the results obtained; as can be clearly observed, the extraction yield gives a first hint regarding the different compositions of the macroalgae studied, not only between countries and distant geographical locations but also within some areas, as in the case of the samples collected on the French coast. The highest extraction yields were obtained with the samples collected in Norway, whereas those collected in Spain possessed the lowest amount of dried matter. As for total phenols, samples collected in Norway possessed the highest amount of total phenols, followed by those harvested in Portugal. These values were significantly higher than the ones obtained for the rest of locations. *S. muticum* samples collected in France possessed the lowest amount of total phenols, less than half of those of the richest samples. Although smaller, statistically significant differences ($p < 0.05$) were also observed among the samples collected in the same country, except those collected in Spain and Norway, that could be considered statistically similar ($p > 0.05$). Next, total phlorotannin contents were estimated in the different extracts; the trend found was rather similar to that of total phenols, that is, the samples collected in Norway and Portugal were the richest. In any case, significant differences were observed between these two countries. For the samples collected from the rest of countries, the values found were closer and lower than those found in the Norwegian samples. As in the case of total phenols, intra-country variations ($p < 0.05$) were observed for the total phlorotannin contents, excepting for those from Spain and Portugal. Previous fingerprints obtained by HR-MAS NMR and FT-IR for the same samples yielded similar conclusions about inter- and intra-site variability [23].

Lastly, the antioxidant capacity of the obtained extracts was determined using the TEAC assay. A good correlation was found between the TEAC values obtained and the total phenols and total phlorotannin contents determined in the extracts. In agreement, the most active extracts were obtained from the samples collected in Norway and Portugal, whereas the rest of extracts possessed lower antioxidant capacity (Table 1). Results obtained in the present work were, in general, well in accordance with those previously presented on *S. muticum* samples [8] in terms of percentage of total phenols per g of dried algae (Table 1). Samples collected in Norway and Portugal were those with higher % of total phenols with respect to the initial dry algae employed, whereas the rest of countries possessed very similar contents (Table 1). However, in the present work, a higher content was found for Norwegian samples compared to those harvested in Portugal. These small differences observed between the two studies could be due to the different extraction process employed to achieve the phenolic-rich extracts.

Looking at the results summarized in this section, it seemed clear that the algae growing in the most extreme locations of this latitudinal gradient along the North-Atlantic coasts, i.e., Norway and Portugal, were the most interesting from a chemical composition perspective. For this reason, the samples collected in those countries (four geographical locations in total) were selected to carry out an in-depth chemical characterization as well as to study their potential anti-proliferative activity. This activity has already been related to the presence of phenolic compounds in general and phlorotannins in particular [12,13].

To do that, a purification protocol was applied as described in Section 2.3 in order to further enrich the selected extracts in

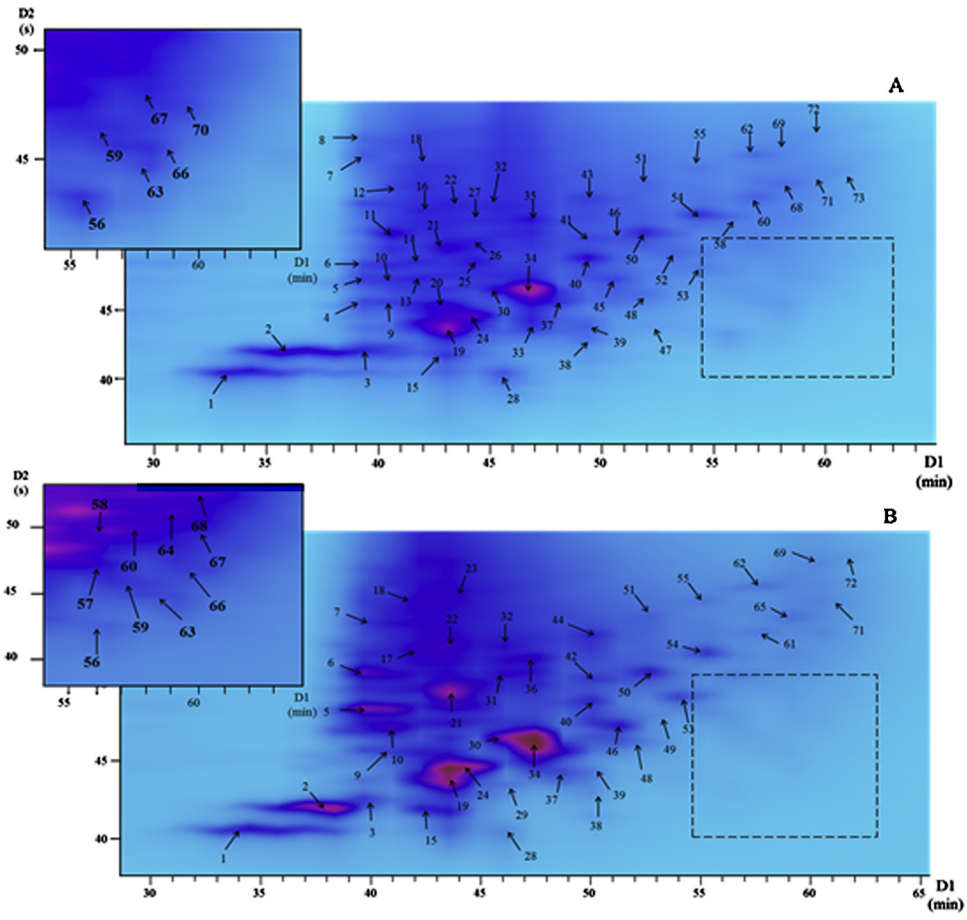

Fig. 1. 2D plot (280 nm) of the *Sargassum muticum* enriched extracts from the samples collected in Norway (A, sample N1 and B, sample N2) obtained using the optimized HILIC × RP-MS/MS method. For peak identification, see Table 2.

those compounds prior analysis. This purification protocol was properly optimized, studying the most influencing variables. To do that, different approaches were studied, including precipitation with several solvents (hexane, dichloromethane, ethyl acetate), use of SPE (different stationary phases) and molecular weight fractionation or combinations thereof. The optimum conditions were selected according to the best results observed in the two-dimensional LC analysis and involved a sample clean-up with dichloromethane followed by precipitations using acetone and ethanol finishing with an ethyl acetate extraction. After this procedure, the total phlorotannin content of the enriched extracts was more than double for Norwegian samples and around 1.5 times the initial content in Portuguese samples, being 11.730 ± 0.141, 12.461 ± 0.264, 5.906 ± 0.324 and 6.4217 ± 0.355 mg PGE g^{-1} for the samples N1, N2, P1 and P2, respectively.

3.2. Chemical characterization of phlorotannins by LC × LC-ESI-MS/MS.

Although the determination of total phlorotannins using the DMBA colorimetric method is able to provide a general estimation of the phlorotannin amount found in the extract, this assay is not able to provide any information about the chemical structure of those compounds. The structural variability known in phlorotannins (see introduction), that includes 5 chemical classes, could be therefore linked to their bioactivity. For this reason, in order to elucidate the compounds present in the most active *S. muticum* extracts, a LC × LC approach was used. We have previously presented the ability of this analytical tool to separate and tentatively identify phlorotannins of other brown algae, *C. abies-marina*, reaching degrees of polymerization of 17 phloroglucinol units (PGU) [16]. By using a combined HILIC separation in the first dimension (D1) and a RP-based separation in the second dimension (D2), 52 different phlorotannins could be effectively separated in *C. abies-marina* extracts. Considering that *C. abies-marina* is a closely related species to *S. muticum*, both belonging to the family Sargassaceae within the class Phaeophyceae, this method was employed as starting point for the optimization of the separation of the purified phlorotannins' extracts from *S. muticum* collected in Portugal and Norway. Different experimental conditions were tested in the two dimensions; D1 optimization included the use of microbore silica, diol and amino columns as well as different combination of acetonitrile and 10 mM ammonium acetate at several pH (6.6 and 8.0). The second dimension optimization was based on the study of several columns (i.e, C_{18} monolithic column, and C_{18} and PFP short partially porous columns) using different flow rates, mobile phases and analysis time. As for the combination of the two dimensions, once the conditions were optimized separately, several transfer volumes (20, 30 and 50 μL) and modulation times (1.3, 1.5 and 2.0 min) were studied.

After the optimization of all the separation conditions, the diol column was selected for the D1 HILIC. Moreover, the best separation conditions for the D2 included the use of a short C_{18} partially porous column adapting the gradient employed to the complexity and composition of the samples studied (see Section 2.6.2). Figs. 1 and 2 show the two-dimensional plots obtained (280 nm) for the samples collected in Norway and Portugal, respectively, under optimized the experimental conditions. At first sight it is

Table 2
Tentative peak assignment of the compounds separated by LC × LC-ESI-MS/MS found in the *S. muticum* samples collected in Norway.

Peak	Identification	D2 t_R (s)	Total t_R (min)	[M-H]$^-$	Main MS/MS fragments detected
1	Trifuhalol	40.30	27.97	389.0	375, 265, 245
2	Trifuhalol	41.85	30.60	389.0	375, 265, 245
3	Trifuhalol	42.00	34.50	389.1	375, 265, 245
4	NI*	45.50	34.56	448.5	415, 385, 321, 245, 196
5	NI	47.10	34.59	566.6	533, 389, 306, 244, 193
6	NI	50.75	34.65	564.3	526, 437, 373, 331, 202
7	NI	55.95	34.73	571.9	526, 449, 383, 319, 261, 193
8	NI	57.30	34.76	625.0	581, 498, 388, 258
9	Hydroxytetrafuhalol	45.30	35.86	529.8	512, 404, 389, 343, 262
10	Hydroxytetrafuhalol	47.10	35.89	529.1	513, 405, 387, 345, 264
11	NI	50.40	35.94	572.6	538, 511, 446, 318, 164
12	Pentafuhalol	53.70	36.00	637.1	621, 513, 385, 262
13	Tetrafuhalol	47.15	37.19	513.0	391, 373, 264, 245, 219
14	Hydroxytetrafuhalol	48.40	37.21	529.4	483, 465, 401, 389, 262, 245
15	Tetrafuhalol	41.60	38.39	513.4	389, 265, 245
16	Pentaphlorethol	52.05	38.57	621.5	603, 493, 357, 245
17	Hydroxytetrafuhalol	52.15	38.58	529.4	513, 389, 262
18	NI	55.25	38.32	590.5	570, 545, 466, 437, 401, 245
19	Tetrafuhalol	43.50	38.43	513.8	389, 263, 245
20	Tetrafuhalol	45.25	38.45	513.3	389, 263, 245
21	Tetrafuhalol	49.50	38.53	513.8	387, 263, 245
22	NI	52.40	38.57	683.3	648, 555, 509, 415, 387, 263, 245
23	NI	57.85	38.66	590.3	573, 547, 446, 333, 245, 195
24	Dihydroxytetrafuhalol	44.45	39.74	545.4	525, 513, 484, 403, 389, 375
25	NI	48.35	39.81	683.9	651, 557, 509, 387, 621, 245
26	NI	49.80	39.83	683.1	652, 543, 389, 302, 263, 245
27	NI	51.30	39.86	588.8	571, 522, 441, 380, 278, 246
28	Hydroxytetrafuhalol	40.20	40.97	529.5	465, 403, 389, 341, 263, 245
29	Hydroxytetrafuhalol	43.35	41.02	529.3	511, 403, 389, 263, 245
30	Pentafuhalol	46.45	41.07	637.3	621, 513, 373
31	Pentafuhalol	50.55	41.14	637.5	633, 513, 273
32	NI	52.30	41.17	807.3	775, 681, 541, 509, 385, 244
33	Pentafuhalol	44.05	42.33	637.3	621, 513, 497, 389
34	Pentafuhalol	46.30	42.37	637.4	513, 374
35	Hexaphlorethol	51.50	42.46	745.3	727, 619, 603, 371, 355, 309
36	NI	51.65	42.46	807.2	775, 757, 681, 509, 385, 245
37	Hydroxypentafuhalol	45.35	43.66	653.8	638, 527, 513, 466, 389, 263, 245
38	Dihydroxypentafuhalol	42.60	44.91	669.6	623, 527, 465, 403, 385, 341, 261
39	Dihydroxypentafuhalol	43.60	44.93	669.6	623, 543, 527, 465, 402, 385, 341, 260
40	Hydroxypentafuhalol	48.65	45.01	653.6	637, 527, 387, 245
41	Hexafuhalol	50.10	45.03	761.6	637
42	Hexafuhalol	50.40	45.04	761.3	745, 637, 498, 389, 245
43	Heptaphlorethol	53.00	45.08	869.2	851, 745, 728, 603, 245
44	Hexafuhalol	53.30	45.09	761.3	747, 637, 621, 513, 497, 245
45	Dihydroxypentafuhalol	47.15	46.29	669.8	621, 541, 527, 463, 401, 337, 271
46	Dihydroxyhexafuhalol	50.00	46.33	793.1	775, 731, 651, 527, 511, 403, 387
47	Hydroxyhexafuhalol	43.65	47.53	777.7	651, 637, 529, 511, 387, 261, 245
48	Dihydroxyhexafuhalol	46.00	47.57	793.3	775, 669, 653, 527, 403, 389, 262
49	Hydroxyhexafuhalol	47.85	47.60	777.3	763, 655, 529, 515, 388
50	NI	50.60	47.64	947.3	915, 821, 651, 527, 385
51	NI	54.00	47.70	894.2	830, 766, 625, 568
52	Dihydroxyhexafuhalol	49.15	48.92	793.7	777, 652, 589, 554, 511, 390, 311
53	Trihydroxyhexafuhalol	47.75	50.20	809.7	791, 765, 747, 667, 543, 527, 405
54	Dihydroxyheptafuhalol	51.90	50.27	917.1	873, 855, 838, 791, 775, 731, 713, 651, 513, 387
55	Octafuhalol	54.94	50.32	1009.2	994, 968, 887, 872, 747, 621
56	Dihydroxyhexafuhalol	42.80	51.41	793.3	667, 653, 529, 403, 387, 263
57	Dihydroxyhexafuhalol	47.80	51.49	794.2	774, 667, 653, 529, 403, 387, 263
58	Hydroxyheptafuhalol	51.70	51.56	901.8	857, 775, 761, 637, 511, 387
59	Dihydroxyhexafuhalol	49.50	52.83	793.9	773, 668, 653, 529, 403
60	Trihydroxyheptafuhalol	53.05	52.88	933.8	889, 793, 747, 651, 525, 385
61	Nonafuhalol	53.25	52.89	1133.9	1115, 1007, 993, 885, 869, 760, 745, 620
62	Nonafuhalol	56.15	52.94	1133.7	1117, 1009, 995, 887, 870, 853, 761, 745, 622
63	Dihydroxyheptafuhalol	45.45	52.76	917.5	874, 777, 651, 527, 387
64	Trihydroxyheptafuhalol	51.90	52.87	933.4	914, 889, 792, 748, 650, 529
65	Trihydroxyoctafuhalol	54.20	52.90	1057.2	1008, 915, 793, 652, 527, 387
66	Dihydroxyheptafuhalol	45.25	54.05	917.5	899, 874, 791, 775, 651, 527, 387
67	Dihydroxyheptafuhalol	51.75	54.16	917.7	873, 791, 777, 653, 527, 387
68	Trihydroxyoctafuhalol	54.05	54.20	1057.3	
69	Decafuhalol	56.75	54.25	1257.7	1239, 1133, 1117, 1007, 885, 624, 573, 387
70	Dihydroxyheptafuhalol	47.30	55.39	917.1	897, 873, 791, 777, 731, 653, 527, 389
71	Dihydroxyoctafuhalol	54.90	55.52	1041.3	979, 915, 901, 853, 777, 731, 651, 637, 528, 389
72	Decafuhalol	57.50	55.56	1257.7	
73	Dihydroxynonafuhalol	55.00	56.82	1165.7	1146, 1040, 1025, 917, 899, 777, 653, 637, 389

*NI, not identified.

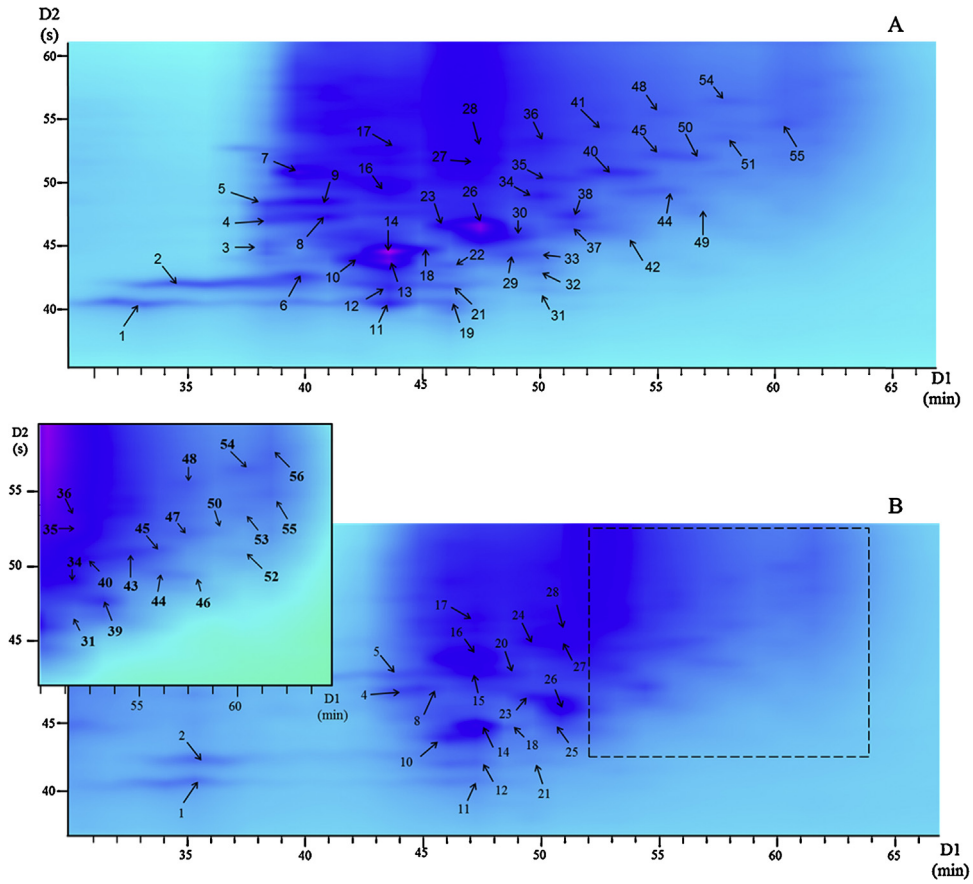

Fig. 2. 2D plot (280 nm) of the *Sargassum muticum* enriched extracts from the samples collected in Portugal (A, sample P1 and B, sample P2) obtained using the optimized HILIC × RP-MS/MS method. For peak identification, see Table 3.

possible to observe that the profiles obtained were significantly different as expected considering the different locations and associated environmental conditions such as sea surface temperature (8–10 °C for Norway and 18–20 °C for Portugal) and photosynthetically available radiation (35–40 mol photons m^{-2} day^{-1} for Norway and 40–45 mol photons m^{-2} day^{-1} for Portugal) [8]. Tables 2 and 3 summarize the data corresponding to the separated compounds in the Norwegian and Portuguese samples, respectively, as well as the tentative assignments of the peaks observed; a first comparison between samples shows important differences in terms of phlorotannin composition.

For instance, samples harvested in Norway were more complex in terms of number of components. As can be observed in Table 2, phlorotannins with a polymerization degree up to 10 units were found. Even if the separation performance achieved was quite satisfactory, the identification of phlorotannins is a very tough task due to their huge chemical variability. In these samples, fuhalol- and hydroxyfuhalol-type phlorotannins were the most-frequently elucidated components, although phlorethols with diverse degree of polymerization were also present (peaks 16, 35 and 43). These two types of phlorotannins are characterized by being formed from phloroglucinol units linked through ether bonds; the difference between phlorethols and fuhalols is the presence of one or more additional hydroxyl groups on the terminal monomer unit [24]. As shown in Table 2, different fuhalols were found in the Norwegian samples, starting from a degree of polymerization of 3 to 10, containing additional hydroxyl group(s). Moreover, other polymers were also elucidated containing up to 4 additional hydroxyl groups. Polymers containing 4–7 phloroglucinol units were the most-frequently found (see Fig. 1 and Table 2). Interestingly, although the profiles were not identical between sites in Norway, they were quite similar, being peaks 2, 19, 24 and 34 among the most intense peaks in both samples, corresponding to trifuhalol (degree of polymerization (DP) = 3, 1 hydroxyl group), tetrafuhalol (DP = 4, 1 hydroxyl group), dihydroxytetrafuhalol (DP = 4, 3 hydroxyl group) and pentafuhalol (DP = 5, 1 hydroxyl group). Sample N2 also contained other very intense peaks (peaks 5, 6) for which an assignment was not attained. In any case, the fragmentation pattern observed for the different peaks was very important for their identification, as they followed a typical fragmentation showing different losses of phloroglucinol units and hydroxyl groups, which helped to achieve a tentative identification. An example is shown in Fig. 3 with the MS/MS fragmentation pattern of dihydroxyheptafuhalol in sample N1 (peak 63). It is also important to note that the relative position of a peak in the 2D plane can be used as a tool for identification since LC × LC allows obtaining 2D patterns in agreement with differential retention in each dimension. For instance, D1 separation shows a distribution according to an increase on degree of polymerization while D2 retention implies that highly hydrophobic compounds elute later, making possible the discrimination, between doubtful identifications, based on peak position. Therefore, this enhanced identification capability of unknown peaks is one of the strongest advantages of 2D approaches over one-dimensional ones.

In the case of the Portuguese samples, less complex 2D plots were obtained (Fig. 2). In this case, the differences between the samples collected in the same country were also more marked. Anyway, peaks 14 and 26 were among the most-intense peaks in both samples, corresponding to an unidentified compound and to a pentafuhalol (DP = 5, 1 hydroxyl group), respectively. From

Table 3
Tentative peak assignment of the compounds separated by LC × LC-ESI-MS/MS found in the *S. muticum* samples collected in Portugal.

Peak	Identification	D2 t_R (s)	Total t_R (min)	[M−H]–	Main MS/MS fragments
1	Trifuhalol	40.70	31.88	389.0	263, 245
2	Trifuhalol	41.90	34.50	389.0	263, 245
3	NI	45.00	38.45	447.8	429, 385, 323, 311, 261
4	Trifuhalol	47.20	38.49	389.0	375, 265, 250
5	NI	48.15	38.50	568.4	552, 537, 443, 305
6	Trifuhalol	42.45	39.71	389.0	375, 251
7	NI	50.50	39.84	570.6	551, 511, 443, 305, 263
8	NI	47.20	41.09	526.8	507, 491, 401, 387, 357, 263, 245
9	NI	48.30	41.11	536.3	520, 475, 411, 333, 268
10	Tetrafuhalol	43.65	42.33	513.7	437, 389, 265, 251
11	Tetrafuhalol	40.30	43.57	513.0	475, 438, 391
12	NI	41.60	43.59	520.0	499, 439, 389, 319, 251
13	Tetrafuhalol	43.55	43.63	513.0	499, 437, 389, 263
14	NI	44.45	43.64	516.3	437, 427, 389, 297, 251
15	NI	48.70	43.73	685.1	651, 633, 509, 387, 245
16	NI	49.55	43.73	685.3	651, 633, 557, 509, 387, 263, 245
17	NI	52.35	43.77	590.4	572, 511, 465, 426, 325, 245
18	Dihydroxytetrafuhalol	44.65	44.94	545.7	529, 513, 389
19	Hydroxytetrafuhalol	40.30	46.17	529.7	403, 389, 277, 262, 245
20	NI	48.55	46.19	687.2	653, 579, 525, 388, 244
21	NI	41.80	46.20	531.4	513, 487, 403, 391, 341, 263, 245
22	NI	43.35	46.22	531.0	515, 486, 405, 391, 363, 307, 265, 245
23	NI	46.55	46.28	646.7	633, 529, 501, 387, 245
24	NI	50.95	46.35	646.5	633, 607, 525, 509, 387, 343, 263, 245
25	Dihydroxypentafuhalol	42.20	47.50	671.0	653, 637, 627, 544, 466, 247
26	Pentafuhalol	46.20	47.57	637.3	623, 513, 373
27	Trihydroxyhexafuhalol	51.55	47.66	809.5	791, 775, 637, 511, 387
28	NI	52.95	47.68	734.3	715, 689, 607, 566, 437, 285
29	Dihydroxypentafuhalol	44.20	48.84	669.0	651, 625, 607, 465, 403, 263
30	Dihydroxypentafuhalol	45.60	48.86	671.3	653, 637, 627, 467, 467, 405, 349
31	Hydroxypentafuhalol	41.40	50.09	653.2	633, 527, 513, 387, 263, 245
32	Hydroxypentafuhalol	42.80	50.11	653.8	637, 527, 513, 387, 263, 245
33	NI	44.20	50.14	655.3	636, 611, 529, 515, 469, 388, 341, 262, 245
34	NI	48.65	50.21	657.0	633, 621, 524, 483, 370, 263
35	NI	50.25	50.24	780.5	638, 611, 532, 388, 217
36	NI	53.05	50.28	877.6	859, 832, 797, 661, 612, 520
37	NI	46.20	51.47	661.2	612, 555, 509, 367, 263
38	NI	47.20	51.49	663.7	647, 574, 537, 505, 374
39	Dihydroxyhexafuhalol	47.70	52.80	793.1	775, 749, 731, 527, 483, 465, 385
40	Dihydroxyhexafuhalol	50.65	52.84	793.2	775, 749, 731, 527, 511, 483, 387, 245
41	NI	53.95	52.89	895.4	
42	NI	44.15	54.02	781.4	763, 701, 499, 437, 263
43	Hydroxyhexafuhalol	50.90	54.08	949.1	
44	Dihydroxyhexafuhalol	49.45	54.12	793.5	777, 730, 634, 513, 485
45	NI	51.05	54.15	948.1	775, 749, 652, 607, 528, 510, 483, 431, 389
46	Dihydroxyheptafuhalol	49.20	55.42	917.3	900, 874, 856, 714, 634, 513
47	Dihydroxyheptafuhalol	52.00	55.47	917.6	898, 873, 791, 777, 634, 513, 403
48	Dihydroxynonafuhalol	55.20	55.52	1165.3	
49	Dihydroxyheptafuhalol	48.00	56.70	919.2	900, 874, 856, 837, 714, 634, 513, 265
50	Dihydroxynonafuhalol	51.90	56.77	1165.7	
51	Dihydroxyhexafuhalol	53.20	56.80	793.1	777, 749, 653, 529, 403, 387, 263
52	Trihydroxyheptafuhalol	53.30	58.09	933.5	914, 871, 773, 667, 651, 623, 511
53	Dihydroxyoctafuhalol	54.60	58.09	1043.1	
54	Nonafuhalol	56.30	58.14	1134.9	
55	Decafuhalol	54.55	60.71	1257.7	
56	Endecaphlorethol	57.70	62.06	1365.3	

*NI, not identified.

the information summarized in Table 3 it is possible to infer that fuhalols and hydroxyfuhalols were also the predominant phlorotannins in these Portuguese samples. Different degrees of polymerization were found, from 3 to 11, whereas the additional hydroxyl groups associated to these structures were up to 4 in some cases. Although the presence of hydroxyfuhalols in *S. muticum* has been reported [25], it is worth to mention that there are no previous studies describing in such detail the phlorotannin content in *S. muticum* samples nor in any other algal sample containing a similar variability on fuhalols, hydroxyfuhalols and phlorethols composition, which gives a clear idea of the difficulty of this task. In this regard, the potential of LC × LC-MS/MS to separate and to tentatively identify such a complex mixture is demonstrated in the present work. NMR spectra (HMBC analysis) obtained with algae collected in different North-Atlantic sites allowed only the determination of phlorethols in the phlorotannin fraction of *S. muticum* [8,15]. Thus, considering the complexity of the polyphenols fraction (as demonstrated by the phlorotannins profile shown in Figs. 1 and 2), we can conclude that the pressurized liquid extraction (PLE) combined to a LC × LC-DAD-MS/MS methodology applied appears a promising tool for the complete separation and identification of phlorotannins in algal samples. This multidimensional tool offers a series of advantages that one-dimensional approaches cannot provide, thanks to the simultaneous use of different separation mechanisms. In fact, the gains obtained through this two-dimensional approach may be illustrated from the peak capacity values achieved for the separations. In this regard, a theoretical peak capacity (n_{c2D}) of 1050 was obtained for N1 sample

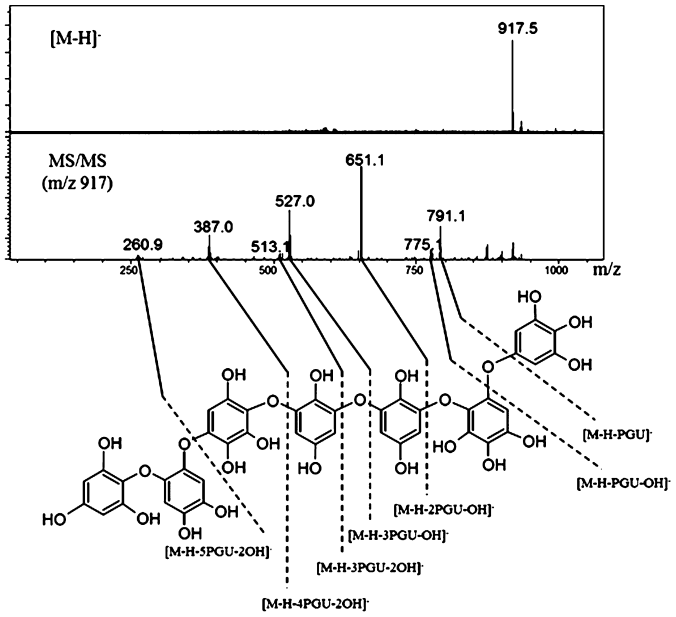

Fig. 3. MS spectrum and MS/MS fragmentation pattern of dihydroxyheptafuhalol in sample N1 (peak 63, fuhalol with DP = 7 with two additional hydroxyl groups) as well as the tentatively proposed chemical structure. PGU: phloroglucinol units.

whereas P1 separation reached a peak capacity of 906; measurements were done according to Li et al. [26] in order to consider the D2 time cycle as well as the influence of undersampling of the D1 eluate. Moreover, to stress the importance of re-optimizing the LC × LC separation according to the sample studied, the values found with the present method and that previously developed [19] were compared for the same sample (N1); results showed that a 50% increase on separation performance was obtained (n_{c2D} 699 vs 1050).

At present, very little is known about the relationship between phlorotannin structure (degree of polymerization, type of bond, branching) and bioactivity [4]. From the published data as well as from the results included in this work, it seems that the antioxidant activity of these components may be more related to their relative abundance than to their different structure [4]. Nevertheless, one should note that in Norwegian populations, a higher variety of smaller compounds compared to Portuguese populations was detected. This observation is in agreement with previous reports that demonstrated that small phlorotannins possess higher antioxidant activity than highly polymerized compounds [27]. Other reports have pointed out some discrepancies between antioxidant activity and other activities, such as hepatoprotective activity, showing that some phlorotannins that presented good antioxidant activity did not possess similar hepatoprotective activity [28]. Besides, to further study the possible relationship between phlorotannin structure and antiproliferative activity, the four purified *S. muticum* extracts (collected in Norway and Portugal) were assayed in order to observe their potential effects against a human colon cancer cell line, HT-29.

3.3. *Antiproliferative activity of phlorotannins from* S. muticum

To determine the antiproliferative effect of the phlorotannins-enriched extracts, HT-29 cells were incubated with increasing concentrations of extracts (from 0 to 100 μg mL^{-1}) for 24, 48 and 72 h and cell proliferation was analyzed by the MTT assay. As can be observed in Fig. 4, after 24 h incubation, the concentration dependence of the antiproliferative activity of the extracts was significant. The extracts demonstrated different *in vitro* antiproliferative effects on HT-29 colon cancer cells. In general, the most enriched extracts

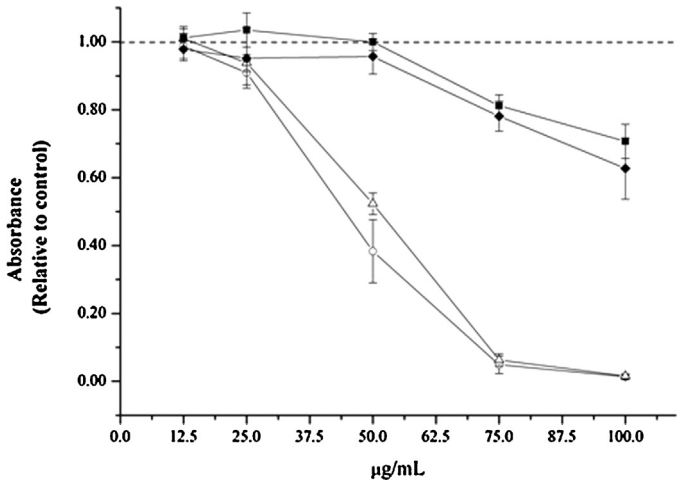

Fig. 4. HT-29 cell viability upon treatment for 24 h with different concentrations of N1 (circle), N2 (triangle), P1 (square) and P2 (diamond) extracts. Error bars are given as 95% confidence interval.

in phlorotannins (those obtained from Norway, sites 1 and 2; N1 11.730 ± 0.141 and N2 12.461 ± 0.264 mg PGE g^{-1}) exerted higher antiproliferative activity. For instance, incubation with N1 and N2 extracts at a concentration of 50 μg mL^{-1}, reduced cell proliferation by roughly 50% after 24 h, while extracts obtained from Portugal, sites 1 and 2 (P1 and P2 samples, total phlorotannin content 5.906 ± 0.324 and 6.4217 ± 0.355 mg PGE g^{-1}, respectively.) did not exert any appreciable effect at this concentration. Furthermore, cell viability was totally reduced after treatments with N1 and N2 extracts at concentrations close to 100 μg mL^{-1} at any of the assayed times, while the same concentration of P1 and P2 extracts reduced cell viability down to *ca.* 40% after 24 h incubation. In order to characterize in more detail the antiproliferative activity of these extracts, the growth inhibition (GI50), the total growth inhibition (TGI) (as an indicator for cytostaticity), and the lethal concentration (LC50) (as an indicator for the cytotoxic level of effect), were also determined at 24, 48 and 72 h incubation times. As it is shown in Table 4, the phlorotannin-enriched extracts exert different *in vitro* cytostatic and cytotoxic effects depending on the type of extract and concentration, exhibiting maximum inhibitory activity after 24 h exposure. In particular, N1 and N2 demonstrated cytotoxic potential at concentrations in the medium micromolar range. The comparison of the results obtained in the present study with those reported in literature for brown seaweeds-derived extracts is not straightforward due to limited information

Table 4
Antiproliferative *in-vitro* effect of *S. muticum* extracts on HT-29 cells. Values represent the concentrations in μg mL^{-1} of each extract that caused 50% growth inhibition (GI50), total growth inhibition (TGI), and 50% cell death (LC50). Results are shown as the mean ± SEM of three independent experiments, each performed in triplicate. Superscripts mean groups not statistically different ($p > 0.05$) for each response.

Sample	Incubation time (h)	GI_{50} (μg mL^{-1})	TGI (μg mL^{-1})	LC_{50} (μg mL^{-1})
N1	24	32.2 ± 1.7^{a}	41.7 ± 1.4^{a}	53.5 ± 0.9^{a}
	48	37.2 ± 1.4^{a}	45.5 ± 0.8^{a,b}	55.0 ± 0.2^{a}
	72	36.4 ± 4.7^{a}	46.3 ± 2.7^{a,b}	59.4 ± 4.2^{a}
N2	24	37.0 ± 2.3^{a}	46.7 ± 1.3^{a,b}	57.9 ± 0.1^{a}
	48	40.3 ± 2.5^{a}	49.2 ± 1.9^{a,b}	57.8 ± 0.2^{a}
	72	46.5 ± 1.1^{a}	56.1 ± 3.2^{b}	74.0 ± 2.6^{b}
P1	24	77.7 ± 4.4^{b}	NC*	NC
	48	72.4 ± 2.7^{b}	NC	NC
	72	81.8 ± 3.1^{b}	NC	NC
P2	24	72.0 ± 3.3^{b}	NC	NC
	48	75.8 ± 2.9^{b}	NC	NC
	72	83.8 ± 4.6^{b}	NC	NC

*NC, not calculated.

available about chemical phlorotannin composition and differences in the *in vitro* cell models used. However, the parameter values obtained in the present study seem to be close to the antiproliferative concentration levels of brown seaweeds extracts published in various reports for other *in vitro* cell studies [11,29,30]. As an example, He et al. [31] reported cell viability inhibition values of 36.9 and 60.5% for the brown seaweed *Saccharina japonica* extracts containing phlorotannins (2.19 and 1.28 mg g^{-1}, respectively) on hepatocellular carcinoma cells following a exposure time of 24 h at the concentration of 60 μg mL^{-1}. Interestingly, data summarized in Table 4 also showed that N1 extract, which contained lower phlorotannin concentration than N2 extract (see Table 1 for the values of TPC and total phlorotannins for the purified N1, N2, P1 and P2 extracts), exerted slightly higher effect on cell proliferation than N2 extract, provided by the lower values obtained for the parameters at the different incubation times. According to the chemical differences in the phlorotannin fraction observed between these extracts, these results suggest that either phlorotannins with selective bioactivity or the presence of other compounds in the extracts might be responsible for the differential antiproliferative effectiveness observed between N1 and N2. In this regard, further work is required to elucidate the active constituents responsible for this differential effectiveness between phlorotannin-enriched extracts.

4. Conclusions

In the present work, the phlorotannin composition of different *S. muticum* samples collected at different locations along the European Atlantic coast was investigated. After PLE extraction, the samples collected at the extreme locations of a latitudinal gradient along North Atlantic coasts, i.e., Portugal and Norway, were found to be the richest in total phenols and, particularly, in phlorotannins. The extracts obtained from these locations were further purified and chemically characterized using a modified HILIC × RP-DAD-MS/MS method. The application of this methodology allowed the tentative identification of phlorotannins with great chemical variability containing different degrees of polymerization and structures; fuhalols, hydroxyfuhalols and phlorethols were the most-abundant phlorotannins on these samples, showing also particularities and important differences depending on the geographical location. This is the first time that these complex structures are separated and characterized with such detail. Afterwards, the antiproliferative activity of these extracts against HT-29 adenocarcinoma colon cancer cells was studied. Results revealed that Norwegian samples of *S. muticum* presented the highest activity, showing a good cytotoxic potential at concentrations in the medium micromolar range.

Acknowledgements

A.P.S.C. thanks to the Administrative Department of Science, Technology and Innovation COLCIENCIAS (Colombia) for her Ph. D. Scholarship. M. H. would like to thank MICINN for his "Ramón y Cajal" research contract. VSP thanks to A. Engelen for the sending of freeze-dried material from Portugal, together with V. Husa and M. Incera for their help in the collection of algae in Norway. The authors would also like to thank Projects AGL2011-29857-C03-01 (MINECO, Spain) and ALIBIRD-CM, S2013/ABI-2728 (Comunidad de Madrid), Interreg IVB Biotecmar (collect of algae along the Atlantic coasts) and Era-net Seas-era INVASIVES for their financial support.

References

[1] M.A. Ragan, K.W. Glombitza, Phlorotannins, brown algal polyphenols, in: F.E. Round, D.J. Chapman (Eds.), Progress in Phycological Research, Biopress Ltd, Bristol; UK, 1986, pp. 129–241.
[2] R. Koivikko, J. Loponen, K. Pihlaja, V. Jormalainen, High-performance liquid chromatographic analysis of phlorotannins from the brown alga *Fucus Vesiculosus*, Phytochem. Anal. 18 (2007) 326–332.
[3] M.S. Tierney, T.J. Smyth, M. Hayes, A. Soler-Vila, A.K. Croft, N. Brunton, Influence of pressurised liquid extraction and solid–liquid extraction methods on the phenolic content and antioxidant activities of Irish macroalgae, Int. J. Food Sci. Technol. 48 (2013) 860–869.
[4] T. Wang, R. Jónsdóttir, H. Liu, L. Gu, H.G. Kristinsson, S. Raghavan, G. Olafsdóttir, Antioxidant capacities of phlorotannins extracted from the brown algae *Fucus vesiculosus*, J. Agric. Food Chem. 60 (2012) 5874–5883.
[5] A. Tanniou, E. Serrano Leon, L. Vandanjon, E. Ibañez, J.A. Mendiola, S. Cerantola, N. Kervarec, S. La Barre, L. Marchal, V. Stiger-Pouvreau, Green improved processes to extract bioactive phenolic compounds from brown macroalgae using *Sargassum muticum* as model, Talanta 104 (2013) 44–52.
[6] G. Lopes, C. Sousa, L.R. Silva, E. Pinto, P.B. Andrade, J. Bernardo, T. Mouga, P. Valentao, Can phlorotannins purified extracts constitute a novel pharmacological alternative for microbial infections with associated inflammatory conditions? PLoS ONE 7 (2012) e31145.
[7] G. Lopes, E. Pinto, P.B. Andrade, P. Valentao, Antifungal activity of phlorotannins against dermatophytes and yeasts: approaches to the mechanism of action and influence on *Candida albicans* virulence factor, PLoS ONE 8 (2013) e72203.
[8] A. Tanniou, L. Vandanjon, M. Incera, E. Serrano Leon, V. Husa, J. Le Grand, J.L. Nicolas, N. Poupart, N. Kervarec, A. Engelen, R. Walsh, F. Guerard, N. Bourgougnon, V. Stiger-Pouvreau, Assessment of the spatial variability of phenolic contents and associated bioactivities in the invasive alga *Sargassum muticum* sampled along its European range from Norway to Portugal, J. Appl. Phycol. 26 (2014) 1215–1230.
[9] S.H. Lee, Y.J. Jeon, Anti-diabetic effects of brown algae derived phlorotannins, marine polyphenols through diverse mechanisms, Fitoterapia 86 (2013) 129–136.
[10] H.A. Jung, H.J. Jung, H.Y. Jeong, H.J. Kwon, M.Y. Ali, J.S. Choi, Phlorotannins isolated from the edible brown alga *Ecklonia stolonifera* exert anti-adipogenic activity on 3T3-L1 adipocytes by downregulating C/EBPa and PPARg, Fitoterapia 92 (2014) 260–269.
[11] M. Zubia, M.S. Fabre, V. Kerjean, K. Le Lann, V. Stiger-Pouvreau, M. Fauchon, E. Deslandes, Antioxidant and antitumoral activities of some *Phaeophyta* from Brittany coasts, Food Chem. 116 (2009) 693–701.
[12] F. Nwosu, J. Morris, V.A. Lund, D. Stewart, H.A. Ross, G.J. McDougall, Antiproliferative and potential anti-diabetic effects of phenolic-rich extracts from edible marine algae, Food Chem. 126 (2011) 1006–1012.
[13] Y. Li, Z.J. Qian, M.M. Kim, S.K. Kim, Cytotoxic activities of phlorethol and fucophlorethol derivatives isolated from *laminariaceae Eklonia cava*, J. Food Biochem. 35 (2011) 357–369.
[14] S.M. Kim, S.W. Kang, J.S. Jeon, Y.J. Jung, W.R. Kim, C.Y. Kim, B.H. Um, Determination of major phlorotannins in *Eisenia bicyclis* using hydrophilic interaction chromatography: seasonal variation and extraction characteristics, Food Chem. 138 (2013) 2399–2406.
[15] V. Stiger-Pouvreau, C. Jégou, S. Cérantola, F. Guérard, K. Le Lann, Phlorotannins in *Sargassaceae* species from Brittany (France): interesting molecules for ecophysiological and valorisation purposes, in: N. Bourgougnon (Ed.), Advances in Botanical Research – Sea Plants, 71, 2014, pp. 379–411 (Chapter 13).
[16] L. Montero, M. Herrero, E. Ibáñez, A. Cifuentes, Separation and characterization of phlorotannins from brown algae *Cystoseira abies-marina* by comprehensive two-dimensional liquid chromatography, Electrophoresis 35 (2014) 1644–1651.
[17] E. Plouguerné, K. Le Lann, S. Connan, G. Jechoux, E. Deslandes, V. Stiger-Pouvreau, Spatial and seasonal variation in density, reproductive status, length and phenolic content of the invasive brown macroalga *Sargassum muticum* (Yendo) Fensholt along the coast of Western Brittany (France), Aquat. Bot. 85 (2006) 337–344.
[18] M. Herrero, A.P. Sánchez-Camargo, A. Cifuentes, E. Ibáñez, Plants, seaweeds, microalgae and food-by-products as natural sources of functional ingredients obtained using pressurized liquid extraction and supercritical fluid extraction. An update, Trends Anal. Chem. (2015), http://dx.doi.org/10.1016/j.trac.2015.01.018 (in press).
[19] A.P. Sanchez-Camargo, L. Montero, V. Stiger-Pouvreau, A. Tanniou, A. Cifuentes, M. Herrero, E. Ibáñez, Considerations on the use of enzyme-assisted extraction in combination with pressurized liquids to recover bioactive compounds from algae, Food Chem. 192 (2016) 67–74.
[20] M. Kosar, H.J.D. Dorman, R. Hiltunen, Effect of an acid treatment on the phytochemical and antioxidant characteristics of extracts from selected *Lamiaceae* species, Food Chem. 91 (2005) 525–533.
[21] R. Re, P. Pellegrini, A. Proteggente, A. Pannala, M. Yang, C. Rice-Evans, Antioxidant activity applying an improved ABTS radical cation decolorization assay, Free Radic. Biol. Med. 26 (1999) 1231–1237.
[22] A. Monks, D. Scudiero, P. Skehan, R. Shoemaker, K. Paull, D. Vistica, C. Hose, J. Langley, P. Cronise, A. Vaigro-Wolff, M. Gray-Goodrich, H. Campbell, M. Boyd, Feasibility of a high-flux anticancer drug screen utilizing a diverse panel of human tumor cell lines in culture, J. Natl. Cancer. Inst. 83 (1991) 757–766.
[23] A. Tanniou, L. Vandanjon, O. Gonçalves, N. Kervarec, V. Stiger-Pouvreau, Rapid geographical differentiation of the European spread brown algae *Sargassum muticum* using HRMAS NMR and Fourier-Transform Infrared spectroscopy, Talanta 132 (2015) 451–456.
[24] J.H. Isaza, H.G. Torres, Preparation and chromatographic analysis of phlorotannins, J. Chromatogr. Sci. 51 (2013) 825–838.

[25] K.W. Glombitza, M. Forster, W.F. Farnham, Polyhydroxyphenyl ethers from brown alga *Sargassum muticum* (Yendo) Fensholt, Bot. Mar. 25 (1982) 449–453.
[26] X. Li, D.R. Stoll, P.W. Carr, A simple and accurate equation for peak capacity estimation in two dimensional liquid chromatography, Anal. Chem. 81 (2009) 845–850.
[27] T. Nakamura, K. Nagayama, K. Uchida, R. Tanaka, Antioxidant activity of phlorotannins isolated from the brown alga *Eisenia bicyclis*, Fish. Sci. 62 (1996) 923–926.
[28] M.S. Lee, T. Shin, T. Utsuki, J.S. Choi, J.S. Choi, D.S. Byun, H.R. Kim, Isolation and identification of phlorotannins from *Ecklonia stolonifera* with antioxidant and hepatoprotective properties in tacrine-treated HepG2 cells, J. Agric. Food Chem. 60 (2012) 5340–5349.
[29] Y.V. Yuan, N.A. Walsh, Antioxidant and antiproliferative activities of extracts from a variety of edible seaweeds, Food Chem. Toxicol. 44 (2006) 1144–1150.
[30] H. Yang, M. Zeng, S. Dong, Z. Liu, R. Li, Anti-proliferative activity of phlorotannin extracts from brown algae *Laminaria japonica* Aresh, Chin. J. Oceanol. Limnol. 28 (2010) 122–130.
[31] Z. He, Y. Chen, Y. Chen, H. Liu, G. Yuan, Y. Fan, K. Chen, Optimization of the microwave-assisted extraction of phlorotannins from *Saccharina japonica Aresch* and evaluation of the inhibitory effects of phlorotannin-containing extracts on HepG2 cancer cells, Chin. J. Oceanol. Limnol. 31 (2013) 1045–1054.

4.4. GENERAL DISCUSSION.

This Chapter presents the development of two on-line LC × LC methods for the chemical characterization of phlorotannins from two seaweed species (*Cystoseira abies-marina* and *Sargassum muticum*) by using HILIC × RP as a highly orthogonal coupling in order to achieve the maximum separation of these compounds regarding to their DP as well as their isomerization level.

Since no previous 2DLC analytical methods for the analysis of phlorotannins were available, a complete optimization study of the on-line LC × LC coupling was necessary.

Based on our previous experience using HILIC × RP, we selected to perform the ^{1}D separation in a microbore column operated at very low flow rates and keeping the modulation time as short as possible. Moreover, the use of sampling loops in the switching valve acting as modulator, with larger volume than strictly needed to collect the ^{1}D effluent, was also selected together with high ^{2}D flow rates. In addition to all the instrumental parameters, the chemical nature of the target compounds was also considered during optimization.

4.4.1. INFLUENCE OF METHOD PARAMETERS.

4.4.1.1. Sample preparation.

The importance of the selection of an adequate extraction/sample preparation process ultimately relies on the fact that the extraction procedure will affect the chromatographic analysis. Consequently, this process has to be selective enough to obtain a final enriched extract in which possible interferences are eliminated, as well as to protect the interesting compounds against degradation during the whole process. In this case, the extraction of phlorotannins from the two studied brown algae was required since macroalgae, in particular brown algae, are complex samples containing mixtures of many different components with diverse physicochemical characteristics, such as carbohydrates, proteins, lipids, carotenoids, chlorophylls, minerals, terpenes and sterols as well as phenolic compounds (Plaza et al. 2008; Polat and Ozogul 2008; El Shoubaky and Salem 2014). Therefore, the co-extraction of many

different compounds together with the target phenolic compounds was unavoidable. For this reason, the use of a purification step after the extraction of the two studied algae was needed to obtain a phlorotannin-rich fraction. In particular, different extractions and sample treatments were employed for each alga, due to the fact that the algal chemical composition greatly varies between species and even between algae from the same species but grown under diverse environmental conditions.

The extraction of phlorotannins from *Cystoseira abies-marina* (Section 4.2.) was carried out by a conventional solid/liquid extraction assisted by magnetic stirring as a fast and simple extraction method. A mixture of acetone/water was selected as extraction solvent. However, this solvent mixture was demonstrated to be effective but not selective for the extraction of phlorotannins, and therefore, a post-extraction sample treatment had to be applied to obtain a phlorotannin pure fraction. In this case, the sample treatment consisted on a sample defatting by liquid/liquid partition with dichloromethane to remove lipids, chlorophylls and carotenoids followed by a SPE concentration, where carbohydrates and proteins were discarded and phlorotannins were retained and afterwards eluted from the cartridge, obtaining a purified extract. Then, before the LC × LC analysis , the phlorotannin content of this extract was measured by reacting with dimethoxybenzaldehyde (DMBA assay), a reagent specific for 1,3- and 1,3,5-substituted phenols, like phloroglucinol.

However, to recover the phlorotannin fraction from *Sargassum muticum* algae (Section 4.3), PLE was selected since it has been demonstrated to present advantages for recovering phenolic-rich fractions from brown algae (Anaëlle et al. 2013). In the work presented in Section 4.3., 13 samples of *Sargassum muticum* brown alga from different locations along the North-Atlantic coast (Portugal, Spain, France, Ireland and Norway) were submitted to PLE. The extraction conditions were carefully studied in a previous work carried out in our lab through the application of an experimental design (Sánchez-Camargo et al. 2016). After that, extracts from Portugal and Norway showing the greater content on phlorotannins as well as higher total phenolic content and antioxidant activity (determined by in-vitro assays) were selected for their further chemical characterization. Different purification methods were applied to those extracts, including the method previously employed for phlorotannins purification from *C.*

abies-marina. However, good results were only achieved with the application of a procedure involving a liquid/liquid extraction of non-polar compounds with dichloromethane followed by solvent precipitation of proteins and carbohydrates with ethanol and acetone, respectively, and a final phlorotannins extraction with ethyl acetate.

4.4.1.2. ^{1}D separation.

First dimension separation was carried out under HILIC mode. Due to our previous experience on the separation of polymeric phenolic compounds using a diol-bonded stationary phase, a microbore diol column was used as HILIC-compatible ^{1}D for the separation of phlorotannins. To the best of our knowledge, just two previous works reported the study of phlorotannins under HILIC mode (Steevensz et al. 2012; Kim et al. 2013). Kim et al. (2013) used a triazole HILIC-compatible bonded phase for the separation of a mixture of six phlorotannins, in particular, six eckols with DP from 3 to 6 PGUs. On the other hand, Steevensz et al. (2012) employed an amide HILIC column achieving the separation of phlorotannins from 3 to 10 PGUs. Therefore, due to the lack of information on the retention behavior of phlorotannins in diol-bonded particles as well as the similar polymeric phenolic nature between proanthocyanidins and phlorotannins, analytical conditions similar to those applied to proanthocyanidin separations were selected as a starting point for the optimization of the ^{1}D separation of phlorotannins. In particular, this first optimization was carried out for the separation of phlorotannins from *Cystoseira abies-marina* brown alga (Section 4.2).

As above mentioned, the separation conditions (mobile phases, flow rates, gradients and temperature) employed for the separation of proanthocyanidins, specifically those used in the application of apple procyanidins (Section 3.3), were tested for the separation of phlorotannins. These preliminary results showed that diol stationary phase could be appropriate for the chromatographic separation of phlorotannins. Moreover, the tested conditions provided relatively good separation results in terms of broad separation of the sample along the whole chromatographic one-dimensional space. Figure 4.4A shows the separation of the phlorotannins found in *C. abies-marina* under those conditions. However, in order to improve

this separation, different mobile phases, mainly buffers at different concentrations and pH, and gradients were studied. Under these latter conditions, the retention of phlorotannins was very strong, and most compounds coeluted at the end of the chromatogram (Figure 4.4.B). Hence, the initial conditions were preliminary retained, and in order to enhance the separation obtained, the careful study and modification of the gradient employed was performed. By applying some changes in the gradient while maintaining, at the same time, mobile phases composition, a good distribution of phlorotannins was obtained, as can be observed in Figure 4.4C, where the optimum ^{1}D separation is depicted. At this point, it is interesting to mention that gradient optimization on HILIC conditions is a difficult task, since little changes in the aqueous mobile phase produce huge modifications on the separation. Thus, the mentioned conditions were finally selected for the ^{1}D separation of the LC × LC methods for phlorotannins analysis from both algae, *C. abies-marina* and *S. muticum*.

However, although the same ^{1}D conditions were finally selected for the separation of phlorotannins from *S. muticum* brown alga, considering that a diverse chemical composition was expected in this alga, different chromatographic conditions were also tested, such as the use of a microbore amino HILIC-compatible stationary phase as well as different mobile phases compositions, including changes on pH.

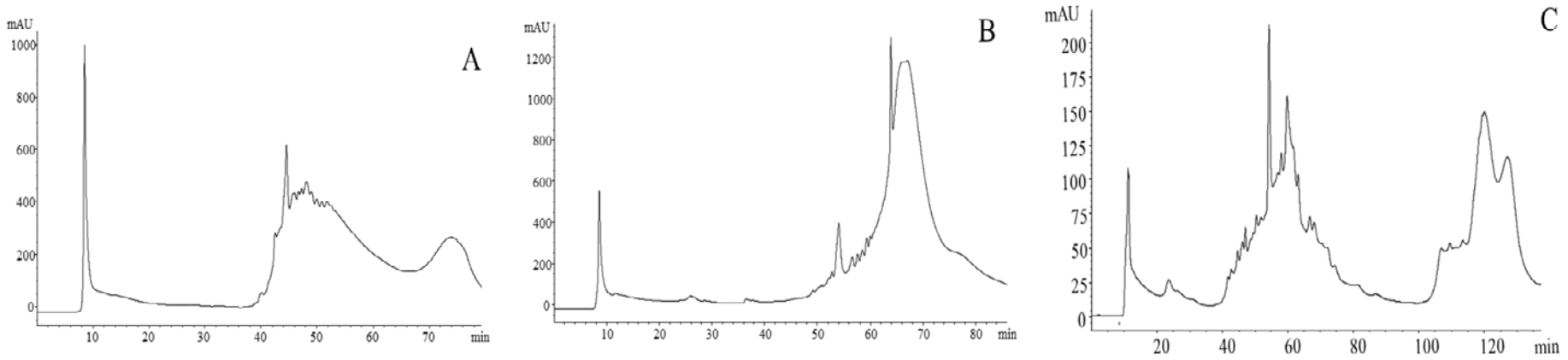

Figure 4.4. Chromatographic separations (280 nm) of the phlorotannins from the alga *Cystoseira abies-marina* obtained during the ^{1}D optimization process. A) Separation obtained employing A) ACN/CH_3COOH, 98:2; B) MeOH/H_2O/ CH_3COOH, 95:3:2 as mobile phases. Eluted according to the following gradient: 0 min, 0 % B; 2 min 0 % B; 5 min, 20 % B; 30 min, 20 % B; 40 min, 30 % B; 50 min, 30 % B, 55 min, 40%B; 65 min, 40%B, 70 min, 100%B, 80 min, 100%B, 90 min, 0%B at a flow rate of 15µL/min. B) Separation employing acetonitrile and ammonium acetate 10 mM at pH 9 as mobile phases. Eluted according to the following gradient: 0 min, 5 % B; 3 min 5 % B; 30 min, 35 % B; 40 min, 35 % B; 45 min, 50 % B; 50 min, 70 % B, 60 min, 100%B; 70 min, 100%B, 75 min, 5%B. C) Optimum separation employed as the ^{1}D in the LC × LC method. (Mobile phases: A) ACN/CH3COOH, 98:2. C) MeOH/H2O/ CH3COOH, 95:3:2. Eluted according to the following gradient: 0 min, 0 % B; 3 min 0 % B; 5 min, 7 % B; 30 min, 15 % B; 70 min, 15 % B; 75 min, 25 % B, 85 min, 25%B; 90 min, 45%B, 95 min, 45%B, 100 min, 60%B, 110 min, 60%B, 115 min, 80%B; 125 min, 80%B; 130 min, 100%B; 135 min, 100%B, 140 min, 0%B at al flow rate of 15µL/min).

4.4.1.3. ^{2}D separation.

RP is theoretically a good chromatographic mode for the separation of isomers of different polymers, such as phlorotannins. However, conventional RP separations are limited to short polymers due to the increased complex isomer composition that occurs as the DP of phlorotannins grows. For this reason, RP may be a good separation option for the ^{2}D of a LC × LC analysis of phlorotannins, considering that just fractions of phlorotannins with similar DP, previously separated on the HILIC-based ^{1}D, are individually analyzed. This way, the separation of isomers containing the same DP, that cannot be separated in the ^{1}D, may be obtained. Consequently, the multidimensionality of natural phlorotannin mixtures, together with the different retention mechanisms that RP and HILIC provide, make the HILIC × RP coupling a highly orthogonal system for the separation of these components.

Therefore, RP was selected as separation mode for the ^{2}D. In the first approach of the analysis of phlorotannins presented in this Chapter (Section 4.2), two RP columns with different stationary phases were tested, namely C_{18} and PFP stationary phases. Both were short (50 mm long) partially porous columns with a wider internal diameter (4.6 mm) than the ^{1}D column internal dimeter (1 mm) (thus, high $^{2}d_c/^{1}d_c$) to enhance the contact and the retention of the analytes present on the injection fraction with the ^{2}D stationary phase particles, which, in turn, helps to limit ^{2}D band broadening.

Different conditions were studied for the separation of phlorotannins in the ^{2}D, including the effect of different mobile phases for each of them. For the optimization of the separation of the C_{18} column, acetonitrile was the organic solvent that offered better separations. Regarding the aqueous mobile phase, different buffers covering the pH range at which the column is stable (pH 3.6-9) were tested as well as water acidified with formic acid. Finally, ultrapure water containing 0.1% of formic acid was selected as mobile phase. In the case of the PFP column, its use was based on its specific selectivity for aromatic compounds thanks to the multiple retention mechanisms that this stationary phase offers (Regos and Treutter 2010). In this column, acetonitrile, methanol and different mixtures of these two organic solvents were studied as mobile phases.

Both stationary phases provided a similar retention of phlorotannin isomers under the tested conditions; however, once more, the C_{18} stationary phase demonstrated a higher separation capability and superior resolution of the separated compounds. A comparison between the two 2D separations obtained using both types of columns can be observed in Figure 4.5.

On the other hand, the best separation for *Sargassum muticum* phlorotannins was achieved by employing similar conditions to those optimized in the previous work, based on the diol × C_{18} configuration with a slight modification of the ^{2}D gradient. These conditions were selected after the study of different experimental conditions. In this second work, the C_{18} and the PFP partially porous columns were tested again, as well as the separation on a C_{18} monolithic column. This latter column could be also tested at different flow rates and analysis times, since monolithic columns allow the use of higher flow rates due to the smaller pressure drops produced by this type of stationary phase compared to particles.

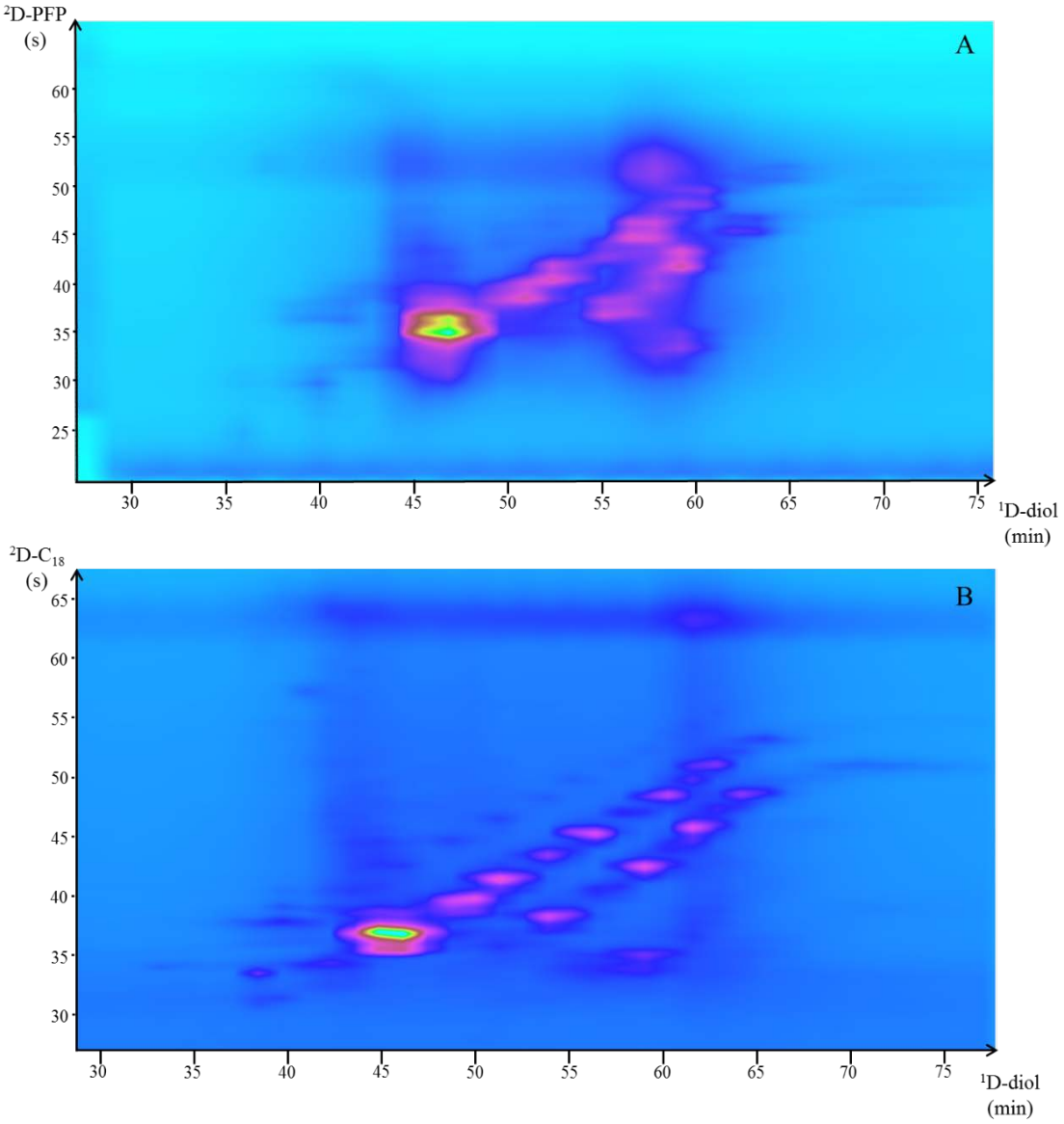

Figure 4.5. Comparison of the 2D separations of phlorotannins from the alga *Cystoseira abies-marina* using in the ^{2}D: A) a PFP column, employing water (0.1% formic acid) and acetonitrile as mobile phases, eluted according to the following gradient: 0 min, 0% B; 0.1 min, 5% B; 0.3 min, 20% B; 0.8 min, 40% B; 0.9 min, 70% B; 1min, 90%; 1.01 min, 0% B; 1.3 min, 0% B; and B) a C_{18} column, employing water (0.1% formic acid) and acetonitrile as mobile phases, eluted according to the following gradient: 0% B; 0.1 min, 10% B; 0.6 min, 30% B; 0.8 min, 50% B; 0.9 min, 70% B; 1 min, 90%; 1.01 min, 0% B; 1.3 min, 0% B. .

4.4.2. CHEMICAL CHARACTERIZATION OF PHLOROTANNINS FROM BROWN ALGAE BY HILIC × RP.

As has widely been demonstrated along Chapter 3, HILIC × RP is a very orthogonal coupling for the separation of polymeric phenolic compounds allowing the separation firstly by their DP on the HILIC-based ^{1}D and then, by according to their hydrophobicity in the RP-based ^{2}D. This characteristic was also advantageous for the separation of phlorotannins from two brown algae.

In both applications a 10-port 2-position switching valve equipped with two sampling loops of 30 μL was used as interface for the transfer process between both dimensions. The advantages associated to the use of sampling loops with this internal volume, higher than the volume required to collect the ^{1}D effluent entering the loop during the collection position, were explained in detail in Chapter 3,

In the first work included in the present Chapter, the objective was the study of the content and the chemical characterization of phlorotannins from the alga *Cystoseira abies-marina* applying an optimized HILIC × RP method. Thanks to the high resolving power offered by this method, 52 compounds could be separated in the complex phlorotannin-rich extract. The information provided by the DAD as well as the position of each peak into the 2D space was useful to tentatively assign the separated compounds. However, in this kind of complex samples the identification of the separated compounds by MS is of utmost importance, taking into consideration the information that this detector is able to provide with. Therefore, the close study of the MS and MS/MS spectra obtained for each separated peak was the key to obtain the compositional information of the phlorotannin extract.

Typical fragmentation pathways of phlorotannins consisted on successive neutral losses of PGUs (126 Da) and of water molecules (18 Da). For example, the most intense peak of the sample (peak 13) was tentatively identified as hepta-phlorethol, fucol or fucophlorethol, due to the detection of its molecular ion at *m/z* 869.4 ($[M-H]^-$). However, phlorotannins with DP = 7 did not suffer a high fragmentation and only one fragment was observed at *m/z* 851, corresponding to a loss of a water molecule. In contrast, the rest of phlorotannins presented a

more extensive fragmentation pathway, and some of them were detected as doubly charged ions ($[M-2H]^{2-}$). For instance, a medium length phlorotannin presented a $[M-2H]^{2-}$ at *m/z* 744.3 whereas its MS/MS fragments detected corresponded to successive losses of PGUs showing *m/z* at 1241, 1177, 993, 867 and 617, corresponding to losses of 2, 3, 4, 5 and 7 PGUs, respectively. Moreover, the MS/MS spectrum of this compound presented some ions corresponding to the losses of PGUs together with a water molecule at *m/z* 1223 (loss of 2PGUs and a water molecule), 726 (6 PGUs plus a water molecule) and 228 (loss of 10 PGUs plus a water molecule). This compound was tentatively identified as a phlorethol, fucol or fucophlorethol with 12 PGUs. The MS, MS/MS spectra and the proposed chemical structure of this molecule is shown in Figure 4.6.

As can be observed, the information provided by the MS and MS/MS spectra is very useful to elucidate the degree of polymerization of each separated phlorotannin, but the identification of the links between PGUs and, therefore, the identification of the specific type of phlorotannin involved is not possible. Alternative chemical structures for the phlorethol shown in Figure 4.6, suggesting the presence of phenyl or ether linkages, or a combination of them in the same molecule, typical from fucols, phlorethols or fucophlorethols, respectively, could not be ruled out, as those molecules would also present similar molecular ions, MS and MS/MS spectra.

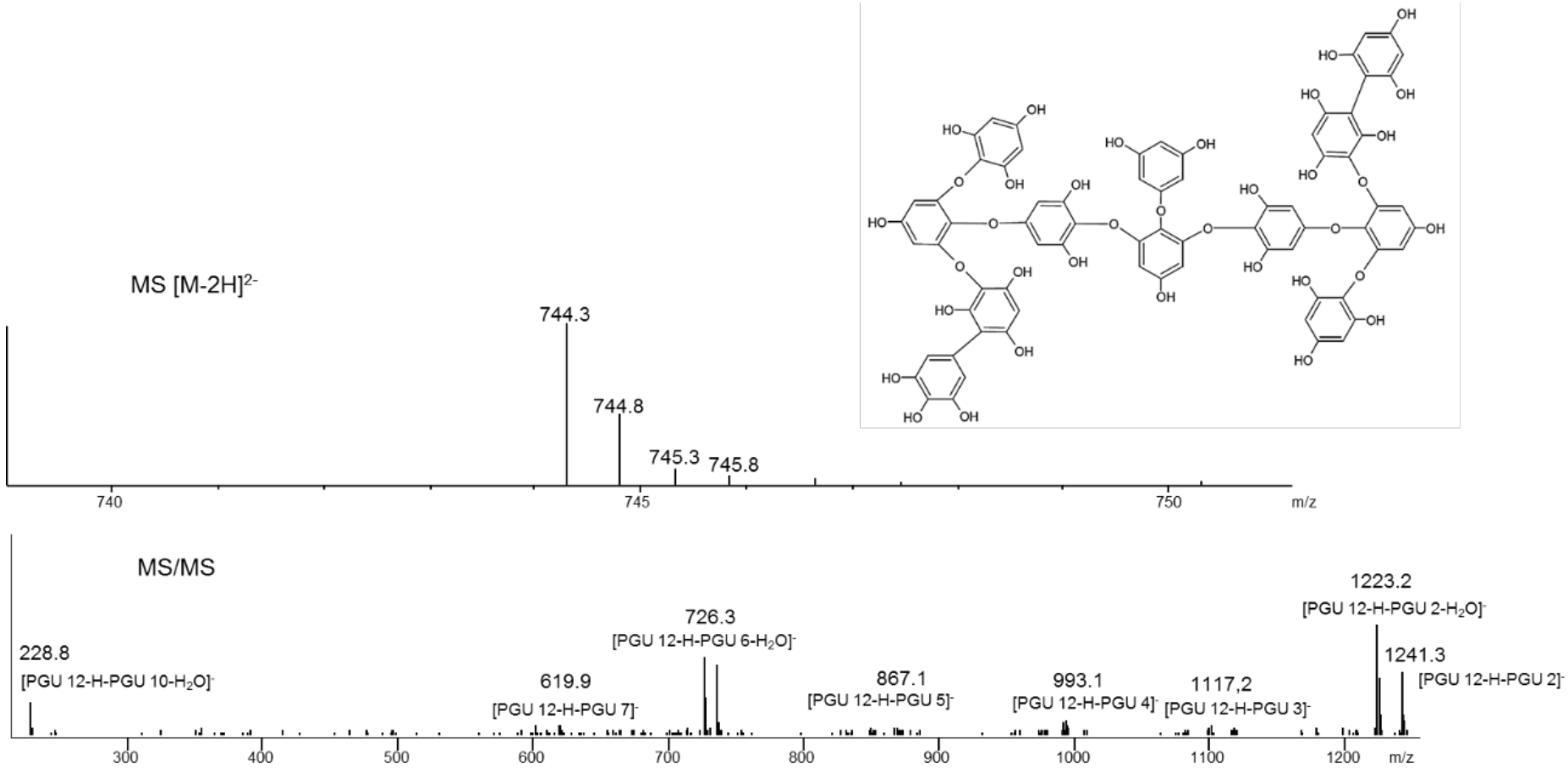

Figure 4.6. MS and MS/MS spectra as well as the proposed chemical structure of a phlorotannin with DP = 12.

Among the 52 separated compounds, the tentatively identification of 43 phlorotannins from 5 to 17 PGUs, namely phlorethols, fucols or fucophlorethols was possible in *Cystoseira abies-marina* brown alga.

On the other hand, phlorotannins contained in *Sargassum muticum* harvested in a total of 13 different geographical locations along the North-Atlantic coast were studied. Two algae samples from Norway and two different samples from Portugal were determined as the richest samples on phlorotannins, using the DMBA in-vitro assay. Interestingly, the harvesting locations in these two countries were those possessing the most-extreme climatological conditions among the studied. Consequently, these four samples were selected to obtain their phlorotannin profiles. The LC × LC phlorotannin profiles of both groups of locations (i.e., Portugal and Norway) were significantly different, as a response to the completely different environmental growing conditions, thus, confirming that phlorotannins compositions are very susceptible to suffer modifications in response to adaptation to the climatologic, nutrient and UV-exposure conditions. In particular, the phlorotannin profiles from the two zones of Norway were more complex (72 and 73 separated compounds, respectively) than those from Portugal (55 and 56 separated compounds, respectively). However, from a qualitative point of view, the phlorotannin composition of samples from both countries was very similar; interestingly, this was the first application in which the simultaneous separation of fuhalol- and hydroxyfuhalol-type phlorotannins as well as phlorethol-, fucol- or fucophlorethol-types, with such a degree of separation, is reported . The identification of fuhalols and hydroxyfuhalols was possible thanks to their characteristic MS and MS/MS spectra, that differs from the rest of phlorotannins types on the presence of one (fuhalols) or more (hydroxyfuhalols) hydroxyl groups, that is, a difference in 18 Da for a given DP. The presence of hydroxyfuhalols with up to 4 hydroxyl groups (several trihydroxyheptafuhalols and trihydroxyoctafuhalols) was observed. An example of the MS-based identification of these complex compounds is illustrated in Figure 4.7.

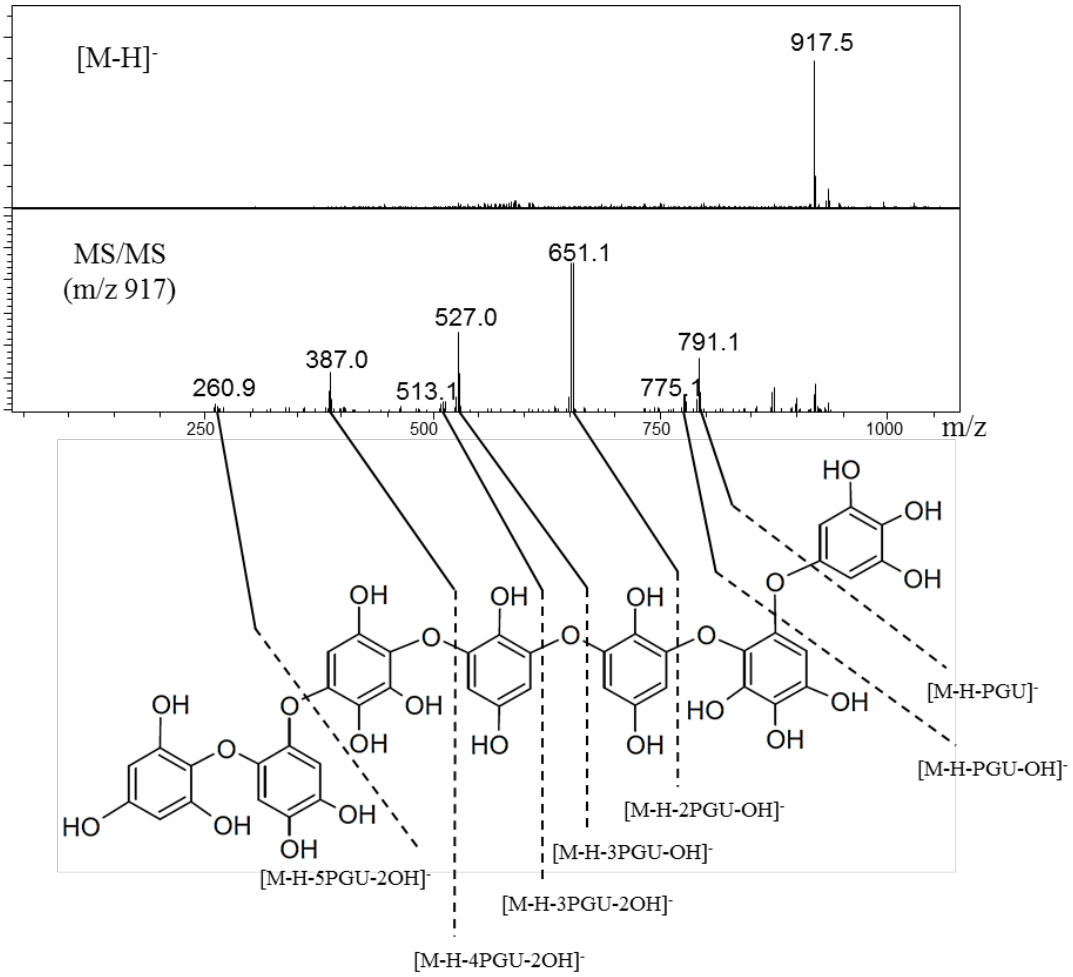

Figure 4.7. MS spectrum and MS/MS fragmentation pattern of dihydroxyheptafuhalol (fuhalol with DP = 7 with two additional hydroxyl groups) as well as the tentatively proposed chemical structure.

In this work the tentative identification of phlorotannins up to 10 and 11 DP in samples from Norway and Portugal, respectively, was achieved.

Besides, as mentioned in the introduction section of this Chapter, the interest on phlorotannins is growing since they present several interesting biological activities. Therefore, in this work, the antiproliferative activity of the purified phlorotannin-rich fractions from *Sargasumm muticum* was studied after their exhaustive chemical characterization by LC × LC. Results showed that one of the extract from Norway, in particular, presented a good antiproliferative effect against human cancer cells. The results achieved in this work could be the beginning of an interesting study on the bioactivities of phlorotannins from *S. muticum*. Further interest on the extraction and valorization of fractions from these compounds relies on the fact that this brown alga in an invasive species and, therefore, is widespread, and has no other uses, although more studies are needed to confirm the positive effects of these extracts.

Thus, in this Chapter the separation of polymeric phlorotannins with a high degree of structural complexity by on-line LC × LC has been presented for the first time. The enormous usefulness of HILIC × RP for the separation of very complex natural samples containing mixtures of polar polymeric phenolic compounds of great chemical complexity and diversity was demonstrated once more attaining similar high peak capacity values of 992 in the HILIC × RP analysis of *Cystoseira abies-marina* alga and 1050 and 906 in the analysis of the Norwegian and Portuguese *Sargassum muticum* samples, respectively. With respect to the orthogonality achieved in these analyses, the separation of *C. abies-marina* phlorotannins arrived to a 71% of orthogonality while the analysis of *S. muticum* phlorotannins attained 81 and 74% of orthogonality in the samples from Norway and Portugal, respectively. It is interesting to note that, although similar, these values show a slight difference. In particular, the two samples of *Sargasum muticum* analyzed under the same analytical conditions present different peak capacity and orthogonality values, showing that not only the correlation level between the two separation mechanisms or the separation conditions selected affect the separation power of the technique, but also the sample has an important weight in the final results.

Moreover, the development and application of this multidimensional methodology allowed the identification of compounds that had not been previously characterized up to date, such as phlorotannins with a high degree of hydroxylation.

In addition, the analytical work presented in this Chapter highlights the essential role that chemical characterization has on bioactivity-related studies, in order to identify the compounds responsible for the observed bioactivity present in the natural extracts.

CHAPTER 5.

Chemical characterization of saponins by HILIC × RP-DAD-MS/MS.

5.2. Metabolite profiling of licorice (*Glycyrrhiza glabra*) from different locations using comprehensive two-dimensional liquid chromatography coupled to diode array and tandem mass spectrometry detection.

5.3. Focusing and non-focusing modulation strategies for the improvement of on-line two-dimensional hydrophilic interaction chromatography × reversed phase profiling of complex food samples.

5.1. INTRODUCTION – SAPONINS.

Saponins are a large and structurally diverse group of secondary metabolites produced by plants, although they have also been found in certain marine organisms such as starfish and sea cucumber. As secondary metabolites, saponins play an important role in the protection and adaptation of plants against external factors of the surrounding environment. In fact, these compounds are considered natural pesticide, insecticide and fungicide agents (Osbourn et al. 2011; Faizal and Geelen 2013; Moses et al. 2014).

The presence of saponins has been described in more than 100 families of plants, being one of the most numerous and diverse groups of plant natural products. Saponins are often present as complex mixtures and their content in plants may significantly vary as a function of genetic, tissue type, age, physiological state of the plant and environmental factors (Faizal and Geelen 2013).

Thanks to their numerous interesting physicochemical properties, these compounds represent a valued natural ingredient for the food industry, due to their sweetness and bitterness characteristics, or for the cosmetic sector where can be used as foaming, surfactant and emulsifying agents. Besides, other interesting properties related to saponins are the wide range of health effects that have been attributed to these natural compounds such as antimicrobial, anti-inflammatory, anticancer, antiviral or hepatoprotective activities, among others (Augustin et al. 2011; Osbourn et al. 2011).

As a result of these interesting properties, saponins are attracting increasing attention. However, different important challenges appear during their analysis and characterization in natural sources, mainly related to the great natural variability that may present. Partially due to this fact, enough scientific evidence of the compound-biological activity relationship has not been sufficiently established yet.

5.1.1. CHEMICAL STRUCTURE OF SAPONINS.

From a chemical point of view, saponins are isoprenoid-derived aglycones, named genins or sapogenins, linked to one or more sugar moieties. This particular composition makes saponins amphiphilic molecules composed by a non-polar part corresponding to the sapogenin aglycone and a hydrophilic saccharide chain. Saponins can be glycosylated by one, two, or more rarely, three sugar chains in different positions of the molecule, with up to 11 monosaccharide units overall (Augustin et al. 2011).

Saponins are divided in two main groups: triterpene saponins and steroid saponins. Both classes derive from the same 30-carbon atoms precursor 2-3-oxidosqualene, a central metabolite for the synthesis of sterols. The difference between triterpene and steroid saponins is that steroid saponins present a skeleton of 27-carbon atoms due to the loss of three methyl groups, whereas triterpene saponins maintain the 30-carbon structure (Figure 5.1) (Vincken et al. 2007; Faizal and Geelen 2013).

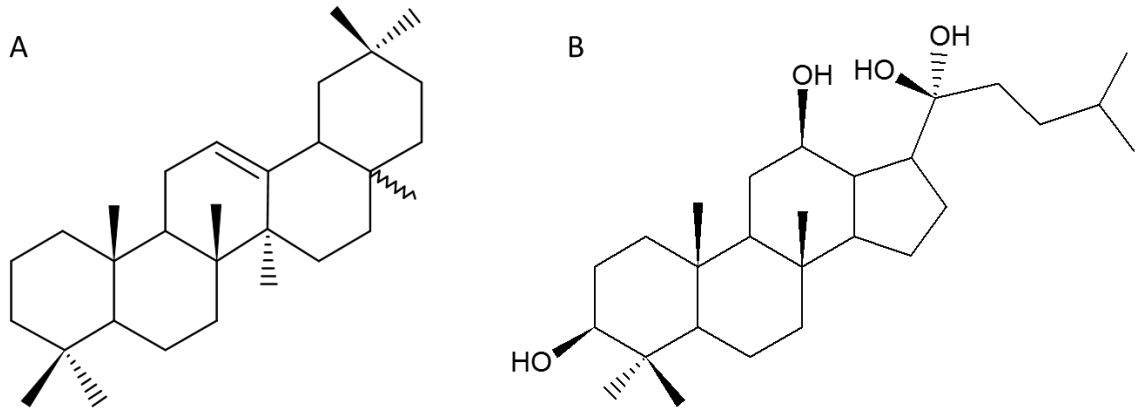

Figure 5.1. Sapogenin structure of triterpene (A) and steroid saponins (B).

Vincken et al. (2007) reported a further classification formed by 11 classes of cyclic carbon skeletons. These new classes consist of modifications of the carbon skeleton by rearrangements, homologations, cleavages and degradations, which besides, present their own subclasses. From all these classes of saponins, oleanane skeleton is the most common structure present in the plant kingdom.

Besides, functionalization of the carbon skeleton, mainly as a result of oxidation reactions, produces further variability, resulting in functional groups like hydroxyl groups, carbonyl groups or carboxylic acids which can be found at different positions in the saponin skeleton (Vincken et al. 2007).

This chemical description shows the evident highly diverse structure of saponins due to their chemical variability and the high number of isomers as well as the diverse number and different possibilities of the sugar chains composition. Hence, the chemical characterization of these natural compounds is hindered by their closely related chromatographic behavior. That is the main reason why the complete composition of saponins in plants is not entirely elucidated; consequently, more information regarding their chemical characterization is required.

5.1.2. CHEMICAL CHARACTERIZATION OF SAPONINS.

LC-MS is the most-employed analytical technique for the analysis of saponins, due to the difficulties to identify saponins by LC-UV methods (Oleszek and Bialy 2006). Therefore, usually, LC is used to separate saponins that are subsequently elucidated by MS and MS/MS experiments (Gafner et al. 2004; Huhman et al. 2005; Khakimov et al. 2016). However, the intrinsic diversity of saponins requires in some cases the use of LC as a purification technique and the combination between MS, NMR and infrared spectroscopy to specifically elucidate the structure of the molecule (Mroczek 2015).

Thus, the study of the particular chemical composition on saponins from natural samples, is an important topic for the characterization and discovering of new high-added value compounds. However, the structural complexity of these molecules hinders their chemical characterization by conventional analytical techniques, mainly due to the insufficient chromatographic resolving power of these techniques to properly separate structurally similar saponins. Besides, the chromatographic separation becomes even more challenging considering that saponins contain complex multisugar chains and that different molecules may present the same molecular weight and glycosylation pattern (Khakimov et al. 2016). Hence, the limited peak capacity and the single separation mechanism used in one-dimensional LC is not enough to

separate these often complex natural mixtures; in this regard, the use of MDLC might be very well suited to the separation of saponins, providing with an impressive increment of separation power.

5.1.3. LICORICE AS A SOURCE OF TRITERPENE SAPONINS.

Medicinal herbs have been used as therapeutic treatments for hundreds and thousands of years. These plants present active ingredients responsible for the associated therapeutic effects. Herbal extracts are usually constituted by a multi-component composition, that is, generally, the therapeutic properties attributed to herbal medicines are associated to different chemical groups such as alkaloids, phenolic compounds, mono- and diterpenes, saponins or glycosides (Li et al. 2011), for example. However, in modern mechanistic studies in which a bioactivity is sought to be associated to the presence of one or more particular compounds, the analysis of the metabolite profile and the major bioactive compounds is essential. This step implies the first approach towards the characterization of the bioactive fraction of an herbal drug.

Among many other plants, licorice is an ancient herb very frequently used in the traditional Chinese medicine. Specifically, three species of licorice, *Glycyrrhiza glabra, Glycyrrhiza uralensis* and *Glycyrrhiza infanta* have centered great interest due to the wide clinical prescriptions associated to those species such as antitumoral, antimicrobial, antiviral, anti-inflammatory, hepatoprotective or neuro-protective functions (Yang et al. 2016). The most abundant secondary metabolites present in licorice are triterpene saponins, being glycyrrhizic acid the main compound. Besides, the secondary metabolite profile of licorice is also composed by a complex mixture of different phenolic compounds, including flavanones, chalcones, flavones, isoflavones and isoprenylated flavonoids, many of them presenting different glycosylations. Both, triterpene saponins and phenolic compounds are considered the bioactive components responsible for the positive health effects of licorice, although a high consumption of licorice could be also associated to some negative consequences, like hypokalemia and hypertension (Sontia et al. 2008).

Besides the beneficial health effects associated to the secondary metabolites of licorice, its precise metabolite profile could be very useful for the differentiation of licorice species as well as for the authentication of the geographical origin of different licorice samples. This differentiation based on the metabolite profile is related to the fact that the metabolite content of licorice, both quali- and quantitatively, may significantly vary depending on the production geographical area, state of the plant, external environmental agents, harvesting and processing (Tanaka et al. 2010; Montoro et al. 2011; Farag et al. 2012).

Although the analysis of licorice metabolites, as many other herbal medicines, has already been widely studied, its entire native composition is far to be completely elucidated (Qiao et al. 2014). LC-MS is the method of choice for the determination of the chemical composition of licorice extracts, up to now. However, there are just a few analytical methods focused on the study of the complete composition of the licorice metabolites, and these available procedures only provide a limited information of the whole native composition due to the limitations of one-dimensional methods (Wei et al. 2015; Jiang et al. 2016).

Therefore, the main objective of this Chapter is to develop a new analytical strategy based on the on-line coupling of HILIC and RP separation modes for the chemical characterization of highly complex natural mixtures of saponins, particularly, from licorice (*Glycyrrhiza glabra*), as well as for the separation of other metabolites to attain an exhaustive characterization of secondary metabolite composition of this plant extract (Section 5.2). Moreover, thanks to the application of this method, not only the separation of up to 89 compounds in a licorice sample, including 47 saponins, could be achieved, but also the obtained profiles were proposed as a means for the comparison of different licorice samples from different geographical locations. In a second work within this Chapter, the previously developed method is employed as a starting point to exhaustively study different modulation options, including focusing and non-focusing modulation approaches, in order to further improve the performance of HILIC × RP methods, using licorice as a model food sample. The results obtained from that study are presented in Section 5.3. paying special attention to the influence of the studied parameters on ^{1}D undersampling, ^{2}D band broadening and sensitivity limitations of today's on-line LC × LC practice.

5.2. Metabolite profiling of licorice (*Glycyrrhiza glabra*) from different locations using comprehensive two-dimensional liquid chromatography coupled to diode array and tandem mass spectrometry detection.

Montero, L.; Ibáñez, E.; Russo, M.; di Sanzo, R.; Rastrelli, L.; Piccinelli, A. L.; Celano, R.; Cifuentes, A.; Herrero, M.

Analytica Chimica Acta. 2016, *913,* 145-159.

Analytica Chimica Acta 913 (2016) 145–159

Contents lists available at ScienceDirect

Analytica Chimica Acta

journal homepage: www.elsevier.com/locate/aca

Metabolite profiling of licorice (*Glycyrrhiza glabra*) from different locations using comprehensive two-dimensional liquid chromatography coupled to diode array and tandem mass spectrometry detection

Lidia Montero [a, b], Elena Ibáñez [a], Mariateresa Russo [b], Rosa di Sanzo [b], Luca Rastrelli [c], Anna Lisa Piccinelli [c], Rita Celano [c], Alejandro Cifuentes [a], Miguel Herrero [a, *]

[a] Laboratory of Foodomics, Institute of Food Science Research (CIAL-CSIC), Nicolás Cabrera 9, 28049 Madrid, Spain
[b] Laboratory of Food Chemistry, Dipartimento di Agraria (QuaSic.A.Tec.), Università Mediterranea di Reggio Calabria, Reggio Calabria, loc. Feo di Vito, 89122 Reggio Calabria, Italy
[c] Dipartimento di Farmacia, Università di Salerno, Via Giovanni Paolo II 132, 84084 Fisciano, Italy

HIGHLIGHTS

- Non-correlated comprehensive LC is applied to licorice roots metabolic profiling for the first time.
- Complex 2D-plots for different licorice samples are attained.
- Typical metabolite patterns potentially helpful to assess origin are obtained.
- Different gradients in D2 are employed to improve separation.
- Up to 89 compounds are separated and detected in the metabolite profile.

GRAPHICAL ABSTRACT

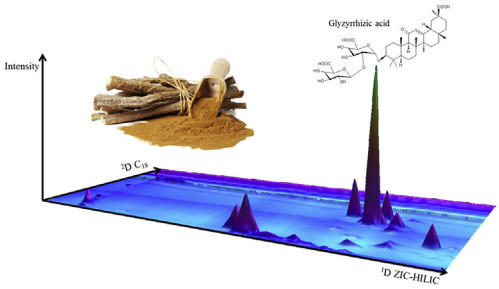

ARTICLE INFO

Article history:
Received 14 October 2015
Received in revised form
19 January 2016
Accepted 24 January 2016
Available online 27 January 2016

Keywords:
LC × LC
Licorice
Metabolite
Triterpene saponins
Phenolic compounds
Authentication

ABSTRACT

Profiling of the main metabolites from several licorice (*Glycyrrhiza glabra*) samples collected at different locations is carried out in this work by using comprehensive two-dimensional liquid chromatography (LC × LC) coupled to diode array (DAD) and mass spectrometry (MS) detectors. The optimized method was based on the application of a HILIC-based separation in the first dimension combined with fast RP-based second dimension separation. This set-up was shown to possess powerful separation capabilities allowing separating as much as 89 different metabolites in a single sample. Identification and grouping of metabolites according to their chemical class were achieved using the DAD, MS and MS/MS data. Triterpene saponins were the most abundant metabolites followed by glycosylated flavanones and chalcones, whereas glycyrrhizic acid, as expected, was confirmed as the main component in all the studied samples. LC × LC-DAD-MS/MS was able to resolve these complex licorice samples providing with specific metabolite profiles to the different licorice samples depending on their geographical origin. Namely, from 19 to 50 specific compounds were exclusively determined in the 2D-chromatograms from the different licorice samples depending on their geographical origin, which can be used as a typical pattern that could potentially be related to their geographical location and authentication.

* Corresponding author.
E-mail address: m.herrero@csic.es (M. Herrero).

http://dx.doi.org/10.1016/j.aca.2016.01.040
0003-2670/

1. Introduction

Licorice (*Glycyrrhiza glabra*) is an herbaceous perennial plant, belonging to the Leguminosae family and is one of the oldest and most popular herbal medicines in the world. A wide array of biological activities have been ascribed to this plant, including anti-ulceric, anti-inflammatory [1], antispasmodic, expectorant, antiallergic, antidepressive [2], antiviral [3], antifungal [4] and antioxidant [5] activities. Besides, licorice has been used in the food industry as a sweetener and a flavor enhancer while it is considered as a safe food ingredient (GRAS) by the US Food and Drug Administration [6]. The mentioned potential health beneficial effects have been associated to the secondary metabolites present in licorice which essentially consist on triterpene saponins and phenolic compounds, including flavanones, chalcones, flavones, isoflavones and isoprenylated flavonoids [7]. Triterpene saponins present in *G. glabra* belong to the oleane-type and are the major active substances. In particular, glycyrrhizic acid is regarded the most important constituent of licorice, pointed out to be the main responsible of the beneficial effects attributed to this plant [8].

There exist around 30 different *Glycyrrhiza* species over the world. Their differentiation based only on root morphology is very complicated. As a consequence, it is important to search metabolic markers that may allow the correct identification of licorice species [9]. The content on secondary metabolites in licorice may vary significantly depending on the geographical area of origin, the stage of maturity of the plant, the environmental conditions and the harvesting/production procedures [7]. In this regard, the content of secondary metabolites could be employed for the geographical identification of licorice, as the product characteristics will be greatly influenced by its particular chemical composition. In relation to these differences, licorice from the region of Calabria (Italy) has been described as one of those with highest quality [10] thanks to the amount of bioactive compounds present on it as well as its typical organoleptic characteristics including volatiles composition. This region presents a Mediterranean climate, characterized by dry summers and mild winters, whereas springs and autumns last only few months, that could provide the special characteristics to the Calabrian licorice [10]. The quality of the Calabrian licorice has been recognized with the Protected Designation of Origin “Licorice from Calabria” in 2011 by the European Union (Reg. (CE) N. 1072/2011 EU) [11].

The metabolic profile of licorice has been widely studied through different analytical techniques such as HPLC-DAD [12,13], HPLC-DAD/MS [10,12–14], UHPLC-DAD [6], UHPLC-MS [6,15–17] or NMR [9,17]. However, aiming the complete profiling of the bioactive phenolics and saponins from licorice is rather difficult since numerous different structures and their isomers are present as well as many compounds with similar retention behavior coexisting in its composition. In this regard, comprehensive two-dimensional liquid chromatography (LC × LC) may be a useful analytical technique to provide a broad separation of the whole composition of the chemically complex licorice extracts. LC × LC allows the separation of a sample through two separation processes simultaneously connected on-line by means of a modulator or interface. This technique provides the advantage of greatly enhancing the peak capacity attainable compared to monodimensional LC due to the use of columns with low correlated separation mechanisms in the first (^{1}D) and the second (^{2}D) dimension, thus, maintaining a high orthogonality degree [18]. Although LC × LC is not still a commonly-employed analytical technique, there are many applications in which this tool has been employed for the successful attainment of the metabolic profile of complex samples [19–21]. However, LC × LC has only been scarcely explored for the separation of licorice compounds. Concretely, a RPLC × RPLC method was developed for the separation of an ethyl lactate fraction of a licorice extract in order to identify flavonoid aglycones present [22]. The developed RPLC × RPLC approach provided a good separation of some components present in a licorice extract fraction, with higher resolving power than one dimensional methods. However, the use of non-correlated separation mechanisms in the two dimensions may significantly increase the attainable peak capacity as well as the orthogonality of the two-dimensional system. Possible combinations of non-correlated mechanisms include NPLC × RPLC [23–25], SEC × RPLC [26], and IEC × RPLC [27–29] approaches. However, these couplings can cause immiscibility and incompatibility problems with the mobile phases employed in both dimensions. The coupling between hydrophilic interaction liquid chromatography (HILIC) and RP separations is useful to partially solve these problems, since the solvents employed in the mobile phases are miscible. In this regard, different HILIC × RP methods have recently been developed for the separation and identification of a variety of compounds in several food-related samples. In particular, HILIC × RPLC methods have been widely demonstrated to be extremely useful for the separation of highly complex and closely related mixtures of phenolic compounds, such as procyanidins [30–33], anthocyanins [34] or phlorotannins [35,36]. The use of DAD and MS detectors connected in series together with the information related to the relative position of each peak in the 2D space allow increasing the identification capabilities of this technique. In this regard, this alternative can be also proposed as a potentially successful approach for the separation and identification of the entire phenolic compounds and saponins profile of licorice samples. The acquisition of these profiles might be later on used to differentiate among samples of different geographical origin. Thus, in the present work, a new HILIC × RPLC method employing a microbore ZIC-HILIC column in the ^{1}D and a C_{18} partially porous column in the ^{2}D has been developed for the characterization of the polyphenol and saponin profile of licorice extracts from different geographical locations with the aim of searching for metabolites that could be pointed out as potential markers for the identification and assignment of the geographical origin as well as for the authentication of each sample.

2. Materials and methods

2.1. Samples and chemicals

Licorice samples (*G. glabra*) from China, Iran and Azerbaijan were produced in 2009, whereas licorice from Crotone and Villapiana (Calabria Region, Italy) were collected in 2007 and 2013, respectively.

HPLC grade ethanol and acetonitrile were purchased from VWR Chemicals (Barcelona, Spain) whereas acetic and formic acids were acquired from Sigma–Aldrich (Madrid, Spain) and ammonium acetate was from Panreac (Barcelona, Spain).

2.2. Sample preparation

The extraction of the metabolites from licorice was carried out following the preparation of the extracts described by Montoro et al. [7]. Briefly, the root material was ground and extracted with a solid–liquid extraction assisted by ultrasonic agitation. The solvent employed was ethanol/water (1:1, *v/v*) with a sample to solvent ratio of 1:5 (*w/v*), and the extraction was carried out during 1 h. Then the mixture was maintained in darkness overnight at room temperature. The extract was vacuum filtered and finally diluted 1:10 with ethanol/water (1:1, *v/v*). Prior to the chromatographic

analysis, an aliquot of each extract was evaporated to dryness and redissolved in ethanol/ACN (1:1, *v/v*).

2.3. LC × LC-DAD-MS/MS

2.3.1. Instrumentation

The LC × LC-DAD instrumentation consisted on a first dimension (^{1}D) composed by an Agilent 1200 series liquid chromatograph (Agilent Technologies, Santa Clara, CA) equipped with an autosampler. In order to obtain more reproducible low flow rates and gradients, a Protecol flow-splitter (SGE Analytical Science, Milton Keynes, UK) was placed between the ^{1}D pump and the autosampler. Additionally, a LC pump (Agilent 1290 Infinity) performed the second dimension (^{2}D). Both dimensions were connected by an electronically-controlled two-position ten-port switching valve acting as modulator equipped with two identical 30 μl injection loops. Modulation time of the switching valve was 1.3 min. A diode array detector was coupled after the second dimension in order to register every ^{2}D analysis. Besides, an Agilent 6320 Ion Trap mass spectrometer equipped with an electrospray interface working in negative ionization mode was coupled in series using the following conditions: dry temperature, 350 °C; dry gas flow rate, 12 L min^{-1}; nebulization pressure, 40 psi; mass range, *m/z* 90–2200 Da. The LC data were elaborated and visualized using LC Image software (version 1.0, Zoex Corp., Houston, TX).

2.3.2. LC × LC separation conditions

The ^{1}D separation was carried out employing a SeQuant ZIC-HILIC (150 × 1 mm, 3.5 μm d.p., Merck, Darmstadt, Germany) column. The analysis was run using (A) acetonitrile and (B) 10 mM ammonium acetate at pH 5.0 as mobile phases, eluted according to the following gradient: 0 min, 3% B; 5 min, 3% B; 10 min, 5% B; 15 min, 10% B; 30 min, 20% B; 40 min, 20% B; 50 min, 30% B; 60 min, 30% B; 65 min, 40% B; 80 min, 40% B. The injection volume was 2.5 μL and the flow rate was set at 15 μL min^{-1}.

On ^{2}D, an Ascentis Express C_{18} (50 × 4.6 mm, 2.7 μm d.p., Supelco, Bellefonte, CA) partially porous column was employed. Mobile phases consisted of (A) water (0.1% formic acid) and (B) acetonitrile, eluted at 3 mL min^{-1}. During the LC × LC analysis two ^{2}D gradients were employed in order to obtain the best ^{2}D separations in agreement with the compounds eluting from the ^{1}D. Therefore, from 0 min to 23.4 min the ^{2}D gradient elution was: 0 min, 0% B, 0.1 min, 5% B; 0.5 min, 35% B; 0.9 min, 70% B; 1 min, 90% B; 1.01 min, 0% B; 1.3 min, 0% B. On the other hand, from 23.4 to 80 min the employed gradient was programmed as follows: 0 min, 0% B; 0.1 min, 5% B; 0.3 min, 35% B; 0.5 min, 40% B; 0.9 min, 50% B; 1 min, 90% B; 1.01 min, 0% B; 1.3 min, 0% B. UV–Vis spectra were collected in the range of 190–550 nm using a sampling rate of 20 Hz, while 254, 280 and 330 nm signals were also independently recorded. The eluent from the ^{2}D column was splitted before entering the MS instrument, so that the flow rate introduced in the MS detector was 0.6 mL min^{-1}.

3. Results and discussion

The metabolic profile of licorice presents compounds with different chemical nature, being the main ones triterpene saponins and phenolic compounds including flavanones, chalcones, flavones, isoflavones and isoprenylated flavonoids [7]. Within this complex mixture, isomers of some compounds may coexist in its composition as well as other compounds with closely related chemical structures. Therefore, they present the same or close molecular weights as well as related chromatographic behavior. For this reason, the exhaustive separation of the whole array of these kinds of compounds present in licorice is difficult to be carried out by conventional analytical techniques such as HPLC or UHPLC. In fact, many of these compounds coelute when separated under a single retention mechanism. Hence, the employment of analytical tools able to separate the sample by two separation process like LC x LC may be effective for obtaining the complete separation of the metabolic profile of licorice.

3.1. Optimization of the 2D profiling of licorice

The combination of HILIC in the ^{1}D and RPLC in the ^{2}D has been shown to provide a high orthogonality degree and therefore good results in terms of peak capacity [30–36]. However, due to the complexity of the samples that are usually analyzed by LC × LC together with the challenging handling of this technique, the development of each new LC × LC application has to be carefully optimized. In this regard, in the present development each dimension was separately studied and optimized.

To obtain appropriate conditions, slow separations are needed in ^{1}D, whereas ^{2}D separations should be as fast as possible; this way, individual ^{2}D analysis time will directly influence the modulation time, and thus, sampling from the ^{1}D eluate. On the other hand, the use of very low flow rates in ^{1}D will allow maintaining the transfer volume to a minimum and also increasing the sampling from each ^{1}D separated peak that could be cut more times into the ^{2}D. Due to these requirements, the use of microbore columns in ^{1}D is advisable as they present several advantages in terms of separation and resolution attainable at very low flow rates. Consequently, the use of these conditions will permit the collection and injection of fractions continuously to the ^{2}D, providing enough time between fractions to completely finish each ^{2}D analysis. Once the basic morphology of the ^{1}D column was selected, three different HILIC-compatible stationary phases were tested, namely silica, diol and ZIC-HILIC columns. For each type of column several gradients and aqueous mobile phases were tested including 10 mM ammonium acetate at pH 5, pH 5.5 and pH 7.5 or mixtures of acetonitrile, methanol, water and acetic acid to find the best conditions independently. Fig. 1 shows a comparison of the separation attainable using each column at the specific optimum conditions. It has to be remarked that the silica column was used for comparison in spite of not having the required dimensions to act a ^{1}D. Still, this test allowed us to discard this stationary phase for further use. After the study and optimization of the experimental conditions that affect the separation, the ZIC-HILIC column was selected employing acetonitrile and 10 mM ammonium acetate at pH 5.0 as the optimum mobile phases for the ^{1}D separation. As it can be observed in Fig. 1, the ZIC-HILIC column provided better resolution than the other columns with reasonable analysis times at 15 μL min^{-1}, which is an appropriate flow rate in order to keep to a minimum the total volume of each transfer to the ^{2}D.

Next, the ^{2}D separation was optimized individually by injecting the whole sample. This provides a good measure of the separation capabilities of the system even if in real conditions no such complex fraction will be transferred into this ^{2}D. Two short RP columns (50 × 4.6 mm), containing C_{18} and PFP (pentafluorophenyl) partially porous particles (2.7 μm), were tested. Typically, the separation carried out in the ^{2}D has to be fast in order to finish each ^{2}D analysis before the next ^{1}D fraction is transferred. In this regard, the employment of short partially porous columns in this kind of separation is advantageous since these columns generate lower backpressures and provide better efficiency in short analysis times. For the optimization of the ^{2}D separation, different mobile phases including acetonitrile, methanol and different combinations of acetonitrile/methanol as well as water and acidified water, and gradients were studied.

After careful comparison of the best attainable separations, C_{18}

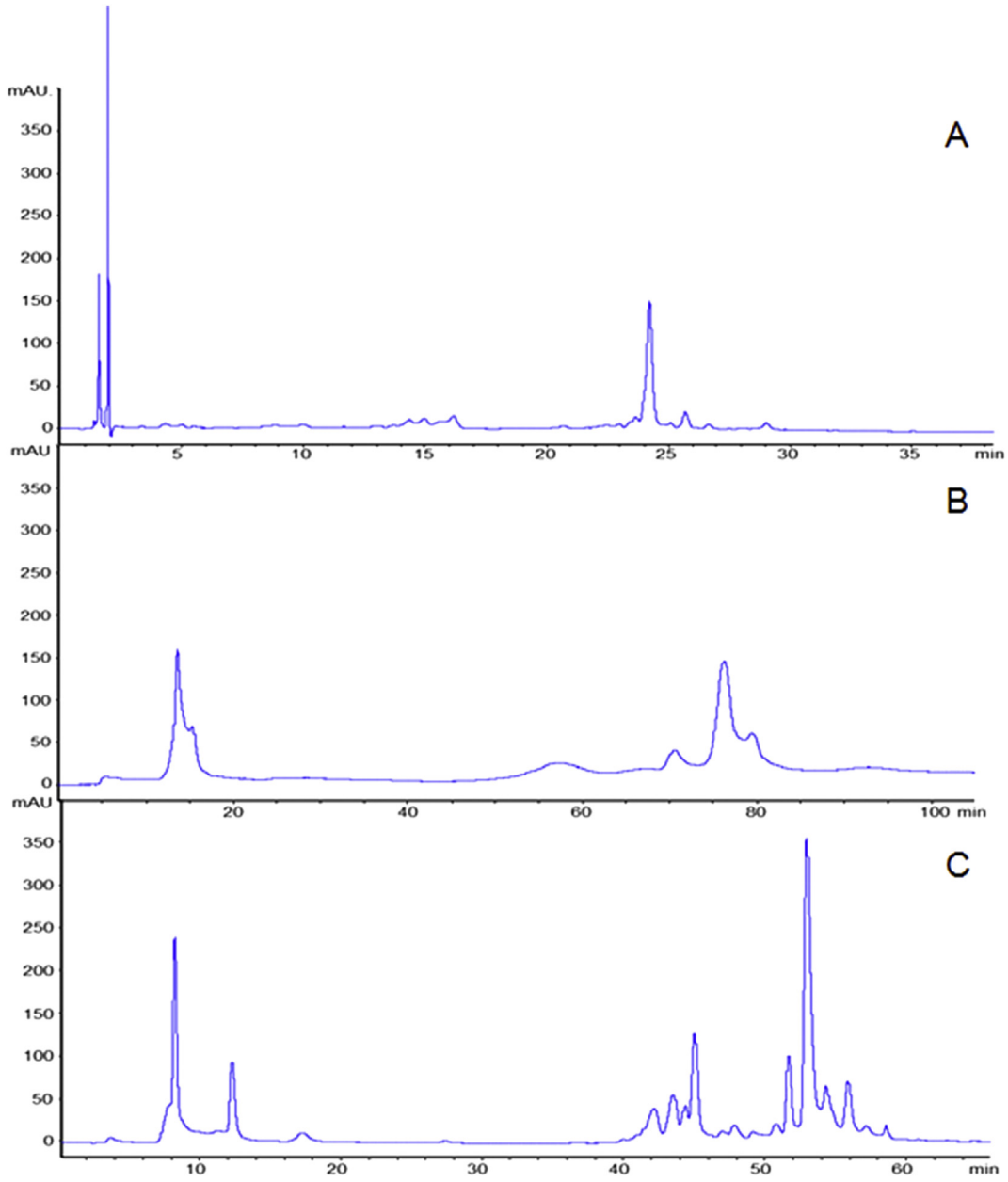

Fig. 1. First dimension chromatograms (280 nm) obtained under optimum conditions for each type of column studied. Separations using: A) Silica column (250 × 2.5 mm, 5 μm d.p., Syncronis HILIC, Thermo Scientific) eluted using acetonitrile (with 0.1% HCOOH), and water (containing 0.1% HCOOH), at 0.5 mL min^{-1}; B) Diol column (150 × 1.0 mm, 5 μm d.p., Lichrospher diol-5, HiChrom) eluted using acetonitrile and 10 mM ammonium acetate at pH 5.5 at 15 μL min^{-1}, and; C) ZIC-HILIC column (150 × 1.0 mm, 3.5 μm d.p., SeQuant ZIC-HILIC, Merck) at the optimum conditions detailed in Section 2.3.2. For other separation conditions, see text.

stationary phase was selected as provided a higher resolution between the compounds contained in such a complex sample. The optimized conditions involved the use of water (0.1% formic acid) and acetonitrile as mobile phases.

Starting from the best possible separation conditions already determined for the separation of licorice compounds in each dimension, the optimization of the LC × LC method as a whole was carried out. After the first analyses it became evident that the huge diversity of compounds contained in the sample meant that the obtained metabolite profiles were clearly grouped in two different areas in the 2D plane (Fig. 2A). Those compounds eluting first from the ^{1}D (low polarity compounds, prenylated flavonoids) were less separated in the ^{2}D under the chosen conditions that those eluting later from the ^{1}D (high polarity compounds, triterpene saponins) that were less retained in the ^{2}D (Fig. 2A). Consequently, with the aim to provide a profile as separated as possible, it was decided to reoptimize the ^{2}D method by including two different gradients along the LC × LC analysis. Fig. 2B and C show a comparison of the two-dimensional separation of licorice compounds eluting first from the ^{1}D (tr ~8–22 min). While in Fig. 2B the same gradient is maintained along the 2D analysis (the same used for the second part of the analysis), in Fig. 2C a newly optimized ^{2}D gradient was used in order to maximize the separation of the compounds eluting in this area (see details in Section 2.3.). As can be seen, significantly better separation could be obtained using the new gradient. Thus, under the finally optimized LC × LC conditions, two different ^{2}D gradients were adopted in order to achieve the best possible separation of the licorice metabolites in agreement with their chemical

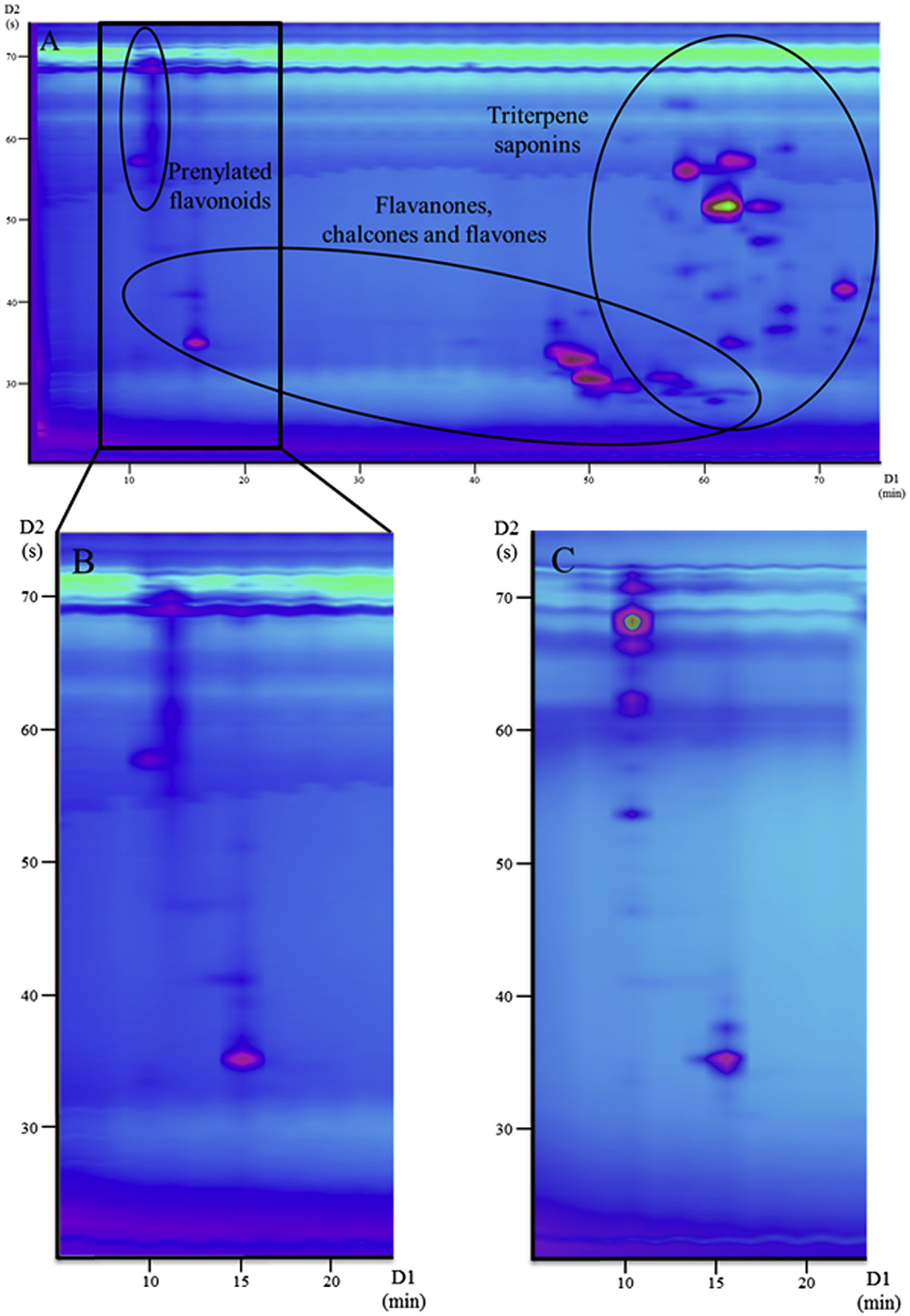

Fig. 2. Two-dimensional licorice metabolites profiles (280 nm) obtained under the studied conditions using the same ^{2}D gradient along the whole analysis (A). Comparison of the separation obtained in the first area using the same ^{2}D gradient (B) and the newly optimized ^{2}D gradient. For separation conditions, see text.

nature, allowing a theoretical peak capacity value of 1306, calculated according to Li et al. [37], which considers the ^{2}D time cycle as well as the influence of undersampling of the ^{1}D eluate. Moreover, as it can be observed from the 2D plots illustrated in Fig. 2, the retention in both dimensions was clearly non-correlated, assuring a good degree of orthogonality.

3.2. Phenolic compounds and saponins profiling of licorice by HILIC × RP-DAD-MS/MS

Once the ZIC-HILIC × C_{18} method was completely optimized, an MS instrument equipped with an ESI interface working in negative ionization mode was coupled in series to the DAD for the

Table 1
Tentatively identified common metabolites present in more than one licorice sample together with their MS and MS/MS information. Source: A) China, B) Iran, C) Crotone (Italy), D) Azerbaijan and E) Villapiana (Italy).

Peak	^{2}D t_R (s)	Total t_R (min)	$[M-H]^-$	Main MS/MS fragments detected	Identification	Structure class	Source	Ref
1	67.9	8.93	409.3	405, 391, 365, 235, 217	Kanzonol Y	Prenylated favonoid	B, C, E	[38]
2	53.3	9.99	576.8	539, 518, 419, 331, 261, 187	NI		B, D	
3	70.9	10.28	409.4	391, 235	NI		C, D, E	
4	40.7	11.08	255.0	134, 119	Liquiritigenin or isomer	Flavanone	B, D. E	[39–42]
5	35.3	12.29	727.7	613, 549, 532, 255	NI	Flavanone	A, B, C, D	
6	37.5	12.33	727.4	549, 531, 389, 255	NI	Flavanone	B, C, D	
7	31.0	14.82	417.2	255, 135	(Iso)liquiritin/Neo(iso)liquiritin	Flavanone	B, E	[43–45]
8	34.4	42.17	725.3	549, 531, 399, 255	Licorice glycoside A/C1/C2 or isomer	Flavanone	B, E	[9,22,42,44]
9	33.3	42.81	725.2	695, 512, 575, 549, 532, 255	Licorice glycoside A/C1/C2 or isomer	Flavanone	B, E	[9,22,42,44]
10	31.1	43.42	419.4	391, 279, 256, 201, 135	NI		B, E	
11	37.3	44.82	725.3	549, 531, 255	Licorice glycoside A/C1/C2 or isomer	Flavanone	B, E	[9,22,42,44]
12	31.0	46.02	633.8	587, 549, 511, 426, 339, 295, 229	Sarcaglaboside D	Sesquiterpene Glycoside	A, D, E	[45]
13	32.6	46.04	549.7	494, 481, 419, 256		Flavanone	A, B, C, D, E	
14	34.1	46.07	695.3	649, 549, 531, 417, 255	Licorice glycoside B/D1/D2	Flavanone	C, E	[9,27,42]
15	29.6	47.28	759.4	549, 467, 209	NI		A, B, E	
16	38.8	47.45	549.2	429, 255	(Iso)liquiritin apioside	Flavanone	A, D	[7,22,44,45]
17	30.5	48.61	549.9	494, 481, 419, 256	NI	Flavanone	B, D, E	
18	32.8	48.65	549.2	429, 417, 297, 255	(Iso)liquiritin apioside	Flavanone	A, B, C, D, E	[7,22,44,44]
19	37.1	48.72	549.8	494, 480, 418, 255	NI	Flavanone	C, D	
20	29.3	51.19	577.3	559, 526, 503, 488, 441, 406	(Iso)violantin	Flavone	B, C, D, E	[9,22]
21	30.3	51.21	665.9	619, 551, 530, 505, 447, 383, 239	NI		A, E	
22	27.1	51.80	721.3	677, 619, 577, 559, 487, 457, 383	NI	Flavone	A, C	
23	60.7	52.36	777.6	715, 627, 538, 470, 427	Apioglycyrrhizin	Triterpene saponin	A, B, C, D, E	[7]
24	29.4	52.49	577.2	559, 526, 503, 488, 441, 406	(Iso)violantin	Flavone	B, C, D	[9,22]
25	27.8	53.76	711.1	674, 649, 591, 549, 531, 443, 423, 298, 255	Glucoliquiritin apioside or isomer	Flavanone	C, E	[39,46]
26	29.4	53.79	837.8	828, 791, 672, 588, 472	Cycloheptaleucyl	Cyclopeptide	A, B, C, D, E	[42]
27	49.2	54.12	983.7	965, 921, 879, 838, 733, 715, 687, 645, 439	NI		A, E	
28	28.5	54.43	563.1	545, 503, 473, 443, 383, 353	Shaftoside/Apigenin 6-C-Glucoside-C-Arabinoside	Flavone	C, D	[22,39,47]
29	52.2	54.82	807.3	745, 627, 609, 583, 537, 469, 351	Licorice saponin B2 or isomer	Triterpene saponin	A, B, C, D, E	[42]
30	63.0	55.00	793.5	775, 732, 645, 522, 351	NI	Triterpene saponin	D, E	
31	28.6	55.08	711.2	674, 649, 591, 549, 531, 443, 423, 298, 255	Glucoliquiritin apioside or isomer	Flavanone	A, B, C, D, E	[39,46]
32	30.9	55.12	649.2	631, 613, 604, 565, 523, 444, 392, 259	NI		A, B, D, E	
33	41.1	55.29	939.6	921, 879, 879, 777, 645, 523, 437	NI	Triterpene saponin	B, C, D	
34	49.0	55.42	865.3	847, 821, 803, 727, 689, 608, 351	22-acetyl licorice saponin B2 or isomer	Triterpene saponin	A, B, D	[47]
35	50.1	55.44	865.3	805, 690, 607, 351	22-acetyl licorice saponin B2 or isomer	Triterpene saponin	A, E	[47]
36	27.0	56.35	711.4	674, 649, 591, 549, 531, 443, 423, 298, 255	Glucoliquiritin apioside or isomer	Flavanone	C, D, E	[39,46]
37	29.6	56.39	707.3	647, 617, 563, 545, 473, 443, 353, 255, 205	3-Hydroxyl-3-methylglutaroyl-(iso) schaftoside	Flavone	C, E	[42]
38	65.1	56.99	807.0	791, 745, 632, 351, 334, 289, 261	Licorice saponin B2 or isomer	Triterpene saponin	A, B, C, D, E	[7,9,42,44]
39	44.5	59.24	865.0	848, 821, 803, 689, 351	22-acetyl licorice saponin B2 or isomer	Triterpene saponin	B, C, E	[47]
40	52.5	59.38	821.0	801, 757, 644, 351, 333	18-α-glycyrrhizin/macedonoside C/ Yunganoside L2/Uralsaponin A/Licorice saponin H2/Licorice saponin K2	Triterpene saponin	B, C	[7,17,42,45]
41	57.6	59.46	807.0	789, 746, 632, 351, 334, 290	Licorice saponin B2 or isomer	Triterpene saponin	A, B, C, D, E	[7,9,42,44]
42	65.6	59.59	939.8	921, 878, 523, 776, 622, 497, 435	NI	Triterpene saponin	A, B, E	
43	28.4	59.63	675.9	549, 531, 255	NI		B, E	
44	37.0	59.77	881.6	864, 819, 705, 351	22-Acetoxyl licorice saponin J2	Triterpene saponin	A, D	[46]
45	41.0	59.83	969.9	953, 925, 909,835, 824, 793, 351	Albiziasaponin B or isomer	Triterpene saponin	B, D	[42]
46	49.4	59.97	1011.6	993, 949, 867, 831, 689, 643, 629, 497, 321	Licorice saponin D3	Triterpene saponin	B, C, E	[7]
47	57.4	60.11	955.8	938, 847, 633, 611, 497, 435, 339	Yunganoside A1/C1/B1	Triterpene saponin	B, C	[9]
48	59.8	60.15	737.3	719, 647, 617, 593, 503, 473, 393, 353	6-(3-Hydroxy-3-methylglutaroyl)-vicenin-2 or isomer	Flavone	C, D, E	
49	57.0	60.21	807.5	789, 745, 631, 611, 351, 289	Licorice saponin B2 or isomer	Triterpene saponin	C, E	[7,9,42,44]
50	60.6	60.27	953.8	937, 892, 849, 790, 633, 497, 339, 321	NI	Triterpene saponin	A, B, C, D	
51	27.9	60.27	593.3	575, 503, 474, 441, 406, 354	Apigenin 6,8-di-C-glucoside (Vicenin-2)	Flavone	B, C, D, E	[47]

Table 1 (*continued*)

Peak	^{2}D t_R (s)	Total t_R (min)	$[M-H]^-$	Main MS/MS fragments detected	Identification	Structure class	Source	Ref
52	35.3	60.39	823.5	805, 779, 761, 647, 539, 351, 333, 289	Licorice saponin J2/Uralsaponin C	Triterpene saponin	A, B, C, D, E	[33,44–46]
53	41.4	60.49	879.8	861, 800, 703, 685, 643, 584, 351, 333, 315	22-Acetoxyl-glycyrrhizin	Triterpene saponin	A, B, C, D, E	[45,47]
54	52.6	60.68	821.5	803, 759, 645, 351	Glycyrrhizic acid	Triterpene saponin	A, B, C, D, E	[17,42,45]
55	60.0	60.80	821.4	803, 759, 645, 351	18-α-glycyrrhizin/Yunnanglysaponin B/ macedonoside C/Yunganoside L2/ Uralsaponin A/Licorice saponin H2/ Licorice saponin K2	Triterpene saponin	A, B, C, D, E	[17,42,45]
56	27.7	62.86	737.3	675, 635, 619, 593, 575, 503, 473, 353	6-(3-Hydroxy-3-methylglutaroyl)-vicenin-2 or isomer	Flavone	B, C, E	
57	28.7	62.88	737.5	675, 635, 619, 593, 575, 503, 473, 353	6-(3-Hydroxy-3-methylglutaroyl)-vicenin-2 or isomer	Flavone	A, B, C, D, E,	
58	49.6	63.23	821.3	803, 759, 645, 351	18-α-glycyrrhizin/macedonoside C/ Yunganoside L2/Uralsaponin A/Licorice saponin H2/Licorice saponin K2	Triterpene saponin	B, C, D, E	[17,42,45]
59	52.6	63.28	821.4	803, 759, 645, 351	18-α-glycyrrhizin/macedonoside C/ Yunganoside L2/Uralsaponin A/Licorice saponin H2/Licorice saponin K2	Triterpene saponin	B, C	[17,42,45]
60	31.8	64.23	969.6	951, 904, 837, 793, 711, 351	Albiziasaponin B or isomer	Triterpene saponin	A, C, D	[42]
61	33.8	64.26	969.1	951, 793, 497, 436, 351	Albiziasaponin B or isomer	Triterpene saponin	D, E	[42]
62	37.0	63.72	1025.7	1007, 956, 908, 645, 497, 321	22-Acetoxyl-rhaoglycyrrhizin	Triterpene saponin	A, C, E	[45,48]
63	47.8	65.80	837.6	819, 776, 704, 661, 485, 351, 333, 289	Licorice saponin G2 or isomers/24-hydroxyl-glycyrrhizin/YunganosideK2/ Macedonoside P/Macedenosin B/ Macedenosin A or isomers	Triterpene saponin	A, B	[7,9,17,22,42,44–47]
64	48.2	73.03	837.5	819, 776, 704, 661, 485, 351, 333, 289	Licorice saponin G2 or isomers/24-hydroxyl-glycyrrhizin/YunganosideK2/ Macedonoside P/Macedenosin B/ Macedenosin A or isomers	Triterpene saponin	A, B, C, D, E	[7,9,17,22,42,44–47]
65	52.3	65.87	821.5	803, 759, 645, 351	18αglycyrrhizin/macedonoside C/ Yunganoside L2/Uralsaponin A/Licorice saponin H2/Licorice saponin K2	Triterpene saponin	A, B, C, D, E	[17,42,45]
66	37.0	66.92	983.5	923, 863, 821, 803, 760, 645, 351, 289	Licorice saponin A3 or isomer	Triterpene saponin	A, B, C, D, E	[45]
67	39.7	66.93	983.5	923, 863, 821, 803, 760, 645, 351, 289	Licorice saponin A3 or isomer	Triterpene saponin	B, C, D, E	[45]
68	48.6	67.11	969.7	951, 904, 837, 793, 711, 351	Albiziasaponin B or isomer	Triterpene saponin	B, C, D, E	[42]
69	52.8	67.18	967.7	949, 906, 833, 645, 497, 321	Yunganoside J1/L1	Triterpene saponin	B, C	[42]
70	44.8	68.35	837.6	819, 781, 661, 351	Licorice saponin G2 or isomers/24-hydroxyl-glycyrrhizin/YunganosideK2/ Macedonoside P/Macedenosin B/ Macedenosin A or isomers	Triterpene saponin	C, D, E	[7,9,17,22,42,44–47]
71	50.3	68.44	837.7	819, 775, 661, 644, 351	Licorice saponin G2 or isomers/24-hydroxyl-glycyrrhizin/YunganosideK2/ Macedonoside P/Macedenosin B/ Macedenosin A or isomers	Triterpene saponin	A, B, C, D, E	[7,9,17,22,42,44–47]
72	59.7	68.60	821.5	803, 759, 645, 351	18αglycyrrhizin/macedonoside C/ Yunganoside L2/Uralsaponin A/Licorice saponin H2/Licorice saponin K2	Triterpene saponin	B, C, D, E	[17,42,45]
73	31.1	70.72	1115.9	1097, 793, 497, 435	NI		A, D	
74	34.6	70.78	999.6	881, 837, 819, 661, 351	22-Hydroxyl-licorice saponin A3	Triterpene saponin	A, B, C, E	[42,45,48]
75	36.9	70.82	989.6	966, 924, 821, 803, 645, 501, 351, 289	Licorice saponin A3 or isomer	Triterpene saponin	A, B, C, D, E	[45]
76	39.9	70.87	969.8	951, 907, 793, 351, 289	Albiziasaponin B or isomer	Triterpene saponin	C, E	[42]
77	41.8	72.19	837.6	821, 776, 661, 485, 351	Licorice saponin G2 or isomers/24-hydroxyl-glycyrrhizin/YunganosideK2/ Macedonoside P/Macedenosin B/ Macedenosin A or isomers	Triterpene saponin	B, C, D, E	[7,9,17,22,42,44–47]
78	36.0	73.40	837.7	821, 776, 661, 485, 351	Licorice saponin G2 or isomers/24-hydroxyl-glycyrrhizin/YunganosideK2/ Macedonoside P/Macedenosin B/ Macedenosin A or isomers	Triterpene saponin	B, C, D, E	[7,9,17,22,42,44–47]
79	38.1	71.74	853.6	837, 835, 677, 502, 351	22-Hydroxy licorice saponin G2	Triterpene saponin	B, C, D, E	[42,48]
80	42.9	74.82	983.7	965, 880, 821, 661, 497, 339, 321	Licorice saponin A3 or isomer	Triterpene saponin	B, C, D, E	[45]

characterization and identification of each separated compound. The employed MS analyzer was an ion trap that offered valuable information about the chemical structure of the separated compounds thanks to its capacity to work in MS/MS mode. However, the use of a high resolution MS detector with high scanning speed could significantly improve the obtained results in terms of reducing the number of non-identified compounds and increasing the certainty of the identifications. The five licorice samples studied, belonging to diverse locations, namely, Calabria-Italy (Villapiana and Crotone), Iran, China and Azerbaijan, were injected and

Table 2
Tentatively identified metabolites exclusively found present in the indicated licorice source.

ID	^{2}D t_R (s)	Total t_R (min)	$[M-H]^-$	Main MS/MS fragments detected	Identification	Structure class	Ref.
China							
A1	51.2	8.65	331.2	311, 293, 229, 211, 171, 139, 99	NI		
A2	53.4	8.69	269.8		Emodin		[49]
A3	72.1	10.30	407.4	379, 284, 235, 177, 135	NI		
A4	74.2	10.34	423.9	391, 347, 322, 229, 207, 193, 177	Kanzonol H or isomer	Prenylated flavonoid	[50,51]
A5	31.2	12.22	417.2	297, 255, 174, 135	(Iso)liquiritin/Neo(iso)liquiritin	Flavanone	[43–45]
A6	34.3	12.27	433.3	385, 301, 271, 176, 151	5-Hydroxyliquiritin	Flavanone	[52]
A7	38.9	12.35	695.3	549, 531, 399, 255	Licorice glycoside B/D1/D2	Flavanone	[9,27,42]
A8	40.7	12.38	417.4	297, 255, 135	(Iso)liquiritin/Neo(iso)liquiritin	Flavanone	[43–45]
A9	43.1	12.42	475.3[a]	417, 345, 311, 267, 252	Ononin	Prenylated flavonoid	[53]
A10	54.2	12.60	255.0	134, 119	Liquiritigenin or isomer	Flavanone	[39–42]
A11	59.1	12.69	369.3	352, 339, 323, 309, 297, 284	NI		
A12	61.0	12.72	423.4	405, 387, 355, 264, 213, 148	NI		
A13	31.4	13.52	419.0	298, 256, 153, 134, 119	NI		
A14	33.3	13.56	551.1	515, 445, 429, 419, 297, 255, 221	NI	Flavanone	
A15	32.0	14.83	586.7	549, 539, 504, 399	NI		
A16	31.0	47.32	481.4	438, 432, 417, 381, 321, 255	NI	Flavanone	
A17	35.3	47.39	551.6	515, 431, 419, 389, 297, 257	NI	Flavanone/Chalcone	
A18	37.3	47.42	551.0	429, 417, 297, 255	NI	Flavanone/Chalcone	
A19	38.5	47.44	478.5	423, 378, 319, 271, 167	NI		
A20	32.7	49.95	777.1	716, 627, 537	Apioglycyrrhizin	Triterpene saponin	[42]
A21	27.5	51.16	579.4	547, 417, 324, 255	Liquiritigenin -7, 4′ diglucoside/Glucoliquiritin	Flavanone	[53]
A22	28.9	51.18	528.7	509, 483, 410, 273, 247	NI		
A23	46.9	51.48	836.0	775, 685, 626	Cycloheptaleucyl	Cyclopeptide	[42]
A24	27.7	53.76	590.8	549, 531, 471, 459, 297, 255	Liquiritigenin 4'-[3-acetylapiosyl-(1-2)] glucoside	Triterpene saponin	
A25	31.8	53.83	881.8	864, 819, 754, 705, 644, 584, 351	22-Acetoxyl glycyrrhizic acid/22β-acetoxyl licorice saponin J2	Triterpene saponin	[43]
A26	46.9	54.08	866.3	805, 626	NI		
A27	50.2	54.14	966.3	947, 896, 863, 757, 717, 671, 629, 579, 537	NI		
A28	60.6	54.31	809.3	745, 627, 537	NI		
A29	37.3	55.22	810.3	629, 540	NI		
A30	40.7	55.28	923.9	905, 877, 861, 777, 716, 627, 609, 537	NI		
A31	41.9	55.30	1014.1	995, 951, 909, 867, 805, 782, 763, 745, 687, 645, 601, 487, 371	NI		
A32	46.9	55.38	997.9	935, 893, 787, 747, 652, 629, 579, 539	NI		
A33	52.1	55.47	868.0	830, 806, 690, 599, 487, 351	NI	Triterpene saponin	
A34	41.0	56.58	982.7	963, 921, 903, 859, 815, 685, 669, 643, 625, 595, 581, 535	NI		
A35	50.5	56.74	864.8	847, 803, 687, 351	22-Acetoxyl licorice saponin C2	Triterpene saponin	[46]
A36	28.7	57.68	709.6	647, 617, 563, 473, 443, 383	NI		
A37	37.5	57.83	1012.2	993, 951, 889, 845, 744, 699, 685, 667, 643, 625, 595, 535, 423	NI		
A38	28.7	58.33	955.8	937, 893, 793, 747, 643, 539	Hederagenin-3-Orhamnosyl glucoryl arabinosyl glucuronide or isomer	Triterpene saponin	
A39	37.7	58.48	837.3	817, 773, 701, 659, 351, 289	Licorice saponin G2 or isomer/24- hydroxyl-glycyrrhizin/ YunganosideK2/Macedonoside P/Macedenosin B/ Macedenosin A	Triterpene saponin	[55,55]
A40	26.4	58.94	676.7	632, 550, 475, 402, 297, 256	NI		[7,9,17,22,42,44–47]
A41	44.7	59.25	823.1	654, 351	Licorice saponin J2/Uralsaponin C or isomer	Triterpene saponin	
A42	28.7	60.28	823.2	806, 761, 647, 351	Licorice saponin J2/Uralsaponin C or isomer	Triterpene saponin	[39,44,46]
A43	40.9	60.48	881.5	862, 819, 575, 705, 643, 466, 351	22-Acetoxyl glycyrrhizic acid/22β-acetoxyl licorice saponin J2	Triterpene saponin	[36,44–46]
A44	35.1	62.99	967.7	933, 907, 794, 351	NI	Triterpene saponin	[46]
A45	37.7	64.33	895.6	877, 833, 721, 351	22-Acetoxyl licorice saponin G2	Triterpene saponin	
A46	33.4	65.56	841.6	821, 663, 351	NI	Triterpene saponin	[46]
A47	41.1	65.69	882.1	863, 803, 351	NI	Triterpene saponin	
A48	33.5	72.06	1129.7	1060, 967, 951, 931, 807, 627, 497, 321	NI	Triterpene saponin	
A49	33.5	73.36	837.2	820, 661, 351	Licorice saponin G2 or isomers/24- hydroxyl-glycyrrhizin/ YunganosideK2/Macedonoside P/Macedenosin B/ Macedenosin A	Triterpene saponin	[7,9,17,22,42,44–47]
A50	30.35	74.61	1132.6	1114, 1072, 1052, 497	NI	Triterpene saponin	
Iran							
B1	40.7	9.78	577.2	559, 539, 472, 386, 329	NI		
B2	61.3	10.12	557.1	539, 521, 499, 381, 323, 261, 173	NI		
B3	67.9	10.23	423.0	403, 352, 309, 229, 193	Kanzonol H or isomer	Prenylated flavonoid	[53]
B4	70.6	10.28	468.4	441, 423, 405, 335, 248, 178	NI		

Table 2 (*continued*)

ID	^{2}D t_R (s)	Total t_R (min)	$[M-H]^-$	Main MS/MS fragments detected	Identification	Structure class	Ref.
B5	32.6	12.24	477.7[a]	443, 433, 317, 271, 252, 176	Naringenin-7-Oglucoside or isomer	Flavanone	[52]
B6	68.6	12.84	742.7	725, 672, 633, 539, 417, 309	NI		
B7	31.2	13.52	496.6	481, 460, 418, 297, 230, 162	NI		
B8	34.4	13.57	725.3	632, 612, 549, 533, 255	Licorice glycoside A/C1/C2 or isomer	Flavanone	[9,22,42,44]
B9	37.6	13.63	695.3	549, 531, 399, 255	Licorice glycoside B/D1/D2	Flavanone	[9,27,42]
B10	68.6	14.14	525.7	456, 334	NI		
B11	30.4	20.01	491.4	446, 283, 267, 211	NI		
B12	35.1	27.89	578.2	534, 387, 326, 283, 268, 194	NI	Isoflavone	
B13	35.2	29.19	695.3	576, 549, 531, 255	Licorice glycoside B/D1/D2	Flavanone	[9,27,42]
B14	33.6	42.16	563.6	483, 427, 310, 267, 253, 183	NI		
B15	34.0	44.77	697.5	662, 551, 533, 255	NI	Flavanone/Chalcone	
B16	39.5	44.86	903.5	885, 873, 725, 531, 255	NI	Flavanone	
B17	29.3	45.99	518.9	446, 385, 307, 205, 153	NI		
B18	31.0	46.02	633.9	587, 549, 417, 339	NI		
B19	33.4	46.06	921.7	903, 873, 725, 549	NI		
B20	37.1	46.12	727.4	685, 550, 532, 309, 255	NI	Flavanone	
B21	38.8	48.75	565.3	471, 433, 271, 161	Naringenin 7-O-(2-β-D-apiofuranosyl)-β-D-glucopyranoside	Flavanone	[42]
B22	52.2	52.87	808.3	745, 627, 539, 469	NI	Triterpene saponin	
B23	40.1	55.27	1013.7	996, 952, 928, 909, 805, 763, 745, 687, 645, 601, 469	NI		
B24	46.9	56.68	824.0	804, 779, 762, 643, 600, 554, 485	NI	Triterpene saponin	
B25	27.0	57.65	563.1	545, 503, 485, 473, 443, 383, 353	Shaftoside	Flavone	[56]
B26	50.7	58.05	924.0	905, 862, 777, 716, 627, 537	NI	Triterpene saponin	
B27	67.3	58.32	805.5	787, 746, 631, 351, 289	Licorice saponin C2	Triterpene saponin	[9]
B28	51.3	59.36	1222.1	1204, 1088, 1045, 965, 869, 789, 352	NI	Triterpene saponin	
B29	45.4	60.56	1027.8	1009, 984, 922, 706, 559, 497, 339	NI	Triterpene saponin	
B30	34.0	64.27	825.6	808, 779, 765, 649, 599, 554, 351, 333, 259	NI	Triterpene saponin	
B31	32.1	65.53	969.7	953, 925, 909,835, 824, 793, 351	Albiziasaponin B or isomer	Triterpene saponin	[42]
B32	45.0	68.35	837.6	819, 661, 485, 351	Licorice saponin G2 or isomers/24- hydroxyl-glycyrrhizin/ YunganosideK2/Macedonoside P/Macedenosin B/ Macedenosin A or isomers	Triterpene saponin	[7,9,17,22,42,44–47]
B33	52.9	68.48	839.1	821, 777, 715, 663, 645, 488, 351, 334, 289, 261, 235	Yunganoside G2 or isomer	Triterpene saponin	[9]
B34	50.2	69.74	969.7	951, 924, 887, 833, 647, 497, 405, 339, 321	Albiziasaponin B or isomer	Triterpene saponin	[42]
B35	56.9	71.15	839.1	837, 821, 663, 351	Yunganoside G2 or isomer	Triterpene saponin	[9]
B36	50.8	73.65	985.8	967, 923, 851, 663, 497, 435, 321	Yunganoside K1 or isomer	Triterpene saponin	[17]
Crotone (Italy)							
C1	53.5	8.69	391.0		Hispaglabridin	Prenylated flavonoid	[43]
C2	62.5	8.84	385.6	367, 340, 311, 162	Glyasperin E	Prenylated flavonoid	[57]
C3	31.2	12.22	419.2	255, 135	NI		
C4	34.1	12.31	420.2	401, 297, 257, 119	NI		
C5	71.5	12.89	667.4	644, 553, 471, 290, 210	NI		
C6	31.3	13.52	659.7	642, 548, 481, 335	NI		
C7	30.1	20.00	549.2	488, 445, 429, 325, 255	NI	Flavanone	
C8	31.2	47.32	549.7	494, 430, 342, 293, 256	NI	Flavanone	
C9	29.4	48.59	634.0	598, 549, 492	NI		
C10	33.1	51.25	724.3[a]	677, 633, 577, 550, 283, 225	NI		
C11	30.8	54.41	721.9	703, 647, 617, 577, 559, 457, 383, 353	Apigenin 6-C-α-L-rhamnopyranoside-8-C-[6‴-(3-methylglutaroyl)-β-D-glucopyranoside]	Flavone	[58]
C12	53.3	54.79	793.7	775, 750, 731, 644, 485, 384, 351	NI	Triterpene saponin	
C13	43.9	55.33	807.3	789, 765, 633, 524, 423, 351	Licorice saponin B2 or isomer	Triterpene saponin	[42]
C14	55.7	55.53	863.5	845, 687, 393, 351, 263	22-Acetoxy-glycyrrhaldehyde	Triterpene saponin	[49]
C15	44.8	59.25	807.3	791, 747, 631, 527, 351	Licorice saponin B2 or isomer	Triterpene saponin	[42]
C16	41.3	59.84	953.6	936, 862, 803, 497, 321	Yunganoside D1/H1/I1	Triterpene saponin	[17]
C17	64.7	60.23	821.4	803, 759, 645, 351	18αglycyrrhizin/Yunnanglysaponin B/Macedonoside C/ Yunganoside L2/Uralsaponin A/Licorice saponin H2/ Licorice saponin K2	Triterpene saponin	[17,42,45]
C18	42.8	64.41	895.6	877, 660, 351	22β-Acetoxyl licorice saponin G2	Triterpene saponin	[46]
C19	40.7	72.68	969.7	952, 922, 793, 351	Albiziasaponin B or isomer	Triterpene saponin	[42]
Azerbaijan							
D1	62.5	10.14	559.0	541, 421, 375, 313, 223	NI		
D2	66.3	10.21	556.9	539, 487, 391, 336, 253	NI		
D3	68.2	10.24	411.5	392, 236, 217, 177	NI		
D4	41.0	11.08	661.3	642, 549, 481, 335	NI		
D5	32.8	12.25	725.2	549, 531, 255	Licorice glycoside A/C1/C2 or isomer	Flavanone	[9,22,42,44]
D6	39.5	12.36	737.3	691, 653, 613, 543, 381, 267	NI		
D7	70.5	12.88	757.1	741, 711, 521, 349, 297	NI		
D8	31.2	13.52	480.9	444, 376, 283, 137	NI		

(*continued on next page*)

Table 2 (*continued*)

ID	^{2}D t_R (s)	Total t_R (min)	$[M-H]^-$	Main MS/MS fragments detected	Identification	Structure class	Ref.
D9	34.4	13.57	727.7	669, 551, 533, 399, 311, 254	NI		
D10	36.6	13.61	697.5	632, 550, 532, 430, 281	NI		
D11	33.8	16.16	648.1	561, 322, 267	NI		
D12	33.8	17.46	598.3	561, 867	NI		
D13	35.1	33.09	561.2	482, 309, 267, 252	Glycyroside or isomer	Isoflavone	[42,51]
D14	33.5	48.66	561.1	484, 401, 309, 267	Glycyroside or isomer	Isoflavone	[42,51]
D15	31.5	48.63	711.1	693, 681, 601, 417, 385	NI		
D16	33.3	48.66	670.8	626, 549, 531, 255	NI	Flavanone/Chalcone	
D17	38.7	54.60	921.4	903, 874, 835, 790, 725, 550, 531	NI		
D18	53.6	55.49	955.6	937, 747, 630	Hederagenin-3-O-rhamnosyl glucoryl arabinosyl glucuronide or isomer	Triterpene saponin	[54,55]
D19	45.1	55.35	867.6	848, 691, 351	NI	Triterpene saponin	
D20	51.1	59.35	867.3	847, 803, 689, 593, 351	NI	Triterpene saponin	
D21	65.9	60.25	807.4	790, 744, 676, 630, 454, 351	NI	Triterpene saponin	
D22	30.2	64.20	713.5	674, 593, 550, 255	NI	Flavanone/Chalcone	
D23	41.6	64.39	985.5	863, 823, 805, 647, 497, 351	Yunganoside K1 or isomer	Triterpene saponin	[17]
D24	43.6	64.43	1027.8	990, 983, 959, 942, 646, 497	NI	Triterpene saponin	
D25	48.4	64.51	837.5	819, 793, 775, 661, 351	Licorice saponin G2/24- hydroxyl-glycyrrhizin/ YunganosideK2/Macedonoside P/ Macedenosin B/Macedenosin A	Triterpene saponin	[7,9,17,22,42,44–47]
D26	49.9	64.53	837.6	819, 793, 775, 661, 351	Licorice saponin G2/24- hydroxyl-glycyrrhizin/ YunganosideK2/Macedonoside P/ Macedenosin B/Macedenosin A	Triterpene saponin	[7,9,17,22,42,44–47]
D27	58.7	64.68	821.4	805, 760, 647, 627, 351	18αglycyrrhizin/Yunnanglysaponin B/macedonoside C/ Yunganoside L2/Uralsaponin A/Licorice saponin H2/ Licorice saponin K2	Triterpene saponin	[17,42,45]
D28	37.2	66.92	983.5	965, 923, 863, 821, 804, 760, 645, 351	Licorice saponin A3	Triterpene saponin	[45]
D29	39.8	68.26	971.2	953, 909, 791, 585, 497, 435, 351	NI	Triterpene saponin	
D30	31.8	70.73	969.7	951, 907, 807, 793, 643, 553, 497, 351	Albiziasaponin B or isomer	Triterpene saponin	[42]
D31	31.1	72.02	1115.9	1098, 981, 951, 858, 793, 497, 435		Triterpene saponin	
D32	30.7	74.61	985.5	983, 967, 924, 810, 496, 405, 351	Yunganoside K1 or isomer	Triterpene saponin	[17]
D33	48.2	76.20	969.7	946, 864, 821, 803, 645, 527, 351, 289	NI	Triterpene saponin	
D34	35.9	77.30	987.2	967, 923, 810, 351	NI	Triterpene saponin	
Villapiana (Italy)							
E1	53.8	8.70	345.4	235, 166	NI		
E2	57.4	8.76	472.2	386, 296, 178			
E3	62.2	8.84	359.0	311, 269, 177			
E4	71.8	9.00	323.2	253, 213, 201, 135, 121	Glabridin	Prenylated flavonoid	[9,43]
E5	35.4	9.69	477.1	432, 353, 268, 253, 221	Naringenin-7-Oglucoside or isomer	Flavanone	[42]
E6	32.5	9.64	592.4	549, 531, 255	NI		
E7	34.7	9.68	725.2	611, 549, 532, 255	Licorice glycoside A/C1/C2 or isomer	Flavanone	[9,22,42,44]
E8	37.3	9.72	695.3	549, 531, 255	Licorice glycoside B/D1/D2 or isomer	Flavanone	[9,27,42]
E9	30.1	42.10	725.4	678, 605, 577, 562, 549, 531, 310, 255	Licorice glycoside A/C1/C2 or isomer	Flavanone	[9,22,42,44]
E10	29.3	43.39	591.5	549, 531, 473, 399, 255	NI	Flavanone	
E11	34.6	51.28	549.2	429, 417, 297, 255	(Iso)liquiritin apioside	Flavanone	[7,22,44,45]
E12	34.6	55.18	723.7[a]	677, 659, 577, 457, 383	Cyclohexaleucyl	Cyclopeptide	[42]
E13	36.7	55.21	925.7	908, 894, 879, 717, 603, 539, 509, 469	NI		
E14	32.9	60.35	939.6	922, 877, 777, 732, 644, 524, 457	dHex-Hex-HexA-Soyasapogenol E	Triterpene saponin	[54]
E15	44.4	60.54	707.2	674, 648, 617, 563, 545, 443, 383, 353, 255	3-Hydroxyl-3-methylglutaroyl-(iso)schaftoside	Triterpene saponin	[42]
E16	34.6	62.98	865.3	847, 804, 689, 582, 351	22-acetyl licorice saponin B2	Triterpene saponin	[47]
E17	40.8	63.08	823.5	805, 761, 648, 351	Licorice saponin J2/Uralsaponin C or isomer	Triterpene saponin	[33,44–47]
E18	57.7	63.36	1011.7	994, 923, 689, 497, 339	Licorice saponin D3	Triterpene saponin	[7]
E19	43.2	65.72	821.3	804, 760, 646, 351	18αglycyrrhizin/Yunnanglysaponin B/Macedonoside C/ Yunganoside L2/ Uralsaponin A/Licorice saponin H2/Licorice saponin K2	Triterpene saponin	[17,42,45]
E20	41.3	73.49	939.2	922, 878, 732, 643, 554, 485, 356	NI	Triterpene saponin	
E21	40.8	74.78	837.5	821, 775, 661, 351	Licorice saponin G2 or isomers/24- hydroxyl-glycyrrhizin/ YunganosideK2/ Macedonoside P/Macedenosin B/Macedenosin A or isomers	Triterpene saponin	[7,9,17,22,42,44–47]

[a] Ions detected as $[M-H+HCOOH]^-$.

analyzed in detail. Table 1 shows the compounds tentatively identified in more than one sample, whereas Table 2 shows those compounds that were exclusively found in just one location (potential markers of geographical origin). Fig. 3 shows the two-dimensional plots obtained for each sample in which the assigned peaks are marked.

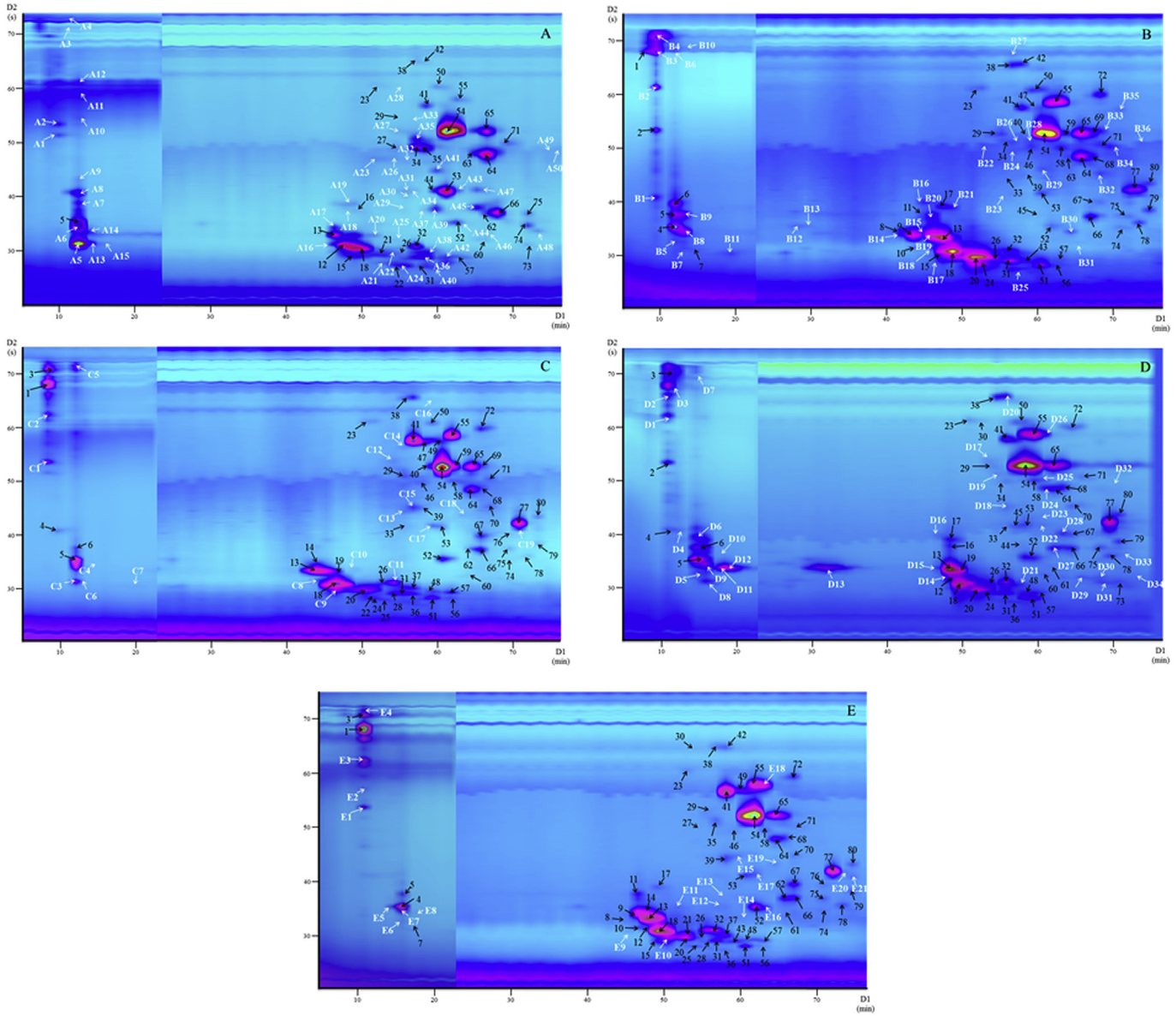

Fig. 3. Two-dimensional HILIC × RP licorice metabolites profiles (280 nm) obtained for licorice samples collected from China (A), Iran (B), Crotone (Italy, C), Azerbaijan (D) and Villapiana (Italy, E). For peak identification, see Tables 1 and 2. Separation details in Section 2.3.

The main licorice metabolites are triterpene saponins and phenolic compounds, including flavanones, chalcones, flavones, isoflavones and isoprenylated flavonoids. Some of these flavonoids may be found as aglycones or glycosylated. Each group of compounds described in licorice can be identified attending to their mass fragmentation pathway [42]. This information was collected and studied in order to tentatively assign the separated peaks in the different samples.

In any case, as can be seen in Fig. 3 the profile of the 5 licorice samples is rather similar being the main detected compounds (those with higher intensities) present in all locations.

3.2.1. *Flavonoid aglycones and prenylated flavonoids*

At the beginning of the analysis, a group of prenylated flavonoids was found together with other flavonoid aglycones, clearly located in the upper side of the 2D plot, as can be observed in Fig. 2. Among prenylated flavonoids, only kanzonol Y (peak 1, *m/z* 409.6) was described in more than a sample. Others were just found to be potential markers of location, such as glabridin (peak E4) from Villapiana, hispaglabridin (peak C1) and glyasperin E (peak C2) from Crotone or kanzonol H (peak A4) from China.

The most relevant flavonoid aglycone found was liquiritigenin (peak 4), a flavanone with $[M-H]^-$ at *m/z* 255.0, which provided fragment ions at *m/z* 135 and 119 through the fragmentation via retro Diels–Alder (RDA) reaction. Fig. 4A shows the MS/MS fragmentation pattern of this compound.

3.2.2. *Glycosylated flavanones and chalcones*

Glycosylated flavanones and their related glycosylated chalcones were found to be the major phenolic compounds in the metabolites profile of all the studied samples. Depending on the position of the OH- groups of the molecule, the fragmentation pathway of these compounds was different. Among them, different peaks presented MS/MS fragmentation patterns that gave rise to a characteristic fragment with *m/z* 255, corresponding to the aglycone liquiritigenin. Thus, the presence of the fragment at *m/z* 255

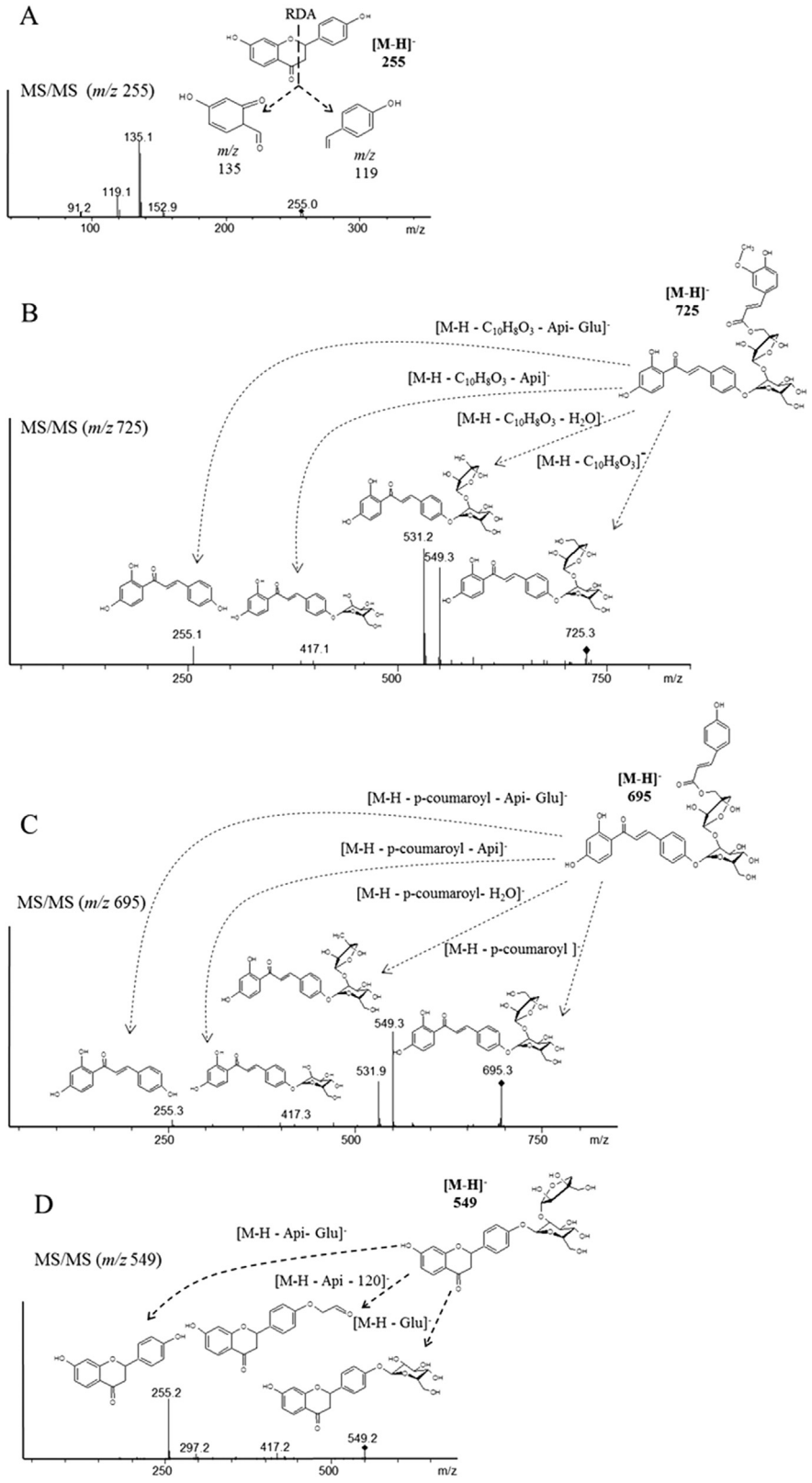

Fig. 4. Chemical structure and MS/MS fragmentation patterns for A) liquiritigenin, B) licorice glycoside A, C) licorice glycoside B, and D) liquiritin apioside, detected in the licorice samples.

meant that these compounds suffered the loss of the saccharide groups. In particular peaks 8, 9 and 11 with $[M-H]^-$ at *m/z* 725.3 were assigned to licorice glycoside A or licorice glycoside C1 or C2. The chemical structure of these compounds presents two glycoside groups (an apiose and a glucose units), and a p-coumaroyl group with a methylated group that decreases their polarity; therefore,

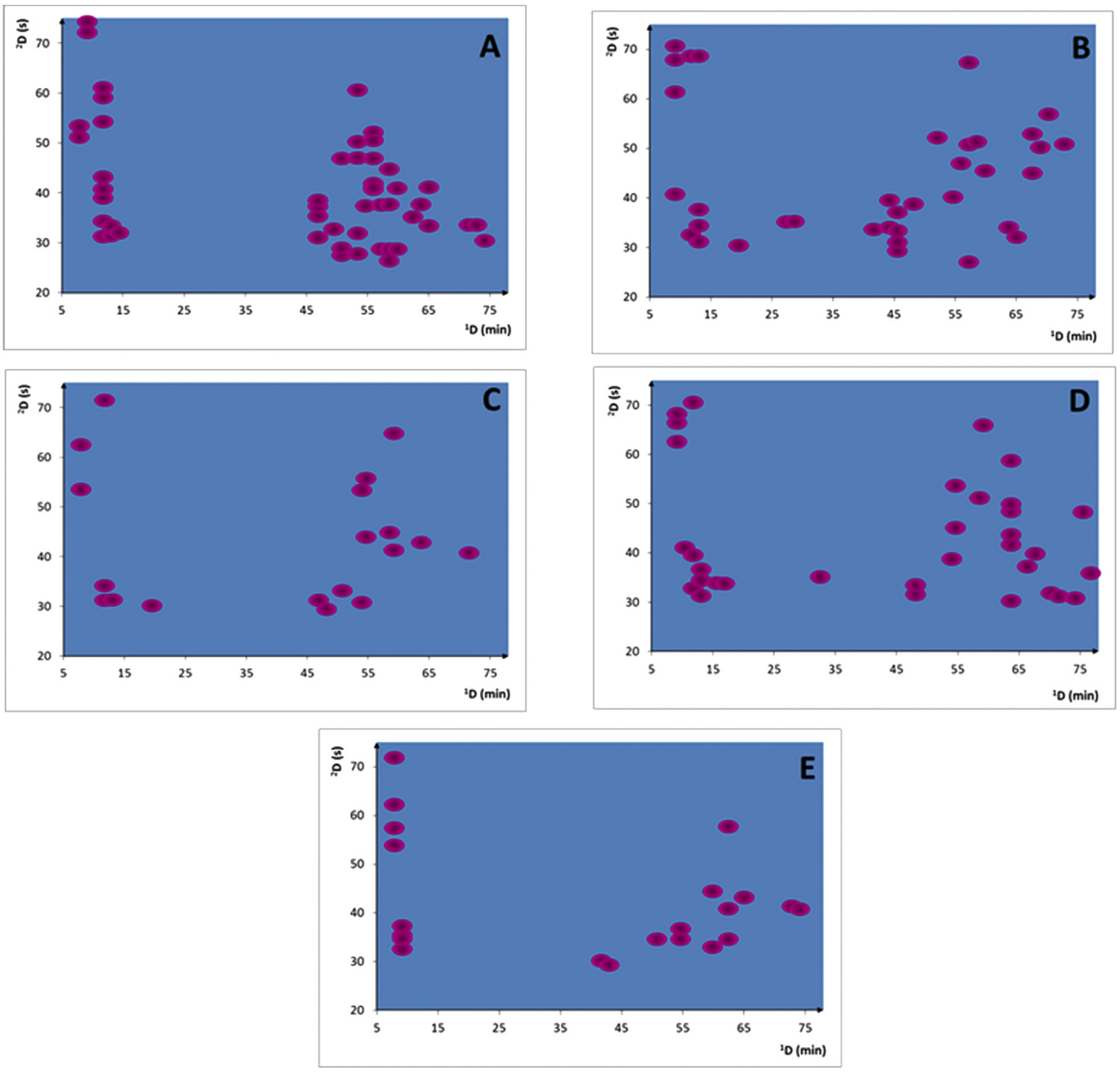

Fig. 5. Reconstructed two-dimensional HILIC × RP traces of metabolites exclusively present in the indicated licorice sample. A) China, B) Iran, C) Crotone (Italy), D) Azerbaijan and E) Villapiana (Italy).

their retention on the HILIC ^{1}D was low. Fig. 4B shows the chemical structure of these components as well as their corresponding MS/MS spectrum. As can be observed, their fragmentation produced ions at *m/z* 549, 531, 417, 255; these fragments could correspond to the loss of 176 Da ($[M-H-C_{10}H_8O_3]^-$), 194 Da ($[M\text{-}H\text{-}C_{10}H_8O_3-H_2O]^-$), 308 Da ($[M\text{-}H\text{-}C_{10}H_8O_3-Api]^-$) and 470 Da ($[M-H-C_{10}O_3H_8-Api-Glu]^-$), respectively.

The same behavior was observed for licorice glycoside B or D1/D2 (peak 14) formed by a liquiritigenin moiety linked to a hexose, a pentose and a p-coumaroyl group. This compound presented a $[M-H]^-$ at *m/z* 695.3 and a fragmentation pattern characterized by ions at *m/z* 549 (loss of p-coumaroyl group), 531 (loss of p-coumaroyl group and a water molecule), 417 (loss of p-coumaryl and pentose molecules) and 255 (removal of the three linked groups: p-coumaroyl, pentose and hexose). Fig. 4C illustrates these data. On the other hand, liquiritin apioside and isoliquiritin apioside (peaks 16 and 18), with $[M-H]^-$ at *m/z* 549.6, have a chemical structure composed by a liquiritigenin and a hexose and a pentose units. As it is shown in Fig. 4D, their MS/MS pattern was characterized by the occurrence of an ion at *m/z* 417 attributed to the loss of apioside (neutral loss of 132 Da), *m/z* 297 to the combination of the loss of the apioside unit and the cleavage of the hexose (−132 Da and −120 Da, respectively) and *m/z* 255 due to the loss of the two glycosidic units [49].

Other compounds belonging to these groups were also tentatively identified or putatively assigned to this group thanks to their MS characteristics, as can be observed in Tables 1 and 2, as well as to their typical UV maxima (270 nm for chalcones and 360 nm for flavanones).

3.2.3. Triterpene saponins

Triterpene saponins are regarded as the main bioactive

metabolites present in licorice, eluting together in the last part of the two-dimensional analyses. The triterpene saponins of licorice belong to oleanane-type triterpene saponins and their chemical structure consist on a 30-carbon aglycone (sapogenin) with multi-sugar attached units. Under MS/MS experiments carried out in negative ionization mode, oleanane-type triterpene saponins mainly give rise to a [M− aglycone − H]$^-$ fragment ion. Glycyrrhizic acid (peak 54) presented a [M−H]$^-$ at *m/z* 821.5 and its fragmentation pattern showed ions at *m/z* 803 ([M−H_2O−H]$^-$), 645 ([M−Glucuronic acid-H]$^-$), 351 ([2 Glucuronic acid − H]$^-$). As mentioned in the introduction section, many compounds and their isomers and compounds with the same molecular weight coexist in the licorice extract, hence, several separated peaks presented [M−H]$^-$ at *m/z* 821. Glycyrrhizic acid is the main licorice metabolite and thus, peak 54 was assigned to this component as it was the most intense peak in all studied samples. Besides this component,18-α-glycyrrhizic acid, macedonoside C, yunganoside L2, uralsaponin A, licorice saponin H2 and licorice saponin K2 presented the same molecular ion and fragmentation pattern, and thus, the peaks that presented this pattern (peaks 40, 55, 58, 59, 65 and 72) could not be unequivocally assigned.

Other important saponins were identified in the samples according to their [M−H]$^-$ values and MS/MS spectra. Table 1 summarizes this information. Among them, 22-acetoxyl-glycyrrhizin (peak 53), licorice saponin A3 (peak 66) and licorice saponin G2 (peak 71) were found in all the studied samples. Additionally, other compounds that could not be identified were putatively assigned as triterpene saponins based on the typical MS/MS behavior.

3.3. Geographical differentiation of licorice by HILIC × RP-DAD-MS/MS

The huge potential that comprehensive two-dimensional LC may provide for the separation of very complex samples, like those studied in the present work, is complemented by the possibility of attaining 2D-plots that may be employed to discriminate among samples. In an effort to avoid frauds when dealing with protected designation of origin foods, metabolite profiling can be used to effectively differentiate samples with different geographical origin. In this work, a first approach to this strategy is employed using the optimized HILIC × RP-DAD-MS/MS method in order to demonstrate the potential of this technique to point out possible markers of geographical origin in different licorice samples. Besides the qualitative information collected described in Section 3.2, the generation of 2D-plots may be used to produce characteristic patterns of each type of sample. Fig. 5 shows reconstructed 2D-plots corresponding to the individual markers found in each sample. Thus, only those compounds that were found in just one sample are included. As can be observed in that Figure, each particular pattern was formed by a variety of peaks at different points along the complete 2D-plot. The use of those points could effectively offer an advantage for the identification of unknown or suspected samples. Consequently, these patterns might be used to visually assign a sample to a particular location, although the analysis of a significantly higher number of samples is required to statistically validate the found candidate markers. Chinese licorice was the one that presented a higher amount of typical compounds (50), whereas the Calabrian samples (C and E) presented just 19 and 22 exclusive peaks, respectively, being clearly more similar.

Once this method has been optimized and its usefulness to analyze licorice samples demonstrated, its extension to a higher number of samples of each location to statistically confirm the validity of the found markers to discriminate according their location will be assessed in a forthcoming paper.

4. Conclusions

The development of a new LC × LC-DAD-MS/MS method to obtain a complete phenolic compounds and saponins profile of licorice samples has been carried out in this work. The optimized method was able to separate a large number of compounds (up to 89 in the Iranian sample), which were grouped in the obtained 2D-plots according to their chemical class. Triterpene saponins were the most abundant metabolites followed by glycosylated flavanones and chalcones. Glyzyrrhizic acid was confirmed as the main component in all the studied samples. Moreover, the developed method not only permitted the assignment of compounds to a particular chemical family according to their position in the 2D-plot, but it was also employed to produce a typical pattern of each sample that could be later on be used to differentiate among geographical locations, once statistically validated. A good number of unique components (from 19 to 50) were found in all the samples. Thus, the usefulness of this method to generate patterns that could be potentially employed to confirm the authenticity and geographical origin of unknown or suspected licorice samples is demonstrated.

Acknowledgments

M. H. would like to thank MICINN for his “Ramón y Cajal” research contract. The authors would like to thank Project AGL2014-53609-P (MINECO, Spain) for financial support. This work was also funded by Italian Ministry of Research and University (MIUR) and European Commission (Project PON01_00636: Anti-counterfeiting technologies and materials and nanotechnologies for authentication and protection of agrifood excellence – “Fingerimball”).

References

[1] S.W. Kim, Y. Jin, J.H. Shin, I.D. Kim, H.K. Lee, S. Park, P.-L. Han, J.-K. Lee, Glycyrrhizic acid affords robust neuroprotection in the postischemic brain via anti-inflammatory effect by inhibiting HMGB1 phosphorylation and secretion, Neurobiol. Dis. 46 (2012) 147–156.
[2] D. Dhingra, A. Sharma, Antidepressant-like activity of *Glycyrrhiza glabra* L. in mouse models of immobility tests, Prog. Neuropsychopharmacol. Biol. Psychiatry 30 (2006) 449–454.
[3] S. Laconi, M.A. Madeddu, R. Pompei, Autophagy activation and antiviral activity by a licorice triterpene, Phytother. Res. 28 (2014) 1890–1892.
[4] R. Mohseni, F. Noorbakhsh, M. Moazeni, A.N. Omran, S. Rezaie, Antitoxin characteristic of licorice extract: the inhibitory effect on aflatoxin production in *Aspergillus parasiticus*, J. Food Saf. 34 (2014) 119–125.
[5] N. Martins, L. Barros, M. Dueñas, C. Santos-Buelga, I.C.F.R. Ferreira, Characterization of phenolic compounds and antioxidant properties of *Glycyrrhiza glabra* L. rhizomes and roots, RSC Adv. 5 (2015) 26991–26997.
[6] S. Zhou, J. Cao, F. Qiu, W. Kong, S. Yang, M. Yang, Simultaneous determination of five bioactive components in radix *Glycyrrhizae* by pressurised liquid extraction combined with UPLC–PDA and UPLC/ESI–QTOF–MS confirmation, Phytochem. Anal. 24 (2013) 527–533.
[7] P. Montoro, M. Maldini, M. Russo, S. Postorino, S. Piacente, C. Pizza, Metabolic profiling of roots of liquorice (*Glycyrrhiza glabra*) from different geographical areas by ESI/MS/MS and determination of major metabolites by LC-ESI/MS and LC-ESI/MS/MS, J. Pharm. Biomed. Anal. 54 (2011) 535–544.
[8] M.A. Farag, A. Porzel, L.A. Wessjohann, Unequivocal glycyrrhizin isomer determination and comparative in vitro bioactivities of root extracts in four *Glycyrrhiza* species, J. Adv. Res. 6 (2015) 99–104.
[9] M.A. Farag, A. Porzel, L.A. Wessjohann, Comparative metabolite profiling and fingerprinting of medicinal licorice roots using a multiplex approach of GC–MS, LC–MS and 1D NMR techniques, Phytochemistry 76 (2012) 60–72.
[10] M. Russo, D. Serra, F. Suraci, R. Di Sanzo, S. Fuda, S. Postorin, The potential of e-nose aroma profiling for identifying the geographical origin of licorice (*Glycyrrhiza glabra* L.) roots, Food Chem. 165 (2014) 467–474.
[11] Commission Implementing Regulation (EU) No 1072/2011 of 20 October 2011, Off. J. Eur. Union (2011), http://dx.doi.org/10.3000/19770677.L_2011.278.eng. ISSN 1977-0677.
[12] W.W. Huang, M.Y. Wang, H.M. Shi, Y. Peng, C.S. Peng, M. Zhang, Y. Li, J. Lu, X.B. Li, Comparative study of bioactive constituents in crude and processed *Glycyrrhizae* radix and their respective metabolic profiles in gastrointestinal tract in-vitro by HPLC-DAD and HPLC-ESI/MS analyses, Arch. Pharm. Res. 35 (2012) 1945–1952.

[13] W.C. Liao, Y.-H. Lin, T.-M. Chang, W.-Y. Huang, Identification of two licorice species, *Glycyrrhiza uralensis* and *Glycyrrhiza glabra*, based on separation and identification of their bioactive components, Food Chem. 132 (2012) 2188–2193.
[14] Y.J. Li, J. Chen, Y. Li, Q. Li, Y.F. Zheng, Y. Fu, P. Li, Screening and characterization of natural antioxidants in four *Glycyrrhiza* species by liquid chromatography coupled with electrospray ionization quadrupole time-of-flight tandem mass spectrometry, J. Chromatogr. A 1218 (2011) 8181–8191.
[15] W. Tao, J. Duan, R. Zhao, X. Li, H. Yan, J. Li, S. Guo, N. Yang, Y. Tang, Comparison of three officinal Chinese pharmacopoeia species of *Glycyrrhiza* based on separation and quantification of triterpene saponins and chemometrics analysis, Food Chem. 141 (2013) 1681–1689.
[16] T. Xu, M. Yang, Y. Li, X. Chen, Q. Wang, W. Deng, X. Pang, K. Yu, B. Jiang, S. Guan, D.-A. Guo, An integrated exact mass spectrometric strategy for comprehensive and rapid characterization of phenolic compounds in licorice, Rapid Commun. Mass Spectrom. 27 (2013) 2297–2309.
[17] S. Ji, Q. Wang, X. Qiao, H.C. Guo, Y.F. Yang, T. Bo, C. Xiang, D.A. Guo, M. Ye, New triterpene saponins from the roots of *Glycyrrhiza yunnanensis* and their rapid screening by LC/MS/MS, J. Pharm. Biomed. Anal. 90 (2014) 15–26.
[18] P.J. Schoenmakers, G. Vivó-Truyols, W.M.C. Decrop, A protocol for designing comprehensive two-dimensional liquid chromatography separation systems, J. Chromatogr. A 1120 (2006) 282–290.
[19] F. Cacciola, P. Jandera, E. Blahovà, L. Mondello, Development of different comprehensive two dimensional systems for the separation of phenolic antioxidants, J. Sep. Sci. 29 (2006) 2500–2513.
[20] P. Dugo, F. Cacciola, M. Herrero, P. Donato, L. Mondello, Use of partially porous column as second dimension in comprehensive two-dimensional system for analysis of polyphenolic antioxidants, J. Sep. Sci. 31 (2008) 3297–3308.
[21] J. Zhang, D. Tao, J. Duan, Z. Liang, W. Zhang, L. Zhang, H. Yushu, Z. Yukui, Separation and identification of compounds in *Adinandra nitida* by comprehensive two-dimensional liquid chromatography coupled to atmospheric pressure chemical ionization source ion trap tandem mass spectrometry, Anal. Bioanal. Chem. 386 (2006) 586–593.
[22] X. Qiao, W. Song, S. Ji, Q. Wang, D.A. Guo, M. Ye, Separation and characterization of phenolic compounds and triterpenoid saponins in licorice (*Glycyrrhiza uralensis*) using mobile phase-dependent reversed-phase× reversed-phase comprehensive two-dimensional liquid chromatography coupled with mass spectrometry, J. Chromatogr. A 10 (2015) 36–45.
[23] F. Cacciola, P. Donato, D. Giuffrida, G. Torre, P. Dugo, L. Mondello, Ultra high pressure in the second dimension of a comprehensive two-dimensional liquid chromatographic system for carotenoid separation in red chili peppers, J. Chromatogr. A 1255 (2012) 244–251.
[24] P. Dugo, D. Giuffrida, M. Herrero, P. Donato, L. Mondello, Epoxycarotenoids esters analysis in intact orange juices using two-dimensional comprehensive liquid chromatography, J. Sep. Sci. 32 (2009) 973–980.
[25] L. Mondello, M. Herrero, T. Kumm, P. Dugo, H. Cortes, G. Dugo, Quantification in comprehensive two-dimensional liquid chromatography, Anal. Chem. 80 (2008) 5418–5424.
[26] B. Winther, J.L.E. Reubsaet, Application of supplementary flow in comprehensive 2D liquid chromatography combining SEC and RPC, J. Sep. Sci. 28 (2005) 477–482.
[27] E.J.C. van der Klift, G. Vivó-Truyols, F.W. Claassen, F.L. van Holthoon, T.A. van Beek, Comprehensive two-dimensional liquid chromatography with ultraviolet, evaporative light scattering and mass spectrometric detection of triacylglycerols in corn oil, J. Chromatogr. A 1178 (2008) 43–55.
[28] Q. Yang, X. Shi, Q. Gu, S. Zhao, Y. Shan, G. Xu, On-line two dimensional liquid chromatography/mass spectrometry for the analysis of triacylglycerides in peanut oil and mouse tissue, J. Chromatogr. B 895 (2012) 48–55.
[29] P. Dugo, T. Kumm, B. Chiofalo, A. Cotroneo, L. Mondello, Separation of triacylglycerols in a complex lipidic matrix by using comprehensive two-dimensional liquid chromatography coupled with atmospheric pressure chemical ionization mass spectrometric detection, J. Sep. Sci. 29 (2006) 1146–1154.
[30] L. Montero, M. Herrero, M. Prodanov, E. Ibáñez, A. Cifuentes, Characterization of grape seed procyanidins by comprehensive two-dimensional hydrophilic interaction× reversed phase liquid chromatography coupled to diode array detection and tandem mass spectrometry, Anal. Bioanal. Chem. (2013) 4627–4638.
[31] L. Montero, M. Herrero, E. Ibáñez, A. Cifuentes, Profiling of phenolic compounds from different apple varieties using comprehensive two-dimensional liquid chromatography, J. Chromatogr. A 1313 (2013) 275–283.
[32] K.M. Kalili, J. Vestner, M.A. Stander, A. de Villiers, Toward unraveling grape tannin composition: application of online hydrophilic interaction chromatography × reversed-phase liquid chromatography–time-of-flight mass spectrometry for grape seed, Anal. Chem. 85 (2013) 9107–9115.
[33] K.M. Kalili, S. de Smet, T. van Hoeylandt, F. Lynen, A. de Villiers, Comprehensive two-dimensional liquid chromatography coupled to the ABTS radical scavenging assay: a powerful method for the analysis of phenolic antioxidants, Anal. Bioanal. Chem. 406 (2014) 4233–4242.
[34] C.M. Willemse, M.A. Stander, J. Vestner, A.G.J. Tredoux, A. de Villiers, Comprehensive two-dimensional hydrophilic interaction chromatography (HILIC) × reversed-phase liquid chromatography coupled to high-resolution mass spectrometry (RP-LC-UV-MS) analysis of anthocyanins and derived pigments in red wine, Anal. Chem. 87 (2015) 12006–12015.
[35] L. Montero, M. Herrero, E. Ibáñez, A. Cifuentes, Separation and characterization of phlorotannins from brown algae *Cystoseira abies-marina* by comprehensive two-dimensional liquid chromatography, Electrophoresis 35 (2014) 1644–1651.
[36] L. Montero, A.P. Sánchez-Camargo, V. García-Cañas, A. Tanniou, V. Stiger-Pouvreau, M. Russo, L. Rastrelli, A. Cifuentes, M. Herrero, E. Ibáñez, Anti-proliferative activity and chemical characterization by comprehensive two-dimensional liquid chromatography coupled to mass spectrometry of phlorotannins from the brown macroalga *Sargassum muticum* collected on North-Atlantic coasts, J. Chromatogr. A (2015), http://dx.doi.org/10.1016/j.chroma.2015.07.053.
[37] X. Li, D.R. Stoll, P.W. Carr, Equation for peak capacity estimation in two-dimensional liquid chromatography, Anal. Chem. 81 (2008) 845–850.
[38] S.S. Azimova, V.I. Vinogradova (Eds.), Natural Compounds. Flavonoids. Plant Sources, Structure and Properties, Springer, New York, Heidelberg Dordrecht, London, 2013, ISBN 978-0-387-49140-0.
[39] Q. Yin, P. Wang, A. Zhang, H. Sun, X. Wu, X. Wang, Ultra-performance LC-ESI/quadrupole-TOF MS for rapid analysis of chemical constituents of Shaoyao-Gancao decoction, J. Sep. Sci. 36 (2013) 1238–1246.
[40] S. Zhou, J. Cao, F. Qiu, W. Kong, S. Yang, M. Yang, Simultaneous determination of five bioactive components in radix Glycyrrhizae by pressurised liquid extraction combined with UPLC–PDA and UPLC/ESI–QTOF–MS confirmation, Phytochem. Anal. 24 (2013) 527–533.
[41] P. Wang, B. Wang, J. Xu, J. Sun, Q. Yan, B. Ji, Y. Zhao, Z. Yu, Detection and chemical profiling of Ling-Gui-Zhu-Gan decoction by ultra performance liquid chromatography-hybrid linear ion trap-orbitrap mass spectrometry, J. Chromatogr. Sci. 53 (2015) 263–273.
[42] S. Wang, L. Chen, J. Leng, P. Chen, X. Fan, Y. Cheng, Fragment ion diagnostic strategies for the comprehensive identification of chemical profile of Gui-Zhi-Tang by integrating high-resolution MS, multiple-stage MS and UV information, J. Pharm. Biomed. Anal. 98 (2014) 22–35.
[43] R. Simons, J. Vincken, E.J. Bakx, M.A. Verbruggen, H. Gruppen, A rapid screening method for prenylated flavonoids with ultra-high-performance liquid chromatography/electrospray ionisation mass spectrometry in licorice root extracts, Rapid Commun. Mass Spectrom. 23 (2009) 3083–3093.
[44] Y. Wang, S. He, X. Cheng, Y. Lu, Y. Zou, Q. Zhang, UPLC–Q-TOF-MS/MS fingerprinting of traditional Chinese formula SiJunZiTang, J. Pharm. Biomed. Anal. 80 (2013) 24–33.
[45] S. Chen, C. Lu, R. Zhao, Identification and quantitative characterization of PSORI-CM01, a Chinese medicine formula for psoriasis therapy, by liquid chromatography coupled with an LTQ orbitrap mass spectrometer, Molecules 20 (2015) 1594–1609.
[46] Y. Qi, S. Li, Z. Pi, F. Song, N. Lin, S. Liu, Z. Liu, Chemical profiling of Wu-tou decoction by UPLC–Q-TOF-MS, Talanta 118 (2014) 21–29.
[47] M. Ye, S. Liu, Z. Jiang, Y. Lee, R. Tilton, Y. Cheng, Liquid chromatography/mass spectrometry analysis of PHY906, a Chinese medicine formulation for cancer therapy, Rapid Commun. Mass Spectrom. 21 (2007) 3593–3607.
[48] Y.F. Zheng, L.W. Qi, J.L. Zhou, P. Li, Structural characterization and identification of oleanane-type triterpene saponins in *Glycyrrhiza uralensis* Fischer by rapid-resolution liquid chromatography coupled with time-of-flight mass spectrometry, Rapid Commun. Mass Spectrom. 24 (2010) 3261–3270.
[49] S. Tao, Y. Huang, Z. Chen, Y. Chen, Y. Wang, Rapid identification of anti-inflammatory compounds from Tongmai Yangxin Pills by liquid chromatography with high-resolution mass spectrometry and chemometric analysis, J. Sep. Sci. (2015), http://dx.doi.org/10.1002/jssc.201401481.
[50] Y.J. Li, J. Chen, Y. Li, Q. Li, Y.F. Zheng, Y. Fu, P. Li, Screening and characterization of natural antioxidants in four *Glycyrrhiza* species by liquid chromatography coupled with electrospray ionization quadrupole time-of-flight tandem mass spectrometry, J. Chromatogr. A 1218 (2011) 8181–8191.
[51] S. Man, S. Guo, W. Gao, J. Wang, L. Zhang, X. Li, Identification of metabolic profiling of cell culture of licorice compared with its native one, Anal. Bioanal. Chem. 405 (2013) 3321–3329.
[52] W. Zhang, M.W. Saif, G.E. Dutschman, X. Li, W. Lam, S. Bussom, Z. Jiang, M. Ye, E. Chu, Y.C. Cheng, Identification of chemicals and their metabolites from PHY906, a Chinese medicine formulation, in the plasma of a patient treated with irinotecan and PHY906 using liquid chromatography/tandem mass spectrometry (LC/MS/MS), J. Chromatogr. A 1217 (2010) 5785–5793.
[53] M. He, H.Y. Lv, Y.P. Li, C.M.V. Gonçalves, N.P. Dong, L.S. Pan, P.L. Liu, Y.Z. Liang, A multiplex approach for the UPLC-PDA-MS/MS data: analysis of licorice, Anal. Methods 6 (2014) 2239–2246.
[54] J. Pollier, K. Morreel, D. Geelen, A. Goossens, Metabolite profiling of triterpene saponins in *Medicago truncatula* hairy roots by liquid chromatography Fourier transform ion cyclotron resonance mass spectrometry, J. Nat. Prod. 74 (2011) 1462–1476.
[55] G. Negri, R. Tabach, Saponins, tannins and flavonols found in hydroethanolic extract from *Periandra dulcis* roots, Rev. Bras. Farmacogn. 23 (2013) 851–860.
[56] G. Tan, Z. Zhu, H. Zhang, L. Zhao, Y. Liu, X. Dong, Z. Lou, G. Zhang, Y. Chai, Analysis of phenolic and triterpenoid compounds in licorice and rat plasma by high-performance liquid chromatography diode-array detection, time-of-flight mass spectrometry and quadrupole ion trap mass spectrometry, Rapid Commun. Mass Spectrom. 24 (2010) 209–218.
[57] S.A. Vasil'ev, M.M. Garazd, V.P. Khilya, 3-Phenoxychromones: natural distribution, synthetic and modification methods, biological properties, Chem. Nat. Compd. 42 (2006) 241–253.
[58] M. Liu, Q. Liu, Y.L. Liu, C.Y. Hou, T.J. Mabry, An acylated flavone C-glycoside from *Glycyrrhiza eurycarpa*, Phytochemistry 36 (1994) 1089–1090.

5.3. Focusing and non-focusing modulation strategies for the improvement of on-line two-dimensional hydrophilic interaction chromatography × reversed phase profiling of complex food samples.

Montero, L., Ibáñez, E., Russo, M., Rastrelli. L., Cifuentes, A., Herrero. M.

Subbmited to Analytica Chimica Acta, 2017

Elsevier Editorial System(tm) for Analytica Chimica Acta

Manuscript Draft

Manuscript Number:

Title: Focusing and non-focusing modulation strategies for the improvement of on-line two-dimensional hydrophilic interaction chromatography × reversed phase profiling of complex food samples.

Article Type: Full Length Article

Section/Category: SEPARATION METHODS

Keywords: Metabolite profiling; two-dimensional LC; licorice; active modulation; trapping columns; resolution

Corresponding Author: Dr. Miguel Herrero, Ph.D.

Corresponding Author's Institution: Institute of Food Science Research (CIAL-CSIC)

First Author: Lidia Montero

Order of Authors: Lidia Montero; Elena Ibañez, PhD; Mariateresa Russo, PhD; Luca Rastrelli, PhD; Alejandro Cifuentes, PhD; Miguel Herrero, Ph.D.

Manuscript Region of Origin: SPAIN

Suggested Reviewers: Oliver J Schmitz PhD
Professor, Applied Analytical Chemistry, Faculty of Chemistry, University of Duisburg-Essen
oliver.schmitz@uni-due.de

Francesco Cacciola PhD
Associate Professor, Dipartimento Farmaco-chimico , University of Messina
francesco.cacciola@unime.it

Tomáš Hájek PhD
Professor, Department of Analytical Chemistry, University of Pardubice
Tomas.Hajek@upce.cz

Michele Camenzuli PhD
Professor, Van 't Hoff Institute for Molecular Sciences, University of Amsterdam
M.Camenzuli@uva.nl

INSTITUTO DE INVESTIGACIÓN
EN CIENCIAS DE LA ALIMENTACIÓN

CSIC Consejo Superior de Investigaciones Científicas
UAM Universidad Autónoma de Madrid

Dr.
Miguel Herrero
Institute of Food Science Research (CSIC)
C/ Nicolás Cabrera, 9
Campus de Cantoblanco
28049 Madrid – SPAIN

Editor
Analytica Chimica Acta

Madrid, April 11th, 2017

Dear Editor,

Please, find attached an electronic copy of our manuscript entitled "**Focusing and non-focusing modulation strategies for the improvement of on-line two-dimensional hydrophilic interaction chromatography × reversed phase profiling of complex food samples.**" by Montero et al. We intend to publish this work as an original *full length article* in Analytica Chimica Acta, if the Editors accept it. The work describes in detail the use of different strategies to improve the performance (resolving power and sensitivity) of HILIC x RP methods applied to food analysis, using the metabolite profiling of licorice as a model sample. Among the different focusing and non-focusing modulation approaches tested, the use of active modulation retains the highest interest as this procedure allows to increase not only the attainable peak capacity but also to improve resolving power and sensitivity. The studied approaches are applied and compared for the first time in the food analysis domain. I confirm that the work is new and original and not under consideration elsewhere.

Sincerely,

Miguel Herrero

*Graphical Abstract

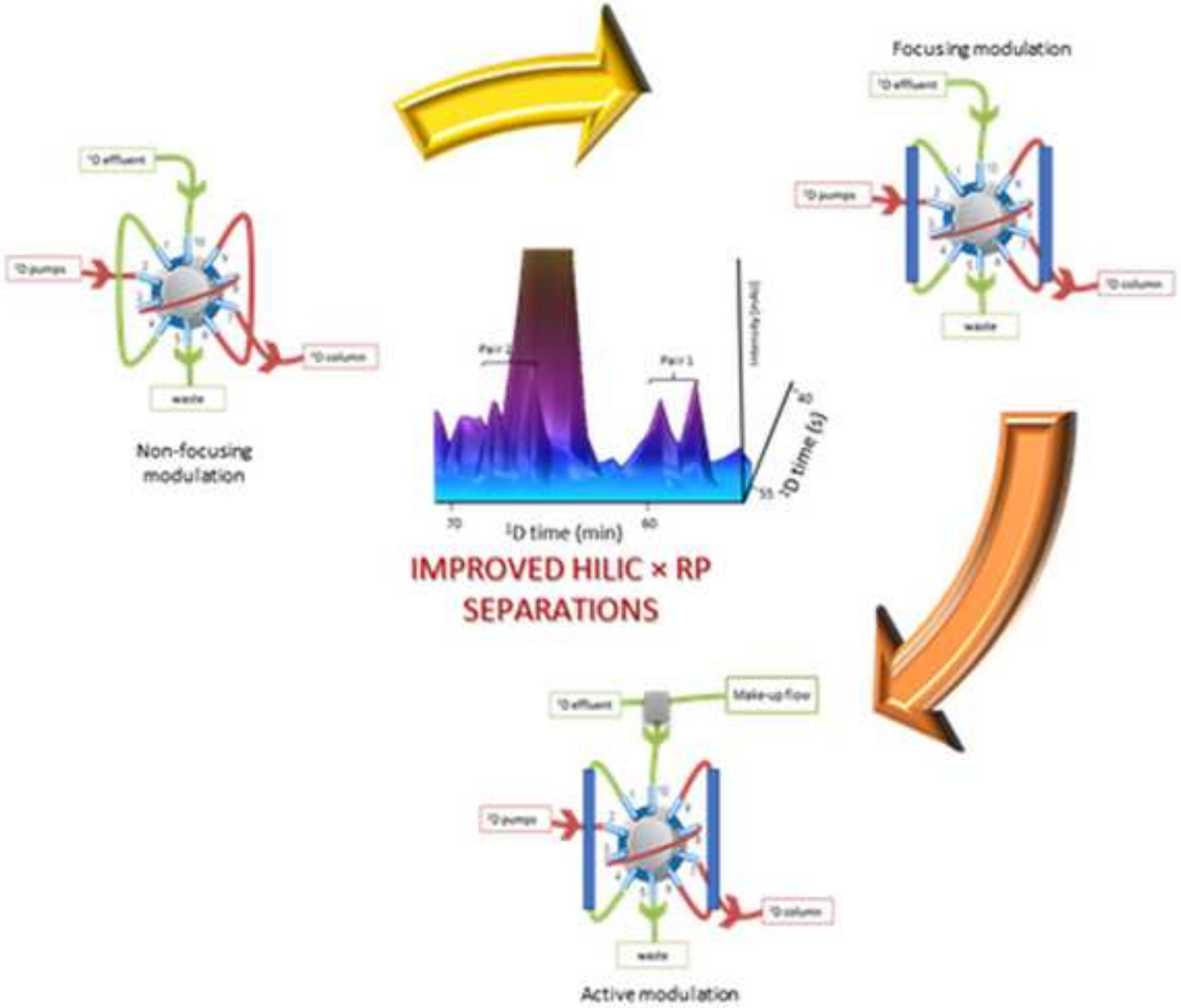

HIGHLIGHTS.

- Different focusing and non-focusing modulations studied to improve HILIC × RP

- Phenyl-hexyl trapping columns provided a satisfactory focusing effect

- Active modulation is demonstrated as the most suitable approach for licorice profiling

- Method sensitivity is improved by using focusing modulation strategies

- Up to 94 compounds can be separated in the metabolite profile of licorice

Focusing and non-focusing modulation strategies for the improvement of on-line two-dimensional hydrophilic interaction chromatography × reversed phase profiling of complex food samples.

Lidia Montero[a], *Elena Ibáñez*[a], *Mariateresa Russo*[b], *Luca Rastrelli*[c], *Alejandro Cifuentes*[a], *Miguel Herrero*[a*]

[a]Laboratory of Foodomics, Institute of Food Science Research (CIAL-CSIC), Nicolás Cabrera 9, 28049 - Madrid, Spain

[b]Laboratory of Food Chemistry, Dipartimento di Agraria (QuaSic.A.Tec.), Università Mediterranea di Reggio Calabria, Reggio Calabria, loc. Feo di Vito, 89122 - Reggio Calabria, Italy

[c]Dipartimento di Farmacia, Università di Salerno, Via Giovanni Paolo II 132, 84084 - Fisciano, Italy

Corresponding author: m.herrero@csic.es (M. Herrero)
TEL: +34 910 017 946
FAX: +34 910 017 905

ABSTRACT.

Comprehensive two-dimensional liquid chromatography (LC × LC) is ever gaining interest in food analysis, as often, food-related samples are too complex to be analyzed through one-dimensional approaches. The use of hydrophilic interaction chromatography (HILIC) combined with reversed phase (RP) separations has already been demonstrated as a very orthogonal combination, which allows attaining increased resolving power. However, this coupling encompasses different analytical challenges, mainly related to the important solvent strength mismatch between the two dimensions, besides those common to every LC × LC method. In the present contribution, different strategies are proposed and compared to further increase HILIC × RP method performance for the analysis of complex food samples, using licorice as a model sample. The influence of different parameters in non-focusing modulation methods based on sampling loops, as well as under focusing modulation, through the use of trapping columns in the interface and through active modulation procedures are studied in order to produce resolving power and sensitivity gains. Although the use of a dilution strategy using sampling loops as well as the highest possible first dimension sampling rate allowed significant improvements on resolution, focusing modulation produced significant gains also in peak capacity and sensitivity. Overall, the obtained results demonstrate the great applicability and potential that active modulation may have for the analysis of complex food samples, such as licorice, by HILIC × RP.

Keywords: Metabolite profiling, two-dimensional LC, licorice, active modulation, trapping columns, resolution.

1. INTRODUCTION

The use of multidimensional liquid chromatography (MDLC) within the food analysis field is gaining interest, as foods and food-related products are normally considered as very complex matrices [1]. That means that under food analysis is frequent to find a sample that is simply too complex to be analyzed by conventional one-dimensional chromatography. In other cases, food-related samples may not be so complex in terms of number of compounds present, but these could be composed by mixtures of closely related components that are also difficult to resolve. Although there are several approaches to MDLC of food, the use of comprehensive two-dimensional liquid chromatography (LC × LC) coupled on-line, presents different advantages over off-line modes as well as over other couplings, such as heart-cutting two-dimensional LC. Most-notably, faster separations may be obtained with high resolving power in a fully-automated way, thus, increasing robustness and reproducibility [2,3]. However, the optimization of a LC × LC method is far from being easy, as there are different inter-related parameters which modification may directly influence others [4]. These optimization challenges are even more pronounced when orthogonal separation mechanisms are coupled, which in practice, is the most-interesting approach. By selecting two independent non-correlated separation modes in both dimensions, significant gains on resolving power and peak capacity are potentially attainable. However, using two very different separation mechanisms in both dimensions means that important solvent incompatibility and/or immiscibility problems may be found. The combination between hydrophilic interaction chromatography (HILIC) in the first dimension (^{1}D) and reversed phase (RP) in the second dimension (^{2}D) has been shown to be characterized by a high degree of orthogonality for the analysis of complex food samples [5], providing with complementary retention. Although in these two separation

modes the same types of mobile phases are employed, their coupling can be termed as fairly incompatible, considering that the relative solvent strength is the opposite in each mode, thus, producing serious solvent mismatch.

In a LC × LC system, both dimensions are physically connected through the modulator. The most-widely employed modulator so far is based on the use of one or more switching valves equipped with two identical volume sampling loops [6]. This configuration allows the effective collection and injection of discrete ^{1}D effluent fractions into the ^{2}D continuously, by alternating the position and function of the two sampling loops. To translate this into practice, different analytical conditions should be established, mainly: i) a ^{1}D slow separation based on the use of very low flow rates, in order to minimize, as much as possible, the effluent fraction volume collected, and; ii) a fast ^{2}D using very high flow rates, in order to achieve fast separations in the shortest possible analysis time to allow a high ^{1}D sampling rate. As a consequence, set-ups involving the use of microbore columns in the ^{1}D combined with short wider columns (e.g., 4.6 mm i.d.) in the ^{2}D have provided good results [5]. This type of coupling implies the additional advantage of injecting relatively small volumes of ^{1}D effluent on the ^{2}D, thus, reducing possible band broadening. However, the main limitation directly related to the application of this approach is the characteristic low sensitivity obtained in LC × LC compared to regular one-dimensional methods, while potential deleterious issues due to solvent mismatch are maintained.

To partially alleviate these problems, different modulators have been designed; among them, thermal modulators are included. Within this group, several improvements have been presented, such as a vacuum-assisted evaporation interface aimed to remove the solvent from the ^{1}D effluent prior transfer to the ^{2}D [7], or the development of an on-column thermal modulation device [8]. This latter device was shown to be able to apply

heating and cooling cycles to capture and elute analytes to the ^{2}D producing narrower bands. However, due to their sophisticated and complicated design, these thermal modulators have not been to date extended to other applications. In parallel, new approaches have been explored taking advantage of the higher robustness and simplicity of valve-based modulation. One of the possibilities to enhance the performance is to substitute the regular sampling loops by trapping columns [9-11]. By using this approach, analytes are adsorbed by the stationary phase of the trap, typically with similar selectivity to that found in the ^{2}D, during the collection position, and are then eluted by the ^{2}D mobile phase in the injection position. Although, theoretically, the injection in ^{2}D mobile phase could also help to produce narrow bands and even focusing at the top of the ^{2}D column, there still may exist solvent incompatibility issues that may imply that not all the analytes contained in the ^{1}D effluent are efficiently retained in the trap. To overcome this issue, recently, a modulation procedure termed Active Modulation has been reported [12]; this approach is based on the introduction of a make-up flow of a weaker solvent after ^{1}D separation and before entrance to the trapping column. This way, a reduction in the solvent strength is fostered, increasing the retention of the trap towards the compounds separated in the ^{1}D. Subsequently, when the valve is actuated, those retained analytes can be eluted from the trap in narrow bands thanks to the ^{2}D mobile phase. From this basic procedure, other modifications can be performed in order not only to improve the transfer of ^{1}D effluent to the ^{2}D, but also to increase sensitivity and decrease analysis time. Although this active modulation approach retains a high potential for the analysis of complex samples, its applicability to food samples is still not demonstrated.

For this reason, the goal of the present work is to explore new possibilities to improve the separation of complex food samples, looking for quantitative improvements on

resolving power, avoiding ^{2}D band broadening, as well as on sensitivity, using licorice as model matrix. To this aim, different modifications at the modulator level are tested and compared, studying their applicability on a HILIC × RP coupling. The influence of the separation and modulation parameters applied on the separation and detection of the secondary metabolite profile of licorice, previously developed in our lab [13], including glycosylated flavanones and chalcones and other polyphenols as well as triterpene saponins, is evaluated.

2. MATERIALS AND METHODS.

2.1. Samples and chemicals.

Licorice samples (*Glycyrrhiza glabra*) from the region of Calabria, Italy, were collected in July 2015 and supplied from a local producer. For the extraction of secondary metabolites from this sample, a simple procedure based on solid-liquid extraction assisted by ultrasounds extraction was followed, as described before [14]. The extraction solvent was a binary mixture ethanol/water (1:1, v/v) using a sample-to-solvent ratio 1:5 (w/v) during 60 min. The resulting extract was filtered and evaporated to dryness. Prior injection, the extract was redissolved in water/acetonitrile (3:7, v/v).

HPLC grade ethanol and acetonitrile were purchased from VWR Chemicals (Barcelona, Spain) whereas ultrapure water was produced from a Milli-Q instrument (Millipore, Billerica, MA). Acetic and formic acids were supplied from Sigma-Aldrich (Madrid, Spain), while ammonium acetate was from Panreac (Barcelona, Spain).

2.2. Instrumentation.

The LC × LC-DAD instrumentation consisted on a first dimension (^{1}D) composed by an Agilent 1200 series liquid chromatograph (Agilent Technologies, Santa Clara, CA)

equipped with an autosampler. A Protecol flow-splitter (SGE Analytical Science, Milton Keynes, UK) was installed between the ^{1}D pumps and the autosampler in order to minimize the gradient delay volume of the pump and to obtain more reproducible low flow rates. The second dimension (^{2}D) was composed by an additional LC pump (Agilent 1290 Infinity). Both dimensions were connected by an electronically-controlled two-position ten-port switching valve (Rheodyne, Rohnert Park, CA, USA) acting as modulator equipped with two identical sampling loops or trap columns, as indicated. A diode array detector was coupled after the second dimension in order to register every ^{2}D analysis, working at a sampling rate of 20 Hz. The system was simultaneously controlled by two different PC running appropriate ChemStation software; one controlled the ^{1}D, the autosampler and DAD, whereas the other controlled the ^{2}D and actuated the switching valve. For the separations involving the use of a make-up flow, a third LC pump (Agilent 1200 Series) was connected through a t-piece between the outlet of ^{1}D and the switching valve. The used additional make-up flow was delivered at five-, seven- and nine-times the ^{1}D flow rate, as indicated.

The LC linear chromatograms were elaborated and visualized as 2D- and 3D-plots using LC Image software (version 1.0, Zoex Corp., Houston, TX).

2.3. HILIC × RP separation conditions.

Different conditions and column combinations were employed during this research, as described in Section 3. The common analytical conditions for each column used in the ^{1}D were the following:

i) SeQuant ZIC-HILIC (150 × 1 mm, 3.5 µm, Merck, Darmstadt, Germany) column, eluted using (A) acetonitrile and (B) 10 mM ammonium acetate at pH 5.0 as mobile phases, according to the following gradient: 0 min, 3% B; 5 min, 3% B; 10 min, 5% B;

15 min, 10% B; 30 min, 20% B; 40 min, 20% B; 50 min, 30% B; 60 min, 30% B; 65 min, 40% B; 80 min, 40% B. The injection volume was 5 µL and the flow rate was set at 15 µL min^{-1}.

ii) ZIC-HILIC (250 × 2.1 mm, 3.5 µm, Merck, Darmstadt, Germany) column, eluted using (A) acetonitrile and (B) 10 mM ammonium acetate at pH 5.0 as mobile phases, according to the following gradient: 0 min, 3% B; 10 min, 3% B; 30 min, 10% B; 50 min, 15% B; 60 min, 20% B; 90 min, 40% B. The injection volume was 15 µL and the flow rate was set at 100 µL min^{-1}.

On the other hand, the common analytical conditions for each column used in the ^{2}D were the following:

i) Ascentis Express C_{18} (50 × 4.6 mm, 2.7 µm, Supelco, Bellefonte, CA) partially porous column using (A) water (0.1% formic acid) and (B) acetonitrile as mobile phases, eluted at 3 mL min^{-1} using two segment gradients: from 0 min to 23.4 min the ^{2}D gradient elution was 0 min, 0% B, 0.1 min, 5% B; 0.5 min, 35% B; 0.9 min, 70% B; 1 min, 90% B; 1.01 min, 0% B; 1.3 min, 0% B; from 23.4 to 80 min the employed gradient was programmed as 0 min, 0% B; 0.1 min, 5% B; 0.3 min, 35% B; 0.5 min, 40% B; 0.9 min, 50% B; 1 min, 90% B; 1.01 min, 0% B; 1.3 min, 0% B.

ii) Ascentis Express C_{18} (30 × 4.6 mm, 2.7 µm, Supelco, Bellefonte, CA) partially porous column using (A) water (0.1% formic acid) and (B) acetonitrile as mobile phases, eluted at 2 mL min^{-1}. Different gradients were applied depending on the modulation time applied. The different step gradients are detailed in Table S1.

When indicated, sets of trapping columns formed by two identical cartridges were employed including C_{18} and phenyl-hexyl (10 × 3 mm, 2.6 µm, Accucore, Thermo Scientific, Waltham,MA) stationary phases.

UV-Vis spectra were collected in the range of 190-550 nm using a sampling rate of 20 Hz, while 254, 280 and 330 nm signals were also independently recorded.

2.4. Calculations.

2.4.1 Peak capacity.

Individual peak capacity for each dimension (n_c) was calculated according to eq. 1:

$$n_c = 1 + \frac{t_G}{\overline{w}} \qquad (1)$$

where t_G is the gradient time and $\overline{w}$ is the average peak width. For ^{1}D peak capacity calculations, the average peak width was obtained from *ca.* 10 representative peaks selected along the analysis. Likewise, for ^{2}D peak capacity, as much as possible peaks were considered (*ca.* 20 peaks, depending on the analysis). Additionally, ^1n_c was also calculated considering the peak broadening factor <β>, giving rise to a corrected ^{1}D peak capacity (eq. 2), that considers the influence of the deleterious effect of undersampling. To estimate <β>, the sampling time (t_s) as well as the average width of ^{1}D peaks as standard deviation in time units ($^1\sigma$) before modulation were considered:

$$^1n_{c,corrected} = \frac{^1n_c}{\sqrt{1+0.21\left(\frac{t_S}{^1\sigma}\right)^2}} \qquad (2)$$

For each two-dimensional set-up, different peak capacity values were estimated. First of all, theoretical peak capacity was obtained following the so-called product rule, using eq. 3, considering the individual peak capacities obtained in each dimension:

$$^{2D}n_{c,theoretical} = {}^1n_c \times {}^2n_c \qquad (3)$$

As eq. 3 does not take into consideration the deleterious effects due to the modulation process as well as possible undersampling, a more realistic peak capacity value was obtained from the equation proposed by Li et al. [15] denominated here as practical peak capacity (eq. 4):

$$ {}^{2D}n_{c,practical} = \frac{{}^{1}n_c \times {}^{2}n_c}{\sqrt{1+3.35\times\left(\frac{{}^{2}t_c\ {}^{1}n_c}{{}^{1}t_G}\right)^2}} \qquad (4) $$

being $^{2}t_c$, the ^{2}D separation cycle time, which is equal to the modulation time. This latter equation also includes the <β> parameter accounting for undersampling. Moreover, to more precisely compare among set-ups and in order to evaluate possible peak clusters along the 2D analysis and, thus, to estimate 2D space coverage, the orthogonality degree (A_O) was considered to offer the denominated 2D corrected (also known as effective) peak capacity, as follows:

$$ {}^{2D}n_{c,corrected} = {}^{2D}n_{c,practical} \times A_O \qquad (5) $$

2.4.2 Orthogonality.

Among the different approaches that have been described and published to quantify the orthogonality degree of a two-dimensional set-up [16], the method proposed by Camenzuli and Schoenmakers [17] was employed in the present work to calculate system orthogonality (A_O). This procedure takes into account the spread of each peak along the four imaginary lines that cross the 2D space forming an asterisk, that is Z_1, Z_2 (vertical and horizontal lines) and Z_{-}, Z_{+} (diagonal lines of the asterisk). Z parameters describe the use of the separation space with respect to the corresponding Z line, allowing to semi-quantitatively diagnose areas of the separation space where sample components are clustered, thus, reducing in practice orthogonality. For the determination of each Z parameter, the S_{Zx} value was calculated, as the measure of

spreading around the Z_x line, using the retention times of all the separated peaks in each 2D analysis.

2.4.3. Two-dimensional resolution.

The resolution metric for two-dimensional separations proposed by Peters et al. [18] was employed to calculate a representative resolution value and the separation quality of each set-up. This measure is based on the valley-to-peak ratio between two neighbor peaks. To establish the valley-to-peak ratio between two peaks (peak 1 and peak 2), three maximum intensities are considered: the maximum of the peak 1 (max1), the saddle point between both peaks (S) and the maximum of peak 2 (max2), as well as the distances between max1 and S, $d_{1,S,}$ and the distance between S and max2, $d_{S,2}$.

$$d_{1,S} = \sqrt{\left(\Delta^1 t_{R1,S}\right)^2 + \left(\Delta^2 t_{R1,S}\right)^2} \quad (6)$$

$$d_{1,S} = \sqrt{\left(\Delta^1 t_{RS,2}\right)^2 + \left(\Delta^2 t_{RS,2}\right)^2} \quad (7)$$

where $\Delta^1 t_{R1,S}$ and $\Delta^2 t_{R1,S}$ are the differences on time between max1 and S in the ^{1}D and ^{2}D and $\Delta^1 t_{RS,2}$ and $\Delta^2 t_{RS,2}$ the difference between S and max2 in both dimensions.

Then, the intensity g is defined in accordance with the graphic showed in Figure S1. Intensity g is calculated by:

$$g = \frac{d_{1,S} h_{max2} + d_{S,2} h_{max1}}{d_{1,s} + d_{2,S}} \quad (8)$$

where h_{max1} and h_{max2} are the maximum intensities of peak 1 and peak 2, respectively.

The valley-to-peak ratio (V) is calculated as:

$$V = \frac{f}{g} = \frac{(g - h_s)}{g} \quad (9)$$

Finally, resolution (Rs) is estimated by the following equation:

$$R\text{s} = \sqrt{-\frac{1}{2}\ln\left(\frac{1-V}{2}\right)} \quad (10)$$

In this work, the resolution measurement of two target critical pairs of peaks was calculated in each instrumental configuration, and results obtained compared among them.

3. RESULTS AND DISCUSSION

In our previous work, the first LC × LC application devoted to the profiling of secondary metabolites in licorice was developed [13]. Although the method was characterized by excellent separation capabilities, being possible to detect around 80 compounds from different metabolite families in just one sample, further optimization is desirable to increase sensitivity and to further improve performance. This is mainly interesting due to the fact that this sample is a very diverse and complex mixture of some closely related components, such as glycosylated flavanones and chalcones among other polyphenols as well as triterpene saponins. In the present work, we have applied several strategies, using licorice as a model complex real food sample in order to quantitatively evaluate the attainable performance by introducing new changes in the interface.

3.1. Non-focusing modulation.

3.1.1. Influence of transfer volume/fraction solvent.

The most-extended approach to interface both dimensions in LC × LC is the use of two identical sampling loops installed on the switching valve(s) acting as modulator. In our original method, two 30 µL sampling loops were employed with satisfactory results. However, modifications at the interface and columns combination levels could further improve two of the most important points in a comprehensive LC separation: ^{1}D undersampling and ^{2}D band broadening. These two parameters have a clear deleterious

effect both on the resolving power as well as on the attainable peak capacity, and thus, should be minimized. The coupling between HILIC and RP is characterized by a very good degree of orthogonality, thus, being very attractive for the analysis of complex samples. Nevertheless, it generates a solvent mismatch during the transfer of ^{1}D effluent, considering that the weaker solvent in the ^{1}D is the stronger one on the ^{2}D environment. According to the intensity of this issue, the resulting ^{2}D separations may be completely ruined, or just worsened to a certain degree depending on the extent of the associated band broadening effect. For this reason, one of the possible strategies to avoid or reduce the mentioned solvent strength mismatch is to dilute the ^{1}D effluent before its transfer to the ^{2}D. When using a non-focusing modulation procedure based on sampling loops, this effect may be obtained through the use of loops with an internal volume higher than the strictly required to collect the ^{1}D effluent during the length of a modulation. That way, ^{1}D effluent supposes only part of the available loop volume whereas the rest is filled with ^{2}D starting mobile phase. However, it has to be also considered that, since short columns are employed in the ^{2}D to obtain fast separations, the increase on the sampling loop volume, which is also the injection volume for each individual ^{2}D separation, may negatively influence the separation [19].

Accordingly, the first step was to study the effects of sampling volume and fraction solvent on the ^{2}D, comparing the separation attainable using sampling loops with different internal volume, i.e., 20, 30 and 50 µL. To do that, experimental conditions based on the use of the ZIC-HILIC microbore column in the ^{1}D and the use of a 50 × 4.6 mm, 2.7 µm C_{18} partially porous column in the ^{2}D, using 78 s as modulation and ^{2}D analysis time, were applied (see Section 2.3). As can be observed in Table 1 and Figure S2A-C, the results in terms of overall separation, resolution and orthogonality were fairly similar. Interestingly, a slight but noticeable increase on theoretical peak capacity

was obtained when the sampling loops volume was bigger. This behavior would correspond to a decrease on average ^{2}D peak widths as a response to higher dilution of the ^{1}D effluent and, thus, to inject each fraction on the ^{2}D in weaker solvent, thus, improving peak shape with respect to less diluted injected fractions. As can be also observed in Table 1, 50 µL fractions injected in the ^{2}D meant an injection volume of 10% of column void volume, considering that partially porous particles may occupy around 40% of the total available column inner volume [20,21]. Thus, the reduction on the fraction solvent strength obtained when using 50 µL sampling loops (a 2.6-fold dilution) was able to make up for the possible deleterious effect due to increased injection volume. In fact, the use of 10% column void volume was significantly higher than the 3% previously reported in order to not get peak distortion [19]. In spite of the increment obtained in theoretical peak capacity, no practical gains on separation were observed (Figure S2A-C).

3.1.2. Influence of sampling frequency.

Possible enhancements on resolving power could be obtained minimizing the effect of ^{1}D undersampling. One of the concepts that characterize the performance of an on-line LC × LC method is the importance of maintaining the separation obtained in the ^{1}D during the transfer of ^{1}D effluent to the ^{2}D. If the sampling process is too slow to collect fractions where two well separated ^{1}D peaks are involved, undersampling arises; in that case, a remix of these previously separated peaks occurs in the transfer process, producing a loss of the ^{1}D separation and peak capacity. To reduce this negative effect, higher sampling frequencies should be applied, in order to obtain more ^{1}D fractions analyzed in the ^{2}D. Murphy et al. [22] established the widely-accepted rule of sampling 3-4 times each ^{1}D peak to solve the remix problem and to maintain the ^{1}D separation.

However, in this case, due to instrumental limitations, it was not possible to reduce the analysis time used with the 50 mm C_{18} partially porous column employed. Changes in the ^{2}D gradient did not produce any noticeable improvement either. For this reason, an even shorter column was tested. A 30 × 4.6 mm C_{18} partially porous column (2.7 µm) was coupled to the formerly optimized ^{1}D. By using this shorter column, a proper separation was obtained allowing a decrease on total ^{2}D analysis time (gradient time + re-equilibration time) to just 60 s. Under these analytical conditions, the use of the three different transfer volumes was studied (Figure S2D-F). As can be observed from the data summarized in Table 1, theoretical peak capacities obtained using the 30 mm column were lower than those attainable using the 50 mm, as a result of the great dependence of $^{2}n_c$ on the available gradient time. However, as a result of the faster ^{1}D sampling rate applied when the shorter column was used, both orthogonality and resolution of pair 1 were improved, independently of the transfer volume employed (see Table 1). This improvement was more pronounced when using 50 µL sampling loops, as deduced from the data shown on Table 1 and illustrated in Figure 1A-B and Figure S2. In this latter set-up, the ^{2}D injection volume was equal to 17% of column void volume. Although this relative injection volume is rather high, no appreciable distorted peaks were detected compared to 20 and 30 µL transfer volumes; indeed, the dilution effect achieved using 50 µL, again allowed better retention of compounds due to the greater dilution in ^{2}D compatible mobile phase could produce a better interaction of the analytes with the stationary phase (see Figure S2D-F and Figure S3).

Although these conditions clearly improved the results attainable using the longer column, the use of higher separation temperature was also explored to investigate if proper ^{2}D separations could be obtained in even shorter analysis times, thus, further increasing ^{1}D sampling rate. To do that, the ^{2}D column was thermostated at 40 ºC and

several changes were applied to the gradient profile to adapt the separation to a total 39 and 50 s analysis times (Table S1). In order to establish a wider evaluation, the results obtained using the different mentioned modulation times (39, 50 and 60 s) were also compared with the longer 78 s ^{2}D modulation time previously employed with the 50 mm column. In this regard, considering that faster ^{1}D sampling rates imply that less ^{1}D effluent volume is transferred to the ^{2}D, the use of sampling loops volume of 50 µL was considered too high; for this reason, to perform these series of experiments, 20 µL sampling loops were installed in the switching valve, allowing more discrete transfers equivalent to 7% of total ^{2}D column void volume. Results are summarized in Table S2 and Figure 2. As can be observed, as the modulation time was reduced, $^{2}n_{c}$ values also decreased, as a result of the great influence that this value retains from the available ^{2}D t_G. In consequence, the practical 2D peak capacity also tended to decrease. However, the observed decrease is not more pronounced thanks to the better peak shapes obtained as consequence of higher dilution effect when using 39 s as modulation time; at those conditions, just 9.5 µL of ^{1}D effluent were transferred in each modulation, whereas the rest of the sampling volume was filled with ^{2}D mobile phase, thus, helping to reduce the solvent strength mismatch. Moreover, the effect of higher sampling rate is also illustrated on the attainable resolution between the two pairs of compounds studied. As illustrated in Figure 2, resolution between pair 1 improved when reducing the modulation time. In addition, compounds in pair 2 remained coletuted using modulation times of 78 and 60 s, but they could be separated using shorter modulation times.

3.2. Focusing modulation using trapping columns.

One of the possible implementations to reduce ^{2}D band broadening and to increase sensitivity limiting dilution is the use of trapping columns in the valve-based modulator.

Reduction on band broadening is accomplished by introducing a focusing effect, considering that the analytes eluting from the ^{1}D would be entrapped in the trapping column during the collection position. Once the valve is actuated, ^{2}D mobile phase would desorb the analytes in discrete bands, injecting them into the ^{2}D column. Even if this approach has a good potential, its use is very limited compared to regular loops-based modulation. In the food analysis field, only C_{18} trapping columns have been reported [11,23], in order to exactly match the selectivity of the ^{2}D column. In the present work, the use of trapping columns-based modulation to increase resolving power and sensitivity is extended to other stationary phases. Namely, the use of C_{18} and phenyl-hexyl trapping columns have been explored. The traps (10 × 3.0 mm, 2.6 µm) were installed in the modulator using the minimum possible extra volume for connections. The trapping columns void volume was 42 µL. Moreover, two elution configurations were compared, namely, forward and backflush elution. The use of the shortest available ^{2}D column was maintained, setting a modulation time of 60 s. Table 2 reports the most important method parameters related to these analyses. As can be observed, very similar results could be obtained using the two stationary phases available as well as both elution modes in terms of peak capacity and orthogonality attainable. Interestingly, using both elution modes resolution of critical pair 1 was maintained with respect to the best value attainable using non-focusing modulation, whereas, pair 2, that coeluted using the same separation conditions (60 s modulation time) with sampling loops, was also resolved. In any case, forward elution produced better resolution results for both tested stationary phases. Moreover, as can be appreciated from Figure S4, in general, ^{2}D peak shapes were improved also under forward elution compared to backflush elution. This effect would be obtained as a result of the longer available interaction allowed under forward elution, bearing in mind that

the trapping column was not fully filled with ^{1}D effluent during the collection position (see Figure 3A,B). In addition, although reduced to a minimum, a 2 µL tube was necessary to connect the trapping columns to the valve; consequently, there was a small fraction of ^{1}D effluent that did not enter the trapping column when backflush elution was employed (Figure 3B).

3.3. Focusing using active modulation.

The use of active modulation is a further evolution of the direct use of trapping columns. This modulation procedure, recently proposed [12], is based on the use of an additional make-up flow of a weak solvent for the ^{2}D in order to reduce the strength of the ^{1}D effluent prior entering the trapping column. This way, the interaction between the analytes and the functional groups in the trap is fostered, as illustrated in Figure 3C. Therefore, considering the high potential and relative simplicity that this implementation may have, it is worth to study its application to complex food samples. Considering the ^{1}D and ^{2}D mobile phases compositions, it was decided to use ultrapure water (0.1% formic acid) as make-up flow. It has been previously observed that a flow rate for the additional make-up flow 7-times higher than the ^{1}D flow rate was appropriate to achieve the desired effect [12]. However, to further study the possible influence of make-up flow rate on the overall separation performance, three different flow rates for each set of trapping columns (C_{18} and phenyl-hexyl) were tested, i.e., 5-, 7- and 9-times the ^{1}D flow rate. Table 3 summarizes the data describing the performance attained using active modulation for the profiling of secondary metabolites in licorice. As can be appreciated, as for trapping columns, the performance attainable using both stationary phases was very similar. In both cases, the use of higher make-up flow rates allowed a slight improvement on peak capacity, whereas orthogonality values

were essentially maintained. More relevant was the improvement observed for the resolution between the two studied pairs; in this regard, the use of make-up flow rates 9-times higher than the ^{1}D flow rate produced the best results (Figure 4).

3.4. Overall comparison.

As already described in the previous sections, different approaches have been considered to further improve the separation capabilities of the initial HILIC × RP method directed towards the profiling of secondary metabolites in licorice. In general, the use of focusing modulation, either using trapping columns or active modulation, allowed a clear improvement on the separation of the complex metabolite profile of this sample (Figure 1). In fact, these two approaches allowed obtaining good degrees of resolution between the studied pairs (Figures 4 and S4). In general, better separations were obtained using trapping columns in forward elution mode and using active modulation with make-up flow rates 9-times the ^{1}D flow rate. Although in both cases, the two stationary phases studied produced comparable performance, the phenyl-hexyl particles were slightly better than C_{18} particles. Under these conditions, similar orthogonality values as well as resolution between the critical pairs were obtained (Tables 2 and 3). However, practical peak capacities were significantly higher using active modulation (2131 vs 1811), and thus, this procedure resulted more favorable. The use of non-focusing modulation by sampling loops could only provide comparable performance in some aspects when modulation time was significantly reduced, thus, increasing ^{1}D sampling rate. However, due to very fast ^{2}D separations, the total 2D peak capacity attainable was severely compromised with respect to active modulation.

With the aim to further obtain more data illustrating the performance of each procedure, the attainable sensitivity under each separation conditions was studied by analyzing

peak S (Figure 5). Values of normalized sensitivity for each set-up are included in Tables 1-3. This value was obtained by considering the sensitivity for peak S in the original method with respect to the sensitivity obtained in each case. As can be observed from those results, the set-up involving the use of active modulation using phenyl-hexyl traps and make-up flow at 9-time ^{1}D flow rate produced the highest sensitivity enhancement. Consequently, active modulation was shown again as the best possible alternative set-up for the profiling of secondary metabolites in licorice by HILIC × RP in order to further enhance both resolving power and sensitivity.

In this regard, theoretically, further sensitivity gains could be obtained if a column with higher sample loadability is used in ^{1}D. For this reason, a last attempt was made using the optimum separation conditions but increasing the ^{1}D column internal diameter to 2.1 mm. That column allowed an increase on the injection volume to 15 µL, although higher ^{1}D flow rates were also needed to maintain the ^{1}D separation. This would have a deleterious effect on the fraction volume transferred to ^{2}D, but considering that active modulation was employed with trapping columns, the fraction volume should not have such a critical influence on the coupling. As shown in Table S3, the normalized sensitivity obtained was further increased with respect to the use of the microbore ^{1}D column (Figure 5F); however, the separation obtained was severely hampered, and the resolution between the critical pairs studied was completely lost (Table S3). Thus, this modification was not considered favorable, bearing in mind that compromises should be always taken between sensitivity, resolving power and overall peak capacity obtainable.

4. CONCLUSIONS.

In the present contribution, different strategies are proposed and compared to further increase HILIC × RP method performance for the analysis of complex food samples, using licorice as a model sample. When using non-focusing modulation based on sampling loops, the use of very short columns (30 mm) in the ^{2}D was shown to be beneficial to increase performance, taking advantage of higher sampling loops volume to increase solvent dilution, thus, minimizing the deleterious effects due to solvent strength mismatch between HILIC and RP. However, the use of focusing modulation procedures was demonstrated to be able to increase not only resolving power but also peak capacity, reducing the effects of solvent mismatch at the same time that producing a focusing effect at the beginning of the ^{2}D analyses. In addition, significant sensitivity gains could be also obtained through the use of active modulation with a relatively high make-up flow rate. A total of 94 peaks were successfully separated in the set-up involving the use of active modulation with phenyl-hexyl trapping columns and a make-up flow rate 9-times higher than the corresponding ^{1}D flow rate, compared to the initial method (79 peaks), increasing sensitivity more than twice. In summary, the results obtained demonstrate the great applicability and potential that active modulation may have for the profiling of complex food samples by HILIC × RP.

ACKNOWLEDGEMENTS.

The authors would like to thank Project AGL2014-53609-P (MINECO, Spain) for financial support.

REFERENCES.

[1] P.Q. Tranchida, P. Donato, F. Cacciola, M. Beccaria, P. Dugo, L. Mondello. Potential of comprehensive chromatography in food analysis. TrAC Trends Anal. Chem. 52 (2013) 186-205.

[2] M. Sarrut, G. Cretier, S. Heinisch. Theoretical and practical interest in UHPLC technology for 2D-LC. TrAC Trends Anal. Chem. 63 (2014) 104-112.

[3] X. Shi, S. Wang, Q. Yang, X. Lu, G. Xu, Comprehensive two-dimensional chromatography for analyzing complex samples: Recent new advances. Anal. Methods 6 (2014) 7112-7123.

[4] F. Bedani, P.J. Schoenmakers, H.G. Jansen. Theories to support method development in comprehensive two-dimensional liquid chromatography – a review. J. Sep. Sci. 35 (2012) 1697-1711.

[5] F. Cacciola, S. Farnetti, P. Dugo, P.J. Marriott, L. Mondello, Comprehensive two-dimensional liquid chromatography for polyphenol analysis in foodstuffs, J. Sep. Sci. 40 (2017) 7-24.

[6] M.J. Egeness, M.C. Breadmore, E.F. Hilder, R.A. Shellie. The modulator in comprehensive two-dimensional liquid chromatography. LC-GC Eur. 5 (2016) 268-276.

[7] H. Tian, J. Xu, Y. Guan. Comprehensive two-dimensional liquid chromatography (NPLC x RPLC) with vacuum-evaporation interface. J. Sep. Sci. 31 (2008) 1677–1685.

[8] M.E. Creese, M.J. Creese, J.P. Foley, H.J. Cortes, E.F. Hilder, R.A. Shellie, M.C. Breadmore. Longitudinal On-Column Thermal Modulation for Comprehensive Two-Dimensional Liquid Chromatography. Anal. Chem. 89 (2017) 1123–1130.

[9] R.J. Vonk, A.F.G. Gargano, E. Davydova, H.L. Dekker, S. Eeltink, L.J. de Koning, P.J. Schoenmakers. Comprehensive Two-Dimensional Liquid Chromatography with Stationary-Phase-Assisted Modulation Coupled to High-Resolution Mass Spectrometry

Applied to Proteome Analysis of *Saccharomyces cerevisiae*. Anal. Chem. 87 (2015) 5387–5394.

[10] Y. Zhao, S.S. W. Szeto, R.P.W. Kong, C.H. Law, G. Li, Q. Qan, Z. Zhang, Y. Wang, I.K. Chu. Online Two-Dimensional Porous Graphitic Carbon/Reversed Phase Liquid Chromatography Platform Applied to Shotgun Proteomics and Glycoproteomics. Anal Chem 86 (2014) 12172-12719.

[11] F. Cacciola, P. Jandera, E. Blahovà, L. Mondello, L. Development of different comprehensive two-dimensional systems for the separation of phenolic antioxidants. J. Sep. Sci. 29 (2006) 2500–2513.

[12] A.F. Gargano, M. Duffin, P. Navarro, P.J. Schoenmakers. Reducing dilution and analysis time in online comprehensive two-dimensional liquid chromatography by active modulation. Anal. Chem. 88 (2016) 1785-1793.

[13] L. Montero, E. Ibañez, M. Russo, R. di Sanzo, L. Rastrelli, A.L. Piccinelli, R. Celano, A. Cifuentes, M. Herrero. Metabolite profiling of licorice (*Glycyrrhiza glabra*) from different locations using comprehensive two-dimensional liquid chromatography coupled to diode array and tandem mass spectrometry detection. Anal. Chim. Acta 913 (2016) 145-159.

[14] P. Montoro, M. Maldini, M. Russo, S. Postorino, S. Piacente, C. Pizza. Metabolic profiling of roots of liquorice (*Glycyrrhiza glabra*) from different geographical areas by ESI/MS/MS and determination of major metabolites by LC-ESI/MS and LC-ESI/MS/MS, J. Pharm. Biomed. Anal. 54 (2011) 535-544.

[15] X. Li, D.R. Stoll, P.W. Carr. Equation for peak capacity estimation in two-dimensional liquid chromatography, Anal. Chem. 81 (2009) 845–850.

[16] M.R. Schure, J.M. Davis, Orthogonal separations: Comparison of orthogonalitymetrics by statistical analysis, J. Chromatogr. A 1414 (2015) 60-76.

[17] M. Camenzuli, P.J. Schoenmakers, A new measure of orthogonality for multi-dimensional chromatography. Anal. Chim. Acta 838 (2014) 93–101.

[18] S. Peters, G. Vivó-Truyols, P.J. Marriott, P.J. Schoenmakers. Development of a resolution metric for comprehensive two-dimensional chromatography. J. Chromatogr. A, 1146 (2007) 232–241.

[19] P. Jandera, T. Hajek, P. Cesla. Effects of the gradient profile, sample volume and solvent on the separation in very fast gradients, with special attention to the second-dimension gradient in comprehensive two-dimensional liquid chromatography. J. Chromatrogr. A 1218 (2011) 1995-2006.

[20] F. Gritti, G. Guiochon. Theoretical investigation of diffusion along columns packed with fully and superficially porous particles. J. Chromatogr. A, 1218 (2011) 3476-3488.

[21] R. Hayes, A. Ahmed, T. Edge, H. Zhang. Core–shell particles: Preparation, fundamentals and applications in high performance liquid chromatography. J. Chromatogr. A 1357 (2014) 36-52.

[22] R.E. Murphy, M.R. Schure, J.P. Foley. Effect of Sampling Rate on Resolution in Comprehensive Two-Dimensional Liquid Chromatography. Anal. Chem.70 (1998) 1585–1594.

[23] F. Cacciola, P. Jandera, Z. Hajdù, P. Česla, L. Mondello, L. Comprehensive two-dimensional liquid chromatography with parallel gradients for separation of phenolic and flavone antioxidants. J. Chromatogr. A 1149 (2007) 73–87.

FIGURE LEGENDS

Figure 1. Resolution obtained for peaks included in critical pair 1 (white oval) and in critical pair 2 (black oval) in the different set-ups studied. A, using 50 µL sampling loops in combination with a 50 mm long column in the ^{2}D; B, using 50 µL sampling loops in combination with a 30 mm long column in the ^{2}D; C, using Phenyl-hexyl trapping columns with forward elution, and; D, using active modulation with phenyl-hexyl traps and make-up flow rate equal to 9-times ^{1}D flow rate.

Figure 2. Dependence of practical peak capacity ($^{2D}n_{c,practical}$) (●), 2D resolution reached for pair 1 (■), and 2D resolution for pair 2 (×) on modulation time. For detailed separation conditions, see section 2.3.

Figure 3. Hypothetical scheme of the retention/elution of secondary metabolites from licorice into the trapping columns under forward elution mode (A), backflush elution mode (B), and active modulation (C) set-ups studied, following the procedure: 1) Trapping column filled with ^{2}D initial mobile phase (injection position, just after valve actuation); 2) Trapping column filled with ^{1}D effluent fraction (collection position) diluted in strong (A and B) or weak (C) solvent; 3) start of ^{2}D gradient. Arrows indicate flow direction.

Figure 4. Resolution obtained by using active modulation with phenyl-hexyl trapping columns of the two pairs of the studied peaks, using make-up flow rates equal to 5- (A), 7- (B) and 9-times (C) ^{1}D flow rate, and practical scheme of the calculation of the valley-to-peak ratio used for the estimation of resolution between critical pairs 1 and 2 (D).

Figure 5. A, 2D-plot (254 nm) of the separation obtained in the original method. Sensitivity comparison (peak S) of the original method with the set-up of each modulation configuration using: B, 50 µL sampling loops in combination with 50 mm length column in the ^{2}D; C, 50 µL sampling loops in combination with 30 mm length column in the ^{2}D; D, C_{18} trapping columns with forward elution; E, active modulation with phenyl-hexyl traps and make-up flow rate equal to 9-times ^{1}D flow rate, and; F, sensitivity gain with the 250 × 2,1 mm, 3,5 µm ^{1}D column. (Retention times of analyses with different ^{2}D gradient are aligned to help the comparison).

Table 1. Comprehensive two-dimensional method parameters applied to the profiling of secondary metabolites from licorice using non-focusing modulation

		^{2}D - C_{18} 50 × 4.6 mm, 2.7 µm			^{2}D - C_{18} 30 × 4.6 mm, 2.7 µm		
	Sampling loop volume	20 µL	30 µL	50 µL	20 µL	30 µL	50 µL
^{1}D	L (mm)	150	150	150	150	150	150
	I.D. (mm)	1.0	1.0	1.0	1.0	1.0	1.0
	Particle size (µm)	3.5	3.5	3.5	3.5	3.5	3.5
	Flow rate (µL min^{-1})	15	15	15	15	15	15
	$\overline{w}$ (min)	2.69	2.69	2.69	2.47	2.47	2.47
	$^{1}n_c$	30	30	30	33	33	33
	<β>	1.34	1.34	1.34	1.25	1.25	1.25
	$^{1}n_c$ corr.	22	22	22	27	27	27
^{2}D	$\overline{w}$ (s)	1.02	0.90	0.78	1.02	1.00	1.00
	$^{2}n_c$	77	88	101	60	61	61
LC × LC	Analysis time (min)	80	80	80	80	80	80
	t_s	1.93σ	1.93σ	1.93σ	1.62σ	1.62σ	1.62σ
	Modulation time (min)	1.3	1.3	1.3	1.0	1.0	1.0
	M – number of modulations	62	62	62	80	80	80
	$^{2}V_{inj}$ (V dilution)	20 µL (0.5 µL)	30 µL (10.5 µL)	50 µL (30.5 µL)	20 µL (5.0 µL)	30 µL (15.0 µL)	50 µL (35.0 µL)
	% ^{2}D column void volume	4%	6%	10%	7%	10%	17%
	Z_1	0,84	0,91	0,92	0,89	0,82	0,85
	Z_2	0,97	0,96	0,99	0,97	0,98	0,97
	Z_-	0,69	0,77	0,81	0,91	0,89	0,86
	Z_+	0,83	0,87	0,84	0,99	0,95	0,99
	A_O	68%	76%	79%	82%	82%	84%
	Resolution pair 1	0.65	0.67	0.70	0.75	0.83	0.89
	Resolution pair 2	-	-	-	-	-	-
	Normalized sensitivity	0.85	1.00	1.37	1.08	1.32	1.61
	$^{2D}n_c$ theoretical	2310	2640	3030	1980	2013	2013
	$^{2D}n_c$ practical	1730	1964	2253	1706	1736	1780
	$^{2D}n_c$ corr.	1176	1493	1780	1399	1424	1495

<β>, average ^{1}D broadening factor; $^{1}n_c$ corr.: calculated according to eq. 2; t_s, sampling time; A_O, orthogonality; $^{2D}n_c$ theoretical: $^{1}n_c \times {}^{2}n_c$; $^{2D}n_c$ practical: calculated according to eq. 4; $^{2D}n_c$ corr.: $^{2D}n_c \times A_0$

Table 2. Comprehensive two-dimensional method parameters applied to the profiling of secondary metabolites from licorice using trapping columns-based focusing modulation.

		Forward elution		Backflush elution	
	Trapping column	C18	Phenyl-hexyl	C18	Phenyl-hexyl
^{1}D	L (mm)	150	150	150	150
	I.D. (mm)	1.0	1.0	1.0	1.0
	Particle size (µm)	3.5	3.5	3.5	3.5
	Flow rate (µLmin^{-1})	15	15	15	15
	$\overline{w}$ (min)	2.11	2.11	2.11	2.11
	$^{1}n_c$	39	39	39	39
	<β>	1.32	1.32	1.32	1.32
	$^{1}n_c$ corr.	30	30	30	30
^{2}D	$\overline{w}$ (s)	0.97	0.96	0.98	0.98
	$^{2}n_c$	63	64	62	62
LC × LC	Analysis time (min)	80	80	80	80
	t_s	1.88σ	1.88σ	1.88σ	1.88 σ
	Modulation time (min)	1.0	1.0	1.0	1.0
	M – number of modulations	80	80	80	80
	Z_1	0,94	0,86	0,83	0,87
	Z_2	0,92	0,94	0,97	0,93
	Z_-	0,94	0,89	0,92	0,97
	Z_+	0,93	0,98	0,92	0,83
	A_0	87%	84%	83%	81%
	Resolution pair 1	0.80	0.80	0.79	0.81
	Resolution pair 2	0.81	0.85	0.72	0.78
	Normalized sensitivity	1.15	0.99	0.59	0.75
	$^{2D}n_c$ theoretical	2457	2496	2418	2418
	$^{2D}n_c$ practical	1792	1811	1777	1777
	$^{2D}n_c$ corr.	1559	1521	1475	1439

<β>, average ^{1}D broadening factor; $^{1}n_c$ corr.: calculated according to eq. 2; t_s, sampling time; A_O, orthogonality; $^{2D}n_c$ theoretical: $^{1}n_c \times {}^{2}n_c$; $^{2D}n_c$ practical: calculated according to eq. 4; $^{2D}n_c$ corr.: $^{2D}n_c \times A_O$

Table 3. Instrumental parameters employed and method performance descriptors from the use of active modulation for the profiling of secondary metabolites from licorice.

		C18 trapping columns			Phenyl-hexyl trapping columns		
	Make-up flow rate	5 × ^{1}F	7 × ^{1}F	9 × ^{1}F	5 × ^{1}F	7 × ^{1}F	9 × ^{1}F
^{1}D	L (mm)	150	150	150	150	150	150
	I.D. (mm)	1.0	1.0	1.0	1.0	1.0	1.0
	Particle size (µm)	3.5	3.5	3.5	3.5	3.5	3.5
	^{1}F (Flow rate, µL min^{-1})	15	15	15	15	15	15
	$\overline{w}$ (min)	2.11	2.11	2.11	2.11	2.11	2.11
	$^{1}n_c$	39	39	39	39	39	39
	<β>	1.33	1.33	1.33	1.32	1.32	1.32
	$^{1}n_c$ corr.	1.32	1.32	1.32	1.32	1.32	1.32
^{2}D	$\overline{w}$ (s)	0.93	0.84	0.81	0.96	0.84	0.81
	$^{2}n_c$	66	73	75	63	73	75
LC × LC	Analysis time (min)	80	80	80	80	80	80
	t_s	1.88σ	1.88σ	1.88σ	1.88σ	1.88σ	1.88σ
	Modulation time (min)	1.0	1.0	1.0	1.0	1.0	1.0
	M – number of modulations	80	80	80	80	80	80
	Z_1	0,87	0,89	0,90	0,87	0,87	0,88
	Z_2	0,98	0,96	0,96	0,96	0,94	0,94
	Z_-	0,91	0,92	0,91	0,87	0,89	0,89
	Z_+	0,93	0,93	0,94	0,96	0,97	0,95
	A_O	85%	86%	86%	84%	84%	84%
	Resolution pair 1	0.69	0.82	0.85	0.71	0.91	0.93
	Resolution pair 2	0.81	0.86	0.88	0.82	0.86	0.88
	Normalized sensitivity	1.46	1.59	1.98	0.91	1.67	2.01
	$^{2D}n_c$ theoretical	2574	2847	2925	2457	2847	2925
	$^{2D}n_c$ practical	1888	2075	2128	1806	2070	2131
	$^{2D}n_c$ corr.	1605	1785	1830	1517	1739	1790

<β>, average ^{1}D broadening factor; $^{1}n_c$ corr.: calculated according to eq. 2; t_s, sampling time; A_O, orthogonality; $^{2D}n_c$ theoretical: $^{1}n_c \times {}^{2}n_c$; $^{2D}n_c$ practical: calculated according to eq. 4; $^{2D}n_c$ corr.: $^{2D}n_c \times A_O$

628

Figure 1

Click here to download high resolution image

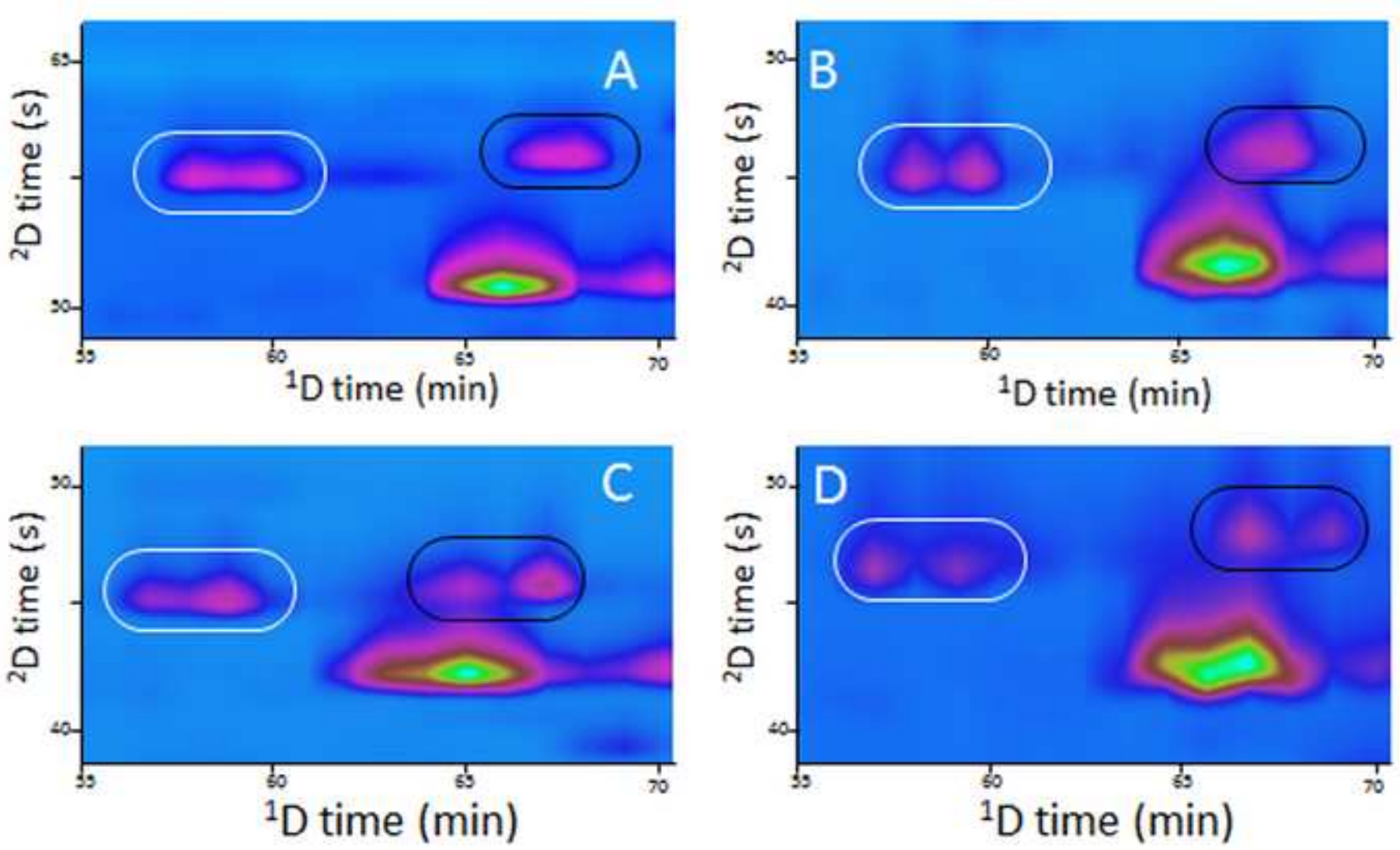

Figure2

Click here to download high resolution image

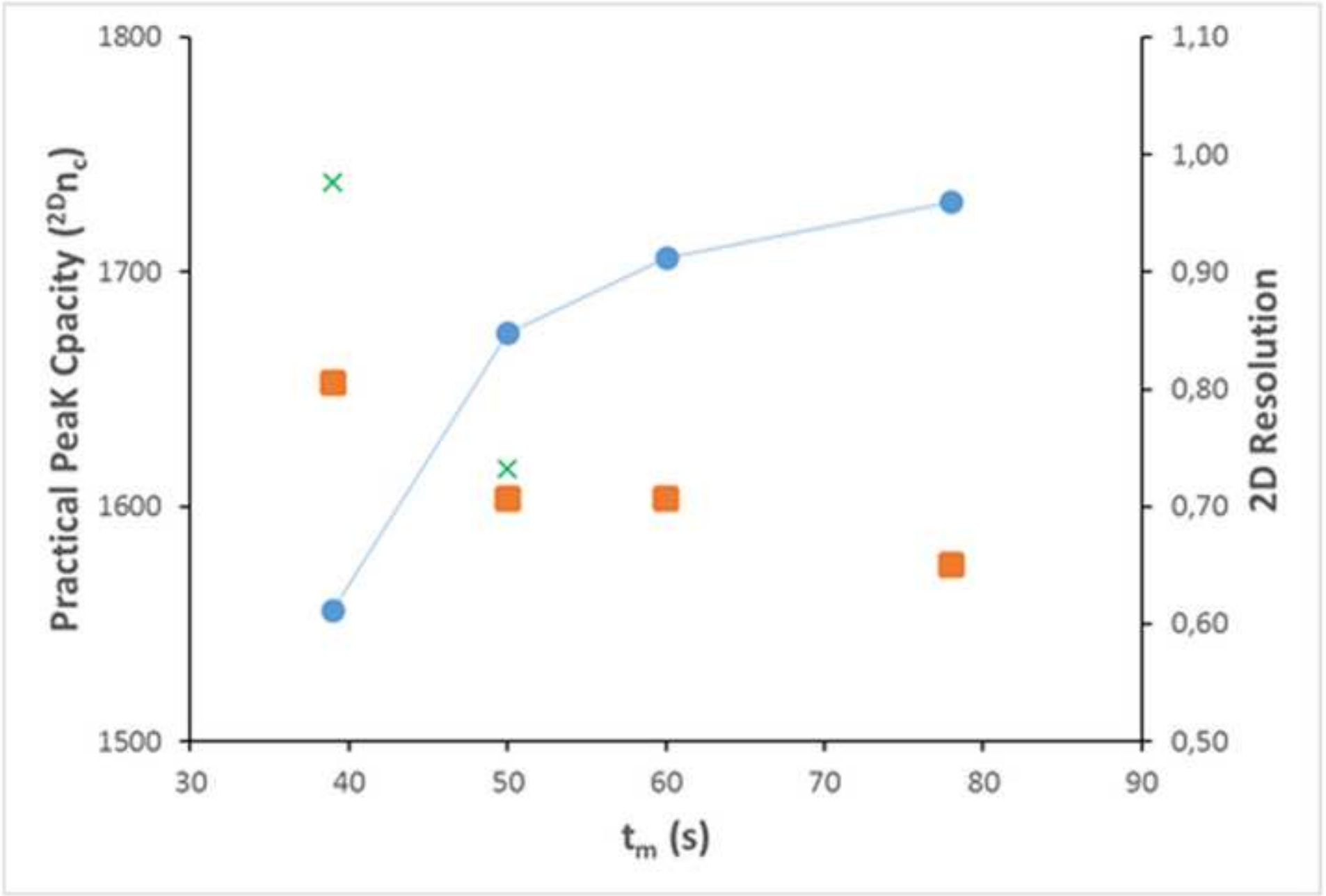

Figure3

Click here to download high resolution image

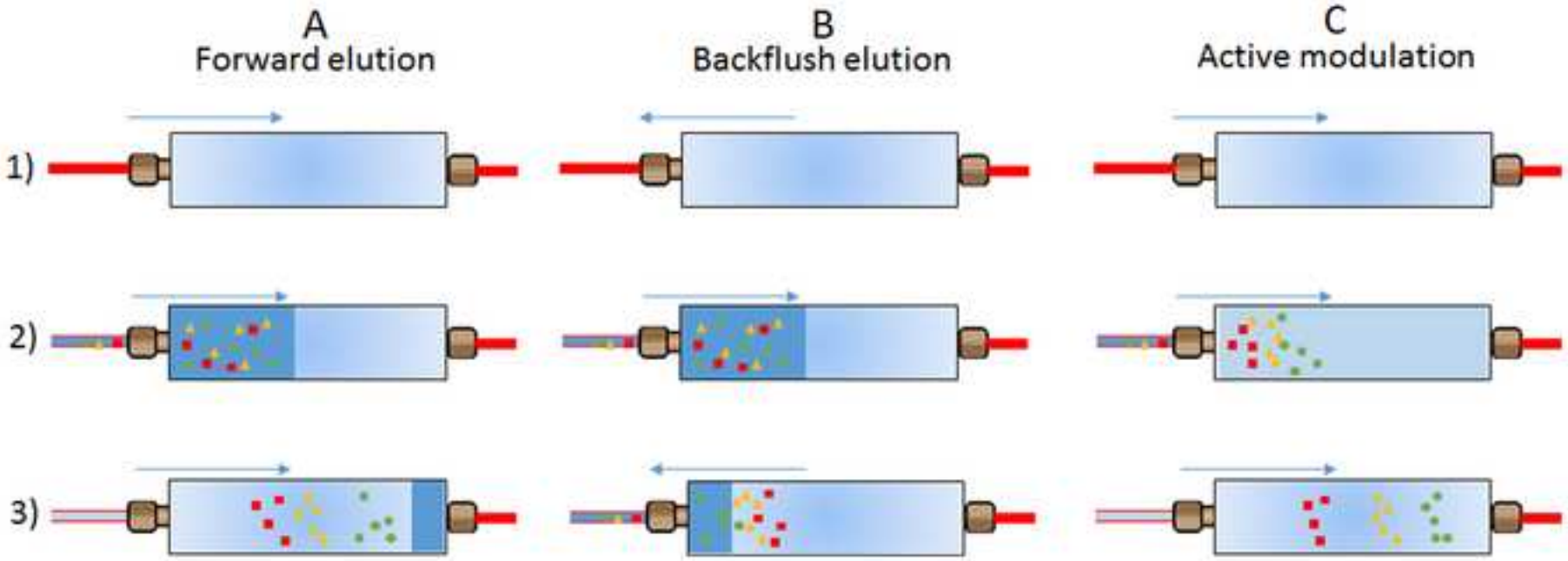

Figure4

Click here to download high resolution image

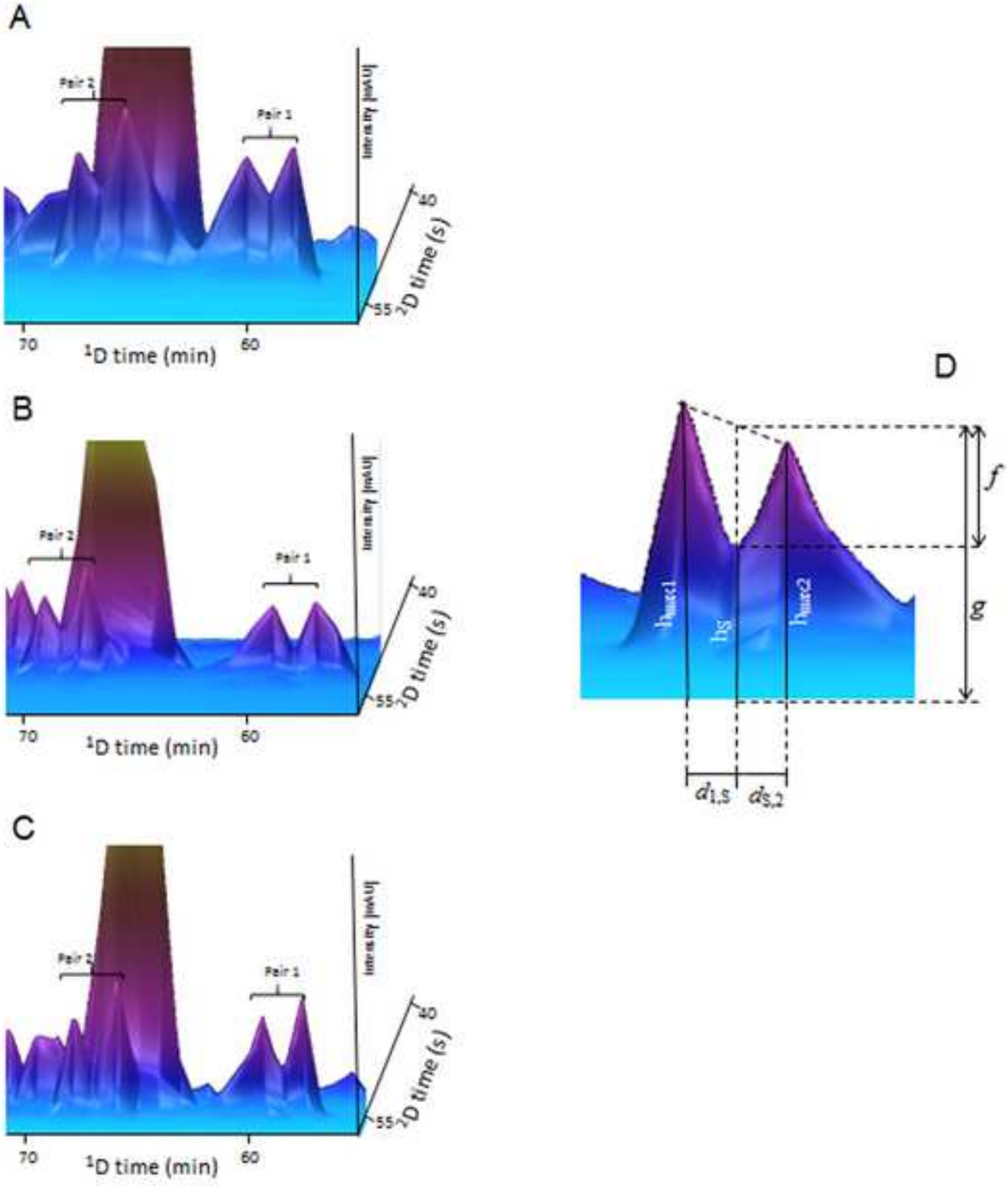

Figure5

Click here to download high resolution image

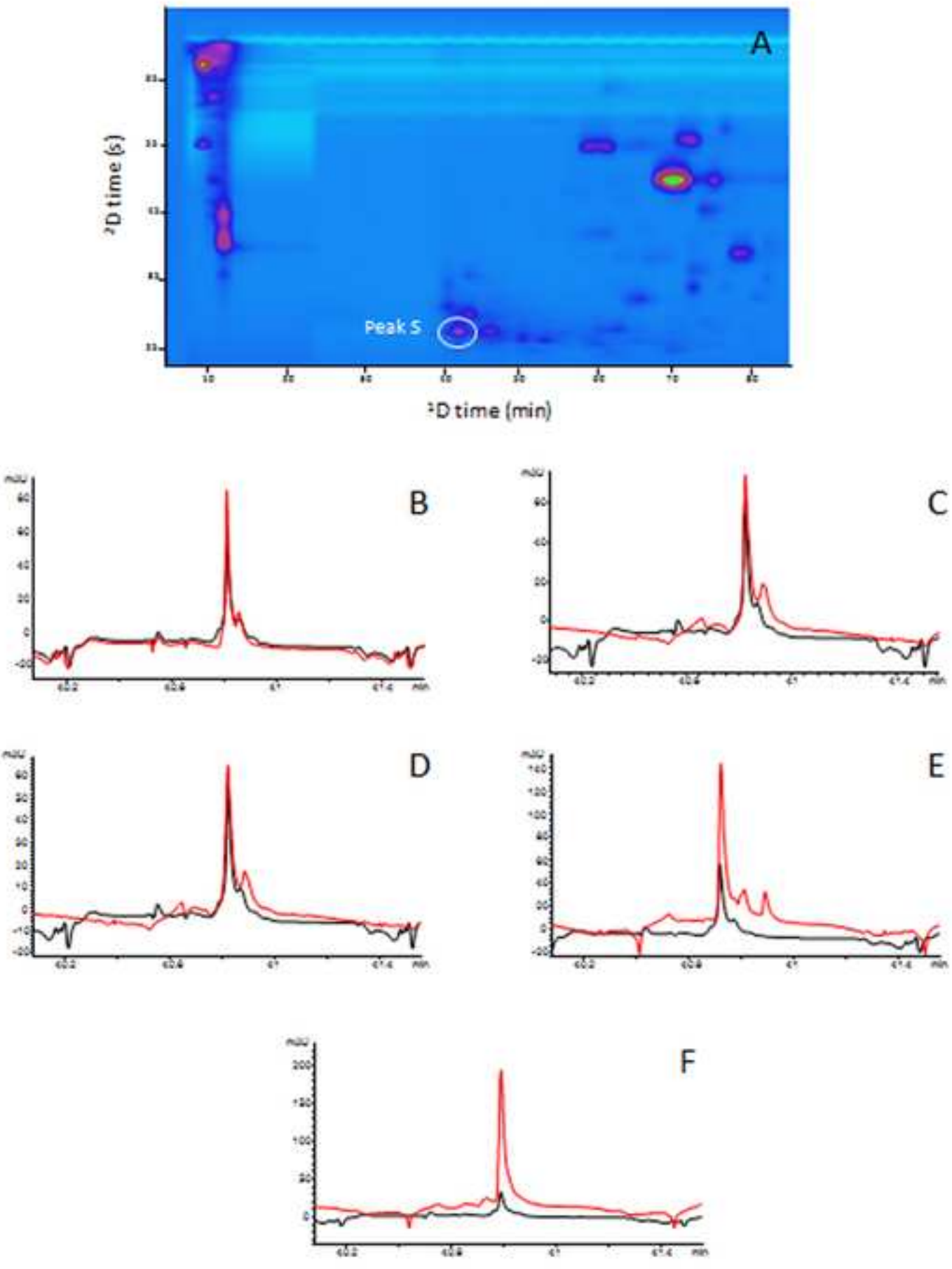

Electronic Supplementary Material (online publication only)

Click here to download Electronic Supplementary Material (online publication only): 10) Supplementary material_Montero et al.p

5.4. GENERAL DISCUSSION.

Licorice is the dried root of *Glycyrrhiza glabra* plant, which is widely used as an important medicinal plant due to its beneficial properties; moreover, it is employed as a natural sweetener and as a flavor additive on the food industry. These characteristics that define licorice are largely related to its composition on triterpene saponins, particularly to its main compound, glycyrrhizic acid, to which some of the important mentioned properties are attributed (Hayashi and Sudo 2009).

Triterpene saponins contained in licorice belong to the oleanane saponins type with diverse glycosylations. Therefore, licorice triterpene saponins are heterogeneous molecules that vary on both, the aglycone structure (sapogenin) and the saccharide moieties that may be composed by various sugars, including glucose, glucuronic acid, galactose, xylose, apiose, rhamnose, fucose and arabinose (Zheng et al. 2010; Tao et al. 2013). However, although saponins represent the major components in licorice, the secondary metabolite composition of these roots is also composed of an important amount of phenolic compounds (Xu et al. 2013).

On-line LC × LC have been employed for the separation of complex formulations of Chinese herbal medicines (Li and Schmitz 2015; Li et al. 2016). However, on-line comprehensive approaches for the complete fingerprinting of licorice have not been developed until date. Only a RP × RP method for the chemical characterization of licorice (*Glycyrrhiza uralensis*) was developed (Qiao et al. 2015); however, in that work, the sample was fractionated during the extraction and sample treatment to simplify the analysis, obtaining a free phenolic compounds-rich fraction and a saponin-rich fraction, that were analyzed individually. Consequently, the comprehensive licorice metabolite profiling in a single run has not previously been carried out.

Regarding to the analysis of saponins in other plant materials, a stop-flow HILIC × RP method has been reported for the analysis of a ginseng extract. The detection of 94 saponins in 122.7 min was possible (Wang et al. 2015). Besides, a HILIC × HILIC analysis for the separation and identification of *Quillaja saponaria* and a RP × RP method for the analysis of saponins from roots of *Platycodon grandiflorum* have been reported (Wang et al. 2008; Jeong et al. 2010).

However, these analyses provided just moderate orthogonality values due to the correlation between the two separation mechanisms selected for both dimensions.

Therefore, a theoretically more orthogonal approach, based on the HILIC × RP coupling was selected for the development of the method studied in this Chapter. Once the method was optimized and its application to the chemical characterization of licorice metabolites demonstrated, it was also applied to the comparison of five licorice samples from different geographical origin (Section 5.2) with the aim to look for potential markers of origin for the authentication of samples. In this first work the instrument configuration previously described for the analysis of proanthocyanidins and phlorotannins was used, that is, a microbore column in the ^{1}D coupled by a 10-port 2-position switching valve equipped with two 30 μL sampling loops to a ^{2}D short partially porous column. Although this approach produced good results, this method was considered as a starting point to study different modifications at the modulator level with the aim to produce further significant gains in resolving power as well as on sensitivity (Section 5.3).

5.4.1. CHEMICAL CHARACTERIZATION OF THE SECONDARY METABOLITE PROFILE OF LICORICE SAMPLES AND GEOGRAPHICAL ORIGIN ASSESSEMENT.

For this work, five samples of licorice (*Glycyrrhiza glabra*) from four different countries, namely Iran, China, Azerbaijan and Italy (two different samples) were considered for their secondary metabolites profile comparison, with the aim to search for possible potential markers of origin of samples produced under Protected Designations of Origin.

Since the success of a LC × LC system largely depends on the orthogonality degree between the two separation mechanisms involved, the coupling between HILIC separation mode in the first dimension and RP mode in the second dimension was selected for the analysis of the metabolite profile of licorice. This selection was also supported by our previous experience with other complex food-related samples, as can be deduced from the information shown in Chapters 3 and 4.

5.4.1.1. Influence of method parameters.

5.4.1.1.1. *Sample preparation.*

In agreement with the particular characteristics of saponins, the use of mixtures of ethanol and water are recommended for the extraction from complex samples in order to have a truthful idea of their native composition (Oleszek and Bialy 2006). The use of hot water is not recommended as it has been shown to produce degradations, whereas methanol could lead to the formation of methyl derivatives, thus, not representing the native chemical composition (Majinda 2012). Consequently, in this work, a simple extraction procedure was applied to obtain the main secondary metabolites from licorice; this procedure was based on the use of ultrasound-assisted extraction with a mixture of ethanol/water (1:1, *v/v*) as extraction solvent. The resulting extract was evaporated and redissolved in an adequate solvent for its direct injection without the need of any other sample treatment or clean-up.

5.4.1.1.2. *^{1}D separation.*

Triterpene saponins are very polar compounds due to the very hydrophilic glycosidic chains present in the molecule. For this reason, HILIC was selected to carry out the separation in the ^{1}D. Considering that HILIC mode was not frequently employed for the separation of saponins, different stationary phases, compatible with HILIC conditions, namely silica, diol and ZIC-HILIC stationary phases, were tested in order to obtain the maximum ^{1}D separation of the sample. After the screening of these three HILIC stationary phases, the ZIC-HILIC column was selected as the optimum ^{1}D column for the LC × LC coupling. In Figure 5.2 the ^{1}D separation of the five licorice samples under the optimum conditions is shown. As can be deduced from this Figure, this preliminary analysis already demonstrated that the chemical composition in each sample could be very variable, as significant differences between the obtained profiles were obtained.

5.4.1.1.3. *^{2}D separation.*

As already mentioned, very fast analyses in the second dimension are needed, and consequently, very high flow rates should be employed. In order to keep the system

backpressure under reachable conditions for the used instrument, a short partially-porous column was selected in the ^{2}D. In this sense, 78 s were available for each separation and re-equilibration on the second dimension column.

Two stationary phases were employed for the study of the separation on the ^{2}D, maintaining the same column morphology (50 × 4.6 mm, 2.7 µm), C_{18} and PFP stationary phases. In each case, different mobile phases (including combinations of acetonitrile, methanol, acetonitrile/methanol mixtures and acidified water), flow rates (2–3 mL min^{-1}) and gradients were tested. According to the obtained results, the C_{18} stationary phase, eluted with mobile phases composed by (A) water (0.1 % formic acid) and (B) acetonitrile at 3 mL min^{-1} provided the best resolution and separation.

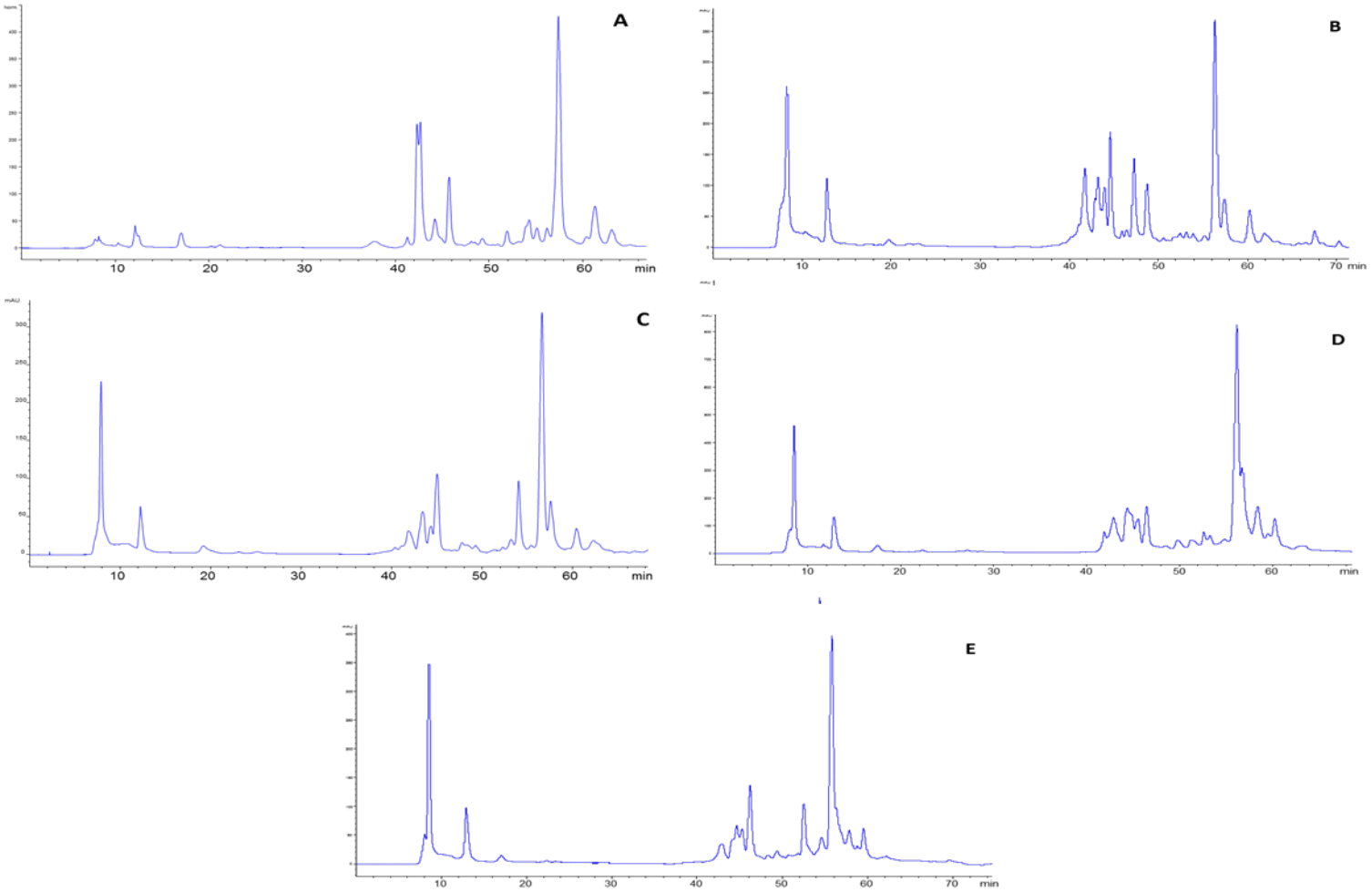

Figure 5.2. [1]D separation of licorice samples from China (A), Iran (B), Crotone (Italy) (C), Azerbaijan (D) and Villapiana (Italy) (E) under the optimum conditions.

5.4.1.2. Chemical characterization of secondary metabolites from licorice by HILIC × RP.

As mentioned in the previous sections, a ZIC-HILIC column was coupled to a C_{18} short partially porous column; during the 2D analysis, SIF gradients were employed in the ^{2}D, in order to match the separation conditions in this dimension to the different polarities of the separated compounds along the ^{1}D analysis. With the use of ^{2}D SIF gradients, an increase on the orthogonality and a more effective peak distribution of the analytes was achieved, reaching a better space coverage. As it can be observed in Figure 5.3, a good separation was obtained, in which the different metabolite groups were well distributed along the 2D plot. Firstly, prenylated flavonoids were eluted, as the less polar compounds, followed by different phenolic compounds, whereas triterpene saponins were eluted at the end of the analysis.

Once the overall LC × LC separation of the compounds of the licorice samples was achieved, the tentative identification of each of the separated peaks was carried out employing the information provided by the UV-Vis and the MS spectra, as well as the relative position of each peak in the 2D plot. At this point it is worth to stress the instrumental limitations that were faced, mainly characterized by the relatively low scanning speed of both DAD (20 Hz) and MS (ion trap working at 26000 m/z s^{-1}) detectors used. The use of higher sampling frequencies in the DAD together with the use of faster high resolution MS instruments, would undoubtedly improve the attainable results even without making any other modification.

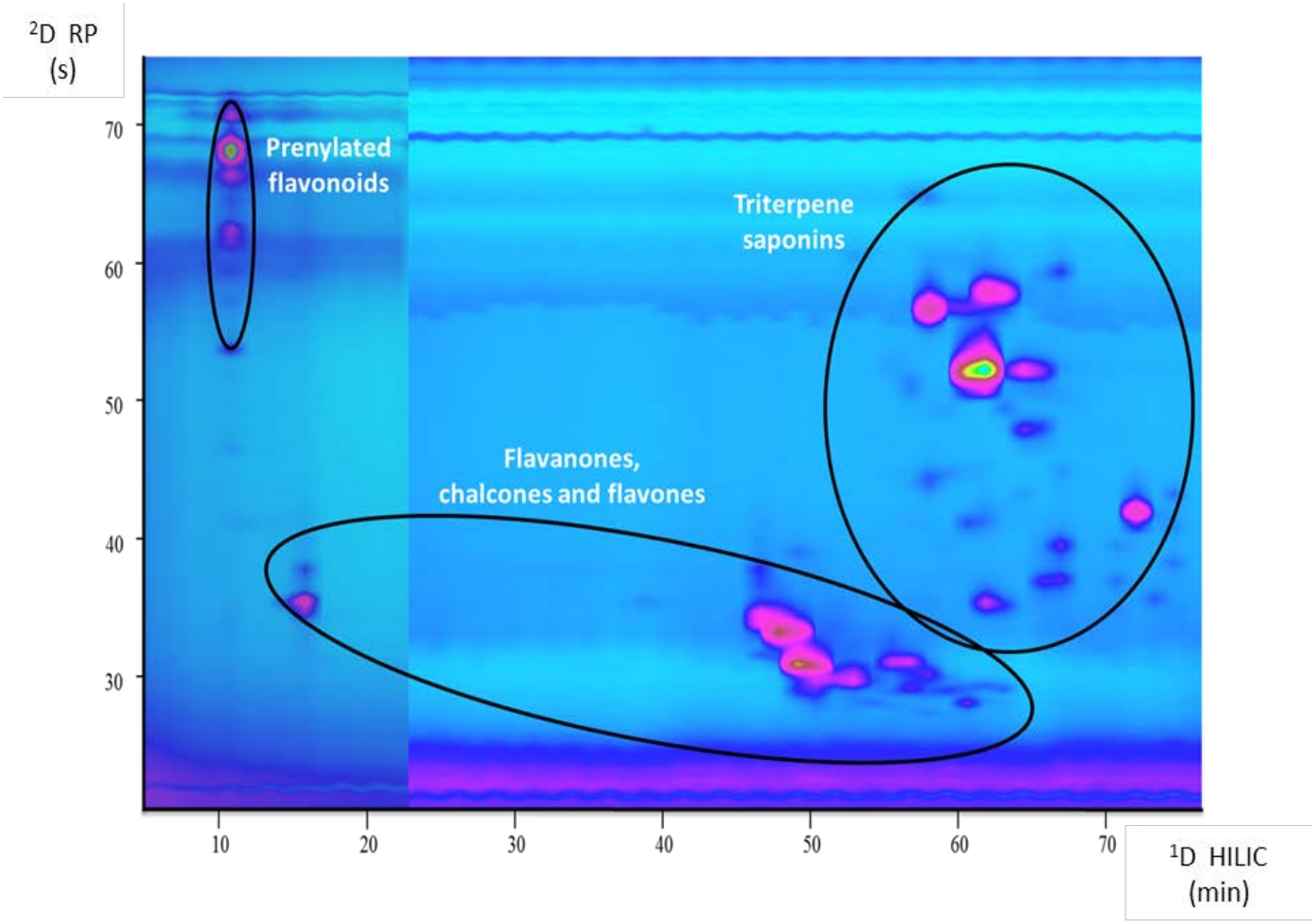

Figure 5.3. 2D-plot of the licorice from Villapiana (Italy). Black ovals group the different families of metabolites present in the sample.

Firstly, the comprehensive characterization of each sample from the 5 geographical origins was carried out, giving as result the tentative identification of 73, 78, 89, 76 and 81 compounds in the licorice from Crotone (Italy), Villapiana (Italy), Iran, China and Azerbaijan, respectively. Within these compounds, the separation and tentative identification of 62 saponins was possible, being the major group of secondary metabolites present in licorice samples. The identification of these saponins was achieved in agreement with their particular MS and MS/MS spectra obtained under negative ionization mode.

The metabolite profile of the samples belonging to the 5 studied locations was relatively similar. For this reason, a comparison between them was performed in order to establish the common compounds to all samples and, mainly, to identify possible biomarkers that could allow attaining the differentiation of each location.

In this regard, most of the separated compounds were identified in two or more samples, whereas 16 compounds were common to all samples, 13 of them corresponding to saponins. However, several differences between samples were also found. Licorice from China was the most different sample in terms of number of exclusive compounds. The chemical characterization of that sample led to the identification of up to 50 unique compounds. Licorice samples from Azerbaijan and Iran presented 34 and 36 exclusive compounds, respectively, while licorice samples from Crotone and Villapiana, both from Italy, were those that presented the lowest number of unique components, with 19 and 21 exclusive compounds, respectively.

Within these differentiating compounds, it is worth noting some compounds that were unique for each sample; for instance, licorocidin, albiflorin and 22β-acetoxyl licorice saponin J2 were detected only in licorice from China, whereas licorice saponin C2 was only present in the sample from Iran and glycyroside in the licorice from Azerbaijan. Besides, other peaks were also unique of each sample, although their identity could not be elucidated.

Although these results were of interest, showing the preliminary existence of compounds that could potentially be considered as biomarkers of origin, proper statistical analysis is necessary to establish if those compounds are robustly found as markers. Unfortunately, not enough

samples from the studied locations were available, and thus, the potential of those compounds to perform a geographical assessment of licorice samples could not be completely demonstrated. To try to solve this problem, a bigger number of samples was analyzed including two different locations for which a wider group of samples could be obtained. This way, the optimized method was extended to the analysis of 11 additional samples from the region of Calabria (Italy), as well as to 11 new licorice samples from Castilla la Mancha (Spain). Figure 5.4 shows the 2D plots obtained for the 11 samples from Italy whereas Figure 5.5 shows the 2D separations of the 11 samples from Spain.

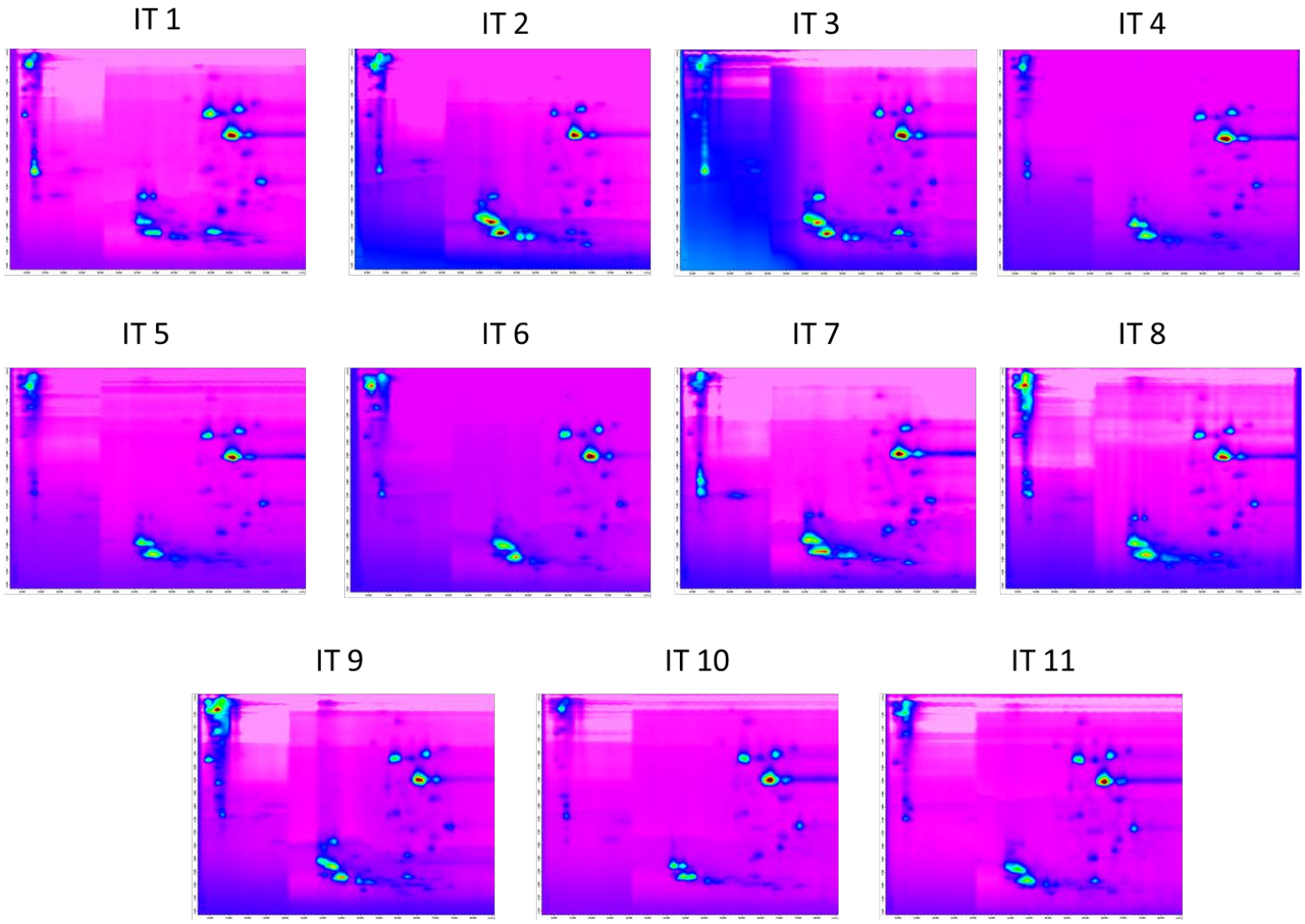

Figure 5.4. 2D separations of the 11 samples from Italy (IT1–IT11).

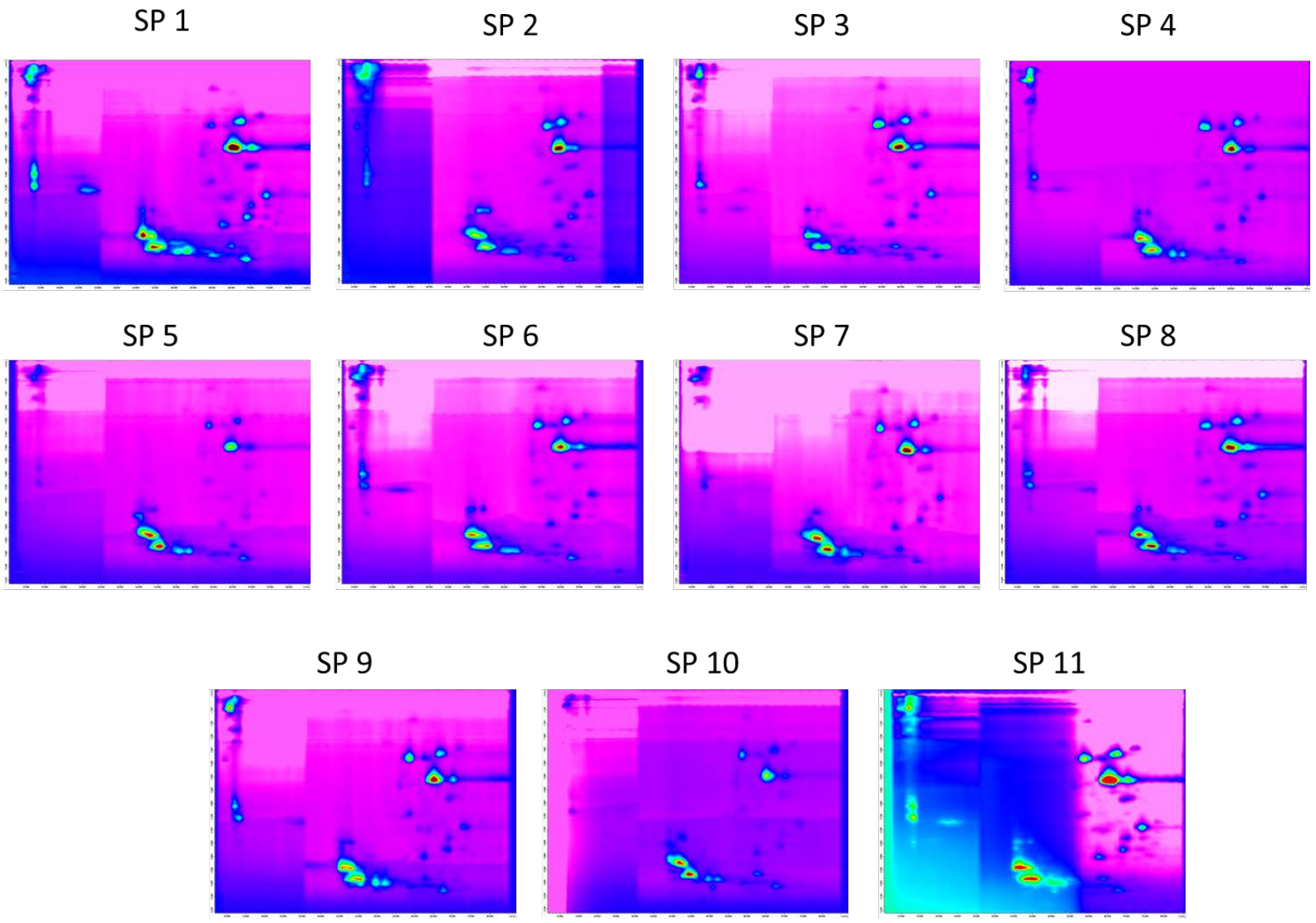

Figure 5.5. 2D separations of the 11 samples from Spain (SP1–SP11).

Data analysis was carried out using multivariate statistical analysis, in particular principal component analysis (PCA) and T-test analysis. However, the statistical study of 2DLC data was revealed as a very difficult task due to different problems, most notably: the statistical comparison of more than two LC × LC images is difficult to be carried out with the available software, and 2D raw data comprise peaks that are sampled into de ^{2}D more than once and, therefore, the use of the raw chromatogram in the same way that are used in one-dimensional LC-MS is not straightforward. Therefore, to try to solve these difficulties, the following procedure was carried out:

i. To make the manual alignment of the chromatograms.

ii. As a first approximation, three samples from each country were randomly selected for the data analysis.

iii. To construct a matrix comprising the aligned retention times, *m/z* values and the intensity of each peak.

iv. To analyze these data by using statistical tools.

Unfortunately, these statistical analyses did not provide with enough differences between the studied samples to support a differentiation based on geographical origin. Therefore, improvements in the data treatment of 2DLC as well as an in-depth study of both, licorice secondary metabolite profile and the LC × LC performance could help to obtain more robust data to confirm the use of the secondary metabolite profiles of licorice as a measure of authenticity for each location.

5.4.2. IMPROVEMENT OF THE HILIC × RP PROFILING OF LICORICE.

As it has been stated throughout this PhD, the analysis of very complex samples requires maximizing the separation power of the analytical method employed; this is the case of licorice samples.

In the work developed in Section 5.3, a more theory-oriented study is described, in which different focusing and non-focusing modulation strategies were studied for the improvement

of the main important parameters of the LC × LC method, i.e., ^{1}D undersampling, ^{2}D band broadening, 2D resolution and sensitivity, using licorice as a real complex food model sample.

Taking the previously developed HILIC × RP method for the analysis of the secondary metabolite profile of licorice as a starting point, different strategies were studied looking for quantitative and significant improvements on method performance. These strategies consisted of the use of diverse non-focusing modulation set-ups using sampling loops installed in the interface, and focusing modulation approaches employing trapping columns in the interface as well as through the use of active modulation.

5.4.2.1. Non-focusing modulation.

In first place, the study of the effect of the transfer volume and the relative strength of the injection solvent on the ^{2}D separation was studied. To this aim, sampling loops with three different internal volumes were tested, namely, 20, 30 and 50 μL. That way, loops with lower internal volume provided the theoretical advantage of lower injection volume, that could help to reduce ^{2}D band broadening considering the relationship between the injection volume and the void volume of the ^{2}D column, but at the same time, the dilution effect of the ^{1}D effluent with ^{2}D mobile phase within the loop was minimized. The opposite situation occurred when using the 50 μL loops, which allowed a greater dilution of the ^{1}D effluent at the cost of a higher ^{2}D injection volume. Table 5.1 shows the ^{1}D effluent fraction dilution obtained with each of the studied sampling loops as well as the relative injection volume into de ^{2}D in each case. Results showed that the use of 50 μL sampling loops produced narrower ^{2}D peak widths as a consequence of injecting the analytes dissolved in a weaker solvent in spite of injecting high volumes (10% of the ^{2}D column void volume, see Table 5.1). Therefore, the efficiency and the ^{2}D peak capacity achieved was higher than those attainable using 20 and 30 μL loops, and hence, practical $^{2D}n_c$ was also higher (Table 5.1).

Table 5.1. Data comparison of the influence of the injection volume and the solvent strength using 50 mm and 30 mm length ^{2}D columns.

	^{2}D – C_{18} 50 × 4.6 mm, 2.7 µm			^{2}D – C_{18} 30 × 4.6 mm, 2.7 µm		
Sampling loop volume	**20 µL**	**30 µL**	**50 µL**	**20 µL**	**30 µL**	**50 µL**
^{1}D flow rate (µL min^{-1})	15	15	15	15	15	15
Modulation time (min)	1.3	1.3	1.3	1.0	1.0	1.0
$^{2}V_{inj}$ (V dilution)	20 µL (0.5 µL)	30 µL (10.5 µL)	50 µL (30.5 µL)	20 µL (5.0 µL)	30 µL (15.0 µL)	50 µL (35.0 µL)
% ^{2}D column void volume	4%	6%	10%	7%	10%	17%
$^{2D}n_{c,}$ practical	1730	1964	2253	1706	1736	1780
Normalized sensitivity	0.85	1.00	1.37	1.08	1.32	1.61

$^{2D}n_{c,}$ practical, calculated according to Eq. 16.

Besides, injection of the fraction in a more compatible solvent resulted in a better retention of the analytes due to an improved analyte-stationary phase contact; this fact together with the better peak shapes obtained, allowed increasing the sensitivity of the analytes. This effect was also confirmed when a 30 × 4.6 mm, 2.7 µm column was employed in the ^{2}D, as can be observed in Figure 5.6 and Table 5.1.

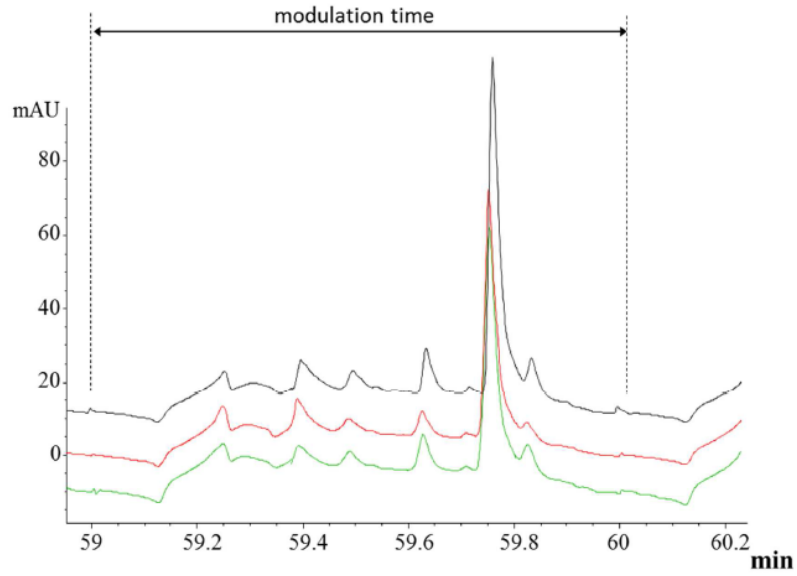

Figure 5.6. Chromatogram of single ^{2}D analyses on a 30 × 4.6 mm, 2.7 µm C_{18} partially porous column comparing the effect of the transfer volume, using 20 µL (green), 30 µL (red) and 50 µL (black) sampling loops.

After that, the effect of the sampling rate from ^{1}D to the ^{2}D was studied in order to observe the influence of the reduction of the sampling time in the $^{1}n_c$ as well as on the overall results. Four different sampling times were tested, namely, 78, 60, 50 and 39 s. However, due to the limitation of the maximum pressure attainable on the switching valve, it was not possible to use the same column employed to carry out the 78 s analysis (50 mm length column) for other shorter analysis times, since higher flow rates were required and, therefore, the pressure drop was significantly increased. Therefore, a shorter column (30 × 4.6 mm, 2.7 µm) was employed for these experiments. It was observed that shorter ^{2}D analysis times (higher sampling frequency) produced higher $^{1}n_c$ values as a result of a better preservation of the separation obtained in the ^{1}D during the fraction transfer, reducing the chance of getting peak re-mix effect and thus, reducing the ^{1}D undersampling and its related deleterious effects. However, the reduction of the ^{2}D analysis time negatively affected to the $^{2}n_c$, achieving values of 40 in the 39 s analyses compared to $^{2}n_c$ of 75 when 78 s were used as ^{2}D analysis time. This effect is due to the great dependence that n_c has on the available gradient time. These results were reflected on the practical $^{2D}n_c$, that is more critically affected by the $^{2}n_c$ than by the $^{1}n_c$.

On the other hand, the resolution of two critical pairs of peaks was also calculated in an effort to illustrate the potential gains on resolving power in each studied set-up. Interestingly, resolution of pair 1 was significantly increased when 60 s fractions were sampled, being this increment greater when 39 s was set as modulation time. On the other hand, pair 2 could only be separated with sampling times lower than 50 s, remaining unresolved with 60 and 78 s (Figure 5.7).

The analysis using 60 s sampling rate was selected for further separation study, since it provided a compromise between resolution and practical ${}^{2D}n_c$.

5.4.2.2. Focusing modulation.

Two focusing modulation approaches were tested using trapping columns installed in the switching valve instead of sampling loops, as well as adding an additional make-up flow to carry out active modulation. Two sets of trapping columns with different RP-compatible stationary phase chemistry were studied: C_{18} and phenyl-hexyl particles.

During the study of the focusing effect of trapping columns, forward and backflush elution configurations were considered. The use of trapping columns helped to retain the analytes in the interface during the collection position of the valve, in a similar separation mechanism than the ^{2}D column, allowing their elution in narrower bands during the injection position, resulting in a reduction of the ^{2}D band broadening. Besides, trapping columns allowed to increase the resolution of pair 2 (Figure 5.8), which was not resolved with the loops-based set-up using 60 s as modulation time, as already illustrated.

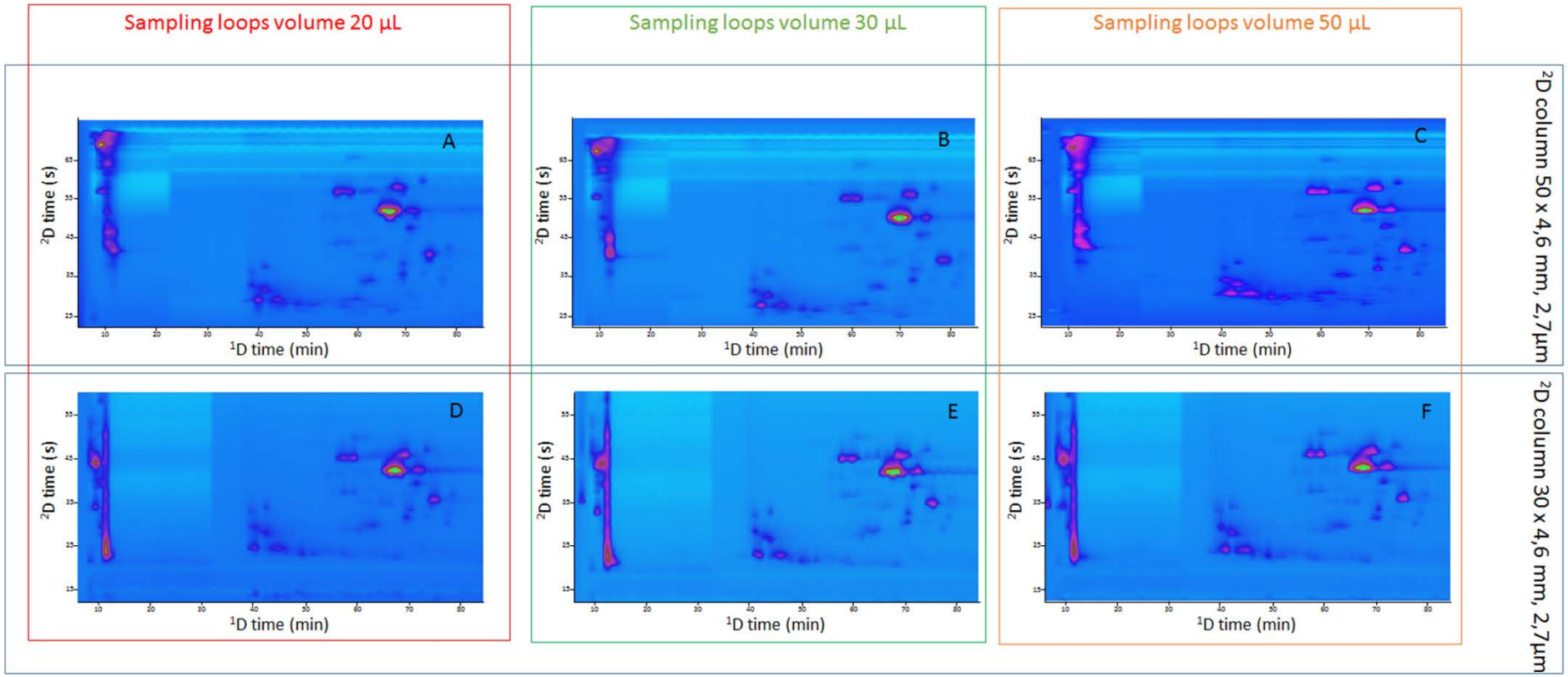

Figure 5.7. 2D-plots (254 nm) of the secondary metabolite profiles of licorice, using different transfer volumes using a 50 x 4.6 mm, 2.7 µm C18 partially porous column (A, 20 µL; B, 30 µL; C, 50 µL), and using a 30 x 4.6 mm, 2.7 µm C18 partially porous column (D, 20 µL; E, 30 µL; F, 50 µL). White ovals indicate the two critical pair of peaks selected for the resolution study.

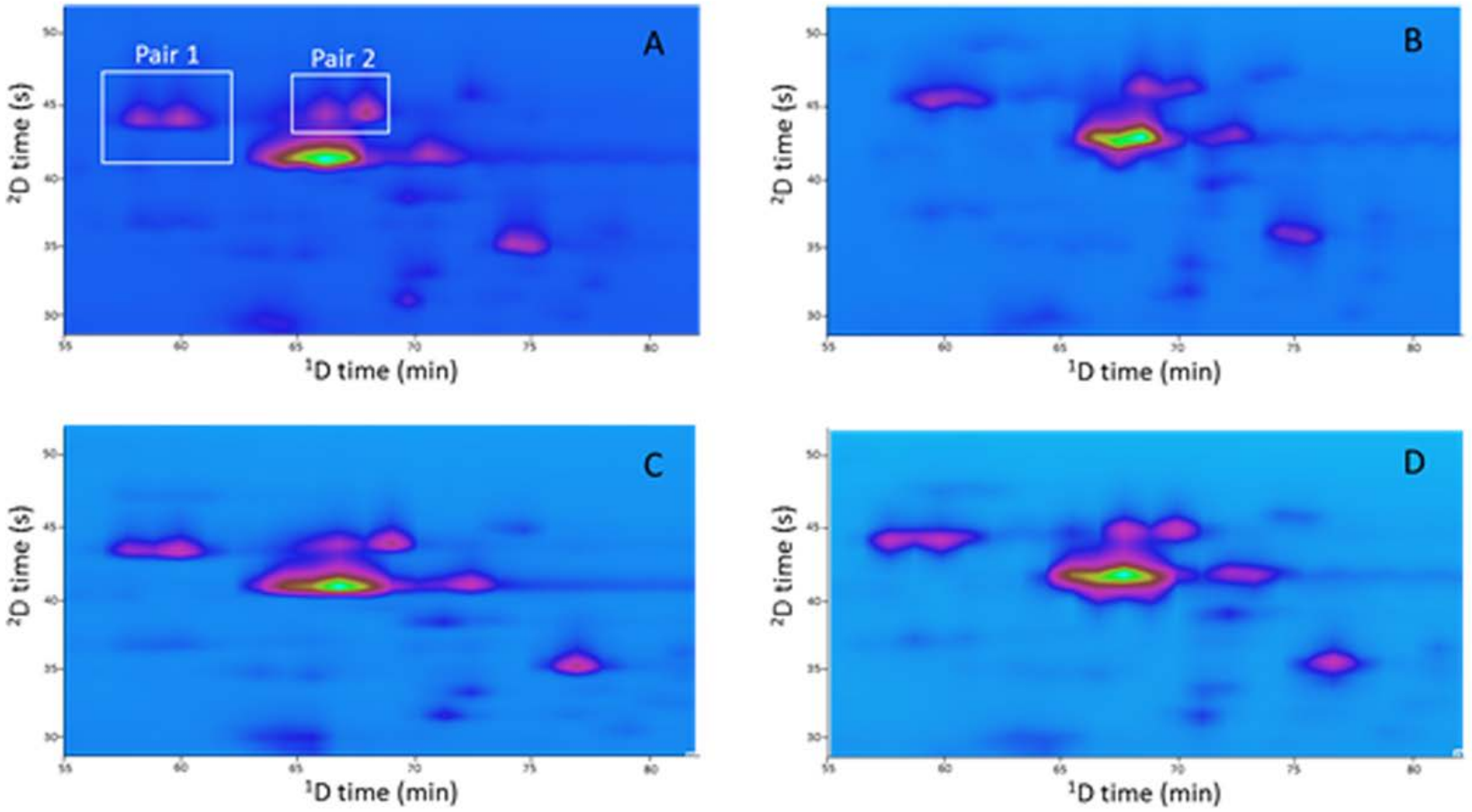

Figure 5.8. Enlarged 2D-plots (254 nm) of the secondary metabolite profiles of licorice, using trapping columns in forward and backflush elution modes. Stationary phases: C_{18} (A, forward elution; B, backflush elution) and phenyl-hexyl (C, forward elution; D, backflush elution).

Comparing forward and backflush configurations, backflush elution resulted in wider ^{2}D peak widths than forward elution as a consequence of the low flow rates used in the ^{1}D as well as the short modulation time and the void volume of the trapping columns. As the trapping column void volume was higher than the fraction volume transferred, analytes were only in contact with a reduced fraction of available particles in the trapping column. Thus, when the fraction was backflushed, the elution did not take advantage of the complete focusing effect that trapping columns could provide.

Although the use of trapping columns clearly improved the attainable results compared to the non-focusing modulation scheme, this set-up did not ensure the complete reduction of the solvent strength mismatch problem. Therefore, with the aim to eliminate this effect that may produce peak distortion or loss of the ^{2}D separation, the procedure so-called *active modulation* was applied as a new strategy. To do that, a new additional make-up flow was included and three different flow rates for its delivery were studied (5-, 7- and 9- times the ^{1}D flow rate) using both, C_{18} and phenyl-hexyl trapping columns.

Best results in terms of practical $^{2D}n_c$, resolution and sensitivity were achieved with the higher make-up flow rate (9-times the ^{1}D flow rate) and, interestingly, using phenyl hexyl trapping columns, as can be observed in Table 5.2, not only compared to focusing strategies, but also to non-focusing approaches.

Table 5.2. Data comparison of the active modulation set-ups using different make-up flow rates.

	C_{18} trapping columns			Phenyl-hexyl trapping columns		
Make-up flow rate	**5 × ^{1}F**	**7 × ^{1}F**	**9 × ^{1}F**	**5 × ^{1}F**	**7 × ^{1}F**	**9 × ^{1}F**
Resolution pair 1	0.69	0.82	0.85	0.71	0.91	0.93
Resolution pair 2	0.81	0.86	0.88	0.82	0.86	0.88
$^{2D}n_c$ practical	1888	2075	2128	1806	2070	2131
Normalized sensitivity	1.46	1.59	1.98	0.91	1.67	2.01

$^{2D}n_c$, practical, calculated according to Eq. 16.

Thus, the results obtained demonstrated the great applicability and potential that active modulation may have for the profiling of complex food samples by HILIC × RP, such as licorice. A total of 94 peaks were successfully separated in the set-up involving the use of active modulation, compared to the initial method (79 peaks), increasing sensitivity more than twice.

Taking advantage of the active modulation performance, the use of a wider ^{1}D column (2.1 mm i.d) was studied with the aim to overcome the limited sample loading of the 1 mm i.d microbore column that directly affects the sensitivity of the method. By using wider columns, more sample can be theoretically loaded, but higher flow rates are needed to obtain proper separations, which would in turn be deleterious for the ^{2}D (either due to increased sampling volume or reduced ^{2}D analysis time). However, by using active modulation the strong ^{1}D solvent is completely removed, and therefore, in theory, these problems can be overcome. After testing that column, it could be confirmed that the use of the 2.1 mm i.d. column allowed a 3.12-fold increase on sensitivity with respect to the initial method, mainly thanks to the injection of a bigger sample volume. However, the resolution of the studied critical pairs of peaks was completely lost compared to the set-up involving the use of the microbore column. Hence, the sensitivity improvement has to be more carefully studed to achieve a good equilibrium between sensitivity and resolution.

In summary, in this Chapter, the separation of a complex mixture of very closely related saponins as well as polyphenols present in licorice has been carried out by applying an optimized HILIC × RP method, arriving to the separation of up to 47 saponins in a single sample and a total of 105 saponins in the 5 samples, including a high number of isomers. Moreover, this method permitted a first approach to a geographical differentiation between licorice samples from different locations based on differential metabolite patterns. In addition, this Chapter provides very interesting results about the importance of the interface performance to significantly improve different parameters that greatly affect any LC × LC separation, like ^{1}D undersampling, ^{2}D band broadening, overall 2D resolution and sensitivity.

CHAPTER 6.

General conclusions

The obtained results described in this PhD Thesis focusing on the development of new LC × LC methods for the chemical characterization of complex food samples, have driven to the following conclusions:

1. The use of microbore columns in the ^{1}D together with an interface equipped with sampling loops with higher inner volume than the strictly required for the collection of the ^{1}D effluent, as well as the use of wider columns in the ^{2}D, is a simple and very useful configuration for the coupling of orthogonal HILIC × RP separations, reducing the solvent strength mismatch problem between dimensions.

2. The chemical characterization of very complex mixtures of proanthocyanidins in different food sources such as grape seeds, apples, grapevine canes and chokeberries samples was successfully achieved by the coupling of HILIC × RP in an on-line approach. The separation of proanthocyanidins was obtained in order of their degree of polymerization in the ^{1}D and according to their relative hydrophobicity in the ^{2}D, attaining very high orthogonality and peak capacities values.

3. The on-line LC × LC-DAD-MS/MS methods developed for the analysis of proanthocyanidins were able to separate, detect and characterize proanthocyanidins with a high degree of polymerization and degree of galloylation in grape seeds as well as other compounds simultaneously detected for the first time in grapevine canes and chokeberries, such as prodelphinidins.

4. The 2DLC methods developed for the analysis of proanthocyanidins, allowed also the separation of the whole metabolite phenolic profile of apples, chokeberry and grapevine canes in a single run, including: dihydrochalcones, flavonols and hydroxycinnamic acids in apples; the complex composition of anthocyanins, flavonoids and phenolic acids in chokeberry, and; stilbene polymers in the case of grapevine canes.

5. The application of MDLC methods for the chemical characterization of phlorotannins from brown algae is reported for the first time. The diol-HILIC compatible stationary phase in

the ^{1}D coupled to a C_{18}-RP column in the ^{2}D provided very good resolving power and separation efficiency of phlorotannins as well as high peak capacity values.

6. The MS and MS/MS spectra obtained as well as the enhanced separation power provided by HILIC × RP allowed a broad separation and the tentative identification of highly polymerized phlorotannins. In particular, the analysis of *Cystoseira abies-marina* revealed phlorotannins from 5 to 17 PGUs, whereas different types of phlorotannins, including fuhalols and hydroxyfuhalols with a relatively high degree of hydroxylation as well as phlorethol-, fucol- and fucophlorethol-types were detected and tentatively identified in *Sargassum muticum*.

7. A novel HILIC × RP method employing a ZIC-HILIC-bonded stationary phase in the ^{1}D and a C_{18} column in the ^{2}D was developed for the characterization secondary metabolite profile of licorice. The new method allowed the separation of up to 89 compounds including 47 closely related triterpene saponins in the Iranian sample.

8. The application of HILIC × RP methods for the chemical characterization of complex food samples, allowed studying the use of 2D plots and the 2D data treatment for the comparison, differentiation and authentication of different samples based on their geographical origin.

9. After an in-depth study of several focusing and non-focusing modulation strategies, the use of active modulation with a make-up flow rate of weaker solvent delivered at 9-times the ^{1}D flow rate allowed the significant improvement of the attainable separation of licorice metabolites, minimizing the non-desired effects related to ^{1}D undersampling and ^{2}D band broadening as well as improving overall 2D resolution and sensitivity, compared to the initial HILIC × RP method.

10. In summary, as **final conclusion**, in this PhD Thesis the huge capability of on-line LC × LC technique, coupling a HILIC-based separation in the ^{1}D and RP-based separation in the ^{2}D, for the chemical characterization of complex food samples that cannot be completely separated by conventional one-dimensional systems has been demonstrated.

CHAPTER 6.

Conclusiones generales

Los resultados obtenidos descritos en esta Tesis Doctoral centrada en el desarrollo de nuevos métodos LC × LC para la caracterización química de muestras alimentarias complejas, han dado lugar a las siguientes conclusiones:

1. El uso de columnas de pequeño diámetro interno en la ^{1}D junto con una interfase equipada con *loops* de muestreo con mayor volumen interno que el estrictamente necesario para almacenar el efluente de la ^{1}D, así como el uso de columnas ^{2}D más anchas, constituye una configuración simple y muy útil para el acoplamiento de separaciones ortogonales HILIC × RP, reduciendo el problema de incompatibilidad en la fuerza de los disolventes entre las dos dimensiones.

2. La caracterización química de muestras muy complejas de proantocianidinas en diferentes muestras alimentarias como las semillas de uva, las manzanas, los sarmientos de vid y la aronia negra se logró satisfactoriamente mediante el acoplamiento en línea de HLIC × RP. Se obtuvo la separación de proantocianidinas en orden de grado de polimerización en la ^{1}D y de acuerdo a su hidrofobicidad relativa en la ^{2}D, alcanzando altos valores de ortogonalidad y capacidad de pico.

3. El método LC × LC-DAD-MS/MS en línea desarrollado para el análisis de proantocianidinas fue capaz de separar, detectar y caracterizar proantocianidinas con un alto grado de polimerización y grado de galoilación en semillas de uva así como otros compuestos detectados simultáneamente por primera vez en las muestras de sarmientos de vid y aronia negra, como son las prodelfinidinas.

4. Los métodos 2DLC desarrollados para el análisis de proantocianidinas, permitieron también la separación del perfil de metabolitos completo de manzanas, aronia negra y sarmientos de vid en un único análisis, incluyendo: dihidrochalconas, flavonoles y ácidos hidroxicinámicos en manzanas; la compleja composición de antocianinas, flavonoides y ácidos fenólicos en aronia negra, y polímeros de estilbenos en el caso del sarmiento de vid.

5. Se ha llevado a cabo la aplicación de métodos MDLC para la caracterización química de florotaninos de algas marrones por primera vez. La fase estacionaria diol compatible con HILIC en la ^{1}D acoplada a una columna C_{18} en modo RP en la ^{2}D proporcionó un poder de resolución

y una eficacia de separación de los florotaninos muy elevados, así como altos valores de capacidad de pico.

6. La buena separación obtenida así como la identificación tentativa de florotaninos altamente polimerizados fue posible gracias al incremento en el poder de separación proporcionado por la combinación HILIC × RP y al uso de los espectros MS y MS/MS obtenidos. En particular, los análisis de *Cystoseira abies-marina* revelaron florotaninos de 5 a 17 PGUs, mientras que diferentes tipo de florotantinos, incluyendo fuhaloles e hidroxifuhaloles con un grado de hidroxilación relativamente alto, así como floretoles, fucoles y fucofloretoles fueron detectados e identificados tentativamente en *Sargassum muticum*.

7. Se desarrolló un nuevo método HILIC × RP empleado en la ^{1}D una fases estacionaria ZIC-HILIC y una C_{18} en la ^{2}D para la caracterización del perfil de metabolitos secundarios de regaliz. El nuevo método permitió la separación de hasta 89 compuestos incluyendo 47 saponinas triterpénicas estrechamente relacionadas en la muestra procedente de Irán.

8. La aplicación de métodos HILIC × RP para la caracterización química de muestras alimentarias complejas, permitió el uso de los cromatogramas 2D y el tratamiento de datos 2D para la comparación, diferenciación y autentificación de diferentes muestras basadas en su origen geográfico.

9. Tras el estudio en profundidad de varios estrategias de modulación con y sin efecto de enfoque, el uso de modulación activa con un flujo compensatorio de un disolvente más débil suministrado con un caudal 9 veces mayor a la velocidad de flujo de la ^{1}D permitió una mejora significativa de la separación obtenida para los metabolitos de regaliz, minimizando los efectos no deseados del submuestreo de la ^{1}D y del ensanchamiento de banda de la ^{2}D, así como una mejora de la resolución y sensibilidad 2D global, comparado con el método HILIC × RP inicial.

10. En resumen, como **conclusión final**, en esta Tesis Doctoral se ha demostrado la enorme capacidad de la LC × LC en línea para la caracterización química de muestras alimentarias complejas que no pueden separarse por completo mediante sistemas unidimensionales convencionales.

REFERENCES

Alarcón-Flores, M. I., Romero-González, R., Martínez Vidal, J. L., & Garrido Frenich, A. (2014). Determination of phenolic compounds in artichoke, garlic and spinach by ultra-high-performance liquid chromatography coupled to tandem mass spectrometry. *Food Analytical Methods*, *7*, 2095–2106.

Ali, F., Ranneh, Y., Ismail, A., & Esa, N. M. (2015). Identification of phenolic compounds in polyphenols-rich extract of Malaysian cocoa powder using the HPLC-UV-ESI—MS/MS and probing their antioxidant properties. *Journal of Food Science and Technology*, *52*, 2103–2111.

Alpert, A. J. (1990). Hydrophilic-interaction chromatography for the separation of peptides, nucleic acids and other polar compounds. *Journal of Chromatography A*, *499*, 177–196.

Amsler, C. D., & Fairhead, V. A. (2006). Defensive and Sensory Chemical Ecology of Brown Algae. *Advances in Botanical Research*, *43*, 1–91.

Anaëlle, T., Leon, E. S., Laurent, V., Elena, I., Mendiola, J. A, Stéphane, C., et al. (2013). Green improved processes to extract bioactive phenolic compounds from brown macroalgae using Sargassum muticum as model. *Talanta*, *104*, 44–52.

Ancillotti, C., Ciofi, L., Rossini, D., Chiuminatto, U., Stahl-zeng, J., Orlandini, S., et al. (2016). Liquid chromatographic/electrospray ionization quadrupole/time of flight tandem mass spectrometric study of polyphenolic composition of different Vaccinium berry species and their comparative evaluation. *Analytical and Bioanalytical Chemistry*, *409*, 1347–1368.

Ard, J. D., Miller, G., & Kahan, S. (2016). Nutrition Interventions for Obesity. *Medical Clinics of North America*, *100*, 1341–1356.

Aron, P. M., & Kennedy, J. A. (2008). Flavan-3-ols: Nature, occurrence and biological activity.

Molecular Nutrition and Food Research, *52*, 79–104.

Asif, A., Farooq, U., Akram, K., Hayat, Z., Shafi, A., Sarfraz, F., et al. (2016). Therapeutic potentials of bioactive compounds from mango fruit wastes. *Trends in Food Science and Technology*, *53*, 102–112.

Augustin, J. M., Kuzina, V., Andersen, S. B., & Bak, S. (2011). Molecular activities, biosynthesis and evolution of triterpenoid saponins. *Phytochemistry*, *72*, 435–457.

Beccaria, M., Costa, R., Sullini, G., Grasso, E., Cacciola, F., Dugo, P., & Mondello, L. (2015). Determination of the triacylglycerol fraction in fish oil by comprehensive liquid chromatography techniques with the support of gas chromatography and mass spectrometry data. *Analytical and Bioanalytical Chemistry*, *407*, 5211–5225.

Bedani, F., Schoenmakers, P. J., & Janssen, H. G. (2012). Theories to support method development in comprehensive two-dimensional liquid chromatography--A review. *Journal of separation science*, *35*, 1697–1711.

Beelders, T., Kalili, K. M., Joubert, E., De Beer, D., & De Villiers, A. (2012). Comprehensive two-dimensional liquid chromatographic analysis of rooibos (Aspalathus linearis) phenolics. *Journal of Separation Science*, *35*, 1808–1820.

Bernal, J., Ares, A. M., Pól, J., & Wiedmer, S. K. (2011). Hydrophilic interaction liquid chromatography in food analysis. *Journal of Chromatography A*, *1218*, 7438–7452.

Betteridge, K., Cao, Y., & Colegate, S. M. (2005). Improved method for extraction and LC-MS analysis of pyrrolizidine alkaloids and their N-oxides in honey: Application to Echium vulgare honeys. *Journal of Agricultural and Food Chemistry*, *53*, 1894–1902.

Bhat, R. V. (2008). Human health problems associated with current agricultural food production. *Asia Pacific Journal of Clinical Nutrition*, *17*, 91–94.

Bretanha, L. C., Piovezan, M., Sako, A. F. V., Pizzolatti, M. G., & Micke, G. A. (2014). Strategy for a Fast and Simple Method for Trace Determination of Senecionine and Senecionine N-Oxide in Honey Using LVI in HPLC-MS/MS. *American Journal of Analytical Chemistry*,

5, 681–687.

Brusotti, G., Cesari, I., Dentamaro, A., Caccialanza, G., & Massolini, G. (2014). Isolation and characterization of bioactive compounds from plant resources: The role of analysis in the ethnopharmacological approach. *Journal of Pharmaceutical and Biomedical Analysis*, *87*, 218–228.

Bushey, M. M., & Jorgenson, J. W. (1990). Automated instrumentation for comprehensive two-dimensional high-performance liquid chromatography of proteins. *Analytical chemistry*, *62*, 161–167.

Cacciola, F., Delmonte, P., Jaworska, K., Dugo, P., Mondello, L., & Rader, J. I. (2011). Employing ultra high pressure liquid chromatography as the second dimension in a comprehensive two-dimensional system for analysis of Stevia rebaudiana extracts. *Journal of Chromatography A*, *1218*, 2012–2018.

Cacciola, F., Donato, P., Giuffrida, D., Torre, G., Dugo, P., & Mondello, L. (2012). Ultra high pressure in the second dimension of a comprehensive two-dimensional liquid chromatographic system for carotenoid separation in red chili peppers. *Journal of Chromatography A*, *1255*, 244–251.

Cacciola, F., Donato, P., Sciarrone, D., Dugo, P., & Mondello, L. (2016a). Comprehensive Liquid Chromatography and other Liquid-based Comprehensive Techniques Coupled to Mass Spectrometry in Food Analysis. *Analytical Chemistry*, *89*, 414–429.

Cacciola, F., Farnetti, S., Dugo, P., Marriott, P. J., & Mondello, L. (2017). Comprehensive two-dimensional liquid chromatography for polyphenol analysis. *Journal of Separation Science*, *40*, 7–24.

Cacciola, F., Giuffrida, D., Utczas, M., Mangraviti, D., Beccaria, M., Donato, P., Bonaccorsi, I., Dugo, P., Mondello, L. (2016b). Analysis of the Carotenoid Composition and Stability in Various Overripe Fruits by Comprehensive Two-Dimensional Liquid Chromatography. *LCGC Europe*, *5*, 252–257.

Cacciola, F., Giuffrida, D., Utczas, M., Mangraviti, D., Dugo, P., Menchaca, D., et al. (2016c). Application of Comprehensive Two-Dimensional Liquid Chromatography for Carotenoid Analysis in Red Mamey (Pouteria sapote). *Food Analytical Methods*, *9*, 2335–2341.

Cacciola, F., Jandera, P., Blahová, E., & Mondello, L. (2006). Development of different comprehensive two dimensional systems for the separation of phenolic antioxidants. *Journal of Separation Science*, *29*, 2500–2513.

Cacciola, F., Jandera, P., Hajdú, Z., Cesla, P., & Mondello, L. (2007). Comprehensive two-dimensional liquid chromatography with parallel gradients for separation of phenolic and flavone antioxidants. *Journal of Chromatography A*, *1149*, 73–87.

Cádiz-Gurrea, M., Borrás-Linares, I., Lozano-Sánchez, J., Joven, J., Fernández-Arroyo, S., & Segura-Carretero, A. (2017). Cocoa and Grape Seed Byproducts as a Source of Antioxidant and Anti-Inflammatory Proanthocyanidins. *International Journal of Molecular Sciences*, *18*, 376-390.

Cai T., Guo Z. Q., Xu X. Y., Wu Z. J. (2016). Recent (2000–2015) developments in the analysis of minor unknown natural products based on characteristic fragment information using LC–MS. *Mass Spectrometry Reviews*, *9999*, 1–15.

Camenzuli, M., & Schoenmakers, P. J. (2014). A new measure of orthogonality for multi-dimensional chromatography. *Analytica Chimica Acta*, *838*, 93–101.

Capriotti, A. L., Cavaliere, C., Foglia, P., Piovesana, S., & Ventura, S. (2015). Chromatographic Methods Coupled to Mass Spectrometry Detection for the Determination of Phenolic Acids in Plants and Fruits. *Journal of Liquid Chromatography & Related Technologies*, *38*, 353–370.

Cardoso, S. M., Pereira, O. R., Seca, A. M. L., Pinto, D. C. G. A., & Silva, A. M. S. (2015). Seaweeds as preventive agents for cardiovascular diseases: From nutrients to functional foods. *Marine Drugs*, *13*, 6838-6865.

Carr, P. W., & Stoll, D. R. (2015). Two-dimensional liquid chromatography: Principles, practical

implementation and applications. *Agilent Technical Note*.

Castro-Puyana, M., & Herrero, M. (2013). Metabolomics approaches based on mass spectrometry for food safety, quality and traceability. *Trends in Analytical Chemistry*, *52*, 74–87.

Castro-Puyana, M., Herrero, M., Urreta, I., Mendiola, J. A., Cifuentes, A., Ibáñez, E., & Suárez-Alvarez, S. (2013a). Optimization of clean extraction methods to isolate carotenoids from the microalga Neochloris oleoabundans and subsequent chemical characterization using liquid chromatography tandem mass spectrometry. *Analytical and Bioanalytical Chemistry*, *405*, 4607–4616.

Castro-Puyana, M., Mendiola, J. A., Ibañez, E., Herrero, M. (2013b). MS-based metabolomics approaches for food safety, quality, and traceability. In A. Cifuentes (Ed.), *Foodomics. Advances mass spectrometry in modern food science and nutrition.* John Wiley & Sons, Inc.

Cavazzini, A., Gritti, F., Kaczmarski, K., Marchetti, N., & Guiochon, G. (2007). Mass-transfer kinetics in a shell packing material for chromatography. *Analytical Chemistry*, *79*, 5972–5979.

Cesla, P., Hájek, T., & Jandera, P. (2009). Optimization of two-dimensional gradient liquid chromatography separations. *Journal of Chromatography A*, *1216*, 3443–3457.

Cesla, P., & Krenková, J. (2017). Fraction transfer process in on-line comprehensive two-dimensional liquid-phase separations. *Journal of Separation Science*, *40*, 109–123.

Cieśla, Ł., & Moaddel, R. (2016). Comparison of analytical techniques for the identification of bioactive compounds from natural products. *Natural Product Reports*, *33*, 1131–1145.

Cifuentes, A. (2009). Food analysis and foodomics. *Journal of Chromatography A*, *1216*, 7109.

Cifuentes, A. (2012). Food Analysis: Present, Future, and Foodomics. *ISRN Analytical Chemistry*, *2012*, 1–16.

Cohen, S. A., & Schure, M. R. (Eds.). (2008). *Multidimensional Liquid Chromatography: Theory*

and Applications in Industrial Chemistry and the Life Sciences. John Wiley & Sons.

Consden, R., Gordon, A. H., & Martin, A. J. (1944). Qualitative analysis of proteins: a partition chromatographic method using paper. *The Biochemical Journal*, *38*, 224–232.

Contarini, G., & Povolo, M. (2013). Phospholipids in milk fat: Composition, biological and technological significance, and analytical strategies. *International Journal of Molecular Sciences*, *14*, 2808–2831.

Cos, P., De Bruyne, T. D., Hermans, N., Apers, S., Berghe, D. V., & Vlietinck, A. J. (2004). Proanthocyanidins in health care: current and new trends. *Current medicinal chemistry*, *11*, 1345–1359.

Counet, C., Ouwerx, C., Rosoux, D., & Collin, S. (2004). Relationship between procyanidin and flavor contents of cocoa liquors from different origins. *Journal of Agricultural and Food Chemistry*, *52*, 6243–6249.

Creese, M. E., Creese, M. J., Foley, J. P., Cortes, H. J., Hilder, E. F., Shellie, R. A., & Breadmore, M. C. (2017). Longitudinal on-column thermal modulation for comprehensive two-dimensional liquid chromatography. *Analytical Chemistry*, *89*, 1123-1130.

Crupi, P., Toci, A. T., Mangini, S., Wrubl, F., Rodolfi, L., Tredici, M. R., et al. (2013). Determination of fucoxanthin isomers in microalgae (Isochrysis sp.) by high-performance liquid chromatography coupled with diode-array detector multistage mass spectrometry coupled with positive electrospray ionization. *Rapid Communications in Mass Spectrometry*, *27*, 1027–1035.

Cuadros-Rodríguez, L., Ruiz-Samblás, C., Valverde-Som, L., Pérez-Castaño, E., & González-Casado, A. (2016). Chromatographic fingerprinting: An innovative approach for food "identitation" and food authentication - A tutorial. *Analytica Chimica Acta*, *909*, 9–23.

Cunliffe, J. M., & Maloney, T. D. (2007). Fused-core particle technology as an alternative to sub-2-μm particles to achieve high separation efficiency with low backpressure. *Journal of Separation Science*, *30*, 3104–3109.

Danezis, G. P., Tsagkaris, A. S., Camin, F., Brusic, V., & Georgiou, C. A. (2016). Food authentication: Techniques, trends & emerging approaches. *TrAC - Trends in Analytical Chemistry*, *85*, 123–132.

Danzer, K. (2007). *Analytical chemistry: Theoretical and metrological fundamentals*. *Springer Science & Business Media.*

Daood, H. G., Bencze, G., Palotás, G., Pék, Z., Sidikov, A., & Helyes, L. (2014). HPLC analysis of carotenoids from tomatoes using cross-linked C18 column and MS detection. *Journal of Chromatographic Science*, *52*, 985–991.

Davis, J. M., & Giddings, J. C. (1983). Statistical theory of component overlap in multicomponent chromatograms. *Analytical Chemistry*, *55*, 418–424.

Davis, J. M., Stoll, D. R., & Carr, P. W. (2008a). Dependence of effective peak capacity in comprehensive two-dimensional separations on the distribution of peak capacity between the two dimensions. *Analytical Chemistry*, *80*, 8122–8134.

Davis J. M,, Stoll, D. R., & Carr, P. W. (2008b). Effect of First-Dimension Undersampling on Effective Peak Capacity in Comprehensive Two-Dimensional Separations. *Analytical Chemistry*, *80*, 461–473.

De Ancos B., Colina-Coca C., González-Peña D., & Sámchez-Moreno, C. (2015). Bioactive compounds from vegetable and fruit by-products. In Gupta, V. K., Tuohy, M. G. (Ed.), *Biotechnology of Bioactive Compounds*. John Wiley & Sons.

de la Iglesia, R., Loria-Kohen, V., Zulet, M. A., Martinez, J. A., Reglero, G., & de Molina, A. R. (2016). Dietary strategies implicated in the prevention and treatment of metabolic syndrome. *International Journal of Molecular Sciences*, *17*, 1877–1892.

De Paepe, D., Servaes, K., Noten, B., Diels, L., De Loose, M., Van Droogenbroeck, B., & Voorspoels, S. (2013). An improved mass spectrometric method for identification and quantification of phenolic compounds in apple fruits. *Food Chemistry*, *136*, 368–375.

Dejaegher, B., Mangelings, D., & Vander Heyden, Y. (2008). Method development for HILIC

assays. *Journal of Separation Science*, *31*, 1438–1448.

Del Bubba, M., Checchini, L., Chiuminatto, U., Doumett, S., Fibbi, D., & Giordani, E. (2012). Liquid chromatographic/electrospray ionization tandem mass spectrometric study of polyphenolic composition of four cultivars of Fragaria vesca L. berries and their comparative evaluation. *Journal of Mass Spectrometry*, *47*, 1207–1220.

Di Stefano, V., Avellone, G., Bongiorno, D., Cunsolo, V., Muccilli, V., Sforza, S., et al. (2012). Applications of liquid chromatography-mass spectrometry for food analysis. *Journal of Chromatography A*, *1259*, 74–85.

Doğu, S. Ö., & Şİrelİ, U. T. (2016). Determination Tools of Origin in the Food Traceability. *Journal of Food and Health Science*, *2*, 140–146.

Donato, P., Rigano, F., Cacciola, F., Schure, M., Farnetti, S., Russo, M., et al. (2016). Comprehensive two-dimensional liquid chromatography-tandem mass spectrometry for the simultaneous determination of wine polyphenols and target contaminants. *Journal of Chromatography A*, *1458*, 54–62.

Dugo, P., Cacciola, F., Kumm, T., Dugo, G., & Mondello, L. (2008a). Comprehensive multidimensional liquid chromatography: Theory and applications. *Journal of Chromatography A*, *1184*, 353–368.

Dugo, P., Favoino, O., Luppino, R., Dugo, G., & Mondello, L. (2004). Comprehensive Two-Dimensional Normal-Phase (Adsorption)-Reversed-Phase Liquid Chromatography. *Analytical Chemistry*, *76*, 2525–2530.

Dugo, P., Fawzy, N., Cichello, F., Cacciola, F., Donato, P., & Mondello, L. (2013). Stop-flow comprehensive two-dimensional liquid chromatography combined with mass spectrometric detection for phospholipid analysis. *Journal of Chromatography A*, *1278*, 46–53.

Dugo, P., Giuffrida, D., Herrero, M., Donato, P., & Mondello, L. (2009). Original Paper Epoxycarotenoids esters analysis in intact orange juices using two-dimensional comprehensive liquid chromatography, *Journal of Separation Science, 32*, 973–980.

Dugo, P., Herrero, M., Giuffrida, D., Kumm, T., Dugo, G., & Mondello, L. (2008b). Application of comprehensive two-dimensional liquid chromatography to elucidate the native carotenoid composition in red orange essential oil. Journal of agricultural and food chemistry, *56*, 3478-3485.

Dugo, P., Herrero, M., Kumm, T., Giuffrida, D., Dugo, G., & Mondello, L. (2008c). Comprehensive normal-phase × reversed-phase liquid chromatography coupled to photodiode array and mass spectrometry detection for the analysis of free carotenoids and carotenoid esters from mandarin, *Journal of Chromatography A, 1189*, *1189*, 196–206.

Dugo, P., Kumm, T., Chiofalo, B., Cotroneo, A., & Mondello, L. (2006a). Separation of triacylglycerols in a complex lipidic matrix by using comprehensive two-dimensional liquid chromatography coupled with atmospheric pressure chemical ionization mass spectrometric detection. *Journal of separation science*, *29*, 1146–1154.

Dugo, P., Kumm, T., Crupi, M. L., Cotroneo, A., & Mondello, L. (2006b). Comprehensive two-dimensional liquid chromatography combined with mass spectrometric detection in the analyses of triacylglycerols in natural lipidic matrixes. *Journal of Chromatography A*, *1112*, 269–275.

Dugo, P., Škeříková, V., Kumm, T., Trozzi, A., Jandera, P., & Mondello, L. (2006c). Elucidation of carotenoid patterns in citrus products by means of comprehensive normal-phase x reversed-phase liquid chromatography. *Analytical Chemistry*, *78*, 7743–7750.

Dugo P. , Mondello L., Cacciola F., Donato P. (2011). Comprehensive two-dimensional liquid chromatography combined with mass spectrometry. In M. Luigi (Ed.), *Comprehensive chromatography in combination with mass spectrometry*. Wiley & Sons, Inc.

Egeness, M. J., Breadmore, M. C., Hilder, E. F., Shellie, R. A. (2016). The Modulator in Comprehensive Two- Dimensional Liquid Chromatography. *LCGC Europe*, *29*, 268–276.

El Shoubaky, G. A., & Salem, E. A. (2014). Terpenes and sterols composition of marine brown

algae Padina pavonica (Dictyotales) and Hormophysa triquetra (Fucales). *International Journal of Pharmacognosy and Phytochemical Research*, *6*, 894–900.

Erni, F., & Frei, R. W. (1978). Two-dimensional column liquid chromatographic technique for resolution of complex mixtures. *Journal of Chromatography A*, *149*, 561–569.

Esparza-Martínez, F. J., Miranda-López, R., Mata-Sánchez, S. M., & Guzmán-Maldonado, S. H. (2016). Extractable and non-extractable phenolics and antioxidant capacity of mandarin waste dried at different temperatures. *Plant Foods for Human Nutrition*, *71*, 294–300.

Faizal, A., & Geelen, D. (2013). Saponins and their role in biological processes in plants. *Phytochemistry Reviews*, *12*, 877–893.

Farag, M. A., Porzel, A., & Wessjohann, L. A. (2012). Comparative metabolite profiling and fingerprinting of medicinal licorice roots using a multiplex approach of GC-MS, LC-MS and 1D NMR techniques. *Phytochemistry*, *76*, 60–72.

Fekete, S., Schappler, J., Veuthey, J. L., & Guillarme, D. (2014). Current and future trends in UHPLC. *Trends in Analytical Chemistry*, *63*, 2–13.

Ferreres, F., Lopes, G., Gil-Izquierdo, A., Andrade, P. B., Sousa, C., Mouga, T., & Valentão, P. (2012). Phlorotannin extracts from fucales characterized by HPLC-DAD-ESI-MS n: Approaches to hyaluronidase inhibitory capacity and antioxidant properties. *Marine Drugs*, *10*, 2766–2781.

Filgueira, M. R., Huang, Y., Witt, K., Castells, C., & Carr, P. W. (2011). Improving peak capacity in fast online comprehensive two-dimensional liquid chromatography with post-first-dimension flow splitting. *Analytical Chemistry*, *83*, 9531–9539.

François, I., de Villiers, A., Tienpont, B., David, F., & Sandra, P. (2008). Comprehensive two-dimensional liquid chromatography applying two parallel columns in the second dimension. *Journal of Chromatography A*, *1178*, 33–42.

François, I., Sandra, K., & Sandra, P. (2009). Comprehensive liquid chromatography:

Fundamental aspects and practical considerations–A review. *Analytica Chimica Acta, 641*, 14–31.

Fraser, P. D., & Bramley, P. M. (2004). The biosynthesis and nutritional uses of carotenoids, *Progress in Lioid Research, 43*, 228–265.

Gafner, S., Bergeron, C., McCollom, M. M., Cooper, L. M., McPhail, K. L., Gerwick, W. H., & Angerhofer, C. K. (2004). Evaluation of the Efficiency of Three Different Solvent Systems to extract triterpene saponins from roots of *Panax quinquefolius* using high-performance liquid chromatography. *Journal of Agricultural and Food Chemistry, 52*, 1546–1550.

Gallo, M., & Ferranti, P. (2016). The evolution of analytical chemistry methods in foodomics. *Journal of Chromatography A, 1428*, 3–15.

Gargano, A. F., Duffin, M., Navarro, P., & Schoenmakers, P. J. (2016). Reducing dilution and analysis time in online comprehensive two-dimensional liquid chromatography by active modulation. *Analytical Chemistry, 88*, 1785–1793.

Gentili, A., Caretti, F., Ventura, S., Pérez-Fernández, V., Venditti, A., & Curini, R. (2015). Screening of carotenoids in tomato fruits by using liquid chromatography with diode array-linear ion trap mass spectrometry detection. *Journal of Agricultural and Food Chemistry, 63*, 7428–7439.

Giddings, J. C. (1995). Sample dimensionality: A predictor of order-disorder in component peak distribution in multidimensional separation. *Journal of Chromatography A, 703*, 3–15.

Gilar, M., Olivova, P., Daly, A. E., & Gebler, J. C. (2005). Orthogonaliy of separation in two-dimensional liquid chromatography. *Analytical Chemistry, 77*, 6426–6434.

Gilbert-López, B., Mendiola, J. A., Fontecha, J., van den Broek, L. A. M., Sijtsma, L., Cifuentes, A., et al. (2015). Downstream processing of Isochrysis galbana: a step towards microalgal biorefinery. *Green Chem., 17*, 4599–4609.

González-Manzano, S., Santos-Buelga, C., Pérez-Alonso, J. J., Rivas-Gonzalo, J. C., & Escribano-Bailón, M. T. (2006). Characterization of the mean degree of polymerization of proanthocyanidins in red wines using Liquid Chromatography-Mass Spectrometry (LC-MS). *Journal of Agricultural and Food Chemistry*, *54*, 4326–4332.

Gu, L., Kelm, M. A., Hammerstone, J. F., Beecher, G., Holden, J., Haytowitz, D., & Prior, R. L. (2003). Screening of foods containing proanthocyanidins and their structural characterization using LC-MS/MS and thiolytic degradation. *Journal of Agricultural and Food Chemistry*, *51*, 7513–7521.

Gu, L., Kelm, M., Hammerstone, J. F., Beecher, G., Cunningham, D., Vannozzi, S., & Prior, R. L. (2002a). Fractionation of polymeric procyanidins from lowbush blueberry and quantification of procyanidins in selected foods with an optimized normal-phase HPLC-MS fluorescent detection method. *Journal of Agricultural and Food Chemistry*, *50*, 4852–4860.

Gu, L., Tao, G., Gu, W., & Prior, R. L. (2002b). Determination of soyasaponins in soy with LC-MS following structural unification by partial alkaline degradation. *Journal of Agricultural and Food Chemistry*, *50*, 6951–6959.

Guajardo-Flores, D., García-Patiño, M., Serna-Guerrero, D., Gutiérrez-Uribe, J. A., & Serna-Saldívar, S. O. (2012). Characterization and quantification of saponins and flavonoids in sprouts, seed coats and cotyledons of germinated black beans. *Food Chemistry*, *134*, 1312–1319.

Guerrero, R. F., Liazid, A., Palma, M., Puertas, B., González-Barrio, R., Gil-Izquierdo, Á., et al. (2009). Phenolic characterisation of red grapes autochthonous to Andalusia. *Food Chemistry*, *112*, 949–955.

Guillarme, D., Schappler, J., Rudaz, S., & Veuthey, J. L. (2010). Coupling ultra-high-pressure liquid chromatography with mass spectrometry. *Trends in Analytical Chemistry*, *29*, 15–27.

Guiochon, G., Marchetti, N., Mriziq, K., & Shalliker, R. A. (2008). Implementations of two-

dimensional liquid chromatography. *Journal of Chromatography A, 1189*, 109–168.

Hájek, T., Jandera, P., Staňková, M., & Cesla, P. (2016). Automated dual two-dimensional liquid chromatography approach for fast acquisition of three-dimensional data using combinations of zwitterionic polymethacrylate and silica-based monolithic columns. *Journal of Chromatography A, 1446*, 91–102.

Hájek, T., Skeríková , V., Cesla, P., Vyňuchalová, K., & Jandera, P. (2008). Multidimensional LC×LC analysis of phenolic and flavone natural antioxidants with UVelectrochemical coulometric and MS detection. *Journal of Separation Science, 31*, 3309–3328.

Hayashi, H., & Sudo, H. (2009). Economic importance of licorice. *Plant Biotechnology, 26*, 101–104.

Heffernan, N., Brunton, N. P., FitzGerald, R. J., & Smyth, T. J. (2015). Profiling of the molecular weight and structural isomer abundance of macroalgae-derived phlorotannins. *Marine Drugs, 13*, 509–528.

Hellstro, J. K., & Mattila, P. H. (2008). HPLC determination of extractable and unextractable proanthocyanidins in plant materials. Journal of Agricultural and Food Chenistry, *56*, 7617–7624.

Hernández-Santos, B., Vivar-Vera, M. A., Rodríguez-Miranda, J., Herman-Lara, E., Torruco-Uco, J. G., Acevedo-Vendrell, O., & Martínez-Sánchez, C. E. (2015). Dietary fibre and antioxidant compounds in passion fruit (Passiflora edulis f. flavicarpa) peel and depectinised peel waste. *International Journal of Food Science and Technology, 50*, 268–274.

Herrero, M., Ibáñez, E., Cifuentes, A., & Bernal, J. (2009). Multidimensional chromatography in food analysis. *Journal of Chromatography A, 1216*, 7110–7129.

Herrero, M., Plaza, M., Cifuentes, A., & Ibáñez, E. (2010). Green processes for the extraction of bioactives from Rosemary: Chemical and functional characterization via ultra-performance liquid chromatography-tandem mass spectrometry and in-vitro assays.

Journal of Chromatography A, *1217*, 2512–2520.

Herrero, M., Sánchez-Camargo, A. P., Cifuentes, A., & Ibáñez, E. (2015). Plants, seaweeds, microalgae and food by-products as natural sources of functional ingredients obtained using pressurized liquid extraction and supercritical fluid extraction. *Trends in Analytical Chemistry*, *71*, 26–38.

HolCapek, M., Velínská, H., Lísa, M., & Cesla, P. (2009). Orthogonality of silver-ion and non-aqueous reversed-phase HPLC/MS in the analysis of complex natural mixtures of triacylglycerols. *Journal of Separation Science*, *32*, 3672–3680.

Horie, K., Kimura, H., Ikegami, T., Iwatsuka, A., Saad, N., Fiehn, O., & Tanaka, N. (2007). Calculating optimal modulation periods to maximize the peak capacity in two-dimensional HPLC. *Analytical Chemistry*, *79*, 3764–3770.

Horváth, K., Fairchild, J. N., & Guiochon, G. (2009). Detection issues in two-dimensional on-line chromatography. *Journal of Chromatography A*, *1216*, 7785–7792.

Hosseinian, F. S., Li, W., Hydamaka, A. W., Tsopmo, A., Lowry, L., Friel, J., & Beta, T. (2007). Proanthocyanidin profile and ORAC values of Manitoba berries, Chokecherries, and Seabuckthorn. *Journal of Agricultural and Food Chemistry*, *55*, 6970–6976.

Huhman, D. V., Berhow, M. A., & Sumner, L. W. (2005). Quantification of saponins in aerial and subterranean tissues of Medicago truncatula. *Journal of Agricultural and Food Chemistry*, *53*, 1914–1920.

Huidobro, A. L., Pruim, P., Schoenmakers, P., & Barbas, C. (2008). Ultra rapid liquid chromatography as second dimension in a comprehensive two-dimensional method for the screening of pharmaceutical samples in stability and stress studies. *Journal of Chromatography A*, *1190*, 182–190.

Hümmer, W., & Schreier, P. (2008). Analysis of proanthocyanidins. *Molecular Nutrition and Food Research*, *52*, 1381–1398.

Ibáñez E., & Cifuentes, A. (2014). Foodomics: Food science and nutrition in the postgenomic

era. *Comprehensive Analytical Chemistry, 64*, 395–440.

Isaza Martínez, J. H., & Torres Castañeda, H. G. (2013). Preparation and chromatographic analysis of phlorotannins. *Journal of Chromatographic Science, 51*, 825-838.

Jaganath, I. B., & Crozier, A. (2009). Dietary Flavonoids and Phenolic Compounds. In Fraga, C. G. *Plant Phenolics and Human Health: Biochemistry, Nutrition, and Pharmacology*. John Wiley & Sons.

Jandera, P. (2011). Stationary and mobile phases in hydrophilic interaction chromatography: A review. *Analytica Chimica Acta, 692*, 1–25.

Jandera, P. (2012). Comprehensive two-dimensional liquid chromatography — practical impacts of theoretical considerations. A review. *Central European Journal of Chemistry, 10*, 844–875.

Jandera, P., Cesla, P., Hájek, T., Vohralík, G., Vynuchalová, K., & Fischer, J. (2008). Optimization of separation in two-dimensional high-performance liquid chromatography by adjusting phase system selectivity and using programmed elution techniques. *Journal of Chromatography A, 1189*, 207–220.

Jandera, P., Hájek, T., & Cesla, P. (2010). Comparison of various second-dimension gradient types in comprehensive two-dimensional liquid chromatography. *Journal of Separation Science, 33*, 1382–1397.

Jandera, P., Hájek, T., Staňková, M., Vyňuchalová, K., & Cesla, P. (2012). Optimization of comprehensive two-dimensional gradient chromatography coupling in-line hydrophilic interaction and reversed phase liquid chromatography. *Journal of Chromatography A, 1268*, 91–101.

Jandera, P., Staňková, M., & Hájek, T. (2013). New zwitterionic polymethacrylate monolithic columns for one- and two-dimensional microliquid chromatography. *Journal of Separation Science, 36*, 2430–2440.

Jeong, E. K., Cha, H. J., Ha, Y. W., Kim, Y. S., Ha, I. J., & Na, Y. (2010). Development and

optimization of a method for the separation of platycosides in Platycodi Radix by comprehensive two-dimensional liquid chromatography with mass spectrometric detection. *Journal of Chromatography A, 1217*, 4375–4382.

Jeong, W. S., & Kong, A. N. T. (2004). Biological Properties of Monomeric and Polymeric Catechins: Green Tea Catechins and Procyanidins. *Pharmaceutical Biology, 42*, 84–93.

Jiang, Z., Wang, Y., Zheng, Y., Yang, J., & Zhang, L. (2016). Ultra high performance liquid chromatography coupled with triple quadrupole mass spectrometry and chemometric analysis of licorice based on the simultaneous determination of saponins and flavonoids. *Jornal of Separation Science, 39*, 2928–2940.

Kalili, K. M., & de Villiers, A. (2009). Off-line comprehensive 2-dimensional hydrophilic interaction × reversed phase liquid chromatography analysis of procyanidins. *Journal of Chromatography A, 1216*, 6274–6284.

Kalili, K. M., & De Villiers, A. (2013). Systematic optimisation and evaluation of on-line, off-line and stop-flow comprehensive hydrophilic interaction chromatography × reversed phase liquid chromatographic analysis of procyanidins. Part II: Application to cocoa procyanidins. *Journal of Chromatography A, 1289*, 69–79.

Kalili, K. M., Vestner, J., Stander, M. A., & De Villiers, A. (2013). Toward unraveling grape tannin composition: Application of online hydrophilic interaction chromatography × reversed-phase liquid chromatography-time-of-flight mass spectrometry for grape seed analysis. *Analytical Chemistry, 85*, 9107–9115.

Kamo, S., Suzuki, S., & Sato, T. (2014). The content of soyasaponin and soyasapogenol in soy foods and their estimated intake in the Japanese. *Food Science & Nutrition, 2*, 289–97.

Kast, C., Dübecke, A., Kilchenmann, V., Bieri, K., Böhlen, M., Zoller, O., et al. (2014). Analysis of Swiss honeys for pyrrolizidine alkaloids. *Journal of Apicultural Research, 53*, 75–83.

Kaur, A., Scarborough, P., Hieke, S., Kusar, A., Pravst, I., Raats, M., & Rayner, M. (2016). The nutritional quality of foods carrying health-related claims in Germany, The Netherlands, Spain, Slovenia and the United Kingdom. *European Journal of Clinical*

Nutrition, *70*, 1388–1395.

Kelm, M. A., Johnson, J. C., Robbins, R. J., Hammerstone, J. F., & Schmitz, H. H. (2006). High-performance liquid chromatography separation and purification of cacao (Theobroma cacao L.) procyanidins according to degree of polymerization using a diol stationary phase. *Journal of Agricultural and Food Chemistry*, *54*, 1571-1576.

Khakimov, B., Tseng, L. H., Godejohann, M., Bak, S., & Engelsen, S. B. (2016). Screening for Triterpenoid Saponins in Plants Using Hyphenated Analytical Platforms. *Molecules*, *21*, 1614-1633.

Khanam, U. K. S., Oba, S., Yanase, E., & Murakami, Y. (2012). Phenolic acids, flavonoids and total antioxidant capacity of selected leafy vegetables. *Journal of Functional Foods*, *4*, 979–987.

Kim, S. M., Kang, S. W., Jeon, J. S., Jung, Y. J., Kim, W. R., Kim, C. Y., & Um, B. H. (2013). Determination of major phlorotannins in Eisenia bicyclis using hydrophilic interaction chromatography: Seasonal variation and extraction characteristics. *Food Chemistry*, *138*, 2399–2406.

Kivilompolo, M., & Hyötyläinen, T. (2008). Comparison of separation power of ultra performance liquid chromatography and comprehensive two-dimensional liquid chromatography in the separation of phenolic compounds in beverages. *Journal of separation science*, *31*, 3466–3472.

Koivikko, R., Loponen, J., Pihlaja, K., & Jormalainen, V. (2007). High-performance liquid chromatographic analysis of phlorotannins from the brown alga Fucus vesiculosus. *Phytochemical Analysis*, *18*, 326–332.

Kok E., van der Spiegel M., Prins T., Manti, V., Groot M., Bremer M., van Raamsdonk L., van der Fels I., van Ruth. S. (2012). Traceability. In Y. Picó (Ed.), *Chemical Analysis of Food: Techniques and Applications*. Elsevier.

Kris-Etherton, P. M., Lefevre, M., Beecher, G. R., Gross, M. D., Keen, C. L., & Etherton, T. D. (2004). Bioactive compounds in nutrition and health-research methodologies for

establishing biological function: the antioxidant and anti-inflammatory effects of flavonoids on atherosclerosis. *Annual Review of Nutrition*, *24*, 511–538.

Krishnamurthy, P., Tsukamoto, C., Takahashi, Y., Hongo, Y., Singh, R. J., Lee, J. D., & Chung, G. (2014). Comparison of saponin composition and content in wild soybean (Glycine soja Sieb. and Zucc.) before and after germination. *Bioscience, Biotechnology, and Biochemistry*, *78*, 1988–1996.

Krska, R., Stubbings, G., MacArthur, R., & Crews, C. (2008). Simultaneous determination of six major ergot alkaloids and their epimers in cereals and foodstuffs by LC-MS-MS. *Analytical and Bioanalytical Chemistry*, *391*, 563–576.

La Barre, S., Potin, P., Leblanc, C., & Delage, L. (2010). The halogenated metabolism of brown algae (phaeophyta), its biological importance and its environmental significance. *Marine Drugs*, *8*, 988-1010.

Lazarus, S. A, Adamson, G. E., Hammerstone, J. F., & Schmitz, H. H. (1999). High-performance liquid Chromatography/Mass spectrometry analysis of proanthocyanidins in foods and beverages. *Journal of agricultural and food chemistry*, *47*, 3693–3701.

Lawal, A., Tan, G. H., & Alsharif, A. M. A. (2016). Recent advances in analysis of pesticides in food and drink samples using LPME techniques couples to GC-MS and LC-MS □: a review. *Journal of AOAC International*, *99*, 1383–1394.

Li, D., Jakob, C., & Schmitz, O. J. (2015). Practical considerations in comprehensive two-dimensional liquid chromatography systems (LC×LC) with reversed-phases in both dimensions. *Analytical and Bioanalytical Chemistry*, *407*, 153–167.

Li, D., & Schmitz, O. J. (2015). Comprehensive two-dimensional liquid chromatography tandem diode array detector (DAD) and accurate mass QTOF-MS for the analysis of flavonoids and iridoid glycosides in Hedyotis diffusa. *Analytical and Bioanalytical Chemistry*, *407*, 231–240.

Li, M., Hou, X. F., Zhang, J., Wang, S. C., Fu, Q., & He, L. C. (2011). Applications of HPLC/MS in the analysis of traditional Chinese medicines. *Journal of Pharmaceutical Analysis*, *1*, 81–

91.

Li, X., Stoll, D. R., & Carr, P. W. (2009). A simple and accurate equation for peak capacity estimation in two-dimensional liquid chromatography. *Analytical Chemistry, 81*, 845–850.

Li, Y. X., Wijesekara, I., Li, Y., & Kim, S.K. (2011). Phlorotannins as bioactive agents from brown algae. *Process Biochemistry , 46, 2219-2224.*

Li, Z., Chen, K., Guo, M., & Tang, D. (2016). Two-dimensional liquid chromatography and its application in traditional Chinese medicine analysis and metabonomic investigation. *Journal of separation science, 39*, 21–37.

Liu, H., & Gu, L. (2012). Phlorotannins from brown algae (*Fucus vesiculosus*) inhibited the formation of advanced glycation endproducts by scavenging reactive carbonyls. *Journal of Agricultural and Food Chemistry, 60*, 1326–1334.

Liu, S. X. & White, E. (2012). Extraction and characterization of Proanthocyanidins from grape seeds. *The Open Food Science Journal, 6*, 5–11.

Liu, Z., Patterson, D. G., & Lee, M. L. (1995). Geometric approach to factor analysis for the estimation of orthogonality and practical peak capacity in comprehensive two-dimensional separations. *Analytical Chemistry, 67*, 3840–3845.

Locatelli, M., Melucci, D., Carlucci, G., & Locatelli, C. (2012). Recent HPLC strategies to improve sensitivity and selectivity for the analysis of complex matrices. *Instrumentation Science & Technology, 40*, 112–137.

Lucci, P., Saurina, J., & Núñez, O. (2016). Trends in LC-MS and LC-HRMS analysis and characterization of polyphenols in food. *Trends in Analytical Chemistry, 88,* 1-24.

Määttä-Riihinen, K. R., Kähkönen, M. P., Törrönen, A. R., & Heinonen, I. M. (2005). Catechins and procyanidins in berries of Vaccinium species and their antioxidant activity. *Journal of Agricultural and Food Chemistry, 53*, 8485–8491.

Majinda, R. R. T. (2012). Extraction and isolation of saponins. In Sarker, S. D., & Nahar, L.

Natural products isolation. Springer

Malerod, H., Lundanes, E., & Greibrokk, T. (2010). Recent advances in on-line multidimensional liquid chromatography. *Analytical Methods*, *2*, 110–122.

Marchetti, N., Cavazzini, A., Gritti, F., & Guiochon, G. (2007). Gradient elution separation and peak capacity of columns packed with porous shell particles. *Journal of Chromatography A*, *1163*, 203–211.

Marchetti, N., Fairchild, J. N., & Guiochon, G. (2008). Comprehensive off-line, two-dimensional liquid chromatography. Application to the separation of peptide digests. *Analytical Chemistry*, *80*, 2756–2767.

Mathon, C., Edder, P., Bieri, S., & Christen, P. (2014). Survey of pyrrolizidine alkaloids in teas and herbal teas on the Swiss market using HPLC-MS/MS. *Analytical and Bioanalytical Chemistry*, *406*, 7345–7354.

Matsui, Y., Kobayashi, K., Masuda, H., Kigoshi, H., Akao, M., Sakurai, H., & Kumagai, H. (2009). Quantitative analysis of saponins in a tea-leaf extract and their antihypercholesterolemic activity. *Bioscience, Biotechnology and Biochemistry*, *73*, 1513–1519.

Milledge, J. J., Nielsen, B. V., & Bailey, D. (2016). High-value products from macroalgae: the potential uses of the invasive brown seaweed, *Sargassum muticum*. *Reviews in Environmental Science and Biotechnology*, *15*, 67–88.

Monagas, M., Quintanilla-López, J. E., Gómez-Cordovés, C., Bartolomé, B., & Lebrón-Aguilar, R. (2010). MALDI-TOF MS analysis of plant proanthocyanidins. *Journal of Pharmaceutical and Biomedical Analysis*, *51*, 358–372.

Mondello, L., Donato, P., Cacciola, F., Dugo, G., & Dugo, P. (2011). Comprehensive two-dimensional liquid chromatography with evaporative light- scattering detection for the analysis of triacylglycerols in Borago officinalis, *Journal of Separation Science*, *34*, 688–692.

Montero, L., Sánchez-Camargo, A. P., Ibáñez, E., Gilbert-López, B. (2017). Phenolic compounds

from edible algae: bioactivity and health benefits. *Current Medicinal Chemistry, In-press*.

Montoro, P., Maldini, M., Russo, M., Postorino, S., Piacente, S., & Pizza, C. (2011). Metabolic profiling of roots of liquorice (*Glycyrrhiza glabra*) from different geographical areas by ESI/MS/MS and determination of major metabolites by LC–ESI/MS and LC–ESI/MS/MS. *Journal of Pharmaceutical and Biomedical Analysis, 54*, 535–544.

Moses, T., Papadopoulou, K. K., & Osbourn, A. (2014). Metabolic and functional diversity of saponins, biosynthetic intermediates and semi-synthetic derivatives. *Critical reviews in biochemistry and molecular biology, 49*, 439–462.

Mroczek, A. (2015). Phytochemistry and bioactivity of triterpene saponins from Amaranthaceae family. *Phytochemistry Reviews, 14*, 577–605.

Murphy, R. E., Schure, M. R., & Foley, J. P. (1998). Effect of Sampling Rate on Resolution in Comprehensive Two-Dimensional Liquid Chromatography. *Analytical Chemistry, 70*, 1585–1594.

Murphy, R. E., & Schure, M. R. (2008). Instrumentation for comprehensive multidimensional liquid chromatography. In Cohen, S. A., & Schure, M. R. (Eds.), *Multidimensional Liquid Chromatography: Theory and Applications in Industrial Chemistry and the Life Sciences*. Wiley & Sons.

Nowik, W., Héron, S., Bonose, M., Nowik, M., & Tchapla, A. (2013). Assessment of bi-dimensional separative systems using nearest neighbor distances approach. Part I: Orthogonality aspects. *Analytical Chemistry, 85*, 9449–9458.

Núñez, O., Gallart-Ayala, H., Martins, C. P., & Lucci, P. (2012). New trends in fast liquid chromatography for food and environmental analysis. *Journal of Chromatography A, 1228*, 298–323.

Oleszek, W., & Bialy, Z. (2006). Chromatographic determination of plant saponins–An update (2002–2005). *Journal of Chromatography A, 1112*, 78–91.

Schmitz, O. J. (2016). LC/MS coupling. In Kromidas, S.(Ed.), *The HPLC Expert: Possibilities and Limitations of Modern High Performance Liquid Chromatography.* John Wiley & Sons.

Ortega, N., Romero, M. P., Macià, A., Reguant, J., Anglès, N., Morelló, J. R., & Motilva, M. J. (2008). Obtention and characterization of phenolic extracts from different cocoa sources. *Journal of Agricultural and Food Chemistry, 56*, 9621–9627.

Osbourn, A., Goss, R. J., & Field, R. A. (2011). The saponins: polar isoprenoids with important and diverse biological activities. *Natural Product Reports, 28*, 1261–1268.

Pardo-Mates, N., Vera, A., Barbosa, S., Hidalgo-Serrano, M., Núñez, O., Saurina, J., et al. (2017). Characterization, classification and authentication of fruit-based extracts by means of HPLC-UV chromatographic fingerprints, polyphenolic profiles and chemometric methods. *Food Chemistry, 221,* 29-38.

Pasch, H. (2000). Hyphenated techniques in liquid chromatography of polymers. In Schmidt, M. (Ed.) New Developmets in Polymer Analytics I, *150*, 1–66.

Petry, F. C., & Mercadante, A. Z. (2016). Composition by LC-MS/MS of new carotenoid esters in mango and citrus, *Journal of Agricultural and Food Chemistry, 64*, 8207-8224.

Piccinelli, A. L., Pagano, I., Esposito, T., Mencherini, T., Porta, A., Petrone, A. M., et al. (2016). HRMS Profile of a Hazelnut Skin Proanthocyanidin-rich Fraction with Antioxidant and Anti-Candida albicans Activities. *Journal of Agricultural and Food Chemistry, 64*, 585–595.

Plaza, M., Cifuentes, A., & Ibáñez, E. (2008). In the search of new functional food ingredients from algae. *Trends in Food Science and Technology, 19*, 31–39.

Polat, S., & Ozogul, Y. (2008). Biochemical composition of some red and brown macro algae from the Northeastern Mediterranean Sea. *International journal of food sciences and nutrition, 59*, 566–572.

Pongsuwan, W., Bamba, T., Harada, K., Yonetani, T., Kobayashi, A., & Fukusaki, E. (2008). High-throughput technique for comprehensive analysis of Japanese green tea quality

assessment using ultra-performance liquid chromatography with time-of-flight mass spectrometry (UPLC/TOF MS). *Journal of Agricultural and Food Chemistry*, *56*, 10705–10708.

Qiao, X., Song, W., Ji, S., Li, Y. jiao, Wang, Y., Li, R., et al. (2014). Separation and detection of minor constituents in herbal medicines using a combination of heart-cutting and comprehensive two-dimensional liquid chromatography. *Journal of Chromatography A*, *1362*, 157–167.

Qiao, X., Song, W., Ji, S., Wang, Q., Guo, D., & Ye, M. (2015). Separation and characterization of phenolic compounds and triterpenoid saponins in licorice (*Glycyrrhiza uralensis*) using mobile phase-dependent reversed-phase×reversed-phase comprehensive two-dimensional liquid chromatography coupled with mass spectromet. *Journal of chromatography. A*, *1402*, 36–45.

Rao, A. V., & Rao, L. G. (2007). Carotenoids and human health. *Pharmacological Research*, *55*, 207–216.

Rasmussen, S. E., Frederiksen, H., Krogholm, K. S., & Poulsen, L. (2005). Dietary proanthocyanidins: Occurrence, dietary intake, bioavailability, and protection against cardiovascular disease. *Molecular Nutrition and Food Research*, *49*, 159–174.

Regos, I., & Treutter, D. (2010). Optimization of a high-performance liquid chromatography method for the analysis of complex polyphenol mixtures and application for sainfoin extracts (*Onobrychis viciifolia*). *Journal of Chromatography A*, *1217*, 6169–6177.

Regulation (EC) no 37/2010 of 22 December 2009, On pharmacologically active substances and their classification regarding maximum residue limits in foodstuffs of animal origin

Regulation (EC) No 178/2002 of the European Parliament and of the Council of 28 January 2002 laying down the general principles and requirements of food law, establishing the European Food Safety Authority and laying down procedures in matters of food safety

Regulation (EC) no 396/2005 of the European parliament and of the council of 23 February

2005 on maximum residue levels of pesticides in or on food and feed of plant and animal origin and amending

Regulation (EC) No 1881/2006 of 19 December 2006 setting maximum levels for certain contaminants in foodstuffs

Regulation (EC) no 1924/2006 of the european parliament and of the Council of 20 December 2006 on nutrition and health claims made on foods

Reis, S. F., Rai, D. K., & Abu-Ghannam, N. (2012). Water at room temperature as a solvent for the extraction of apple pomace phenolic compounds. *Food Chemistry*, *135*, 1991–1998.

Ribeiro, L. F., Ribani, R. H., Francisco, T. M. G., Soares, A. A., Pontarolo, R., & Haminiuk, C. W. I. (2015). Profile of bioactive compounds from grape pomace (*Vitis vinifera* and *Vitis labrusca*) by spectrophotometric, chromatographic and spectral analyses. *Journal of Chromatography B*, *1007*, 72–80.

Robbins, R. J., Leonczak, J., Johnson, J. C., Li, J., Kwik-Uribe, C., Prior, R. L., & Gu, L. (2009). Method performance and multi-laboratory assessment of a normal phase high pressure liquid chromatography-fluorescence detection method for the quantitation of flavanols and procyanidins in cocoa and chocolate containing samples. *Journal of Chromatography A*, *1216*, 4831–4840.

Rodríguez-Mateos, A., Cifuentes-Gomez, Tabatabaee, S., T., Lecras, C., & Spencer, J. P. E. (2011). Procyanidin , anthocyanin and chlorogenic acid content of highbush and lowbush blueberries, *Journal of Agricultural and Food Chemistry, 60*, 5772-5778.

Rzeppa, S., Von Bargen, C., Bittner, K., & Humpf, H. U. (2011). Analysis of Flavan-3-ols and procyanidins in food samples by reversed phase high-performance liquid chromatography coupled to electrospray ionization tandem mass spectrometry (RP-HPLC-ESI-MS/MS). *Journal of Agricultural and Food Chemistry*, *59*, 10594–10603.

Saha, S., Walia, S., Kundu, A., Sharma, K., & Paul, R. K. (2015). Optimal extraction and fingerprinting of carotenoids by accelerated solvent extraction and liquid chromatography with tandem mass spectrometry. *Food Chemistry*, *177*, 369–375.

Saini, R. K., Nile, S. H., & Park, S. W. (2015). Carotenoids from fruits and vegetables: Chemistry , analysis , occurrence , bioavailability and biological activities. *Food Research International*, *76*, 735–750.

Sánchez-Camargo A. P., Ibáñez E., Cifuentes A., Herrero. M. (2017). Bioactives obtained from plants, seaweeds, microalgae and food by-products using pressurised liquid extraction and supercritical fluid extraction. In D. S. A. Rocha Teresa (Ed.), *Comprehensive Analytical Chemistry*. Elsevier.

Sánchez-Camargo, A. P., Montero, L., Stiger-Pouvreau, V., Tanniou, A., Cifuentes, A., Herrero, M., & Ibáñez, E. (2016). Considerations on the use of enzyme-assisted extraction in combination with pressurized liquids to recover bioactive compounds from algae. *Food Chemistry*, *192*, 67–74.

Sánchez-Rabaneda, F., Jáuregui, O., Lamuela-Raventós, R. M., Viladomat, F., Bastida, J., & Codina, C. (2004). Qualitative analysis of phenolic compounds in apple pomace using liquid chromatography coupled to mass spectrometry in tandem mode. *Rapid communications in mass spectrometry*, *18*, 553–563.

Santos-Buelga, C., & Scalbert, A. (2000). Proanthocyanidins and tannin-like compounds - Nature, occurrence, dietary intake and effects on nutrition and health. *Journal of the Science of Food and Agriculture*, *80*, 1094–1117.

Sarker, S. D., & Nahar, L. (2012). Hyphenated techniques and their applications in natural products analysis. In Sarker, S. D., & Nahar, L. (Eds.) *Natural Products Isolation*. Springer.

Sarrut, M., Crétier, G., & Heinisch, S. (2014). Theoretical and practical interest in UHPLC technology for 2D-LC. *Trends in Analytical Chemistry*, *63*, 104–112.

Schmidt, S., Zietz, M., Schreiner, M., Rohn, S., Kroh, L. W., & Krumbein, A. (2010). Identification of complex, naturally occurring flavonoid glycosides in kale (Brassica oleracea var. sabellica) by high-performance liquid chromatography diode-array detection/electrospray ionization multi-stage mass spectrometry. *Rapid*

Communications in Mass Spectrometry, *24*, 2009–2022.

Schoenmakers, P., Marriott, P., & Beens, J. (2003). Nomenclature and conventions in comprehensive multidimensional chromatography. *LCGC Europe*, *25*, 1–4.

Schure, M. R. (1999). Limit of detection, dilution factors, and technique compatibility in multidimensional separations utilizing chromatography, capillary electrophoresis, and field-flow fractionation. *Analytical Chemistry*, *71*, 1645–1657.

Schure, M. R. (2011). The dimensionality of chromatographic separations. *Journal of Chromatography A*, *1218*, 293–302.

Schure, M. R., & Davis, J. M. (2015). Orthogonal separations: Comparison of orthogonality metrics by statistical analysis. *Journal of Chromatography A*, *1414*, 60–76.

Seeley, J. V. (2002). Theoretical study of incomplete sampling of the first dimension in comprehensive two-dimensional chromatography. *Journal of Chromatography A*, *962*, 21–27.

Shan, Y. (2016). Functional components of citrus peel. In Shan, Y. (Ed.), *Comprehensive Utilization of Citrus By-Products*. Elsevier.

Shibata, T., Kawaguchi, S., Hama, Y., Inagaki, M., Yamaguchi, K., & Nakamura, T. (2004). Local and chemical distribution of phlorotannins in brown algae. *Journal of Applied Phycology*, *16*, 291–296.

Shoji, T., Mutsuga, M., Nakamura, T., Kanda, T., Akiyama, H., & Goda, Y. (2003). Isolation and structural elucidation of some procyanidins from apple by low-temperature nuclear magnetic resonance. *Journal of Agricultural and Food Chemistry*, *51*, 3806–3813.

Siddiqui, A. J., Musharraf, S. G., Choudhary, M. I., & Rahman, A. (2017). Application of analytical methods in authentication and adulteration of honey. *Food Chemistry*, *217*, 687–698.

Singh, T., Sharma, S. D., & Katiyar, S. K. (2011). Grape proanthocyanidins induce apoptosis by loss of mitochondrial membrane potential of human non-small cell lung cancer cells In

Vitro and In Vivo. *PLoS ONE*, *6*, e27444.

Slonecker, P. J., Li, X., Ridgway, T. H., & Dorsey, J. G. (1996). Informational orthogonality of two-dimensional chromatographic separations. *Analytical chemistry*, *68*, 682–689.

Snyder, L. R., Dolan, J. W., & Carr, P. W. (2004). The hydrophobic-subtraction model of reversed-phase column selectivity. *Journal of Chromatography A*, *1060*, 77–116.

Sontia, B., Mooney, J., Gaudet, L., & Touyz, R. M. (2008). Pseudohyperaldosteronism, Liquorice, and Hypertension. *The Journal of Clinical Hypertension*, *10*, 153–157.

Spiridon, I., Colceru, S., Anghel, N., Teaca, C. A., Bodirlau, R., & Armatu, A. (2011). Antioxidant capacity and total phenolic contents of oregano (*Origanum vulgare*), lavender (*Lavandula angustifolia*) and lemon balm (*Melissa officinalis*) from Romania. *Natural product research*, *25*, 1657–1661.

Stavrianidi, A., Stekolshchikova, E., Porotova, A., Rodin, I., & Shpigun, O. (2017). Combination of HPLC-MS and QAMS as a new analytical approach for determination of saponins in ginseng containing products. *Journal of Pharmaceutical and Biomedical Analysis*, *132*, 87–92.

Steevensz, A. J., MacKinnon, S. L., Hankinson, R., Craft, C., Connan, S., Stengel, D. B., & Melanson, J. E. (2012). Profiling phlorotannins in brown macroalgae by liquid chromatography-high resolution mass spectrometry. *Phytochemical Analysis*, *23*, 547–553.

Stengel, D. B., Connan, S., & Popper, Z. A. (2011). Algal chemodiversity and bioactivity: Sources of natural variability and implications for commercial application. *Biotechnology Advances, 29, 483-501.*

Stephan, S., Hippler, J., Köhler, T., Deeb, A. A., Schmidt, T. C., & Schmitz, O. J. (2016a). Contaminant screening of wastewater with HPLC-IM-qTOF-MS and LC+LC-IM-qTOF-MS using a CCS database. *Analytical and Bioanalytical Chemistry*, *408*, 6545–6555.

Stephan, S., Jakob, C., Hippler, J., & Schmitz, O. J. (2016b). A novel four-dimensional analytical approach for analysis of complex samples. *Analytical and Bioanalytical Chemistry*, *408*,

3751–3759.

Stevenson, P. G., Mnatsakanyan, M., Francis, A. R., & Shalliker, R. A. (2010). A discussion on the process of defining 2-D separation selectivity. *Journal of Separation Science*, *33*, 1405–1413.

Stiger-Pouvreau, V., Jégou, C., Cérantola, S., Guérard, F., & Le Lann, K. (2014). Phlorotannins in sargassaceae species from brittany (France): Interesting molecules for ecophysiological and valorisation purposes. *Advances in Botanical Research*, *71*, 379–411.

Stoll, D. R., & Carr, P. W. (2005). Fast, comprehensive two-dimensional HPLC separation of tryptic peptides based on high-temperature HPLC. *Journal of the American Chemical Society*, *127*, 5034–5035.

Stoll, D. R., & Carr, P. W. (2016). Two-Dimensional Liquid Chromatography: A State of the Art Tutorial. *Analytical Chemistry*, *89*, 519-531.

Stoll, D. R., Li, X., Wang, X., Carr, P. W., Porter, S. E. G., & Rutan, S. C. (2007). Fast, comprehensive two-dimensional liquid chromatography. *Journal of Chromatography A*, *1168*, 3–43.

Stoll, D. R., Talus, E. S., Harmes, D. C., & Zhang, K. (2015). Evaluation of detection sensitivity in comprehensive two-dimensional liquid chromatography separations of an active pharmaceutical ingredient and its degradants. *Analytical and Bioanalytical Chemistry*, *407*, 265–277.

Strain, H. H., & Manning, W. M. (1942). Chlorofucine (chlorophyll γ), a green pigment of diatoms and brown algae. *Journal of Biological Chemistry, 144,* 625-636.

Sun, C., Zhao, Y. Y., & Curtis, J. M. (2015). Characterization of phospholipids by two-dimensional liquid chromatography coupled to in-line ozonolysis-mass spectrometry. *Journal of Agricultural and Food Chemistry*, *63*, 1442–1451.

Tanaka, K., Ina, A., Hayashi, K., & Komatsu, K. (2010). Comparison of chemical constituents in Glycyrrhiza uralensis from various sources using a multivariate statistical approach.

Journal of Traditional Medicine, 27, 210–216..

Tao, W., Duan, J., Zhao, R., Li, X., Yan, H., Li, J., et al. (2013). Comparison of three officinal Chinese pharmacopoeia species of Glycyrrhiza based on separation and quantification of triterpene saponins and chemometrics analysis. *Food Chemistry, 141*, 1681–1689.

Tian, H., Xu, J., & Guan, Y. (2008). Comprehensive two-dimensional liquid chromatography (NPLC x RPLC) with vacuum-evaporation interface. *Journal of Separation Science, 31*, 1677–1685.

Tian, Y., Liimatainen, J., Alanne, A. L., Lindstedt, A., Liu, P., Sinkkonen, J., et al. (2017). Phenolic compounds extracted by acidic aqueous ethanol from berries and leaves of different berry plants. *Food Chemistry, 220*, 266–281.

Tierney, M. S., Soler-Vila, A., Rai, D. K., Croft, A. K., Brunton, N. P., & Smyth, T. J. (2014). UPLC-MS profiling of low molecular weight phlorotannin polymers in Ascophyllum nodosum, *Pelvetia canaliculata* and *Fucus spiralis*. *Metabolomics, 10*, 524–535.

Tucker, G., & Robards, K. (2008). Bioactivity and structure of biophenols as mediators of chronic diseases. *Critical Reviews in Food Science and Nutrition, 48*, 929–66.

Uliyanchenko, E., Cools, P. J., Van Der Wal, S., & Schoenmakers, P. J. (2012). Comprehensive two-dimensional ultrahigh-pressure liquid chromatography for separations of polymers. *Analytical Chemistry, 84*, 7802–7809.

Valls, J., Millán, S., Martí, M. P., Borràs, E., & Arola, L. (2009). Advanced separation methods of food anthocyanins, isoflavones and flavanols. *Journal of Chromatography A, 1216*, 7143–7172.

Vallverdú-Queralt, A., Martínez-Huélamo, M., Casals-Ribes, I., & Lamuela-Raventós, R. M. (2014a). Differences in the carotenoid profile of commercially available organic and conventional tomato-based products. *Journal of Berry Research, 4*, 69–77.

Vallverdú-Queralt, A., Regueiro, J., Martínez-Huélamo, M., Rinaldi Alvarenga, J. F., Leal, L. N., &

Lamuela-Raventos, R. M. (2014b). A comprehensive study on the phenolic profile of widely used culinary herbs and spices: Rosemary, thyme, oregano, cinnamon, cumin and bay. *Food Chemistry, 154*, 299–307.

van der Klift, E. J., Vivó-Truyols, G., Claassen, F. W., van Holthoon, F. L., & van Beek, T. A. (2008). Comprehensive two-dimensional liquid chromatography with ultraviolet, evaporative light scattering and mass spectrometric detection of triacylglycerols in corn oil. *Journal of Chromatography A, 1178*, 43–55.

Van Gyseghem, E., Van Hemelryck, S., Daszykowski, M., Questier, F., Massart, D. L., & Vander Heyden, Y. (2003). Determining orthogonal chromatographic systems prior to the development of methods to characterise impurities in drug substances. *Journal of Chromatography A, 988*, 77–93.

Verardo, V., Cevoli, C., Pasini, F., Gómez-Caravaca, A. M., Marconi, E., Fabbri, A., & Caboni, M. F. (2015). Analysis of oligomer proanthocyanidins in different barley genotypes using high-performance liquid chromatography-fluorescence detection-mass spectrometry and near-infrared methodologies. *Journal of Agricultural and Food Chemistry, 63*, 4130–4137.

Vincken, J. P., Heng, L., de Groot, A., & Gruppen, H. (2007). Saponins, classification and occurrence in the plant kingdom. *Phytochemistry, 68*, 275–297.

Visioli, F., Poli, A., Peracino, A., Luzi, L., Cannella, C., & Paoletti, R. (2007). Assessment of nutritional profiles: a novel system based on a comprehensive approach. *The British Journal of Nutrition, 98*, 1101–1107.

Vivó-Truyols, G., & Schoenmakers, P. J. (2006). Chemical variance, a useful tool for the interpretation and analysis of two-dimensional chromatograms. *Journal of Chromatography A, 1120*, 273–281.

Vivó-Truyols, G., Van Der Wal, S., & Schoenmakers, P. J. (2010). Comprehensive study on the optimization of online two-dimensional liquid chromatographic systems considering losses in theoretical peak capacity in first- and second-dimensions: A pareto-optimality

approach. *Analytical Chemistry, 82*, 8525–8536.

Vonk, R. J., Gargano, A. F., Davydova, E., Dekker, H. L., Eeltink, S., De Koning, L. J., & Schoenmakers, P. J. (2015). Comprehensive two-dimensional liquid chromatography with stationary-phase-assisted modulation coupled to high-resolution mass spectrometry applied to proteome analysis of saccharomyces cerevisiae. *Analytical Chemistry, 87*, 5387–5394.

Wachtel J. L., & Cassidy, H. G. (1943). Chromatography as a means of separating amino acids. *Journal of the American Chemical Society, 65*, 665–668.

Wallace, T. C., & Giusti, M. M. (2010). Extraction and normal-phase HPLC-fluorescence-electrospray MS characterization and quantification of procyanidins in cranberry extracts. *Journal of Food Science, 75*, 690–696.

Waltenberger, B., Mocan, A., Šmejkal, K., Heiss, E. H., & Atanasov, A. G. (2016). Natural products to counteract the epidemic of cardiovascular and metabolic disorders. *Molecules, 21*, 807-831.

Wang, S., Qiao, L., Shi, X., Hu, C., Kong, H., & Xu, G. (2015). On-line stop-flow two-dimensional liquid chromatography-mass spectrometry method for the separation and identification of triterpenoid saponins from ginseng extract. *Analytical and Bioanalytical Chemistry, 407*, 331–341.

Wang, T., Jónsdóttir, R., Liu, H., Gu, L., Kristinsson, H. G., Raghavan, S., & Ólafsdóttir, G. (2012). Antioxidant capacities of phlorotannins extracted from the brown algae Fucus vesiculosus. *Journal of Agricultural and Food Chemistry, 60*, 5874–5883.

Wang, X., Wang, S., & Cai, Z. (2013). The latest developments and applications of mass spectrometry in food-safety and quality analysis. *Trends in Analytical Chemistry, 52*, 170–185.

Wang, Y., Lu, X., & Xu, G. (2008). Development of a comprehensive two-dimensional hydrophilic interaction chromatography / quadrupole time-of-flight mass spectrometry

system and its application in separation and identification of saponins from *Quillaja saponaria*, *Journal of Chromatography A, 1181*, 51-59.

Weber, H. A., Hodges, A. E., Guthrie, J. R., O'Brien, B. M., Robaugh, D., Clark, A. P., et al. (2007). Comparison of proanthocyanidins in commercial antioxidants: Grape seed and pine bark extracts. *Journal of Agricultural and Food Chemistry*, *55*, 148–156.

Wei, S. S., Yang, M., Chen, X., Wang, Q. R., & Cui, Y. J. (2015). Simultaneous determination and assignment of 13 major flavonoids and glycyrrhizic acid in licorices by HPLC-DAD and Orbirap mass spectrometry analyses. *Chinese Journal of Natural Medicines*, *13*, 232–240.

Wei, Y., Lan, T., Tang, T., Zhang, L., Wang, F., Li, T., et al. (2009). A comprehensive two-dimensional normal-phase × reversed-phase liquid chromatography based on the modification of mobile phases. *Journal of Chromatography A*, *1216*, 7466–7471.

Willemse, C. M., Stander, M. A., Vestner, J., Tredoux, A. G. J., & De Villiers, A. (2015). Comprehensive two-dimensional hydrophilic interaction chromatography (hilic) × reversed-phase liquid chromatography coupled to high-resolution mass spectrometry (RP-LC-UV-MS) analysis of anthocyanins and derived pigments in red wine. *Analytical Chemistry*, *87*, 12006–12015.

Winther, B., & Reubsaet, J. L. E. (2005). Application of supplementary flow in comprehensive 2D liquid chromatography combining SEC and RPC. *Journal of Separation Science*, *28*, 477–482.

Wishart, D. S. (2008). Metabolomics: applications to food science and nutrition research. *Trends in Food Science and Technology , 19*, 482-493.

Wu, H., Guo, J., Chen, S., Liu, X., Zhou, Y., Zhang, X., & Xu, X. (2013). Recent developments in qualitative and quantitative analysis of phytochemical constituents and their metabolites using liquid chromatography-mass spectrometry. *Journal of Pharmaceutical and Biomedical Analysis*, *72*, 267–291.

Xu, T., Yang, M., Li, Y., Chen, X., Wang, Q., Deng, W., et al. (2013). An integrated exact mass

spectrometric strategy for comprehensive and rapid characterization of phenolic compounds in licorice. *Rapid Communications in Mass Spectrometry*, *27*, 2297–2309.

Yanagida, A., Shoji, T., & Shibusawa, Y. (2003). Separation of proanthocyanidins by degree of polymerization by means of size-exclusion chromatography and related techniques. *Journal of Biochemical and Biophysical Methods*, *56*, 311–322.

Yang, R., Yuan, B. C., Ma, Y. S., Zhou, S., & Liu, Y. (2016). The anti-inflammatory activity of licorice, a widely used Chinese herb. *Pharmaceutical Biology, 55, 5-18.*.

Yang, W., Zhang, J., Yao, C., Qiu, S., Chen, M., Pan, H., et al. (2016). Method development and application of offline two-dimensional liquid chromatography/quadrupole time-of-flight mass spectrometry-fast data directed analysis for comprehensive characterization of the saponins from Xueshuantong Injection. *Journal of Pharmaceutical and Biomedical Analysis*, *128*, 322–332.

Zhang, M., Sun, J., & Chen, P. (2017). A Computational tool for accelerated analysis of oligomeric proanthocyanidins in plants. *Journal of Food Composition and Analysis*, *56*, 124–133.

Zheng, Y. F., Qi, L. W., Zhou, J. L., & Li, P. (2010). Structural characterization and identification of oleanane- type triterpene saponins in *Glycyrrhiza uralensis* Fischer by rapid-resolution liquid chromatography coupled with time-of-flight mass spectrometry. *Rapid Communications in Mass Spectrometry*, *24*, 3261–3270.

Annexes

Annex A. Curriculum Vitae

Lidia Montero finished her studies in the degree in Food Science and Technology in 2011in Universidad Autónoma de Madrid (UAM). Thereafter, Lidia started her Master studies in Agricultural Chemistry and Novel Foods in Universidad Autónoma de Madrid (2011-2012) thanks to the "Starting postgraduate studies program" scholarship, granted by UAM (2011-2013). During this period, Lidia began to work in the Foodomics lab belonging to the Spanish National Research Council (CSIC) at the Institute of Food Science Research (CIAL)where she acquired an extensive knowledge about green extraction techniques for food applications as well as a deep knowledge about different analytical techniques. With this scholarship, Lidia started her PhD in the Foodomics Lab under the supervision of Dr Elena Ibáñez and Dr Miguel Herrero. Her PhD is focused on the development of comprehensive two-dimensional liquid chromatography coupled to mass spectrometry methods for the chemical characterization of complex food matrices.

From 2014 to 2017, Lidia obtained a contract from the Mediterranean University of Reggio Calabria (Italy), thanks to which she could continue her PhD studies. This contract was associated to two Italian research projects. In addition, she has participated in a Spanish research project. The results obtained during this PhD period are presented in the present Dissertation.

Annex B.

B.1 List of publications. included in the Doctoral dissertation.

1. Montero, L.; Herrero, M.; Prodanov, M.; Ibáñez, E.; Cifuentes, A. (2013). Characterization of grape seed procyanidins by comprehensive two-dimensional hydrophilic interaction × reversed phase liquid chromatography coupled to diode array detection and tandem mass spectrometry. *Analytical and Bioanalytical Chemistry, 405*, 4627-4638.

2. Montero, L.; Herrero, M.; Ibáñez, E.; Cifuentes, A. (2013). Profiling of phenolic compounds from different apple varieties using comprehensive two-dimensional liquid chromatography. *Journal of Chromatography A.131,* 275-283.

3. Montero, L.; Herrero, M.; Ibáñez, E.; Cifuentes, A. (2014). Separation and characterization of phlorotannins from brown algae *Cystoseira abies-marina* by comprehensive two-dimensional liquid chromatography. *Electrophoresis, 35*, 1644–1651.

4. Montero, L.; Sánchez-Camargo, A. P., García-Cañas, V.; Tanniou, A.; Stiger-Pouvreau, V., Russo, M; Rastrelli, L.; Cifuentes, A.; Herrero, M.; Ibáñez, E. (2016) Anti-proliferative activity and chemical characterization by comprehensive two-dimensional liquid chromatography coupled to mass spectrometry of phlorotannins from the brown macroalga *Sargassum muticum* collected on North-Atlantic coasts. *Journal of Chromatography A. 1428,* 115–125.

5. Montero, L.; Ibáñez, E.; Russo, M.; di Sanzo, R.; Rastrelli, L.; Piccinelli, A. L.; Celano, R.; Cifuentes, A.; Herrero, M. (2016). Metabolite profiling of licorice (*Glycyrrhiza glabra*) from different locations using comprehensive two-dimensional liquid chromatography coupled to diode array and tandem mass spectrometry detection. *Analica Chimica Acta, 913*, 145-159.

6. Brazdauskas, T.; Montero, L.; Venskutonis, P.R.; Ibañez, E.; Herrero, M. (2016). Downstream valorization and comprehensive two-dimensional liquidchromatography-based chemical characterization of bioactives fromblack chokeberries (*Aronia melanocarpa*) pomace. *Journal of Chormatography A, 6*,126-135.

7. Montero, L.; Sáez, V.; von Baer, D.; Cifuentes, A.; Herrero, M. (2017). Profiling of *Vitis vinifera L.* canes (poly)phenolic compounds using comprehensive two-dimensional liquid chromatography. *Journal of Chormatography A,* Subbmited.

8. Montero, L.; Ibáñez, E.; Russo, M.; Rastrelli, L.; Cifuentes, A.; Herrero M. (2017). Focusing and non-focusing modulation strategies for the improvement of on-line two-dimensional hydrophilic interaction chromatography × reversed phase profiling of complex food samples. *Analytica Chimica Acta,* Subbmited.

B.2 Other publications in SCI Journals.

9. Sánchez-Camargo, A. P.; Montero, L.; Stiger-Pouvreau, V.; Tanniou, A.; Cifuentes, A.; Herrero, M.; Ibáñez, E. (2016). Considerations on the use of enzyme-assisted extraction in combination with pressurized liquids to recover bioactive compounds from algae. *Food Chemistry, 192*, 67–74.

10. Sánchez-Camargo, A. P.; Montero, L.; Cifuentes, A.; Herrero, M.; Ibáñez, E. (2016). Application of Hansen solubility approach for the subcritical and supercritical selective extraction of phlorotannins from *Cystoseira abies-marina*. *RSC Advances*, *6*, 94884-94894.

11. Montero, L.; Sánchez-Camargo, A.P.; Ibáñez, E.; Gilbert-López, B. (2016). Phenolic compounds from edible algae: bioactivity and health benefits. Current Medicinal Chemistry, Special Issue Polyphenols and Human Diseases: From Kitchen to Clinic. CMC-2016-0163. In-Press. Ed. Bentham Science.

12. Gabriele, M.; Frassinetti, S.; Caltavuturo, L.; Montero, L.; Dinelli, G.; Di Gioia, D.; Longo,

V.; Pucci, L. (2017). *Citrus bergamia* powder: antioxidant, antimicrobial and anti-inflammatory properties. *Journal of Functional Foods*, *31*, 255-265.

13. Castro-Puyana, M.; Montero, L.; Pérez-Míguez, R.; Herrero, M. (2017). Application of mass spectrometry-based metabolomics approaches for food safety, quality and traceability. *Trends in Analytical Chemistry*. Subbmited.

B.3. Book chapters.

1. Montero, L.; Sánchez-Camargo, A.P.; Mendiola, J.A.; Herrero, M.; Ibáñez E. (2016). Novel extraction techniques for bioactive compounds from herbs and spices in "Herbs and Spices: Processing Technology and Health Benefits", Mohammad Hossain, Dilip Rai and Nigel P Brunton, Eds., Wiley. ISBN: 978-1-119-03661-6.

B.4. Dissemination of results.

Oral Communications (PhD-related)

* Indicates the lecturer

1.- Montero, L.*; Herrero M.; Prodanov, M.; Cifuentes, A.; Ibáñez, E. Development of a comprehensive two-dimensional liquid chromatography method for the characterization of grape seed procyanidins based on the coupling of hydrophilic interaction and reversed phase separations (HILIC × RP). XII Scientific Meeting of the Spanish Society of Chromatography and Related Techniques. Tarragona, Spain. November, 2012.

2.- Montero, L.*. Aplicaciones alimentarias de la cromatografía de líquidos bidimensional completa acoplada a espectrometría de masas (LC × LC-MS). III Cycle of Research Institute of Food Science Seminars. Madrid. September, 2013.

3.- Montero, L.*; Herrero, M.; Cifuentes, A.; Ibáñez, E. Phlorotannins characterization from

Cystoseira abies-marina brown algae by comprehensive two-dimensional liquid chromatography coupled to mass spectrometry. XIII Scientific Meeting of the Spanish Society of Chromatography and Related Techniques. Tenerife, Spain . October, 2013.

4.- Herrero, M.*; Montero, L.; Ibáñez, E.; Cifuentes, A. Analysis of complex food samples with comprehensive two-dimensional liquid chromatography (LC × LC) using hydrophilic interaction and reversed phase. ITP2013-20th International Symposium on Electro- and Liquid Phase-Separation Techniques. Tenerife, Spain. October, 2013.

5.- Montero, L.*; Sánchez Camargo, A.P.; Cifuentes, A.; Ibáñez, E.; M. Herrero. Comprehensive two-dimensional liquid chromatography to characterize polyphenols from *Sargassum muticum* brown algae. 14th Instrumental Analysis Conference. Barcelona, Spain. October, 2014.

6.- Montero, L.*; Ibáñez, E.; Russo, M.; Rastrelli, L.; Piccinelli, A.; Celano, R.; Cifuentes, A.; Herrero, M. Fingerprinting analysis of extracts of licorice by comprehensive two-dimensional liquid chromatography. XV Scientific Meeting of the Spanish Society of Chromatography and Related Techniques (SECyTA2015). Castellón de la Plana, Spain. October, 2015.

7.- Montero, L.; Ibáñez, E.; Russo, M.; di Sanzo, R.; Rastrelli, L.; Cifuentes, A.; Herrero, M.*. Comprehensive two-dimensional liquid chromatography coupled to mass spectrometry (LC × LC-MS/MS) for geographical origin assignment of licorice. '40th international symposium on capillary chromatography' and '13th GC×GC symposium'. Riva del Garda, Italy. May, 2016.

8.- Montero, L.*; Ibáñez, E.; Russo, M.; di Sanzo, R.; Rastrelli, L.; Cifuentes, A.; Herrero, M. Metabolic Classification of Licorice as Function of Geographical Origin by Comprehensive Two-dimensional Liquid Chromatography Coupled to Mass Spectrometry (LC × LC-MS/MS). 44th International Symposium on High Performance Liquid Phase Separations and Related Techniques (HPLC 2016). San Francisco, California (USA). June, 2016.

9.- Montero, L.*; Herrero, M.; Ibáñez, E.; di Sanzo, R.; Carabetta, S.; Rastrelli, L.; Cifuentes, A.; Russo, M. Characterization of the metabolite profile of licorice from different geographical origin by comprehensive two-dimensional liquid chromatography coupled to mass spectrometry (LC × LC-MS/MS). XI Italian congress of food chemistry. Cagliari, Italy. October,

2016.

10.- Montero, L.*; Brazdauskas, T.; Venskutonis, P. R.; Ibáñez, E.; Herrero, M. Valorization of black chokeberries (*Aronia melanocarpa*) pomace and chemical characterization by comprehensive two-dimensional liquid chromatography coupled to mass spectrometry. XVI Scientific Meeting of the Spanish Society of Chromatography and Related Techniques (SECyTA2016). Sevilla, Spain. November, 2016.

Other Oral Communications

1.- Sánchez-Camargo, A. P. *; Montero, L.; Barranco, A.; Cifuentes, A.; Ibáñez, E.; Herrero, M. Green process to obtain polyphenols from *Sargassum muticum* macroalgae collected of different geographic Europe sites. VI Meeting of Experts on Compressed Fluids Technology (FLUCOMP). Barcelona, Spain. June, 2014.

2.- Herrero, M.; Mendiola, J. A.*; Cediel, A. L.; Montero, L., López-Expósito, I.; Ibáñez, E. New green technologies to extract bioactives from *Isochrysis galbana* microalgae. VII Meeting of Experts on Compressed Fluids Technology (FLUCOMP). Barcelona, Spain. June, 2014.

3.- Herrero, M.; Sánchez-Camargo, A. P.; Montero, L.; Mendiola, J. A.; Cifuentes, A.; Ibáñez, E.*. Green Foodomics Applied to the Discovery of New Functional Food Ingredients with Antiproliferative Activity. XVI Latin-American Congress on Chromatography (COLACRO). Lisbon, Portugal. January, 2016.

4.- Sánchez-Camargo, A. P.; Montero, L.; Cifuentes, A.; Herrero, M.; Ibáñez, E. Development of new strategies of integrated green processes for obtaining phlorotannin-enriched extracts from brown algae *Cystoseira abies-marina*. IV Iberoamerican Conference on Supercritical Fluids. Viña del Mar, Chile. March-April, 2016.

5.- Sánchez-Camargo, A. P.; Herrero, M.; Montero, L.; Mendiola, J. A.; García-Cañas, V.; Cifuentes, A.; Ibanez, E.*. Green foodomics: new approaches for the isolation and purification of bioactive compounds with antiproliferative activity using green technologies.

Conference: '40th international symposium on capillary chromatography' and '13th GC×GC symposium'. Riva del Garda, Italy. May, 2016.

Poster Presentations (PhD-related)

1.- Montero, L.; Sánchez Camargo, A. P.; Cifuentes, A.; Ibáñez, E.; Herrero, M. Chemical characterization of particular phlorotannins of Sargassum muticum by LC × LC-DAD-MS/MS. Conference: VII National Meeting of the Spanish Society of Mass Spectrometry (SEEM2015). Castellón de la Plana, Spain. October, 2015.

2.- Montero, L.; Ibáñez, E.; Cifuentes, A.; Herrero, M. Acoplamiento HILIC × RP en cromatografía de líquidos bidimensional completa para el análisis de muestras alimentarias complejas. **I**I Cientific Meeting CIAL Forum. Madrid, Spain, November, 2016.

Other Poster Presentations

3.- Montero, L.; López-Expósito, I.; A. L. Cediel, Ibáñez, E.; Herrero, M. Pressurized liquid extraction to obtain antioxidant and anti-inflamatory fractions from *sochrysis galbana* microalga. I Cientific Meeting CIAL Forum. Madrid, Spain. June, 2014.

2.- Sánchez-Camargo, A. P.; Montero, L.; Alejandro Cifuentes, Miguel Herrero, Elena Ibáñez. Development of new strategies for obtaining phlorotannin-enriched extracts from brown algae *Cystoseira abies-marina*. VIII Meeting of Experts on Compressed Fluids Technology (FLUCOMP). Cádiz, Spain. September, 2015.

4.- Alioto, F.; Sánchez-Camargo, A. P.; Mendiola, J. A.; Montero, L.; Bonaccorsi, I.; Mondello, L.; Ibáñez, E. Flavonoids from citrus seeds obtained using compressed fluids. VIII Meeting of Experts on Compressed Fluids Technology (FLUCOMP). Cádiz, Spain. September, 2015.

5.-Celano, R, Di Sanzo, R., Carabetta, S., Montero, L., Campone, L., pagano, L., Piccinelli, A. L., Rastrelli, L., Russo, M. Metabolic profiling of Calabrian licorice (Glycyrrhiza glabra) and related product by UHPLC-HRMS and tándem mass spectrometry MS^n). XI Italian congress of food chemistry. Cagliari, Italy. October, 2016.

6.- Calixto, M. R.; Montero, L.; Soberón, M.; Arnao, I. Chemical analysis, antioxidant activity and characterization of polyphenolic compounds from "uvilla" (*Pourouma cecropiifolia Mart*) by HPLC-MS. 28° Peruvian Conference of Chemistry. Lima, Peru. March, 2017.